RESEARCH FOUNDATION

RESEARCH FOR THE NFPA MISSION

Fire Safety Challenges of Tall Wood Buildings – Phase 2: Task 2 & 3 – Cross Laminated Timber Compartment Fire Tests

FINAL REPORT BY:

Joseph Su and Pier-Simon Lafrance

National Research Council of Canada
Ottawa, Ontario, Canada

Matthew Hoehler and Matthew Bundy

National Institute of Standards and Technology
Gaithersburg, MD, USA

February 2018

Fire Protection Research Foundation
1 Batterymarch Park, Quincy, MA 02169-7417, USA
Email: research@nfpa.org | Web: nfpa.org/foundation

RESEARCH FOUNDATION

RESEARCH FOR THE NFPA MISSION

Errata

Report:

Fire Safety Challenges of Tall Wood Buildings – Phase 2: Task 2 & 3 – Cross Laminated Timber Compartment Fire Tests

Author(s)

Joseph Su and Pier-Simon Lafrance
National Research Council of Canada
Ottawa, Ontario, Canada

Matthew Hoehler and Matthew Bundy
National Institute of Standards and Technlogy
Gaithersburg, MD USA

February 2018

Errata No.: FPRF-2018-01-01

Reference:

Erratum

This is to correct typos in the heat flux equation in Task 2&3 Report FPRF-2018-01 (i.e. NRC A1-010659.1). On page 40, the sign in front of the second term of the heat flux equation should be minus (not plus) and the units of heat flux are W/m^2 (not W). The corrected text should read:

The incident heat flux at the plate thermometer at step i ($\left[\dot{q}''_{inc}\right]^i$, in W/m^2) is calculated using the measured temperature of the plate thermometer (T_{PT}, in K) and the gas temperature near the plate thermometer (T_{gas}, in K) as follows:

$$\left[\dot{q}''_{inc}\right]^i = \sigma\left[T_{PT}^4\right]^i - \frac{(h + K_{PT})\left(\left[T_{gas}\right]^i - \left[T_{PT}\right]^i\right) - C_{PT}\dfrac{\left[T_{PT}\right]^{i+1} - \left[T_{PT}\right]^{i-1}}{\left[t\right]^{i+1} - \left[t\right]^{i-1}}}{\varepsilon_{PT}}$$

The published results in both the report and data sets for heat flux are correct and not affected by the typos in the body of the report.

Issue date: April 22, 2020

Phone: 617-984-7281
E-mail: foundation@nfpa.org

FOREWORD

Recent architectural trends include the design and construction of increasingly tall buildings with structural components comprised of engineered wood referred to by names including; cross laminated timber (CLT), laminated veneer lumber (LVL), or glued laminated timber (Glulam). These buildings are cited for their advantages in sustainability resulting from the use of wood as a renewable construction material.

Research and testing are needed to evaluate the contribution of mass timber elements to room/compartment fires with the types of structural systems that are expected to be found in tall buildings (e.g. CLT, etc.). Previous research has shown that timber elements contribute to the fuel load in buildings and can increase the initial fire growth rate. This has the potential to overwhelm fire protection systems, which may result in more severe conditions for occupants, fire fighters, property and neighboring property.

There is a need to quantify the contribution of timber elements to compartment fires to assess the relative performance compared to noncombustible structural materials. The contribution of exposed timber to room fires should be quantified for the full fire duration using metrics such as charring rate, visibility, temperature and toxicity. This will allow a designer to quantify the contribution, validate design equations and develop a fire protection strategy to mitigate the level of risk to occupants, fire fighters, property and neighboring property. In addition, the effect of encapsulating the timber as means of preventing or delaying involvement in the fire (e.g. gypsum, thermal barrier) needs to be characterized.

Therefore, the Research Foundation initiated a research program with the goal to quantify the contribution of Cross Laminated Timber (CLT) building elements (wall and/or floor-ceiling assemblies) in compartment fires. This Task 3 report summarizes the results from a series of fire tests conducted with CLT compartments.

The Fire Protection Research Foundation expresses gratitude to the report authors Joseph Su and Pier-Simon Lafrance, who are with National Research Council (NRC) of Canada located in Ottawa, Ontario, Canada and Matthew Hoehler and Matthew Bundy, who are with the National Institute of Standards and Technology (NIST) located in Gaithersburg, MD, USA. The Research Foundation appreciates the guidance provided by the Project Technical Panelists, the funding provided by the project sponsors, and all others that contributed to this research effort. Special thanks are expressed to the US Department of Agriculture (USDA), Forest Service for being a sponsor of this study. Donations of gypsum board from USG Corporation and simulated thermal elements from FM Global are gratefully acknowledged. The Foundation would also like to acknowledge the substantial in-kind contribution by NRC to conduct the test program.

About the Fire Protection Research Foundation

The Fire Protection Research Foundation plans, manages, and communicates research on a broad range of fire safety issues in collaboration with scientists and laboratories around the world. The Foundation is an affiliate of NFPA.

About the National Fire Protection Association (NFPA)

Founded in 1896, NFPA is a global, nonprofit organization devoted to eliminating death, injury, property and economic loss due to fire, electrical and related hazards. The association delivers information and knowledge through more than 300 consensus codes and standards, research, training, education, outreach and advocacy; and by partnering with others who share an interest in furthering the NFPA mission.

All NFPA codes and standards can be viewed online for free.

NFPA's membership totals more than 65,000 individuals around the world.

Keywords: tall wood buildings, fire safety, tall timber, cross laminated timber, CLT, compartment fire, fire test

Report number: FPRF-2018-01-REV

PROJECT TECHNICAL PANEL

Carl Baldassarra, Wiss, Janney, Elstner Associates
David Barber, Arup
Jim Brinkley, International Association of Fire Fighters
Charlie Carter, American Institute Steel Construction
Kim Clawson, Jensen Hughes
Ronny Coleman, Fireforce One
Sean DeCrane, Battalion Chief (Retired), Cleveland Fire Department, OH
Michael Engelhardt, University of Texas at Austin
Patricia Layton, Clemson University
Steven Lohr, Fire Chief, Hagerstown Fire Department, MD
Rick McCullough, Fire Chief (Retired), City of Regina, Saskatchewan, Canada
Kevin McGrattan, NIST
Ben Johnson, Skidmore, Owings & Merrill LLP
Paul Shipp, USG Corporation
Ray Walker, Fire Marshal, Vernon, CT, International Fire Marshals Association
Tracy Vecchiarelli, NFPA Staff Liaison

PROJECT SPONSORS

American Wood Council (AWC)

US Department of Agriculture, Forest Service

National Research Council (NRC) of Canada

Property Insurance Research Group (PIRG):
American International Group, Inc. (AIG)
CNA Insurance
FM Global
Liberty Mutual Insurance
Tokio Marine America
Travelers Insurance
XL Group
Zurich Insurance Group

NRC·CNRC CONSTRUCTION

Fire Safety Challenges of Tall Wood Buildings – Phase 2:

Task 2 & 3 - Cross Laminated Timber Compartment Fire Tests

Joseph Su, Pier-Simon Lafrance, Matthew Hoehler and Matthew Bundy

12 February 2018

National Research Council Canada | Conseil national de recherches Canada

Canada

Fire Safety Challenges of Tall Wood Buildings – Phase 2

Task 2 & 3 - Cross Laminated Timber Compartment Fire Tests

Lead Author

Joseph Su, PhD

Approved

Ahmed Kashef, PhD
Director
Fire Safety
NRC Construction Research Centre

Report No: A1-010659.1
Report Date: 12 February 2018
Contract No: A1-010659 (formerly A1-006599)
Agreement date: 1 July 2015

388 pages

Table of Contents

List of Figures

List of Tables

Executive Summary

The Fire Protection Research Foundation (FPRF) initiated the project “Fire Safety Challenges of Tall Wood Buildings - Phase 2” to address the need for evaluating the contribution of mass timber elements to compartment fires. In part, this is linked to the concern that timber elements in tall wood buildings could increase the fire load, affect the fire growth rate, and potentially compromise fire protection systems in buildings, all of which could result in more severe conditions for occupants and responding fire fighters and increase the threat of damage to the property and adjacent properties. This project aimed to quantify the contribution of cross laminated timber (CLT) building elements to compartment fires, and to characterize the fire protection of the CLT structural elements using physical barrier (e.g., gypsum board) for delaying or preventing their involvement in the fire.

As part of the project, six large CLT compartment fire tests were conducted. The fire tests were conducted without any sprinklers and without firefighting intervention until the end of the tests in order to quantify the CLT contribution to compartment fires. Note that it would be the typical arrangement and requirement for tall wood buildings to be equipped with automatic sprinklers in North America.

For this FPRF test series, CLT test compartments (9.1 m long x 4.6 m wide x 2.7 m high or 30 ft long x 15 ft wide x 9 ft high) were constructed using 175-mm thick 5-ply CLT structural panels. The CLT panels were manufactured using 2 x 4 spruce-pine-fir lumber glued with a polyurethane structural adhesive (with a brand name of HBE[1], 1% of the CLT panel weight), conforming to American National Standard ANSI/APA PRG 320 manufacturing standard. The compartment had a rough opening of 1.8 m wide x 2.0 m high (6 ft wide x 6.7 ft high) in four tests and 3.6 m wide x 2.0 m high (12 ft wide x 6.7 ft high) in two tests, with a ventilation factor of 0.03 $m^{½}$ and 0.06 $m^{½}$, respectively. The CLT surfaces in the compartments were fully or partially protected using multiple layers of 15.9-mm (5/8 in.) thick Type X gypsum board as the physical barrier. Real residential contents and furnishings were used in the compartment tests with a moveable fire load density of 550 MJ/m^2.

Two baseline tests (Test 1-1 and Test 1-2) with all CLT surfaces protected in the compartments, defined the contribution of the moveable fire load to the compartment fires and provided baseline data for quantifying the CLT contribution to the compartment fires in the tests involving various amounts of exposed CLT surfaces. Protecting the CLT surfaces using the physical barrier was an effective means to delay and/or prevent the ignition and involvement of the timber structural elements in the fires, limiting and/or eliminating their contribution to the fires.

Ventilation conditions had significant impacts on the fire development in the compartments. The smaller opening, which was used in four of the six tests, provided a longer duration of interior compartment fire than the larger opening, since the fire was more ventilation-limited with the smaller opening and a longer duration of fully-developed fire exposure conditions ensued. The larger opening provided a higher overall peak heat release rate, albeit for a shorter duration. As expected, with the smaller opening, the CLT elements were exposed to a longer duration of fully-developed fire, and therefore the CLT became more involved over the duration of the test(s), which made it more likely to distinguish and quantify the CLT contribution.

---

[1] Certain commercial products are identified in this report to specify the materials used and the procedures employed. In no case does such identification imply endorsement or recommendation by the National Research Council Canada or the National Institute of Standards and Technology, nor does it indicate that the products are necessarily the best available for the purpose.

The CLT contribution to the compartment fire increased with the increasing surface area of the CLT panels that were exposed and involved in the fires, and was also influenced by the ventilation condition.

The impact of the ventilation opening size on the CLT contribution to the compartment fires was demonstrated by Test 1-3 and Test 1-5, where the same long wall was exposed in both tests. The peak temperatures in the compartments were similar in both tests. In Test 1-3, with the larger ventilation opening, the fire exhibited a general trend of decay following the fully-developed phase although the initial heat release rate and exterior heat fluxes were higher and two small transient increases occurred (due to the delamination of two plies of CLT from the exposed wall). In Test 1-5, with the smaller ventilation opening, more heat was trapped inside the compartment and, after the initial decay, a large re-flash occurred on the exposed wall with delamination of the second ply of the CLT, which caused the second flashover and induced the full involvement of all originally protected CLT panels in the fire.

The area and orientation of exposed CLT surface had a large impact on the CLT contribution to compartment fires. In all tests with exposed CLT surface(s), flashover occurred approximately 3 min to 5 min earlier than the two baseline tests (i.e., ≈ 15 min). The peak compartment temperatures were similar to the baseline. However, the heat release rates and heat fluxes to the exterior façade were higher than the baseline; the exposed CLT panels increased the fuel load in the test compartments. The unprotected (exposed) CLT surface exhibited heat delamination, which led to one or more periods of fire regrowth after decay in Test 1-3, Test 1-4 and Test 1-5 and no decay of the fire prior to suppression in Test 1-6.

Although the CLT compartment fire tests were conducted without sprinklers, simulated thermal elements (STE) were used in the tests to replicate the time temperature response of a quick-response (QR) sprinkler element. In all the tests, the STEs reached 68 °C (a typical temperature rating for residential sprinklers) well before the flashover while the fire was still limited to the first item ignited, predicting a likely time for sprinkler activation if sprinklers had been installed in the tests.

The CLT compartment fire tests produced a large amount of technical information. The test data can be used to compare the fire performance of CLT structural systems with other types of structural systems used in tall buildings, to validate design equations and models and to develop a fire protection strategy to mitigate potential fire hazards to occupants, fire fighters and properties.

Fire Safety Challenges of Tall Wood Buildings – Phase 2: Task 2 & 3 - Cross Laminated Timber Compartment Fire Tests

Joseph Su, Pier-Simon Lafrance, National Research Council of Canada, Canada

Matthew Hoehler, Matthew Bundy, National Institute of Standards and Technology, USA

1. INTRODUCTION

Recent architectural trends include the design and construction of increasingly tall buildings with structural components comprised of mass timber including cross laminated timber (CLT). These buildings are cited for their advantages for sustainability resulting from the use of wood as a renewable construction material.

Research and testing are needed to evaluate the contribution of mass timber elements to room/compartment fires with the types of structural systems that are expected to be found in tall buildings (e.g., CLT, etc.). The Fire Protection Research Foundation (FPRF) initiated the project "Fire Safety Challenges of Tall Wood Buildings – Phase 2". It is recognized that current and future tall wood buildings in North America will use various structural wood elements which may include timber beams and columns, CLT walls and CLT floors, or other mass timber products. This phase of the research project aimed to quantify the contribution of CLT building elements (wall and/or floor-ceiling assemblies) to compartment fires, and also to characterize the fire protection of the CLT using physical barriers (e.g., gypsum board) for delaying or preventing its involvement in the fire. Six large-scale CLT compartment fire tests (unsprinklered) were planned in consultation with the Project Technical Panel (PTP) [1-3] and in consideration of gaps identified by a literature review [4]. Modeling was also conducted to support the choice of test parameters [5].

North American codes require that all tall buildings be fully sprinklered in accordance with National Fire Protection Association (NFPA) standard NFPA 13 [6] and that fire services are required to respond to fire incidents in accordance with NFPA 1710 and 1720 [7, 8]. However, in order to achieve the project objective to quantify the contribution of CLT building elements, the CLT compartment fire tests were conducted without sprinklers and without firefighting intervention. Although the CLT compartment fire tests used no sprinklers, simulated thermal elements (STEs) were used in the tests to replicate the time temperature response of a quick-response (QR) sprinkler element. This report documents the results of the CLT compartment fire tests.

It is worthy of note that, in support of code development efforts of the International Code Council's Ad Hoc Committee on Tall Wood Buildings, US Department of Agriculture's Forest Products Laboratory recently conducted another series of CLT compartment fire tests at the Bureau of Alcohol, Tobacco, Firearms, and Explosives Fire Test Laboratory (ATF). The fire test series at ATF included tests with various levels of exposed CLT elements as well as tests of fully exposed CLT compartments with sprinklers [9].

2. TEST SETUP AND PROCEDURE

Under a collaborative agreement between the National Research Council Canada (NRCC) and National Institute of Standards and Technology (NIST), the CLT compartment fire tests were

conducted by a joint NRCC-NIST team at NIST's National Fire Research Laboratory [10]. Computer modelling was conducted by the RISE Research Institutes of Sweden to help determine experimental parameters [5].

2.1 CLT Compartment

In the original request for proposals, a steel-framed compartment structure had been specified as a baseline to determine the contribution from the CLT compartment structure to the fire severity. However, the project team and the Project Technical Panel agreed that, for the purpose of quantifying CLT contributions to the compartment fires, a steel baseline test was not absolutely necessary. Instead, a fully protected CLT compartment would have the same fire dynamics as a compartment with noncombustible construction, and therefore could be used as a baseline to define the contribution of all movable fire loads (room contents) to the compartment fires and then to quantify the contributions of CLT structural elements to the fires in other tests. This allowed more CLT compartment tests with better use of limited resources.

Figure 1 is a schematic of the test compartments, which simulated studio sized apartments. A total of four CLT compartments were constructed in two series, with two compartments constructed simultaneously in each series under the calorimeter hood.

2.1.1 CLT Compartment Structure

Each CLT test compartment was 9.1 m x 4.6 m x 2.7 m high (30 ft x 15 ft x 9 ft), representing a studio sized apartment unit. The size of the fire compartments was chosen by the Project Technical Panel from two options presented in the discussion paper [1]. The original request for proposals called for a compartment size of not less than a 4 m x 4 m (13 ft x 13 ft) footprint and not less than 2.4 m (8 ft) in height. After reviewing the literature survey by Brandon and Östman [4] and relevant references, the Panel decided that the CLT compartment size specified in the request for proposals was similar in size to most CLT compartments tested previously and that the size of 9.1 m x 4.6 m x 2.7 m (30 ft x 15 ft x 9 ft) would be more representative of current and future CLT structures in tall buildings [1, 11].

Test compartments were constructed using 175-mm (7 in.) thick 5-ply CLT structural panels manufactured using 2 x 4 spruce-pine-fir (SPF) lumber glued with a polyurethane adhesive (with a brand name of HBE[2], 1% of the panel weight) for all wall and ceiling assemblies. All CLT panels conformed to American National Standard ANSI/APA PRG-320 [12]. The ceiling assembly spanned in the 4.6-m (15 ft) direction parallel to walls W2 and W4. Figure 2 to Figure 7 show construction details.

As shown in Figure 2 to Figure 4 each compartment consisted of twelve CLT wall panels, one CLT header, and four CLT ceiling panels. Figure 5 shows the construction sequence. The connection details are shown in Figure 6. The wall panels were connected using lap joints and the adjacent walls were connected using butt joints with screws. The ceiling panels were connected to the walls using butt joints with screws. The ceiling panels were connected to each other using spline joints with strips of 12.7 mm (1/2 in.) thick plywood nailed on each panel every 300 mm (12 in.). Figure 7 are photographs of the spline joints on top of the ceiling.

[2] Certain commercial products are identified in this report to specify the materials used and the procedures employed. In no case does such identification imply endorsement or recommendation by the National Research Council Canada or the National Institute of Standards and Technology, nor does it indicate that the products are necessarily the best available for the purpose.

Although sealants are normally required to seal the CLT panel joints in field applications, no sealant was used in the construction of the test compartments. The project focused on the contribution of CLT elements to a compartment fire and the structural performance was secondary. The absence of the sealant could allow minor smoke and flame leakage from the compartment, but would be unlikely to cause a significant difference in quantifying the CLT contribution. Test 1-3 was an exception where caulking was used to repair the compartment after a preceding fire test (the compartment was used twice; see Section 3.3 for details). For the two tests (Test 1-4 and Test 1-6) which involved an exposed CLT ceiling on the interior side, gypsum concrete was poured along each joint on top of the ceiling panels (see Section 2.1.3 for details).

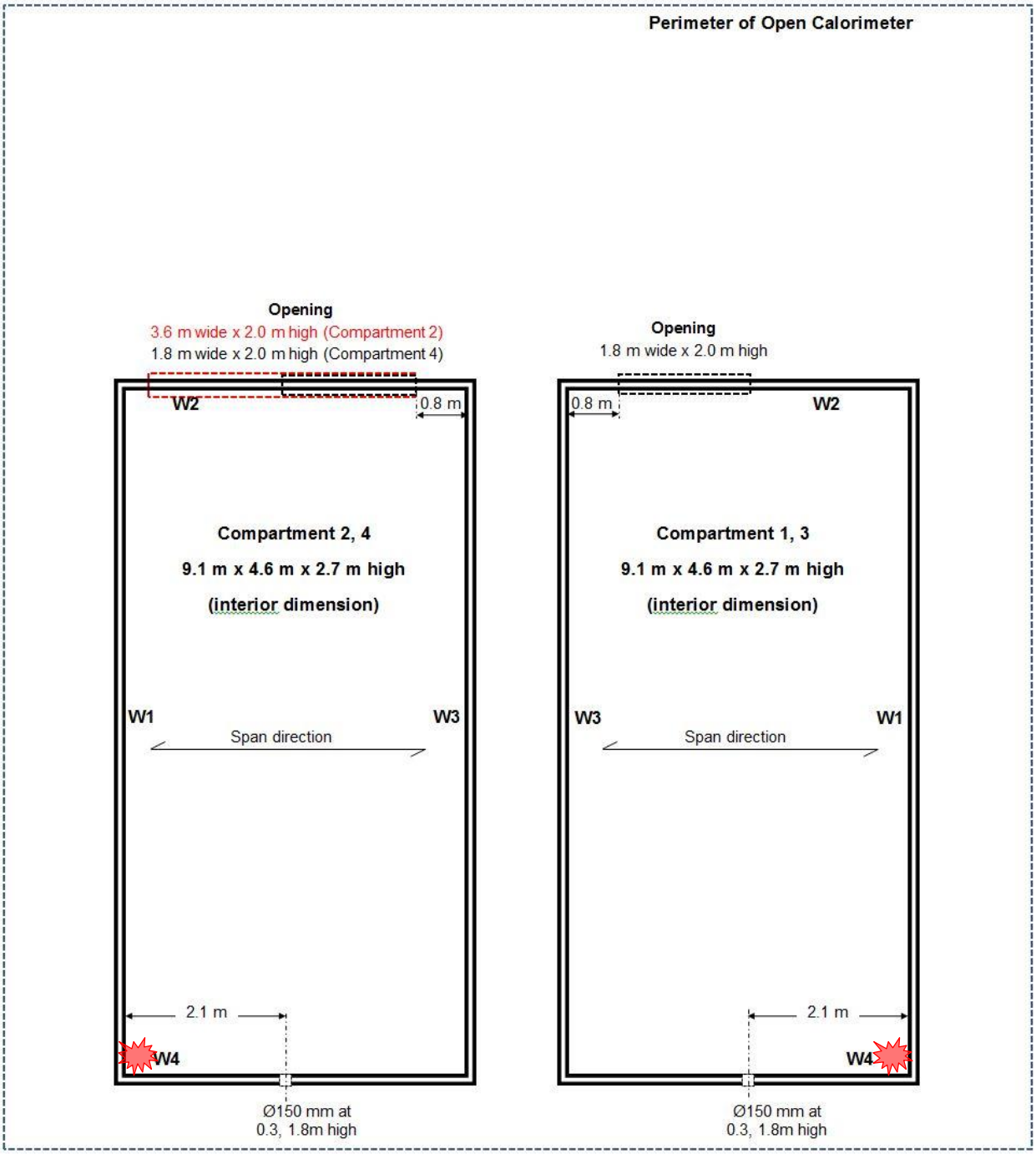

Figure 1. Schematic of test compartments.

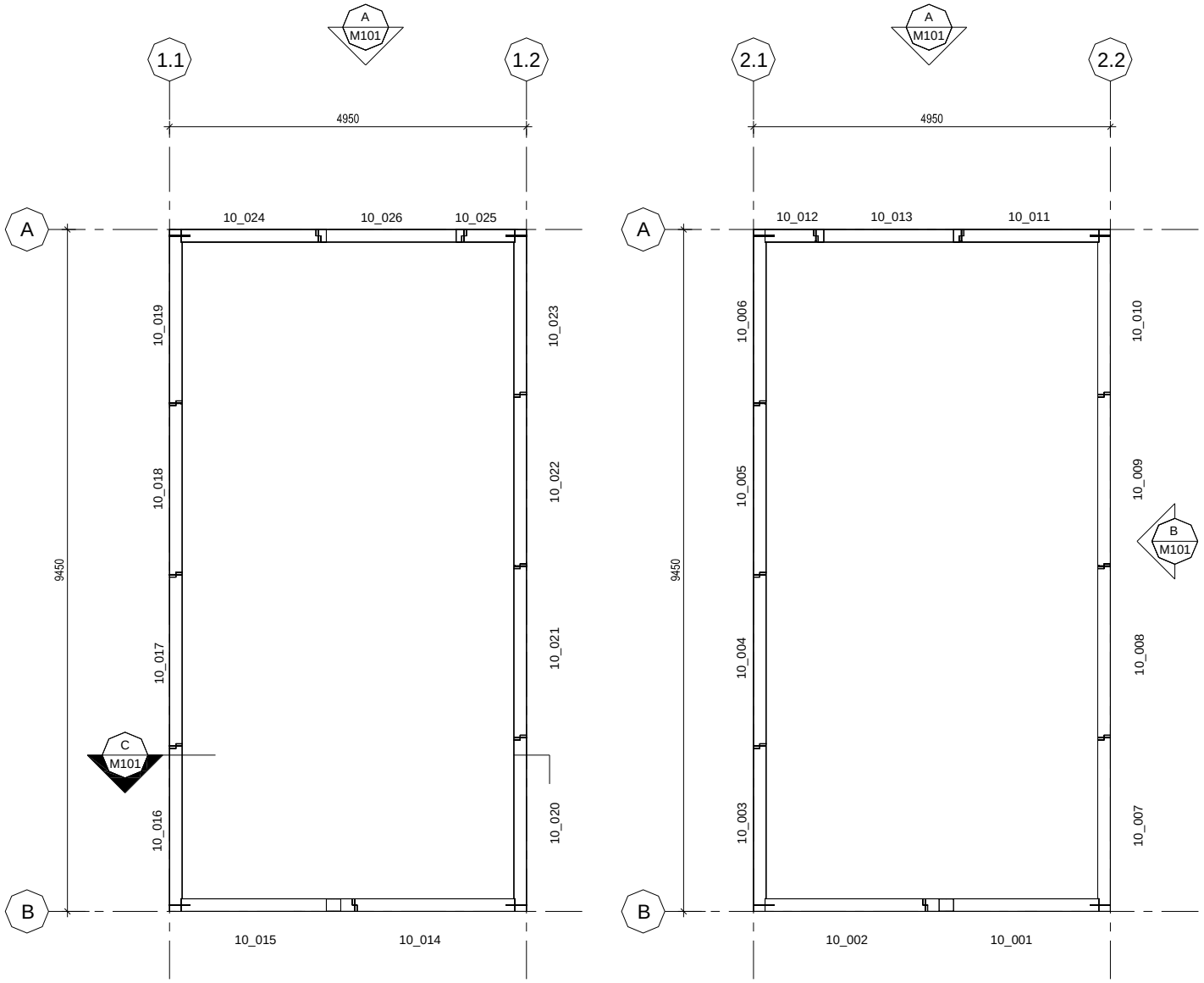

Figure 2. Wall Panels of CLT Compartments.

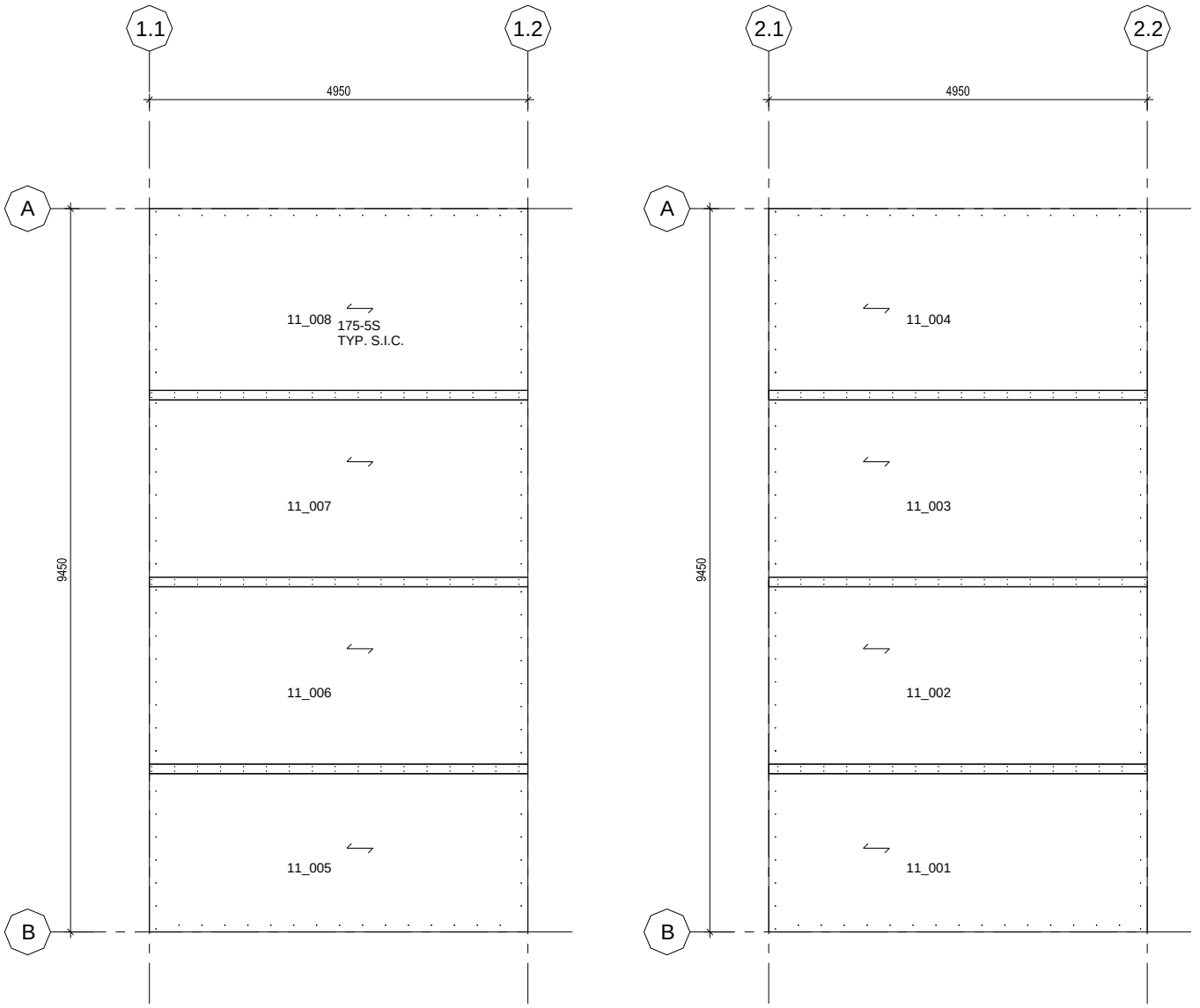

Figure 3. Ceiling Panels of CLT Compartments.

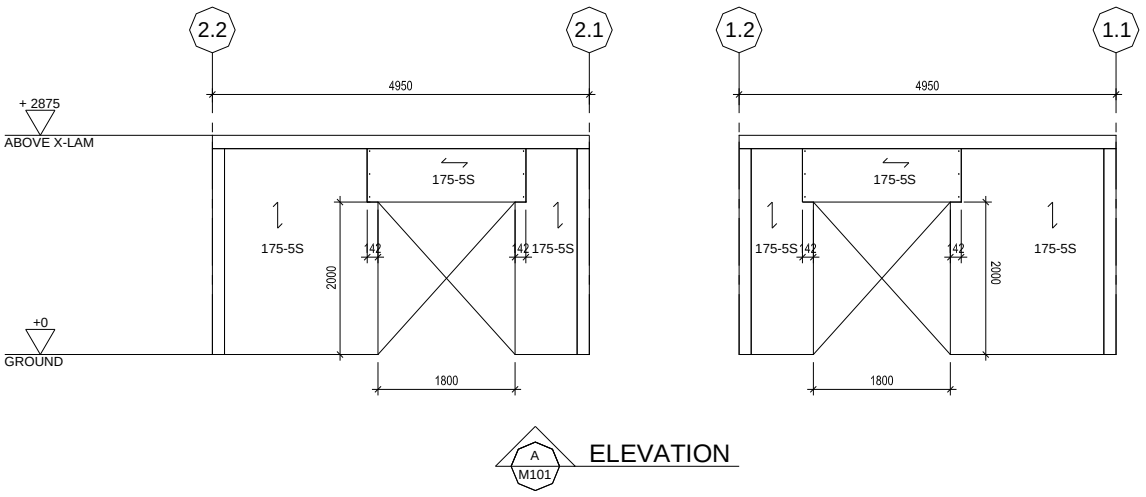

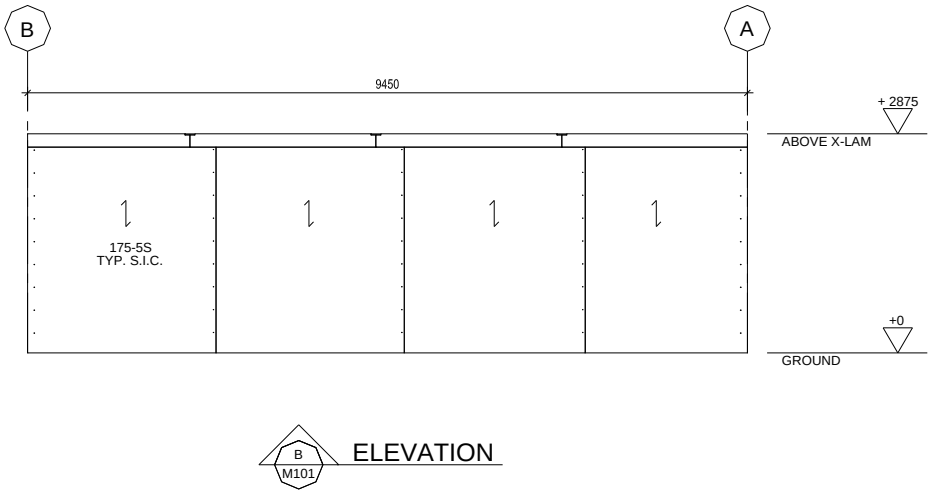

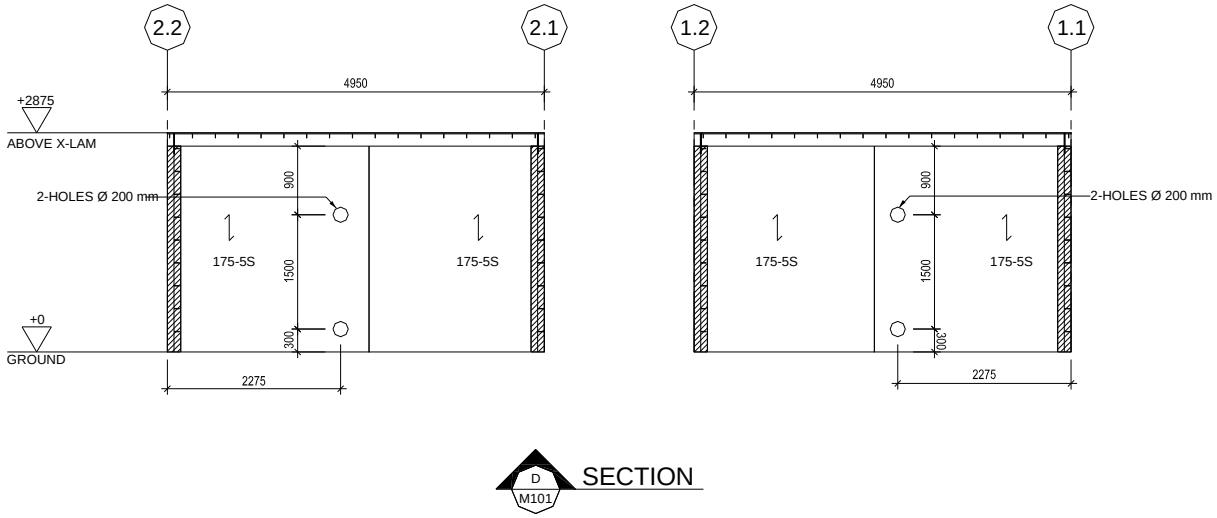

Figure 4. Elevation and Section View of CLT Compartments.

(a)

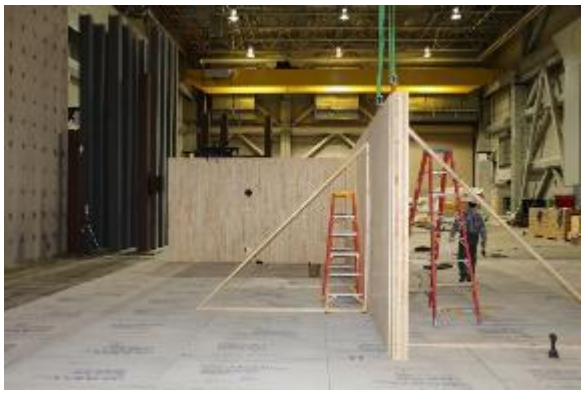

(b)

(c)

(d)

(e)

(f)

Figure 5. Photographs of compartment construction sequence.

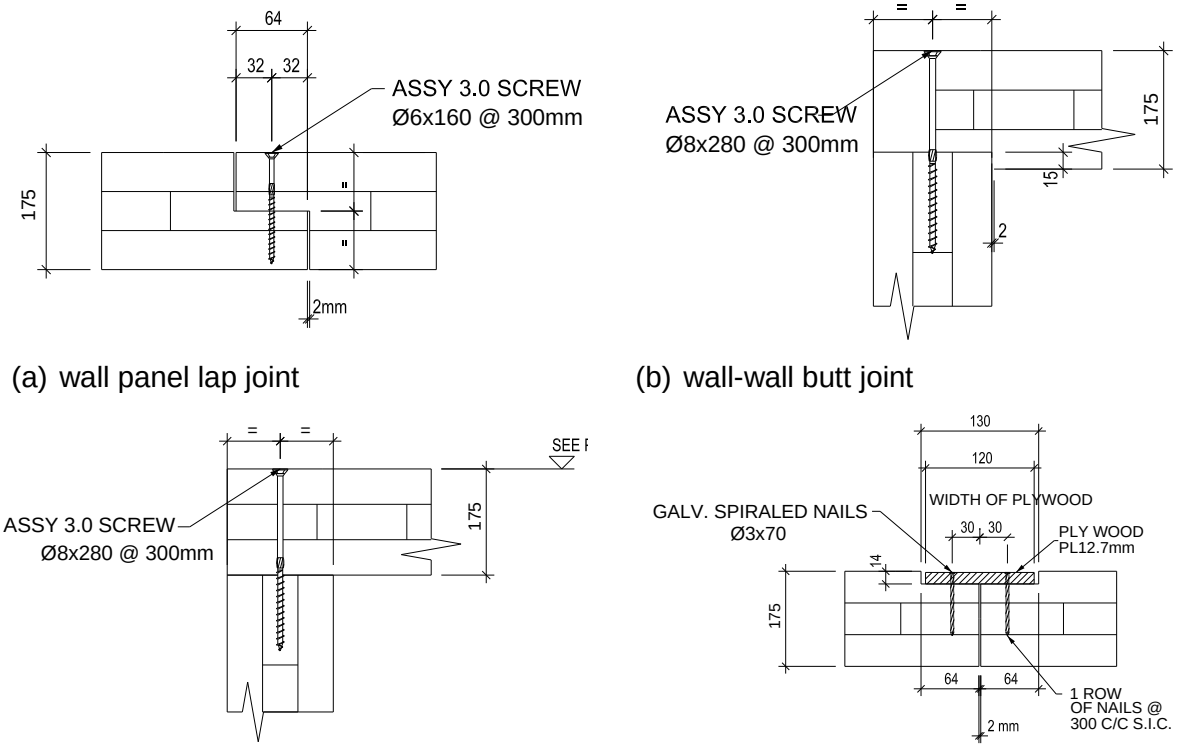

(a) wall panel lap joint

(b) wall-wall butt joint

(c) ceiling-wall butt joint

(d) ceiling panel spline joint

Figure 6. Details of CLT Panel Connections.

Figure 7. Ceiling panels connected with spline joints.

2.1.2 Ventilation

Ventilation is one of the key parameters which has significant impact on the duration of each fire stage, heat release rate and total heat release as well as charring of timber elements in compartment fires. Due to a limited number of tests, two ventilation configurations were used in the compartment fire tests. Ventilation openings were created in the W2 and W4 walls. Other ventilation configurations could be addressed by computer modelling.

2.1.2.1 **Equivalent leakage in W4 to simulate entrance doorway**

Doorways can provide ventilation air to a fire. In high-rise apartment buildings, an entrance door to an apartment unit would normally be a fire-protection rated door (0.8 m wide by 2.0 m high, or 32 in. wide by 80 in. high).

In fire tests, however, if the duration of the fully developed fire is too long, even a rated door may fail and may introduce an undesirable ventilation test-to-test variable. PTP agreed with an alternative approach – using small openings to simulate an equivalent leakage area around a door. Two small openings of 150-mm (6 in.) diameter were created in wall W4 at 0.3 m and 1.8 m (1 ft and 6 ft) heights as shown in Figure 1 (the 150-mm diameter was the finished dimension of the small openings after installing a protective ceramic fibre blanket around the edge). These openings provided an equivalent leakage of 0.035 m^2 (54 $in.^2$) without actually having a door located in the wall.

2.1.2.2 **Rough opening in W2 exterior wall**

A rough opening was located in the exterior wall (W2). Ventilation to the fire compartment was mainly through the rough opening.

In order to compare the results from test-to-test it is critical to create similar ventilation conditions between these tests. Since the focus was on what would be happening inside the compartment, the exterior wall used in each test was a protected CLT wall to keep a constant size of the ventilation opening during the test.

Previous studies of residential fires in both noncombustible and protected CLT compartments [13, 14] show that a rough opening of 1.5 m x 1.5 m (5 ft x 5 ft) maximized the fire severity and its impact to the fire compartment wall and floor-ceiling assemblies, in terms of peak temperature and duration of the fully developed fire stage. A smaller opening size would result in an under-ventilated fire with lower temperatures inside the compartment; a larger size would lead to an increased burning rate (faster burn out of the room content) and earlier fire decay – both creating a lower fire impact on the wall and floor assemblies inside. Computer modelling conducted by RISE also indicated that temperatures in the compartment would increase with the increase of the opening size but reach a plateau beyond the size of 1.5 m x 1.5 m and that the total charring depth would be maximized with a 1.5 m x 1.5 m opening size [5].

During the deliberation of ventilation options, the PTP voted in favor of using a larger opening similar to the size of a sliding door, and also pointed out that the minimum opening area should be at least 8% of the floor area as required by the International Building Code. This led to a decision to use an opening size of 1.8 m wide x 2.0 m high (6 ft wide x 6.7 ft high) in four tests. There was no actual door installed in the rough opening in order to reduce test-to-test ventilation variables. This also represented a scenario of the door being left fully open.

Several PTP members expressed a desire to have more ventilation as some buildings being built or considered would have even larger openings. To accommodate this suggestion and to obtain data under this ventilation condition, two tests were conducted with a rough opening of

3.6 m wide x 2.0 m high (12 ft wide x 6.7 ft high). This large opening was expected to result in a more intense but shorter duration fire.

The ventilation factor for the fire tests was 0.03 $m^{½}$ with the 1.8 m x 2.0 m opening, and 0.06 $m^{½}$ with the 3.6 m x 2.0 m opening, respectively. The ventilation factors are calculated using $A_0\sqrt{H_0}\ /\ A_t$, where A_o and H_o are the area and height of the opening and A_t the total area of the boundary surfaces. Most previous fire tests involving exposed CLT were conducted for compartments with a ventilation factor close to 0.04 $m^{½}$.

2.1.3 Fire Protection and Flooring Materials

The CLT compartments used in the tests were either fully or partially protected using multiple layers of 15.9 mm x 1.22 m x 3.05 m (5/8 in. x 4 ft x 10 ft) Type X gypsum board on the walls and ceiling. The gypsum board was directly applied to the CLT panels using type S drywall screws. Detailed drawings of the gypsum board layout and screw patterns for each test are shown in Appendix A. In general:

- The gypsum board was applied to the CLT ceiling and wall panels in a staggered fashion so that no joint would line up with any joint of the CLT panels and other gypsum board layers.
- The gypsum board was always installed onto the ceiling (horizontal board) first followed by the W1, W4, W3 and W2 walls (vertical board) for each layer. After a layer of gypsum board was complete on the ceiling and walls, the next layer of gypsum board was then installed in the same sequence to the ceiling and walls. This sequence was repeated until all layers were installed. This multiple layer installation sequence is known as the stair-step sequence, illustrated schematically in Figure 8.
- Type S drywall screws were 41 mm, 51 mm and 76 mm (1 5/8 in., 2 in. and 3 in.) long for a three-layer gypsum board installation; 41 mm and 51 mm (1 5/8 in. and 2 in.) long for a two-layer gypsum board installation (see Section 3.3 on Test 1-3 for exception on the ceiling). These screw lengths achieved a minimum of 19 mm (3/4 in.) penetration into the wood elements. The screws were spaced at 305 mm (12 in.) on centre. Near the joints, screws were placed at 38 mm (1 ½ in.) from the edges of the gypsum board sections. Care was taken not to over drive the screw head into the gypsum board (to prevent damaging the board surface).
- On the face layer, the joints between gypsum board sections were covered with tape and joint compound and the screw heads were also covered with joint compound.

The concrete floor of the lab was protected using two layers of 15.9 mm (5/8 in.) thick Type X gypsum board and then two layers of 12.7 mm (1/2 in.) thick cement board (see Figure 5 and Figure 9). Laminated wood flooring was installed on top of the cement board in the CLT compartments. The laminated flooring was 7 mm thick (each piece had a dimension of 7 mm x 194 mm x 1290 mm (9/32 in. x 7-9/16 in. x 50-25/32 in.)).

CLT wall surfaces outside the fire compartment were bare for the W1 and W3 walls. The outside surface of the W4 wall was mostly bare except for limited areas surrounding the two small openings where one layer of 15.9 mm (5/8 in.) thick Type X gypsum board was installed.

The exterior wall (W2) was covered with one layer of 15.9 mm (5/8 in.) thick Type X gypsum board. The edges of the rough opening were lined with two layers of 15.9 mm (5/8 in.) thick Type X gypsum board followed by a layer of 25 mm thick ceramic fiber insulation wrapped around. A 2-m high extension was added on top of the W2 exterior wall to better simulate the geometry of exterior façade, as shown in Figure 9.

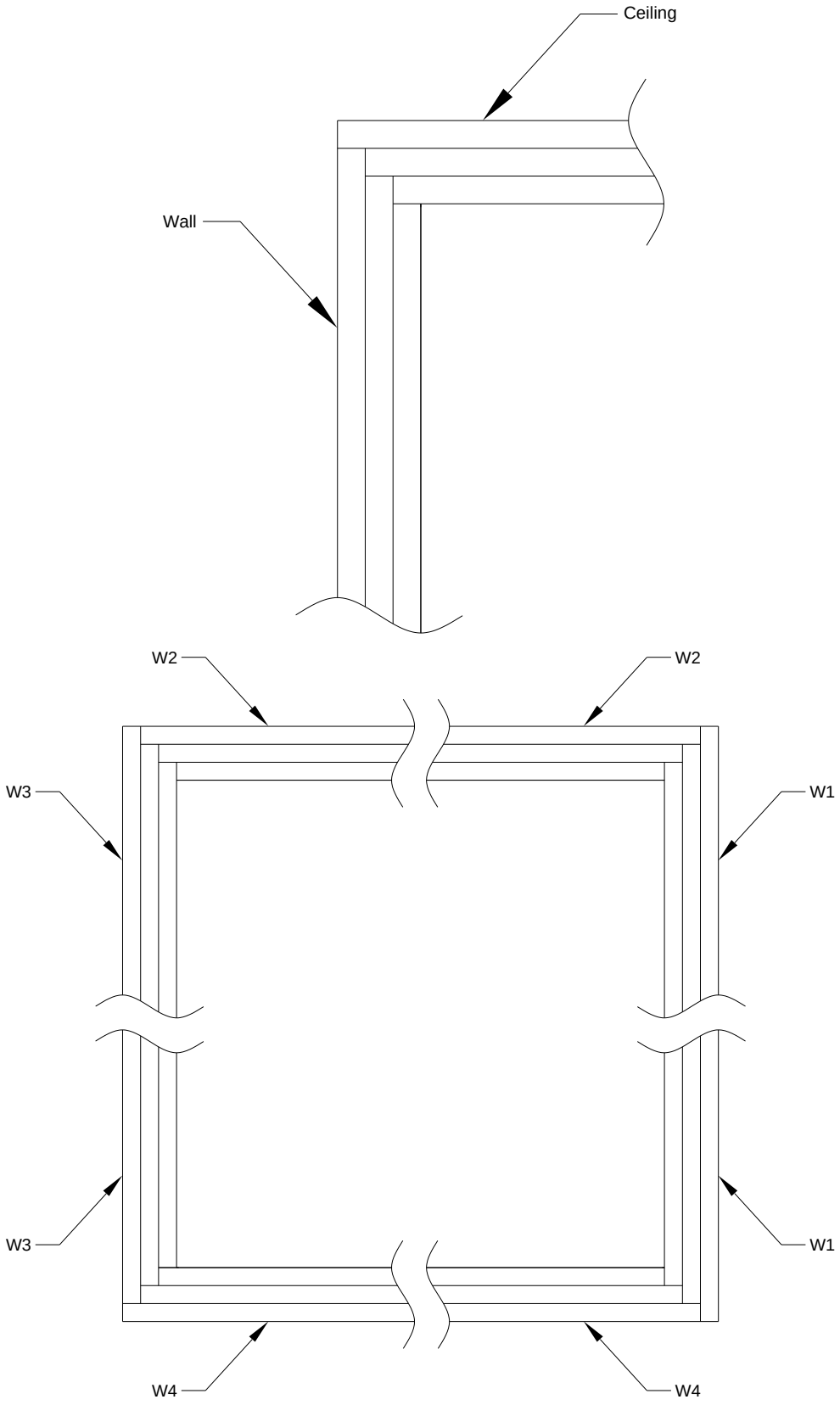

Figure 8. Stair-step installation for multilayer gypsum board (cross section view).

On the top of the fire compartment, as shown in Figure 9(a), the CLT ceiling panels were covered by one layer of 12.7 mm (1/2 in.) thick cement board fastened with 38 mm (1½ in.) long wood screws of size 8 with 610 mm (24 in.) spacing in the two baseline tests (cement board was not used in other tests). For the two tests (Test 1-4 and Test 1-6) with exposed CLT ceiling on the interior side, 38 mm (1-1/2 in.) thick and 305 mm (12 in.) wide gypsum concrete was poured on top of each of the ceiling panel joints, as shown in Figure 9(b).

(a) cement board on top of ceiling

(b) gypsum concrete on top of ceiling joints

(c) W2 exterior wall with extension

(d) W2 exterior wall with extension

Figure 9. Ceiling top and exterior wall extension.

2.1.4 Structural Load

As the project focused on the contribution of CLT elements to a compartment fire and the effect of fire protection using gypsum board as the physical barrier on delaying or preventing CLT involvement, the structural performance of the compartments was secondary. Nevertheless, a structural load of 0.95-kN/m^2 (20-psf), which is one half of the design live load for a residential occupancy, was superimposed on top of the ceiling using eight cylindrical water tanks 1.5 m tall and 0.78 m in diameter. Each water tank weighed approximately 510 kg (1125 lbs). Two tanks were placed along the centerline (parallel to spanning direction) of each of the four ceiling CLT panels and positioned at one third and two third of the CLT span distance.

2.2 Test Matrix

The CLT compartments were fully or partially protected using multiple layers of 15.9-mm (5/8 in.) thick Type X gypsum board. Table 1 is a test matrix for the CLT compartments.

Table 1. Test Matrix of CLT Compartments for Fire Tests.

Rough Opening in Wall W2	Compartment Surface					Test	CLT Compart-ment	Date
	W1 9.1 m x 2.7 m	W2 4.6 m x 2.7 m	W3 9.1 m x 2.7 m	W4 4.6 m x 2.7 m	Ceiling 9.1 m x 4.6 m			
1.8 m wide x 2.0 m high	3GB	3GB	3GB	3GB	3GB	1-1	1	Feb. 16
	3GB	3GB	3GB	3GB	**exposed**	1-4*	1*	Mar. 21
	exposed	3GB	3GB	3GB	**3**GB	1-5	4	Apr. 13
	exposed	3GB	3GB	3GB	**exposed**	1-6	3	Apr. 18
3.6 m wide x 2.0 m high	2GB	2GB	2GB	2GB	2GB	1-2	2	Feb. 23
	exposed	2GB	2GB	2GB	3GB	1-3*	2*	Mar. 16

GB: 15.9 mm (5/8 in.) thick Type X gypsum board; 2GB: 2 layers of GB; 3GB: 3 layers of GB
** Reused CLT structure.*

Test 1-1 served as a baseline for the tests with the 1.8 m x 2.0 m (6 ft x 6.7 ft) rough opening. Three layers of the gypsum board were used to fully protect the CLT compartment in Test 1-1 so that the CLT structure would neither contribute to the compartment fire nor develop char during the test and could then be re-used for another test. Test 1-2 served as a baseline for the tests with the 3.6 m x 2.0 m (12 ft x 6.7 ft) rough opening.

An exposed W1 wall was tested in both ventilation configurations (Test 1-3 and Test 1-5). The room corner formed by the W1 and W4 walls was the ignition location (see section 2.4). Therefore, the exposed W1 wall was right beside the first item ignited in Test 1-3 and Test 1-5 as well as Test 1-6. Test 1-4 and Test 1-6 involved an exposed ceiling and a combination of exposed ceiling and W1 wall, respectively, with the 1.8 m x 2.0 m rough opening, as data available in the literature for the exposed ceiling (alone or in combination) was lacking.

2.3 Moisture Content

Prior to fire testing the compartments, the moisture content of each wall was sampled using a handheld moisture meter (Figure 10). For Test 1-1 and Test 1-2, the measurements were made on the outside surface of the compartment after the gypsum board had been applied because there was no longer access to the inside surfaces. In Test 1-3 to Test 1-6, the measurements were made on the inside surfaces of the compartments shortly prior to installation of the gypsum board. Three measurements were made at random locations on each wall.

Figure 10. Measurement of panel moisture content using Delmhorst (BD-2100) meter.

Table 2 summarizes the mean values for panel moisture content. For the entire test series, the mean moisture content of the panels was 7.7 % with a standard deviation of less than 1.1 %. The complete data can be found in Appendix B. It should be noted that the device used to sample the moisture content reports the value measured between the instrument pins, which just penetrate the surface of the CLT panel. Therefore, any gradient in the moisture content through the panel thickness is not captured and the measurements are potentially susceptible to transient variations in the panel surface moisture.

Table 2. Pretest panel moisture content.

	Mean moisture content, %						
	Wall					Compartment	
	W1	W2	W3	W4	Roof	Mean	SD
Test 1-1	7.2	-	8.2	7.9	6.2	7.4	1.0
Test 1-2	8.0	-	7.6	8.1	6.9	7.7	0.9
Test 1-3	8.2	7.5	8.6	6.8	6.4	7.5	1.0
Test 1-4	9.9	8.7	8.8	8.8	7.2	8.7	1.1
Test 1-5	7.8	7.7	7.6	7.9	7.9	7.8	0.7
Test 1-6	7.2	7.7	6.4	6.7	7.9	7.2	0.7

2.4 Contents Fire Load and Ignition Scenario

Since the primary objective of the experiments was to evaluate the effect of the CLT structural elements on the fire growth and fire dynamics, the contents fire load and ignition scenario was designed to produce a medium fire growth rate. Movable fuel refers to all combustible material inside of the compartment (including the laminated flooring) that is not a CLT structural element.

2.4.1 Composition and location of contents fire load

The movable fuel represented residential contents in a studio apartment with sleeping, living and kitchen areas. Figure 11 illustrates the arrangement and location of the furnishings. The furnishings included a queen size bed with mattress and wooden bedframe and large storage drawers underneath, night tables, dressers, shelves, desk, upholstered sofa, coffee table, dining table and chairs, and kitchen counters. A floating laminated wood floor (without underlay) was installed in the compartment. The movable contents and furnishings target a fire load density (FLD) of 550 MJ/m^2 in the compartment. This corresponds to the average fire load density for a bedroom, living room and kitchen from a survey on residential fire load by Bwalya [15], assuming a quarter of the space as kitchen, a quarter as sleeping area, and half as living area. This value is consistent with those used in previous studies by Su and Lougheed [14] and Janssens [16].

Complete listings of all movable fuel in the compartment, including the item manufacturer, article number or description, dimensions, material and mass, are provided in Appendix C. A limited number of supplemental wood cribs were placed in the shelves to achieve the target fuel load density. Dimensionally accurate 2D and 3D representations of the as-tested fuel locations are shown in Figure 11 and Figure 12. The positions were verified using a tape measure prior to each test and varied less than +/- 25 mm. The measured positions and dimensions used to generate these figures are provided in Appendix C. A photograph of a furnished compartment

(mirrored furniture layout) is provided in Figure 13 and photographs of select furnishings in Figure 14.

Three small CLT blocks (305 mm x 203 mm x 175 mm) were also positioned on the floor in the front, middle and rear sections of the compartment in the two baseline tests for char measurements. Each block had its top surface exposed and all other surfaces were protected using ceramic fiber wraps.

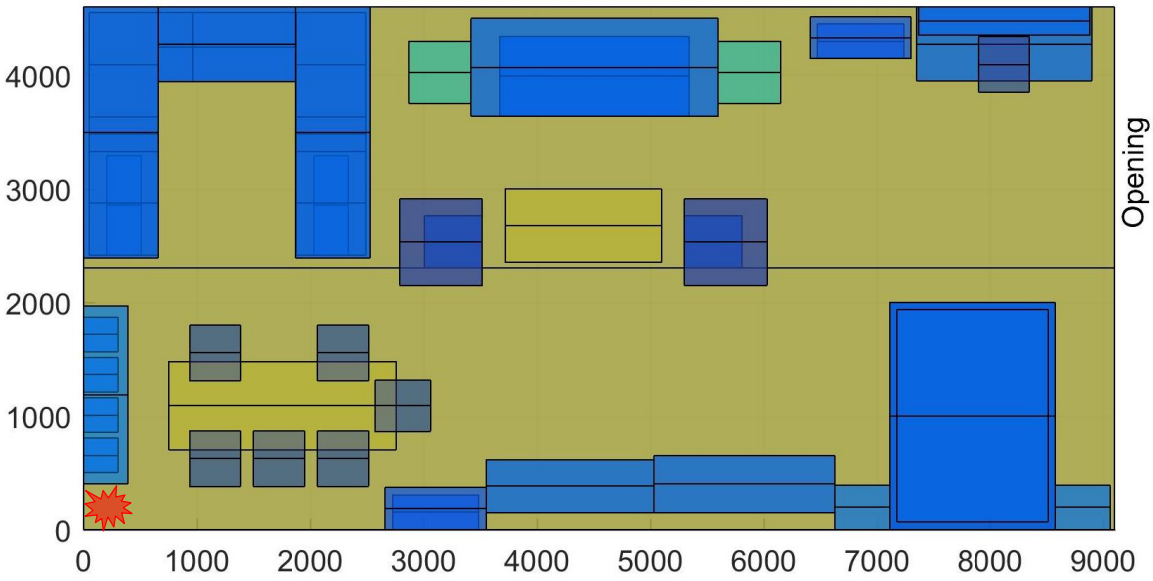

Figure 11. Plan view of a model of the moveable fuel as installed (units in mm).

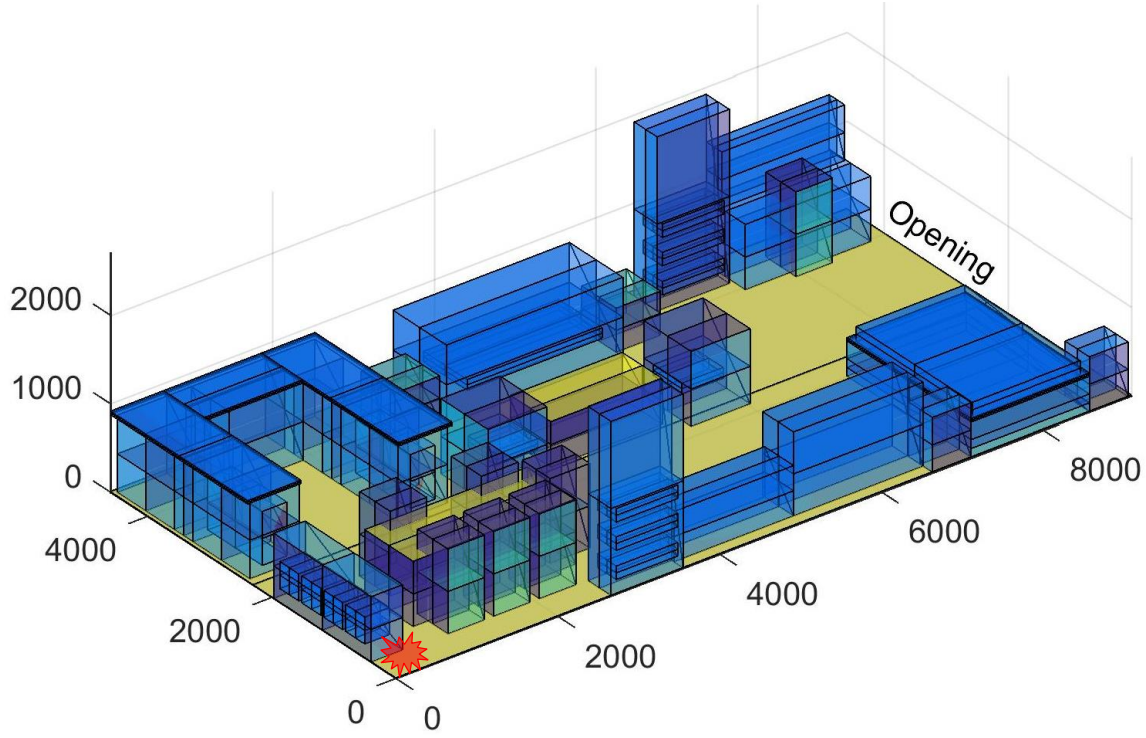

Figure 12. Isometric view of a model of the moveable fuel as installed (units in mm).

Figure 13. Photograph of the movable fuel as installed.

(a)

(b)

(c)

(d)

Figure 14. Photographs of (a) installation of wood flooring, (b) kitchen cabinets with end cabinet placed inside to increase walkway, (c) and (d) detailed interior views.

Every piece of combustible material was weighed prior to placement. The total weight of the combustible material in each compartment was 1,169 kg +/- 8 kg (standard uncertainty). Using the calorific values in Table 3 [17], the estimated energy for each item was determined (see Appendix C). Accounting for the paper on the innermost layer of drywall (the layer participating during flashover) which constituted less than 1.6 % of the total fuel by energy, the total estimated energy for the movable fuel was 23,074 MJ +/- 161 MJ (standard uncertainty). Table 4 summarizes the fuel load density used in each test, which varied between 548 MJ/m^2 and 556 MJ/m^2.

The detailed measured dimensional and mass information for the movable fuel was used to generate fuel energy distributions for Test 1-1. The distributions for the other tests were similar. The 3D model in Figure 12 split each piece of fuel into 8 surfaces (6 sides plus a vertical and a horizontal plane through the centre). The mass distribution to each surface was estimated. The values used are provided in Appendix C. The compartment was arbitrarily divided into 101 (length) by 51 (width) regions and the energy of the content (from floor to ceiling) in each region was calculated. A 3D bar plot of the resulting energy distribution is shown in Figure 15. Figure 16 shows the same data viewed as a 2D contour plot. At this high resolution, the non-homogenous nature of the fuel distribution for real contents is highlighted, however, if one increases the region size to result in only eight regions, the fuel energy distribution appears more homogenous; except for a higher contribution in the back corner at the kitchen (Figure 17).

Table 3. Calorific values used to determine energetic content of moveable fuel.

Material	Calorific Value	Units
Hardboard	19.9	MJ/kg
White pine	19.2	MJ/kg
Douglas fir	21.0	MJ/kg
Polyurethane foam	29.0	MJ/kg
Cotton	20.3	MJ/kg
Paper	17.0	MJ/kg

Table 4. Contents fire load density (FLD, MJ/m^2).

Test	FLD (w/o paper)*	FLD (w/ paper)*
1-1	540	549
1-2	539	548
1-3	549	556
1-4	543	548
1-5	549	556
1-6	546	550

* w/o paper – without drywall paper; w/ paper – with drywall paper.

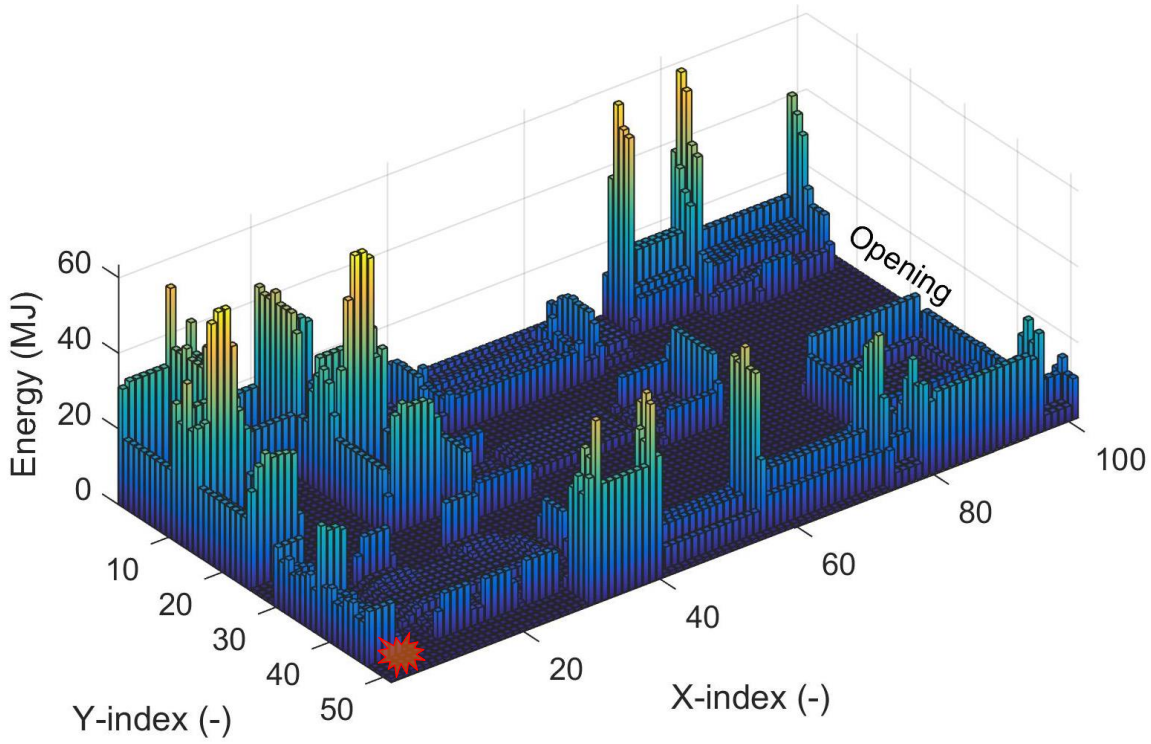

Figure 15. Isometric view of the movable fuel energy as installed (101 × 51 regions).

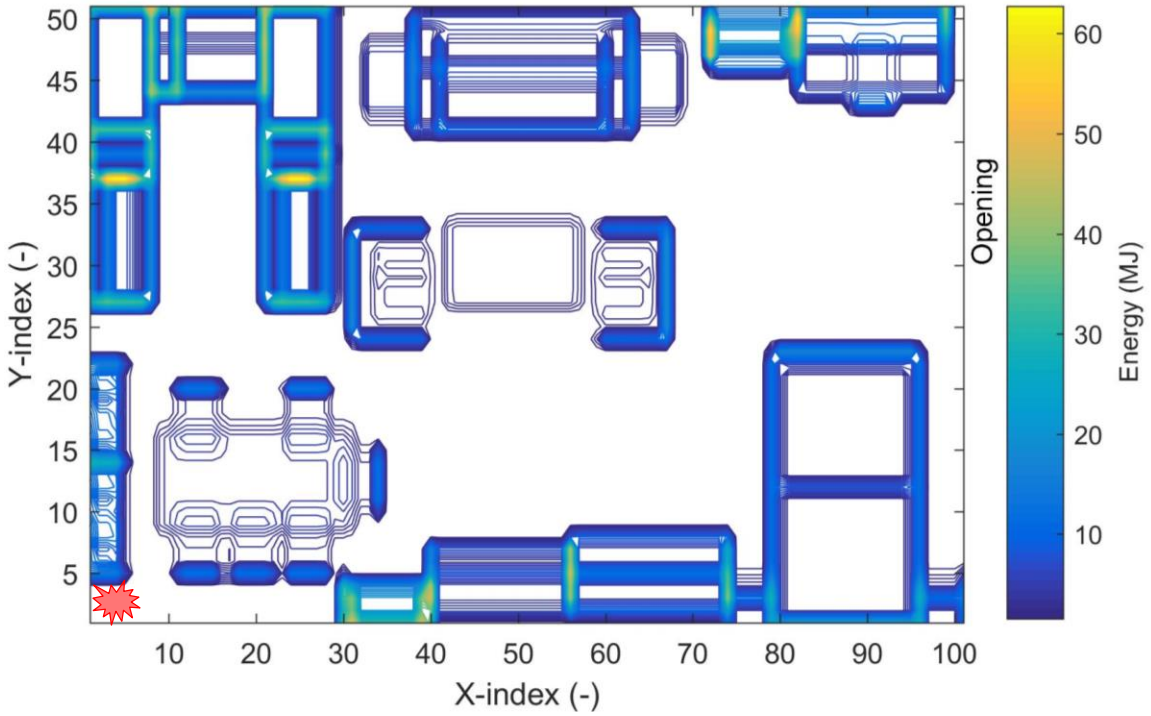

Figure 16. Plan view of the movable fuel energy as installed (101 × 51 regions).

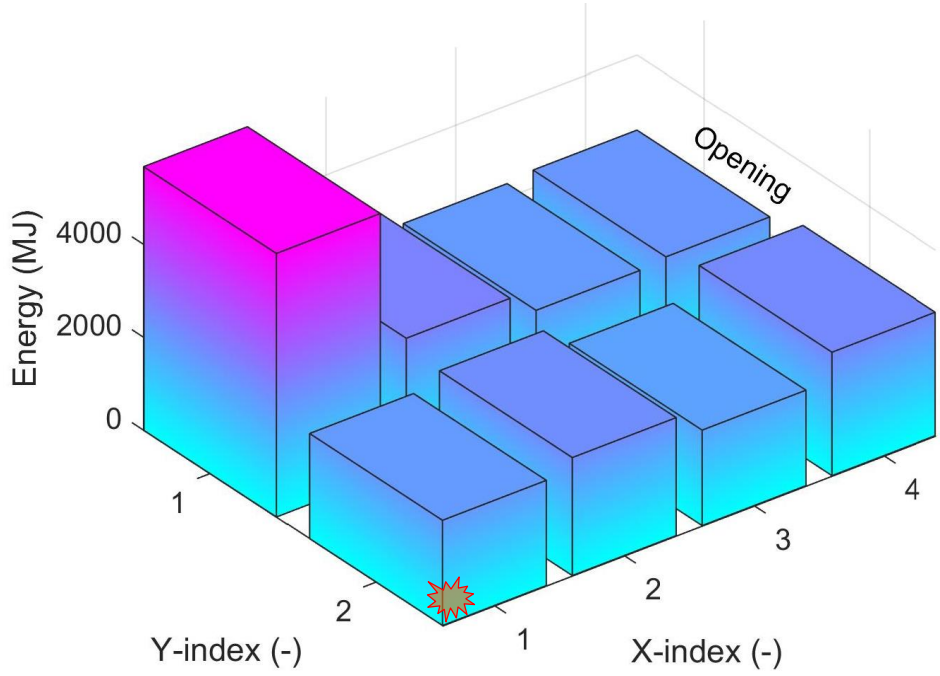

Figure 17. Isometric view of the movable fuel energy as installed (4 × 2 regions).

2.4.2 Ignition source and first item ignited

A room corner ignition scenario was used in the CLT compartment fire tests. The ignition corner was formed by the adjacent W1 and W4 walls. The ignition source used was a natural gas diffusion burner (200 mm x 400 mm or 8 in. x 16 in.) placed in the corner partially under the shelving unit (console table). The natural gas flowed into a cavity below porous ceramic plates in the burner and then diffused upward. A small pilot flame was used to ignite the burner. The shelving unit (console table) was the first item ignited (Figure 18). A heat release rate of 50 kW (similar to a burning waste basket) from the burner was maintained until the total measured heat release rate from the compartment exceeded 1000 kW (due to ignited contents), at which time the burner was shut off. Four small wood cribs (85 MJ each) were placed in the console table to achieve a reliable ignition (Figure 18b). Two 'mock-up' tests of the ignition scenario were performed using a corner burn setup prior to the compartment test (Figure 19). The mock-up tests showed a reproducible fire growth and heat release sufficient to ignite neighboring contents in the compartment.

(a) (b)

Figure 18. Photographs of (a) burner with copper tube for pilot flame and (b) the object of first ignition (console table with wood cribs).

(a) (b)

Figure 19. Photographs of (a) mock-up corner burn setup and (b) the object of first ignition catching fire.

2.5 Instrumentation and Measurement Systems

Various measurement devices were installed inside and outside the fire compartment in each test. Figure 20 to Figure 27 illustrate a general instrumentation plan for the tests. Some minor adjustments were made to the general plan from test to test; a more specific instrumentation plan for each test is detailed in Appendix A.

Data was collected from multiple systems during the experiments. These systems can be grouped into four categories related to: (1) the NFRL calorimeter – dedicated to measuring fuel flow to the small burner and performing oxygen depletion calorimetry, (2) gas sampling in the compartment, (3) the constituent measurements for the test specimens, and (4) imaging and video. Because these systems often captured more data than was germane to the experiments, in additional to storage of all data locally, key channels were digitized and ported to a single data acquisition system for recording. Information about measurement uncertainties is provided in the following sections and in the Appendices. Where expanded uncertainty is reported, a coverage factor of 2 corresponding to an approximately 95 % confidence interval is used.

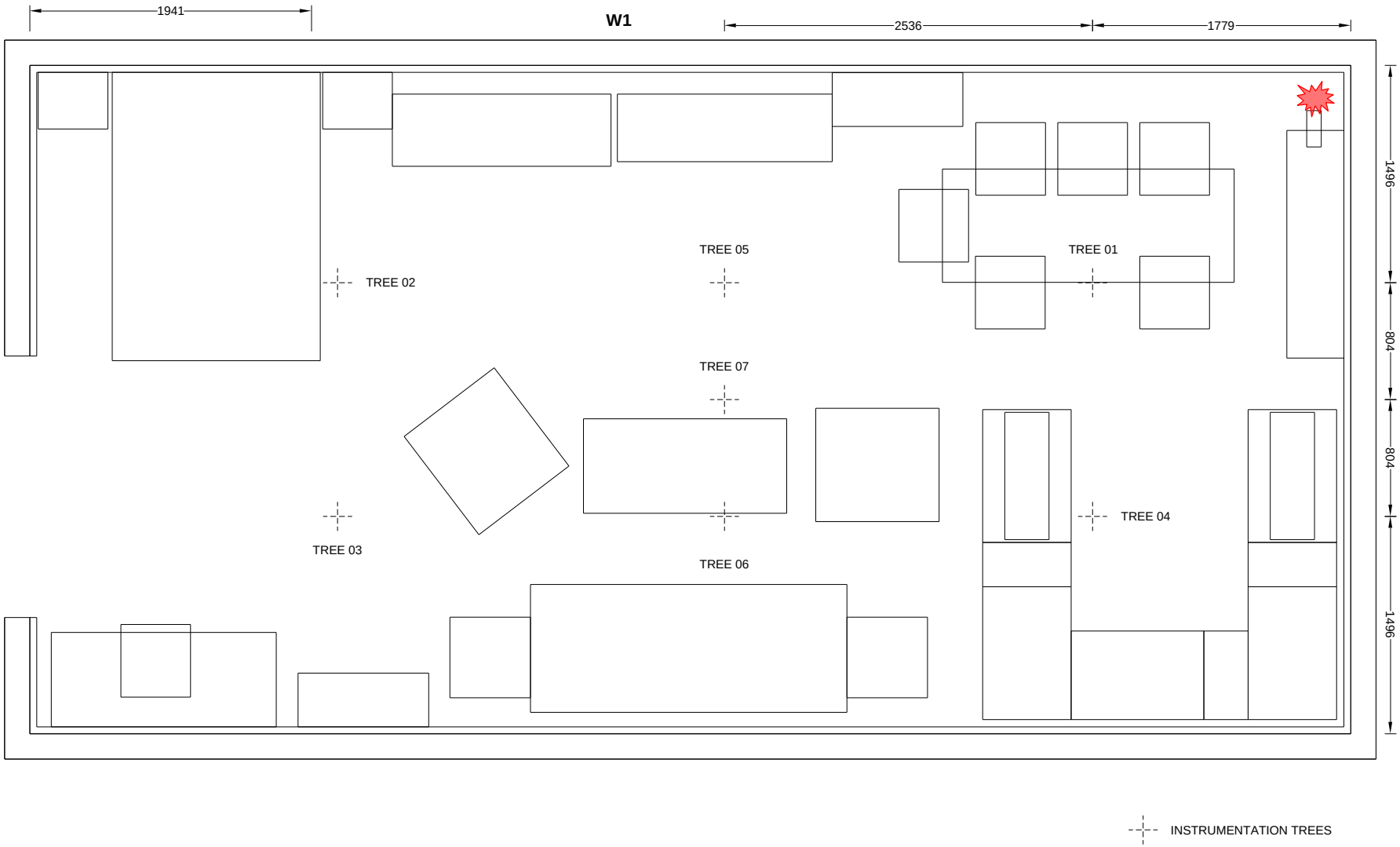

Figure 20. Locations of thermocouple trees and gas sampling tree inside the compartment.

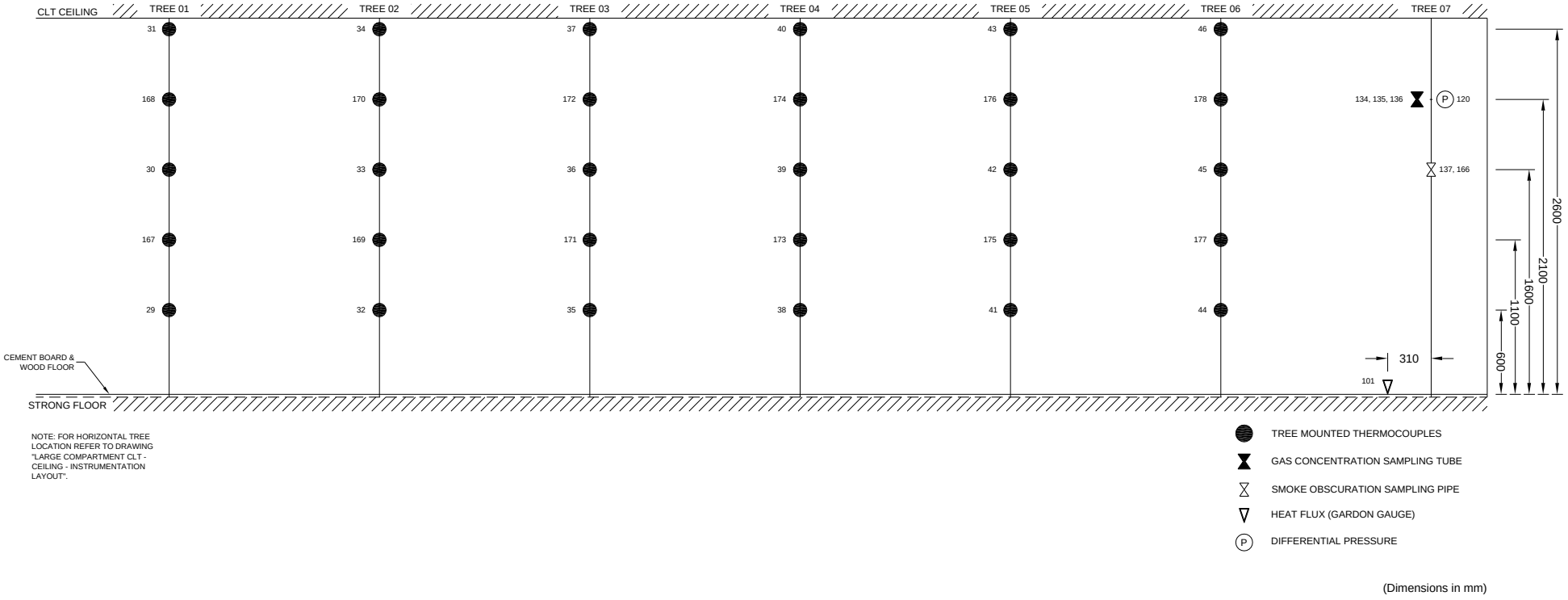

Figure 21. Illustration of heights of thermocouples and smoke-gas sampling ports on the trees inside the compartment.

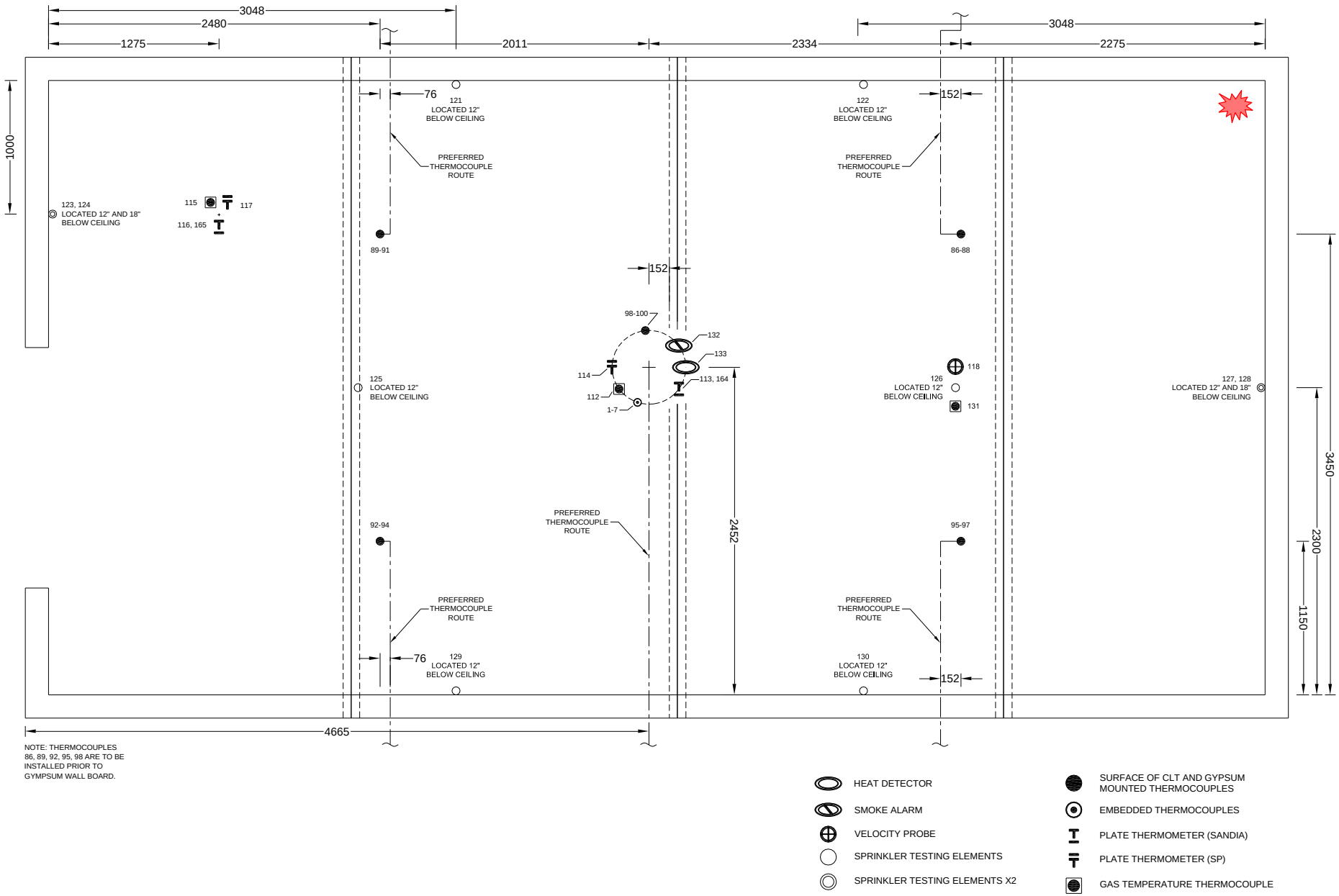

Figure 22. Measurement devices on the ceiling and inside the ceiling assembly in the compartment.

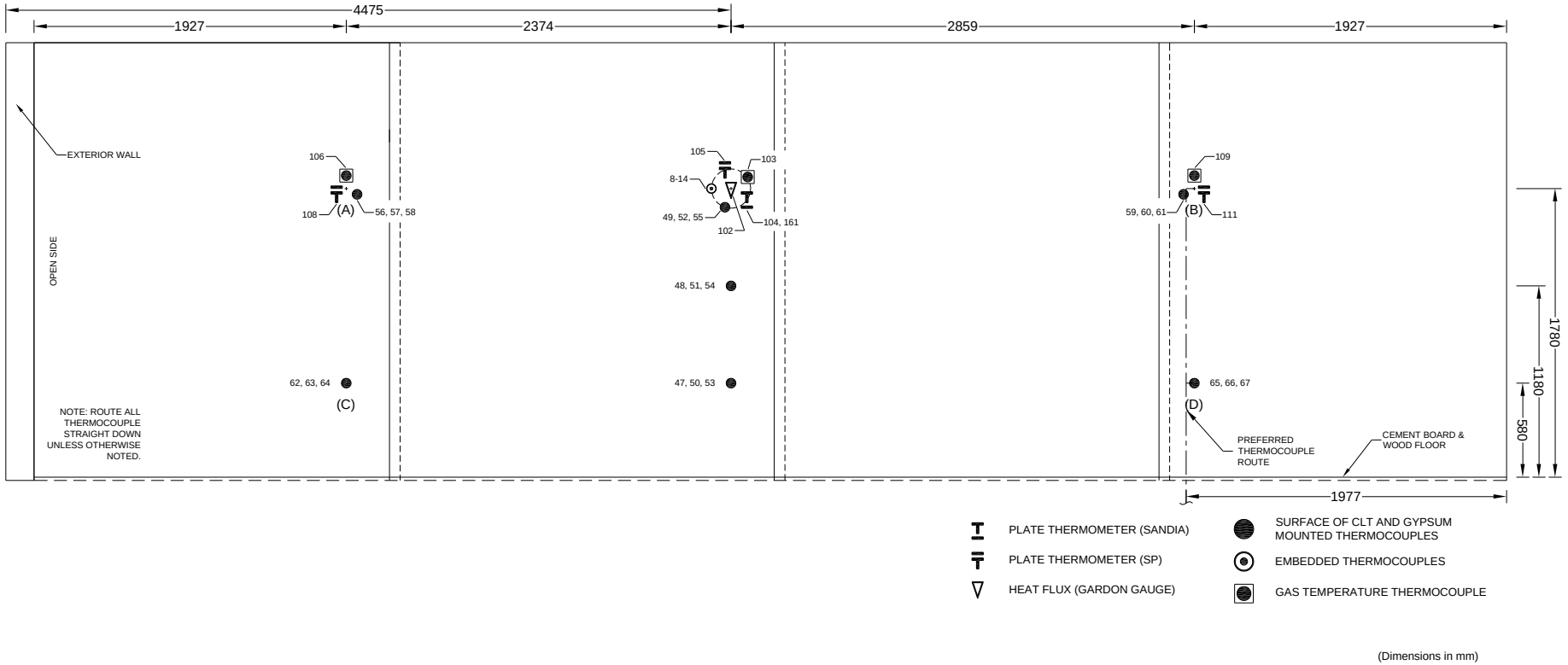

Figure 23. Measurement devices in W1 wall.

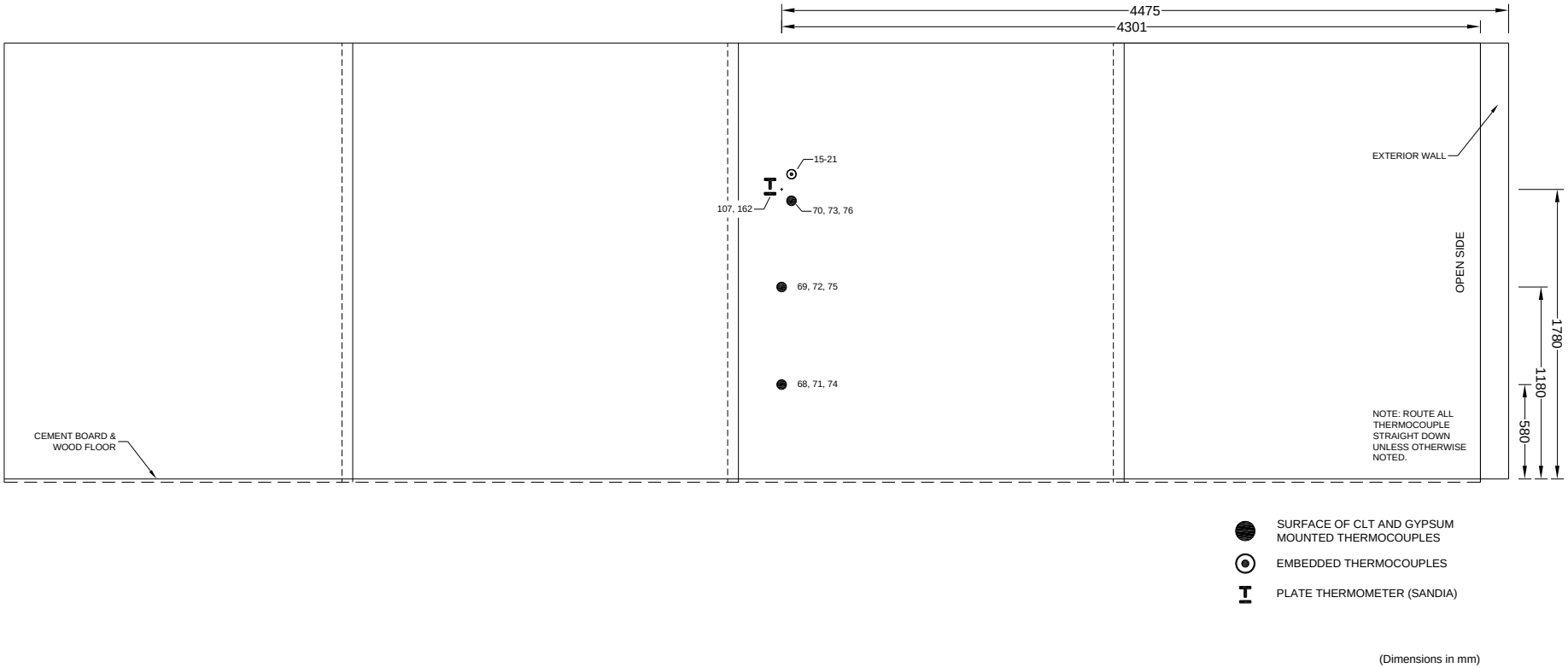

Figure 24. Measurement devices in W3 wall.

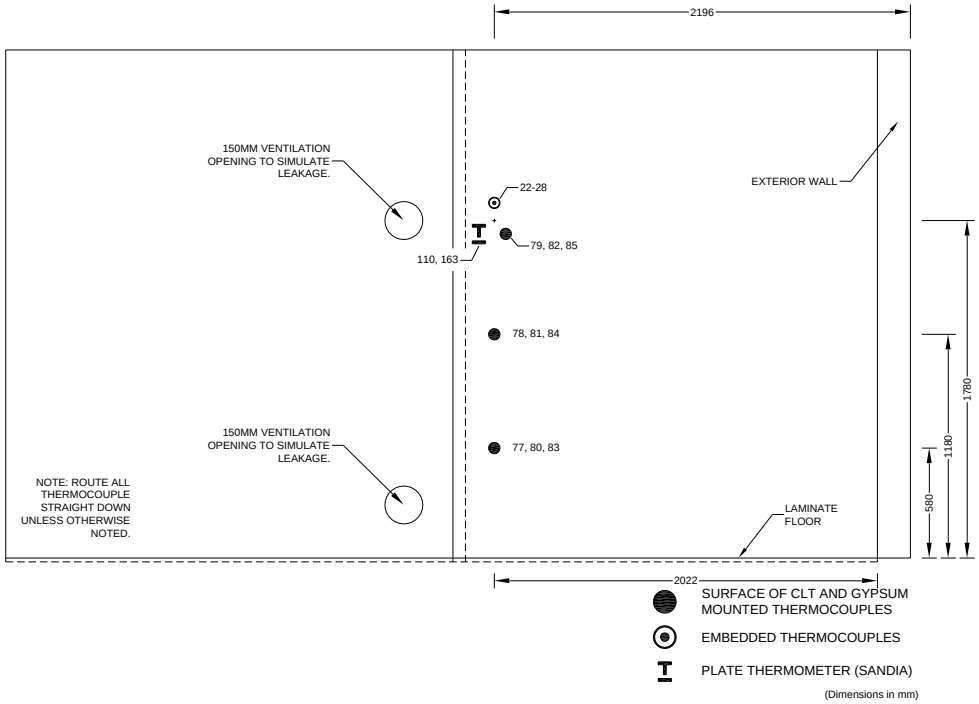

Figure 25. Measurement devices in W4 wall.

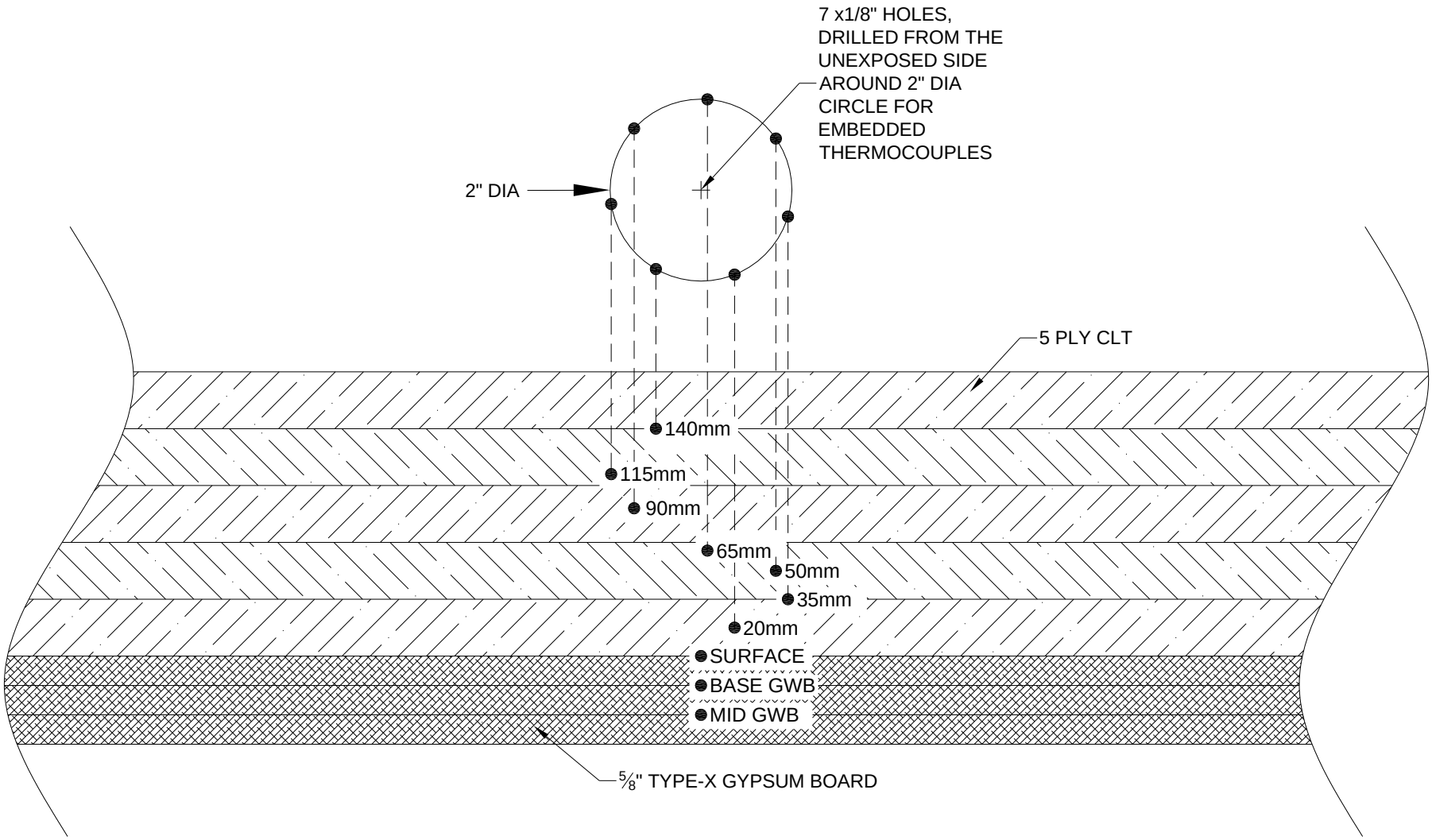

Figure 26. Details of embedded thermocouples in ceiling and walls with the drilled holes sealed from the outside (additional thermocouples added at the 2nd and 3rd gluelines in Test 1-5 and Test 1-6).

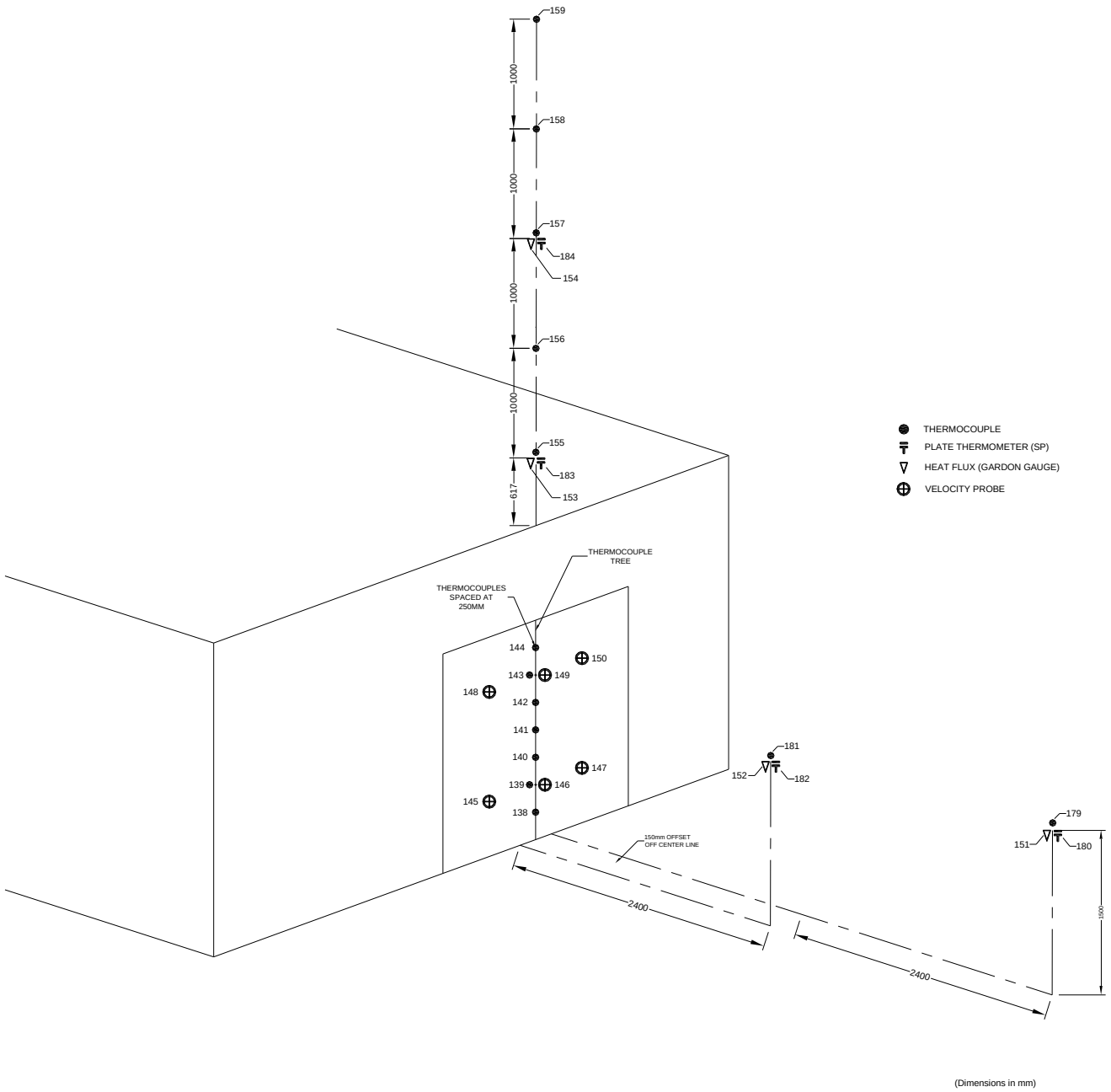

Figure 27. Measurements in the doorway and outside the compartment.

2.5.1 Data acquisition

The constituent measurements from the test specimens were acquired using three National Instruments cDAQ-9188 data acquisition (DAQ) chassis populated with the following I/O-Modules: NI 9213 for thermocouples and NI-9205 for sensors with voltage outputs (Figure 28a). Additional details are provided on National Instruments' website.

In addition to measurements of oxygen (O_2), carbon dioxide (CO_2), and carbon monoxide (CO) ported from the gas analyzer and the Heat Release Rate (HRR) and the burner heat release rate (HRRburner) ported from the NFRL calorimeter, 185 specimen-related data channels were recorded. These included data from thermocouples, simulated thermal elements, heat flux sensors, bi-directional velocity probes, a pressure transducer, and smoke and heat alarms. Both raw and processed data was recorded. A listing of the channels for each test is provided in the 'Hardware Configurations' in Appendix D.

An in-house software developed in LabVIEW™ called MIDAS (Modular In situ Data Acquisition System) was used to allocate channels and control the data acquisition (Figure 28b). Each channel was sampled at 90 Hz and data were averaged and recorded at a rate of 1 Hz along with the standard deviations from the averaging process. The I/O-Modules had at least 16-bit precision, resulting in uncertainties from the DAQ that were orders of magnitude lower than those from other sources in all of the measurements reported here.

(a) (b)

Figure 28. Photographs of (a) cDAQ-9188 chassis populated with I/O-modules and (b) setup used to control the NFRL calorimeter and data acquisition.

2.5.2 NFRL calorimeter

Heat release rate measurements were performed using an oxygen consumption fire calorimeter. The calorimeter consisted of a 15 m square canopy style smoke collection hood, a 2.42 m diameter exhaust duct instrumented for mass flow measurements and a gas sampling system for measuring exhaust gas composition. The smoke collection hood was located 12.5 m above the test floor and was equipped with 6 m retractable side curtains (Figure 29a). The measurement section of the duct was located on the roof 25 m downstream of the hood. The total straight run of the roof duct was 35 m (Figure 29b).

A 9.5 mm diameter sample tube was used to extract 38 splm (standard L/min) of exhaust gas from the duct to the gas analyzers located in the instrumentation room. A 5 slpm sample stream of exhaust gas was conditioned to remove particles and water before entering the gas analyzers. High efficiency particle filters and multistage dryers, consisting of Nafion membrane

tube dryers and desiccant, were used to condition the sample to a dryness of less than 100 micro L of water.

The oxygen was measured using a paramagnetic oxygen analyzer. Carbon dioxide and carbon monoxide were measured using a nondispersive infrared (NDIR) analyzer. The gas analyzers were calibrated prior to each test using ultra high purity nitrogen zero gas (99.999% N_2) and high precision span gases. The oxygen span gas was 21.397% +/- 0.021% with a balance of nitrogen. The CO_2 span gas was 1.0025% +/- 0.00022% and the CO span gas was 0.09970% +/- 0.00022% with a balance of nitrogen. The sample gas delay time was 25 s. Heat release rate measurements were adjusted to account for this delay time.

The exhaust gas mass flow rate was determined using a pressure based velocity measurement in the duct and four Type K thermocouple temperature sensors (Figure 29b). Two averaging pitot tube flow velocity sensors were installed in the duct measurement section. The velocity probes were separated by a distance of 2.4 m and offset by 90°. The pressure from each velocity probe was measured using a high precision capacitance manometer. The pressure transducers had a range of 0 Pa to 1333.3 Pa and an accuracy of 0.15 % of the reading per manufacturer's specification. The exhaust duct velocity was taken as the average of these two measurements. The exhaust flow was set to approximately 100 kg/s prior to each test. The exhaust flow rate measurement standard deviation was 0.5 kg/s.

The heat release rate measurement system was verified using a natural gas burner reference fire. The heat release rate of the reference fire had a measurement combined standard uncertainty of less than +/- 1%. Calorimeter verification tests were performed on 2 separate days at heat release rate values of 1 MW, 5 MW, 10 MW, 15 MW and 20 MW. The maximum relative difference between the measured heat release rate and reference fire was less than 4.5%. The relative standard deviation of the heat release rate varied from 6.5 % at 1 MW to 3 % at 20 MW for a steady reference fire over a period of 180 s. The combined standard relative uncertainty for the heat release rate measurements was determined to be 7.4 % for this set of experiments. This uncertainty estimate is valid for near steady state fires. Transient events (< 30 s) have larger uncertainty due to the effect of system response time. Additional time delays and smearing of heat release rate data related to transport of the combustion gases out of the test compartment are not quantified in this report.

(a) (b)

Figure 29. (a) 15-m exhaust hood with natural gas reference burner at 5 MW and (b) 2.42-m diameter calorimeter exhaust duct with averaging pitot tubes and temperature sensors (gas sample tube not shown).

2.5.3 Gas sampling

Gas samples inside the compartment were taken using metal tubes attached to a steel stand located at the centre of the room (Figure 20, Figure 21 and Figure 30). Samples for the gas analyzer and differential room pressure were drawn from two 6-mm (1/4 in) diameter stainless steel tubes with their opening 210 cm from the floor. Samples for the smoke meter were drawn from a 50-mm (2 in.) diameter steel pipe with an opening 160 cm from the floor.

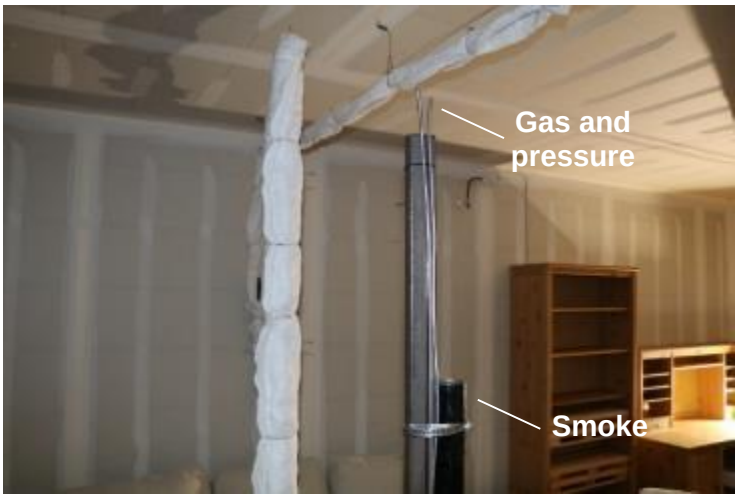

Figure 30. Photograph of stand with gas sampling tubes.

2.5.3.1 **Gas analyzer (O_2, CO_2, CO)**

Room gases were extracted and analyzed using the gas measurement rack shown in Figure 20, Figure 21 and Figure 30. A Permapure MiniGASS sample conditioning system was used to filter and dry the sample gas. The sample gas flow rate was set to 1 slpm for these tests. The delay time from the room inlet port to the gas rack was approximately 60 s. The oxygen was measured using a paramagnetic oxygen analyzer. Carbon dioxide and carbon monoxide were measured using a nondispersive infrared (NDIR) analyzer. The analyzers were calibrated prior to each test using calibrated zero and span gases. Nitrogen gas was used to zero each analyzer and room air was used to span the oxygen analyzer. Room air was assumed to have an oxygen concentration of 20.95% +/- 0.05 %. The carbon dioxide span gas consisted of 9.0% +/- 0.09% CO_2 in N_2 and the carbon monoxide span gas consisted of 4.0 % +/- 0.04% CO in N_2. A high pressure air line was used to blow out the sample line during the test if the sample line became clogged by soot. The maximum range of the CO and CO_2 measurements was 20 %. This range was exceeded during several of the tests. There were other periods where gas sample data was invalid due to loss of sample flow and loss of sample tube support. The sample tube deformed and fell onto the room floor during several of the tests. The gas sample measurements were more reliable early in the tests. All gas measurements are reported on a dry basis.

Figure 31. Photograph of gas analyzer rack.

2.5.3.2 **Differential pressure**

The pressure difference between the inside and outside of the compartment was made using a Greisinger (Model GMH 3181-01) manometer (Figure 32). For these experiments, we used the 0 V to 1 V analog output to record the data and scaled the data range to +/- 200 Pa. The combined standard uncertainty for this measurement was +/- 1.1 Pa.

Figure 32. Photograph of Greisinger model GMH 3181-01 handheld manometer.

2.5.3.3 **Smoke density**

Smoke sample was drawn from the compartment to the smoke meter, consisted of a completely enclosed black measuring chamber with a white light source (light emitting diode (LED)), aperture and silicon PIN diode as the detector inside. The LED source approximates the light sensitivity of the human eye. Each smoke meter was calibrated using neutral density filters and also calibrated at 100% and 0% transmission.

Visibility through smoke can be related to the optical density of smoke (*OD* in m^{-1}) expressed as [17]:

$$OD = \frac{1}{L}\log_{10}\left(\frac{I_0}{I}\right)$$

where I_0 is the intensity of the incident light, I is the intensity of the light transmitted through the path length, L (m), of the smoke. The optical density is related to the extinction coefficient k (m^{-1}) by $OD = k/2.303$. The combined standard uncertainty for this measurement is around +/- 10 % for full-scale fire tests.

Figure 33. Photograph of smoke density meter (PVC pipe) and manometers mounted outside of the compartment.

2.5.4 Specimen sensors

In this section, the specimen sensors are described and photographs of representative applications for each sensor are shown. Detailed drawings of the location of each sensor are provided in Figure 20 to Figure 27. The key relating the sensor wire numbers in the drawings to the specific sensor can be found in the ‘Hardware Configurations’ in Appendix D. It is noted that wire numbers 119 and 160 were not assigned. These wire numbers were assigned to channels in the original test plan that were eliminated (channel 119) or did not require wiring (channel 160).

2.5.4.1 **Thermocouples**

Temperatures were measured using four types of thermocouples. All of them were Type K thermocouples from Omega Engineering with a measurement range from -200 °C to 1250 °C and a standard uncertainty of the greater of +/- 0.75 % or 2.2 °C. No correction for radiation on the bead temperature was performed.

The majority of the thermocouples were glass-sheathed, 24-gauge, 0.5-mm diameter bare-bead thermocouples (Model GG-K-24-SLE-1000). The wire was purchased in 305 m (1000 ft) spools, cut to length and a bead was created in-house using a thermocouple welder. These thermocouples were used to measure the temperatures at the interface between gypsum layers (Figure 34a), CLT panel temperatures (Figure 34b) as well as other gas-phase temperatures (e.g., Figure 34c,e).

- Eighteen of these thermocouples were installed on the interior side of the CLT panels: (1) five thermocouples located at the centre and four quarter points of the ceiling assembly, respectively, (2) three thermocouples located at the centre of each of the W1, W3 and W4 wall assemblies at 0.6 m, 1.2 m and 1.8 m above the floor, and (3) extra four thermocouples installed at the quarter points of the W1 wall assembly.
- Another eighteen thermocouples were installed at each interface between two adjacent gypsum board layers at the same positions as on the interior side of the CLT ceiling and walls.
- The thermocouples were also embedded in the CLT panels at the depths of 20 mm, 35 mm, 50 mm, 65 mm, 90 mm, 115 mm, 140 mm (interior side as 0) at the centre of the ceiling and at the mid length of the W1, W3 and W4 walls 1.8 m above the floor, respectively. The embedded thermocouples were also added at the 70 mm depth in some CLT panels for the last two tests. The drilled holes were sealed from the outside after embedding the thermocouples.
- One thermocouple was installed beside each plate thermometer (see Section 2.5.4.3).
- Five thermocouples were located at the 3.5 m, 4.5 m, 5.5 m, 6.5 m and 7.5 m height above the rough opening along its vertical centerline on a vertical metal pole. The thermocouples at the 3.5 m and 4.5 m height were flush against the exterior wall; the thermocouples at the 5.5 m, 6.5 m and 7.5 m height were open to the air.

The thermocouples used on the trees inside the compartment (Figure 34f) and in the doorway were stainless steel sheathed, 3.175 mm (1/8 in.) diameter, grounded junction thermocouples (Model HKQSS-18G-400) purchased in fixed lengths. The sheathing allowed the trees to be reused in multiple tests, with replacement of individual thermocouples as required.

- Six trees using these thermocouples were installed in the fire compartment, each tree with five thermocouples at 0.6 m, 1.1 m, 1.6 m, 2.1 m and 2.6 m above floor.
- A vertical array of these thermocouples was located at the centreline of the rough opening with 7 thermocouples spaced at intervals of 1/8 the height of the rough opening.

Stainless steel sheathed (Model KMQSS-040) or plastic coated thermocouples (Model EXPP-K-24-SLE-1000) were used to measure cooling water temperatures for various instruments (Figure 34d). These thermocouples were used for monitoring and the data is not reported.

(a)

(b)

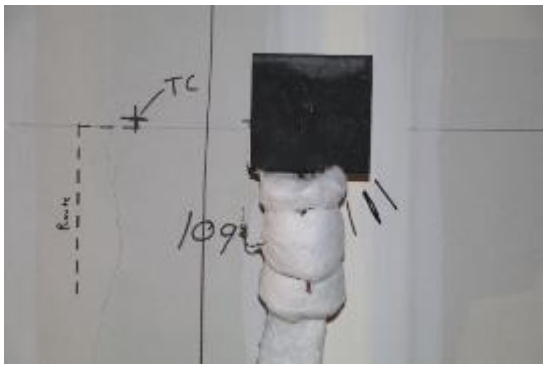

(c)

(d)

(e)

(f)

Figure 34. Photographs of typical thermocouple applications; (a) layer interface temperature, (b) temperature through panel, (c) gas temperature near plate thermometer, (d) cooling water temperature, (e) roof tree, and (f) compartment tree.

2.5.4.2 **Simulated thermal elements**

Simulated Thermal Elements (STEs) manufactured by FM Global were installed to replicate the time temperature response of a quick-response (QR) sprinkler element. STEs were constructed of spring steel having a diameter of 25.4 mm (1 in.) and a thickness of 0.46 mm (0.018 in.), with type K chromel-alumel thermocouple wires tack welded to one side (Figure 35a). The response time index (RTI) of QR STEs was established with plunge tunnel testing to have an average and standard deviation of 28.4 $(m\,s)^{1/2}$ +/- 1.1 $(m\,s)^{1/2}$ (i.e., 51.4 $(ft\,s)^{1/2}$ +/- 2.0 $(ft\,s)^{1/2}$).

Ten STEs were located at 305 mm (12 in.) or 457 mm (18 in.) from the ceiling (Figure 35b) at various locations for each test, with the disk plate in horizontal orientation parallel to the ceiling. For the eight STEs near walls, they were installed 100 mm (4 in.) away the wall..

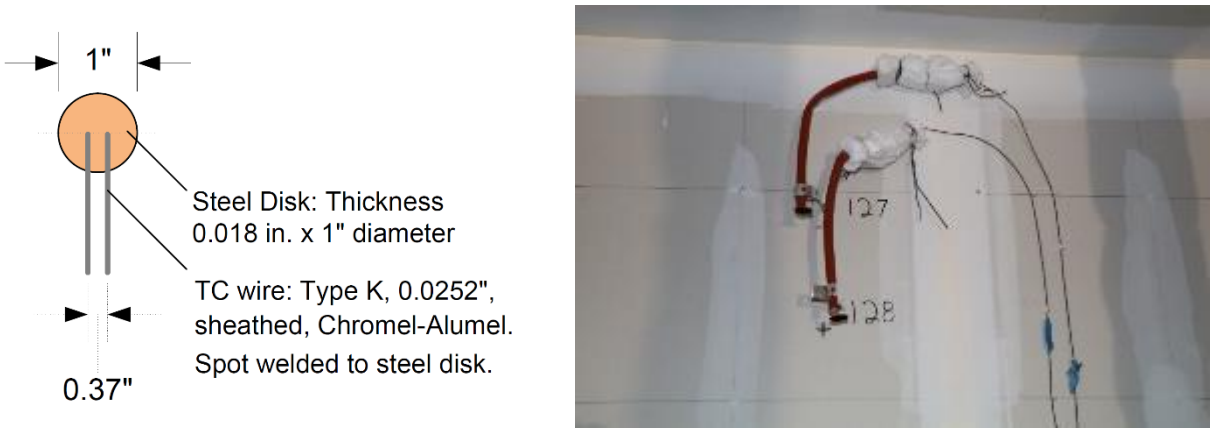

(a) (b)

Figure 35. (a) Sketch of back view of simulated thermal element (STE) and (b) photograph of STEs located 305 mm (12 in.) and 457 mm (18 in.) from the ceiling (1 inch = 25.4 mm).

2.5.4.3 **Heat flux**

Total heat flux was measured at twelve locations during each experiment (Figure 36). Eight locations were inside of the compartment: five wall locations (the W1 wall at the approximate ¼, ½ and ¾ lengths at a height of 1.8 m; the W3 wall at the approximate ½ length at a height of 1.8 m; the W4 wall at the approximate ½ length at a height of 1.8 m), two ceiling locations (the ceiling centre and above the bed) and one floor centre location. Two locations were outside the compartment 2.4 m and 4.8 m away facing the doorway at the 1.5 m height. Two locations were outside the compartment in the W2 wall above the doorway along its vertical centerline at the 3.5 m and 5.5 m heights from the ground level.

This provided three different environments for the measurement with respect to the surrounding gas temperature. Three different sensor types were used to measure heat flux: Gardon gauges, plate thermometers and differential flame thermometers. In some instances, multiple types of heat flux gauges were co-located to investigate the various techniques; the locations of the sensors are shown in Figure 20 to Figure 25 and Figure 27.

Gardon gauge

The Gardon gauges were 25.4 mm (1 in.) diameter water cooled sensors manufactured by Medtherm (Model 64-20-18). The nominal range for the gauges was 227 kW/m^2 from a field of view of 180° with a manufacturer-reported standard uncertainty of 1.5 % in the responsivity (the slope in kW/m^2/mV). Heat fluxes as high as approximately 300 kW/m^2 were observed. These heat fluxes are beyond the stated range of the gauges. According to the manufacturer, the calibrations remain linear and valid beyond the stated range as long as the materials do not degrade and change the sensitivity of the gauge. Gauges located inside the compartment – where the highest heat fluxes were observed – were replaced after each test. Gauges located outside of the compartment were reused.

The wall mounted Gardon gauges inside the compartment were placed in steel pipes with a 25.4 mm (1 in.) inside diameter, wrapped with a 25 mm thick thermal ceramic blanket and covered with aluminum foil (Figure 36b). Floor mounted Gardon gauges were either installed like the wall mounted gauges or were boxed-out with multiple layers of gypsum board and covered with a thermal ceramic blanket to protect the cooling water tubes and wiring. Gardon gauges located outside the compartment were either placed in steel pipes with a 25.4 mm (1 in.) inside diameter (Figure 36d) or attached to a stand on the roof of the compartment with the front face of the probe flush with the wall above the doorway (Figure 34e, Figure 36f).

Cooling water to the gauges was supplied at 43 °C +/- 5 °C. Water flowing out of the gauges was monitored for the gauges that experienced the highest heat flux. During testing, for gauges located outside the compartment, the outflow water temperature rose to no more than 56 °C in all tests, except Test 1-5, where a peak outflow water temperature of 71 °C was observed. For Gardon gauges located inside the compartment, the outflow water approached 100 °C in all tests. In several cases, the cooling lines failed and the measurement was lost.

For the gauges where the water temperatures increased to 100 °C, the heat fluxes were on the order of 100 kW/m^2 to 300 kW/m^2 which represent blackbody temperatures in the 950 °C to 1300 °C range. The most extreme combination (affecting uncertainty) of cooling water and environment temperature would be a 55 °C increase in cooling water in a 950 °C environment. This combination would have less than a 0.5 % effect on the measured heat flux. The effect was determined by calculating the ratio of the T^4 difference between 950 °C and the 55 °C cooling water with 950 °C and the 100 °C cooling water. This is a simplified comparison which assumes everything else is equal, but generates an approximation of the magnitude of the cooling water effect under specified conditions [18].

Heat flux uncertainty due to soot and dust deposition on the gauges is difficult to quantify. Bundy [18] estimated that the soot coating on the gauge would add an additional uncertainty of +/- 10 % due to variations in surface emissivity, and soot agglomerates shadowing the surface of the gauge.

Plate thermometers

The plate thermometers (PT) manufactured by Pentronic (Model 5928060) were in conformance with EN 1363-1 [19] or ISO 834 [20]. The nominal range of the probe was 1200 °C. Sensors that exceeded this temperature (i.e., all sensors inside of the compartment), were replaced after each test. A manufacturer-reported standard uncertainty is not available.

Three different mounting conditions were used. Inside of the compartment, the sensors were affixed to a metal bracket such that the plate was parallel to the mounting surface (wall or ceiling) with a standoff of 100 mm (Figure 36a). The bracket and sensor wiring were wrapped in

a thermal ceramic blanket. In this configuration, heating of the probe from all sides was possible. In front of the doorway (outside the compartment), the sensors were attached to metal stands with the probe face oriented toward the doorway (Figure 36c,d). In this configuration, heating of the probe was one-directional. Above the doorway (outside the compartment), the sensors were attached to a stand on the roof of the compartment with the front face of the probe flush with the wall above the doorway (Figure 34e, Figure 36e,f). Any gap between the probe and the wall was filled with a thermal ceramic blanket and the back of the probe was surrounded with a thermal ceramic blanket as well. In this configuration, heating of the probe was one-directional.

The gas temperature near the probe (T_{gas}) was measured using a glass-sheathed, 24-gauge, bare-bead thermocouple (Figure 36a) with a measurement range from -200 °C to 1250 °C and a standard uncertainty of the greater of +/- 0.75 % or 2.2 °C.

The incident heat flux at the plate thermometer at step i ($[\dot{q}''_{inc}]^i$, in W/m^2) is calculated, using the measured temperature of the plate thermometer (T_{PT}, in K) and the gas temperature near the plate thermometer (T_{gas}, in K), as follows:

$$[\dot{q}''_{inc}]^i = \sigma[T_{PT}^4]^i - \frac{(h + K_{PT})\left([T_{gas}]^i - [T_{PT}]^i\right) - C_{PT}\frac{[T_{PT}]^{i+1} - [T_{PT}]^{i-1}}{[t]^{i+1} - [t]^{i-1}}}{\varepsilon_{PT}}$$

where the time (t) is in seconds, the Stefan Boltzmann constant (σ) is 5.6704E-8 W/m^2/K^4, the convection coefficient (h) is taken to be 10 W/m^2/K, the heat transfer coefficient due to heat losses of the plate thermometers (K_{PT}) is taken to be 8 W/m^2/K [21], the lumped heat capacity of the plate thermometers (C_{PT}) is taken to be 4200 J/m^2/K [21], and the emissivity of the plate thermometer (ε_{PT}) is taken to be 0.9. The emissivity was suggested by the inventor of the plate thermometers based on experience. The convective portion of the heat flux was relatively small inside the compartment as the gas temperature was relatively close to the plate thermometer temperature, resulting in a small convective heat flux. The convective heat flux was also low away from the compartment since no significant airflow or wind occurred in the lab space. The convective heat flux above the ventilation opening had more influence on the total heat flux.

Differential flame thermometers

The differential flame thermometers (DFT) manufactured by Fire Instrument Research (Model TN-TN-K) were in conformance with American Society for Testing and Measurement (ASTM) standard E3057-16 [22]. These sensors were only used in Test 1-1 and Test 1-2 and were not reusable after the test. A manufacturer-reported standard uncertainty is not available.

All sensors were installed inside the compartments. The sensors were affixed to a metal bracket such that both plates (front and back) were parallel to the mounting surface (wall or ceiling) with a standoff of 100 mm to the back plate (Figure 36b). The bracket and sensor wiring were wrapped in a thermal ceramic blanket. In this configuration, heating of the probe from all sides was possible.

The incident heat flux at the plate thermometer was determined using the measured temperature of the front ($T_{DFT.front}$) and back plate ($T_{DFT.back}$) of the DFT using a proprietary software package purchased with the sensors.

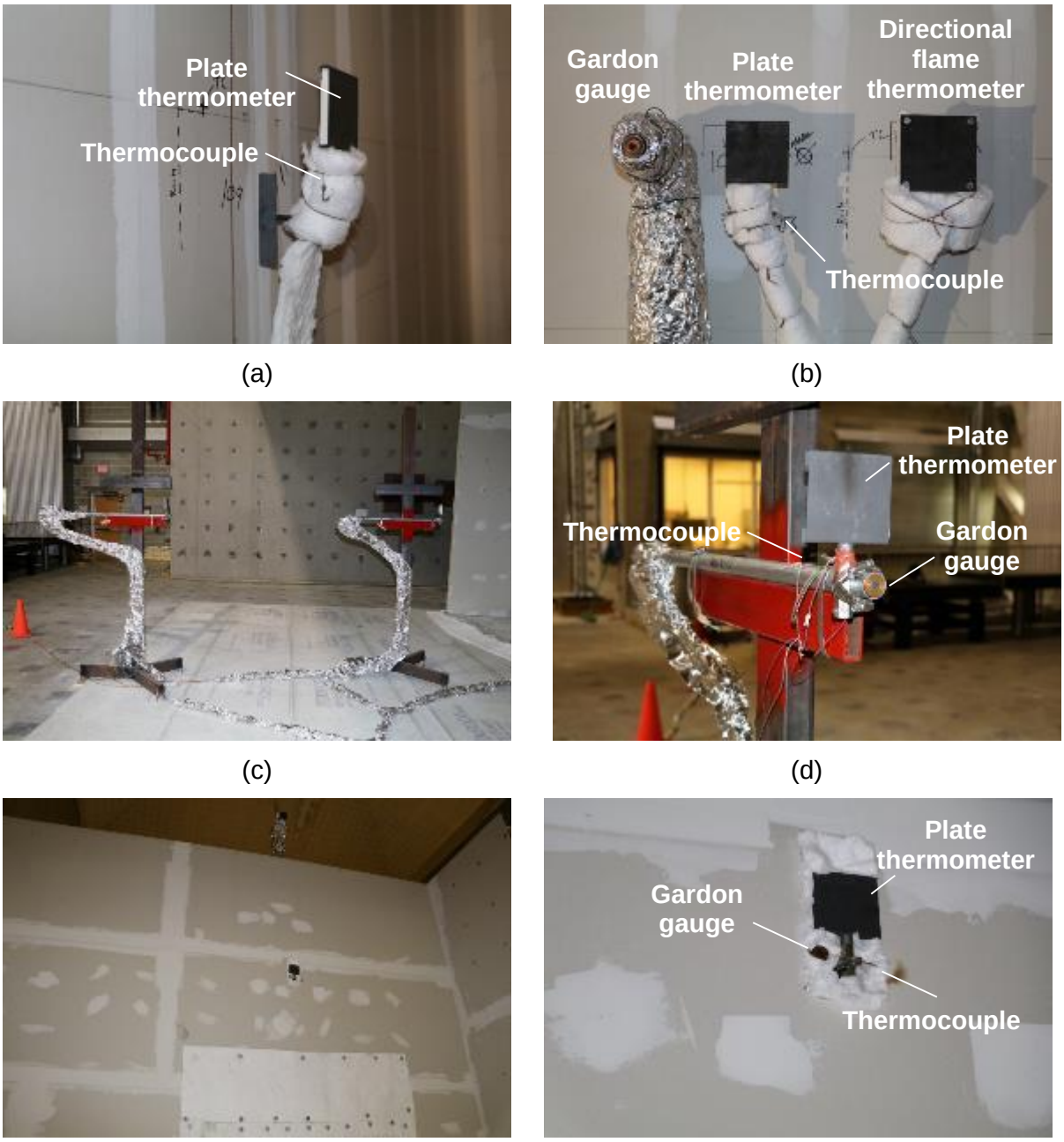

Figure 36. Photographs of heat flux sensors: (a) plate thermometer on wall inside compartment, (b) co-located Gardon gauge, plate thermometer and differential flame thermometer on wall inside compartment, (c) heat flux sensors on stands facing the doorway, (d) detail of heat flux sensors facing the doorway, (e) heat flux sensors in the wall above the doorway and (f) detail of heat flux sensors above the doorway.

2.5.4.4 **Bi-directional velocity probes**

Dynamic pressure was measured 305 mm from the ceiling 227.5 cm from the rear of the compartment along the centerline (Figure 37a) and at 6 locations in the doorway of the compartment (Figure 37b) to determine velocities. The six locations in the doorway included: (1) three bi-directional velocity probes installed at 1.5 m height, one on the centerline of the opening and one on each side, 0.5 m from the centerline; (2) three bi-directional velocity probes installed at the 1.5 m height, one on the centerline of the opening and one on each side, 0.5 m from the centerline.

The differential pressure transducers (0 V to 1 V output) were the same type as that used to measure the differential pressure in the room; Greisinger Model GMH 3181-01. The output voltage was scaled to achieve a range of +/- 200 Pa with a combined standard uncertainty of +/- 1.1 Pa. Each pressure transducer was mounted outside of the compartment (Figure 33). Each transducer produced a voltage, V_{bdp}, related to the exposed differential pressure by the following equation: $\Delta P_{bdp} = 13.332\left(V_{bdp} - V_{bdp,zero}\right)$, where the pressure difference is in Pascals and the voltages are measured in volts. The zero voltage, $V_{bdp,zero}$, condition is created when the positive and negative ports of the transducer are connected so there can be no pressure difference between them.

The transducers were connected to 1.3 cm diameter bi-directional probes [23] with 4.7 mm diameter stainless steel (inside compartment) or copper (outside compartment) tubing. Probe leads were routed close to each other so each lead was exposed to the same levels of heating. This installation care minimized differential heating and any resulting non-flow induced pressure differences between the leads.

Bi-directional probes enable the measurement of dynamic pressure, which is the difference between the total pressure on the face where flow impinges and the static pressure on the downstream face of the probe. Using Bernoulli's principle and including a calibration factor, velocity, v, can be obtained from the dynamic pressure and a local gas temperature through the following relation: $v = C\sqrt{\Delta P_{bdp} T_{bdp}}$ where ΔP_{bdp} is the measured pressure across the bi-directional probe, T_{bdp} is the temperature (in K) of the gases flowing past the probe and C is defined as: $C = \frac{1}{C_{bdp}}\sqrt{\frac{2R}{P_{ref} MW_{gas}}}$.

The calibration coefficient, C_{bdp}, for a bi-directional probe is equal to 1.08 +/- 0.05 [23] when the local Reynolds number (defined by the probe diameter) is greater than 1000. R is the ideal gas constant, P_{ref} is the reference pressure and MW_{gas} is the molecular mass of the gas.

To generate the velocity from the differential pressure, the temperature near the bi-directional probe is required. Assuming standard atmosphere values for air:

$$v = sign\left(\Delta P_{bdp}\right)\frac{1}{1.08}\sqrt{2\left|\Delta P_{bdp}\right| T_{bdp}\frac{R}{P_{ref} MW_{gas}}} = sign(\Delta P_{bdp})\frac{1}{1.08}\sqrt{\frac{2\left|\Delta P_{bdp}\right| T_{bdp}}{353.06}}$$

The measured velocities had a combined standard uncertainty of +/- 15.2 %.

(a) (b)

Figure 37. Photographs of bi-directional velocity probes located (a) on the ceiling (co-located STE visible) and (b) on stand in doorway (tubes for zeroing sensor visible).

2.5.4.5 **Smoke and heat alarms**

A commercially-available photoelectric non-ionizing smoke detector (Kidde PE120) and heat alarm (Kidde HD135F) were located on the ceiling near the centre of the compartment in each test (Figure 38a). The devices were modified to generate a voltage drop when the alarms triggered, which could be measured by the data acquisition system (Figure 38b).

(a) (b)

Figure 38. Photographs of (a) installed smoke and heat alarms and (b) circuit for power supply and signal extraction from alarms.

2.5.5 Imaging and video

Various networked high-definition video cameras (Figure 39) and handheld cameras were used to document the experiments.

(a) (b)

Figure 39. Photographs of (a) networked video camera and (b) web USB camera.

2.5.5.1 **Water cooled GoPro cameras**

High-definition video footage of the inside of the compartment during the fire was captured from the doorway using a waterproof GoPro camera placed in a water bath. The water served dual purposes of cooling the camera and filtering out the thermal radiation produced by the fire; water is very efficient at absorbing energy in the infrared spectrum. For the first test, a partially-filled borosilicate (Pyrex) container supported on a stand was continuously supplied with tap water (23 °C +/- 5 °C) and a pump was used to extract the water as it heated (Figure 40a). This worked for about 10 min after flashover, but the high thermal gradient caused the vessel to fracture. For the subsequent tests, a thinner borosilicate container was filled completely to the top with water that could overflow out the back of the container where it was collected and drained (Figure 40b). Additionally, the field of view for the camera was minimized using thermal ceramic boards to reduce the view factor. This approach allowed the camera to capture images indefinitely (limited by battery life).

(a) (b)

Figure 40. Photographs of water-cooled camera setup (a) 1st attempt and (b) improved setup.

2.6 Test Procedure

The following procedure was used for the fire tests.

(1) Start data acquisition and instrumentation system;

(2) Ignite the gas burner with the small pilot flame;

(3) Turn off the gas burner once the combustion of the room contents reaching 1 MW in heat release rate;

(4) Let the fire continue to a total burnout where possible and practicable;

(5) Terminate the test based on the following criteria:

   a. Any safety threat to personnel and facilities;

   b. An elapsed time of 4 h;

   c. Total burnout to self-extinguishment; or,

   d. Continuous fire decay with temperatures in CLT and/or compartment falling below 250 °C and heat release rate falling below 1 MW.

(6) Examine debris and take necessary measurements (photographs, charring depth of selected samples, etc.) after the fire test.

3. RESULTS AND DISCUSSIONS

Six large-scale CLT compartment fire tests were conducted as part of the FPRF project “Fire Safety Challenges of Tall Wood Buildings – Phase 2”. A large amount of technical data was produced, including the heat release rate, interior and exterior heat fluxes, gas and flow conditions, temperatures inside and outside the compartment and through the ceiling and wall assemblies, and char depth, etc. All the measurement data is included in Appendixes E-K. Table 5 summarizes some selected data. This section presents key results of the tests and analysis to quantify the contribution of the CLT structural panels to the compartment fires.

Table 5. CLT Compartment Fire Tests (February to April 2017).

Opening size in W2 wall	1.8 m wide x 2.0 m high								3.6 m wide x 2.0 m high			
Test	1-1 (Feb 16)		1-4*(Mar 21)		1-5 (Apr 13)		1-6 (Apr 18)		1-2 (Feb 23)		1-3*(Mar 16)	
W1 wall	3GB		3GB		exposed		exposed		2GB		exposed	
W2, W3 and W4 walls	3GB		3GB		3GB		3GB		2GB		2GB	
Ceiling	3GB		exposed		3GB		exposed		2GB		3GB	
Exposed CLT surface versus total ceiling and wall area (%)	0		36%		21%		57%		0		21%	
Smoke / heat alarms (min)	2.1 / 3.5		2.5 / 1.5		1.8 / 2.5		2.0 / 3.0		3.4 / 2.9		5.5 / 2.9	
STEs reaching 68 °C (min)	1.3-5.4		1.3-3.5		1.2-3.6		1.6-3.9		1.5-4.6		2.4-5.8	
Smoke OD > 3.4 m^{-1} (min)	12.6		11.6		11.0		9.4		15.2		12.4	
Flashover (min)	14.9		11.5		11.5		9.8		15.3		12.5	
Fully developed fire stage(min)	14.9 - 45		11.5 - 57 ☼		11.5 - 50 ☼		9.8 - 160		15.3 - 37		12.5 - 35	
HRR initial peak (MW)	9.5		13.1		9.6		12.9		12.4		14.2	
HRR fully developed (MW)	> 5		> 6		> 5		> 6		> 8		> 9	
HRR near end (MW)	0.34		5.1		10		9.5		0.43		0.7	
HF ceiling centre; bed (kW/m^2)	160; 240		>100↘		190; 180		220; 200		170; 230		n/a; 220	
HF W1 front; mid; rear (kW/m^2)	250; 275; 260		320; 320; 235		270; 290; 270		280; 270; 290		220; 275; 275		245; 320; 320	
HF W3 (kW/m^2)	180		-		250		280		200		n/a	
HF W4 (kW/m^2)	250		150		175		>170↘		230		210	
HF floor (kW/m^2)	190		205		190		170		190		200	
HF 3.5 m; 5.5 m high (kW/m^2)	70; 20		120; 30		120; 30		190; 60		105; 37		115; 45	
HF 2.4 m; 4.8 m away(kW/m^2)	40; 12		45; 17		40; 15		55; 20		65; 22		65; 25	
GB back reaching 300 °C	ceiling	walls	ceiling	walls	ceiling	walls	W3	W4	ceiling	walls	ceiling	walls
face layer (min)	30-40	32-60	-	31-58	28-35	36-60	37-68	48-82	32-36	31-43	13-17	30-92
mid layer (min)	50-68	65†	-	53-80	46-56	58-72	60-102	83-120	-	-	30-91	-
base layer (min)	No	No	-	77-141 rear only	70-85	98-191	86-123	102-130	53-67 rear only	No	118-221 rear only	95-123 upper only
GB fall-off time	ceiling	walls	ceiling	walls	ceiling	walls	W3	W4	ceiling	walls	ceiling	walls
face layer (min)	34-44	Nfo	-	46-73	32-45	50-70	55-108	77-120	36-40	Nfo	25-35	Nfo
mid layer (min)	Nfo	Nfo	-	Nfo	70-144	155-180	85-120	93-120	-	-	Nfo	-
base layer (min)	Nfo	Nfo	-	Nfo	144-155	185-195	125	125-130	Nfo	Nfo	Nfo	Nfo
Test duration (min)	134		159		202		160		104		242	
W1 char (mm)	0		0-14		102-141		88-143		0		60-86	
W3 char (mm)	0		0-10		0-52		5-66		0		0-10	
W4 char (mm)	0		0-2		25-51		25-68		0		0-20	
Ceiling char (mm)	0		66-90		25-79		116-154		0-15		0-20	
CLT contribution to HRR (MW)	0		5.5		3.3; 6.3; 9.5		7.5; 10		0		2.5	

GB: 15.9 mm (5/8 in.) thick Type X gypsum board; 2GB: 2 layers of GB; 3GB: 3 layers of GB
*Nfo: no fall-off (i.e., GB stayed intact during test); * Reused CLT structure; † W1 front upper portion only; ↘gauge failed;*
☼ re-flashed after 140 min.

3.1 Test 1-1

Test 1-1 was conducted on February 16th, 2017 using CLT compartment #1 with 3 layers of the gypsum board and the 1.8 m x 2.0 m ventilation opening. All CLT surfaces on the walls and ceiling were fully protected so that the CLT structure would neither contribute to the compartment fire nor develop char during the test and then be re-used for another test. Test 1-1 served as a baseline to define the contribution of the movable fire loads (residential furnishings) and to quantify CLT contribution to the fire in subsequent tests for the compartments with the same ventilation conditions.

3.1.1 Fire development

The test started with ignition. The first item ignited was the shelf (console table) in the room corner (Figure 18). The smoke alarm and heat alarm activated at 2.1 min and 3.5 min, respectively. Between 1.3 min and 5.4 min, all ten STEs reached 68 °C, which is a typical temperature rating for residential sprinklers. By this time, the fire involved only a portion of the console table (first item ignited). The console table was fully involved at 7 min with the smoke layer descending to mid height in the compartment. At 12.6 min, the smoke optical density measured at the 1.6 m height in the room centre reached 3.4 m^{-1}, at which occupants would not be able to see their hands in front of their faces [24]. The loss of visibility resulted from the first item ignited alone. At 14 min, the fire spread from the shelf to the adjacent dining table and chairs and dark smoke completely filled the room with dramatic changes of O_2, CO_2 and CO concentrations. Flashover occurred at 14.9 min and a large fire plume issued from the opening. After flashover, an intense burning of room contents lasted for approximately 30 min. The fire started to decay at 45 min and the fire plume ceased to issue from the opening at 50 min and thereafter; O_2 recovered to above 15% in the compartment. The test lasted over 2 h and was terminated at 134 min after continuous fire decay (the heat release rate falling to 300 kW at the end). A household garden hose was used to mist water over the debris on the floor to terminate the test. Figure 41 shows some photographs during and after Test 1-1.

(a) at 7 min after ignition

(b) at 14.5 min – just before flashover

(c) at 15 min – flashover

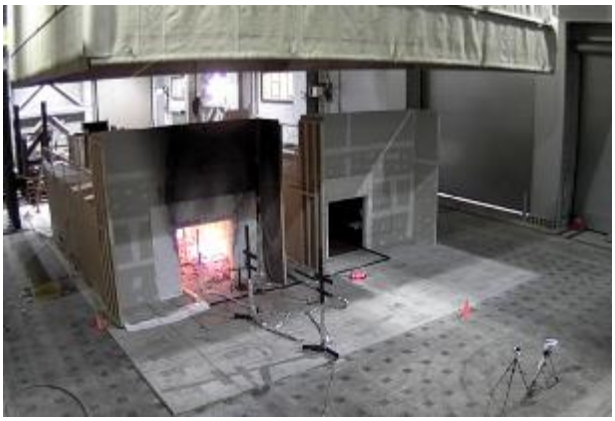

(d) at 60 min

(e) at 130 min – near end of test, gypsum board remained: 2 layers on ceiling; 3 layers on walls

(f) after Test 1-1 – gypsum board remained: 2 layers on ceiling; 3 layers on walls

(g) after cleanup and removal of gypsum board

(h) after cleanup and removal of gypsum board

Figure 41. Photographs (a)-(h) of the CLT compartment during and after Test 1-1 including subsequent cleanup and removal of gypsum board.

3.1.2 Compartment temperatures

Figure 42 shows temperatures in the compartment, measured using six thermocouple (TC) trees with thermocouples at 60 cm, 110 cm, 160 cm, 210 cm and 260 cm heights. TC trees 2 and 3 were in the front section of the compartment (near the rough opening), TC trees 5 and 6 in the middle section (living area), and TC trees 1 and 4 in the rear section (dinning and kitchen area).

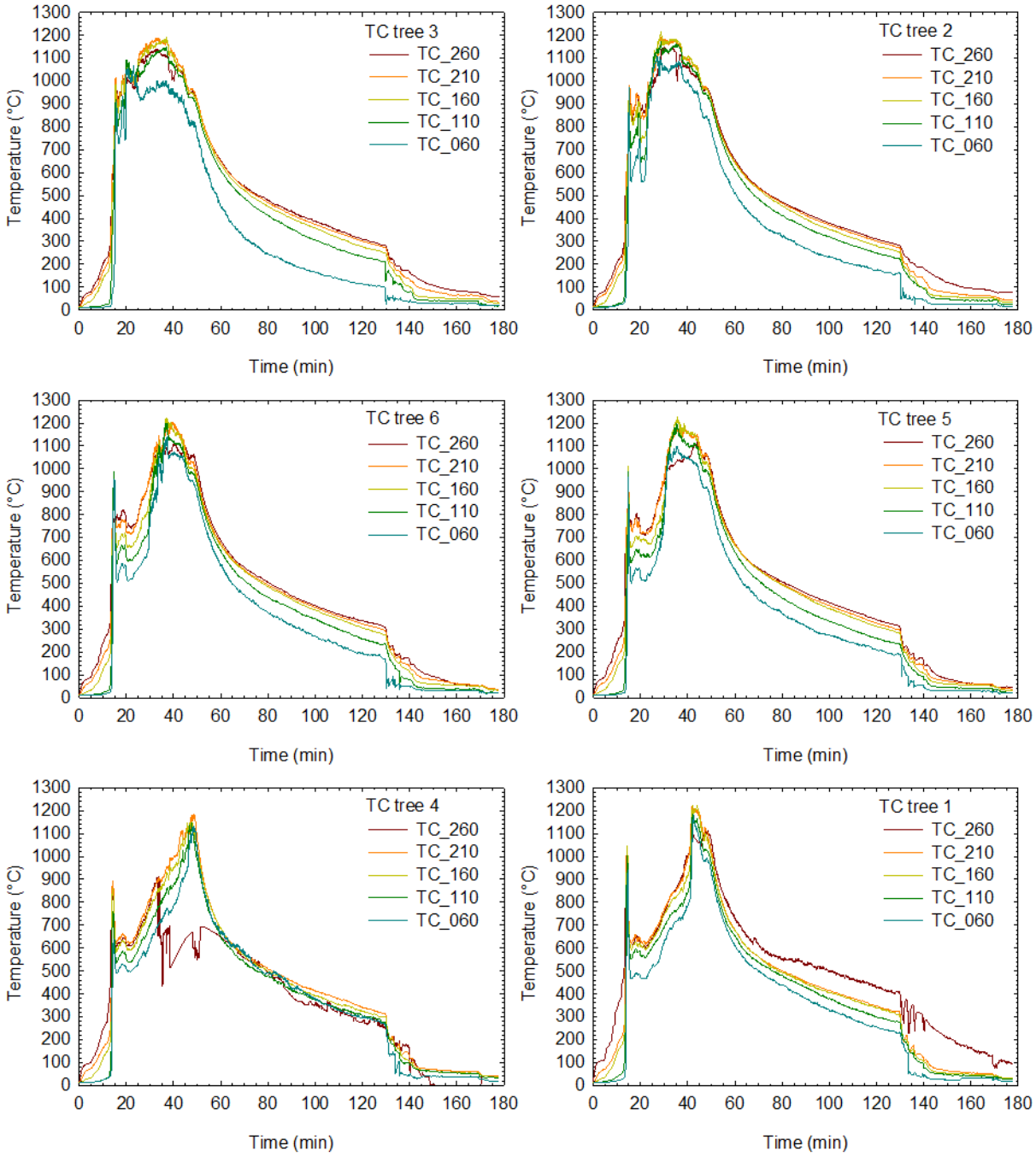

Figure 42. Temperatures in the compartment space during Test 1-1 (height in cm, test terminated at 134 min).

During the intense burning period (from flashover to decay at 15 min to 50 min), the vertical temperature difference along each TC tree was relatively small; for example, temperatures at 160 cm, 210 cm and 260 cm height were almost identical; while the lateral temperature difference across the room at difference TC trees was much larger. As time elapsed, the hottest area was moving from the front section of the room (with TC trees 2 and 3), to the middle section (with TC trees 5 and 6), and then to the rear section (with TC trees 1 and 4). The temperature reached 1200 °C, respectively, in the front, middle and rear sections at approximately 30 min, 40 min and 50 min.

The temperature measured by TC tree 4 at the 2.6 m height (TC_260) had a sudden drop and oscillation (see Figure 42) at 34 min and thereafter, which corresponded to the fall-off of the face layer gypsum board from the ceiling (see Section 3.1.5), indicating that the falling gypsum board covered that thermocouple.

3.1.3 Heat release rate

Figure 43 shows the heat release rate (HRR) during Test 1-1. The HRR was 9.5 MW at the initial peak right after the flashover and maintained above 5 MW until 45 min. As the fire decayed, the HRR reduced to 2 MW at 55 min and to 1 MW at 90 min. The test was terminated when HRR reduced to 0.3 MW at 134 min.

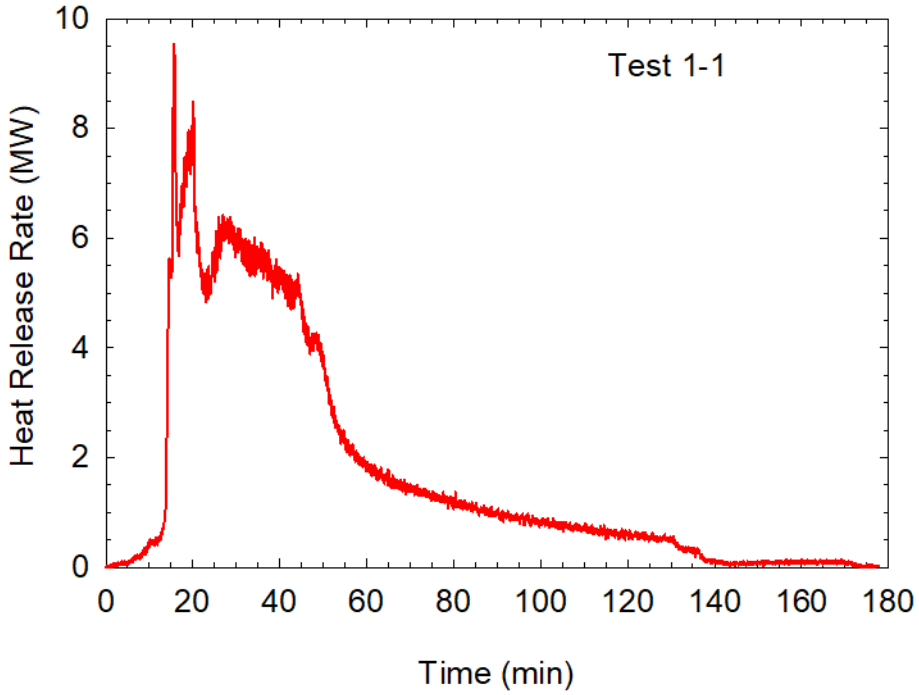

Figure 43. Heat release rate during Test 1-1 (test terminated at 134 min).

3.1.4 Heat flux inside and outside fire compartment

Various combinations of Gardon gauges, plate thermometers and differential flame thermometers provided measurements of heat flux at co-located positions. Figure 44 shows heat fluxes measured at the twelve locations inside and outside the fire compartment during Test 1-1. The initial spike of each curve corresponded to the flashover. Table 5 provides the

peak heat flux values at the fully developed fire stage after the flashover. The heat fluxes ranged from 160 kW/m^2 to 275 kW/m^2 inside the compartment and from 12 kW/m^2 to 70 kW/m^2 outside the compartment during the fully developed fire stage, depending on the locations. Comparisons of measurements made by different types of co-located heat flux gauges can be found in the appendices.

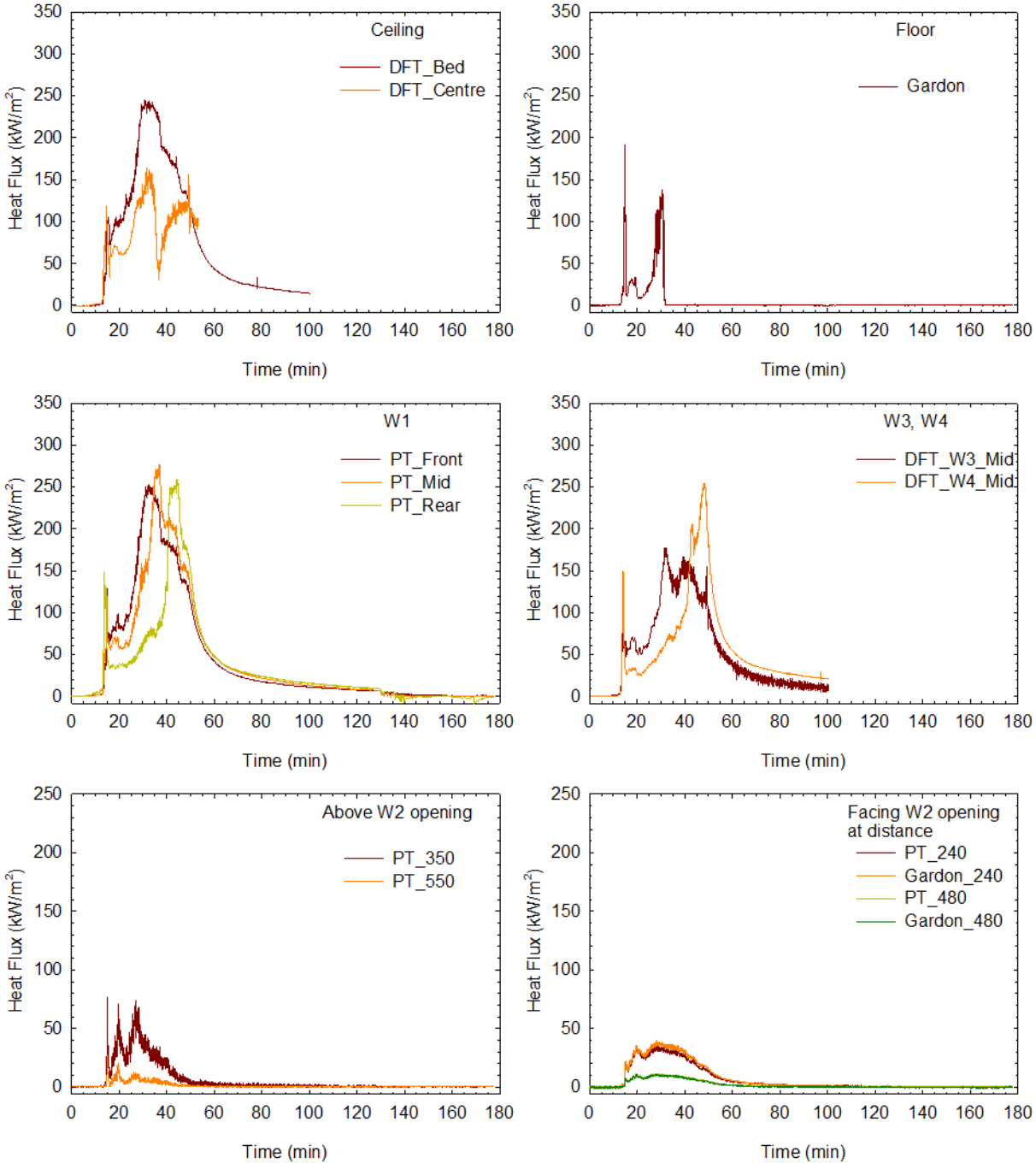

Figure 44. Heat fluxes inside and outside the compartment during Test 1-1 (test terminated at 134 min).

3.1.5 Temperatures at gypsum board interfaces and inside of CLT assemblies

The temperatures measured at the interfaces between the adjacent gypsum board layers and between the CLT interior surface and the gypsum board base layer, as well as inside CLT panels at various depths, are shown in Figure 45.

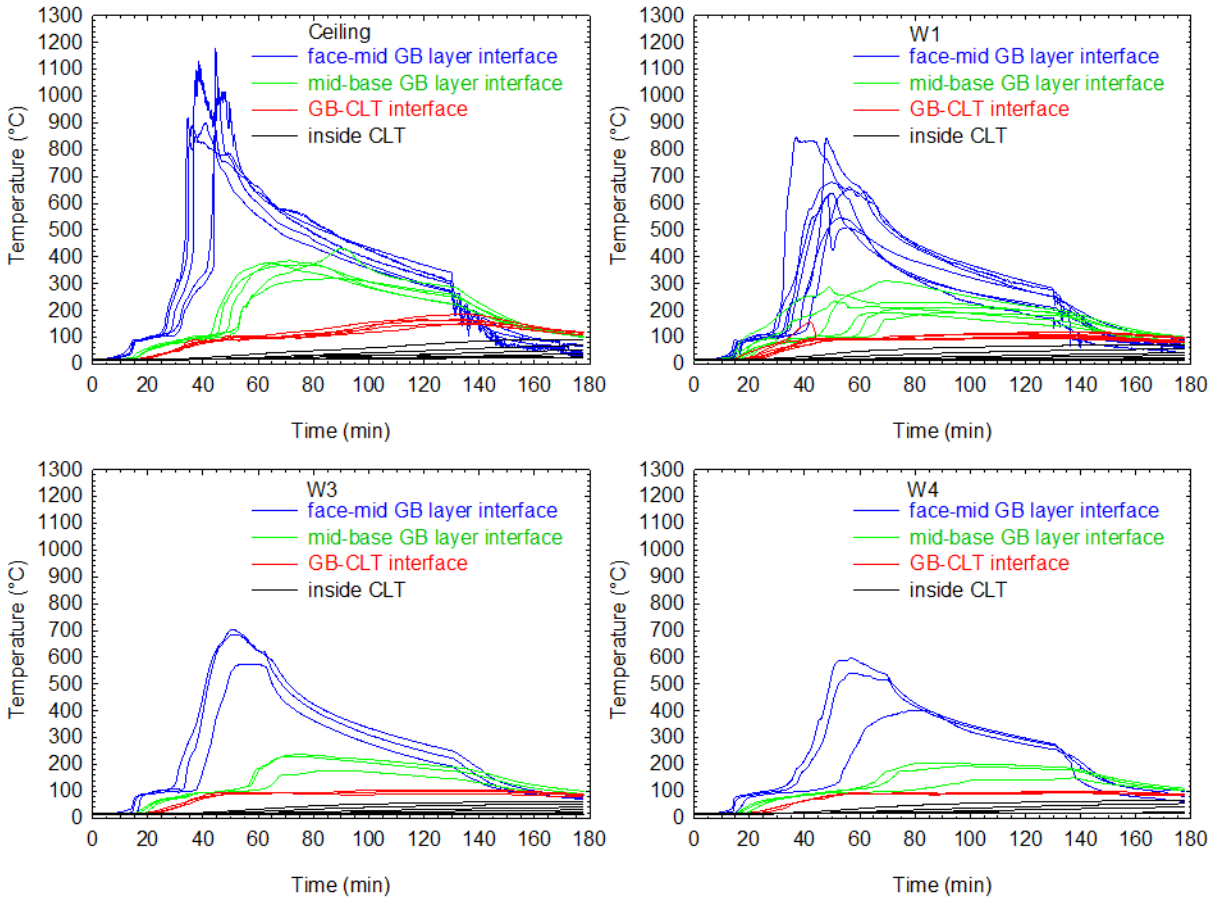

Figure 45. Temperatures in CLT and at gypsum board interfaces in Test 1-1 (test terminated at 134 min).

The temperature profiles at the interfaces indicated a typical three-stage heat transfer pattern through the gypsum board. There was an initial temperature rise up to 100 °C, followed by a period of gypsum calcinations (removal of water from gypsum board) during which the temperatures stayed at 100 °C. After the calcination, the temperatures increased rapidly.

In the ceiling assembly, the temperatures at the interface between the face and mid layers of gypsum board increased sharply at 34-44 min to equal to the compartment temperatures, indicating the fall-off of the face layer gypsum board. The fall-off of the face layer gypsum board resulted in the mid layer gypsum board being directly exposed to the fire and also increased the rate of conductive heat transfer through the mid layer to its interface with the base layer gypsum board. The temperatures at the mid and base layer interface reached 320-430 °C at 50-68 min in the ceiling assembly. If only two layers of the gypsum board had been used, the CLT ceiling panels would have been subjected to these temperatures (320-430 °C) and charred after these times. With the three layer gypsum board system, the CLT ceiling panels were kept below 180 °C on the interior surface and at the ambient temperature on the exterior surface.

In the wall assemblies, although the temperatures at the interface between the face and mid layers of gypsum board increased significantly up to 500-800 °C, the face layer gypsum board stayed intact until the end of the test. The CLT wall panels stayed below 120 °C on the interior surface and at the ambient temperature on the exterior surface.

As shown in Figure 41 (e) and (f), two layers of gypsum board remained on the ceiling except the absence of small pieces of the mid layer, and all three layers of gypsum board remained on the walls, until the end of the test. Figure 41 (g) and (h) show CLT compartment #1 after Test 1-1 with gypsum board removed, indicating no char was developed during the test. This CLT structure was re-used later in Test 1-4 with an exposed CLT ceiling.

The three layer gypsum board system successfully protected the CLT structure, preventing the ignition and involvement of CLT structural elements in the fire. Test 1-1 provided a baseline to quantify CLT contribution to the compartment fire in subsequent tests.

3.1.6 Char depth of CLT panels and small CLT blocks

As shown in Figure 41 (g) and (h), the entire interior surface of the CLT compartment had no char; neither did the exterior surface. Although no sealant was used to seal the compartment, there was no char developed at any CLT panel joints. However, there was minor smoke deposition outside the two back corners at the wall-ceiling junction, which could have been prevented if the joint had been sealed.

Three small CLT blocks (305 mm x 203 mm x 175 mm) were placed on the floor in Test 1-1 for char measurements (only the top surface was exposed). After the test, each block was cut to half at the middle. Figure 46 shows the remaining thickness of the CLT blocks after Test 1-1. The char depth was 55 mm, 45 mm and 42 mm for the blocks placed at the front, middle and rear sections of the compartment floor, respectively.

(a) CLT block near a TC Tree

(b) front block near TC Tree 3 charred 55 mm

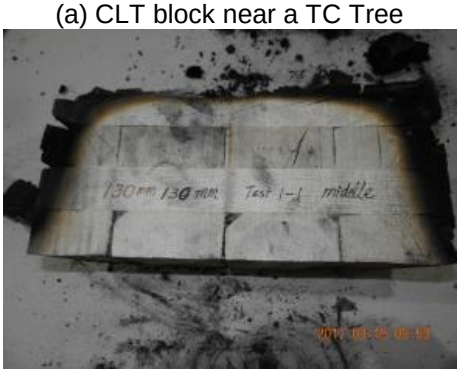

(c) middle block near TC Tree 6 charred 45 mm

(d) rear block near TC Tree 4 charred 42 mm

Figure 46. Char of small CLT blocks in Test 1-1 (cut to half to show remaining thickness).

3.2 Test 1-2

Test 1-2 was conducted on February 23rd, 2017 using CLT compartment #2. All CLT surfaces on the walls and ceiling were fully protected using two layers of the gypsum board and the 3.6 m x 2.0 m ventilation opening. Test 1-2 served as a baseline to define the contribution of the movable fire loads (residential furnishings) and to quantify CLT contribution to the fire in a subsequent test for the compartment with the same ventilation conditions.

In the test plan [3], this test had originally been designed to incorporate the same ventilation opening (1.8 m x 2.0 m) in the W2 wall and the only intended difference between the two baseline tests in the original plan was the number of layers of gypsum board. However, based on the interface temperatures measured between gypsum board layers during Test 1-1 (see Figure 45), two layers of gypsum board lining would very likely result in significant charring to the CLT compartment with the 1.8 m x 2.0 m opening, at least causing damages to the ceiling and the upper portion of the W1 wall.

This test was adjusted to incorporate the 3.6 m wide x 2.0 m high ventilation opening in order to address two needs. Firstly, during the development of the test plan, fire service representatives in the PTP expressed an interest of using a larger ventilation opening for the test series in order to collect data on the more intense exterior exposure that would result. Secondly, to better use the project resources, the CLT structure was intended to be restored after this baseline test for another test. A larger opening was expected to accelerate combustion of the room contents and shorten the intense burning duration thus reducing potential damages to the CLT structure. At the same time, the need of fire services would be addressed.

3.2.1 Fire development

The test also started with the ignition of the console table in the room corner. The smoke alarm and heat alarm activated at 3.4 min and 2.9 min, respectively. Between 1.5 min and 4.6 min, all ten STEs reached 68 °C, which is a typical temperature rating for residential sprinklers. The console table (first item ignited) was fully involved at 5 min. As the fire progressed in the dining area, the smoke layer descended to the mid height in the compartment and stayed at this height until flashover. At 15.2 min, the smoke optical density measured at the 1.6 m height in the room centre reached 3.4 m^{-1}. Flashover occurred at 15.3 min with dramatic changes of O_2, CO_2 and CO concentrations; large fire plume was issued from the opening. After flashover, an intense burning of room contents lasted for approximately 24 min. As expected, the combustion of the room contents accelerated with the larger opening. The fire started to decay at 37 min and fire plume ceased to issue from the opening at 40 min and thereafter; O_2 recovered to above 15% in the compartment at 47 min. The test lasted for 104 min and was terminated after continuous fire decay (the heat release rate falling to below 500 kW at the end). A fire hose was used to lightly spray water over the debris on the floor to terminate the test. Figure 47 shows some photographs during and after Test 1-2.

(a) at 7 min 49 s after ignition

(b) at 15 min 9 s – just before flashover

(c) at 15 min – flashover

(d) at 67 min

(e) at 100 min – near end of test, gypsum board remained: base layer on ceiling; 2 layers on walls

(f) after Test 1-2 – gypsum board remained: 1 layer on ceiling; 2 layers on walls

Figure 47. Photographs of the CLT compartment during and after Test 1-2.

3.2.2 Compartment temperatures

Figure 48 shows temperatures in the compartment, measured using six thermocouple (TC) trees with thermocouples at 60 cm, 110 cm, 160 cm, 210 cm and 260 cm heights in Test 1-2. TC trees 2 and 3 were in the front section of the compartment (near the rough opening), TC trees 5 and 6 in the middle section (living area), and TC trees 1 and 4 in the rear section (dining and kitchen area).

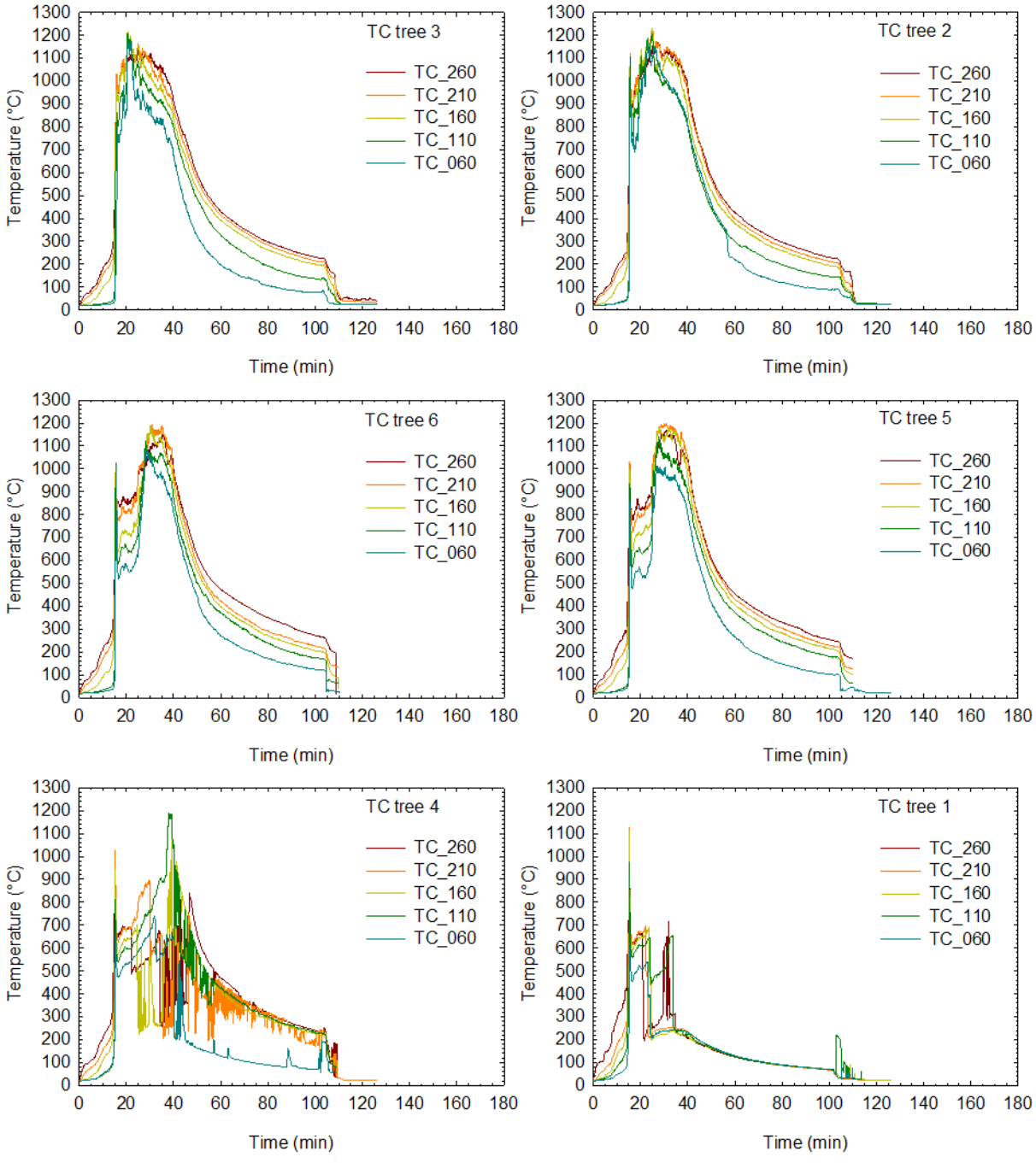

Figure 48. Temperatures in the compartment space during Test 1-2 (height in cm, test terminated at 104 min).

During the intense burning period (from flashover to decay, 15-40 min), the vertical temperature difference along each TC tree was relatively small, compared to the lateral temperature difference across the room at different TC trees. As time elapsed, the hottest area was moving from the front section of the room, to the middle section and then to the rear section of the compartment. The temperature reached 1200 °C, respectively, in the front, middle and rear sections at approximately 20 min, 30 min and 40 min. This hot area movement was similar in both Test 1-1 and Test 1-2.

The temperatures measured by TC trees 1 and 4 had sudden drops and oscillations at 21 min and thereafter (see Figure 48). There appeared to be a malfunction with some thermocouples on these two TC trees.

3.2.3 Heat release rate

Figure 49 shows the heat release rate during Test 1-2. The HRR was 12.4 MW at the initial peak right after the flashover and maintained above 7.5 MW until 37 min. As the fire decayed, the HRR reduced to 2 MW at 52 min and to 1 MW at 70 min. The test was terminated when HRR reduced to 0.43 MW at 104 min.

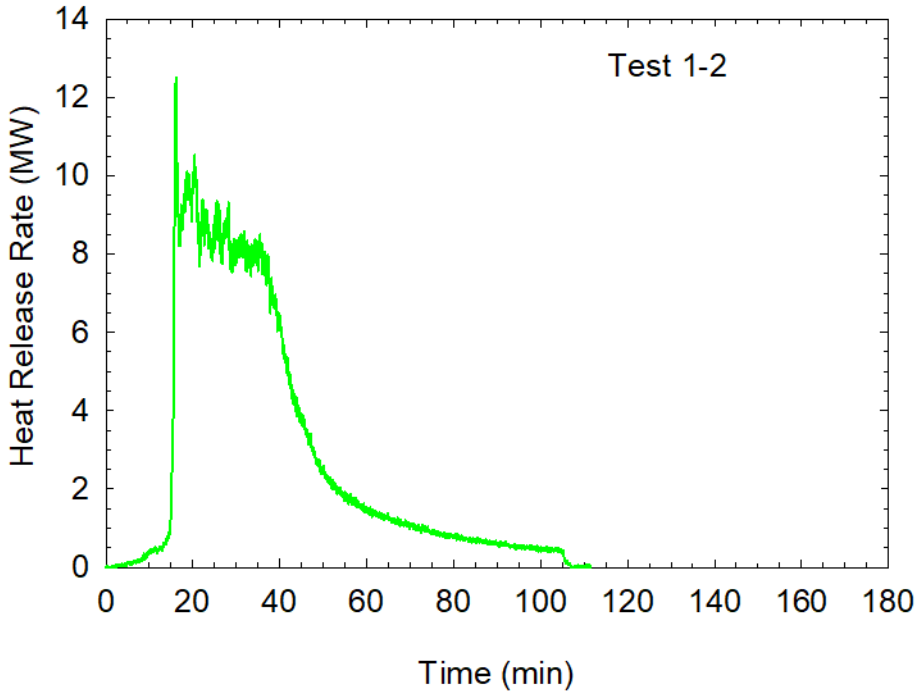

Figure 49. Heat release rate during Test 1-2 (test terminated at 104 min).

3.2.4 Heat flux inside and outside fire compartment

Various combinations of Gardon gauges, plate thermometers and differential flame thermometers provided measurements of heat flux at their co-located positions. Figure 50 shows heat fluxes measured at the twelve locations inside and outside the fire compartment during Test 1-2. The initial spike of each curve corresponded to the flashover. Table 5 provides the peak heat flux values at the fully developed fire stage after the flashover. The heat fluxes

ranged from 170 kW/m^2 to 275 kW/m^2 inside the compartment and from 22 kW/m^2 to 105 kW/m^2 outside the compartment during the fully developed fire stage, depending on the locations. The heat fluxes inside the compartment were comparable between Test 1-1 and Test 1-2. However, the heat fluxes outside the compartment were much higher in Test 1-2 than in Test 1-1. Comparisons of measurements made by different types of co-located heat flux gauges can be found in the appendices.

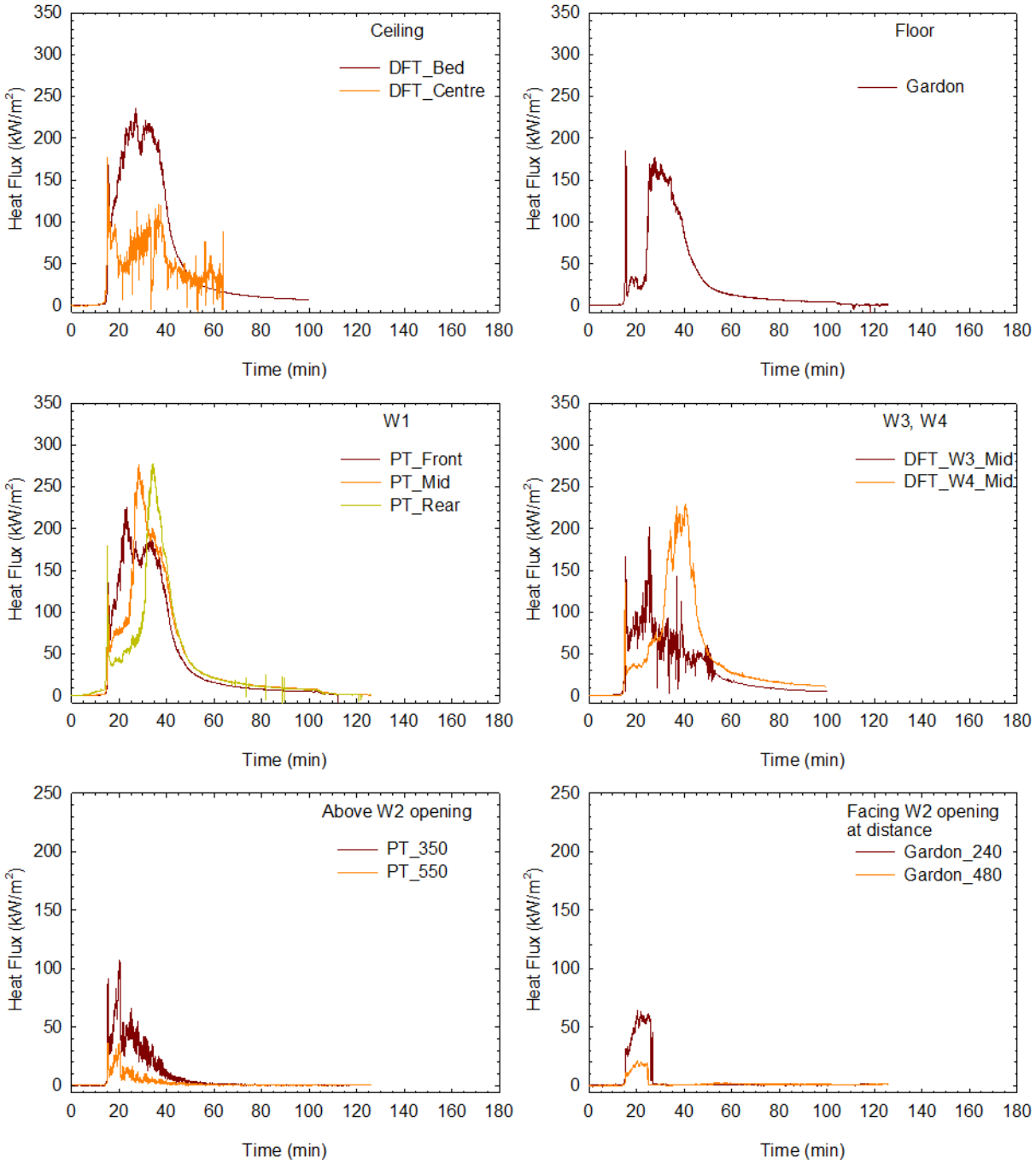

Figure 50. Heat fluxes inside and outside the compartment during Test 1-2 (test terminated at 104 min).

3.2.5 Temperatures at gypsum board interfaces and inside of CLT assemblies

The temperatures measured at the interfaces between the adjacent gypsum board layers, and between the CLT interior surface and the gypsum board base layer, as well as inside CLT panels at various depths are shown in Figure 51. The heat transfer through the gypsum board also followed the typical three-stage pattern as indicated by the temperature profiles at the interfaces: an initial temperature rise up to 100 °C, a period of gypsum calcinations at the constant temperature of 100 °C, then temperature increasing again after the calcination. As shown in Figure 47 (e) and (f), the base layer of gypsum board remained on the ceiling, and all two layers of gypsum board remained on the walls, to the end of the test.

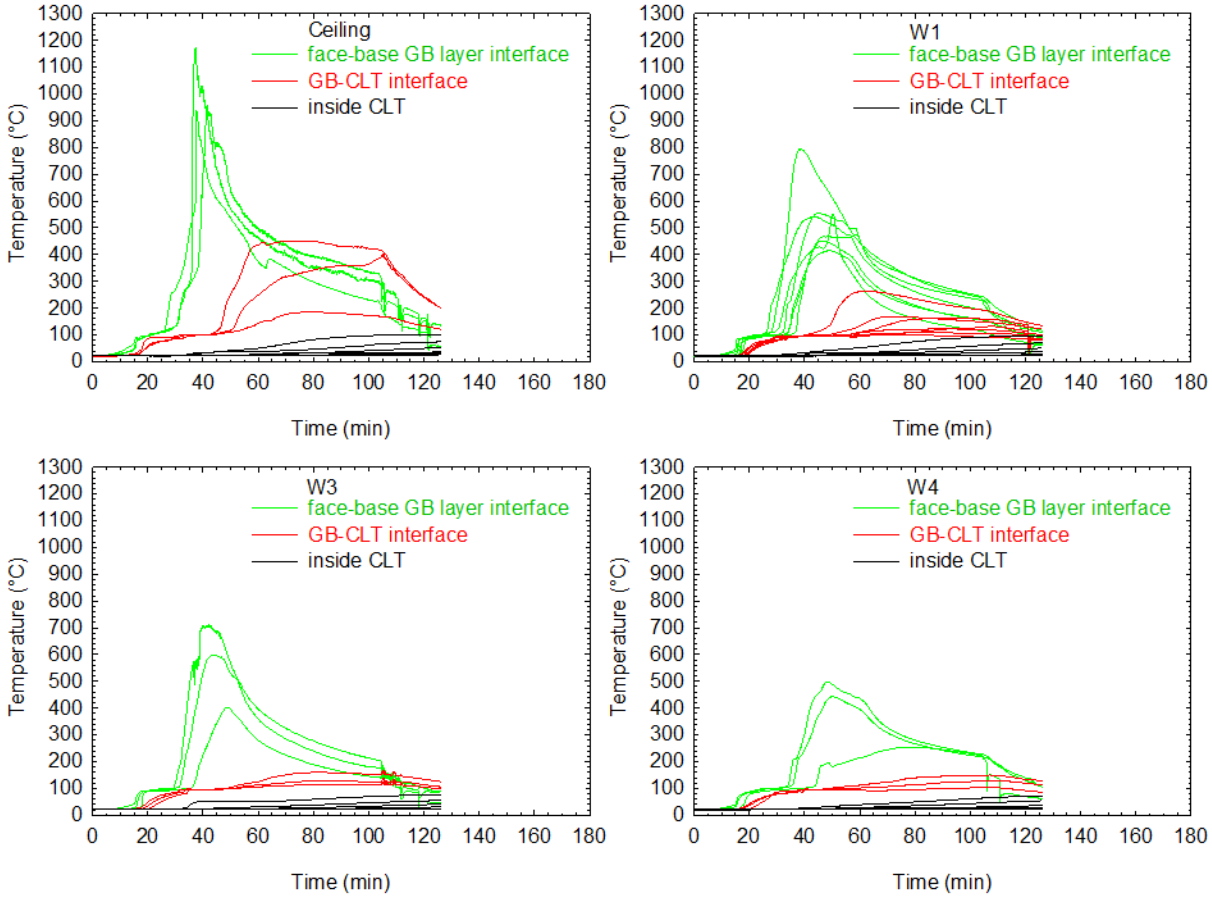

Figure 51. Temperatures in CLT and at gypsum board interfaces in Test 1-2 (test terminated at 104 min).

In the ceiling assembly, the temperatures at the interface between the face and base layers of gypsum board increased sharply at 36-40 min to the compartment temperatures, indicating the fall-off of the face layer gypsum board. The fall-off of the face layer gypsum board resulted in the base layer gypsum board being directly exposed to the fire, resulting in an increased rate of conductive heat transfer through the base layer to its interface with the CLT surface. The temperatures at the gypsum board base layer and CLT interface reached 300 °C at 53-67 min in the rear and middle sections of the ceiling assembly and increased to a peak temperature of 450 °C afterwards. This indicated that CLT ceiling panels started charring behind the base layer

gypsum board in the rear and middle sections of the ceiling assembly but had no flaming combustion at the CLT surface, which had negligible contribution to the compartment fire. The CLT interface temperatures in the front section of the ceiling were less than 185 °C (well below the wood charring temperature of 300 °C). The temperatures inside the CLT ceiling panels were quite low: below 100 °C at the 20 mm depth, below 32 °C at the 140 mm depth, and at the ambient temperature on the exterior surface.

In the wall assemblies, although the temperatures at the interface between the face and base layers of gypsum board increased significantly to 200-800 °C at different locations, the face layer gypsum board stayed intact until the end of the test. The maximum temperature measured at the CLT interface with gypsum board was 263 °C on wall W1 at the 1.8 m height; at other measurement locations, the CLT wall interface temperatures were 100-170 °C. The CLT wall panels were at the ambient temperature on the exterior surface.

3.2.6 Char depth of CLT panels and small CLT blocks

Figure 52 (a) and (b) show CLT compartment #2 after Test 1-2 with gypsum board removed. No char was developed on the CLT walls (except some smoke deposition). However, the CLT ceiling had surface char in the rear and middle sections, which were consistent with the CLT interface temperatures shown in Figure 51. The char depth ranged from 0 mm to 15 mm. The char pattern generally reflected the gypsum board joint layout. The char was more pronounced along the gypsum board joints and the CLT panel joints. However, there was deeper charring (approximately 50 mm) at two spots – the mid ceiling joint between panels 11_006 and 11_007 and the ceiling-wall corner joint – as shown in Figure 52 (c) and (d). Two layers of gypsum board were used for the CLT protection and one layer was lost in this test. Although the base layer gypsum board remained in place but the tape and joint compound were not applied on the base layer gypsum board joints, hot gases could get through these joints to reach the CLT joints which were also not sealed. This could be the reason for the deeper charring at the two spots. The exterior surface of the CLT compartment had no char except for some smoke deposition along the middle spline joint of the ceiling (no burn through). Had the panel joints been sealed, the char at these two spots could have been reduced.

(a) after cleanup and removal of gypsum board

(b) after cleanup and removal of gypsum board

(c)) joint of ceiling panels 11_006 and 11_007

(d) corner joint at ceiling and W1 and W4 walls

Figure 52. Photographs of CLT compartment #2 with localized charring after Test 1-2 after cleanup and removal of gypsum board.

Although there was some charring of the CLT ceiling panels, it did not contribute to the compartment fire as the fire conditions in the compartment were not affected. This test provides a baseline for quantifying CLT contribution to the compartment fire for a subsequent test with the larger ventilation opening.

Figure 53 shows the remaining thickness of the three small CLT blocks placed on the floor (only the top surface was exposed), each cut to half at the middle after Test 1-2. The char depth was 46 mm, 35 mm and 35 mm for the blocks placed at the front, middle and rear sections of the compartment, respectively.

(a) CLT block near a TC Tree

(b) front block near TC Tree 3 charred 46 mm

(c) middle block near TC Tree 6 charred 35 mm

(d) rear block near TC Tree 4 charred 35 mm

Figure 53. Char of small CLT blocks in Test 1-2 (cut to half to show remaining thickness).

3.2.7 Comparison of two baselines Test 1-1 and Test 1-2

While the differences in experimental variables between Test 1-1 and Test 1-2 included the number of gypsum board layers for protecting the fire compartment and the size of the ventilation opening as well as the test duration, the ventilation opening difference accounted for almost all of the differences in the fire development, energy release and compartment temperatures.

Figure 54 shows comparisons of the heat release rates and total heat releases (THR) during both tests. Test 1-2 with the larger ventilation opening had a higher heat release rate but earlier fire decay than Test 1-1. The two tests released virtually the same amount of total heat of 18 000 MJ, which is equivalent to the total energy of the movable fuel with 80% combustion efficiency. This indicates that the combustion of room contents was faster but the fully developed fire stage was shorter in Test 1-2 than in Test 1-1.

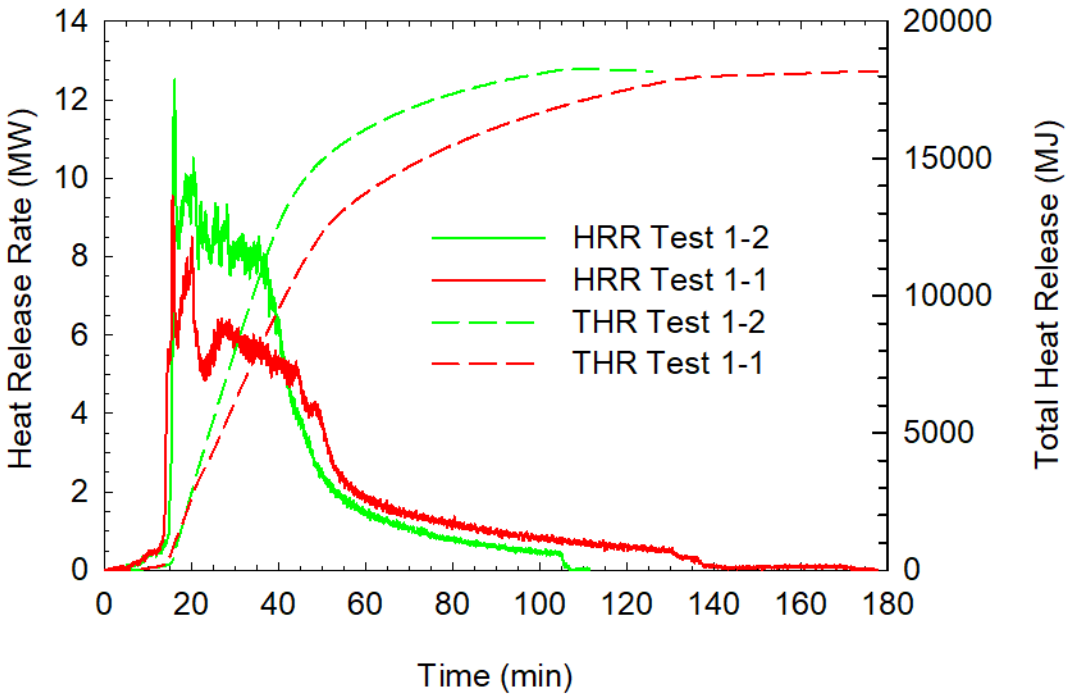

Figure 54. Heat release rates and total heat releases in Test 1-1 and Test 1-2.

The heat exposure conditions inside the fire compartment were more severe in Test 1-1 than in Test 1-2. Figure 55 shows hot layer temperatures in the fire compartments in both tests; the peak temperatures were similar in both test but the duration of the fully developed fire stage was longer in Test 1-1 than in Test 1-2. This was also demonstrated by the heat fluxes inside the fire compartments as shown in Figure 56. In addition, the char depths of the small CLT blocks placed on the floor were 7-10 mm more in Test 1-1 than in Test 1-2.

There was more intense burning outside the fire compartment in Test 1-2. Figure 57 and Figure 58 show comparisons of the temperatures and heat fluxes outside the fire compartments in both tests. The exterior heat fluxes and temperatures were higher in Test 1-2 than in Test 1-1.

All these show that the larger opening increased exterior fire challenges but reduced the fire challenges to the CLT compartment structure inside. This would have implications on exterior façade and adjacent buildings.

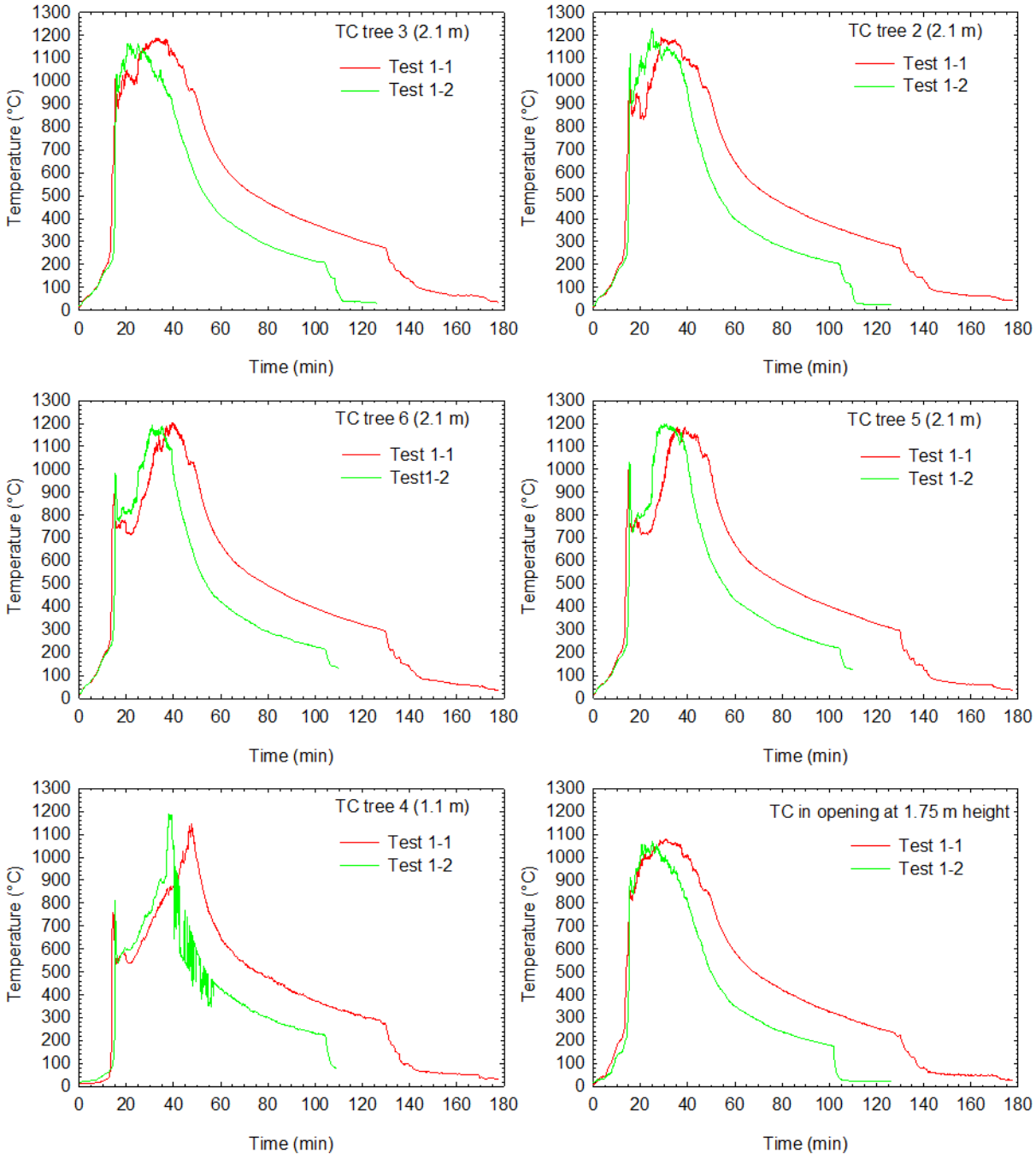

Figure 55. Hot layer temperatures in fire compartments in Test 1-1 and Test 1-2.

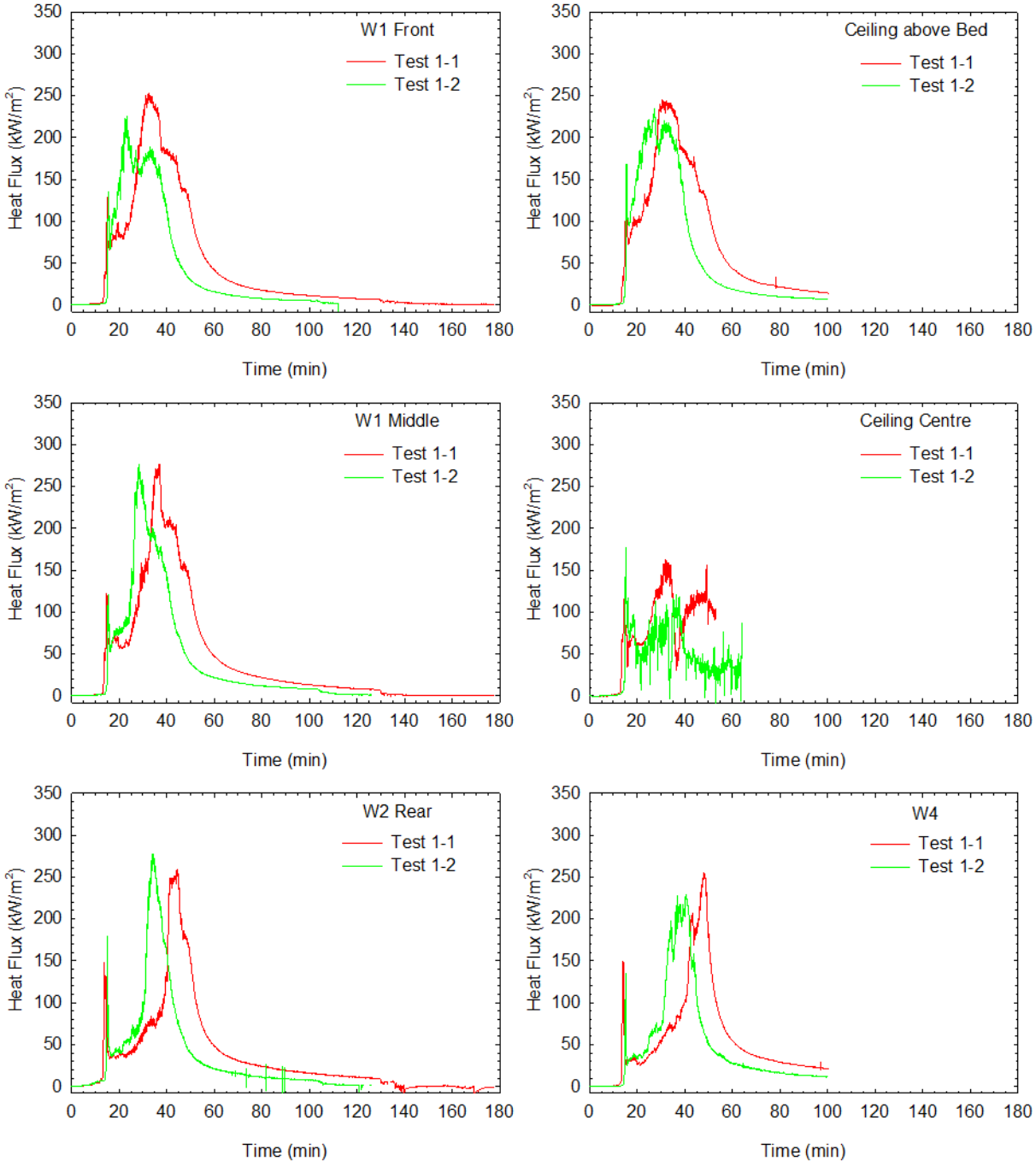

Figure 56. Heat fluxes inside fire compartments in Test 1-1 and Test 1-2.

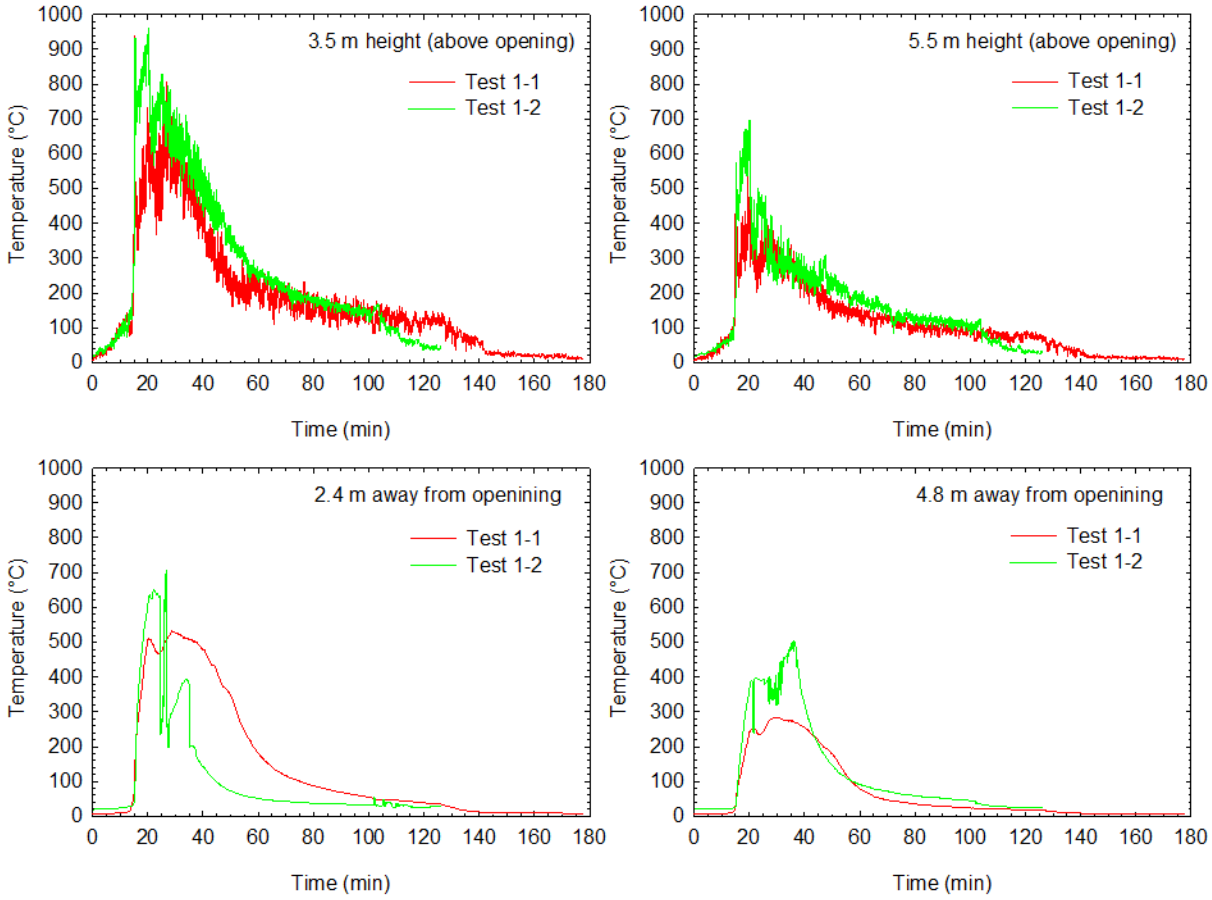

Figure 57. Temperatures outside fire compartments in Test 1-1 and Test 1-2.

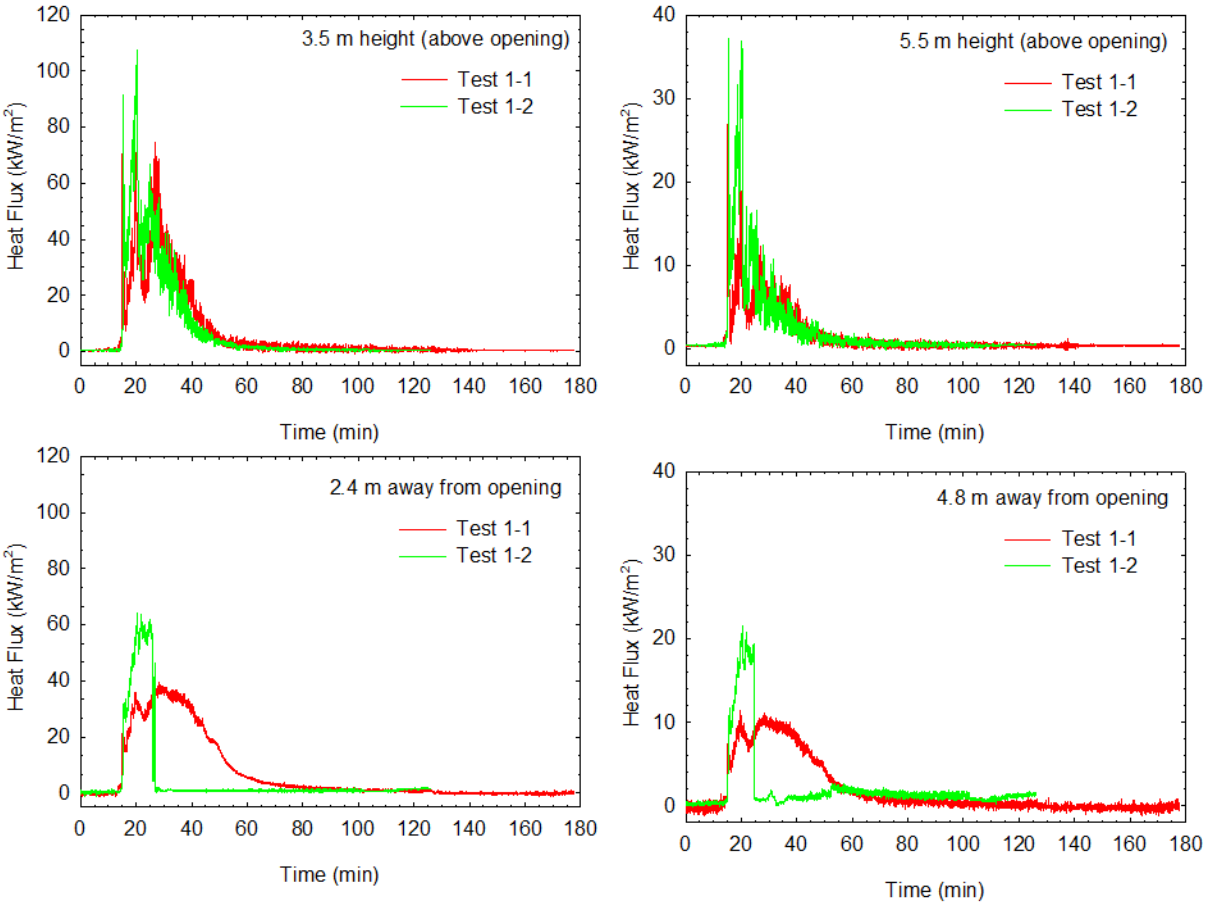

Figure 58. Heat fluxes outside fire compartments in Test 1-1 and Test 1-2.

3.3 Test 1-3

After Test 1-2, a cleanup operation was conducted in the CLT compartment #2 and all the remaining gypsum board was removed. The CLT compartment #2 was repaired, as shown in Figure 59. The deep charred spots between ceiling panels 11_006 and 11_007 and at the ceiling-W1-W4 corner joint were chiseled out. Plywood (0.3 m x 0.3 m) was screwed into the chiseled spot between panels 11_006 and 11_007. Fire caulking was used in repairing these two damaged spots. Ceramic fiber material was also filled into the ceiling-W1-W4 corner spot. Fire caulking was also used (only in this test) to seal limited CLT panel joints – between ceiling panels 11_006 and 11_007, between ceiling panels 11_007 and 11_008, and along the ceiling joint with the W1 wall.

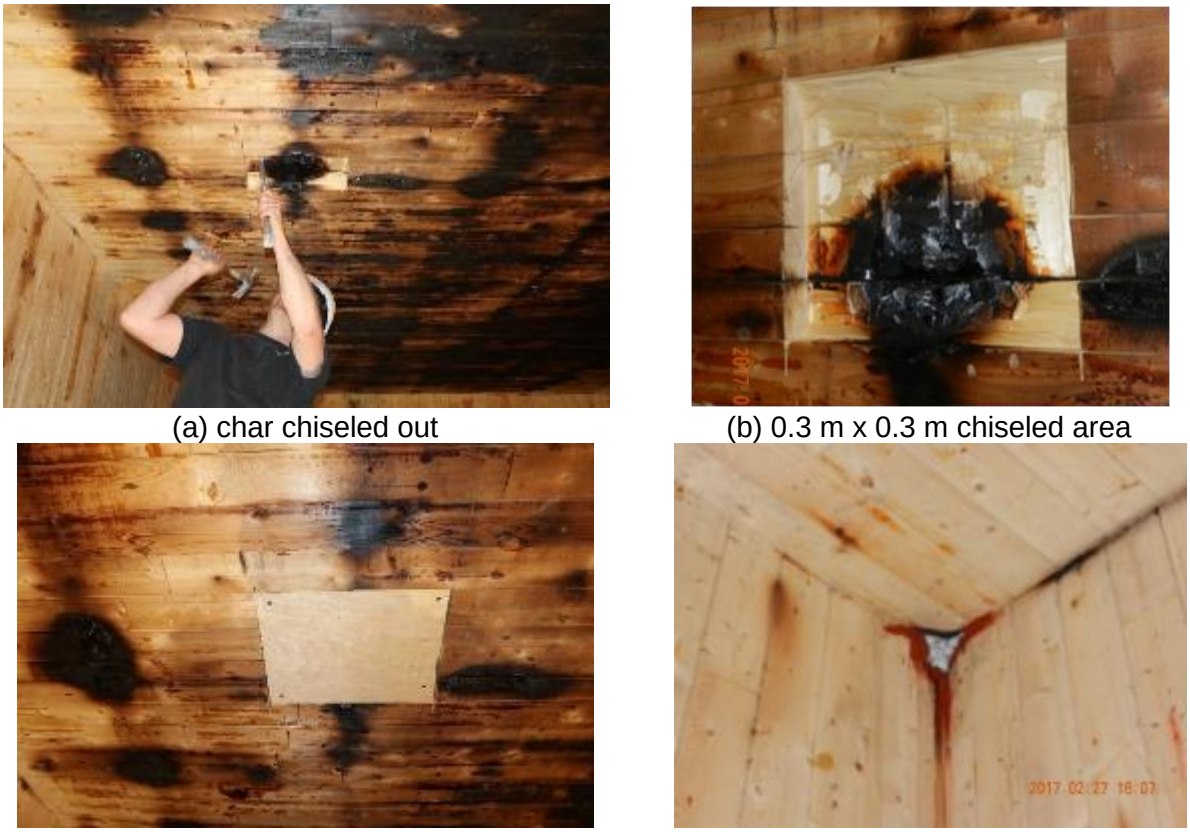

(a) char chiseled out

(b) 0.3 m x 0.3 m chiseled area

(c) plywood piece screwed in

(d) ceiling-W1-W4 corner spot filled

Figure 59. Repair of localized charring on ceiling after Test 1-2 before Test 1-3.

(a) CLT structure after repair

(b) CLT structure after repair

Figure 60. Photographs of CLT structure before Test 1-3.

Figure 60 shows photographs of the CLT structure after the repair. The repaired CLT compartment #2 was relined with new gypsum board and re-used in Test 1-3. Three layers of 15.9 mm (5/8 in.) thick Type X gypsum board were installed on the ceiling, two layers on the W2, W3 and W4 walls. The entire W1 wall was exposed – bare CLT surface on W1.

Because of some surface char on the ceiling, longer type S drywall screws were used to line the ceiling gypsum board. The gypsum board base layer was attached using 51 mm (2 in.) long screws, the middle layer 57 mm (2 ¼ in.) long screws, and the face layer 76 mm (3 in.) long screws to the ceiling. For the installation of the two-layer gypsum board on the walls, type S drywall screws were still 41 mm and 51 mm (1 5/8 and 2 in.) long.

Test 1-3 was conducted on March 16th, 2017 and designed to quantify the contribution of the exposed W1 wall to the compartment fire with Test 1-2 as the baseline with the 3.6 m x 2.0 m ventilation opening. Figure 61 shows the fully furnished CLT compartment before Test 1-3.

Figure 61. Photograph of CLT compartment with exposed W1 wall for Test 1-3.

3.3.1 Fire development

The test started with ignition of the console table in the dining area corner. The smoke alarm and heat alarm activated at 5.5 min and 2.9 min, respectively. Between 2.4 min and 5.8 min, all ten STEs reached 68 °C, which is a typical temperature rating for residential sprinklers. The console table was fully involved at 6 min and the smoke layer descended to the mid height in the compartment and stayed at this height until flashover. At 11.3 min, the fire from the console table ignited the upper portion of the W1 wall and the tall bookcase in the dining area. At 12 min, the dining table and chairs were fully involved in the fire. The smoke optical density measured at the 1.6 m height in the room centre reached 3.4 m^{-1} at 12.4 min. Flashover occurred at 12.5 min with dramatic changes of O_2, CO_2 and CO concentrations. Large fire plume issued from the opening. Figure 62 shows some photographs of the CLT compartment during Test 1-3.

After flashover, an intense burning of room contents, along with the exposed W1 wall, lasted for approximately 23 min. The gypsum board face layer was seen to start falling off the ceiling at 31 min. The fire started to decay at 35 min. Fire plume ceased to issue from the opening at 38 min and the compartment became visible inside. From 40 min to 80 min, the exposed W1 wall surface was noticeably charred but had little visible flame during this period as shown in Figure 62(c). O_2 was recovered to above 15% in the compartment. From 80 min to 100 min, flaming combustion re-occurred to the W1 wall (Figure 62(d)), starting at the joint between panels 10_018 and 10_019; then, the charred first ply stared to fall off and the flame diminished on the W1 wall. Fire decayed again in the subsequent 80 min (from 100 min to 180 min (Figure 62(e)). At 190 min, another flaming combustion occurred to the charred second ply of CLT panels on the W1 wall (Figure 62(f)), starting at the joint between panels 10_017 and 10_018. This flaming of the charred second ply lasted for 20 min and was less intense than the first re-occurrence. When the charred second ply started to fall off, the flame on the W1 wall diminished again from 205 min to the end of the test (Figure 62(g)). The test was terminated at 242 min (4 h after ignition). A fire hose was used to lightly spray water over the W1 wall and the debris on the floor to terminate the test. At the end of the test, two layers of gypsum board were still on the W3 and W4 walls and the ceiling (Figure 62(h)).

(a) just before flashover at 12 min

(b) flashover at 12.5 min

(c) exposed W1 at 48 min: charred, no visible flame

(d) exposed W1 at 85 min before 1st ply falling off

(e) exposed W1 at 120 min after 1st ply falling off

(f) exposed W1 at 190 min before 2nd ply falling off

(g) exposed W1 at 240 min after 2nd ply falling off

(h) two GB layers on ceiling and W3 and W4 at 240 min

Figure 62. Photographs of the CLT compartment during Test 1-3.

3.3.2 Compartment temperatures

Figure 63 shows temperatures in the compartment, measured using six thermocouple (TC) trees with thermocouples at 60 cm, 110 cm, 160 cm, 210 cm and 260 cm heights in Test 1-3. During the fully developed fire stage (12.5 min to 35 min), the hottest area was also moving from the front section of the room, to the middle section and then to the rear section of the compartment as time elapsed. The peak temperature reached 1200 °C.

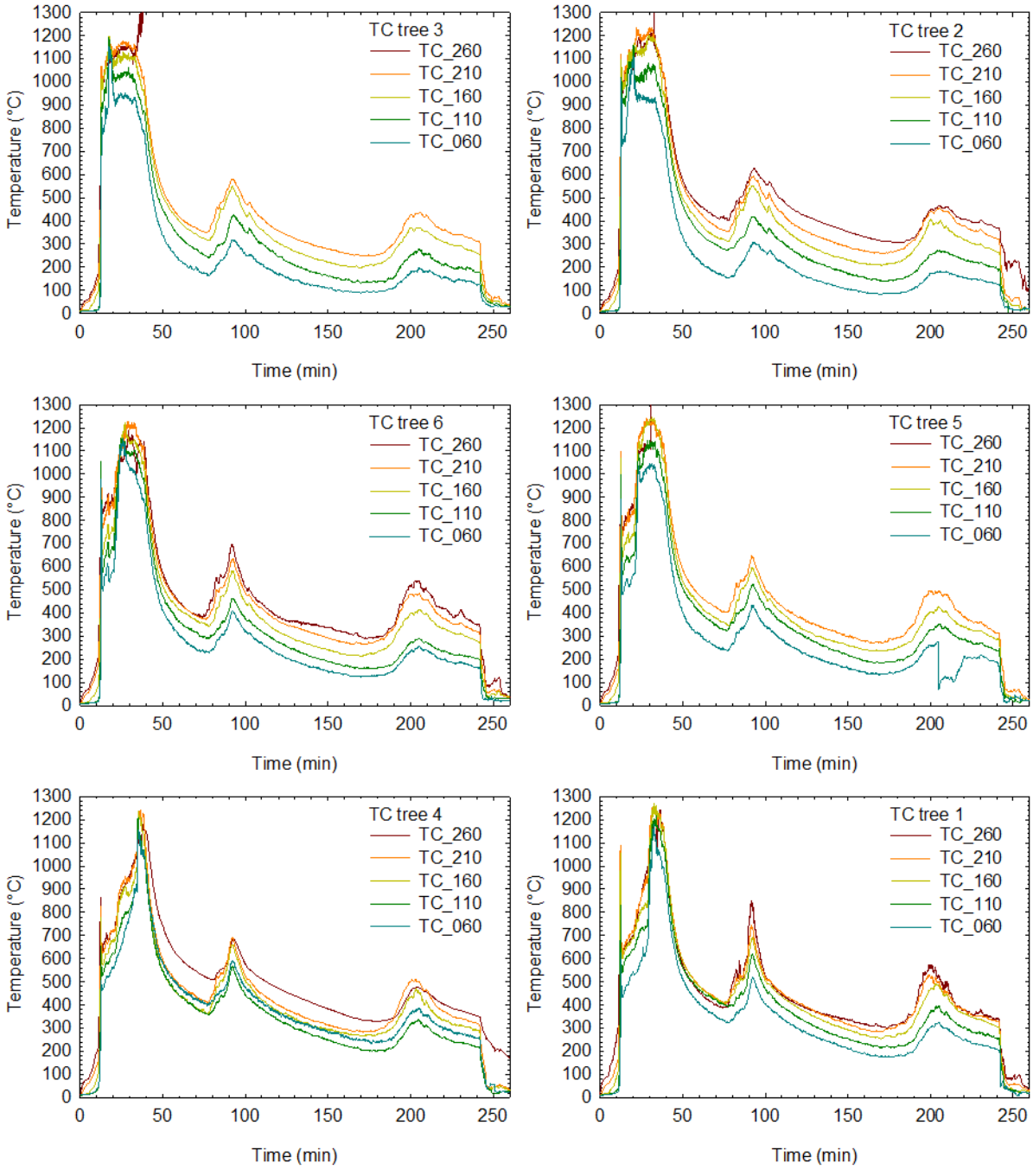

Figure 63. Temperatures in the compartment space during Test 1-3 (height in cm, test terminated at 242 min).

As the fire started to decay at 35 min, the compartment temperatures decreased to below 400 °C at 80 min with little visible flame on the W1 wall. The two subsequent peaks at 90 min and 200 min corresponded to the re-occurred burning and fall-off of the charred first and second ply of CLT on the W1 wall, respectively. Once the charred ply started to fall off, the flame on the W1 wall diminished and the room temperatures decreased again.

3.3.3 Heat release rate

Figure 64 shows the heat release rate during Test 1-3. The HRR was 14.2 MW at the initial peak right after the flashover and maintained above 9 MW until 35 min. As the fire decayed, the HRR reduced to 1.2 MW at 75 min. The two subsequent peaks of 3 MW at 92 min and 1.7 MW at 200 min corresponded to the charred first and second plies of CLT on W1 transitioned from smouldering to flaming before falling off, respectively. The HRR was reduced to 0.7 MW at the end of the test.

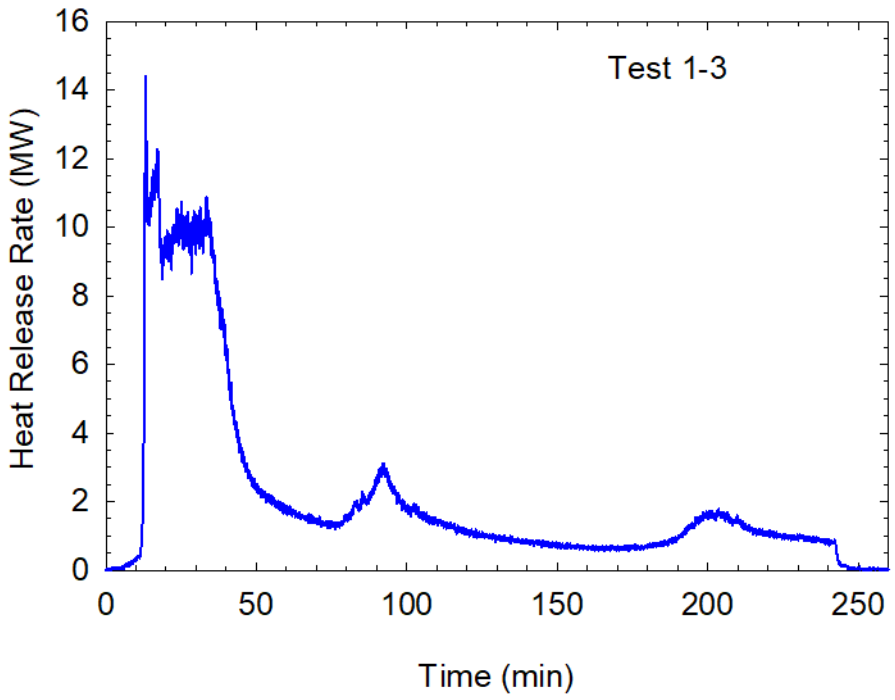

Figure 64. Heat release rate during Test 1-3 (test terminated at 242 min).

3.3.4 Heat flux inside and outside fire compartment

Figure 65 shows heat fluxes measured inside and outside the fire compartment during Test 1-3. The initial spike of each curve corresponded to the flashover. Table 5 provides the peak heat flux values at the fully developed fire stage after the flashover (note that the artificial initial spikes for the floor and the W4 wall are discounted as they were caused by a single data point). The heat fluxes ranged from 200 kW/m^2 to 320 kW/m^2 inside the compartment and from 25 kW/m^2 to 115 kW/m^2 outside the compartment during the fully developed fire stage, depending on the locations. Due to the exposed W1 wall, the heat fluxes to the W1 wall, the floor and the exterior façade were higher in Test 1-3 than in Test 1-2.

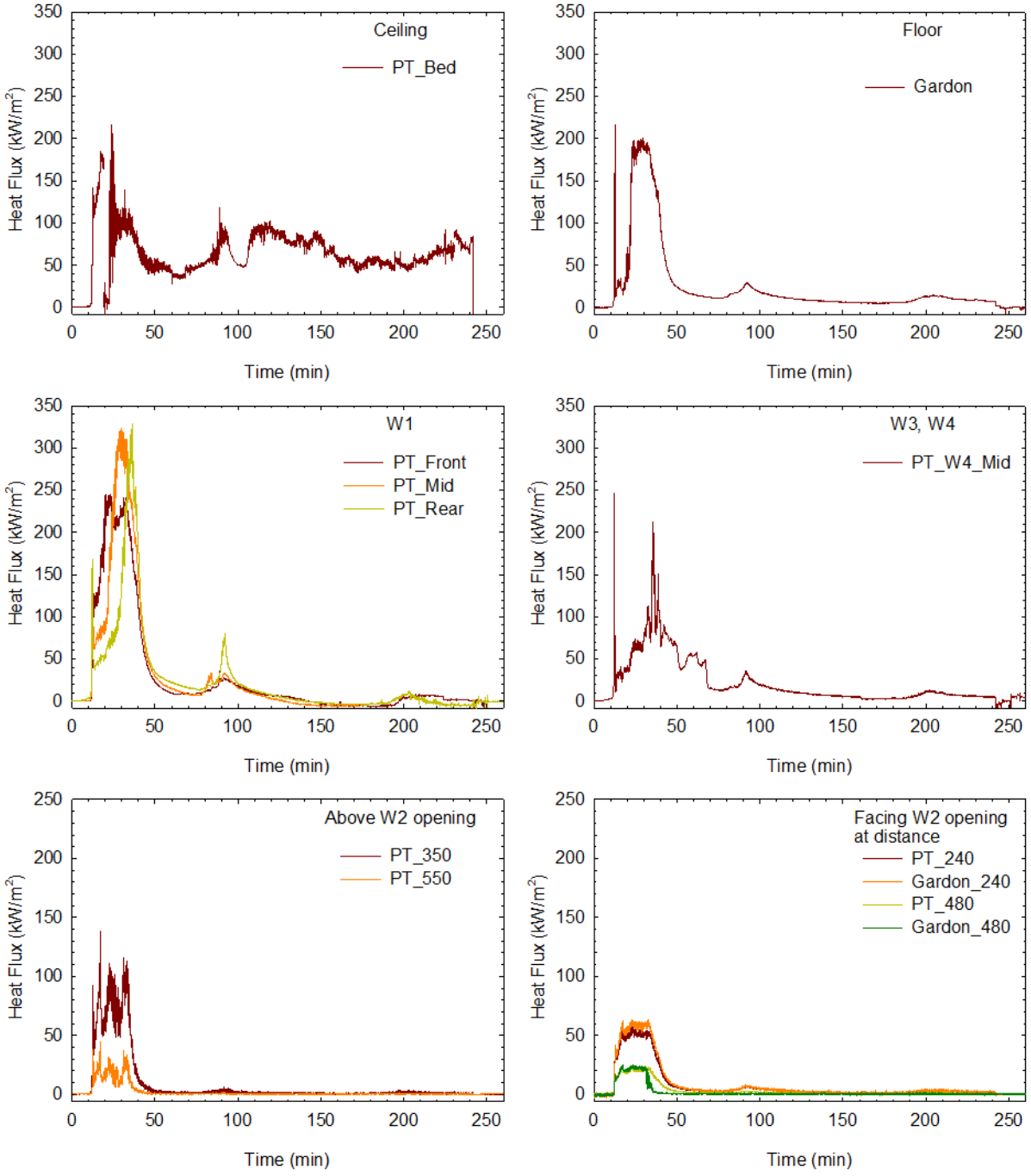

Figure 65. Heat fluxes inside and outside the compartment during Test 1-3 (test terminated at 242 min).

3.3.5 Temperatures at surface and in depth of CLT as well as gypsum board interfaces

Figure 66 shows the temperatures measured at the CLT surfaces, interfaces between gypsum board layers and inside CLT panels. The temperature profiles show that before the flashover the upper portion of the exposed W1 wall was already ignited.

Based on the timing when the embedded thermocouples in the W1 wall (mid-length at 1.8 m height) measured 300 °C, the char front reached 20 mm, 35 mm, 50 mm and 65 mm deep at 32 min, 83 min, 172 min and 213 min, respectively, in the CLT panel 10_018. The embedded thermocouple in 35 mm depth of the W1 wall shows a sharp temperature rise at around 80 min, from approximately 220 °C to 500 °C. The starting point of this temperature rise, 220 °C, is below the wood charring temperature. The end point of this temperature rise, 500 °C, is the prevailing compartment temperature. Given that 35 mm inside CLT corresponds with a glueline and that the char front should be at around 300 °C, this temperature rise indicates that the delamination of the first ply of the CLT occurred prior to the char front reaching the first glueline. The embedded thermocouple in 65 mm depth of the W1 wall shows a similar temperature rise at around 210 min, indicating the delamination of the second ply of the CLT prior to the char front reaching the second glueline. At the end of the test (242 min), the temperatures at the 90 mm, 115 mm and 140 mm depths in the CLT panel were 132 °C, 80 °C and 40 °C. This indicated that the char front would move into the third ply of the CLT panel at that location (65 mm < char depth <90 mm), which was confirmed in the post test observation.

In the ceiling assembly, the temperatures at the interface, between the face and middle layers of gypsum board, increased sharply to the compartment temperatures at 25-35 min, indicating the fall-off of the face layer gypsum board. The fall-off of the face layer gypsum board resulted in the middle layer gypsum board being directly exposed to the fire, resulting in an increased rate of conductive heat transfer through the middle layer to its interface with the gypsum board base layer. The temperatures at the gypsum board base layer and CLT interface reached 300 °C at 118-221 min in the rear section of the ceiling assembly and increased to 320-375 °C afterwards. This indicated that the CLT ceiling panels started charring behind the base layer gypsum board in the rear section of the ceiling assembly but the ceiling contribution to the compartment fire was not significant as no flaming combustion occurred at the CLT surface. The CLT interface temperatures in the front section of the ceiling were 200-260 °C (well below the wood charring temperature of 300 °C). The maximum temperatures inside the CLT ceiling panels were 115 °C at the 20 mm depth, 19 °C at the 140 mm depth, and the ambient temperature on the exterior surface.

In the W3 and W4 wall assemblies, although the temperatures at the interface between the face and base layers of gypsum board increased significantly at different locations, the two layers of gypsum board stayed on the walls until the end of the test. The temperatures at the gypsum board base layer and CLT interface reached 300 °C at 95 min in the upper portion of the W3 wall (in the middle length) and increased to 490 °C afterwards; this indicated that CLT panel 10_022 started charring behind the base layer gypsum board in the upper portion of the W3 wall but had no flaming combustion occurring at the CLT surface and the contribution to the compartment fire was not significant. In the upper portion of the W4 wall (1.8 m height), the maximum temperature at the CLT interface with gypsum board just reached 300 °C at 123 min for a short period (approximately 7 min). The CLT interface temperatures in the lower portion of the W3 and W4 walls were 182-238 °C (well below the wood charring temperature of 300 °C). The maximum temperatures inside the CLT panels were 185 °C at the 20 mm depth, 19 °C at the 140 mm depth, and the ambient temperature on the exterior surface of the W3 and W4 walls.

As shown in Figure 62(h), two layers of gypsum board remained on the ceiling and W3 and W4 walls until the end of the test. In general, the CLT panels in the ceiling, W2, W3 and W4 walls did not contribute to the growth of the compartment fire during the test. The exposed W1 wall was fully involved and contributed to the fire.

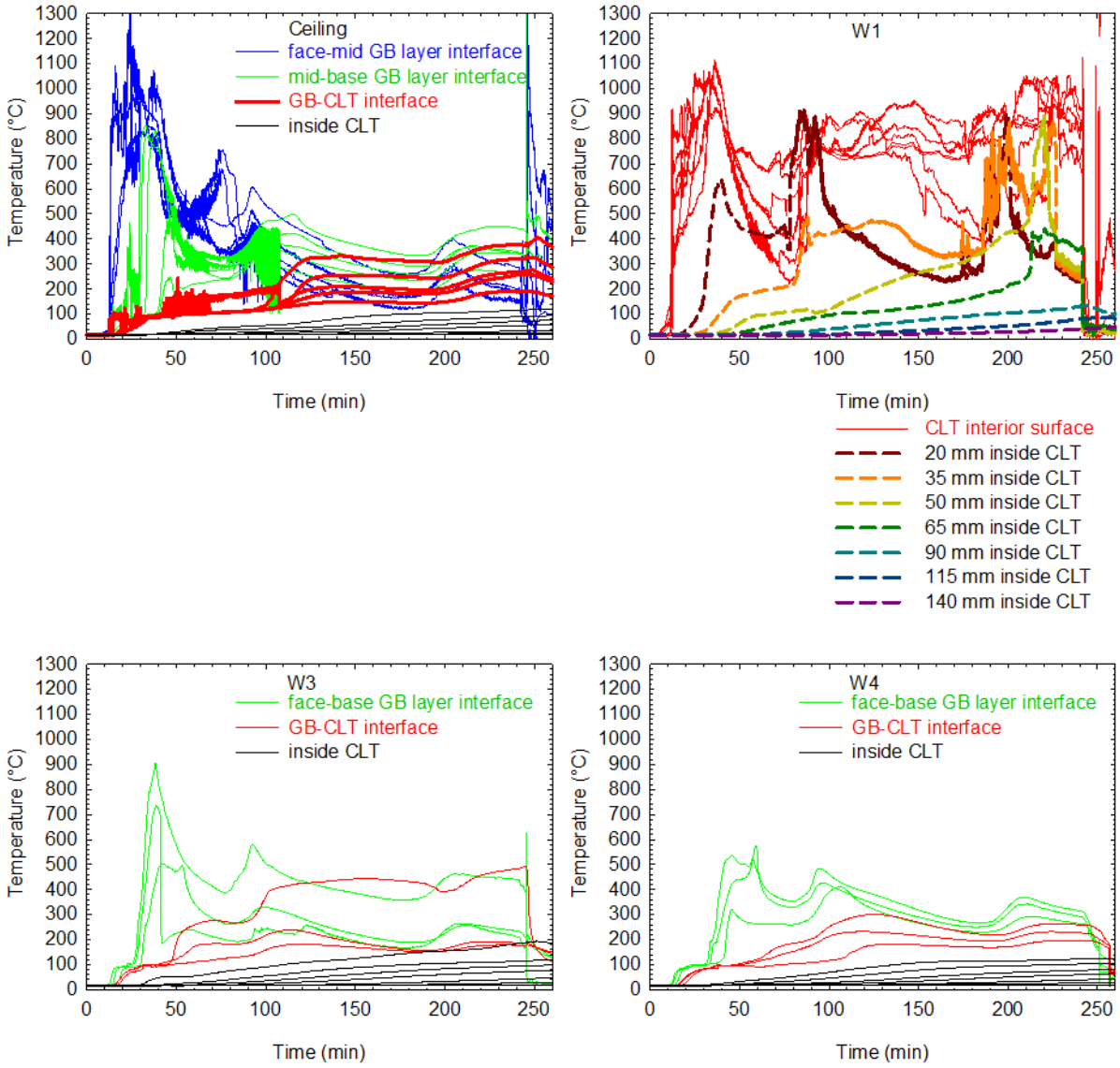

Figure 66. Temperatures in CLT and at gypsum board interfaces in Test 1-3 (test terminated at 242 min).

3.3.6 Char depth of CLT panels

After the fire test, the CLT compartment was examined for char. Figure 67 shows photographs of the CLT compartment interior surface before and after Test 1-3. On the exposed W1 wall, 85% of the CLT surface charred to the third ply of the CLT panels with a total char depth of approximately 80 mm; 15% of the surface close to the opening in the upper portion of the wall charred to the second ply with a total char depth of approximately 60 mm. On the W3 wall,

protected with two layers of gypsum board, only 35% of the CLT surface at the upper portion had char of 10 mm maximum; the remaining 65% had no char. On the W4 wall, 50% of the CLT surface developed char of up to 20 mm deep mainly in the section close to the W1 wall. For the ceiling, which was protected using three layer of the gypsum board, most of the CLT surface was unaffected by the fire; the char shown in the photo was mostly left from the previous Test 1-2. However, the ceiling surface adjacent to the W1 wall charred another 10 mm depth in Test 1-3. The char was measured more accurately at several selected positions and the results are shown in Table 6 and Table 7.

(a) W3, W4 W1 and ceiling CLT before Test 1-3.

(b) W3, W4 W1 and ceiling CLT after Test 1-3.

(c) W1 and ceiling after Test 1-3.

(d) W1, W2, W3 and ceiling CLT after Test 1-3.

Figure 67. Char in CLT compartment before and after Test 1-3.

Table 6. Char depth (mm) of CLT wall panels in Test 1-3.

Measurement locations	W3 Panel 10_022	W4 Panel 10_014	W4 Panel 10_015	W1 Panel 10_016	W1 Panel 10_018	W1 Panel 10_019
1.6 m height	10*	1*	18	80*	80*	60*
1.1 m height	0*	0*	15	80	78*	78
0.6 m height	0*	0*	20	83*	85*	80*

* TC nearby on wall

Table 7. Accumulated char depth (mm) of CLT ceiling panels in Test 1-2 and Test 1-3.

Measurement locations	7/8 span (close to W3)	5/8 span	3/8 span	1/8 span (close to W1)
Ceiling Panel 11_008	0	0	0	0
	0	0	0	1
Ceiling Panel 11_007	0	0*	1*	1
	0	1	1*	2
Ceiling Panel 11_006	0	3	10	17
	0	1*	3*	6
Ceiling Panel 11_005	0	1	5	7
	1	0	5	6

* TC nearby on ceiling

Table 8. Char depth (mm) of cut CLT samples in Test 1-3.

CLT cut sample	Remaining thickness (mm)	Char depth (mm)	Image
Test 1-3 W1 – mid length 1.8 m high Panel 10_018 (TC 49, 8-14)	89	86	

The photo in Table 8 shows the CLT sample that was cut from the W1 panel 10_018 where the embedded thermocouples were installed. The thickness of the char was 86 mm (remaining CLT thickness was 89 mm). This confirms the measurement of the char depth by the embedded thermocouples (65 mm < char depth < 90 mm).

As the test lasted for 4 h, there were deeper chars involving the W1 wall at some panel-to-panel joints, including some spots where the W1 and ceiling panels met as well as wall-ceiling corner joints. At 150 min, a small hole was burnt through the ceiling spline joint between panels 11_006 and 11_007 near the exposed W1 wall. At the end of the test, the size of this hole became 125 mm x 200 mm (5 in. x 8 in.). Figure 68 shows the exterior of the W1 wall with flame through wall-ceiling panel joints after 3 h into the test. However, there was no burn through at the repaired corner (only smoke was leaked from there). Although fire caulking was used to seal limited CLT panel joints before the test, no adhesive was applied to the panel joints during construction. Had the panel joints been well sealed, the char could have been reduced at the joints and the flame through could have been delayed. Nevertheless, this had limited impact on the CLT contribution to the compartment fire in Test 1-3.

Figure 68. Exterior of the W1 wall at 198 min in Test 1-3.

3.3.7 Contribution of the CLT structure to compartment fire

Based on the volume (depth x area) of the CLT charred, which was measured after the test, the CLT panels were estimated to contribute approximately 1100 kg of timber to the fire (mainly by the W1 wall panels), which translated to 540 MJ/m^2 fuel load density to the floor area in addition to the movable fuel load. This brought the effective fuel load density to 1090 MJ/m^2 in Test 1-3.

With the exposed W1 wall in Test 1-3, flashover occurred 3 min earlier and the heat release rate was approximately 2 MW higher than the baseline (Test 1-2) in the growth and fully developed fire stages, as shown in Figure 69. However, the compartment temperatures and heat fluxes (to

W3, W4 and ceiling) in the growth, developed and initial decay stages were similar to the baseline. The heat fluxes to the exterior façade were higher in Test 1-3 than the baseline.

Figure 70 shows the CLT contribution to the heat release rate during Test 1-3, by subtracting the baseline. A time shift was made to the baseline in order to line up the flashover time with Test 1-3 for proper subtraction. The CLT structure contributed a maximum of 2.5 MW to the heat release rate (mainly due to the exposed W1 wall), which is 18% of the peak heat release rate and does not appear to be a significant contribution. The contribution occurred at three occasions: (1) during the growth and fully developed stages, (2) during the reoccurred flaming of the charred first ply of the CLT panels in the W1 wall, and (3) during the reoccurred flaming of the charred second ply of the CLT panels in the W1 wall.

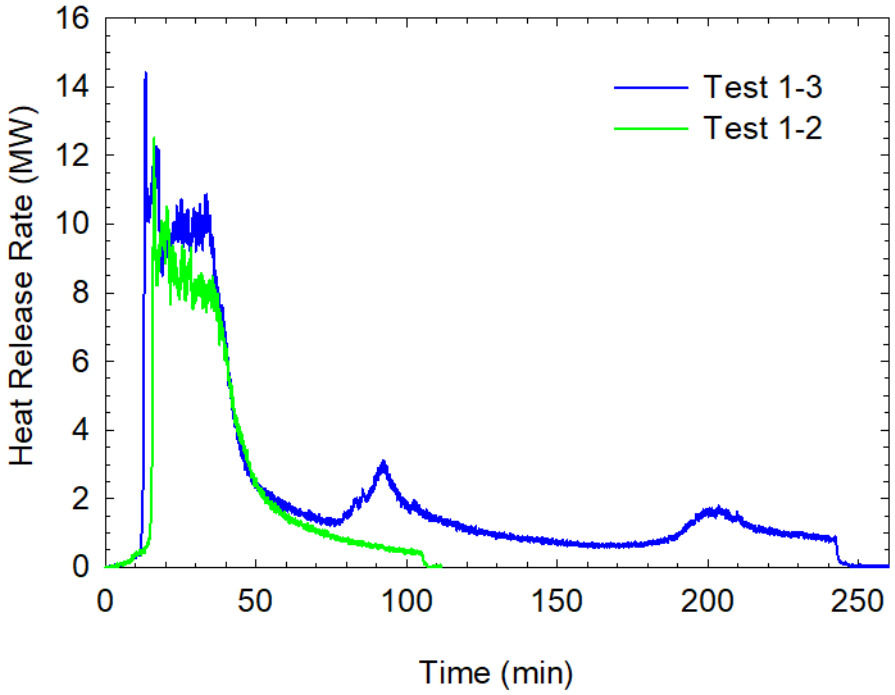

Figure 69. Heat release rate of Test 1-3 superimposed over baseline (Test 1-2).

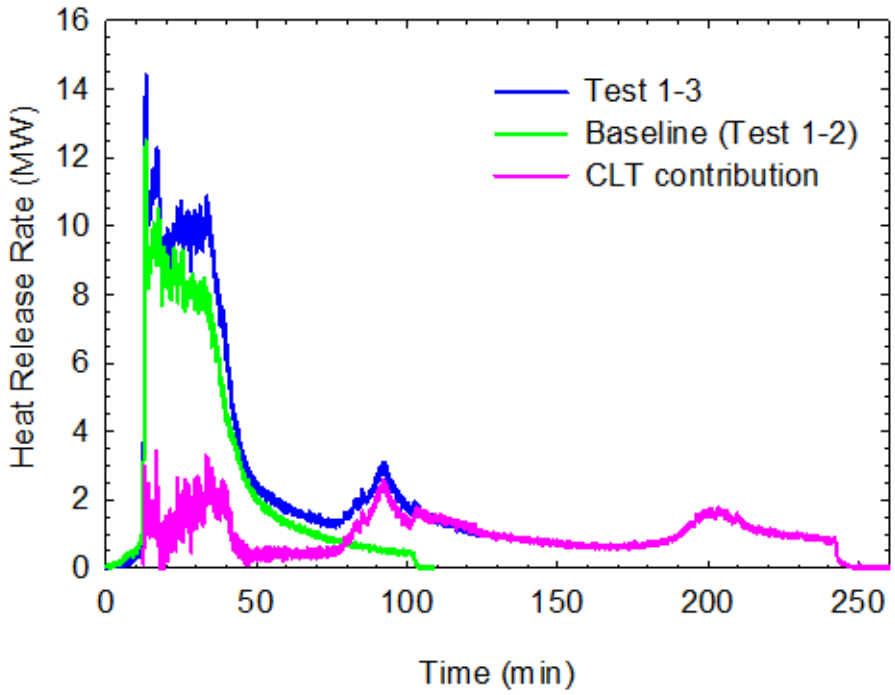

Figure 70. CLT contribution to heat release rate in Test 1-3 (baseline time shifted).

3.4 Test 1-4

After the previous Test 1-1, a cleanup operation was conducted in the CLT compartment #1 and all the remaining gypsum board was removed, as shown in Figure 41 (g) and (h). The compartment was relined with new gypsum board. Three layers of 15.9 mm (5/8 in.) thick Type X gypsum board were installed on all walls. The entire ceiling was exposed – bare CLT surface on the ceiling. Gypsum concrete (38 mm thick x 305 mm wide or 1-1/2 in. thick x 12 in. wide) was poured on the top of each spline joint of the ceiling panels on the outside,

In a recent standard fire test conducted in accordance with ASTM E119-15 and CAN/ULC-S101-14 [25, 26], a bare 175-mm thick 5-ply CLT floor assembly provided a fire resistance time of 128 min under a superimposed load of 4.40 kN/m^2 (91.8 psf) [27]. This superimposed load combined with the dead load (the self-weight of the CLT assembly) corresponded to approximately 30% of the bending moment capacity. Note that the full load capacity of the bare 175-mm thick 5-ply CLT floor/ceiling was 16.0 kN/m^2 (333 psf) for the tested span of 4.8 m (16 ft).

Test 1-4 was conducted on March 21st, 2017 for quantifying the contribution of the exposed CLT ceiling to the compartment fire with Test 1-1 as the baseline using the 1.8 m x 2.0 m ventilation opening. Figure 71 shows the fully furnished CLT compartment before Test 1-4.

Figure 71. Photograph of CLT compartment with exposed ceiling for Test 1-4.

3.4.1 Fire development

Test 1-4 started with ignition of the console table in the corner. The smoke alarm and heat alarm activated at 2.5 min and 1.5 min, respectively. Between 1.3 min and 3.5 min, all ten STEs reached 68 °C, which is a typical temperature rating for residential sprinklers. The fire ignited the ceiling above the dining area at 10.1 min, the dining table at 10.4 min, dining chairs at 10.7 min, and the tall bookcase near the dining area at 11.1 min. The exposed ceiling was fully involved. The smoke optical density measured at the 1.6 m height in the room centre reached 3.4 m^{-1} at 11.6 min. Figure 72 shows some photographs of the CLT compartment during Test 1-4.

Flashover occurred at 11.5 min with the exposed ceiling fully involved. Large fire plume issued from the opening (Figure 72(b)). The concentrations of O_2, CO_2 and CO concentrations changed dramatically. At 50 min, pieces of the charred first ply of the ceiling CLT panels started to gradually fall off. By 55 min, the flame issued from the opening was solely due to the burning of the ceiling (Figure 72(c)). The fire started to decay at 75 min after the charred first ply of the CLT panels fell off the ceiling (Figure 72(d)(e)). At 85 min, the fire plume ceased to issue from the opening and O_2 was recovered to above 15% in the compartment.

From 90 to 140 min, the exposed second ply of the CLT ceiling continued to char with intermittent localized burning, as shown in Figure 72(f)(g). At 150 min, flaming combustion reoccurred on the CLT ceiling (Figure (h)), causing the second flashover with a large fire plume issuing from the opening again. The test was terminated by manual fire suppression at 159 min after the second ply of the CLT panels fell off the ceiling and the third ply became involved. Two fire hoses were used to spray water to the compartment to terminate the test. (The laboratory safety criterion was to terminate the test when more than two plies of CLT ceiling were charred or lost.) At the end of the test, two layers of gypsum board were still on all the walls. After the test, there was a 46-mm (1 7/8”) deflection occurred and two and half plies of CLT were lost at the centre of the ceiling.

3.4.2 Compartment temperatures

Figure 73 shows temperatures in the compartment during Test 1-4, measured using six thermocouple (TC) trees with thermocouples at 60 cm, 110 cm, 160 cm, 210 cm and 260 cm heights. During the fully developed fire stage (11.5 min to 75 min), the hottest area was also moving from the front section of the room, to the middle section and then to the rear section of the compartment as time elapsed. The peak temperature reached 1200 °C in the front, middle and rear section, respectively, at 30 min, 40 min and 50 min.

Once the fire started to decay at 75 min, the compartment temperatures decreased continuously until 140 min. After the second ply of the CLT panels fell off the ceiling and the third ply started flaming combustion, the compartment temperatures increased again rapidly to over 900 °C after 150 min. The test was terminated at 159 min.

(a) ceiling ignited in corner

(b) just before flashover

(c) at 11.8 min; just after flashover

(d) at 60 min

(e) at 85 min

(f) at 90 min

(g) at 122 min

(h) at 151 min, second flashover

Figure 72. Photographs of the CLT compartment during Test 1-4.

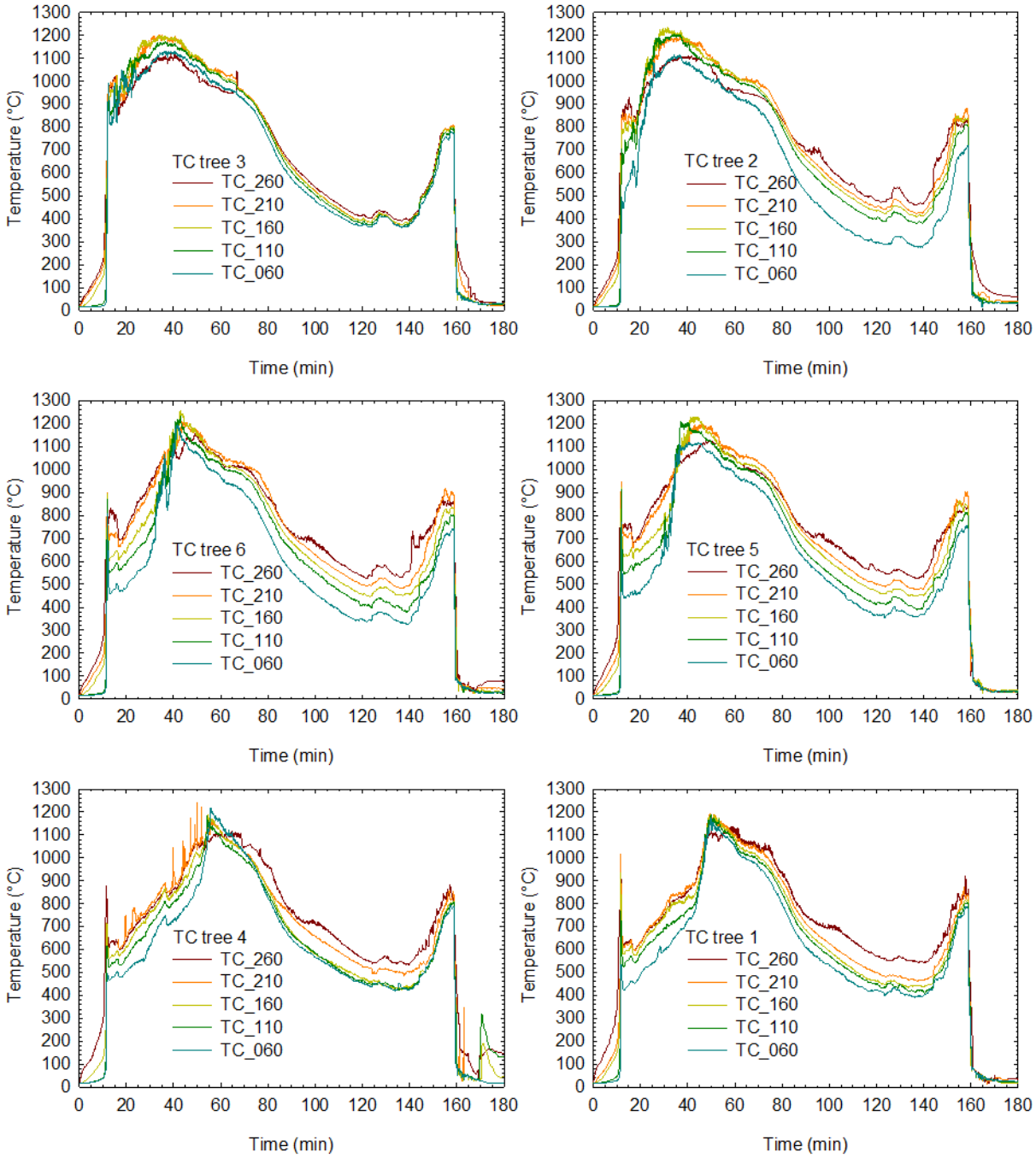

Figure 73. Temperatures in the compartment space during Test 1-4 (height in cm, test terminated at 159 min).

3.4.3 Heat release rate

Figure 74 shows the heat release rate during Test 1-4. The HRR was 13.1 MW at the initial peak right after the flashover and maintained above 6 MW until 70 min. As the fire decayed, the HRR reduced to 1 MW at 140 min. The subsequent peak corresponded to the second flashover due to the flaming and fall-off of the charred second ply and involvement of the third ply of the ceiling in the fire, which led to the second flashover. The test was terminated at 159 min by suppressing the fire, which grew to 6 MW before the suppression.

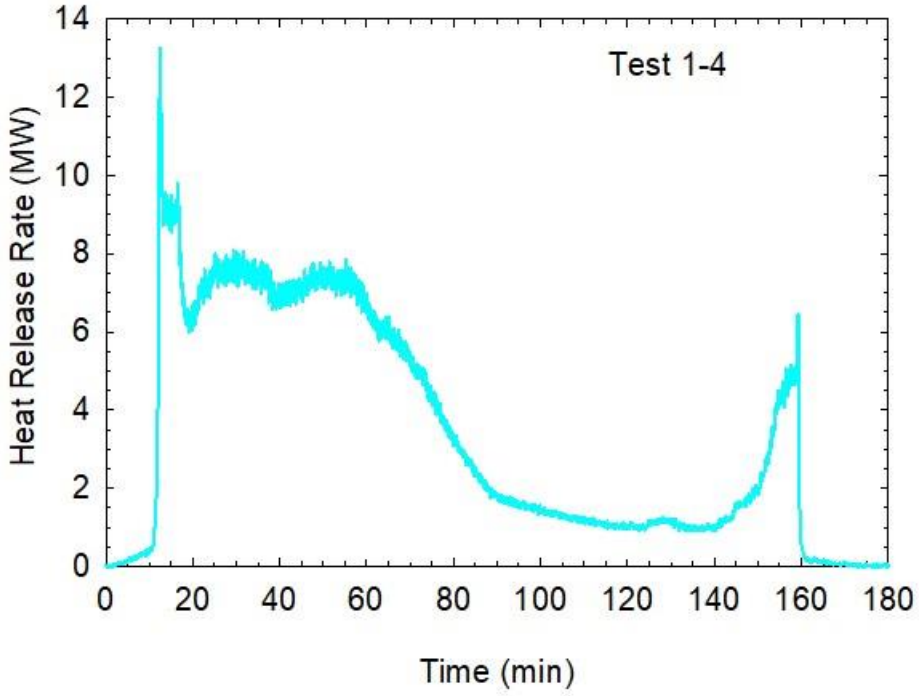

Figure 74. Heat release rate during Test 1-4 (test terminated at 159 min).

3.4.4 Heat flux inside and outside fire compartment

Figure 75 shows heat fluxes measured inside and outside the fire compartment during Test 1-4. The initial spike of each curve corresponded to the flashover. Table 5 provides the peak heat flux values at the fully developed fire stage after the flashover (note that the spikes for the ceiling and the W4 wall are discounted as they were caused by a single odd data point). The heat fluxes ranged from 150 kW/m^2 to 320 kW/m^2 inside the compartment and from 17 kW/m^2 to 120 kW/m^2 outside the compartment during the fully developed fire stage, depending on the locations. Due to the exposed ceiling, the heat fluxes to the exterior façade were higher in Test 1-4 than in Test 1-1.

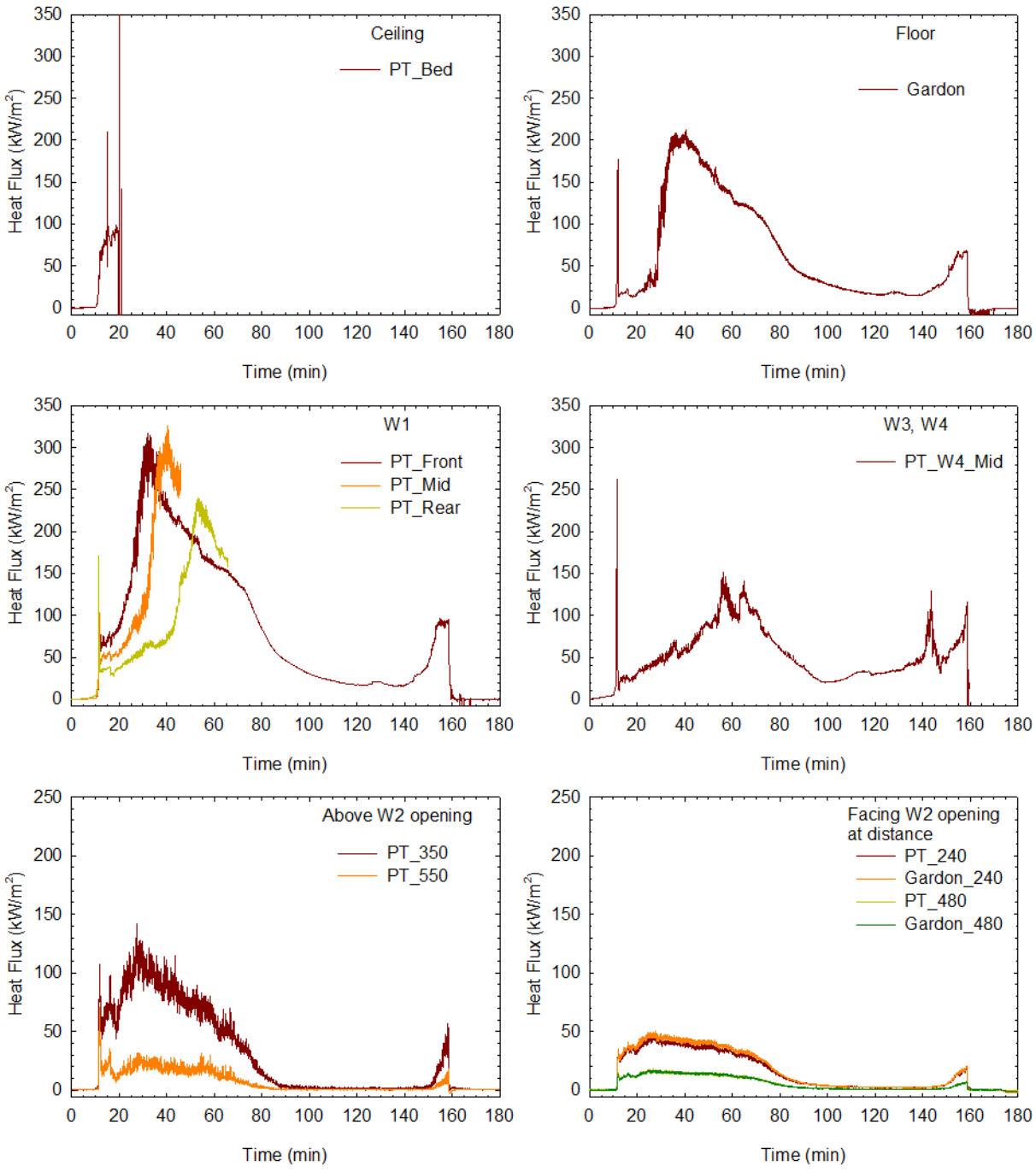

Figure 75. Heat fluxes inside and outside the compartment during Test 1-4 (test terminated at 159 min).

3.4.5 Temperatures at surface and in depth of CLT as well as gypsum board interfaces

Figure 76 shows the temperatures measured at the CLT surfaces, interfaces between gypsum board layers and inside CLT panels. The temperature profiles show that, before the flashover, the exposed ceiling was already ignited.

Based on the timing when the embedded thermocouples in the ceiling measured 300 °C, the char front reached 20 mm, 35 mm, 50 mm and 65 mm deep at 37 min, 58 min, 116 min and 153 min, respectively, in the CLT ceiling panel 11_003. The embedded thermocouple in 35 mm depth of the ceiling shows a relatively gradual increase of the temperature at the first glueline in the CLT from 100°C to 600 °C while the prevailing compartment temperature stayed at above 1000 °C. The delamination of the first ply of the CLT might have occurred after the char front passing the first glueline at that location. However, the embedded thermocouple in 65 mm depth of the ceiling does show a sharp temperature rise at around 150 min, from approximately 240 °C to 500 °C. This indicates that the delamination of the second ply of the CLT occurred prior to the char front reaching the second glueline. At the end of the test (159 min), the temperatures at the 90 mm, 115 mm and 140 mm depths in the CLT ceiling panel were 113 °C, 76 °C and 49 °C. This indicated that the char front would move into a depth in-between 65 mm and 90 mm at that location (65 mm < char depth <90 mm), which was confirmed in the post test observation.

In the wall assemblies, the heat transfer through the gypsum board also followed the typical three-stage pattern as indicated by the temperature profiles at the interfaces: an initial temperature rise to 100 °C, a period of gypsum calcinations at the constant temperature of 100 °C, then temperature increasing again after the calcination. The temperatures at the interface between the face and mid layers of gypsum board, increased sharply to the compartment temperatures at 46-60 min in the W1 wall and 73 min in the W4 wall, indicating the fall-off of the face layer gypsum board from the W1 and W4 walls. The fall-off time of the face layer gypsum board from the W3 wall was not obvious based on the interface temperature but should be 70-80 min as the interface temperatures reached the compartment temperatures at this time. At the end of the test, two layers of gypsum board remained on the W1, W2, W3 and W4 walls.

In the W1 and W3 walls, the temperatures at the gypsum board base layer and CLT interface reached 300 °C at 77-141 min in the middle and rear sections of the W1 and W3 walls and increased to 400-530 °C afterwards. This indicated that the W1 and W3 wall panels started charring on the surface behind the base layer gypsum board in the middle and rear sections of the walls. Inside the W1 and W3 panels, the maximum temperatures were 143 °C at the 20 mm depth, 20 °C at the 140 mm depth, and the ambient temperature on the exterior surface (well below the wood charring temperature of 300 °C). This indicated that the char in the W1 and W3 walls was less than 20 mm deep and should have negligible contribution to the compartment fire since there were still two layers of gypsum board covering the CLT surface (no flaming combustion occurred at the CLT wall surface). In the W4 wall, the temperatures at the gypsum board base layer and CLT interface were less than 240 °C and should have no contribution to the compartment fire.

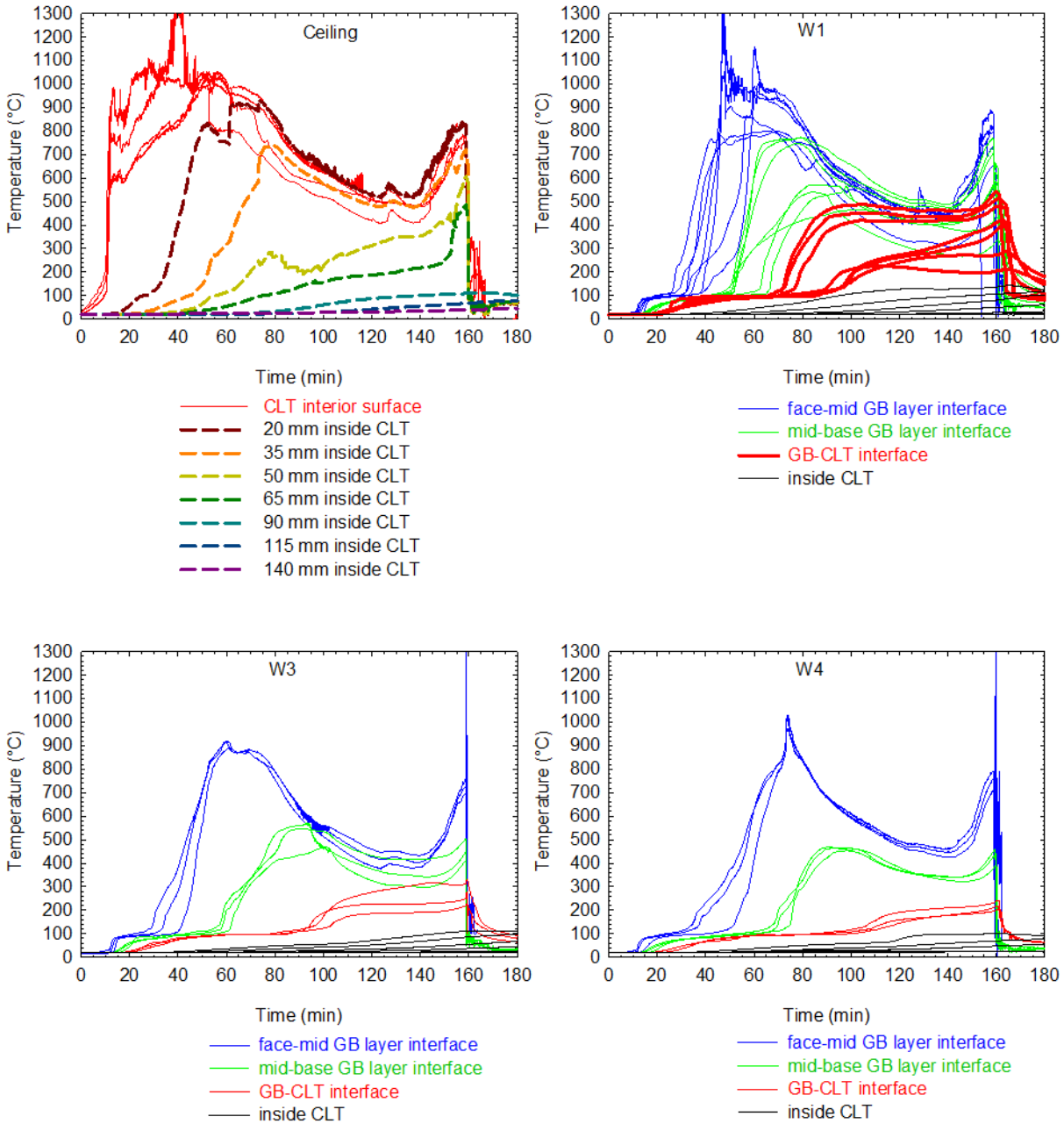

Figure 76. Temperatures in CLT and at gypsum board interfaces in Test 1-4 (test terminated at 159 min).

3.4.6 Char depth of CLT panels

After the fire test, the CLT compartment was examined for char. Figure 77 shows photographs of the CLT compartment after Test 1-4. Table 9 and Table 10 list the char depths measured at several selected positions. Most areas of the ceiling lost more than two plies (70 mm) of CLT and 55% of the area charred to the third ply with a total char depth of up to 90 mm. On the W1 wall, 40% of the surface had char of 4 mm to 14 mm depth; 60% of the surface had no char. On

the W3 wall, 25% of the CLT surface had char of 2 mm to 10 mm; the rest of 75% had no char. On the W4 wall, 90% of the CLT surface had no char and 10% of the CLT had only surface char. Additional charring would have occurred if the test had been allowed to continue.

(a) top of ceiling

(b) exterior of W1 wall

(c) interior with gypsum board removed

(d) interior with gypsum board removed

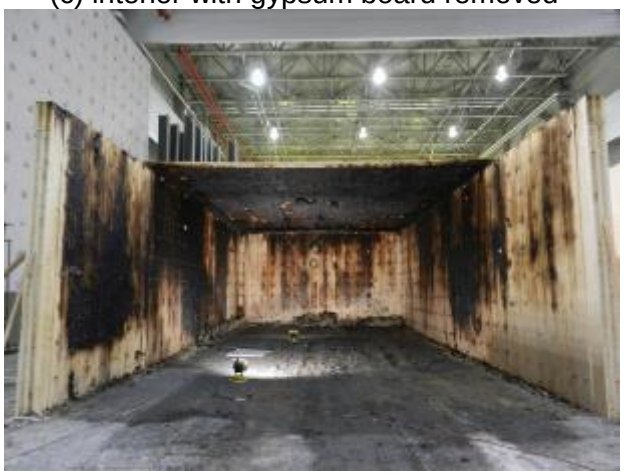

(e) during demolition

(f) ceiling panels

Figure 77. Photograph of CLT compartment and panels after Test 1-4.

Table 9. Char depth (mm) of CLT wall panels in Test 1-4.

Measurement locations	W1 Panel 10_010		W1 Panel 10_009		W1 Panel 10_007		W4 Panel 10_002		W3 Panel 10_005	
1.6 m height	0	0*	-	14*	4*	-	0*	-	2*	0
1.1 m height	9	0	-	12*	1	-	0*	-	0*	10
0.6 m height	8	0*	-	10*	5*	-	0*	-	0*	10

* TC nearby on wall

Table 10. Char depth (mm) of CLT ceiling panels in Test 1-4.

Measurement locations	1/8 span (close to W1)	3/8 span	5/8 span	7/8 span (close to W3)
Ceiling Panel 11_004	72	74	81	70
	78	80	82	81
Ceiling Panel 11_003	73	85*	90*	90
	79	90	86*	86
Ceiling Panel 11_002	75	70 (78)	80	81
	72 (78)	70*	80*	70 (81)
Ceiling Panel 11_001	71 (79)	71 (84)	66 (83)	79
	68 (72)	66 (78)	68 (72)	68 (79)

* TC nearby on ceiling; nearby maximum in brackets

Table 11 shows the CLT sample that was cut from the ceiling panel 11_003 where the embedded thermocouples were installed. The thickness of the char was 71 mm (remaining CLT thickness was 104 mm). This confirms the char depth (65 mm < char depth < 90 mm) measured by the embedded thermocouples.

Table 11. Char depth (mm) of cut CLT samples in Test 1-4.

CLT cut sample	Remaining thickness (mm)	Char depth (mm)	Image
Test 1-4 Ceiling centre Panel 11_003 (TC 98, 1-7)	104	71	

As shown in Figure 77, the exterior surface of the CLT ceiling and walls had no char; neither did the exterior surface. The ceiling panel spline joints were covered with gypsum concrete on top but no sealant was used at any CLT joint of the compartment. Neither the wall panel joints nor the ceiling panel joints developed char. However, there was minor surface char developed outside the two back corners at the wall-ceiling junction (no burn through), which could have been prevented if the wall-ceiling joint had been sealed.

3.4.7 Contribution of the CLT structure to compartment fire

Based on the volume (depth x area) of the CLT charred, which was measured after the test, the CLT panels were estimated to contribute approximately 1800 kg of timber to the fire (mainly by the ceiling panels), which translated to 900 MJ/m^2 fuel load density to the floor area in addition to the movable fuel load. This brought the effective fuel load density to 1450 MJ/m^2 in Test 1-4.

With the exposed ceiling in Test 1-4, flashover occurred earlier than in the baseline (Test 1-1). The peak compartment temperatures were similar to the baseline. However, the heat fluxes to the exterior façade were higher in Test 1-4 than in Test 1-1. With the involvement of the exposed ceiling in the fire, the fully developed stage (initial intense burning period) was much longer than the baseline. The initial decay of the fire came after 75 min, compared to 45 min in baseline test.

The heat release rate was higher than the baseline, as shown in Figure 78. By subtracting the baseline, Figure 79 shows the CLT contribution to the heat release rate during Test 1-4. A time shift was made to the baseline in order to line up the flashover time with Test 1-4 for proper subtraction. The CLT structure contributed a maximum of 5.5 MW to the heat release rate (mainly due to the exposed ceiling) in the fully developed fire stage and in the second flashover at the end.

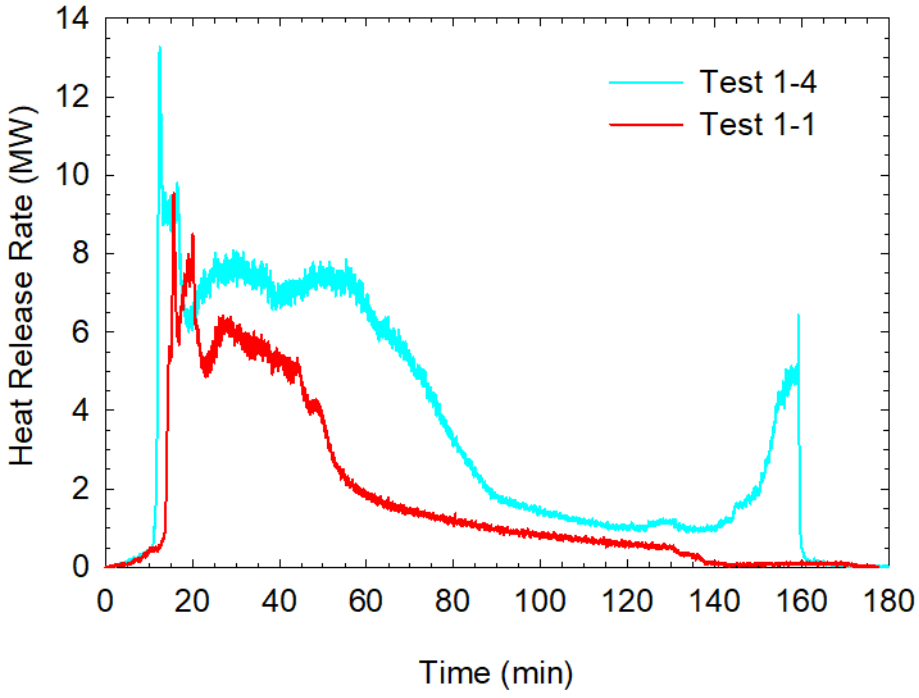

Figure 78. Heat release rate of Test 1-4 superimposed over baseline (Test 1-1).

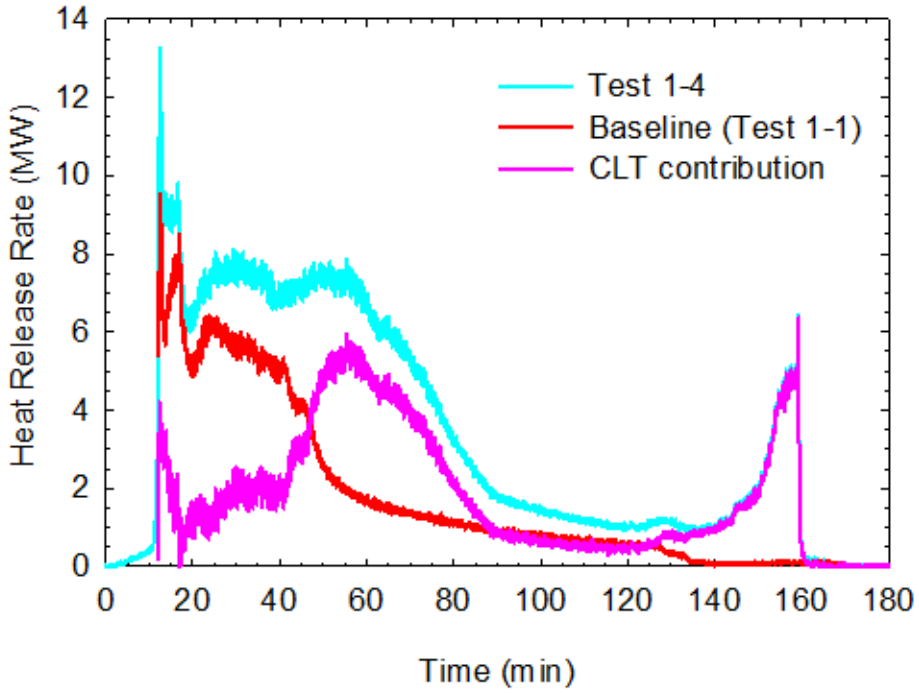

Figure 79. CLT contribution to heat release rate in Test 1-4 (baseline time shifted).

3.5 Test 1-5

A new CLT compartment was constructed using 5-ply 175 mm thick CLT panels for Test 1-5. As shown in Figure 80, the entire W1 wall was exposed – bare CLT surface. Three layers of 15.9 mm (5/8 in.) thick Type X gypsum board were installed on the ceiling and the W2, W3 and W4 walls. Necessary adjustment was made to thermocouple locations for Test 1-5. For the gypsum protected W3 and W4 walls and ceiling, the embedded thermocouples, originally planned for 140 mm depth, were moved to the second glueline at 70 mm deep in the CLT. Additional thermocouples were embedded in the exposed W1 wall to the CLT's first and second gluelines (35 mm and 70 mm) at ten locations. Test 1-5 was conducted on April 13th, 2017 and designed to quantify the contribution of the exposed W1 wall to the compartment fire with Test 1-1 as the baseline (1.8 m x 2.0 m ventilation opening). (Test 1-5 had the same exposed wall surface (W1) as Test 1-3 but a smaller ventilation opening and one more layer of gypsum board on the W2, W3 and W4 walls than Test 1-3.)

Figure 80. Photograph of CLT compartment with exposed W1 wall for Test 1-5.

3.5.1 Fire development

Figure 81 shows some photographs of the CLT compartment during Test 1-5. The test started with ignition of the console table in the corner (Figure 81(a)). The smoke alarm and heat alarm activated at 1.8 min and 2.5 min, respectively. Between 1.2 min and 3.6 min, all ten STEs reached 68 °C, a typical temperature rating for residential sprinklers.

As shown in Figure 81(b), the fire ignited the exposed W1 wall panels in the dining area at 9.2 min. The first dining chair nearest to the corner was ignited by the fire at 10 min, the tall bookcase near the dining area at 10.2 min, and the dining table at 10.3 min. By 10.5 min, the whole dining area was on fire. The smoke optical density measured at the 1.6 m height in the room centre reached 3.4 m^{-1} at 11.0 min. The W1 wall was then fully involved.

Flashover occurred at 11.5 min, as shown in Figure 81(c) and (d). The concentrations of O_2, CO_2 and CO concentrations changed dramatically. Large fire plume issued from the opening. While the room content was consumed by 40 min, the W1 wall continued to burn. At 52 min, pieces of the charred first ply of the W1 panels started to fall off gradually and the fire started to decay significantly. The fire plume ceased to issue from the opening at 67 min and the W1 wall was clearly seen burning inside the compartment. Char of the CLT first ply was falling off the W1 wall until 75 min. The CLT second ply continued to burn on the W1 wall until 100 min. From 100 min to 130 min, the CLT second ply showed charring but little visible flame (Figure 81(e)).

From 130 min to 140 min, visible flame re-occurred and spread over the W1 wall again. Fire plume re-issued from the front opening at 140 min. The ceiling started full involvement in the fire at 150 min and the W3 and W4 walls also became fully involved at 185 min, after losing all gypsum board protection (see subsection 3.5.5). By this time, all CLT panels in the compartment contributed to the compartment fire. The test was terminated at 202 min with fire suppression using two fire hoses spraying water to the compartment.

(a) ignition

(b) W1 wall ignited at 9 min.

(c) just before flashover

(d) flashover at 11.5 min

(e) exposed W1 wall at 111 min.

(f) second flashover at 155 min

Figure 81. Photographs of the CLT compartment during Test 1-5.

3.5.2 Compartment temperatures

Figure 82 shows the compartment temperatures during Test 1-5. After the flashover, the peak temperatures reached 1200 °C in the front, middle and rear sections of the compartment sequentially. After the room contents were consumed and as the CLT charred first ply were falling off the W1 wall, the compartment temperatures decreased at 50-70 min. A small transient increase occurred at approximately 70 min as shown by each curve when the CLT second ply started flaming on the W1 wall. The compartment temperatures continued to decrease even with the CLT second ply visibly flaming from 75 min to 100 min. As the CLT second ply ceased flaming on the W1 wall, the compartment temperatures further dropped, reaching the minimum temperatures at 130 min. With the flames re-occurring on the W1 wall and the fire involving the ceiling, the compartment temperatures grew to over 1000 °C at 150 min. The temperatures further increased to above 1100 °C when the W3 and W4 walls got involved in the fire after 180 min.

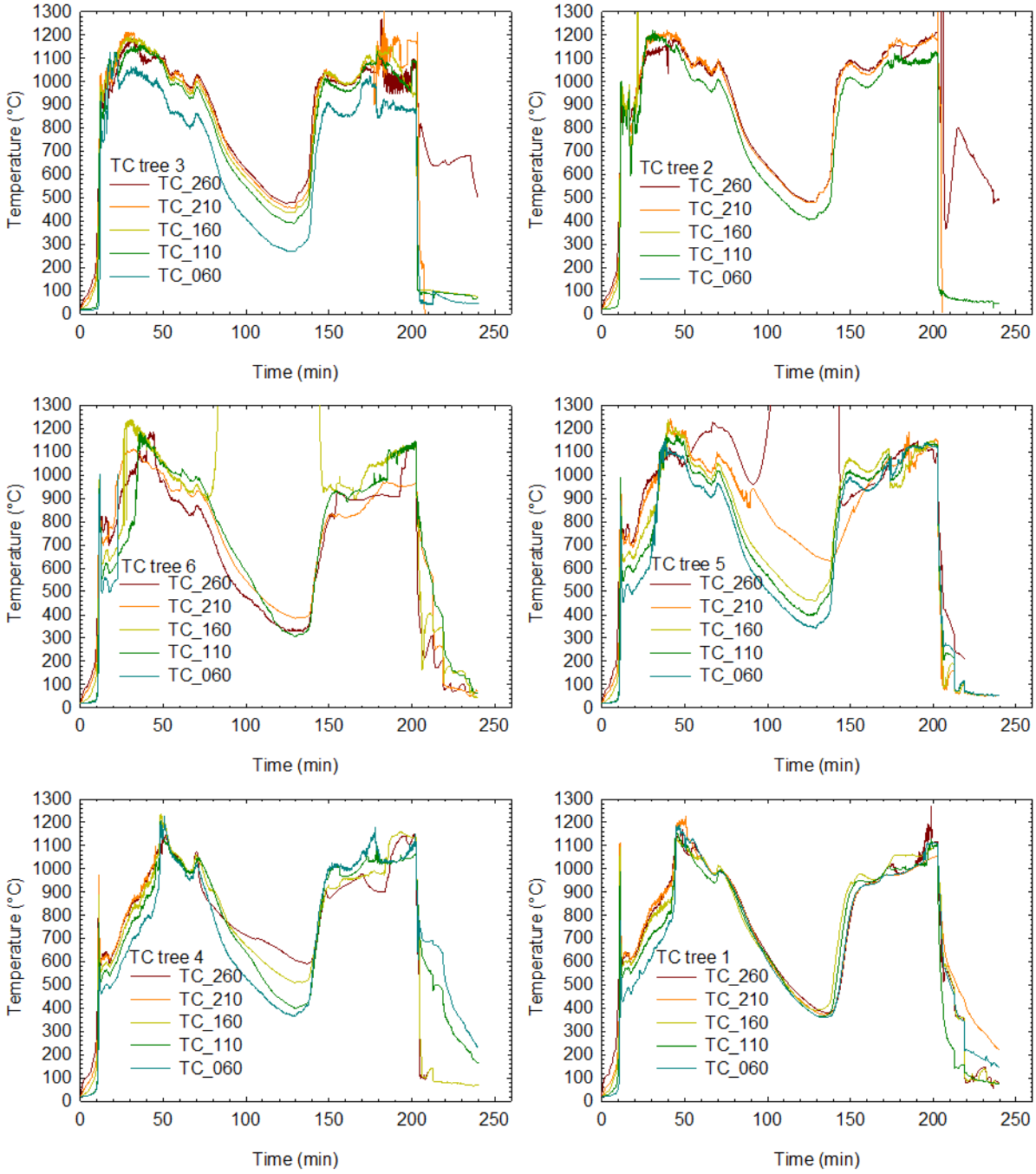

Figure 82. Temperatures in the compartment space during Test 1-5 (height in cm, test terminated at 202 min).

3.5.3 Heat release rate

Figure 83 shows the heat release rate during Test 1-5. The HRR was 9.6 MW at the initial peak right after the flashover and maintained above 5 MW until 50 min. As the fire decayed, the HRR reduced to 1 MW at 130 min. A second flashover occurred at 150 min and the HRR rose to over 6 MW after the re-occurred flaming on the W1 wall and involvement of the ceiling in the fire. With the W3 and W4 walls involved in the fire after 180 min, the HRR further climbed to 10 MW. The test was terminated at 202 min by suppressing the fire.

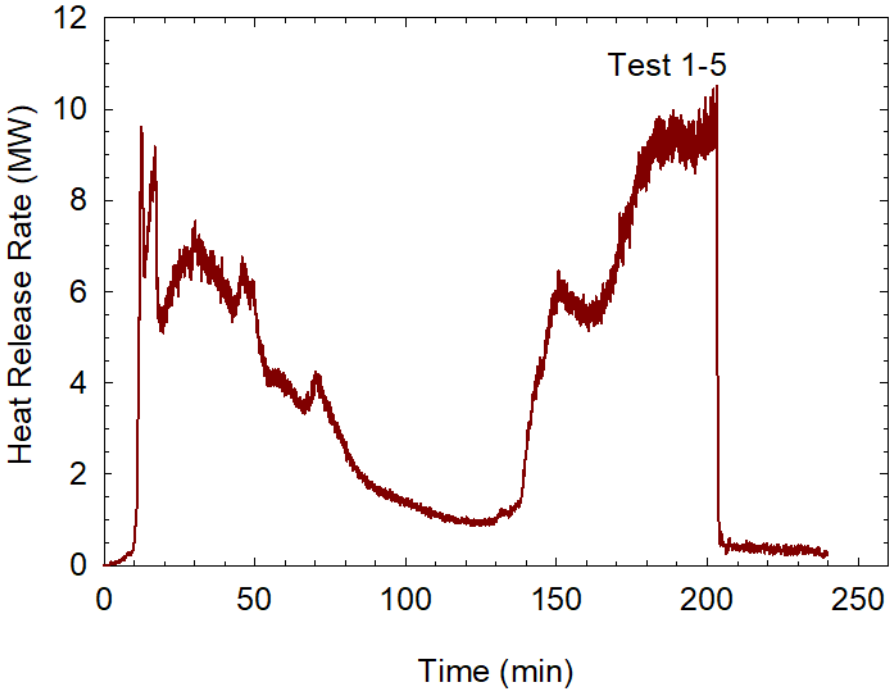

Figure 83. Heat release rate during Test 1-5 (test terminated at 202 min).

3.5.4 Heat flux inside and outside fire compartment

Figure 84 shows heat fluxes measured inside and outside the fire compartment during Test 1-5, displaying similar shapes as the heat release rate and the compartment temperatures. The initial spike of each curve corresponded to the flashover. Table 5 provides the peak heat flux values at the fully developed fire stage after the flashover (note that the large vertical spikes for the ceiling and the W3 and W4 walls are discounted as they were caused by odd data points). During the initial fully developed fire stage, the heat fluxes ranged from 175 kW/m^2 to 290 kW/m^2 inside the compartment and from 15 kW/m^2 to 120 kW/m^2 outside the compartment, depending on the locations. During the second flashover, the heat fluxes to the exterior façade were even higher than the initial peaks.

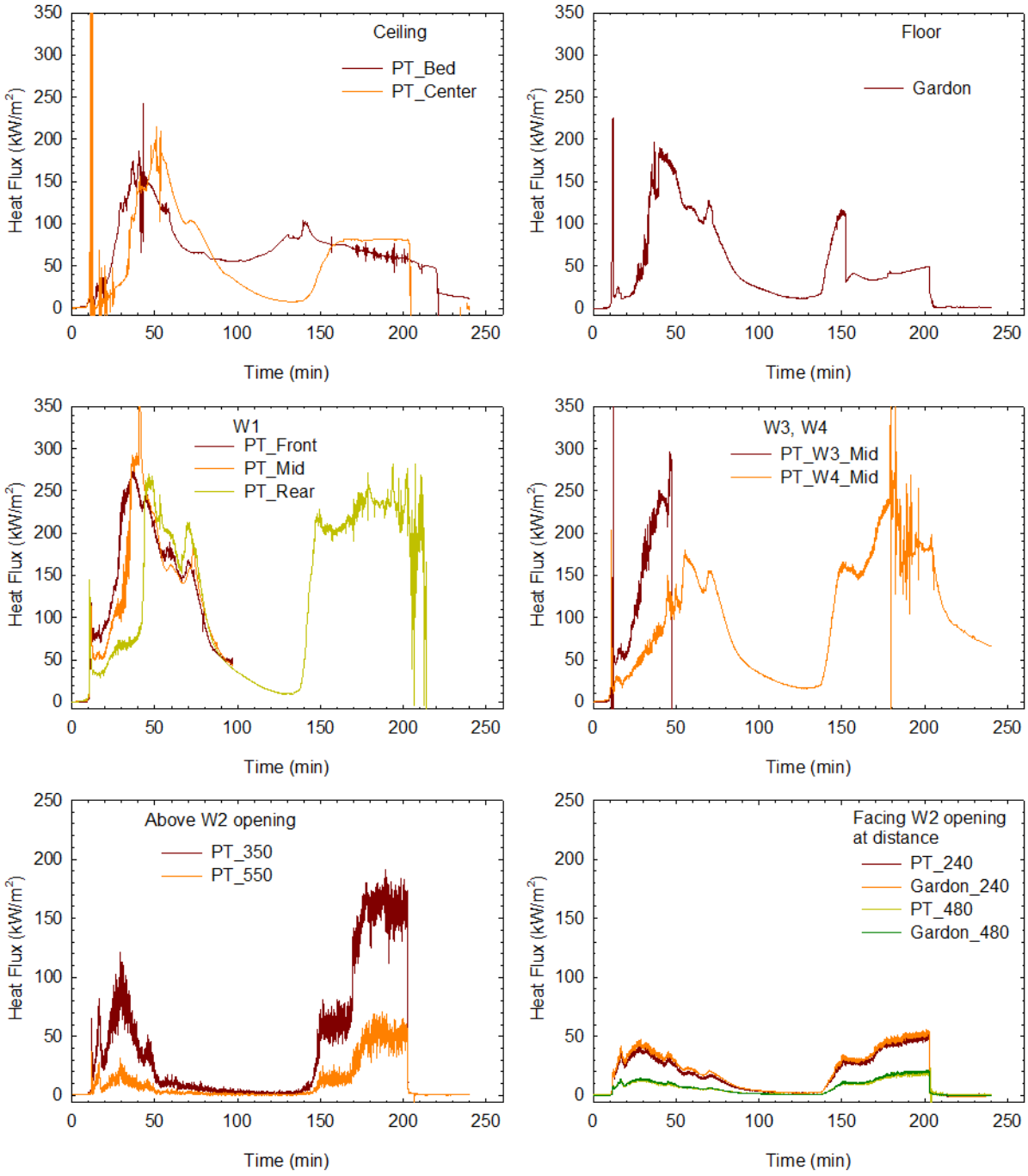

Figure 84. Heat fluxes inside and outside the compartment during Test 1-5 (test terminated at 202 min).

3.5.5 Temperatures at surface and in depth of CLT as well as gypsum board interfaces

Figure 85 shows the temperatures measured at the CLT surfaces, interfaces between gypsum board layers and inside CLT panels. The temperature profiles show that, before the flashover, the exposed W1 wall was already ignited. Based on the timing when the embedded thermocouples in the W1 wall at the mid-length and 1.8 m height measured 300 °C, the char front reached the depths of 20 mm, 35 mm, 50 mm, 70 mm, 90 mm and 115 mm at 43 min, 59 min, 80 min, 142 min, 175 min and 202 min, respectively, in CLT panel 10_018. At the end of the test, the temperature at 140 mm depth in the CLT panel was 85 °C.

The embedded thermocouples in 35 mm depths at the five locations in the W1 wall reached 300 °C at 49 min to 72 min, indicating that the char front reached the first glueline in the CLT panels. By visual observation, the charred CLT first ply was falling off the W1 wall from 52 min to 75 min. The embedded thermocouples in 70 mm depth at the five locations in the W1 wall reached 300 °C at 140-154 min during the second flashover with sharp temperature rises from below 300 °C to the prevailing compartment temperature. This indicated delamination of the second ply of the CLT prior to the char front reaching the second glueline. The third ply of CLT on the W1 wall started charring as well.

In the ceiling assembly, the temperatures at the interface between the face and middle layers of gypsum board increased sharply to the compartment temperatures at 32-45 min, indicating the fall-off of the face layer gypsum board. The fall-off of the face layer gypsum board resulted in the middle layer gypsum board being directly exposed to the fire, resulting in an increased rate of conductive heat transfer through the middle layer to its interface with the gypsum board base layer. The middle layer gypsum board fell off the rear section of the ceiling at 70 min, as indicated by the interface temperatures. The temperatures at the gypsum board base layer and CLT interface reached 300 °C at 70-85 min and the ceiling CLT panels started charring behind the base layer gypsum board. At 144-155 min, as indicated by the interface temperatures, the base layer gypsum board fell off the ceiling, exposing the CLT ceiling panels to the compartment fire which led to the second flashover. The embedded thermocouples in the ceiling centre (CLT panel 11_007) reached 300 °C in the depths of 20 mm, 35 mm and 50 mm at 163 min, 175 min and 186 min, respectively, during the second flashover. As indicated by the sharp temperature increase at the 35-mm depth, the delamination of the first ply of the charred CLT occurred prior to the char front reaching the first glueline, and the charred first ply of the CLT fell off the ceiling at 175 min. The second ply of the ceiling panels started charring as well.

Based on the temperatures at the interface between the face and middle layers of gypsum on the W3 and W4 walls, the face layer gypsum board fell off the W3 and W4 walls at 50 and 70 min, respectively. The CLT interfaces reached the charring temperature of 300 °C in the W3 and W4 walls at 98 min and 148 min, respectively. During the second flashover, the middle layer of the gypsum board fell off the W3 and W4 wall at 155-180 min; the base layer of the gypsum board fell off the W3 and W4 walls at 185-190 min, fully exposing the CLT wall panels and further intensifying the compartment fire until the end of the test. However, the temperatures at the CLT first glueline were less than 175 °C in the W3 and W4 walls. The temperatures on the W3 and W4 exterior surfaces were less than 40 °C during the test.

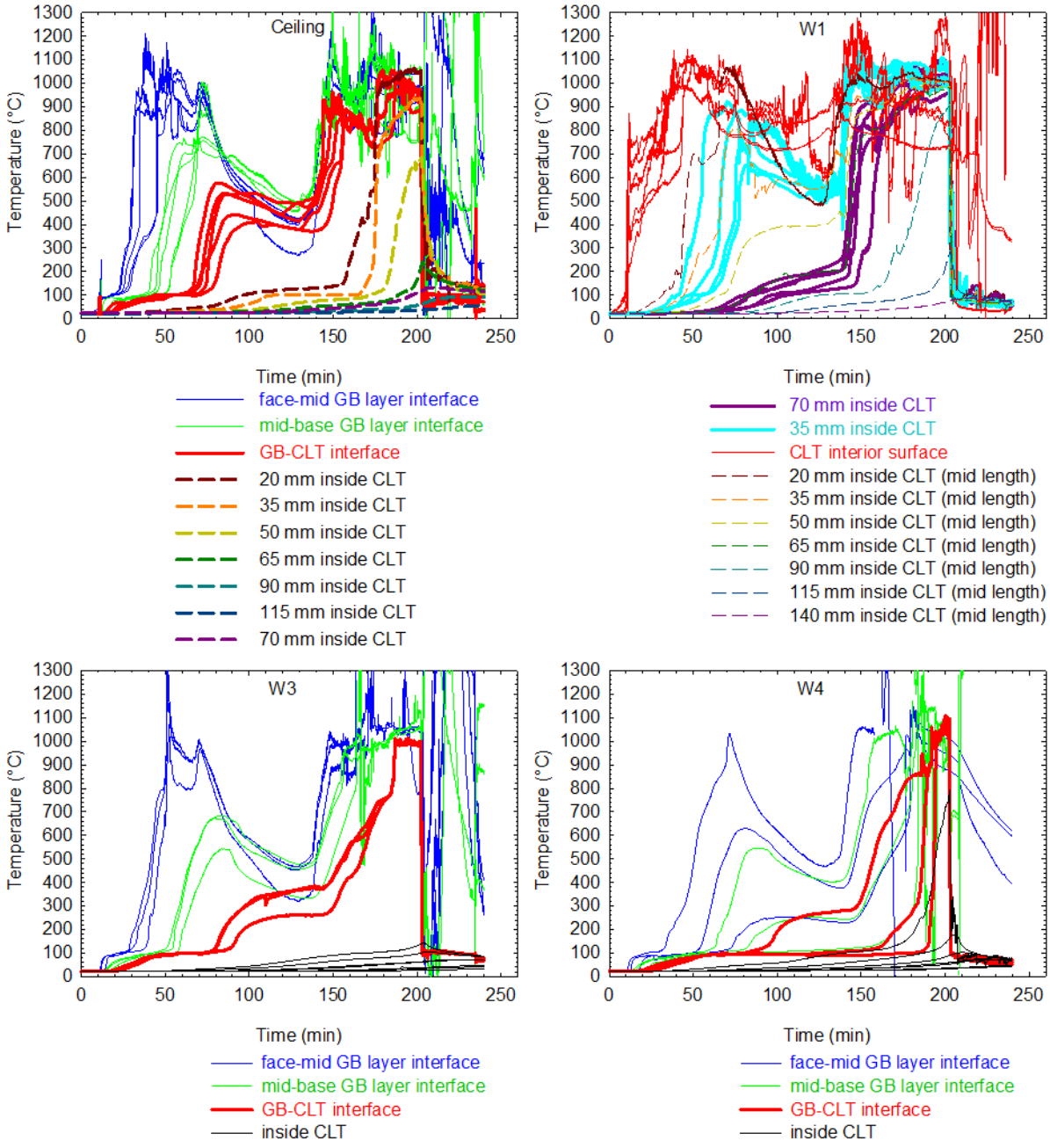

Figure 85. Temperatures in CLT and at gypsum board interfaces in Test 1-5 (test terminated at 202 min).

3.5.6 Char depth of CLT panels

After the fire test, the CLT compartment was examined for char. Figure 86 shows photographs of the CLT compartment and char measurement after Test 1-5. Eight sampling holes were drilled through each CLT panel for char measurements. Table 12 and Table 13 list the char depths measured at the sampling-hole locations for each panel. The exposed W1 wall charred up to 141 mm (with the last ply supporting the ceiling structure), the ceiling up to 79 mm, the W3

and W4 walls up to 52 mm, at the sampling locations. Additional charring would have occurred if the test had been allowed to continue.

(a) interior of CLT compartment after Test 1-5

(b) exterior of exposed W1 after Test 1-5

(c) drilling holes through ceiling panels

(d) char measurement by drilled holes

(e) drilled holes through wall panels

(f) cutting sample for char measurement

Figure 86. Observation and measurement of char after Test 1-5.

Table 12. Char depth (mm) of CLT wall panels in Test 1-5.

	W3 Panels								W4 Panels				W1 Panels							
Height	**10_023**		**10_022**		**10_021**		**10_020**		**10_014**		**10_015**		**10_016**		**10_017**		**10_018**		**10_019**	
2.1 m	9	13	15	22	30	22	25	18	25	43	49	48	130	138	138	130	133	137	132	126
1.6 m	13	15	26	33*	41	48	27	25	37	37*	51	47	130	141*	139	138	134*	141	132*	129
1.1 m	13	16	52	38*	45	42	39	35	40	35*	45	44	133	134	135	138	135*	138	132	130
0.6 m	5	0	38	33*	32	37	33	30	33	32*	44	45	115	120*	102	125	128*	129	138*	121

* TC nearby on wall

Table 13. Char depth (mm) of CLT ceiling panels in Test 1-5.

Measurement locations	7/8 span (close to W3)	5/8 span	3/8 span	1/8 span (close to W1)
Ceiling Panel 11_008	25	45	60	70
	35	55	60	70
Ceiling Panel 11_007	47	60*	72*	76
	55	62	72*	79
Ceiling Panel 11_006	58	64	70	73
	62	62*	72*	74
Ceiling Panel 11_005	53	54	67	68
	51	58	66	66

* TC nearby on ceiling

Table 14 shows the CLT samples that were cut from the ceiling and wall panels where the embedded thermocouples were installed. The thickness of the char was 117-130 mm in the W1 wall panels, 69 mm in the ceiling panels, and 33-39 mm in the W3 and W4 wall panels. This confirmed the char depths measured by the embedded thermocouples.

Table 14. Char depth (mm) of cut CLT samples in Test 1-5.

CLT cut sample	Remaining thickness (mm)	Char depth (mm)	Image
Test 1-5 Ceiling centre Panel 11_007 (TC 98, 1-7)	106	69	
Test 1-5 W1 – front 0.6 m high Panel 10_019 (TC 62, 63, 64)	47	128	
Test 1-5 W1 – rear 0.6 m high Panel 10_016 (TC 65, 66, 67)	52	123	
Test 1-5 W1 – front 1.8 m high Panel 10_019 (TC 56, 57, 58)	45	130	
Test 1-5 W1 – mid length 1.8 m high Panel 10_018 (TC 49, 8-14, 55)	57	118	

CLT cut sample	Remaining thickness (mm)	Char depth (mm)	Image
Test 1-5 W1 – rear 1.8 m high Panel 10_016 (TC 59, 60, 61)	58	117	
Test 1-5 W3 – mid length 1.8 m high Panel 10_022 (TC 70, 15-21)	142	33	
Test 1-5 W4 – mid length 1.8 m high Panel 10_014 (TC 79, 22-28)	136	39	

Figure 87 shows the exterior surface of the CLT ceiling and walls after the test. Although no sealant was used at any CLT joints of the compartment, there were only a few spots at the ceiling-wall joints and at the W1 panel joints where smoke escaped and char appeared. However, there was no burn through during the test.

(a) W1 wall

(b) ceiling panels 11_007 and 11_008

(c) W3 wall

(d) ceiling panels 11_006 and 11_007

(e) W4 wall

(f) ceiling panels 11_005 and 11_006

Figure 87. Exterior surface and joints of CLT compartment after Test 1-5.

3.5.7 Contribution of the CLT structure to compartment fire

In addition to the exposed W1 wall panels, the protected ceiling panels contributed to the compartment fire after 140 min and the protected wall panels contributed after 170 min. Based on the volume (depth x area) of the CLT charred, which was measured after the test, the CLT panels in the exposed W1 wall were estimated to contribute approximately 1800 kg of timber to the fire, the CLT ceiling panels approximately 1400 kg, and the CLT panels in all other walls approximately 830 kg, which translated to 2000 MJ/m^2 fuel load density to the floor area in addition to the movable fuel load.

With the exposed W1 wall in Test 1-5, flashover occurred earlier than in the baseline (Test 1-1). The peak compartment temperatures were similar to the baseline. The initial heat release rate was similar to the baseline, as shown in Figure 88, because the burning rate was largely controlled by the ventilation. However, the initial decay occurred later and the heat fluxes to the exterior façade were higher in Test 1-5 than the baseline. The exposed W1 wall extended the fully developed stage (initial intense burning period) 10 min longer than the baseline before reaching the decay stage. During the second flashover, which was caused by the re-flash on the W1 wall and the full involvement of the ceiling panels in the fire, the heat release rate rebounded to over 6 MW from 140 min to 155 min. The HRR further climbed to 10 MW with the full involvement of all other walls in the fire after 185 min.

By subtracting the baseline, Figure 89 shows the CLT contribution to the heat release rate during Test 1-5. A time shift was made to the baseline in order to line up the flashover time with Test 1-5 for proper subtraction. The CLT structure contributed a maximum of 3.3 MW, 6.3 MW and 9.5 MW to the heat release rate at the fully developed fire stage, second flashover and near the end of the test, respectively.

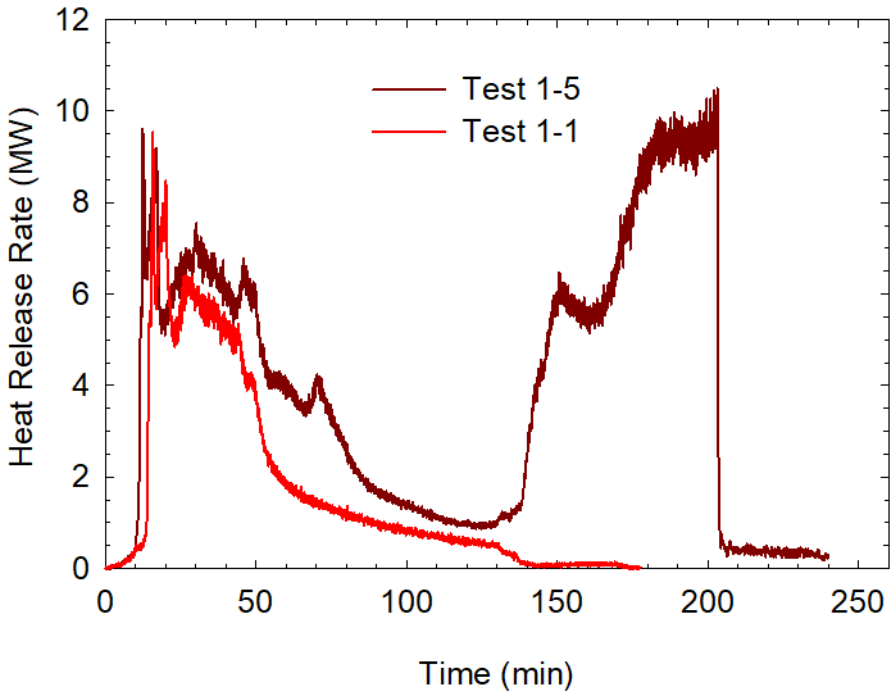

Figure 88. Heat release rate of Test 1-5 superimposed over baseline (Test 1-1).

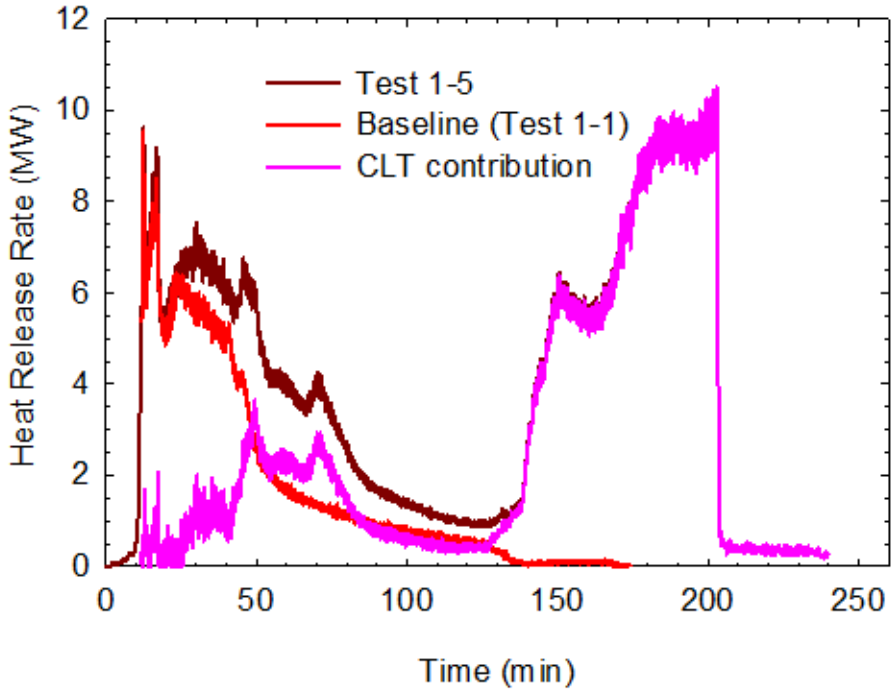

Figure 89. CLT contribution to heat release rate in Test 1-5 (baseline time shifted).

Ventilation conditions had a great impact on the compartment fires as shown in Figure 90, Figure 91 and Figure 92. The figures demonstrate the effect of two different ventilation conditions in Test 1-3 and Test 1-5 on the fire development and on the CLT contribution to the fires, with the same exposed wall surface. In the initial period after flashover, the peak temperatures in the compartments and openings were similar in both tests. However, the heat release rate and exterior heat fluxes (especially those away from the opening) were higher in Test 1-3 (with the larger ventilation opening) than Test 1-5 (with the smaller ventilation opening), suggesting more exterior combustion in Test 1-3. The fire started to decay quickly in Test 1-3 at 37 min. In Test 1-5, the fire was only reduced slightly at 40 min and continued with the flaming and delamination of the CLT first ply from the W1 wall until 75 min, followed by a 60-min period of decay. In Test 1-3, the CLT first ply on the W1 wall did not delaminated until 90-100 min; the second ply delaminated at 190-205 min, after which the fire continued to decay with the flame detached from the wall. With more heat trapped inside the compartment due to the smaller ventilation opening used in Test 1-5, the second ply of the CLT on the W1 wall re-flashed and delaminated earlier at 140-150 min, which further induced the full involvement of the ceiling and all other walls in the fire. The amount of char in Test 1-5 was approximately 3.6 times of that in Test 1-3.

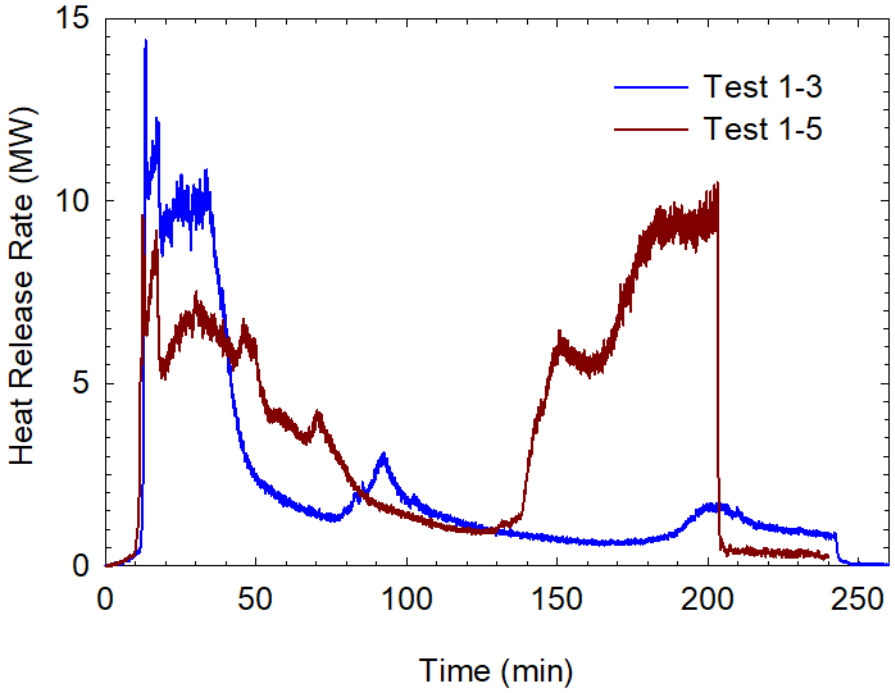

Figure 90. Effect of ventilation – Heat release rates in Test 1-3 and Test 1-5.

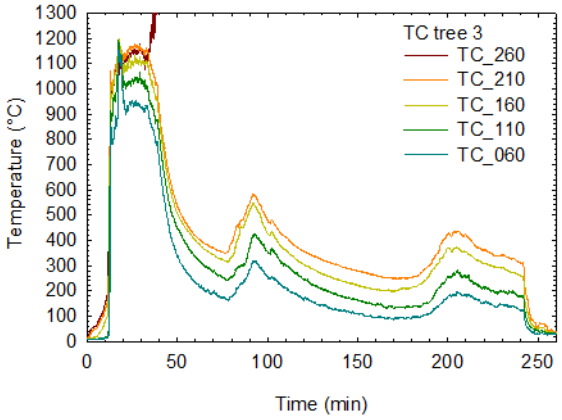

(a) compartment temperatures (Test 1-3)

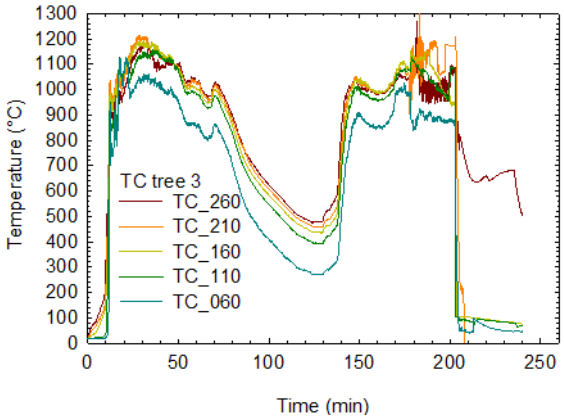

(b) compartment temperatures (Test 1-5)

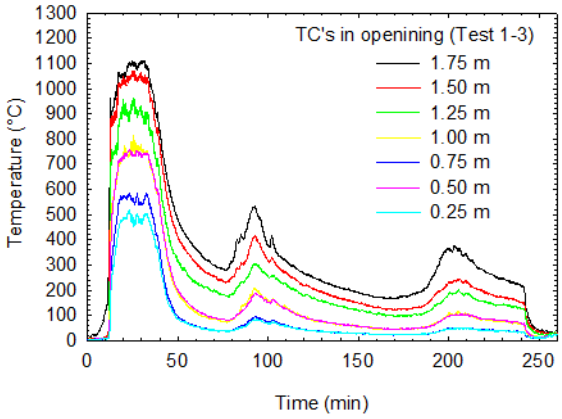

(c) temperatures at opening (Test 1-3)

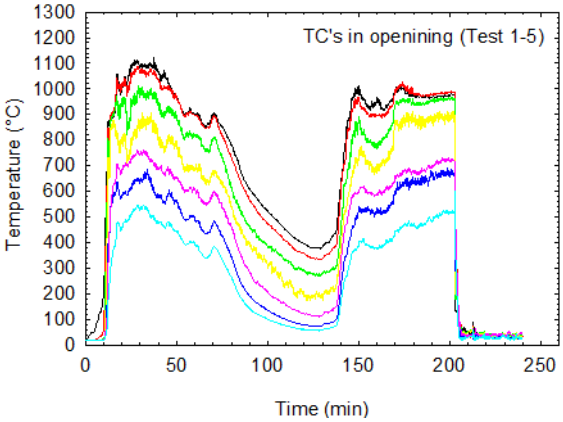

(d) temperatures at opening (Test 1-5)

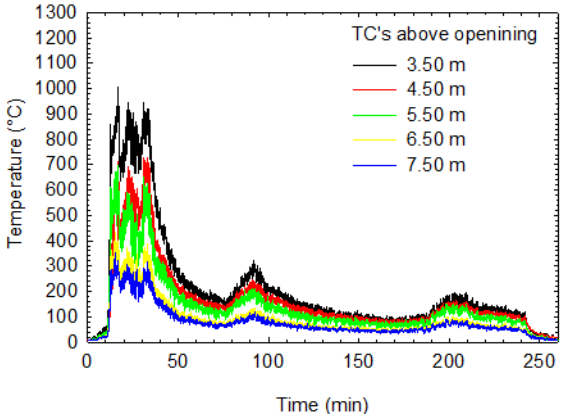

(e) exterior temperatures on façade (Test 1-3)

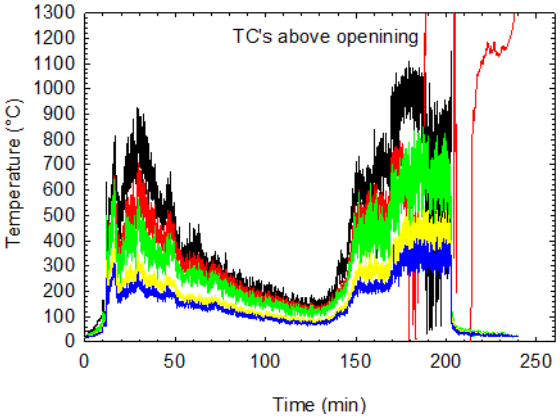

(f) exterior temperatures on façade (Test 1-5)

Figure 91. Effect of ventilation – Temperatures in Test 1-3 and Test 1-5.

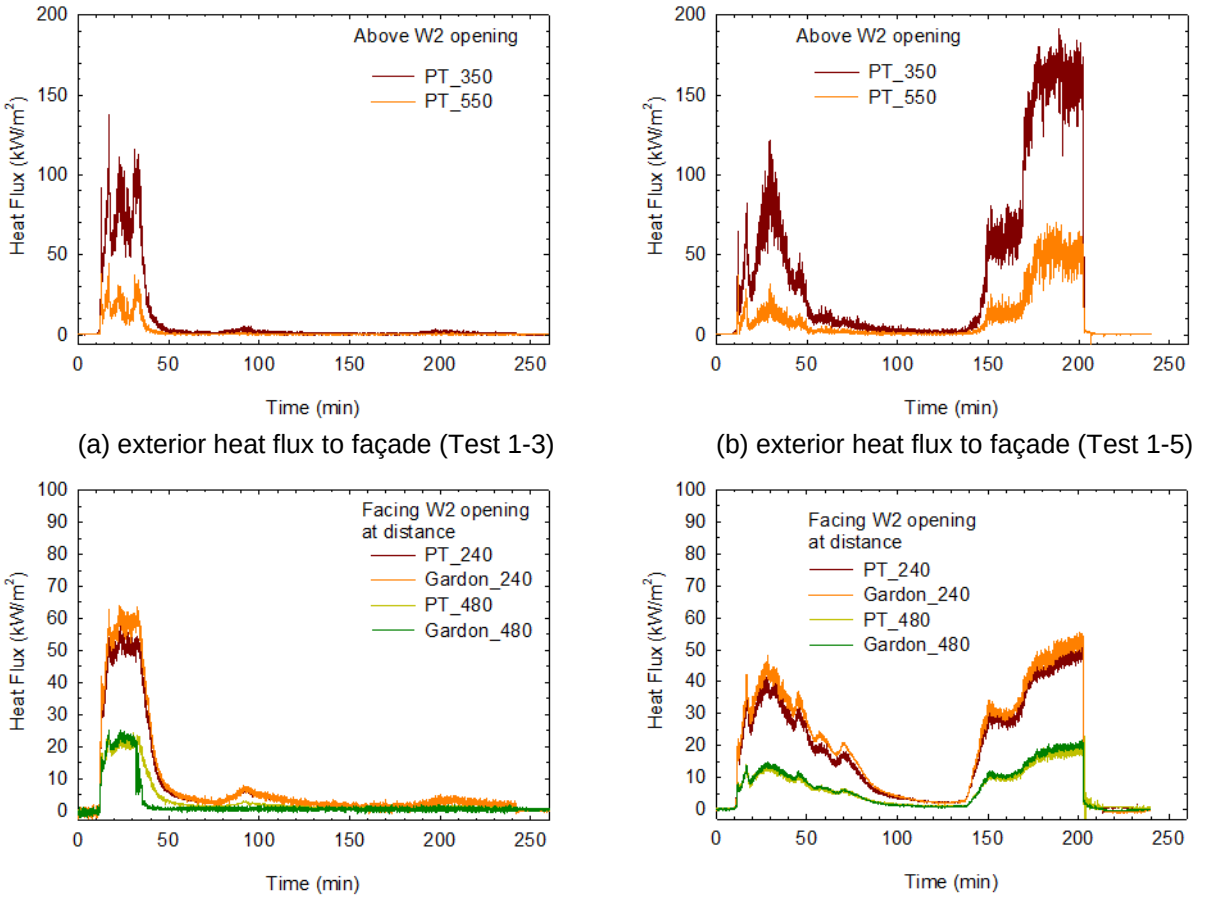

(a) exterior heat flux to façade (Test 1-3)

(b) exterior heat flux to façade (Test 1-5)

(c) exterior heat flux at distance (Test 1-3)

(d) exterior heat flux at distance (Test 1-5)

Figure 92. Effect of ventilation – Exterior heat fluxes in Test 1-3 and Test 1-5.

3.6 Test 1-6

A new CLT compartment was constructed using 5-ply 175 mm thick CLT panels for Test 1-6. The entire ceiling and W1 wall were exposed (bare CLT surface), as shown in Figure 93. Three layers of 15.9 mm (5/8 in.) thick Type X gypsum board were installed on the W2, W3 and W4 walls. Gypsum concrete (38 mm thick x 305 mm wide or 1-1/2 in. thick x 12 in. wide) was poured on the top of each spline joint of the ceiling panels on the outside,

Necessary adjustment was made to thermocouple locations for Test 1-5. For the gypsum protected W3 and W4 walls, the embedded thermocouples originally planned for 140 mm depth were moved to the second glueline at 70 mm deep in the CLT. Additional thermocouples were embedded in the exposed ceiling and W1 wall to the CLT's first and second gluelines (35 mm and 70 mm) at twenty locations.

Test 1-6 was conducted on April 18th, 2017 and designed to quantify the contribution of the exposed ceiling and W1 wall to the compartment fire with Test 1-1 as the baseline (1.8 m x 2.0 m ventilation opening).

Figure 93. CLT compartment with exposed ceiling and W1 wall for Test 1-6.

3.6.1 Fire development

Figure 94 shows some photographs of the CLT compartment during Test 1-6. The test started with ignition of the console table in the dining area corner. The smoke alarm and heat alarm activated at 2 min and 3 min, respectively. Between 1.6 min and 3.9 min, all ten STEs reached 68 °C, a typical temperature rating for residential sprinklers.

The fire ignited the exposed W1 wall near the corner at 7.3 min and the exposed ceiling above at 8.5 min. The dining table and chairs, as well as the tall bookcase near the dining area, were ignited by the fire at 9.2 min. The smoke optical density measured at the 1.6 m height in the room centre reached 3.4 m^{-1} 9.4 min.

Flashover occurred at 9.8 min. Large fire plume issued from the opening. After the room content was consumed, the exposed ceiling and W1 wall continued to burn with large fire plume issuing from the opening. At 80 min, the fire plume reduced in size and mainly issued from the upper right part of the opening and the interior of the compartment became partly visible. Most of the face layer gypsum board already fell off the W3 wall while the face layer gypsum board on the W4 wall started to fall. At 90 min, the W3 wall was seen to have lost some middle layer gypsum board with flare at several gypsum board joints on the base layer. At 100 min, the fire plume increased in size obstructing the view into the compartment. As the fire continued to grow, the ceiling appeared to sag at 120 min. At 150 min, flames burnt through a hole at the ceiling-wall junction between panels 10_009 and 11_003 near the ceiling spline joint. At 156 min flames burnt through the ceiling joint between ceiling panels 11_003 and 11_004.

The test was terminated at 160 min with fire suppression. Ceiling panel 11_003 (one of the four ceiling panels) collapsed into the compartment at 30 s after commencing the fire suppression. The large flame was extinguished within 1 min and glowing debris were extinguished within 5 min of the fire suppression operation. Connected to a stand pipe opening at 690 kPa (100 psi), two charged hose lines (38 mm diameter or 1.5 in. diameter) delivered 6.3 L/s (100 gpm) of water each through two low-pressure nozzles (517 kPa or 75 psi). Lower flow rates and pressures were used for overhaul.

(a) first item ignited in the corner

(b) outside view of ignition

(c) ceiling ignited above the dining area

(d) just before flashover

(e) flashover

(f) at 60 min

(g) at 120 min

(h) at 160 min

Figure 94. Photographs of the CLT compartment during Test 1-6.

3.6.2 Compartment temperatures

Figure 95 shows the compartment temperatures during Test 1-6. After the flashover, the peak temperatures reached 1200 °C in the front, middle and rear sections of the compartment, consecutively. The compartment temperatures stayed above 1000 °C until the end of the test, including a transient decrease in the vicinity of 90 min.

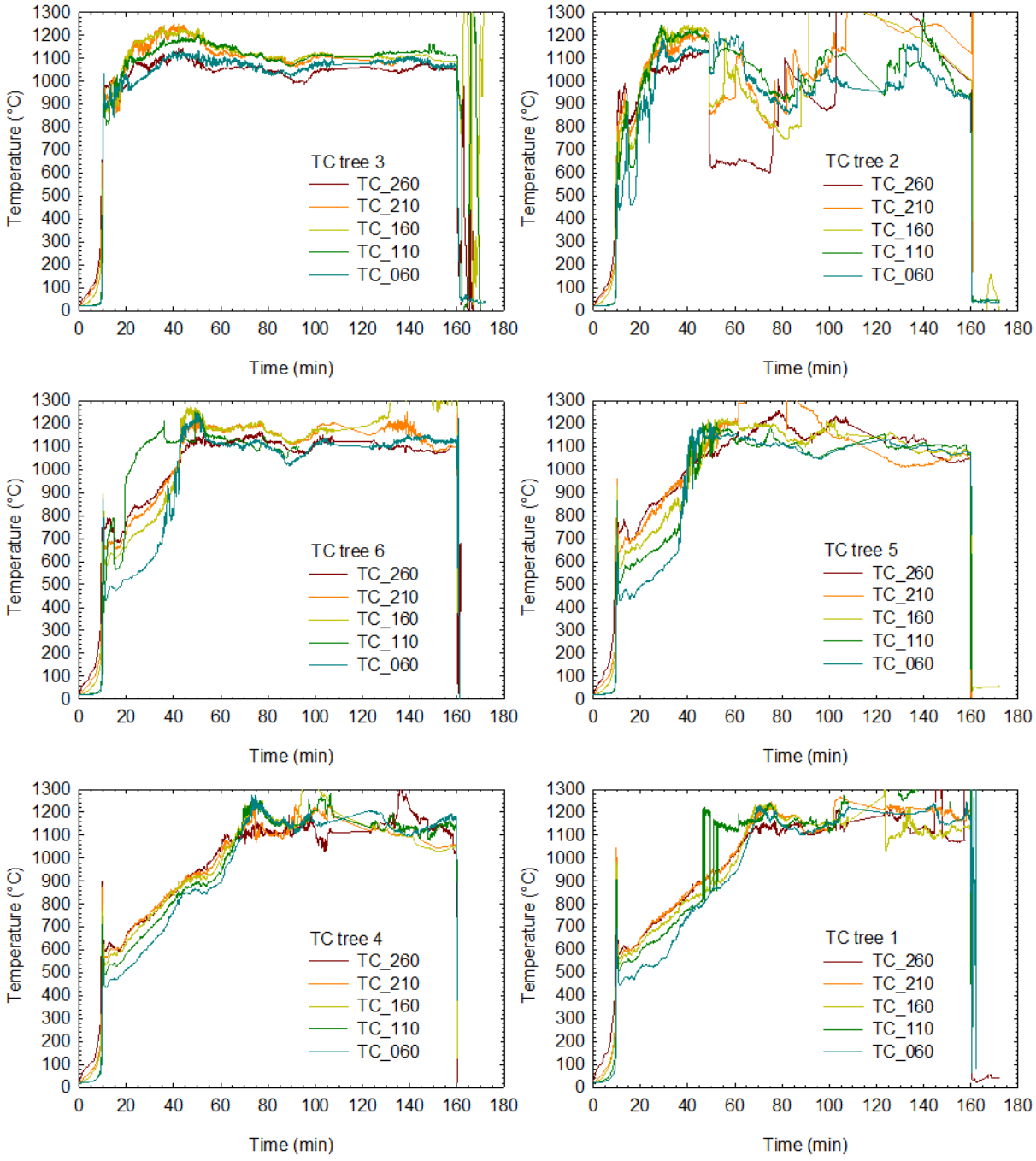

Figure 95. Temperatures in the compartment space during Test 1-6 (height in cm, test terminated at 160 min).

3.6.3 Temperatures at surface and in depth of CLT and gypsum board interfaces

Figure 96 shows the temperatures measured at the CLT surfaces, interfaces between gypsum board layers and inside CLT panels. Before the flashover, the exposed ceiling and W1 wall were already ignited by the fire.

Based on the timing when the embedded thermocouples in the ceiling measured 300 °C, the char front reached the depths of 20 mm, 35 mm, 50 mm, 65 mm, 70 mm, 90 mm and 115 mm at 44 min, 59 min, 67 min, 84 min, 98 min, 126 min and 160 min, respectively, in the CLT ceiling panel 11_003 (near the centre of the compartment). The thermocouples embedded in 35 mm depths at the five locations in the ceiling reached 300 °C at 52 min to 68 min, respectively, indicating that the char front reached the first glueline in the CLT ceiling. Some of the five locations in 35 mm depth show relatively gradual temperature rises after reaching 220 °C at the first glueline while others show sharp temperature rises to the prevailing compartment temperature. The thermocouples embedded in 70 mm depth at the five locations of the ceiling, which reached 300 °C at 88 min to 101 min, respectively, also show similar changes of temperatures. The data from the ceiling indicate that delamination may occur before or after the char front passing the glueline (i.e., below or above the charring temperature) in the test. The third ply and forth ply of the CLT ceiling panels started charring at 126 min and 160 min, respectively. At the end of the test (160 min), the temperatures at the 140 mm depth in the CLT ceiling panel 11_003 (the glueline to the last ply of the CLT) was 83 °C. This indicated that the char depth would be less than four plies of the CLT panel (115 mm < char depth <140 mm), which was confirmed in the post test observation.

The embedded thermocouples in the W1 wall panel 10_009 measured 300 °C in the depths of 20 mm, 35 mm, 50 mm, 65 mm, 70 mm, 90 mm and 115 mm at 49 min, 65 min, 85 min, 101 min, 105 min, 133 min and 154 min, respectively. The embedded thermocouples in 35 mm depths at the five locations in the W1 wall reached 300 °C at 54 min to 79 min, indicating that the char front reached the first glueline in the CLT panels. The embedded thermocouples in 70 mm depth at the five locations in the wall panels reached 300 °C at 99 min to124 min, indicating the third ply of the CLT ceiling panels started charring. At the end of the test (160 min), the temperatures at the 140 mm depth in the CLT panel 10_009 was 75 °C. This indicated that the char front moved into the fourth ply of the CLT panel (115 mm < char depth < 140 mm), which was confirmed in the post test observation.

In the protected W3 and W4 wall assemblies, the heat transfer through the gypsum board also followed the typical three-stage pattern as indicated by the temperature profiles at the interfaces: an initial temperature rise to 100 °C, a period of gypsum calcinations at the constant temperature of 100 °C, then temperature increasing again after the calcination. The temperatures at the interface between the face and middle layers of gypsum board increased sharply to the compartment temperatures at 55 min and 77 min in the upper portion of the W3 and W4 walls, respectively, indicating the beginning of fall-off of the face layer gypsum board from the W3 and W4 walls. The fall-off of the face layer gypsum board resulted in the middle layer gypsum board being directly exposed to the fire, resulting in an increased rate of conductive heat transfer through the middle layer to its interface with the gypsum board base layer. The middle layer gypsum board started falling off the W3 and W4 walls at 85 min and 93 min, respectively, as indicated by the interface temperatures. The temperatures at the gypsum board base layer and CLT interface reached 300 °C at 86 min and 102 min in the W3 and W4 walls, respectively, and the CLT panels started charring behind the base layer gypsum board. At 125-130 min, as indicated by the interface temperatures, the base layer gypsum board fell off the W3 and W4 walls, fully exposing the CLT panels to the compartment fire. The charring temperature of 300 °C was reached in the CLT panels: 20 mm, 35 mm and 50 mm depths in the W3 panel 10_005 at 127 min, 142 min and 157 min (50 mm < char < 70 mm), and

20 mm and 35 mm depths in the W4 panel 10_002 at 140 min and 154 min (35 mm < char < 70 mm), respectively. The temperature measured using the embedded thermocouples in other depths were all below 135 °C. The temperatures on the W3 and W4 exterior surfaces were less than 30 °C during the test.

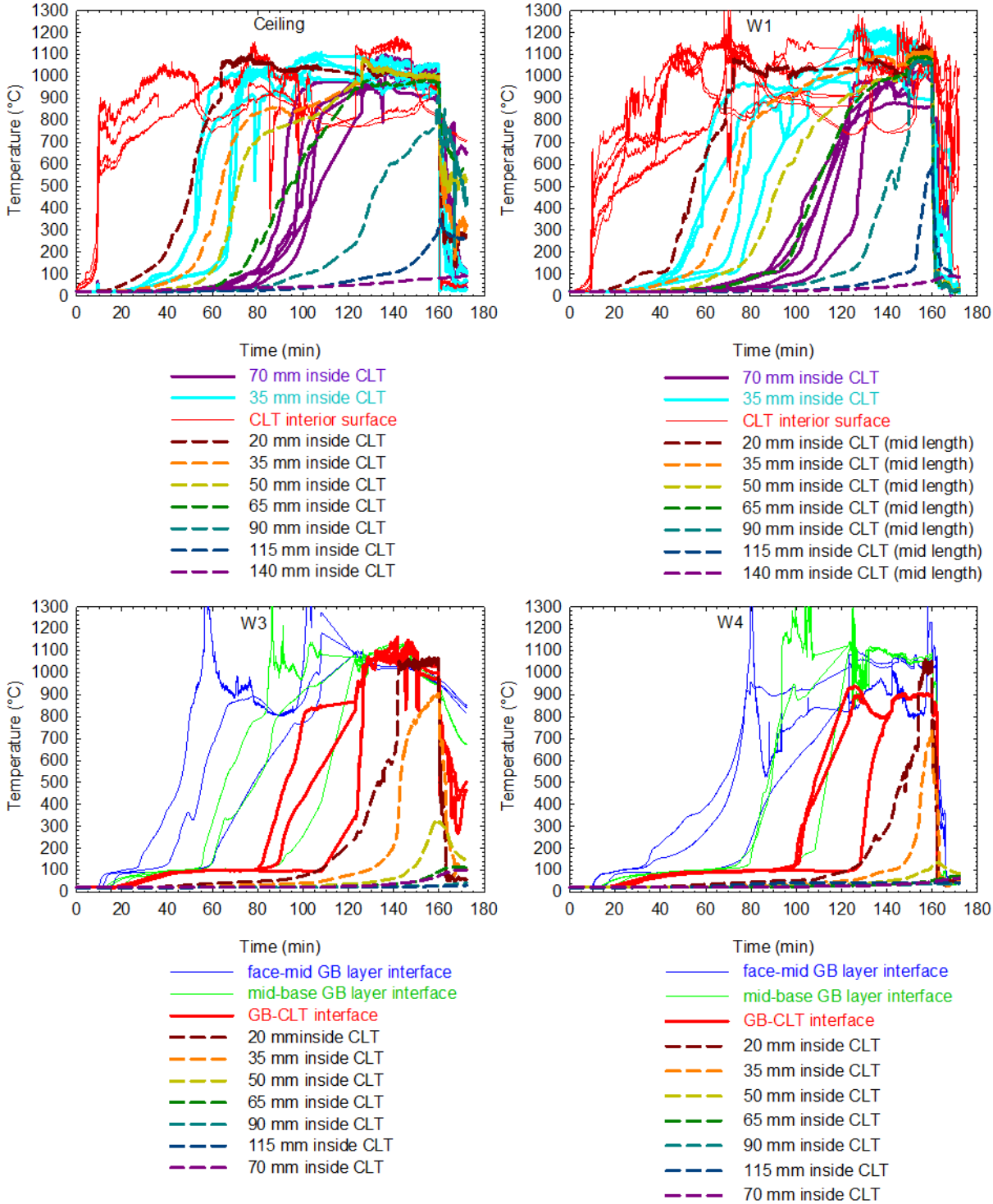

Figure 96. Temperatures in CLT and at gypsum board interfaces in Test 1-6 (test terminated at 160 min).

3.6.4 Heat release rate

Figure 97 shows the heat release rate during Test 1-6. The heat release rate had an initial peak of 12.9 MW right after the flashover and maintained above 6 MW during the test. The heat release rate varied with time. The intense burning of the surface ply of the exposed ceiling and W1 wall panels kept the HRR at 8 MW initially. Starting at 55 min, the charred CLT surface ply delaminated from the ceiling and W1 wall and the second ply started to be involved in the fire, increasing the HRR to 9 MW. After the surface ply completely delaminated from the ceiling and W1 wall, the HRR started to decrease at 75 min and dropped to 6.5 MW at 90 min. From 90 min to 100 min, the HRR climbed back to 9 MW as the second ply on the ceiling charred through and delaminated with the third ply involved. From 100 min to 125 min, the HRR stayed at 9 MW while the second ply on the W1 wall charred through and delaminated, exposing the third ply. At 125 min to 130 min, the protected W3 and W4 walls lost the last layer of gypsum board and the CLT panels were fully exposed to the fire, which further increased the HRR to 10 MW. At 147 min, the HRR decreased to 9 MW, which corresponded to charring through and delamination of the third ply from the ceiling and W1 wall. All CLT panels contributed to the compartment fire from this point.

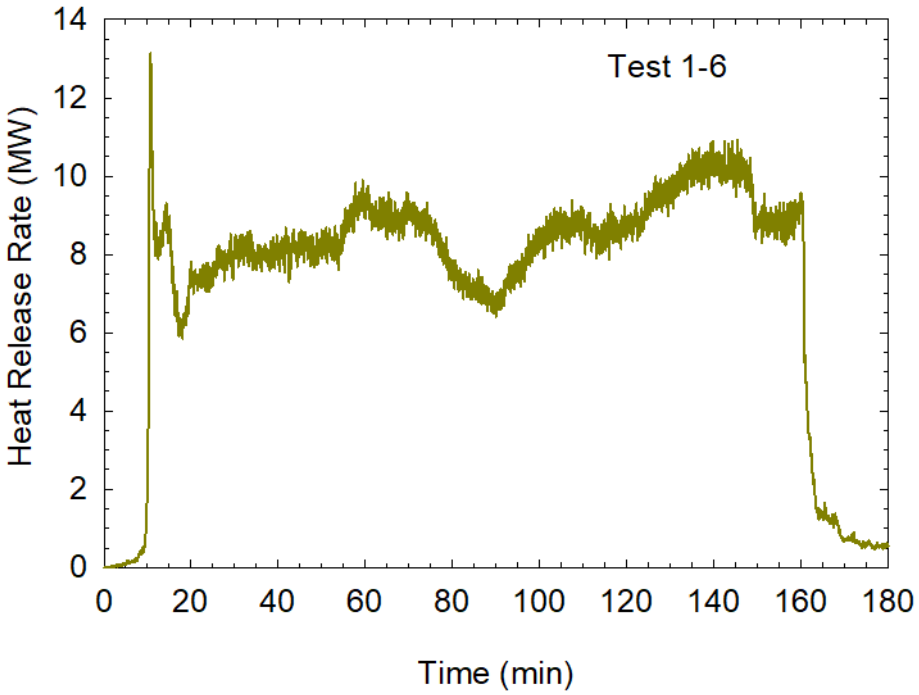

Figure 97. Heat release rate during Test 1-6 (test terminated at 160 min).

3.6.5 Heat flux inside and outside fire compartment

Figure 98 shows heat fluxes measured inside and outside the fire compartment during Test 1-6. The initial spike of each curve corresponded to the flashover. Table 5 provides the peak heat flux values at the fully developed fire stage after the flashover (note that the large vertical spikes for the ceiling and the W3 and W4 walls as well as above the opening are discounted as they were caused by odd data points). The heat fluxes ranged from 170 kW/m^2 to 290 kW/m^2 inside the compartment and 20 kW/m^2 to 120 kW/m^2 outside the compartment during the fully developed fire stage, depending on the locations.

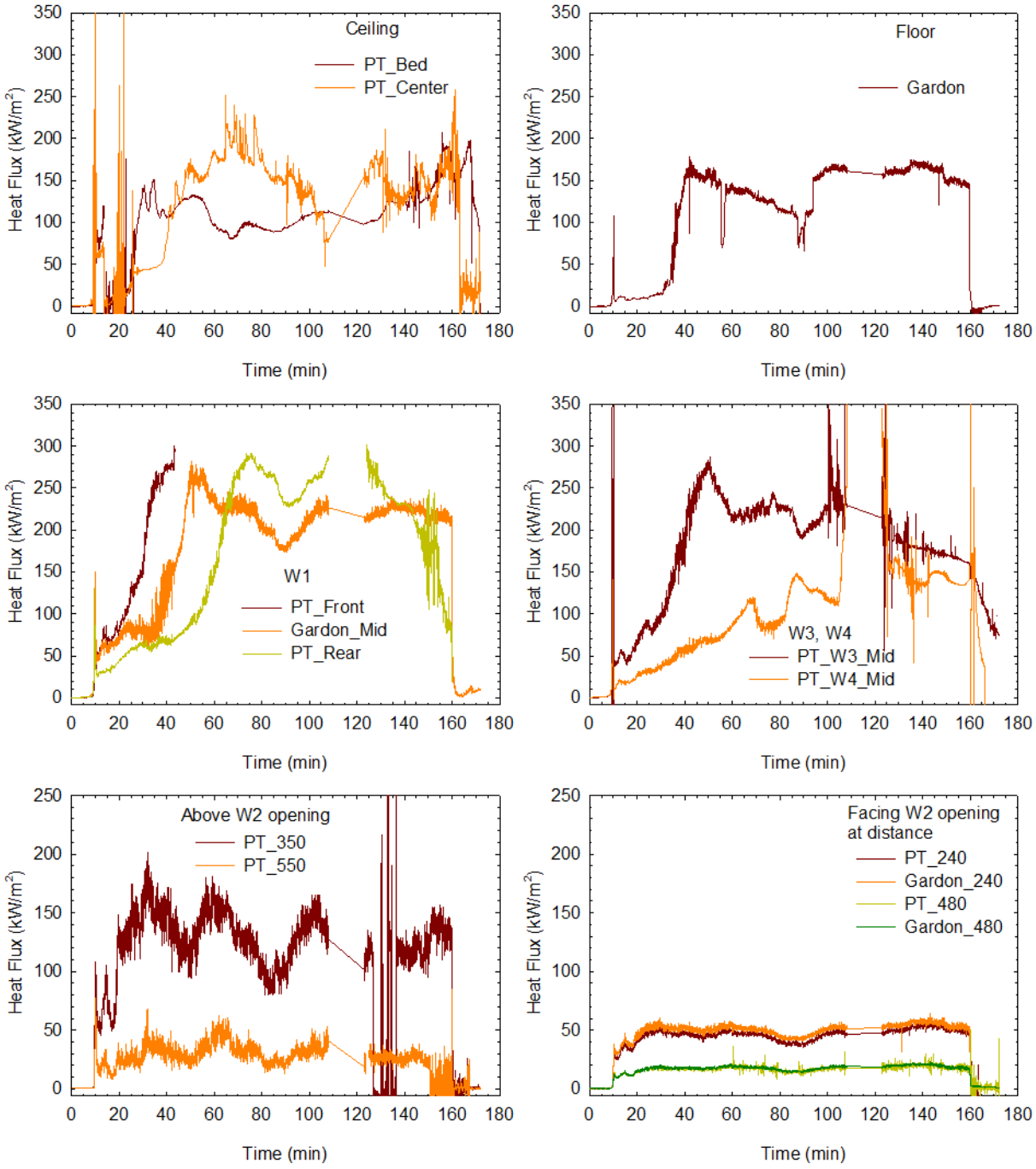

Figure 98. Heat fluxes inside and outside the compartment during Test 1-6 (test terminated at 160 min).

3.6.6 Char depth of CLT panels

After the fire test, the CLT compartment was examined for char. Figure 99 shows photographs of the CLT compartment after Test 1-6. After the test, there was a 406-mm (16 in.) deflection for the remaining ceiling panels.

(a) Compartment interior surface

(b) Ceiling exterior surface

(c) W1 exterior surface

(d) W2 exterior surface

(e) W3 exterior surface

(f) W4 exterior surface

Figure 99. CLT compartment after Test 1-6.

As shown in Figure 99, eight sampling holes were drilled through each CLT panel for char measurements. Table 15 and Table 16 list the char depths measured at the sampling-hole locations for each panel. The exposed ceiling charred 116-154 mm, the exposed W1 wall 88-143 mm, the W3 wall 5-66 mm and the W4 wall 25-68 mm at the sampling locations. Additional charring would have occurred if the test had been allowed to continue.

Table 15. Char depth (mm) of CLT wall panels in Test 1-6.

	W1 Panels								W4 Panels				W3 Panels							
Height	**10_010**		**10_009**		**10_008**		**10_007**		**10_001**		**10_002**		**10_003**		**10_004**		**10_005**		**10_006**	
2.1 m	133	139	134	141	138	126	127	124	59	44	42	43	47	45	50	55	45	36	9	5
1.6 m	143	134*	136	141*	131	130	129*	125	65	54	49*	50	52	59	58	63	59*	35	6	16
1.1 m	138	135	130	132*	138	125	120	126	68	60	48*	45	54	57	64	64	66*	50	6	16
0.6 m	89	99*	92	88*	95	93	96*	94	40	42	25*	33	28	48	53	52	48*	48	10	13

* TC nearby on wall

Table 16. Char depth (mm) of CLT ceiling panels in Test 1-6.

Measurement locations	1/8 span (close to W1)	3/8 span	5/8 span	7/8 span (close to W3)
Ceiling Panel 11_004	131	124	116	117
	123	132	129	125
Ceiling Panel 11_003	147	154*	135*	130
	147	-	132*	135
Ceiling Panel 11_002	133	133	144	129
	141	130*	131*	134
Ceiling Panel 11_001	132	129	131	129
	132	123	122	123

* TC nearby on ceiling

Table 17 shows the CLT samples that were cut from the ceiling and wall panels where the embedded thermocouples were installed. The thickness of the char was 124-154 mm in the ceiling panels, 107-123 mm in the W1 wall panels, and 47-56 mm in the W3 and W4 wall panels. This confirmed the char depth measured by the embedded thermocouples.

Table 17. Char depth (mm) of cut CLT samples in Test 1-6.

CLT cut sample	Remaining thickness (mm)	Char depth (mm)	Image
Test 1-6 Ceiling centre Panel 11_003 (TC 98, 1-7, 100)	51	124	
Test 1-6 Ceiling above Tree 1 Panel 11_002 (TC 86, 87, 88)	36	139	
Test 1-6 Ceiling above Tree 2 Panel 11_003 (TC 89, 90, 91)	21	154	
Test 1-6 Ceiling above Tree 3 Panel 11_003 (TC 92, 93, 94)	42	133	
Test 1-6 Ceiling above Tree 4 Panel 11_002 (TC 95, 96, 97)	44	131	
Test 1-6 W1 – front 0.6 m high Panel 10_010 (TC 62, 63, 64)	66	109	

CLT cut sample	Remaining thickness (mm)	Char depth (mm)	Image
Test 1-6 W1 – rear 0.6 m high Panel 10_007 (TC 65, 66, 67)	68	107	
Test 1-6 W1 – front 1.8 m high Panel 10_010 (TC's 56, 57, 58)	52	123	
Test 1-6 W1 – mid length 1.8 m high Panel 10_009 (TC 49, 8-14, 55)	52	123	
Test 1-6 W1 – rear 1.8 m high Panel 10_007 (TC 59, 60, 61)	53	122	
Test 1-6 W3 – mid length 1.8 m high Panel 10_005 (TC 70, 15-21)	119	56	
Test 1-6 W4 – mid length 1.8 m high Panel 10_002 (TC 79, 22-28)	128	47	

As shown in Figure 99, other than the char formed around the openings, the exterior surface of the CLT panels had char localized at the joint between the W1 wall and ceiling near the ceiling spline locations, Had sealant been used in the joints, the smoke leaked from the W1-ceiling junction could have been reduced and the burn through at the W1-ceiling junction spot and at one of the ceiling spline joints could have been delayed. However, based on the amount of char formed at these locations, the absence of sealant in joints had a negligible impact on the quantification of CLT contribution to the compartment fire.

3.6.7 Contribution of the CLT structure to compartment fire

In addition to the exposed ceiling and W1 wall panels, the protected panels in the W3 and W4 walls contributed to the compartment fire after 125 min. Based on the volume (depth x area) of the CLT charred, which was measured after the test, the CLT panels in the exposed ceiling were estimated to contribute approximately 3020 kg of timber to the fire, the exposed W1 wall panels approximately 1680 kg, and the protected CLT panels in other walls approximately 1070 kg, which translated to 2850 MJ/m^2 fuel load density to the floor area in addition to the movable fuel load.

With the exposed ceiling and W1 wall in Test 1-6, flashover occurred 5 min earlier than in the baseline (Test 1-1). The peak compartment temperatures were similar to the baseline, however, the compartment stayed at the peak temperatures until the end of the test. The heat release rate was higher than the baseline as shown in Figure 100. The heat fluxes to the exterior façade and to the targets away from the opening were much higher than the baseline. There was no decay of the fire during this test. The HRR was close to 10 MW at the end of the test before fire suppression.

By subtracting the baseline, Figure 101 shows the CLT contribution to the heat release rate during Test 1-6. A time shift was made to the baseline in order to line up the flashover time with Test 1-6 for proper subtraction. The CLT structure contributed a maximum of 7.5 MW when only the exposed ceiling and W1 wall were involved in the fire (55 min to 75 min), and a maximum of 10 MW when all ceiling and wall panels were involved in the fire (after 130 min), to the heat release rate.

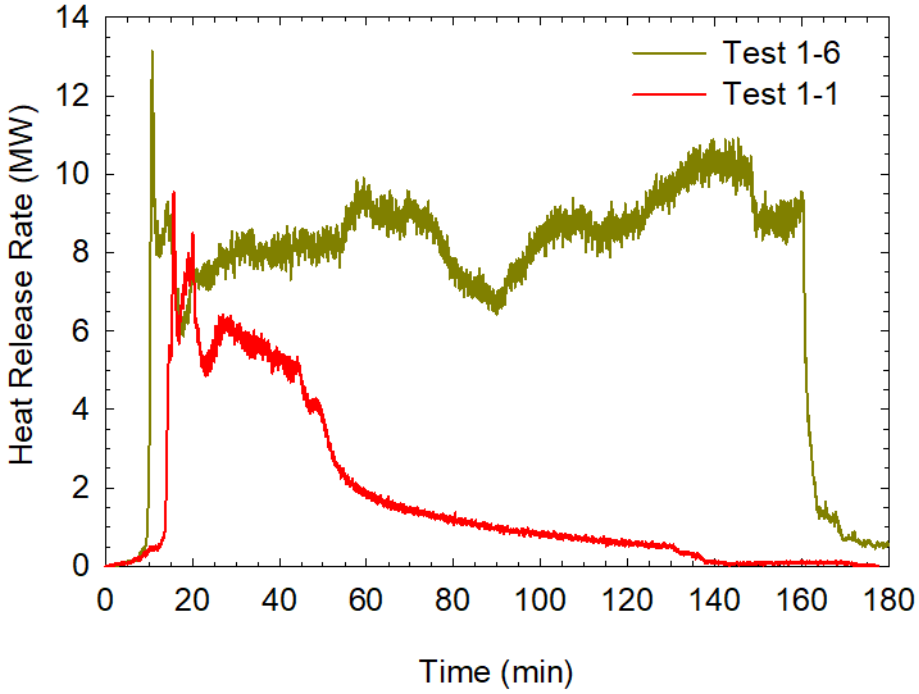

Figure 100. Heat release rate of Test 1-6 superimposed over baseline (Test 1-1).

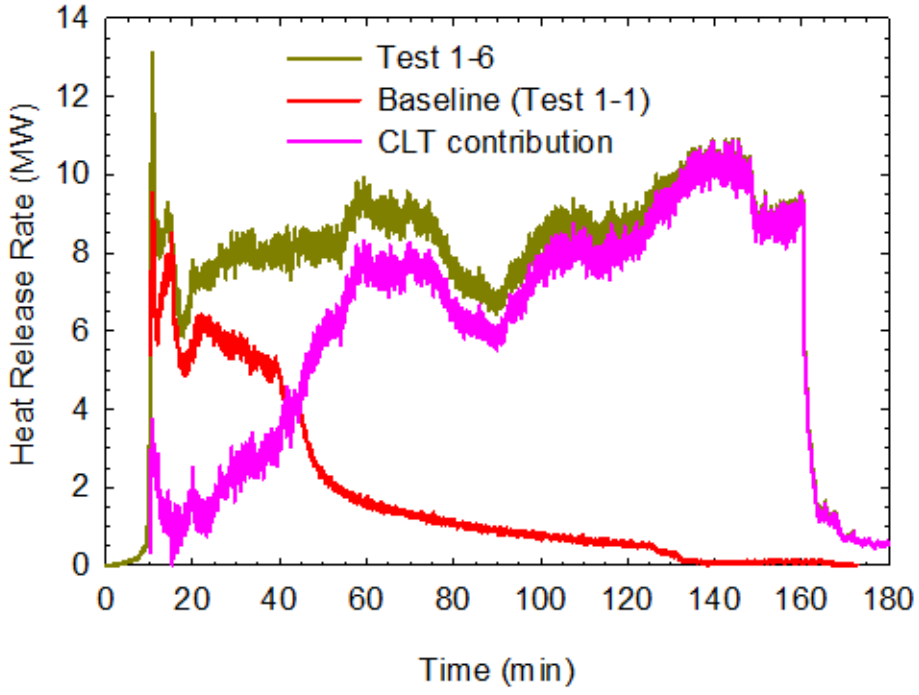

Figure 101. CLT contribution to heat release rate in Test 1-6 (baseline time shifted).

3.7 Responses of Simulated Thermal Elements

Although the CLT compartment fire tests were conducted without sprinklers, simulated thermal elements (STE) donated by FM Global were used in the tests to replicate the time temperature response of a quick-response (QR) sprinkler element. In each test, ten STEs were installed at various locations. Between 1.2 min and 5.8 min, all the STEs reached 68 °C (a typical temperature rating for residential sprinklers). Figure 102 shows the temperature profiles measured using the STEs in each test. Table 18 shows the timing for each STE to reach the temperature of 68 °C. At these times, the fires in the tests were still limited to the first item ignited. Had sprinklers been installed in the tests, flashover would not have occurred with effective sprinkler operations.

Table 18. Simulated thermal element activation times.

		Simulated Thermal Element (STE)									
		STE_1	**STE_2**	**STE_3**	**STE_4**	**STE_5**	**STE_6**	**STE_7**	**STE_8**	**STE_9**	**STE_10**
Distance below ceiling, mm	-	305	305	305	457	305	305	305	457	305	305
Distance from ignition source, mm	X	6052	2275	9100	9100	6620	2275	0	0	6052	2275
	Y	0	0	1000	1000	2300	2300	2300	2300	4600	4600
	Z	2395	2395	2395	2243	2395	2395	2395	2243	2395	2395
	Diagonal	6509	3303	9463	9426	7406	4025	3321	3213	7970	5663
		Time to exceed 68 °C, s									
	Test 1-1	131	77	324	307	226	97	113	266	187	160
	Test 1-2	152	101	262	278	189	114	92	234	145	113
	Test 1-3	240	141	350	349	341	214	144	271	336	210
	Test 1-4	128	82	210	203	155	102	76	177	135	105
	Test 1-5	111	74	213	205	160	91	90	198	130	114
	Test 1-6	151	96	231	236	187	111	106	235	156	115
	Mean	152	95	265	263	210	122	104	230	182	136
	SD	46	25	59	59	69	46	24	37	78	41

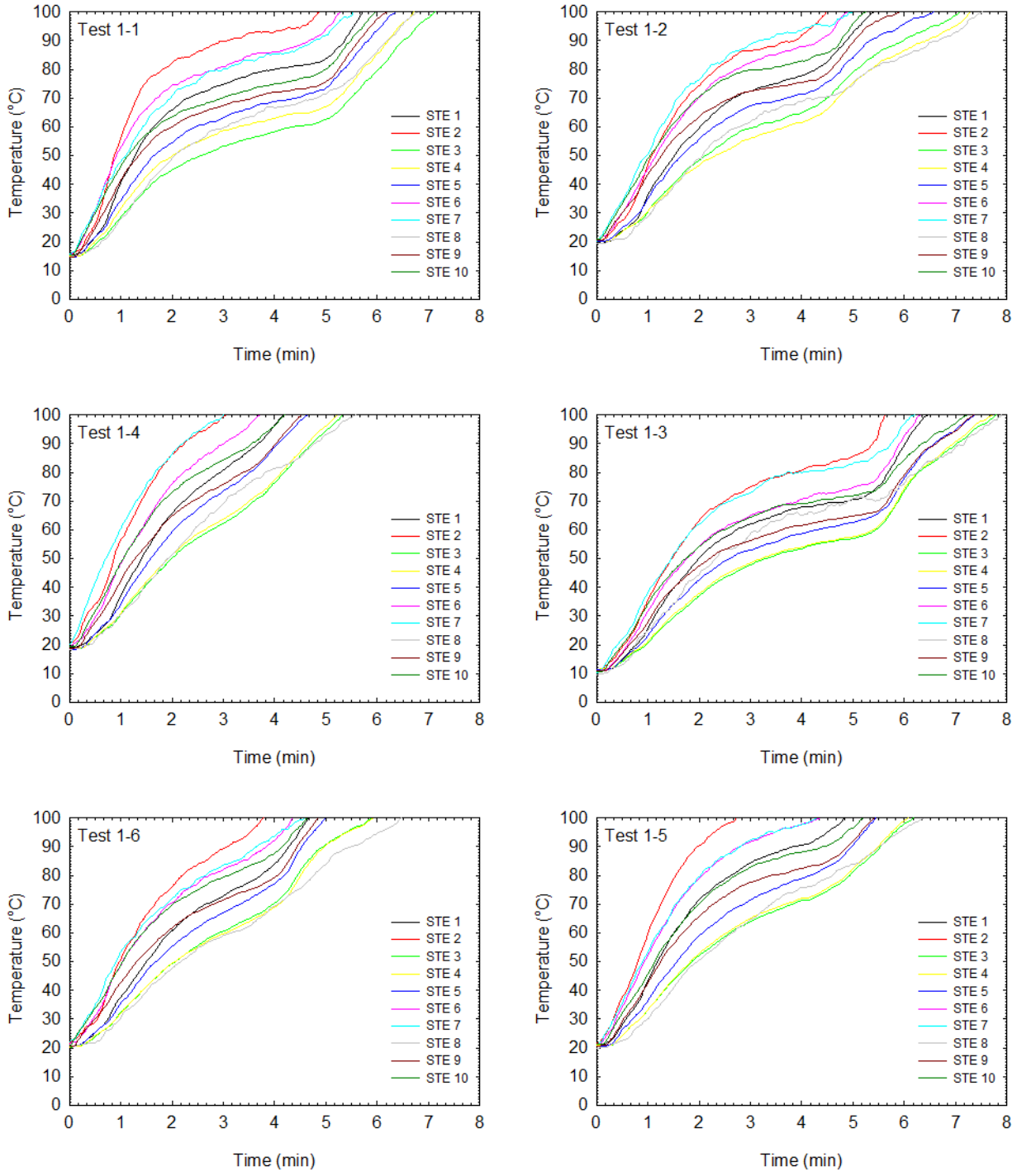

Figure 102. Responses of simulated thermal elements (STE's) in CLT compartment tests.

4. SUMMARY AND CONCLUSIONS

As part of Phase 2 of the FPRF project, a series of six large CLT compartment fire tests were conducted, with the goal to quantify the contribution of CLT building elements to the compartment fires. The fire tests were conducted without sprinklers and without firefighting intervention until the end of the tests in order to achieve this goal. Note that it would be the typical arrangement and requirement for tall wood buildings to be equipped with automatic sprinklers in North America.

The CLT compartment fire tests produced a large amount of technical data, including the heat release rate, interior and exterior heat fluxes, gas and flow conditions, temperatures inside and outside the compartment, temperatures between gypsum board layers and inside the CLT structural panels, as well as char depth, etc., under various exposure conditions. The fire test data was analyzed to quantify the contribution of CLT building elements to the compartment fires, with the following conclusions.

Test 1-1 and Test 1-2, with fully protected CLT compartments, defined the contribution of the movable fire load to the compartment fires and provided baselines to quantify the CLT contribution to the compartment fires in the tests involving various amounts of exposed CLT surfaces. Fully protecting the CLT compartments using gypsum board as the physical barrier was an effective means to delay and/or prevent the ignition and involvement of the timber structural elements in the fires, limiting and/or eliminating their contribution to the fires. In baseline Test 1-1, the three-layer gypsum board system completely prevented the ignition and involvement of the CLT structural elements in the fire and performed as well as non-combustible structural systems. In baseline Test 1-2, the two-layer gypsum board system successfully protected the CLT structure and limited the impact of the fire on the CLT structure with only surface char (less than 15 mm) in the rear section of the ceiling but no contribution to the compartment fire.

Ventilation conditions had significant impacts on the fire development in the compartments. In baseline Test 1-2, the larger ventilation opening accelerated combustion of the room contents, which intensified the exterior exposure, while shortening the intense burning duration. The peak temperatures and the heat fluxes inside the fire compartments were similar in both baseline tests but the fire decayed earlier in Test 1-2 with the larger opening. The heat release rate was higher but more intense burning occurred outside the fire compartment in Test 1-2 with the larger opening. The larger opening increased exterior fire exposure, which would have implications on the exterior façade and adjacent buildings. The smaller opening, as used in Test 1-1, delayed the onset of the decay phase, thereby extending the duration of the fully-developed phase.

Partially exposed CLT structure in Test 1-3, Test 1-4, Test 1-5 and Test 1-6 contributed to compartment fires to an extent depending on the area and orientation of exposed CLT surface and ventilation conditions. Note that Test 1-3 was terminated at 242 min (over 4 h), later than Test 1-4, Test 1-5 and Test 1-6. The impact of the ventilation opening size on CLT contribution to the compartment fires was clearly demonstrated by Test 1-3 and Test 1-5 with the same long wall exposed (W1 wall). The peak temperatures in the compartments were similar in both tests. However, the heat release rate and exterior heat fluxes were higher, and the fire exhibited a general trend of decay in Test 1-3 with the larger ventilation opening although there were two small transient increases due to the delamination of two plies of CLT from the exposed wall. In Test 1-5, with the smaller ventilation opening, more heat was trapped inside the compartment and, after the initial decay, a large re-flash occurred on the exposed wall with delamination of the second ply of the CLT, which caused the second flashover and induced the full involvement of the ceiling and all other walls in the fire. Over the full test duration, the volume (depth x area)

of the CLT charred in Test 1-5 with the smaller opening, was approximately 3.6 times of that in Test 1-3 with the larger opening although Test 1-5 was terminated 40 min earlier than Test 1-3.

In all the tests with the exposed CLT surface, flashover occurred earlier than in the baseline. The exposed CLT panels translated to more fuel loads in addition to the movable fuel load (room contents) in the compartment. The peak compartment temperatures were similar to the baseline. However, the heat release rates and heat fluxes to the exterior façade were higher than the baseline. Other than Test 1-3, which had the larger opening and exhibited a general trend of decay, all tests with exposed CLT surface either had a second flashover due to the re-flash on the exposed surface or an intense fire continuously without any decay period. The heat-release-rate curves of the tests are given in Figure 103, while the total heat releases are shown in Figure 104. The data presented in these figures include contribution from both the contents and the CLT. The quantified contributions of the partially exposed CLT to the compartment fires are illustrated by Figure 105.

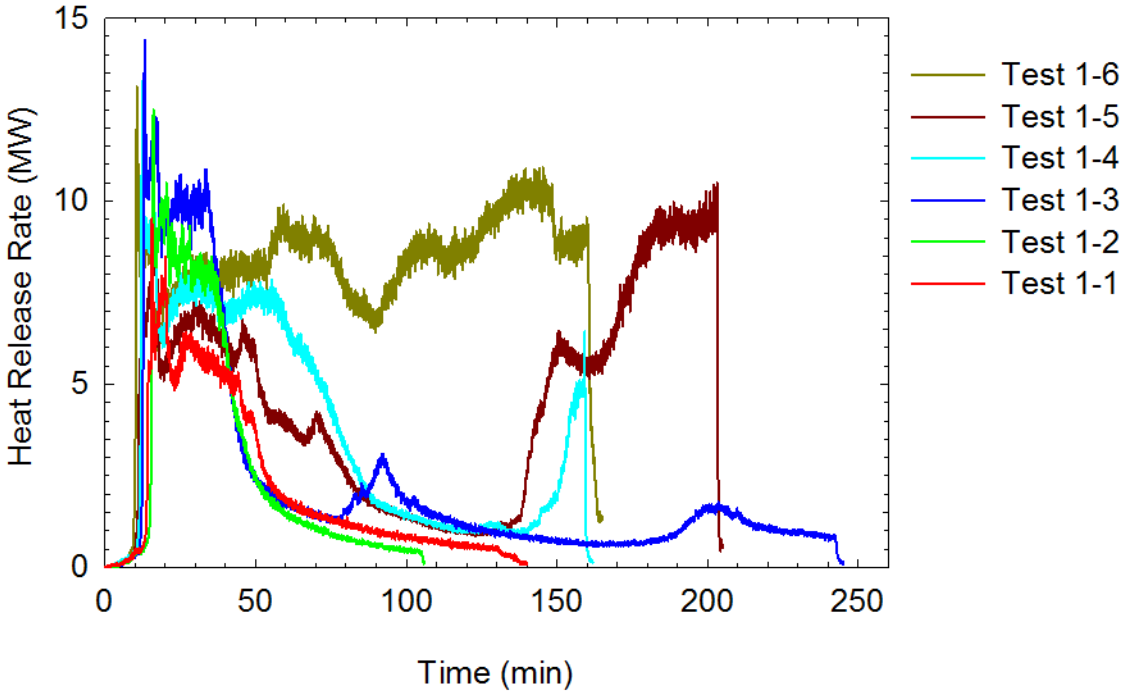

Figure 103. Heat release rates in CLT compartment tests.

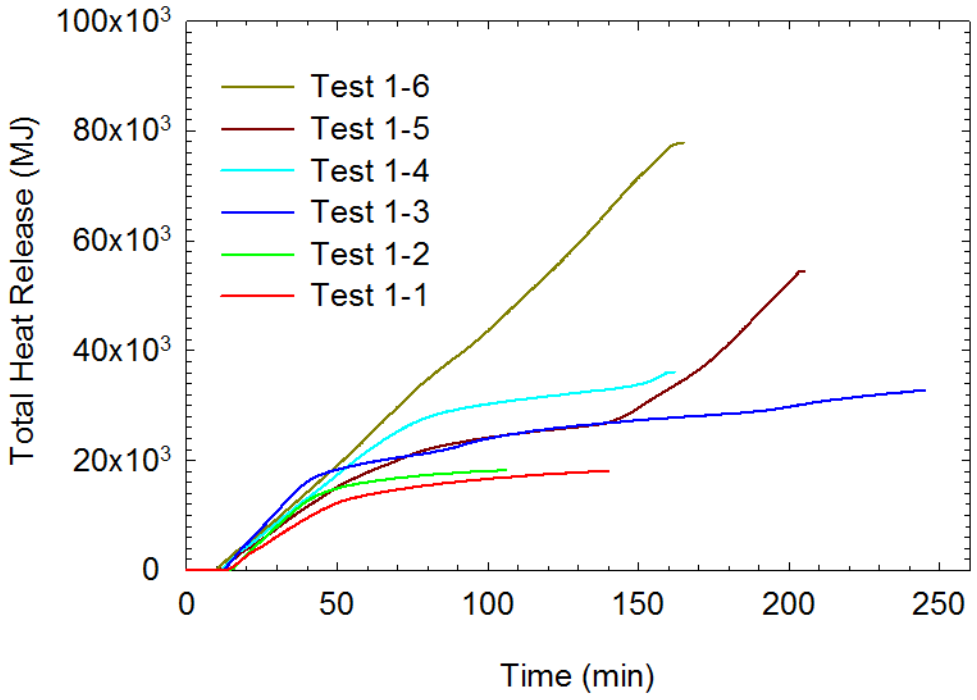

Figure 104. Total heat releases in CLT compartment tests.

Figure 105 shows the heat release rates attributed to the CLT contributions. The quantified values for the CLT contributions are derived from Figure 70, Figure 79, Figure 89 and Figure 101. The peak contributions to HRR, associated times, attributed CLT panels and surface areas are illustrated in Figure 105. For Test 1-5, only the W1 wall was involved in the fire initially, however, all walls and ceiling were involved in the fire at a later stage. Therefore, Figure 105 includes two data entries from Test 1-5 – the peak when only the W1 wall panels were contributing during the first 70 min, and the peak when all the CLT panels in the compartment were contributing during the last 10 min (see Figure 89). Similarly, Figure 105 has two data entries from Test 1-6 – the peak when only the W1 wall and ceiling panels were contributing during the first 75 min, and the peak when all the CLT panels in the compartment were contributing during the last 25 min (see Figure 101). Two curves fitting the data points are plotted in Figure 105 for the two ventilation conditions. The CLT contribution to the compartment fire increased with the increasing surface area of the CLT panels that were involved in the fires, and was also influenced by the ventilation condition.

The CLT panels used in this series of the compartment tests were manufactured using 2 x 4 SPF lumber glued with a polyurethane adhesive (with a brand name of HBE). The delamination of unprotected (exposed) CLT panels led to re-flare and/or re growth of the fire after a period of decay in Test 1-3, Test 1-4 and Test 1-5 and no decay of the fire in Test 1-6.

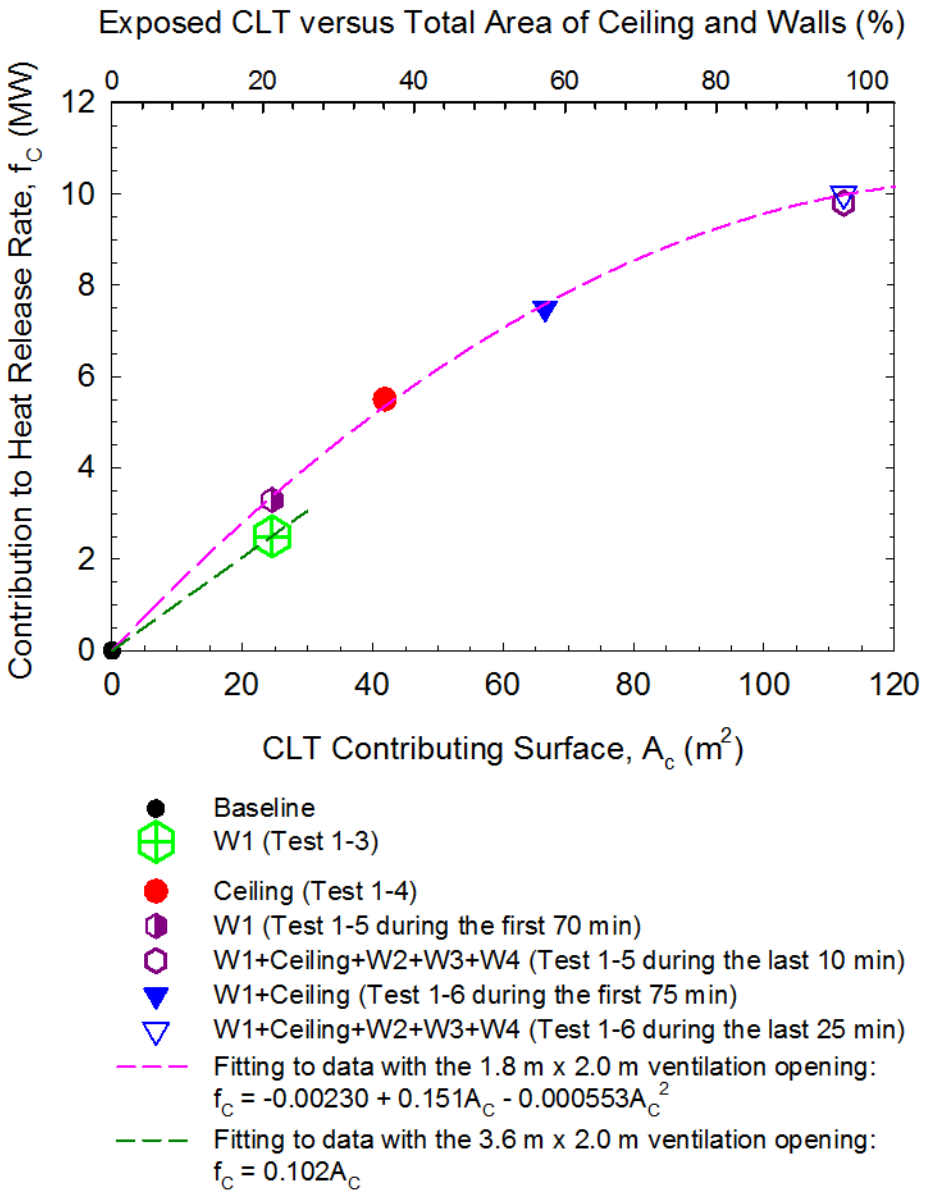

Figure 105. CLT contributions to heat release rates in compartment tests.

During Test 1-3, Test 1-5 and Test 1-6, the heat flux measured at 2.4 m and 4.8 m away from the rough opening reached 60 kW/m^2 and 25 kW/m^2, respectively. During Test 1-3, a video camera positioned at 9 m away from the opening was damaged due to its polycarbonate casing melting. Based on the configuration factor, the heat flux would be 9 kW/m^2 at the camera location (9 m away). To support the fire service request for a large opening factor, a stand-off distance should be at least 12 m away from the rough opening for staging firefighting as the heat flux would be attenuated to 5 kW/m^2 at 12 m away from the opening.

Although the CLT compartment fire tests were conducted without sprinklers, simulated thermal elements (STE) donated by FM Global were used in the tests to predict the time temperature response of a quick-response sprinkler element. In all the tests, the STEs reached 68 °C (a typical temperature rating for residential sprinklers) in between 1.2 min and 5.8 min while the fires were still limited to the first item ignited (the console table). Had sprinklers been installed in the tests, flashover would not have occurred with effective sprinkler operations. Recent fire tests, conducted in support of code development efforts of the International Code Council's Ad Hoc Committee on Tall Wood Buildings by US Department of Agriculture's Forest Products Laboratory at the Bureau of Alcohol, Tobacco, Firearms, and Explosives Fire Test Laboratory collected additional data on the effectiveness of sprinklers in controlling and suppressing fires in fully exposed CLT compartments [9].

The CLT compartment fire test data from this FPRF project can be used to compare the fire performance of CLT structural systems with other types of structural systems used in tall buildings, to validate design equations and to develop a fire protection strategy to mitigate potential fire hazards to occupants, fire fighters and properties. As part of Phase 2 of the FPRF project, the test data is being used to develop and validate a modeling tool for predicting the influence of exposed CLT elements on the severity and duration of compartment fires.

5. FURTHER WORK

Heat delamination of the exposed CLT affected its fire performance as observed in this series of the large-scale compartment fire tests. Further study is necessary to quantify the contribution of the CLT structural members that do not exhibit heat delamination. Reduced-scale fire tests are currently being conducted as part of the FPRF project to further study the delamination behavior of CLT with different adhesive types using the heat exposure conditions from Test 1-4 described in this report.

Acknowledgments

The authors gratefully acknowledge the auspices of the Fire Protection Research Foundation and the technical oversight of its Project Technical Panel. Financial support from the Fire Protection Research Foundation, Property Insurance Research Group, U.S. Department of Agriculture, U.S. Forest Service, American Wood Council, and National Research Council Canada is gratefully acknowledged. Donations of STE devices from FM Global and gypsum board from USG Corporation are also gratefully acknowledged.

The authors acknowledge Daniel Brandon and Birgit Östman of the RISE Research Institutes of Sweden for their valuable contributions to the test planning. The authors would like to thank technical and research staff of the National Research Council Canada and the National Institute of Standards and Technology: Ryan Kroeker, Michael Ryan, Yoon Ko, Eric Gibbs, Johnathon Gillis, Steve Cassidy, Daniel Frampton, Audrey Roy-Poirier and Lisette Seguin of NRCC, Artur Chernovsky, Laurean DeLauter, Anthony Chakalis, Marco Fernandez, Philip Deardorff, Brian Story, Doris Rinehart and Rodney Bryant of NIST, for their contributions to the fire testing.

References

1. Su, J.Z. and Lougheed, G.D. Fire Safety Challenges of Tall Wood Buildings – Phase 2, Test Options for Task 2 – A Discussion Paper, CLIENT REPORT A1-006599-03.1, National Research Council Canada, Ottawa, Ontario, 2016.

2. Su, J.Z. and Lougheed, G.D. Fire Safety Challenges of Tall Wood Buildings – Phase 2, Test Options for Task 2 – Second Discussion Paper, CLIENT REPORT A1-006599-03.2, National Research Council Canada, Ottawa, Ontario, 2016.
3. Su, J.Z. and Lougheed, G.D. Test Plan for Fire Safety Challenges of Tall Wood Buildings - Phase 2, CLIENT REPORT A1-006599-03.3 (revised version, 14 September 2016), National Research Council Canada, Ottawa, Ontario, 2016.
4. Brandon, D. and Östman, B. FPRF Project Fire Safety Challenges of Tall Wood Buildings – Phase 2, Task 1 – Literature review: The contribution of CLT to compartment fires, SP Technical Research Institute of Sweden, 2015.
5. Brandon, D. and Östman, B. FPRF Project Fire Safety Challenges of Tall Wood Buildings – Phase 2, Task 2 – Test plan, modeling: The contribution of CLT to compartment fires, SP Technical Research Institute of Sweden, 2016.
6. NFPA 13. Standard for the Installation of Sprinkler Systems, National Fire Protection Association, Quincy, MA, 2016.
7. NFPA 1710. Standard for the Organization and Deployment of Fire Suppression Operations, Emergency Medical Operations, and Special Operations to the Public by Career Fire Departments, National Fire Protection Association, Quincy, MA, 2016.
8. NFPA 1720. Standard for the Organization and Deployment of Fire Suppression Operations, Emergency Medical Operations and Special Operations to the Public by Volunteer Fire Departments, National Fire Protection Association, Quincy, MA, 2014.
9. Zelinka, S.L., Hasburgh, L.E., Bourne, K.J., Tucholski, D.R., Ouellette, J.P. Compartment fire testing of a two-story cross laminated timber (CLT) building. General Technical Report FPL-GTR-247. Madison, WI: U.S. Department of Agriculture, Forest Service, Forest Products Laboratory. (In press)
10. Bundy, M., Hamins, A., Gross, J., Grosshandler, W. and Choe, L. Structural Fire Experimental Capabilities at the NIST National Fire Research Laboratory, Fire Technology, Volume 52, 2016, pp. 959–966.
11. Sumathipala, K. Fire Safety Challenges of Tall Wood Buildings- Phase 2, Review of Contribution of Mass Timber Surfaces to Compartment Fires, American Wood Council, January 31st, 2016.
12. ANSI/APA PRG 320-2012. Standard for Performance-Rated Cross-Laminated Timber, American National Standards Institute, 2012.
13. Bwalya, A., Gibbs, E., Lougheed, G. and Kashef, A. Characterization of Fires in Multi-Suite Residential Dwellings - Part 1: A Compilation of Post-Flashover Room Fire Test Data, Research Report, National Research Council Canada, Ottawa, Ontario, 2013.
14. Su, J.Z. and Lougheed, G.D. REPORT TO RESEARCH CONSORTIUM FOR WOOD AND WOOD-HYBRID MID-RISE BUILDINGS: Fire Safety Summary – Fire Research Conducted for the Project on Mid-Rise Wood Construction, CLIENT REPORT A1- 004377.1, National Research Council, Ottawa, Ontario, 2014.
15. Bwalya, A., Lougheed, G., Kashef, A. and Saber, H. Survey Results of Combustible Contents and Floor Areas in Canadian Multi-Family Dwellings, Fire Technology, Volume 47, 2011, pp. 1121-1140.
16. Janssens, M. CLT compartment fire test results, webinar, American Wood Council, 2015.

17. The SFPE Handbook of Fire Protection Engineering, ed. P.J. DiNenno, D. Drysdale, C.L. Beyler, W.D. Walton, R.L.P. Custer, J.R. Hall, Jr. and J.M. Watts, Jr., 3rd edition, Society of Fire Protection Engineers/National Fire Protection Association, Quincy, Massachusetts, 2002.
18. Bundy, M.F., Hamins, A., Johnsson, E.L., Kim, S.C., Ko, G.H. and Lenhert, D.B. Measurements of Heat and Combustion Products in Reduced-Scale Ventilation-Limited Compartment Fires, National Institute of Standards and Technology, NIST TN 1483, 2007.
19. EN 1363-1 (2012). Fire Resistance Tests - Part 1 General Requirements, Brussels.
20. ISO 834. Fire resistance tests -- Elements of building construction, International Organization for Standardization, Geneva.
21. Häggkvist, A., Sjöström, J. and Wickström, U. Using plate thermometer measurements to calculate incident heat radiation, Journal of Fire Science 31 (2013) p. 166–177.
22. ASTM E3057-16. Standard Test Method for Measuring Heat Flux Using Directional Flame Thermometers with Advanced Data Analysis Techniques, ASTM International, West Conshohocken, PA, 2016.
23. McCaffrey, B.J. and Heskestad, G. Robust Bidirectional Low-Velocity Probe for Flame and Fire Applications, Combustion and Flame 1125-127 (1976).
24. ISO 13571. Life-threatening Components of Fire-Guidelines for the Estimation of Time Available for Escape Using Fire Data, International Organization for Standardization, Geneva, 2007.
25. ASTM E119-15. Standard Test Methods for Fire Tests of Building Construction and Materials, ASTM International, West Conshohocken, PA, 2015.
26. CAN/ULC-S101-14. Standard Methods of Fire Endurance Tests of Building Construction and Materials, ULC Standards, National Standard of Canada, ULC Standards, Ottawa, ON, 2014.
27. Su, J.Z. Fire Endurance of Exposed Cross-Laminated Timber Floor for Tall Buildings, CLIENT REPORT A1-008570.1, National Research Council, Ottawa, Ontario, 2016.

Appendix A - Instrumentation and gypsum board layout

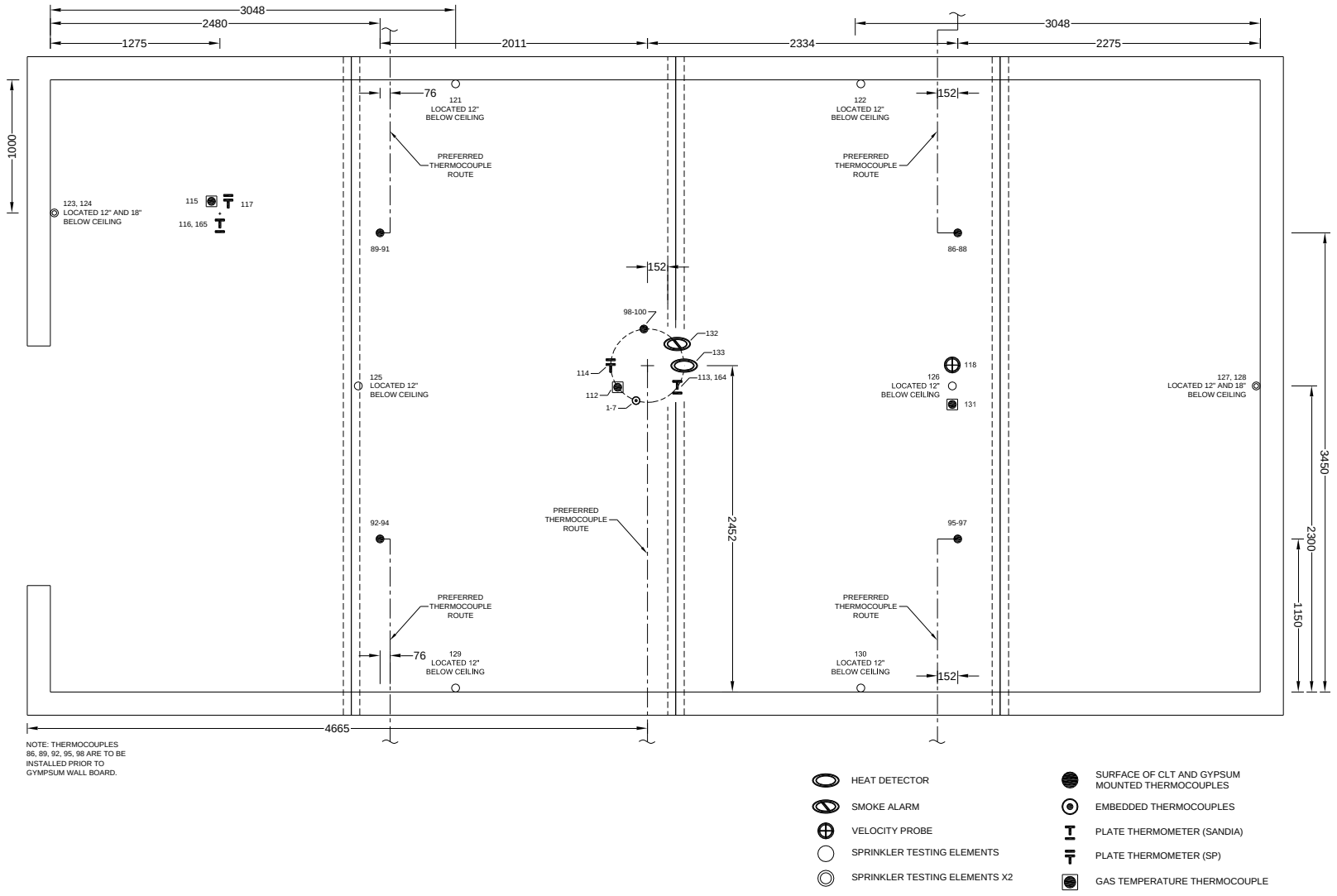

Figure A 1. Test 1-1 Large Compartment CLT - Ceiling - Instrumentation Layout

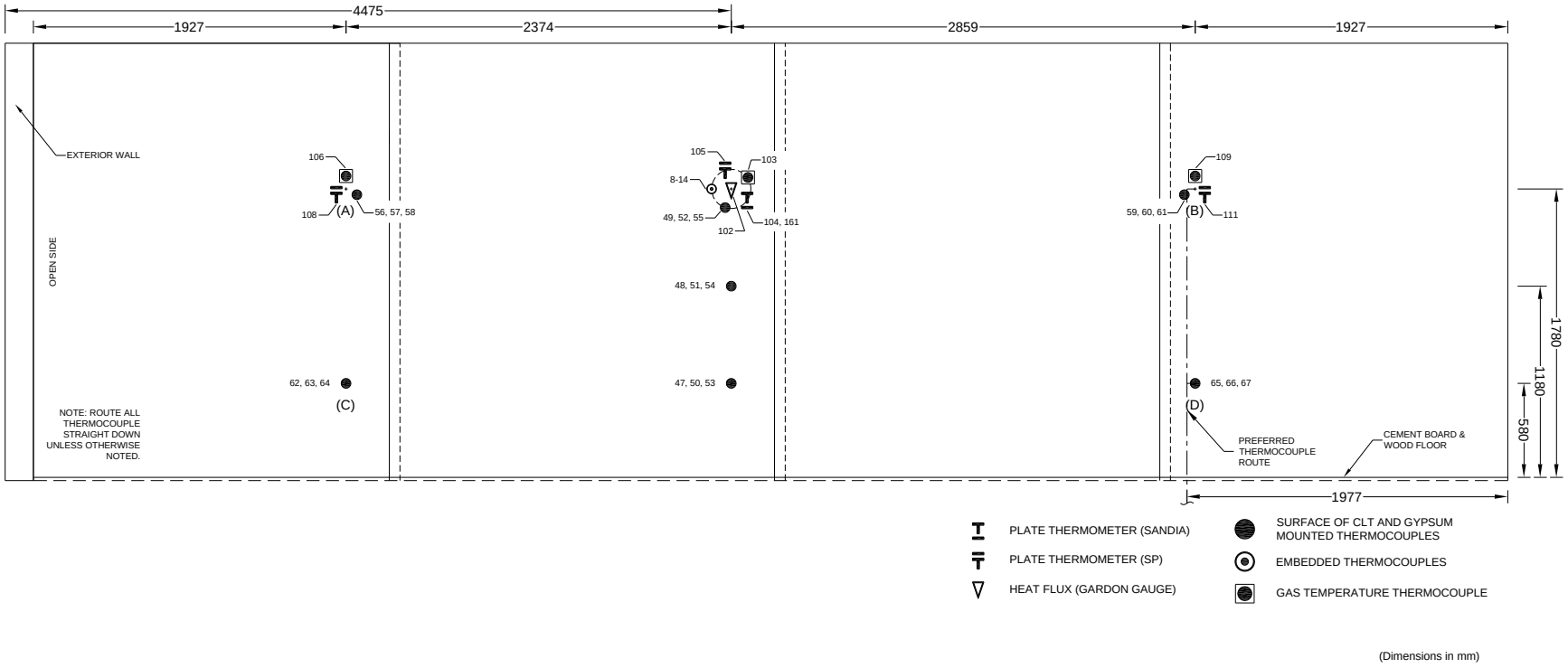

Figure A 2. Test 1-1 Large Compartment CLT - W1 - Instrumentation Layout

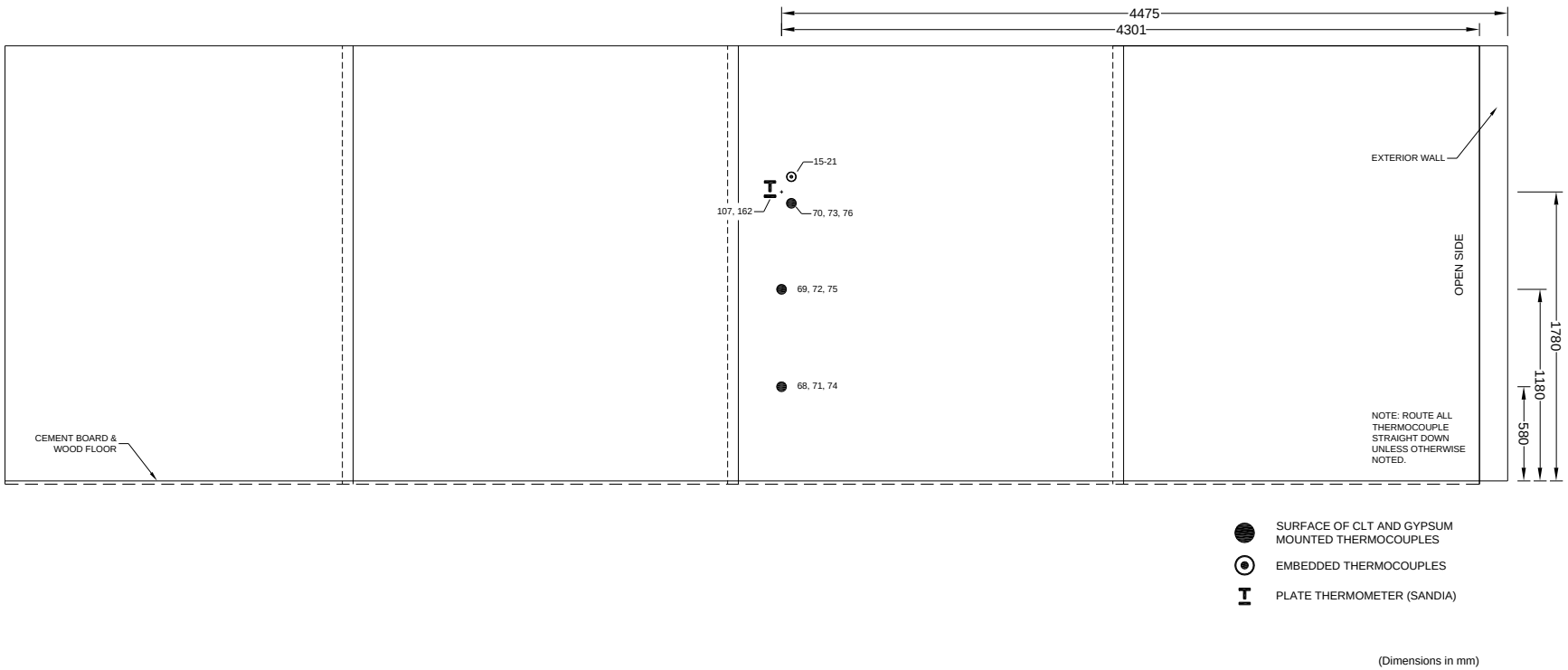

Figure A 3. Test 1-1 Large Compartment CLT - W3 - Instrumentation Layout

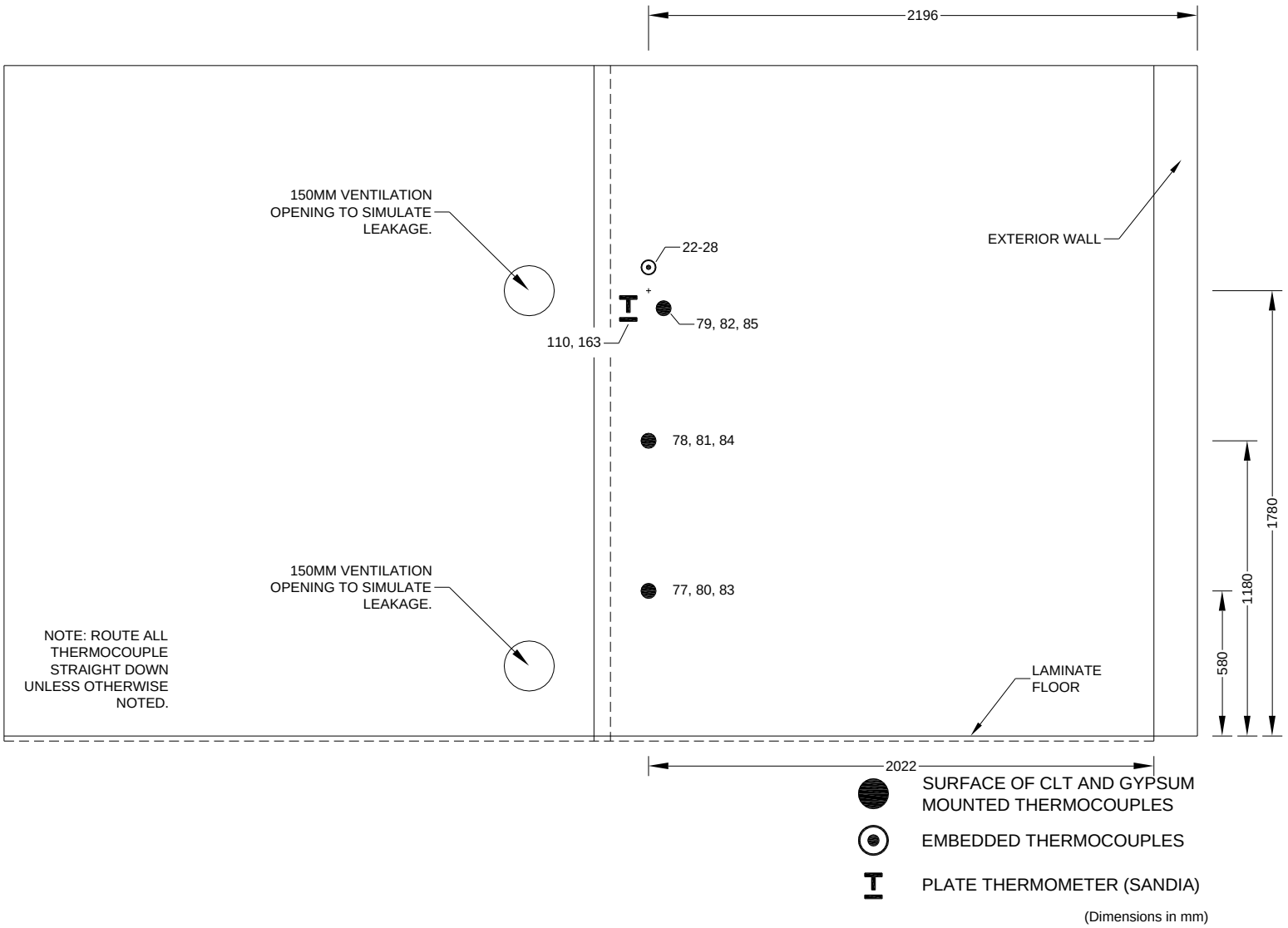

Figure A 4. Test 1-1 Large Compartment CLT - W4 - Instrumentation Layout

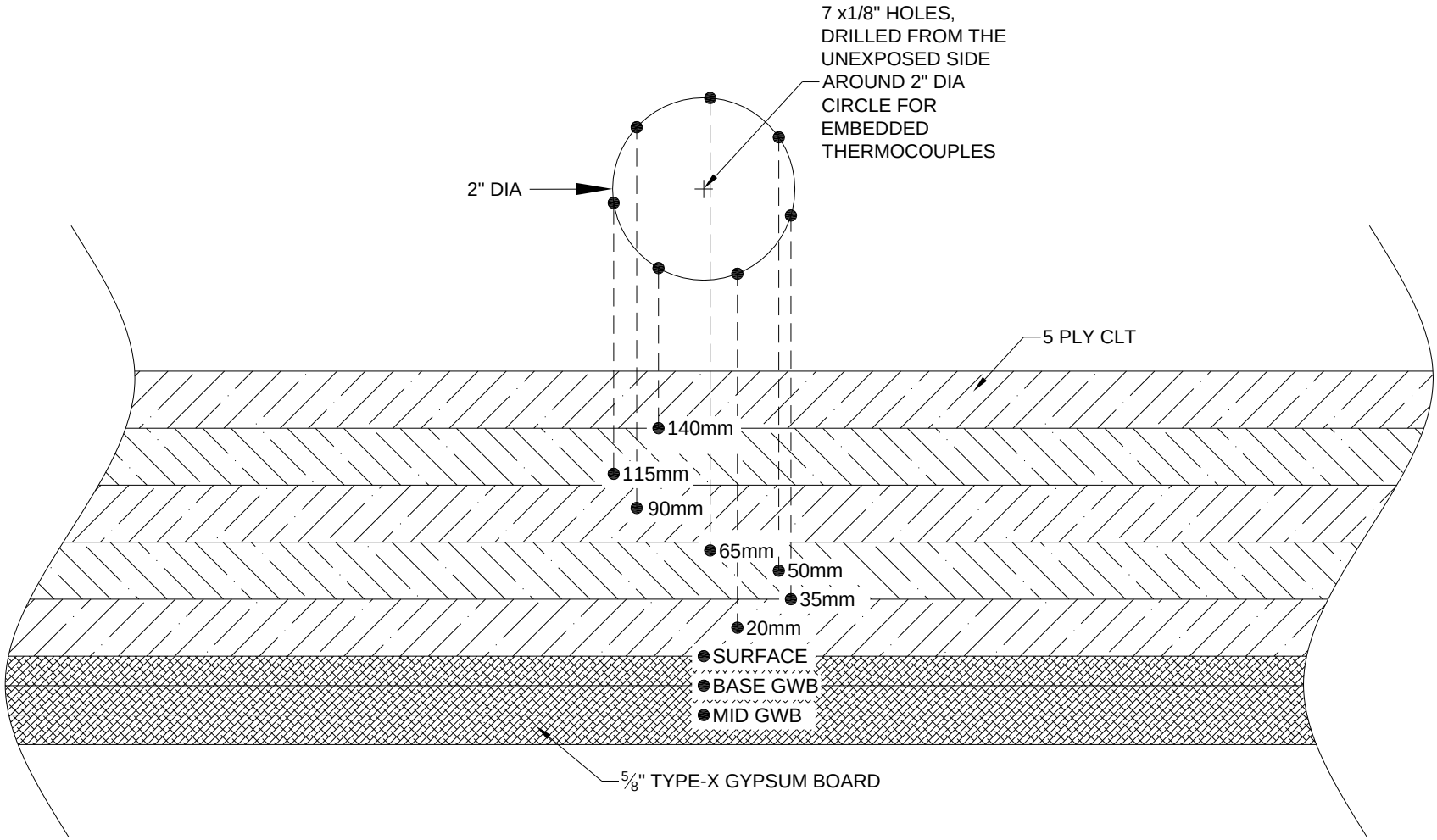

Figure A 5. Test 1-1 Large Compartment CLT - Embedded Thermocouple Detail

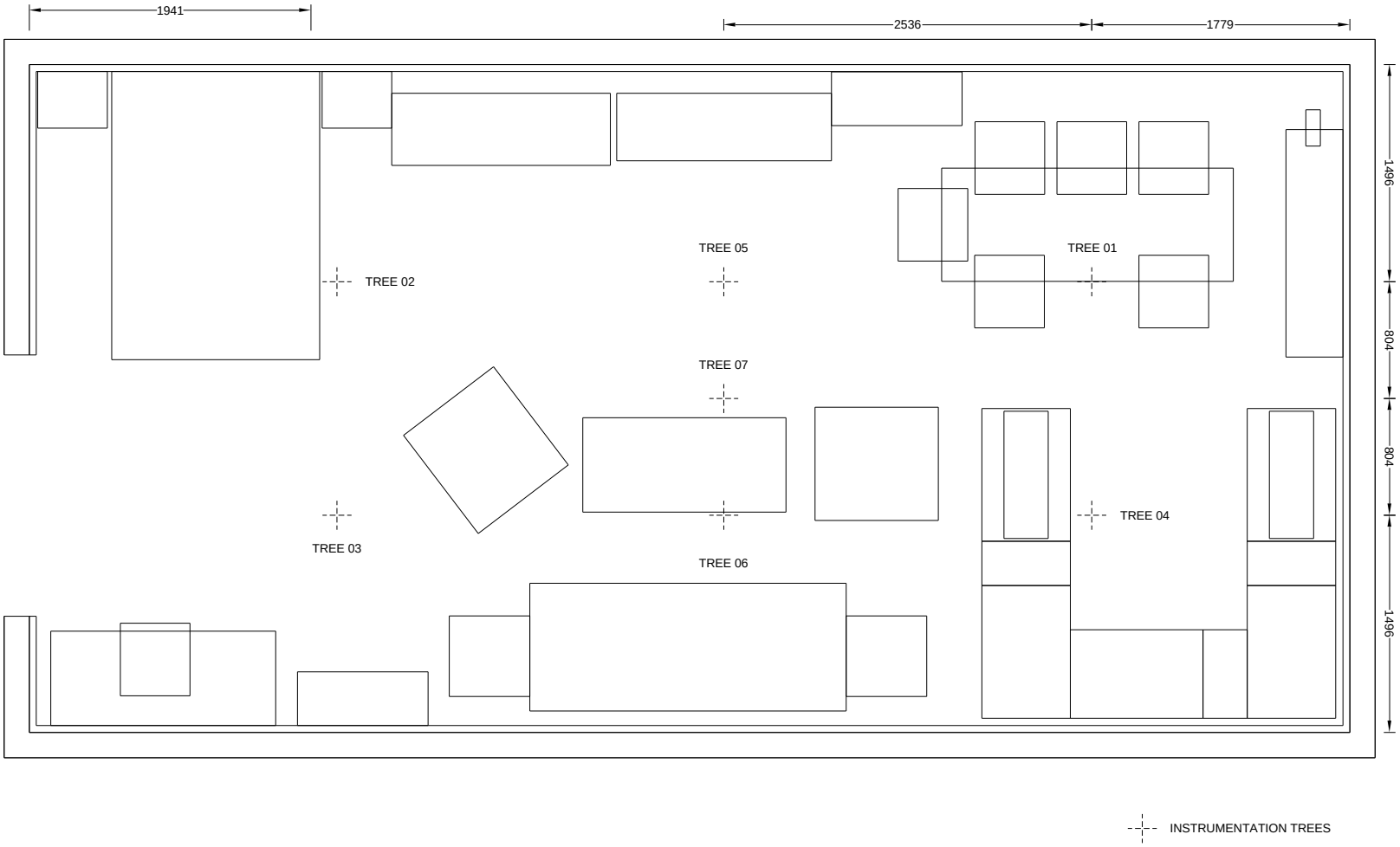

Figure A 6. Test 1-1 Large Compartment CLT - Instrumentation Tree Layout

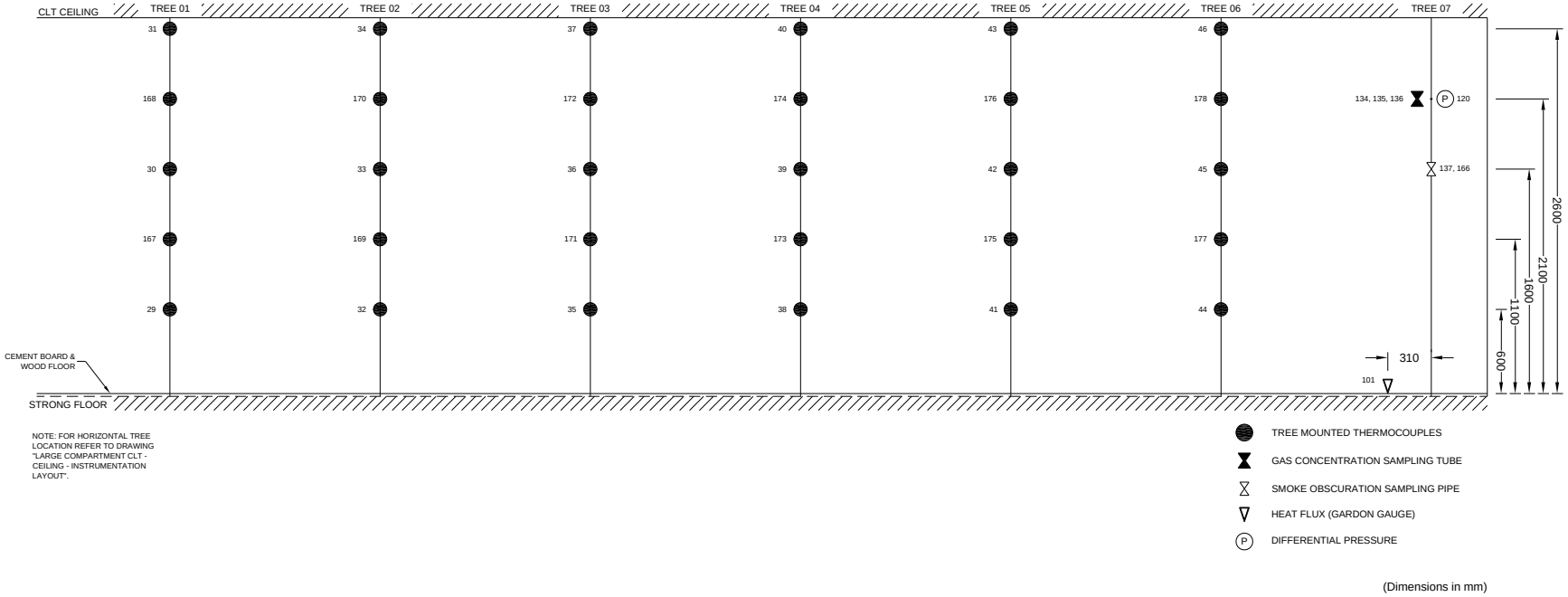

Figure A 7. Test 1-1 Large Compartment CLT - Instrumentation Tree Specifications

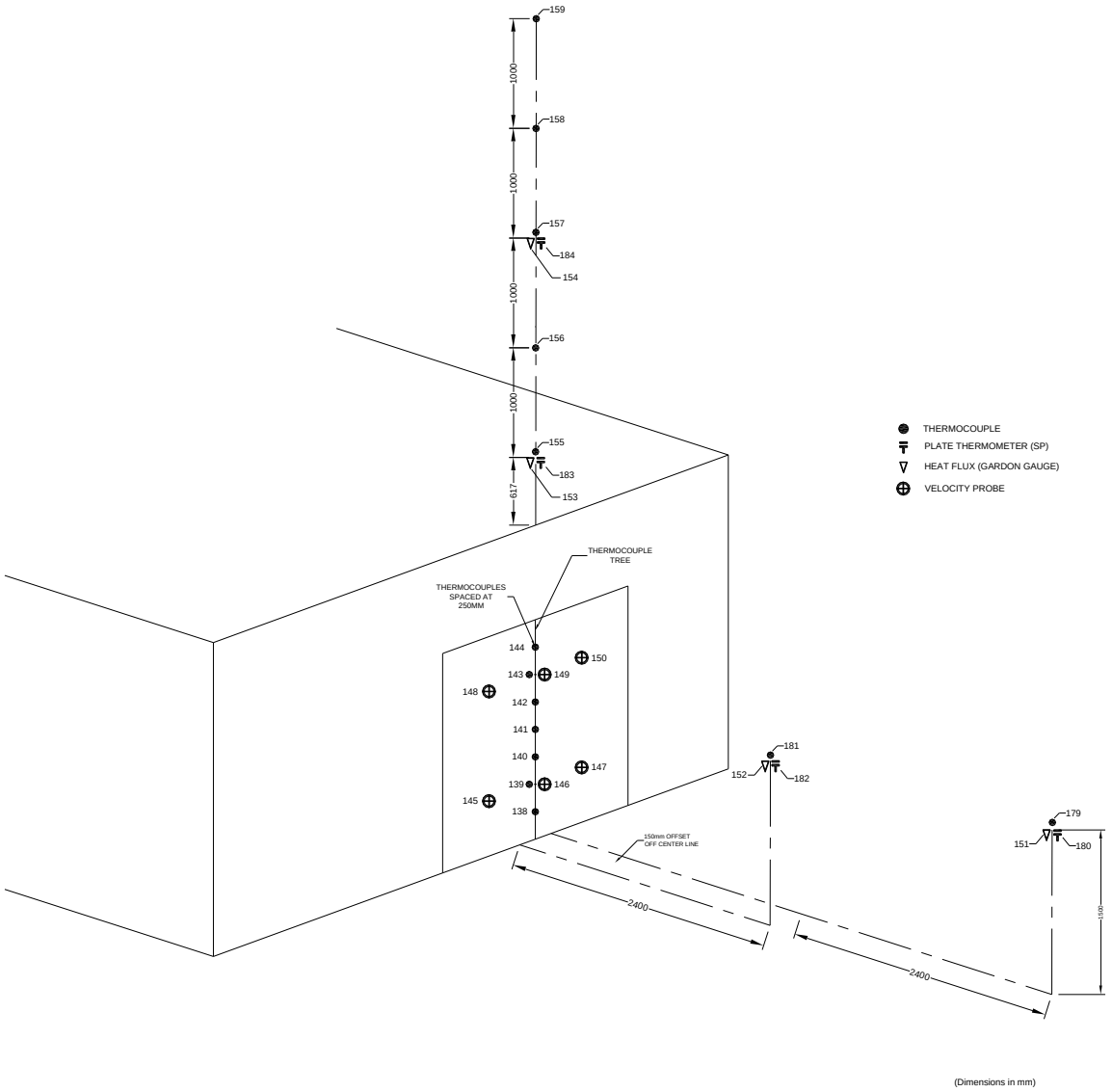

Figure A 8. Test 1-1 Large Compartment CLT - Exterior Instrumentation Layout

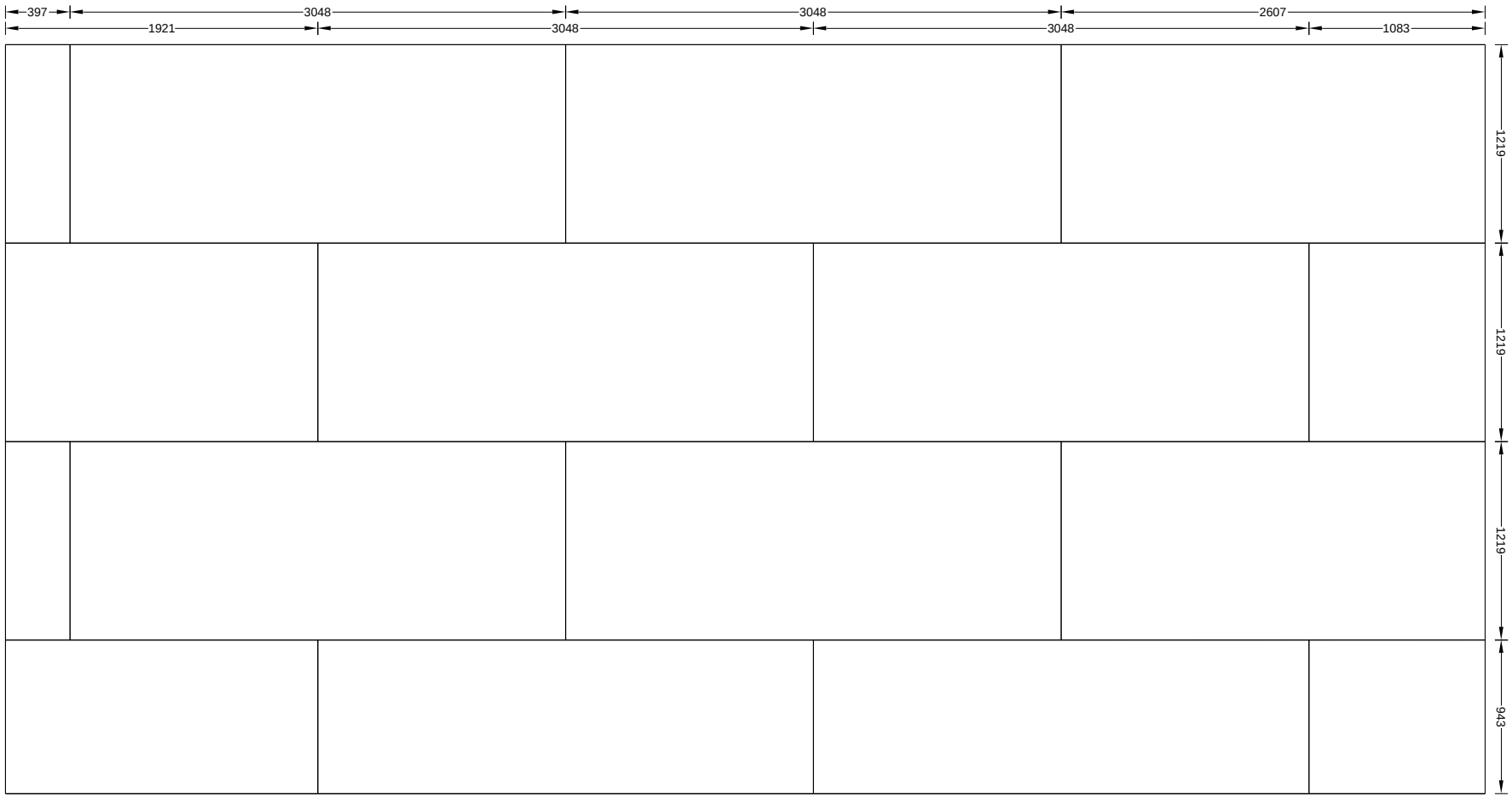

Figure A 9. Test 1-1 Large Compartment CLT - Ceiling - Gypsum Layout - Base Layer

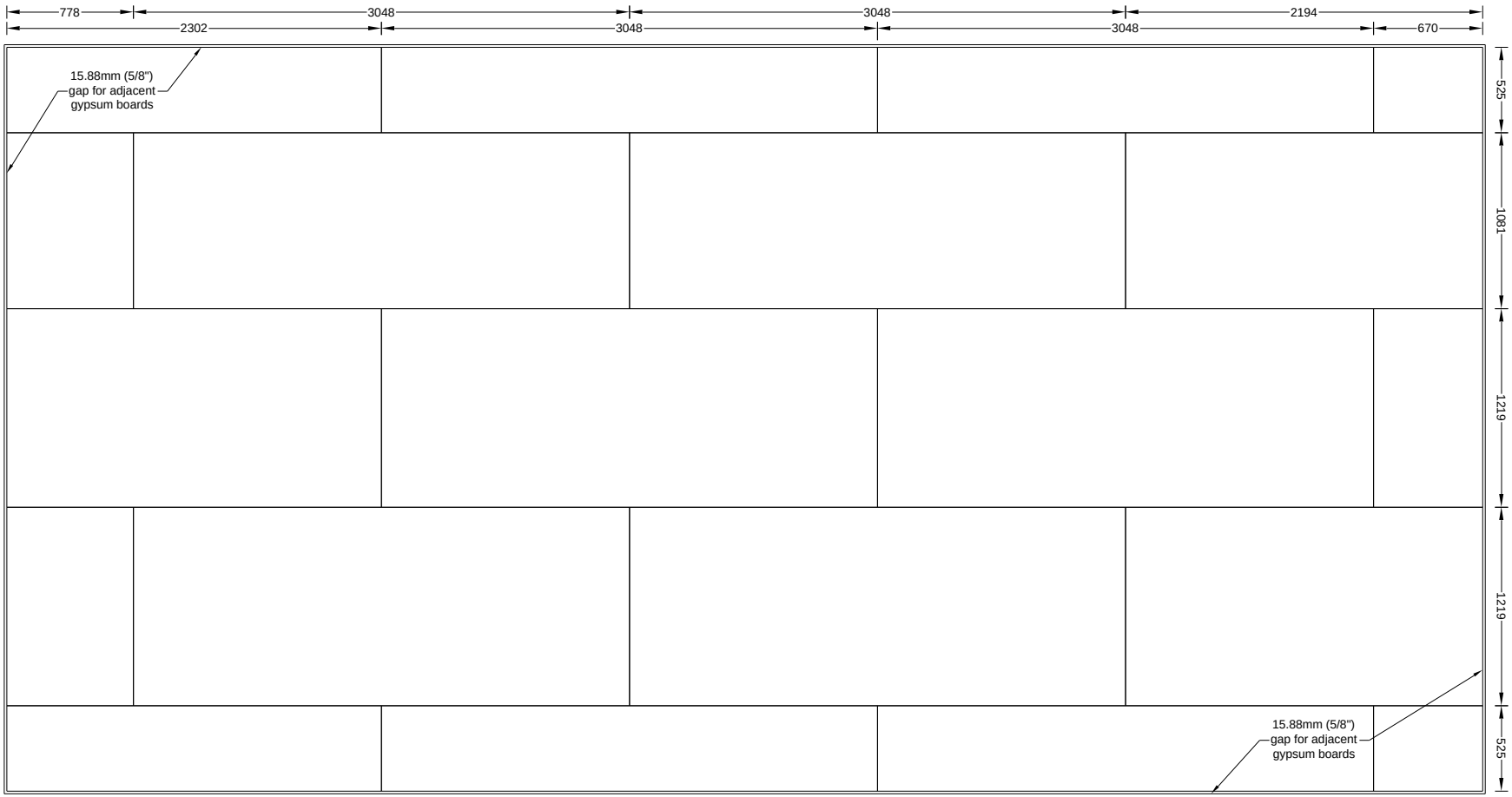

(Dimensions in mm)

Figure A 10. Test 1-1 Large Compartment CLT - Ceiling - Gypsum Layout - Middle Layer

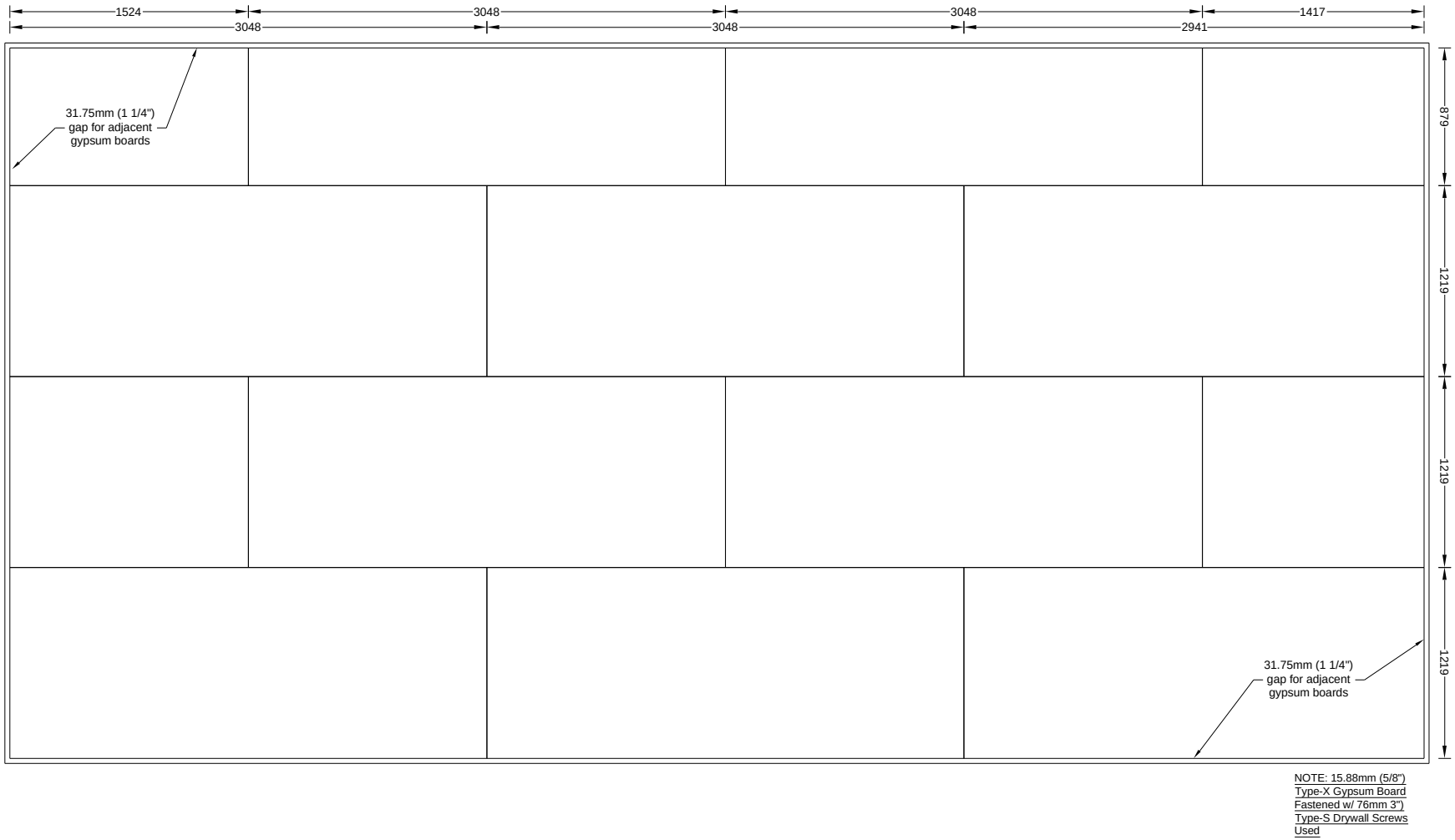

Figure A 11. Test 1-1 Large Compartment CLT - Ceiling - Gypsum Layout - Face Layer

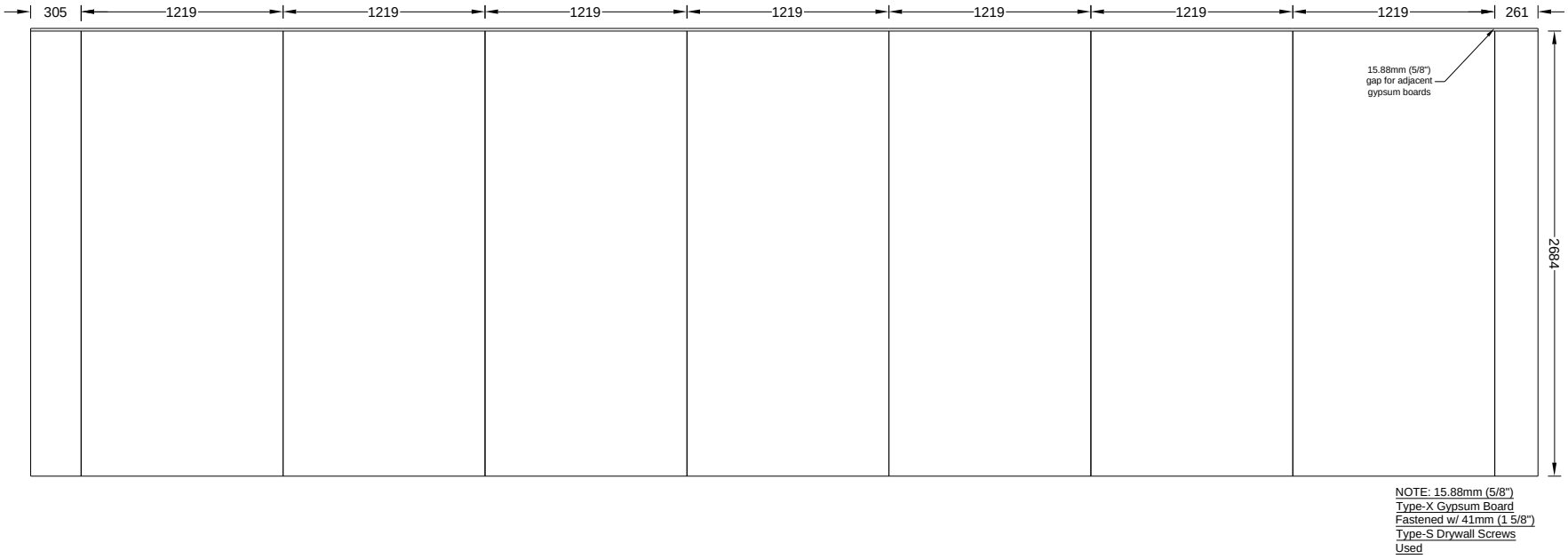

Figure A 12. Test 1-1 Large Compartment CLT - W1 - Gypsum Layout - Base Layer

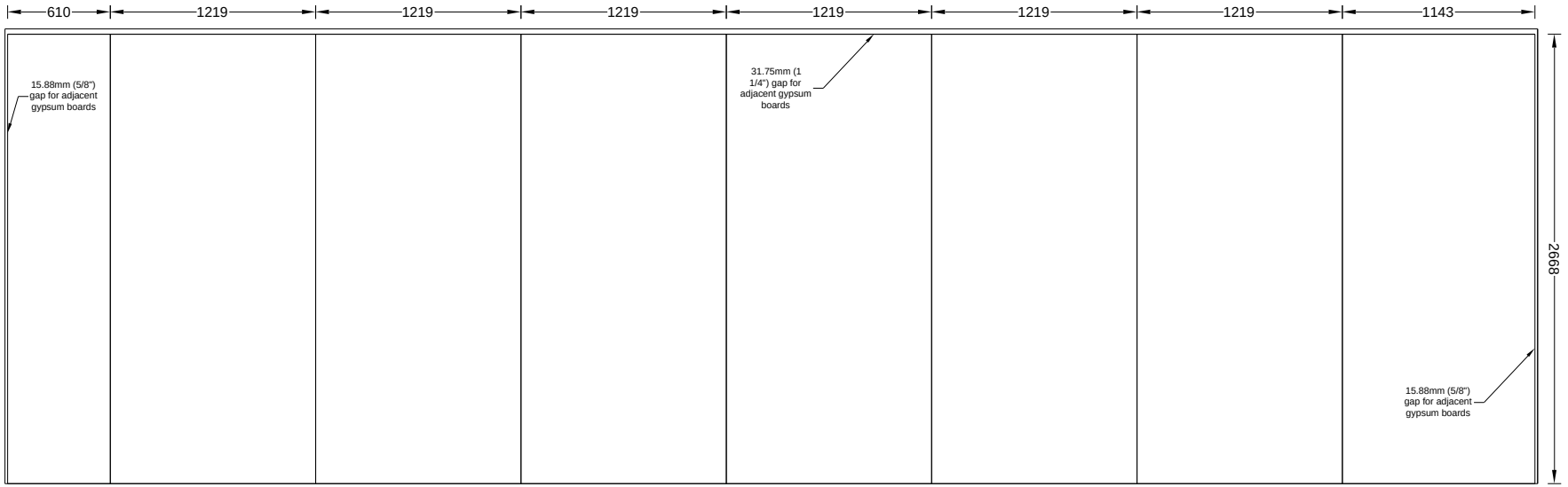

Figure A 13. Test 1-1 Large Compartment CLT - W1 - Gypsum Layout - Middle Layer

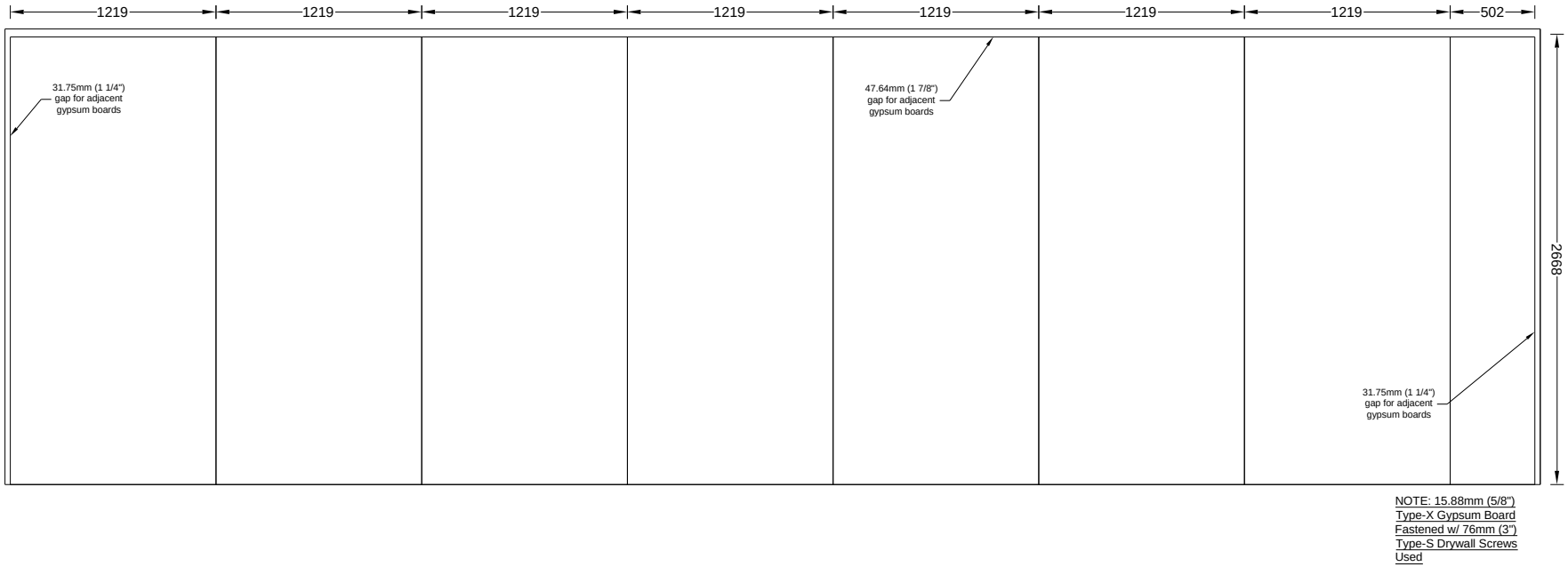

Figure A 14. Test 1-1 Large Compartment CLT - W1 - Gypsum Layout - Face Layer

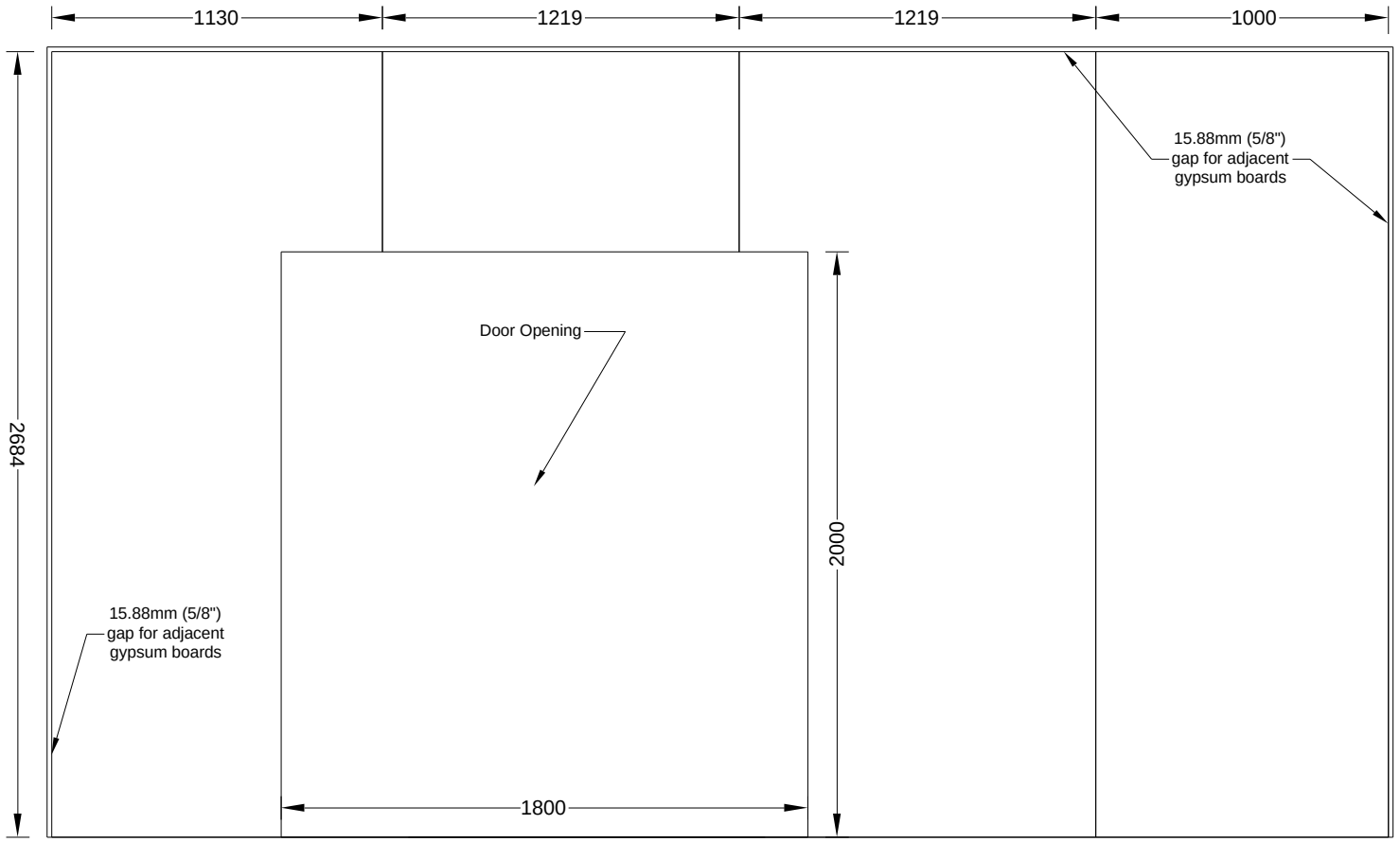

(Dimensions in mm)

Figure A 15. Test 1-1 Large Compartment CLT - W2 - Gypsum Layout - Base Layer

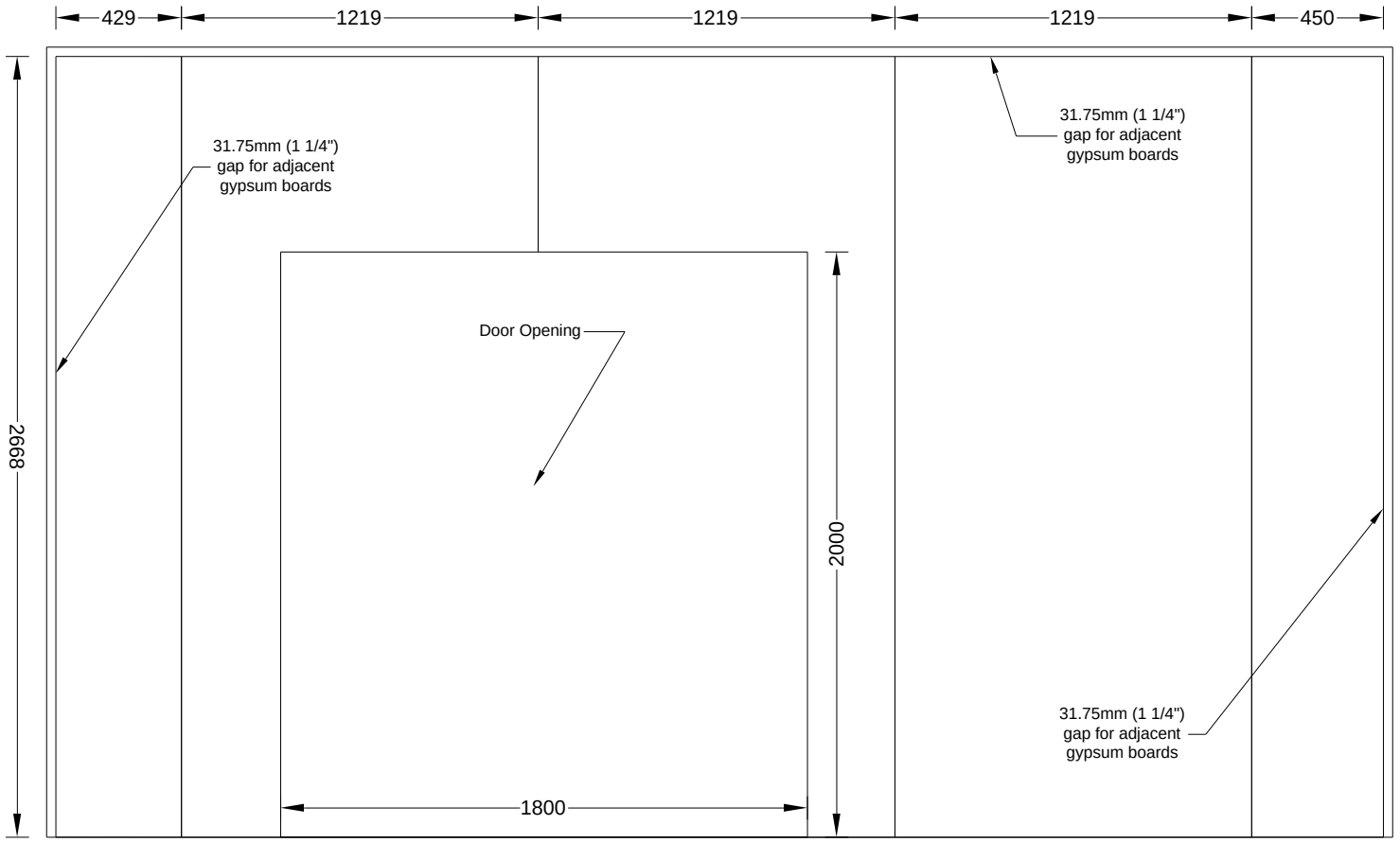

Figure A 16. Test 1-1 Large Compartment CLT - W2 - Gypsum Layout - Middle Layer

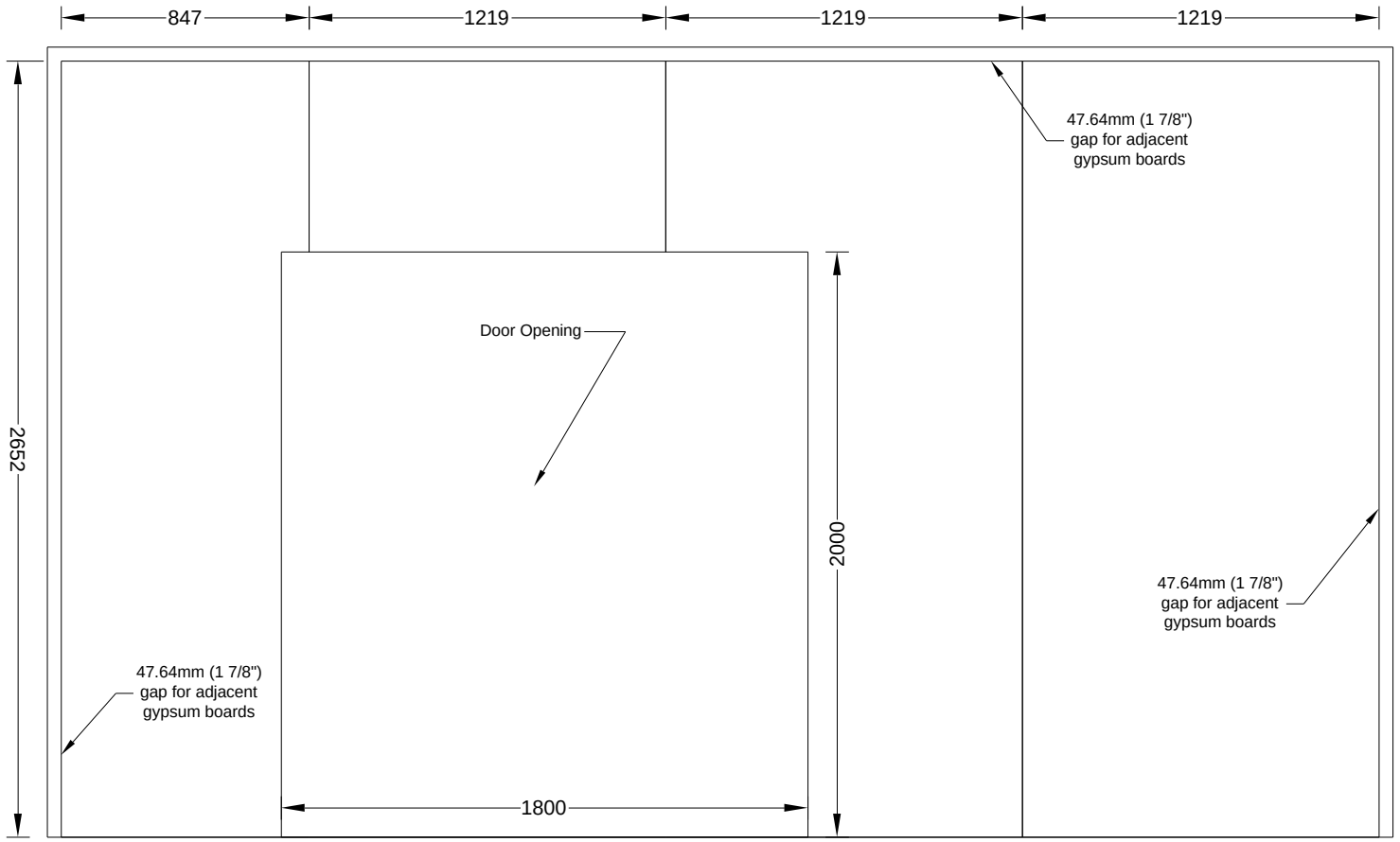

(Dimensions in mm)

Figure A 17. Test 1-1 Large Compartment CLT - W2 - Gypsum Layout - Face Layer

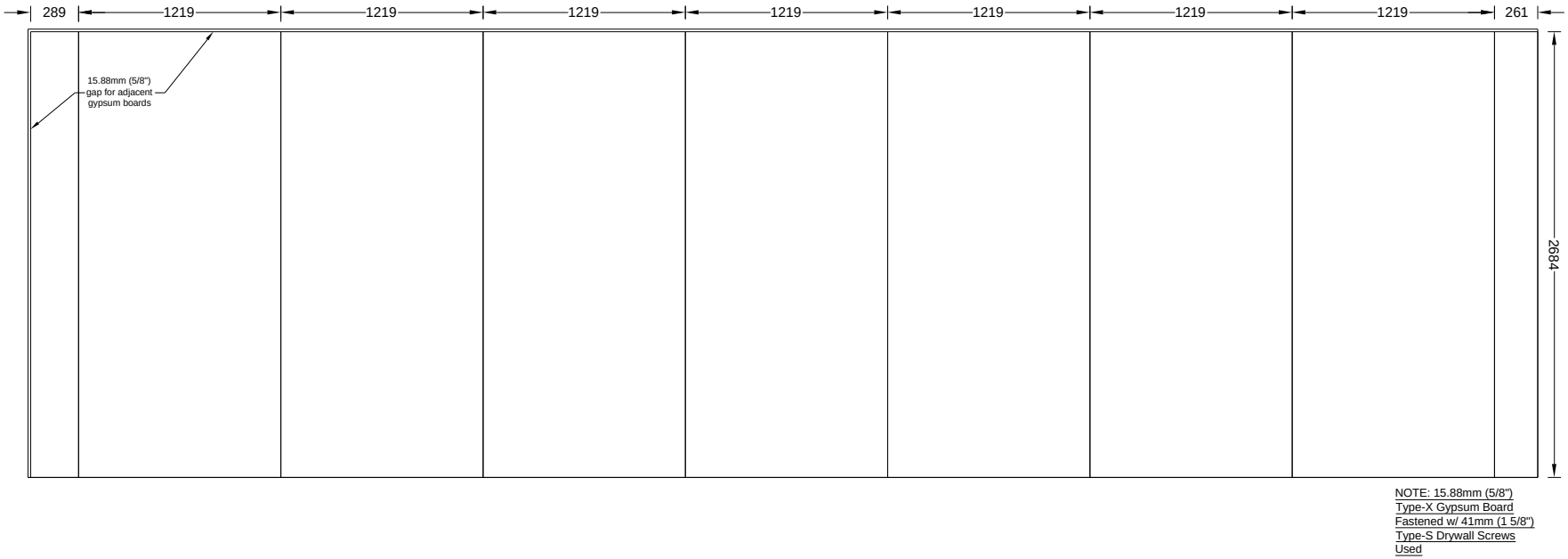

Figure A 18. Test 1-1 Large Compartment CLT - W3 - Gypsum Layout - Base Layer

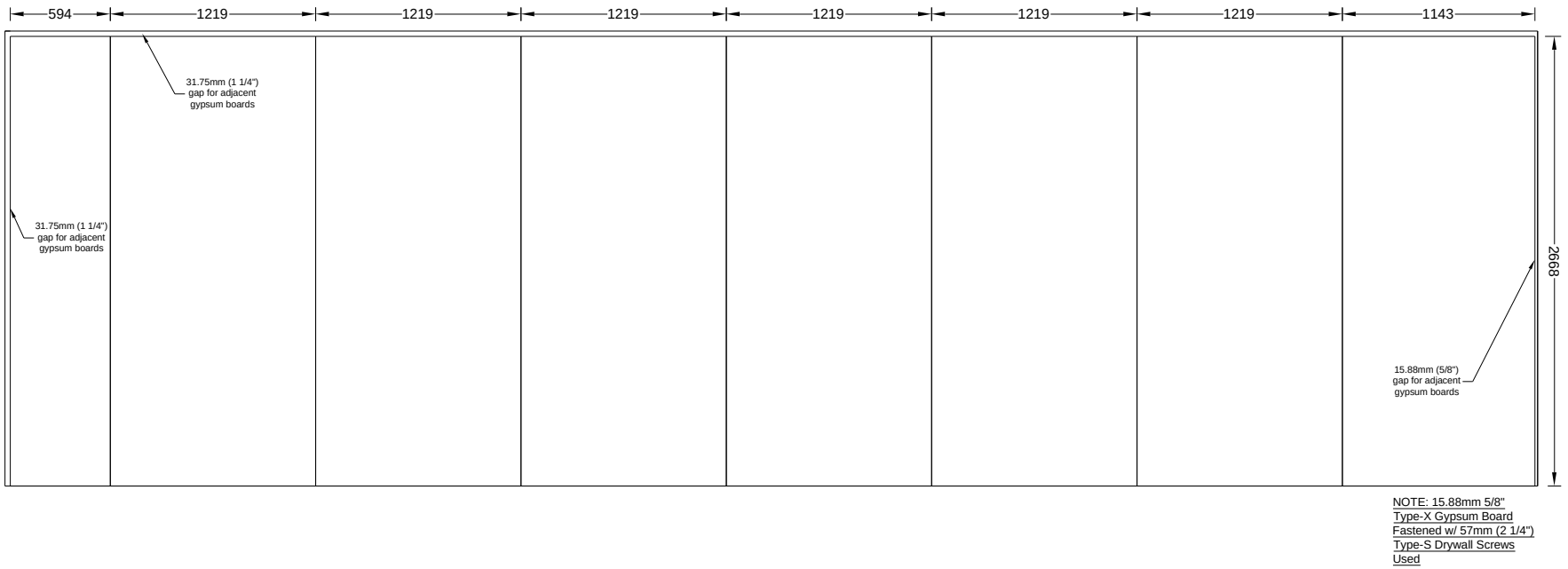

Figure A 19. Test 1-1 Large Compartment CLT - W3 - Gypsum Layout - Middle Layer

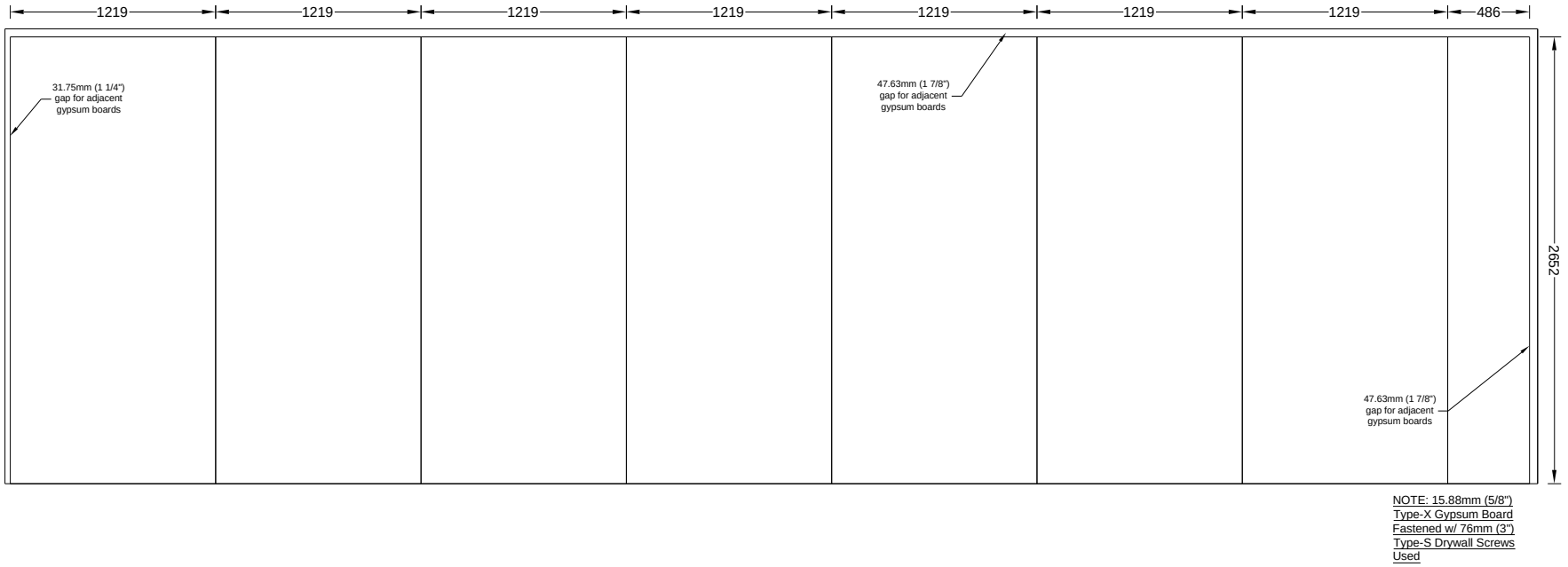

Figure A 20. Test 1-1 Large Compartment CLT - W3 - Gypsum Layout - Face Layer

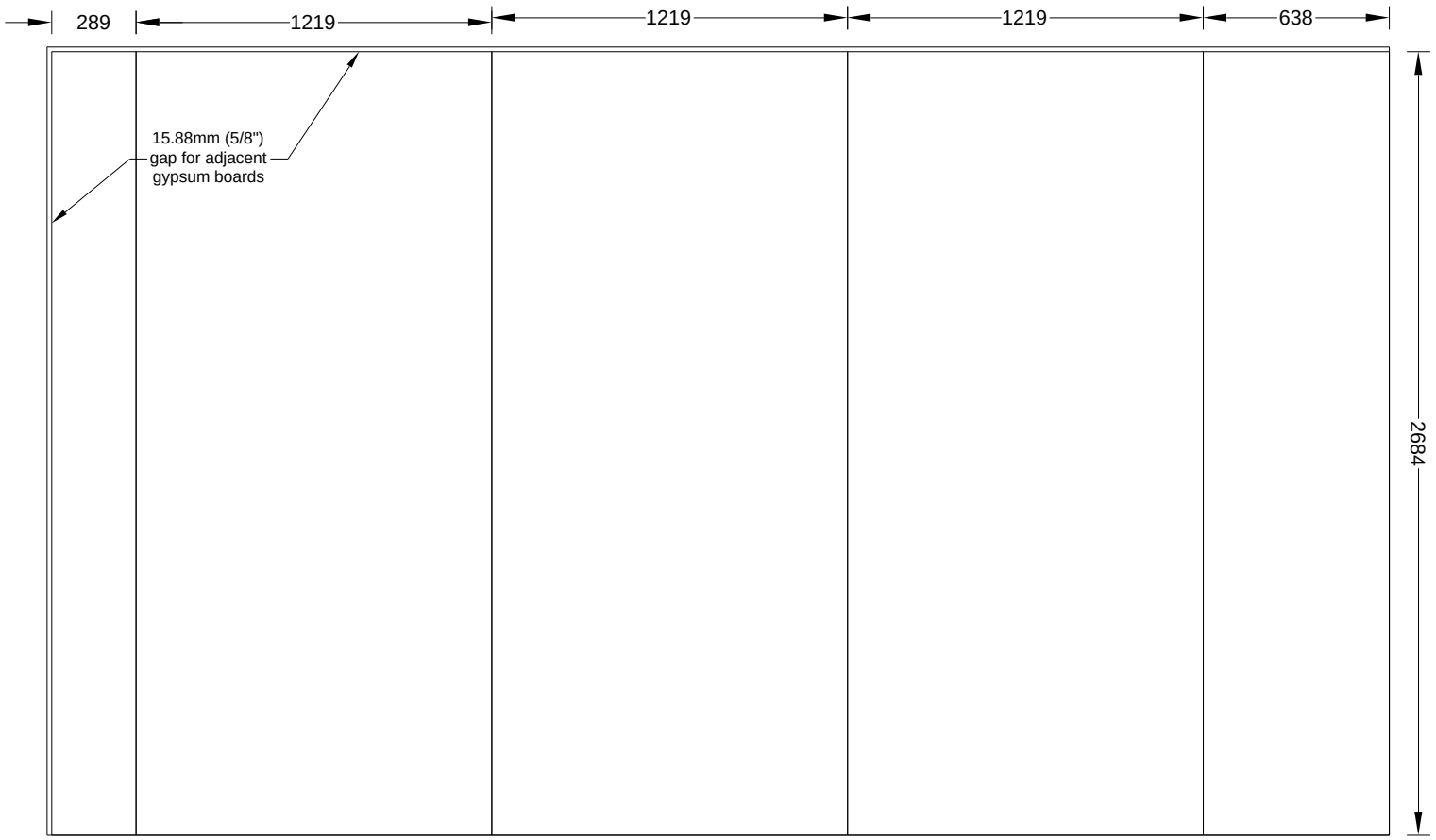

(Dimensions in mm)

Figure A 21. Test 1-1 Large Compartment CLT - W4 - Gypsum Layout - Base Layer

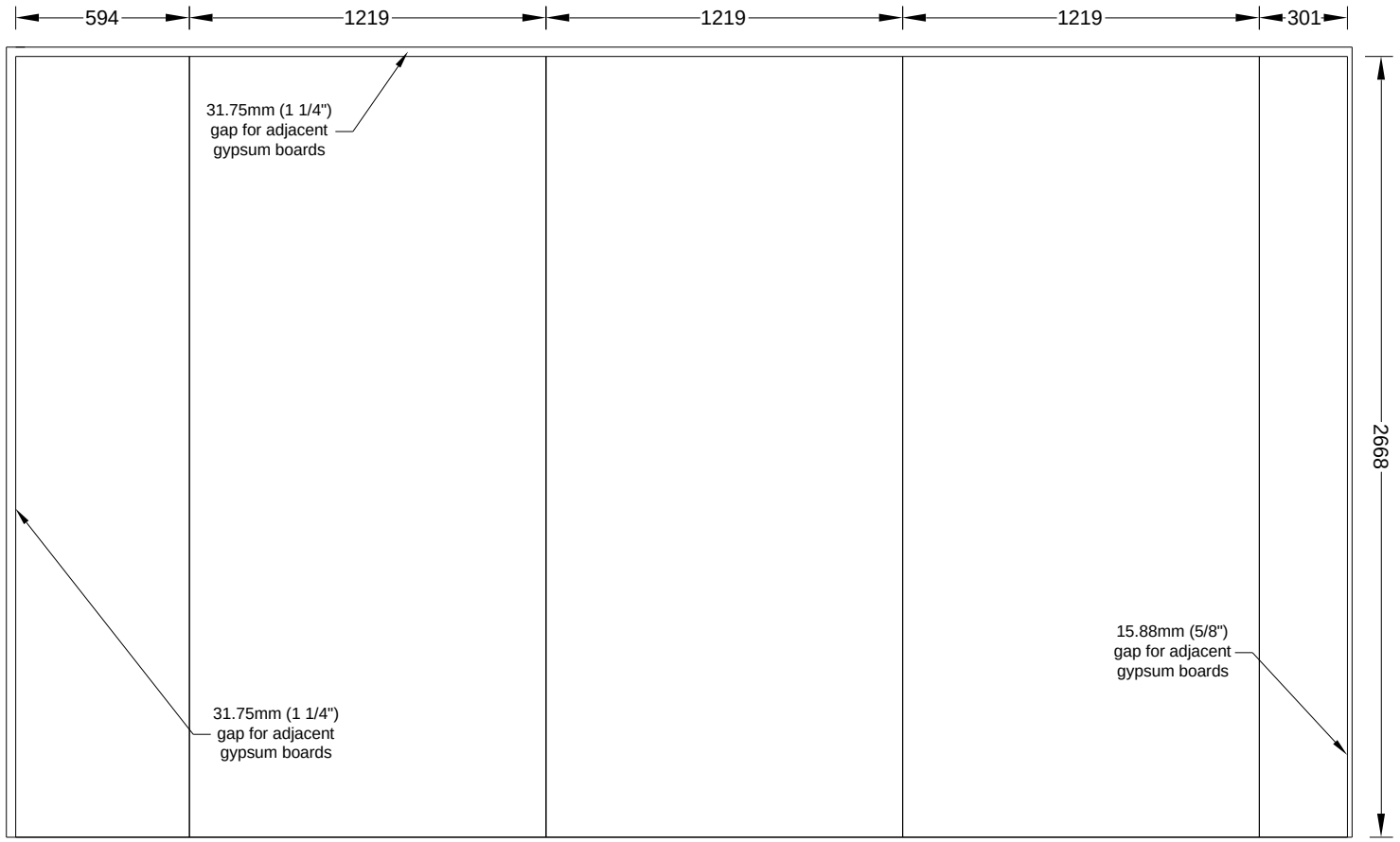

Figure A 22. Test 1-1 Large Compartment CLT - W4 - Gypsum Layout - Middle Layer

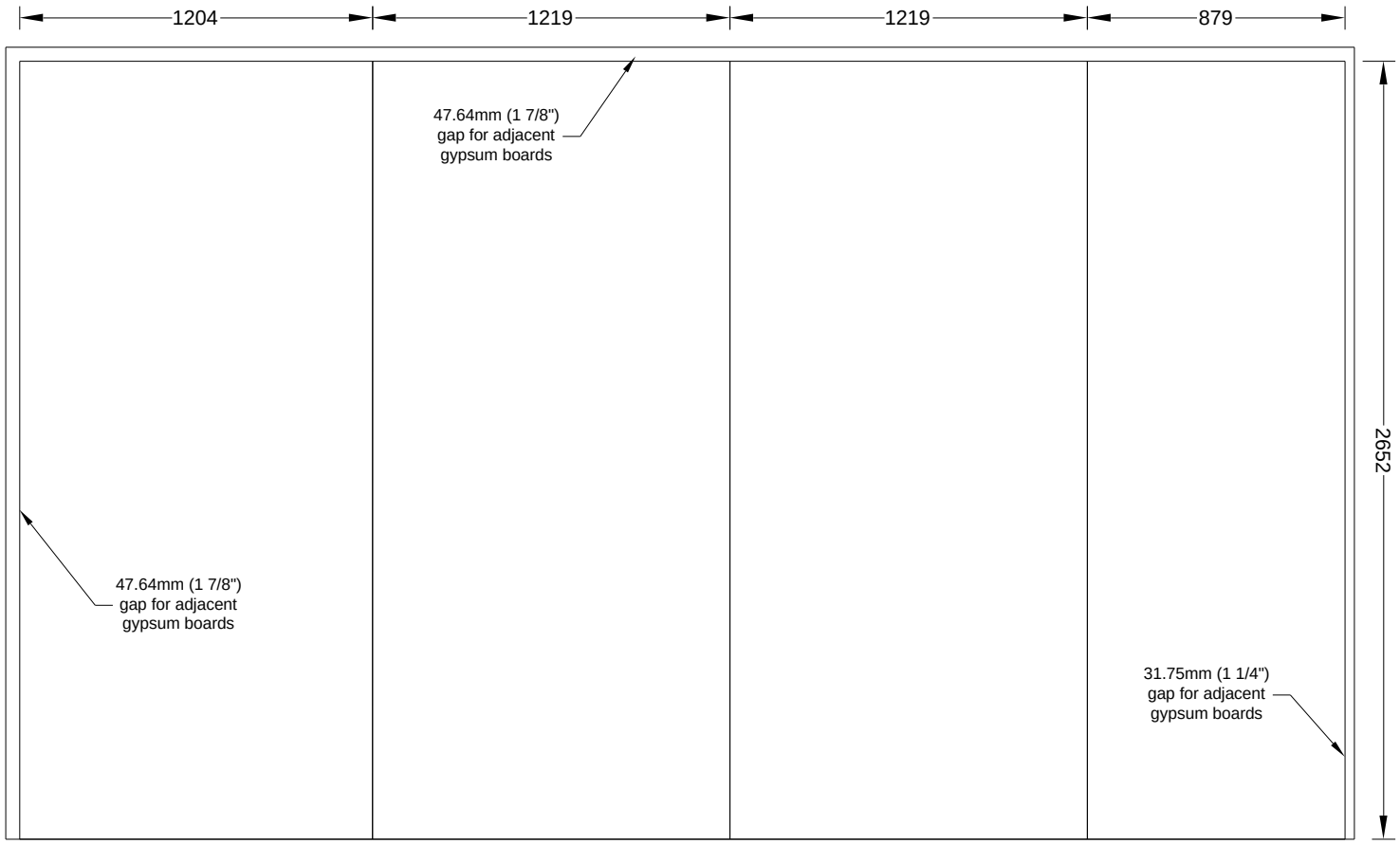

Figure A 23. Test 1-1 Large Compartment CLT - W4 - Gypsum Layout - Face Layer

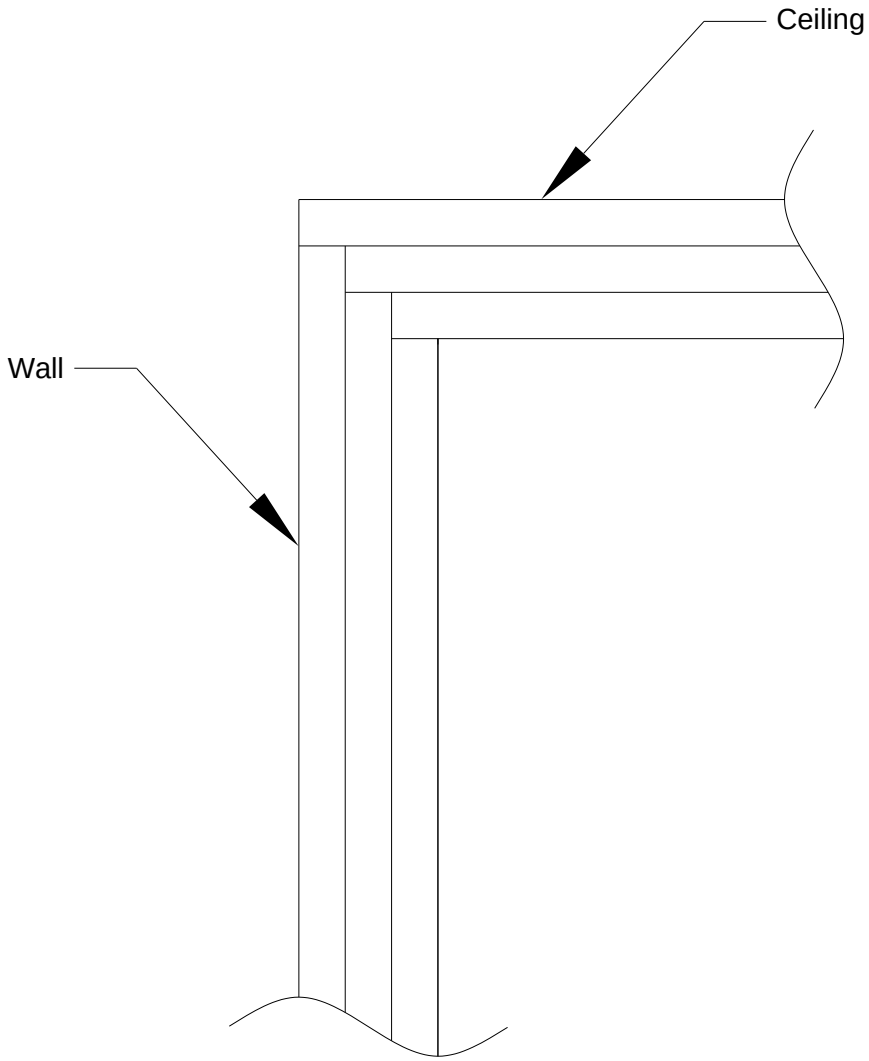

Note: Cross Section View

Figure A 24. Test 1-1 Large Compartment CLT - Wall - Gypsum Stagger at Ceiling

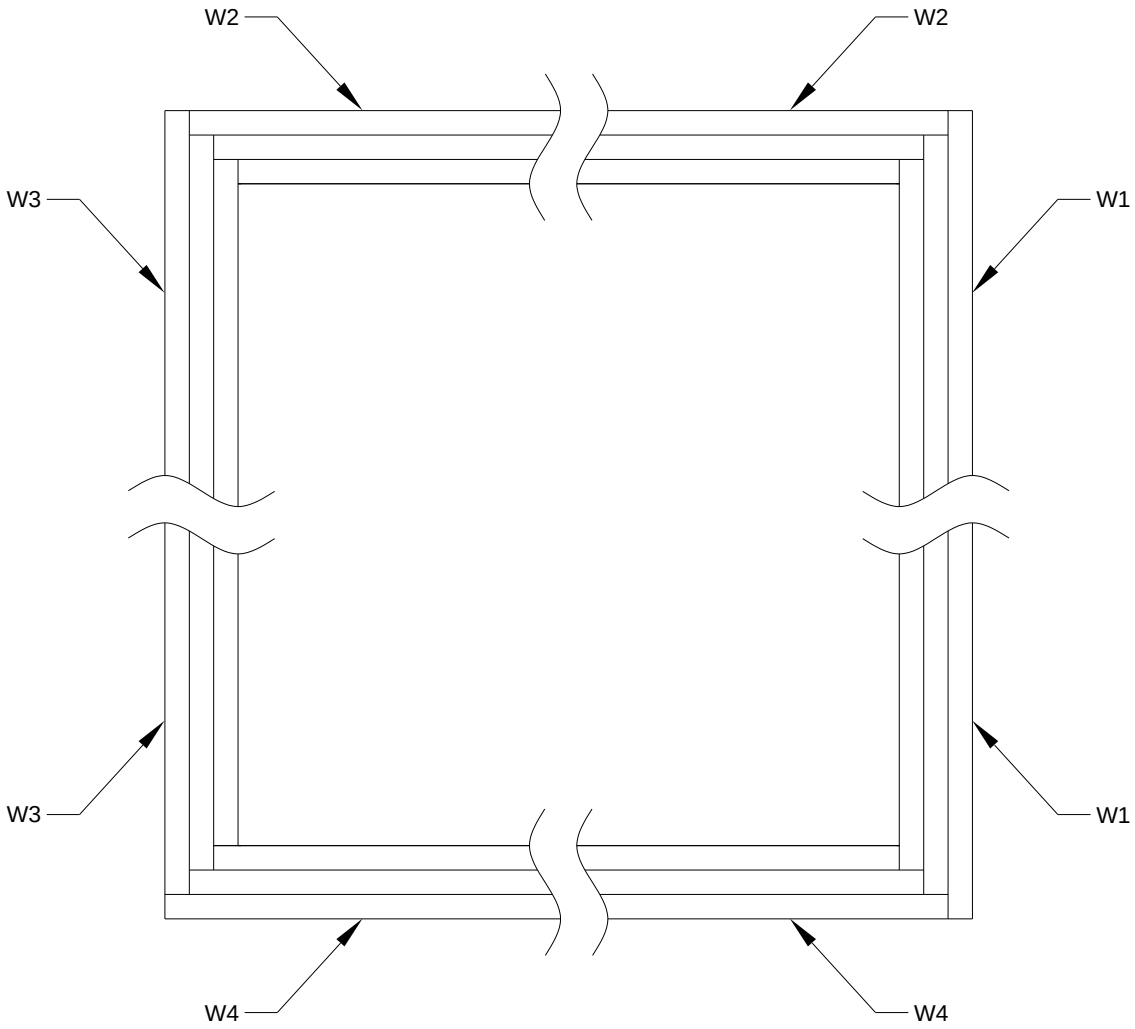

Figure A 25. Test 1-1 Large Compartment CLT - Wall - Gypsum Stagger in Corners

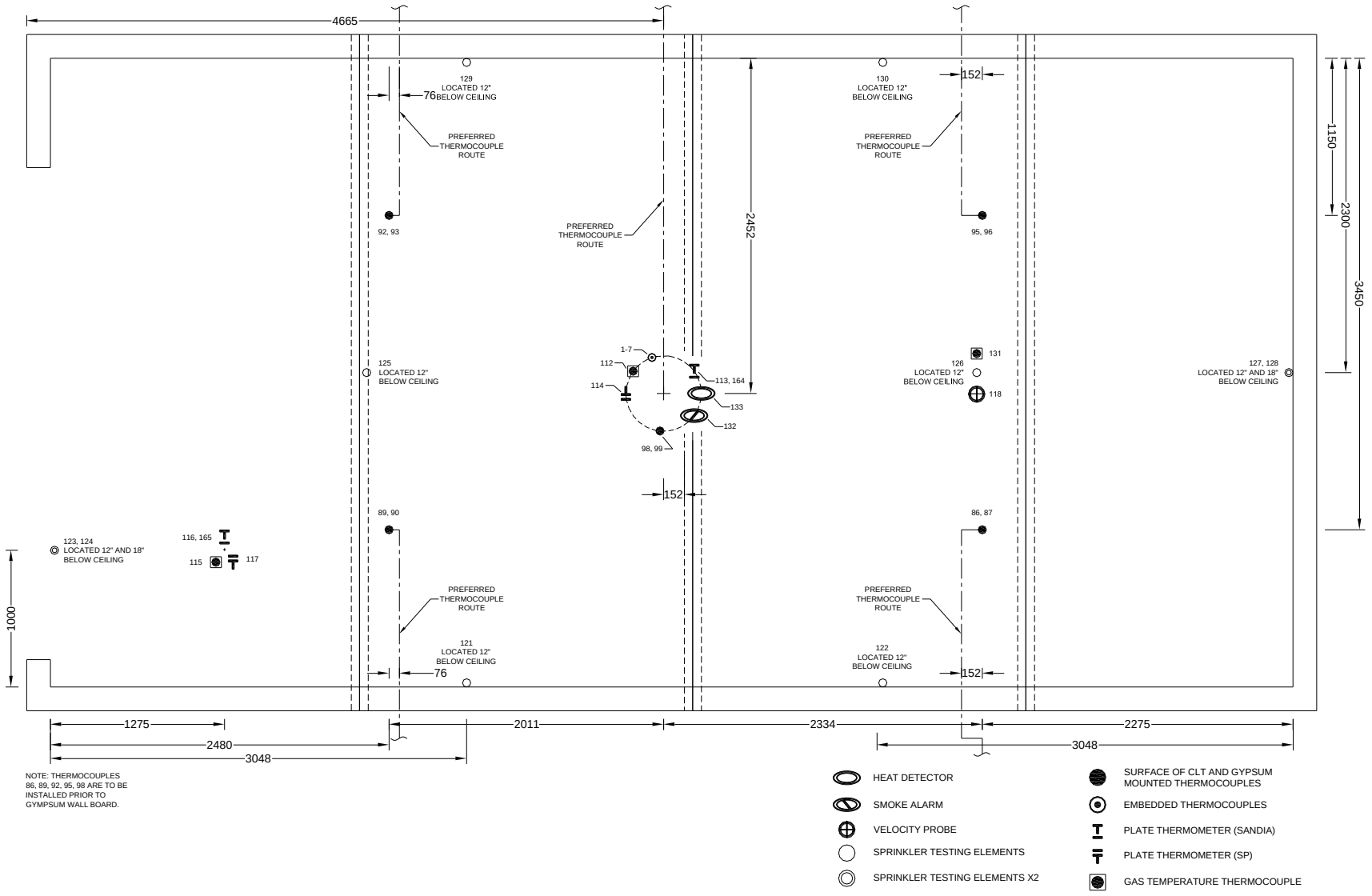

(Dimensions in mm)

Figure A 26. Test 1-2 Large Compartment CLT - Ceiling - Instrumentation Layout

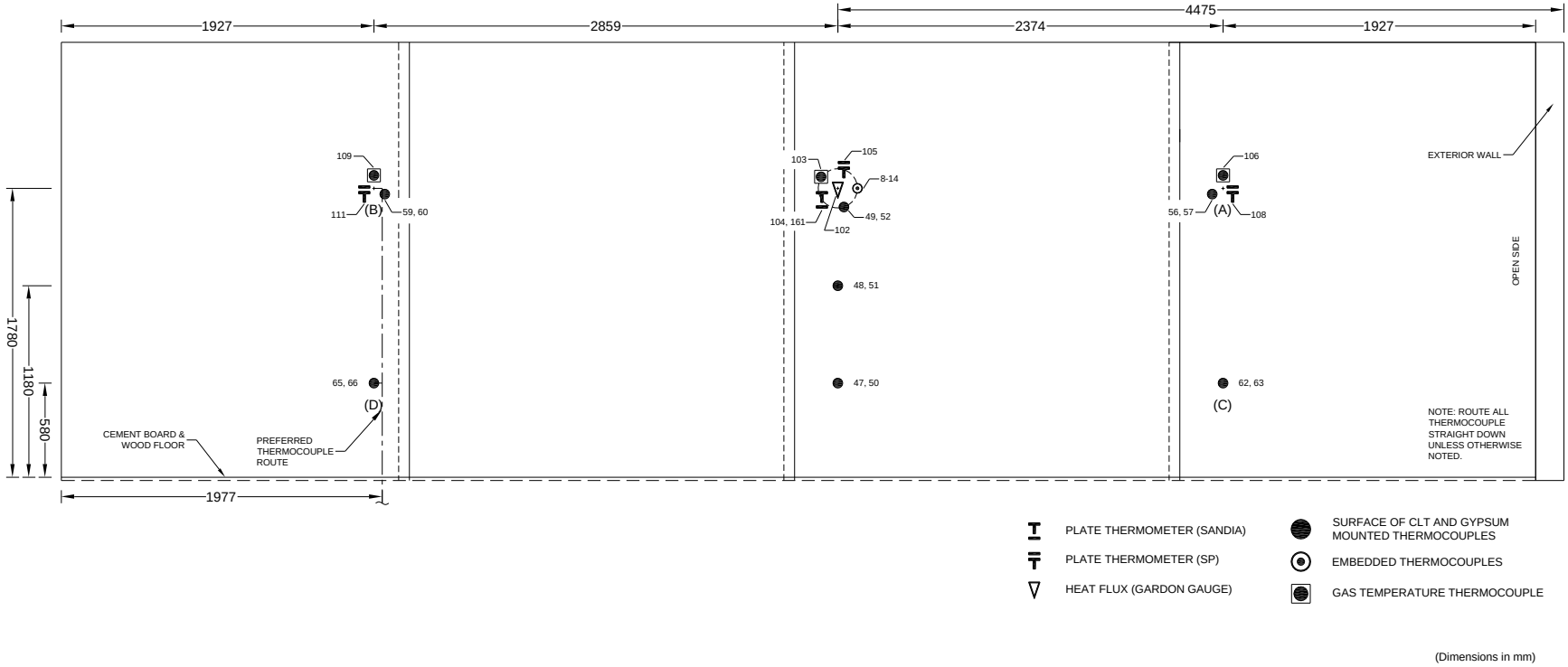

Figure A 27. Test 1-2 Large Compartment CLT - W1 - Instrumentation Layout

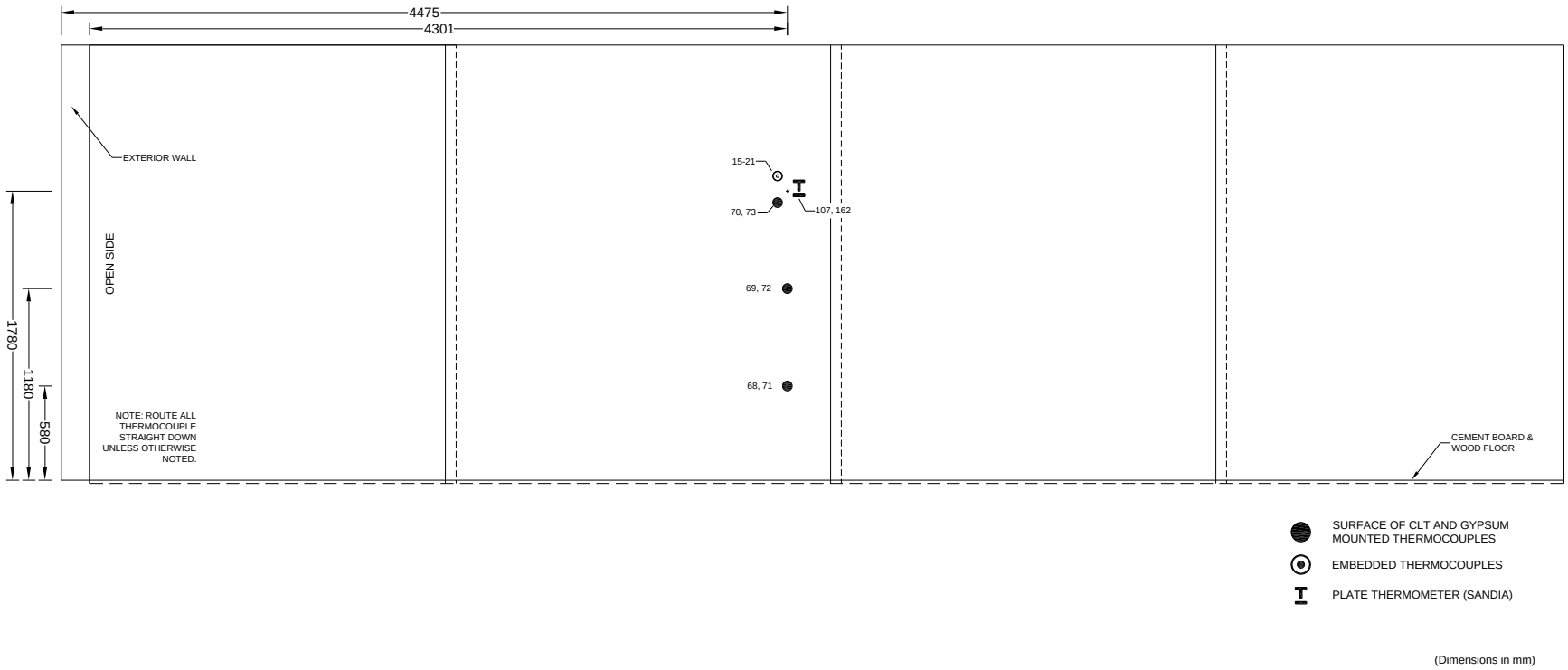

Figure A 28. Test 1-2 Large Compartment CLT - W3 - Instrumentation Layout

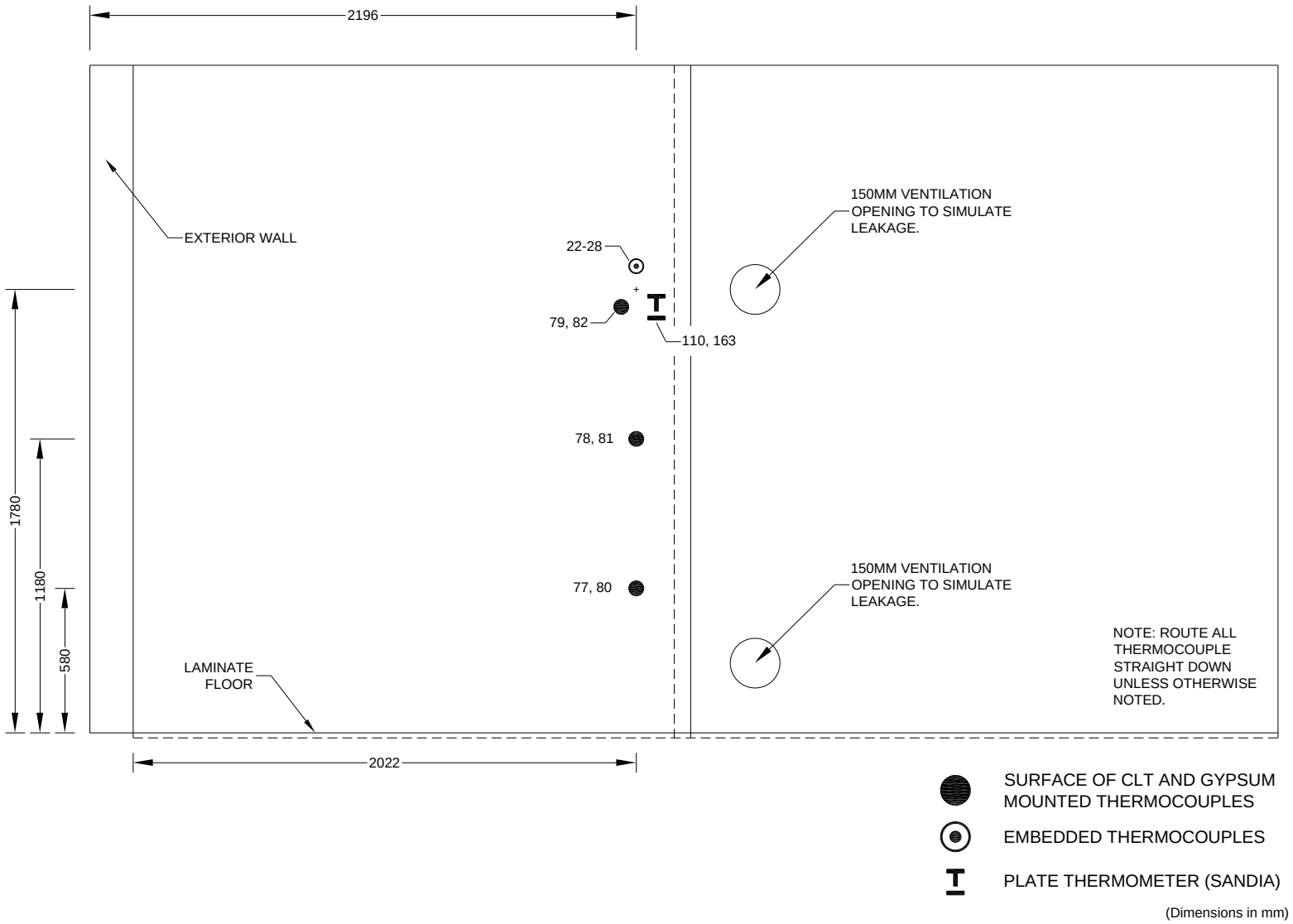

Figure A 29. Test 1-2 Large Compartment CLT - W4 - Instrumentation Layout

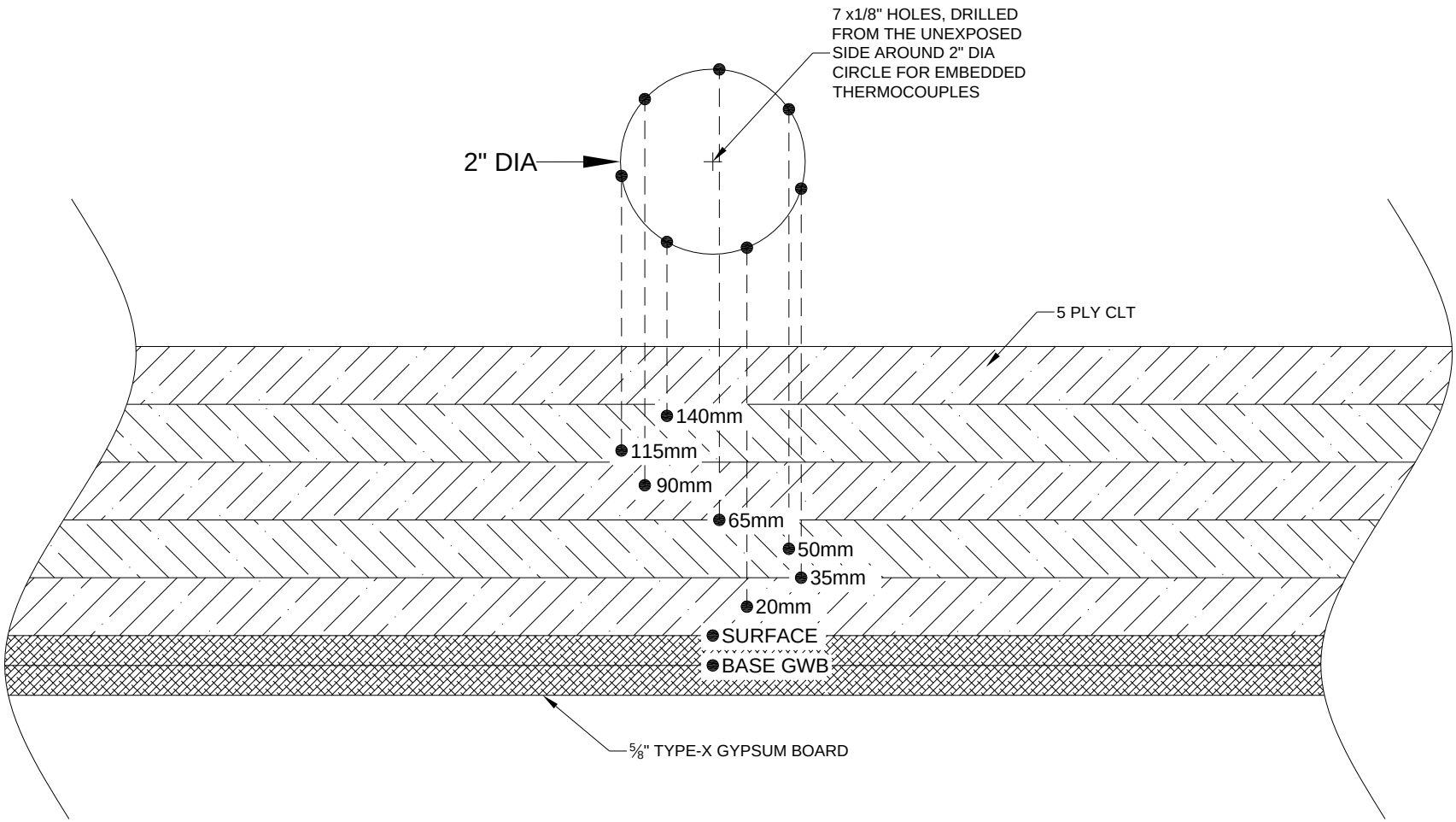

Figure A 30. Test 1-2 Large Compartment CLT - Embedded Thermocouple Detail

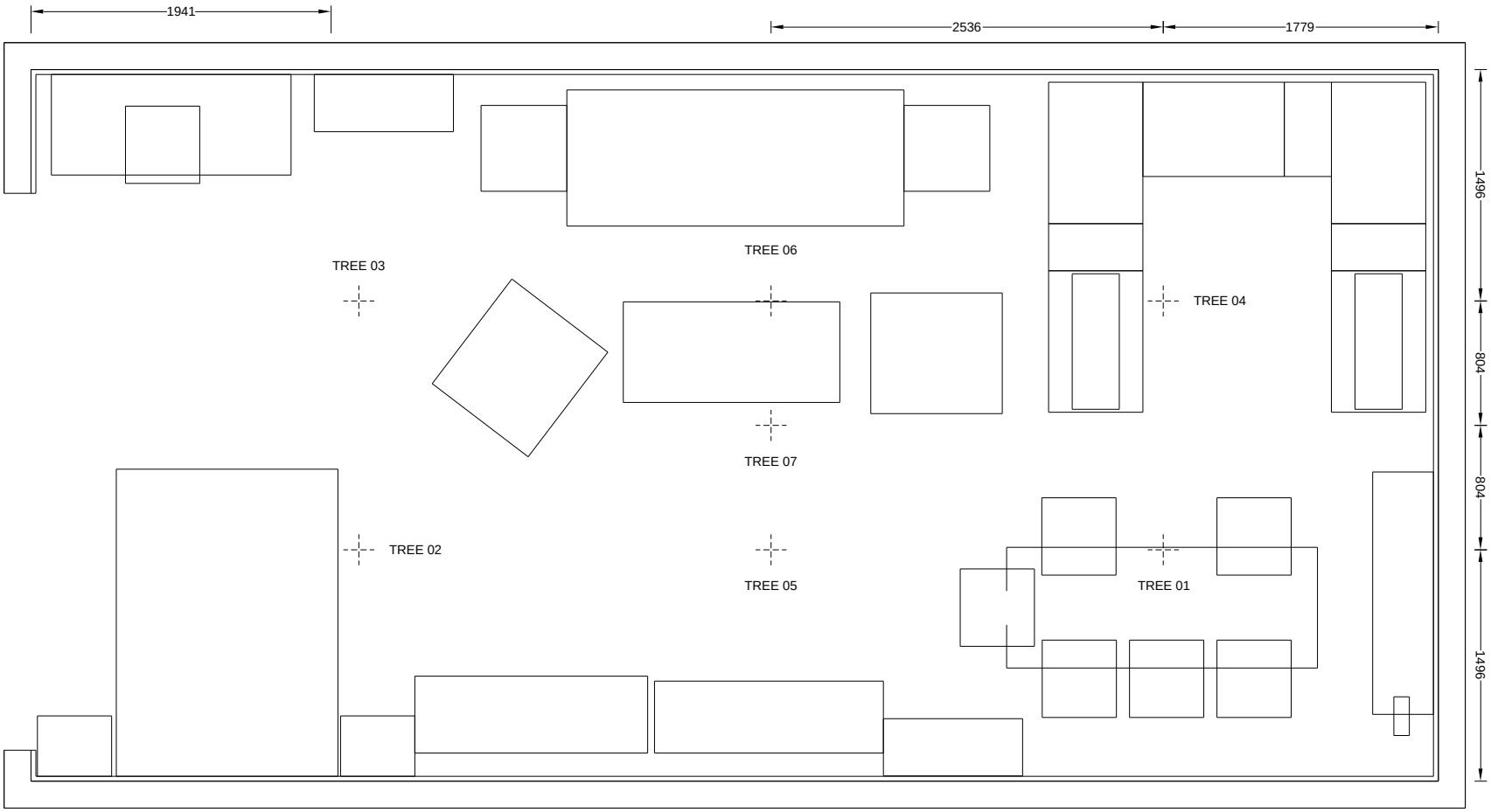

Figure A 31. Test 1-2 Large Compartment CLT - Instrumentation Tree Layout

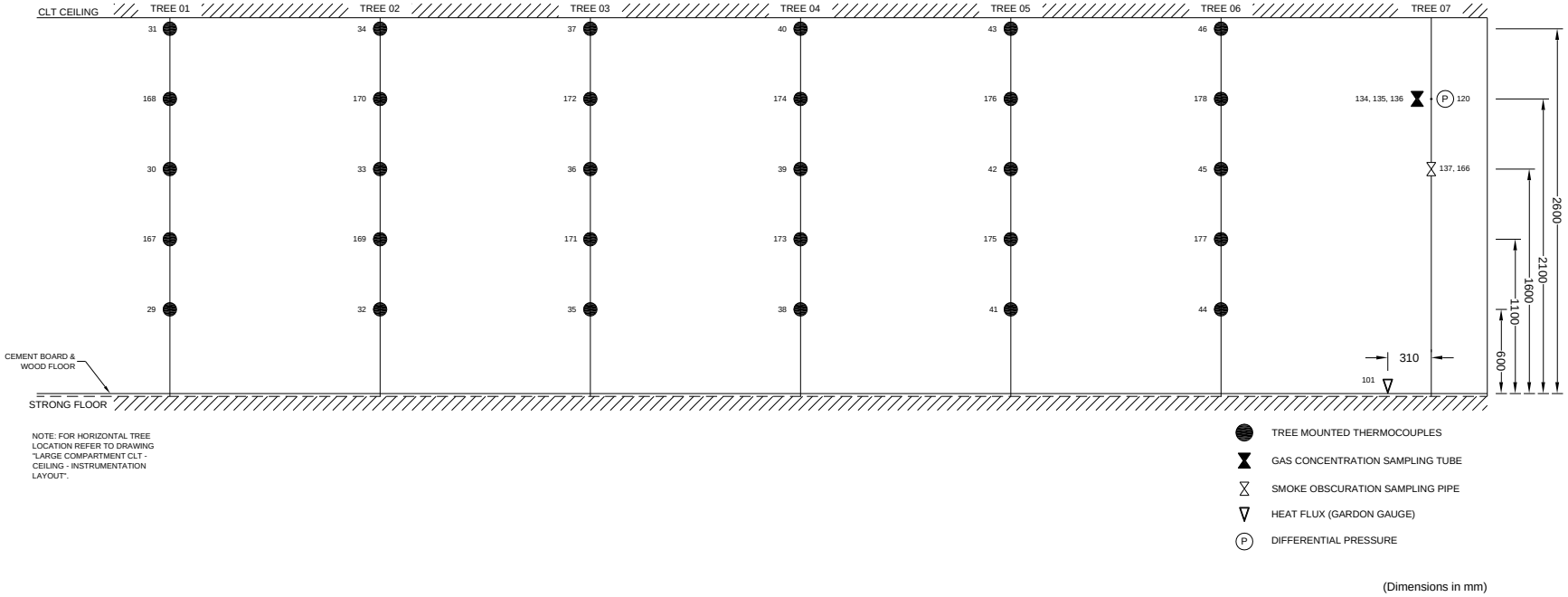

Figure A 32. Test 1-2 Large Compartment CLT - Instrumentation Tree Specifications

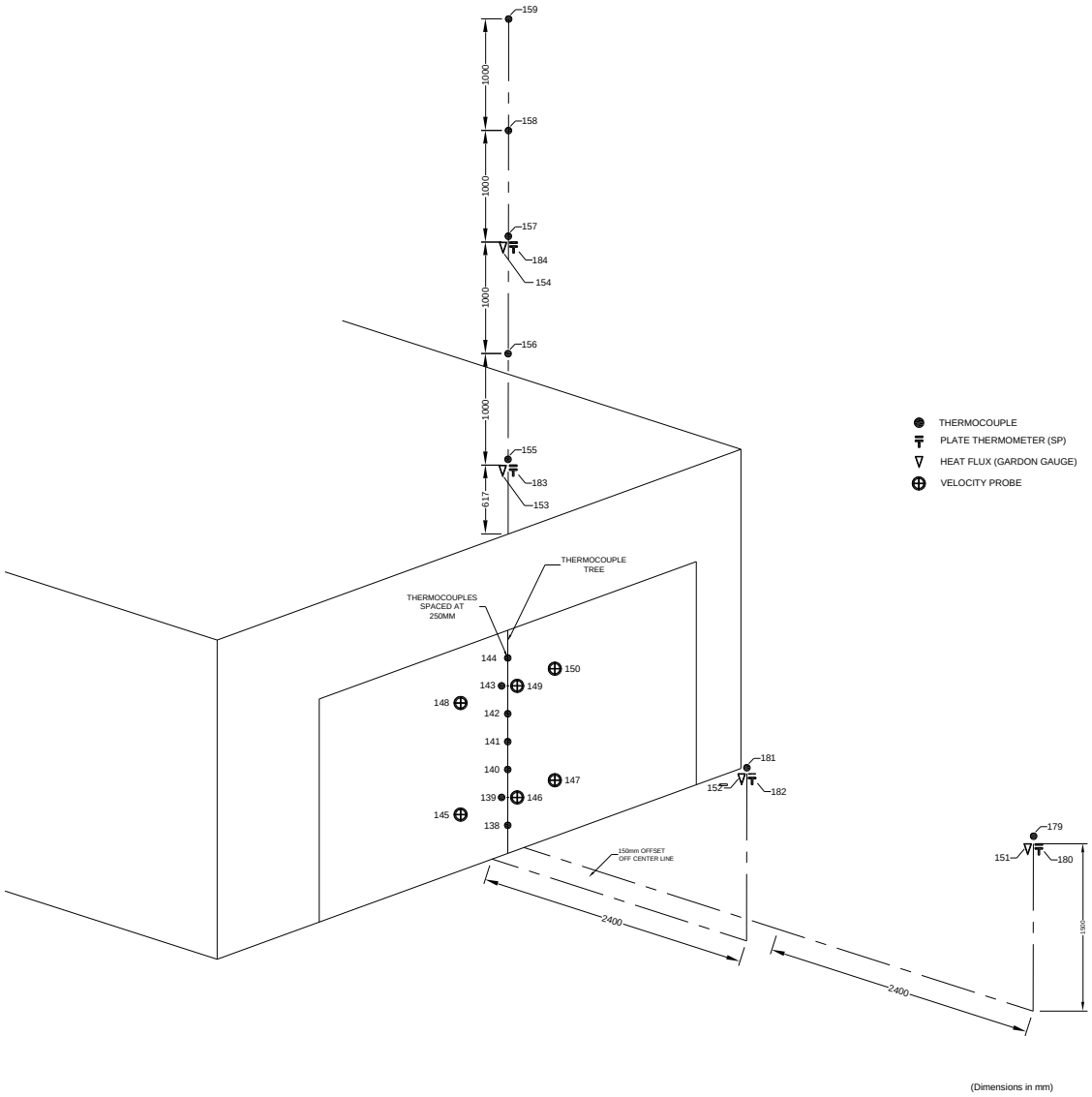

Figure A 33. Test 1-2 Large Compartment CLT - Exterior Instrumentation Layout

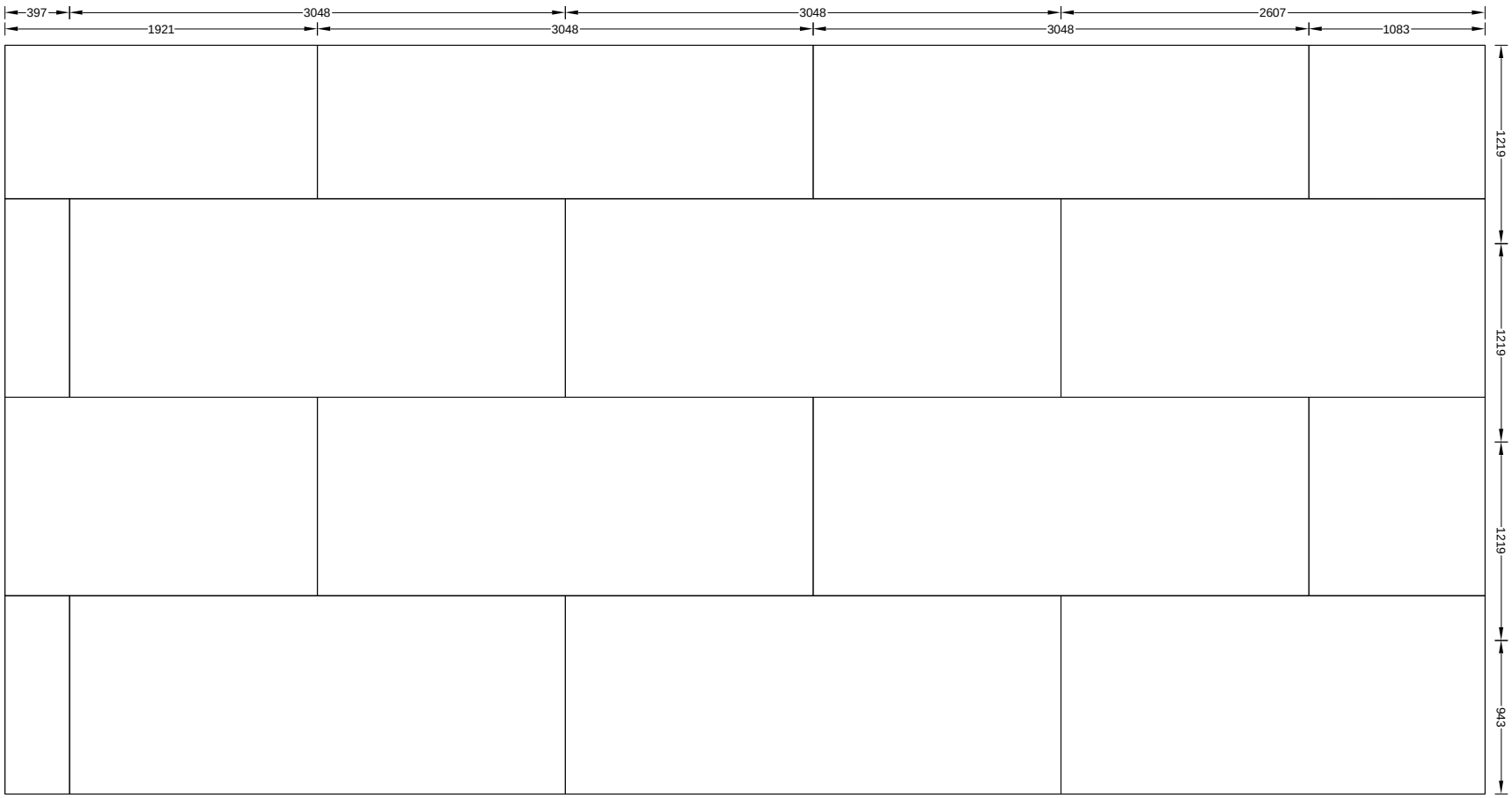

(Dimensions in mm)

Figure A 34. Test 1-2 Large Compartment CLT - Ceiling - Gypsum Layout - Base Layer

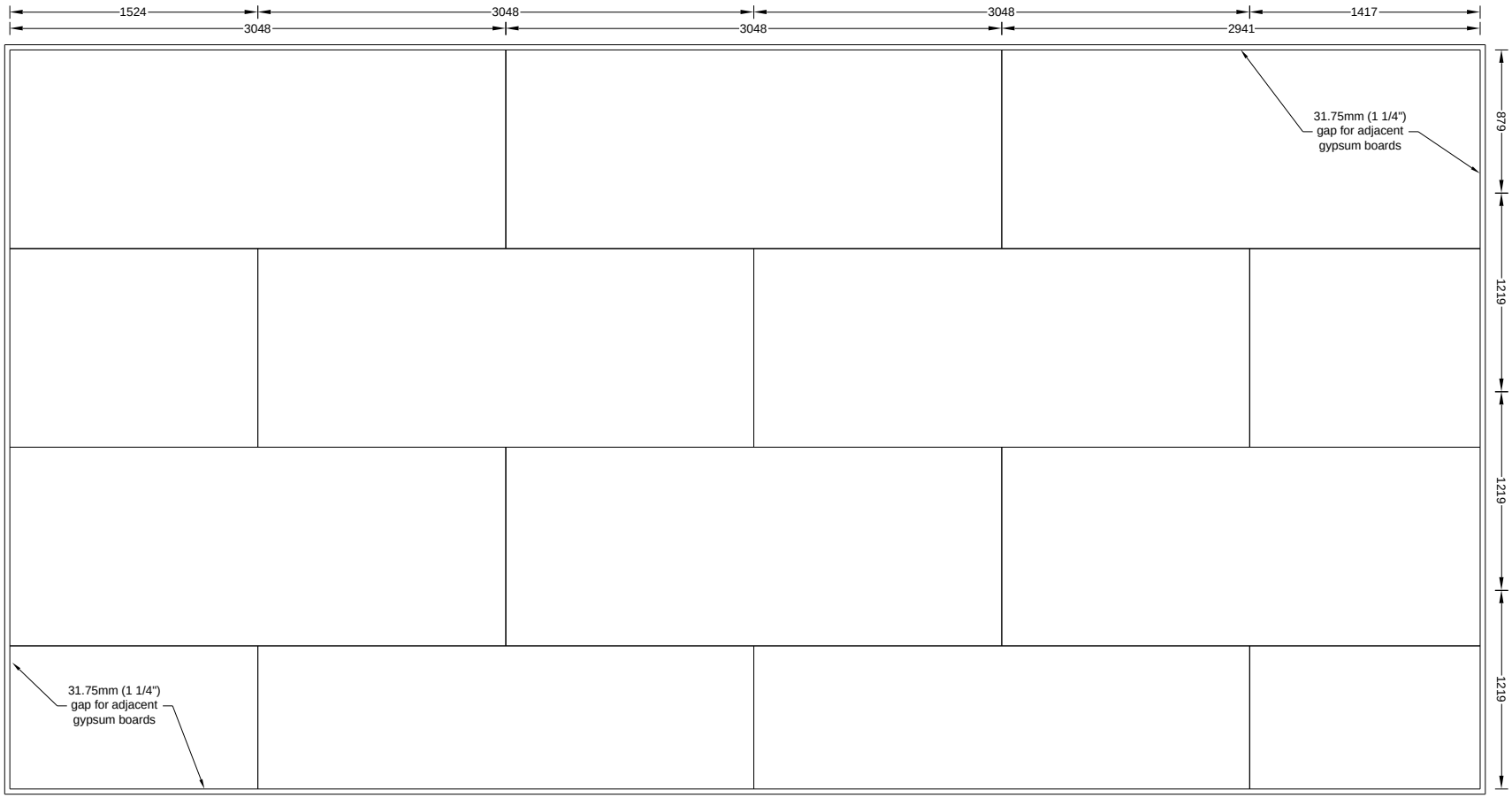

(Dimensions in mm)

Figure A 35. Test 1-2 Large Compartment CLT - Ceiling - Gypsum Layout - Face Layer

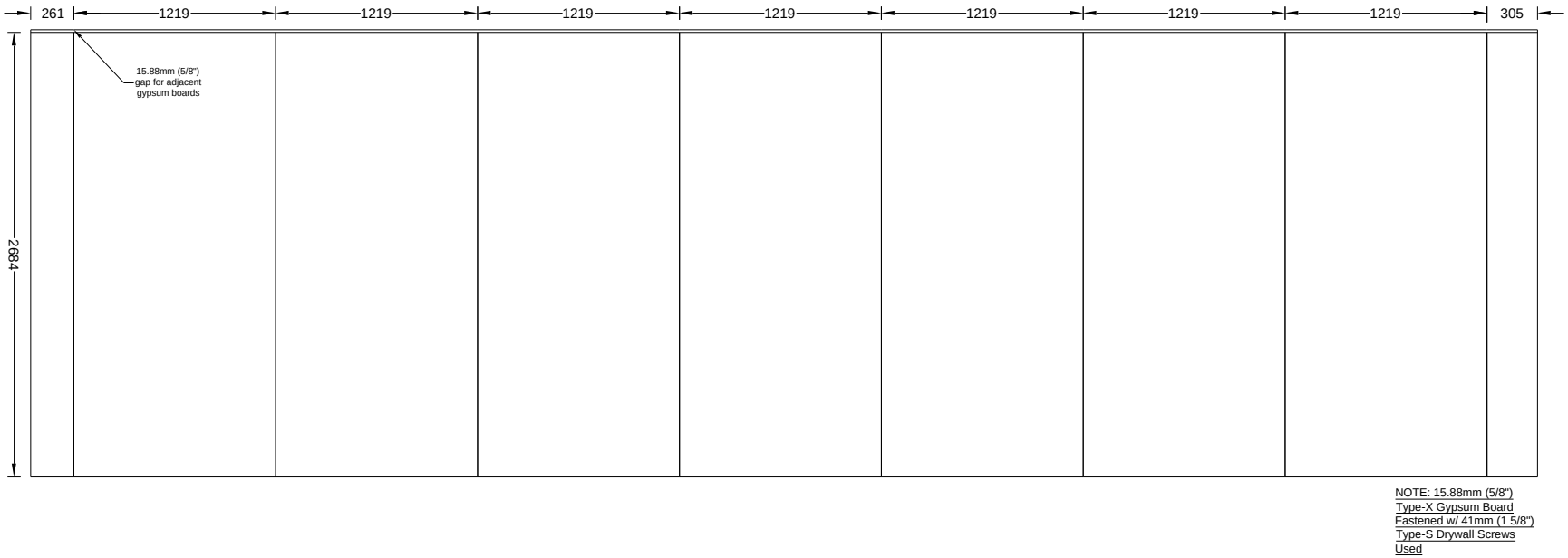

Figure A 36. Test 1-2 Large Compartment CLT - W1 - Gypsum Layout - Base Layer

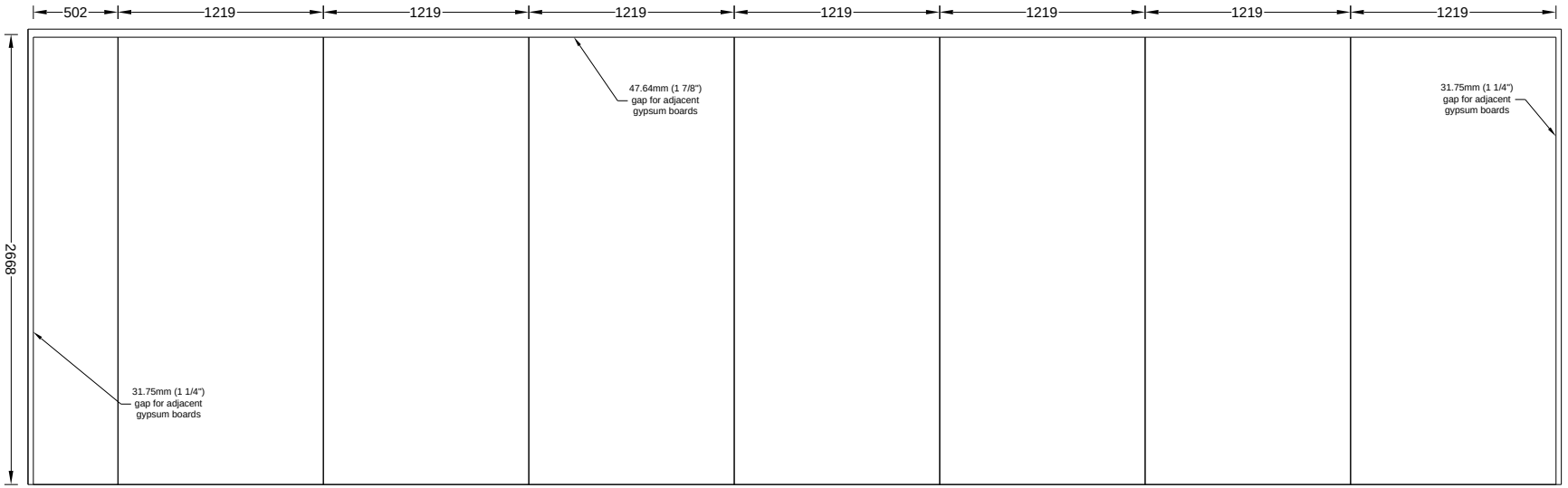

Figure A 37. Test 1-2 Large Compartment CLT - W1 - Gypsum Layout - Face Layer

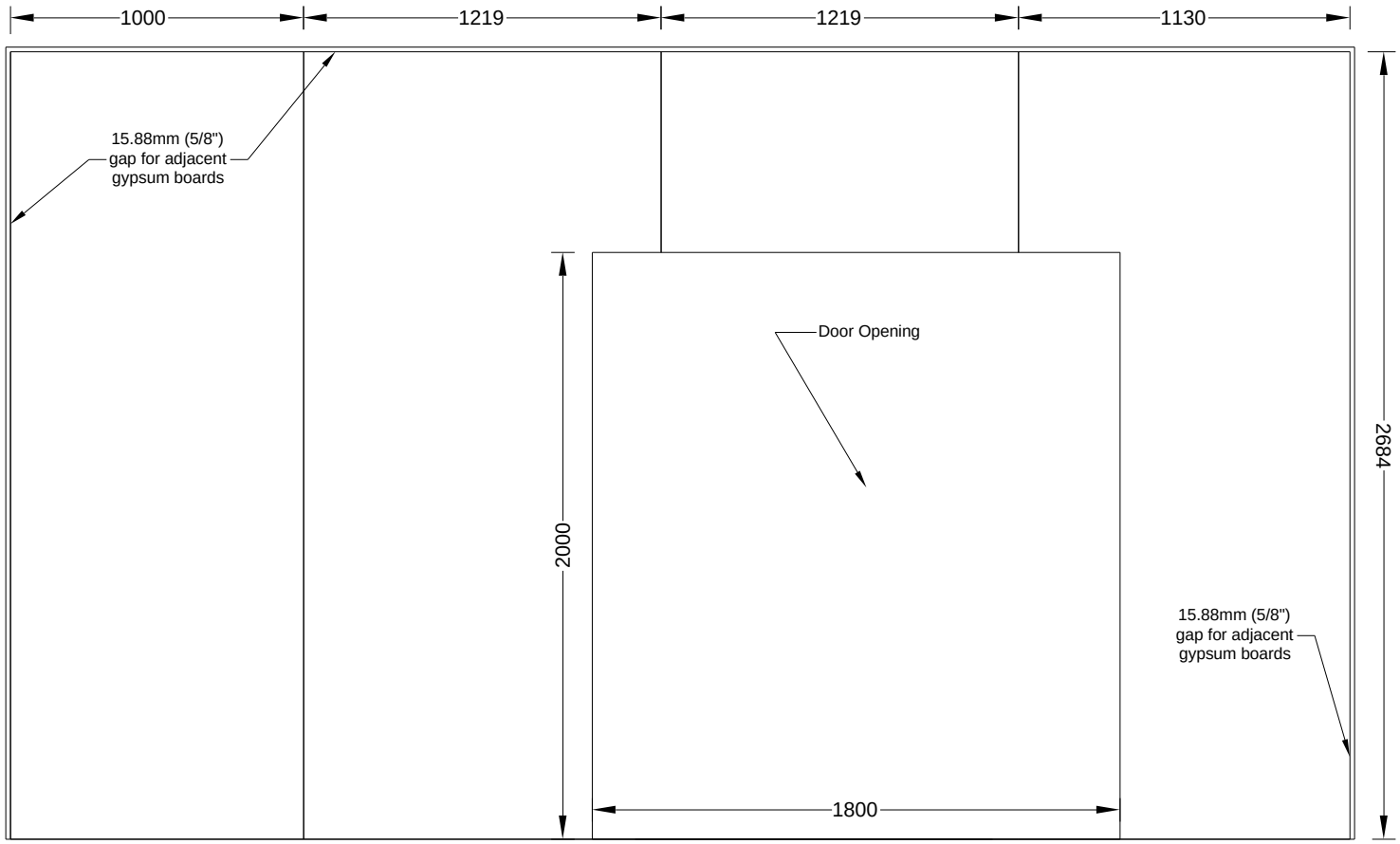

(Dimensions in mm)

Figure A 38. Test 1-2 Large Compartment CLT - W2 - Gypsum Layout - Base Layer

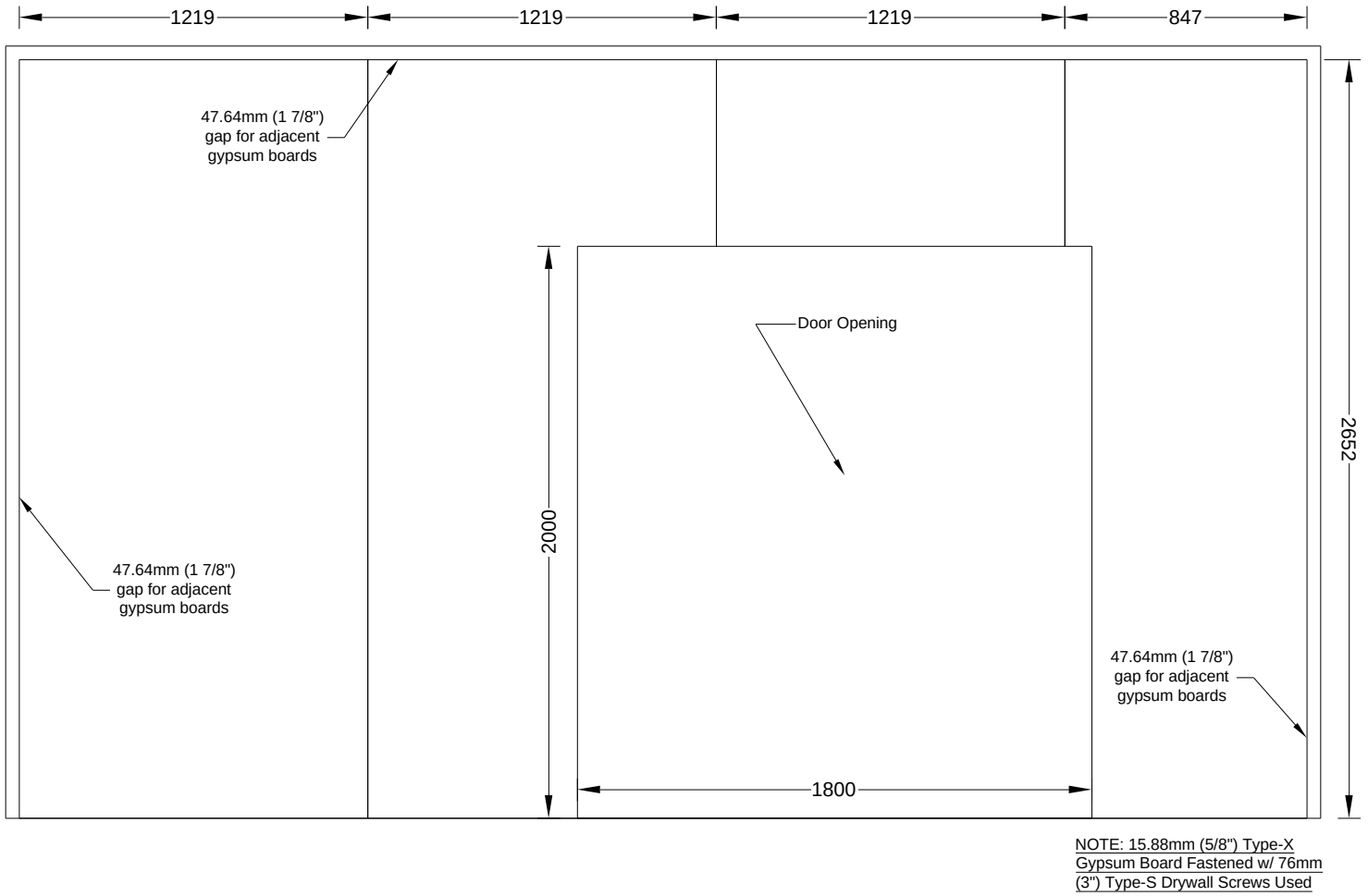

(Dimensions in mm)

Figure A 39. Test 1-2 Large Compartment CLT - W2 - Gypsum Layout - Face Layer

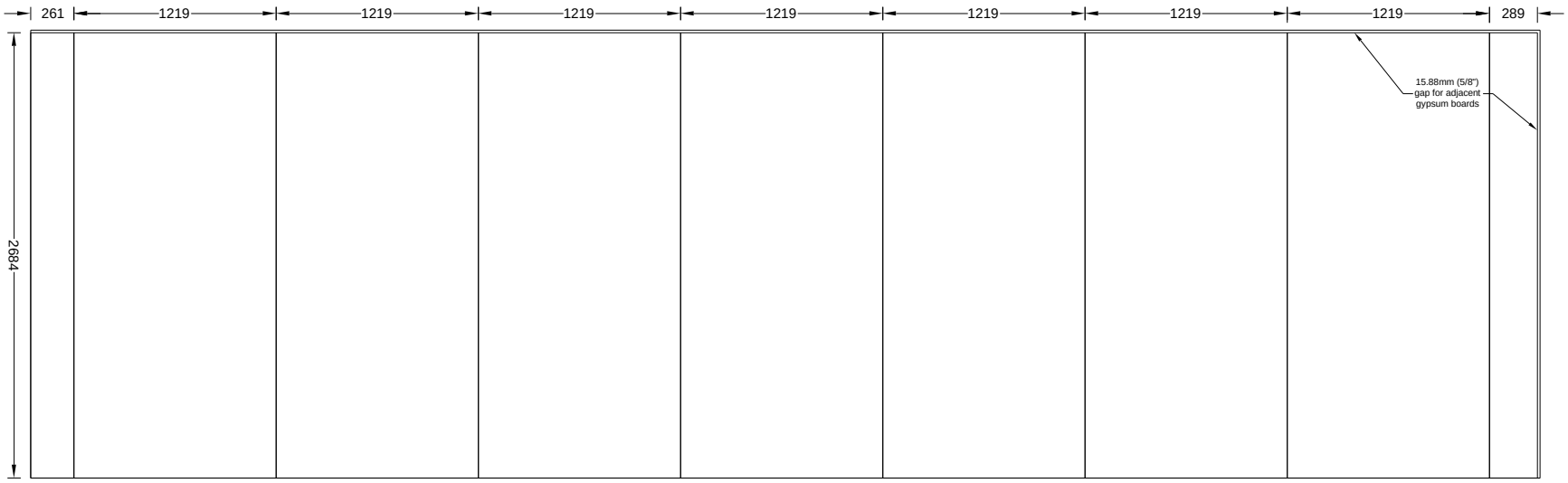

Figure A 40. Test 1-2 Large Compartment CLT - W3 - Gypsum Layout - Base Layer

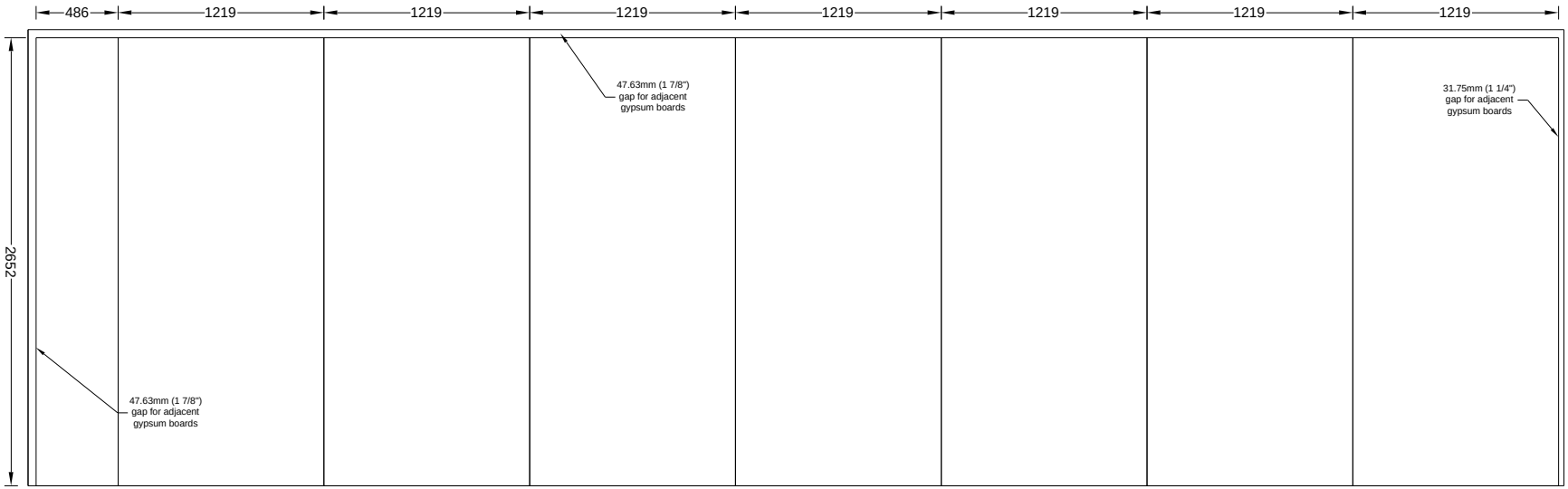

(Dimensions in mm)

Figure A 41. Test 1-2 Large Compartment CLT - W3 - Gypsum Layout - Face Layer

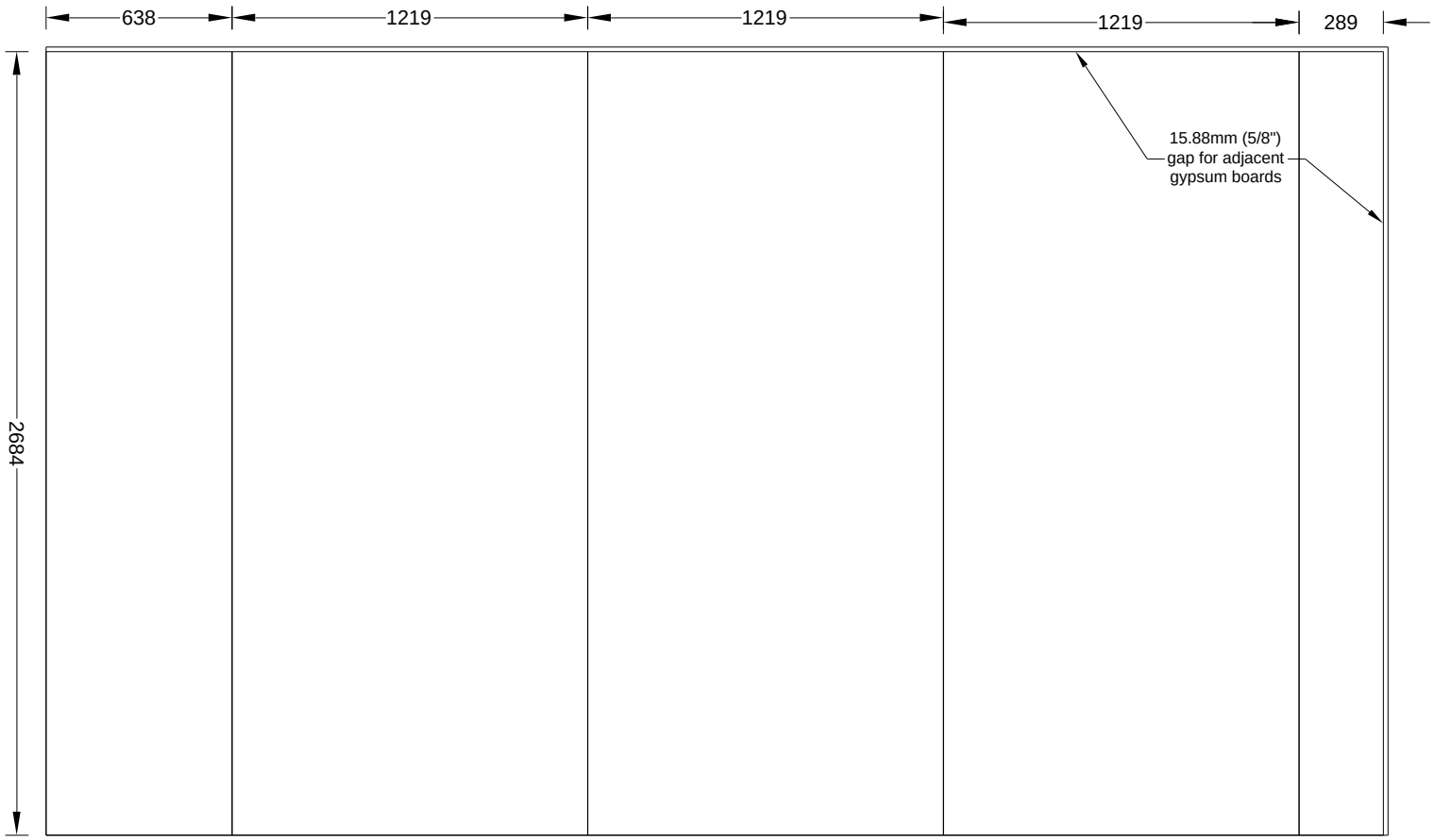

(Dimensions in mm)

Figure A 42. Test 1-2 Large Compartment CLT - W4 - Gypsum Layout - Base Layer

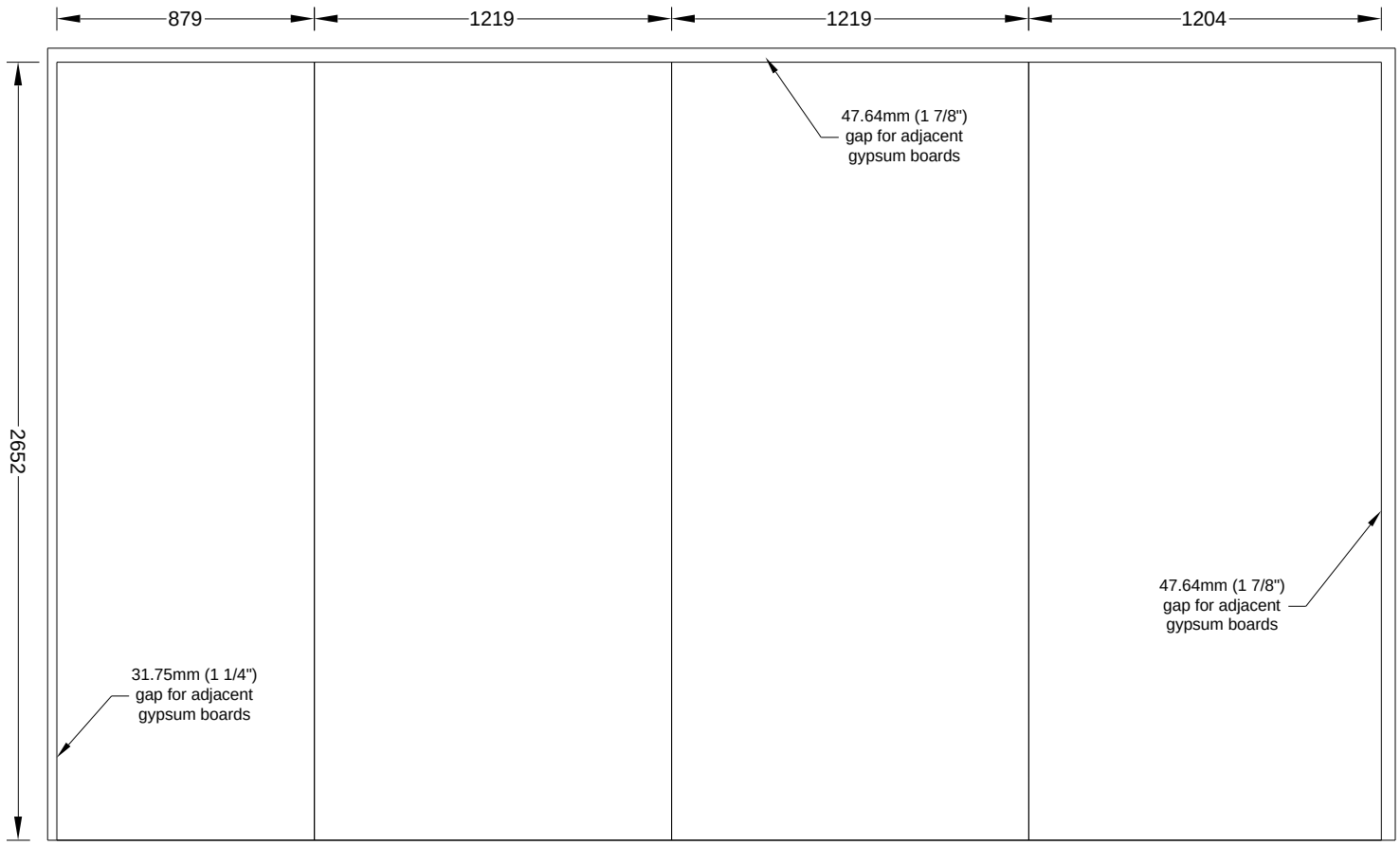

(Dimensions in mm)

Figure A 43. Test 1-2 Large Compartment CLT - W4 - Gypsum Layout - Face Layer

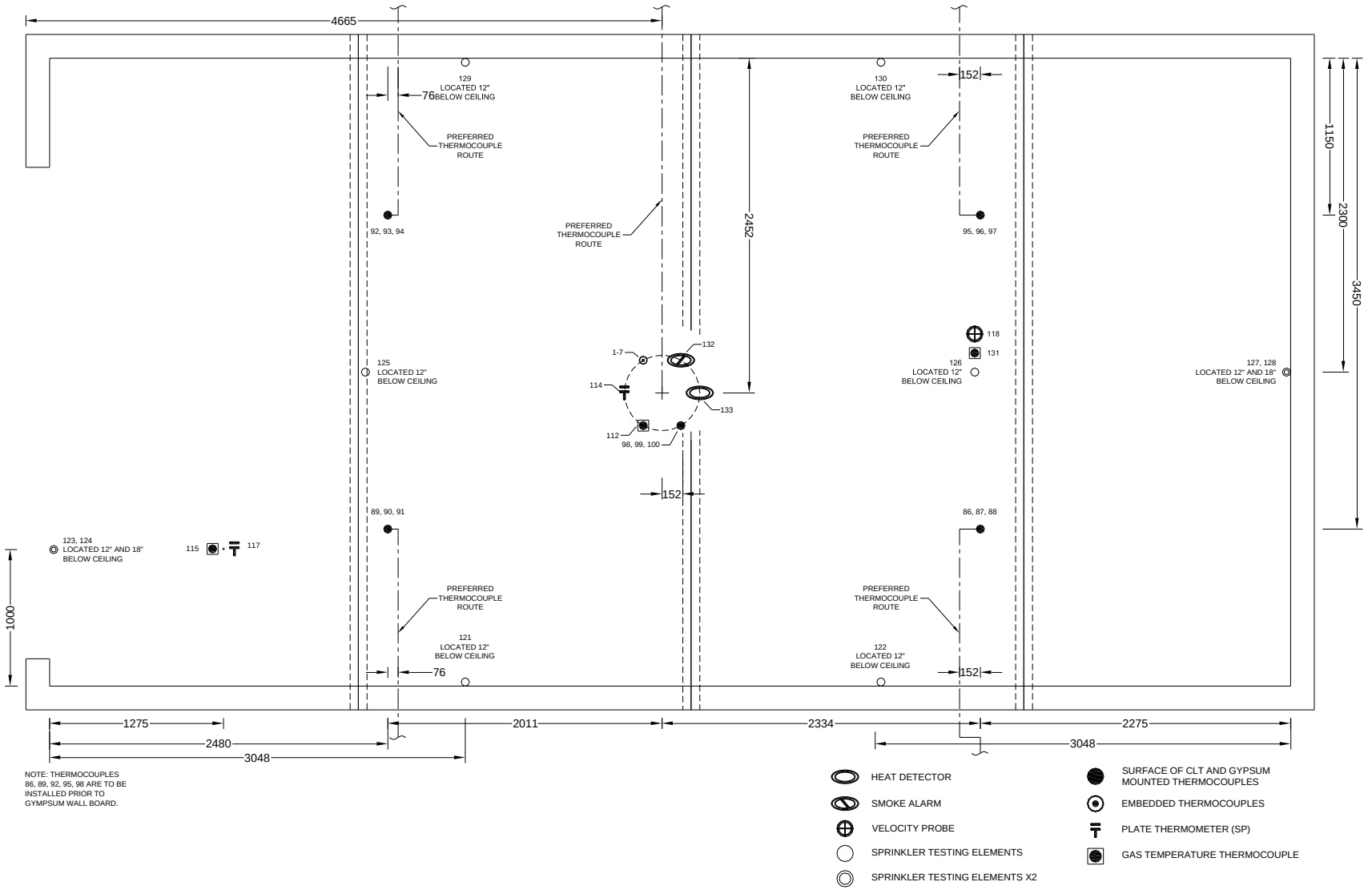

(Dimensions in mm)

Figure A 44. Test 1-3 Large Compartment CLT - Ceiling - Instrumentation Layout

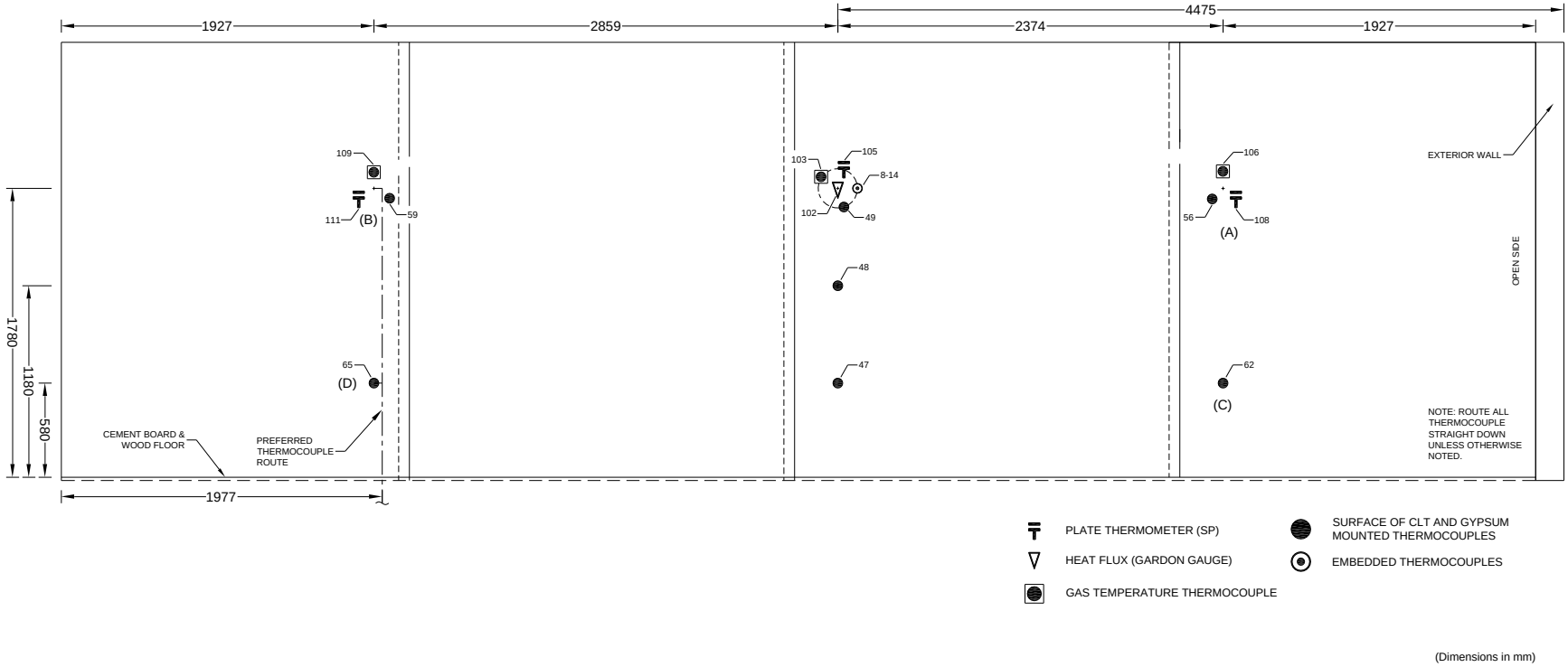

Figure A 45. Test 1-3 Large Compartment CLT - W1 - Instrumentation Layout

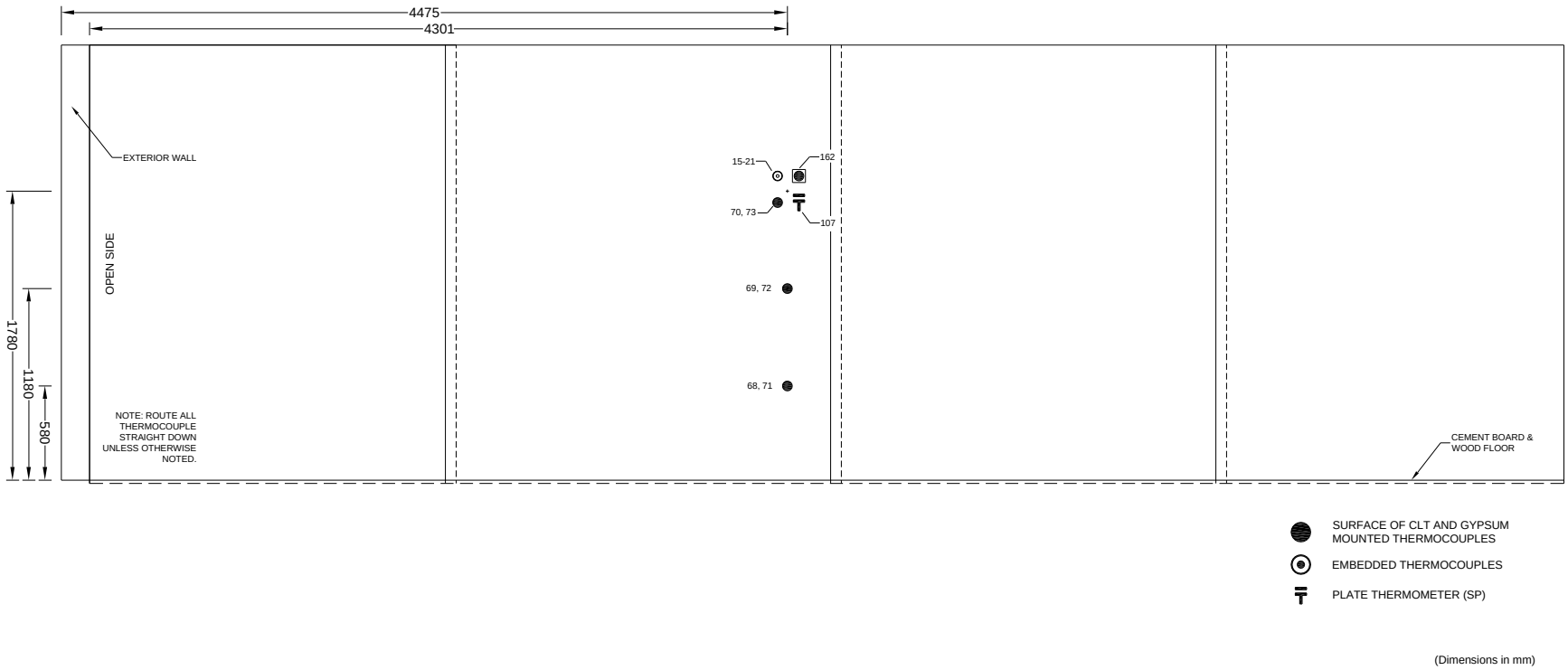

Figure A 46. Test 1-3 Large Compartment CLT - W3 - Instrumentation Layout

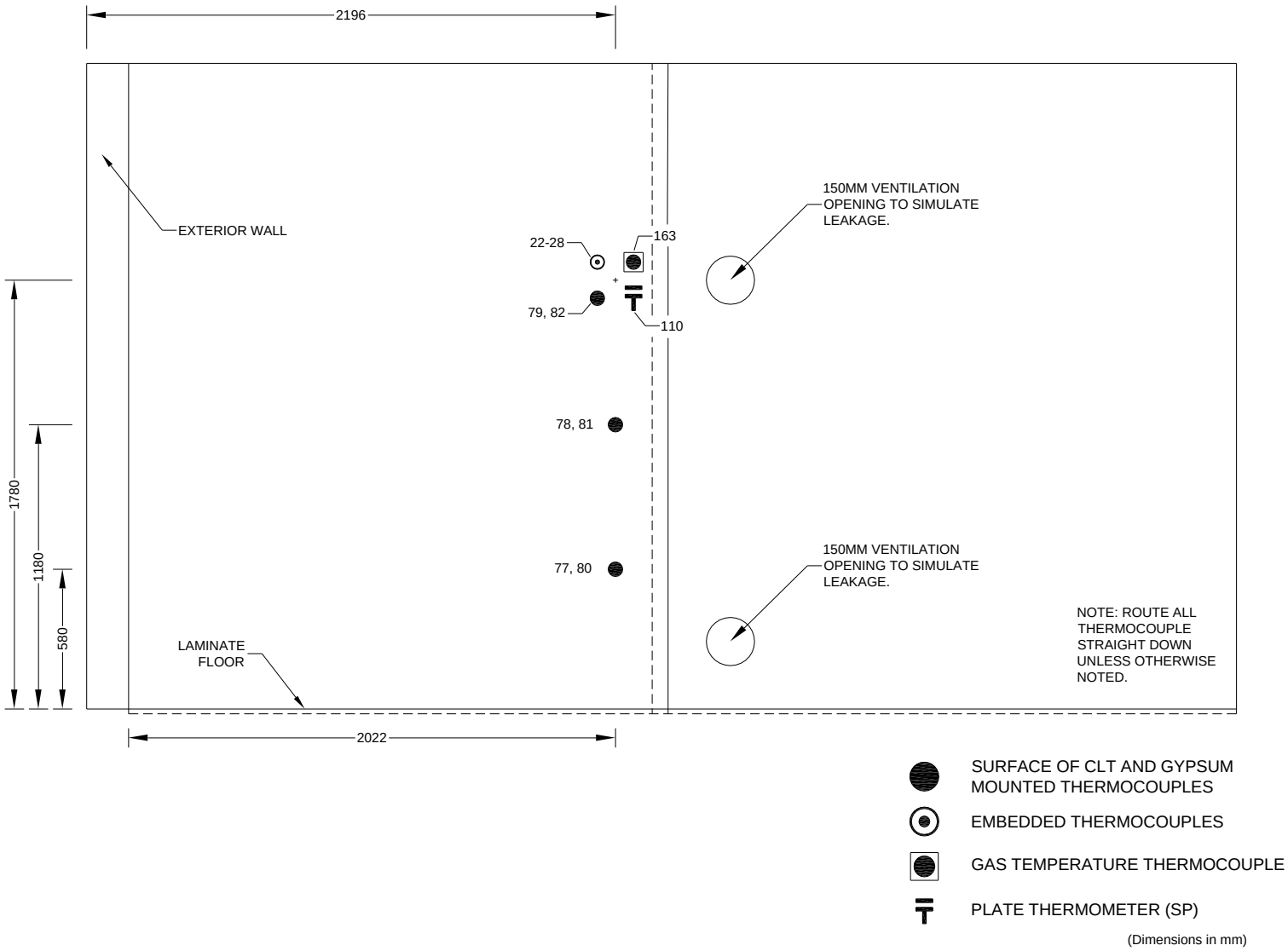

Figure A 47. Test 1-3 Large Compartment CLT - W4 - Instrumentation Layout

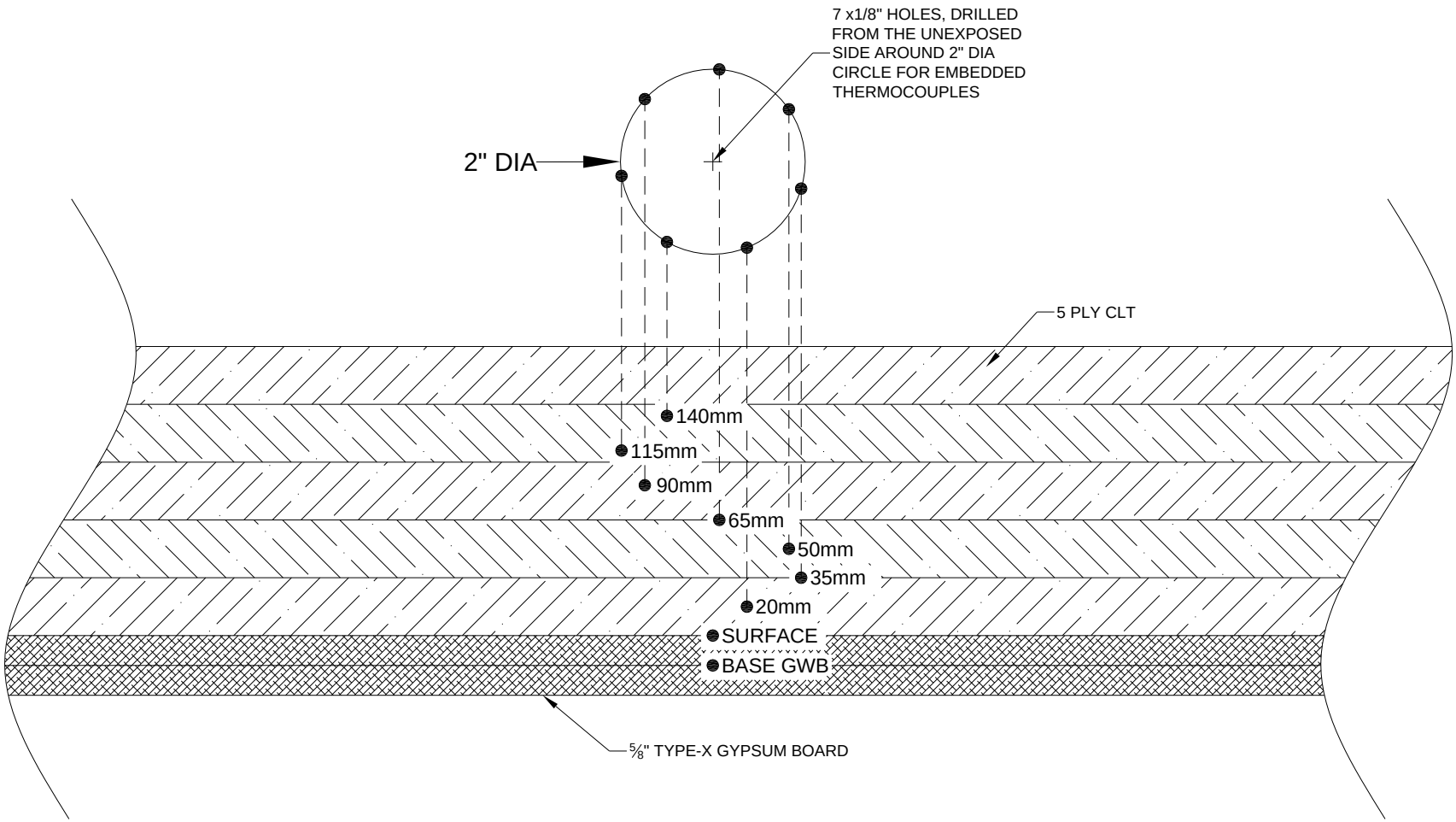

Figure A 48. Test 1-3 Large Compartment CLT - Embedded Thermocouple Detail

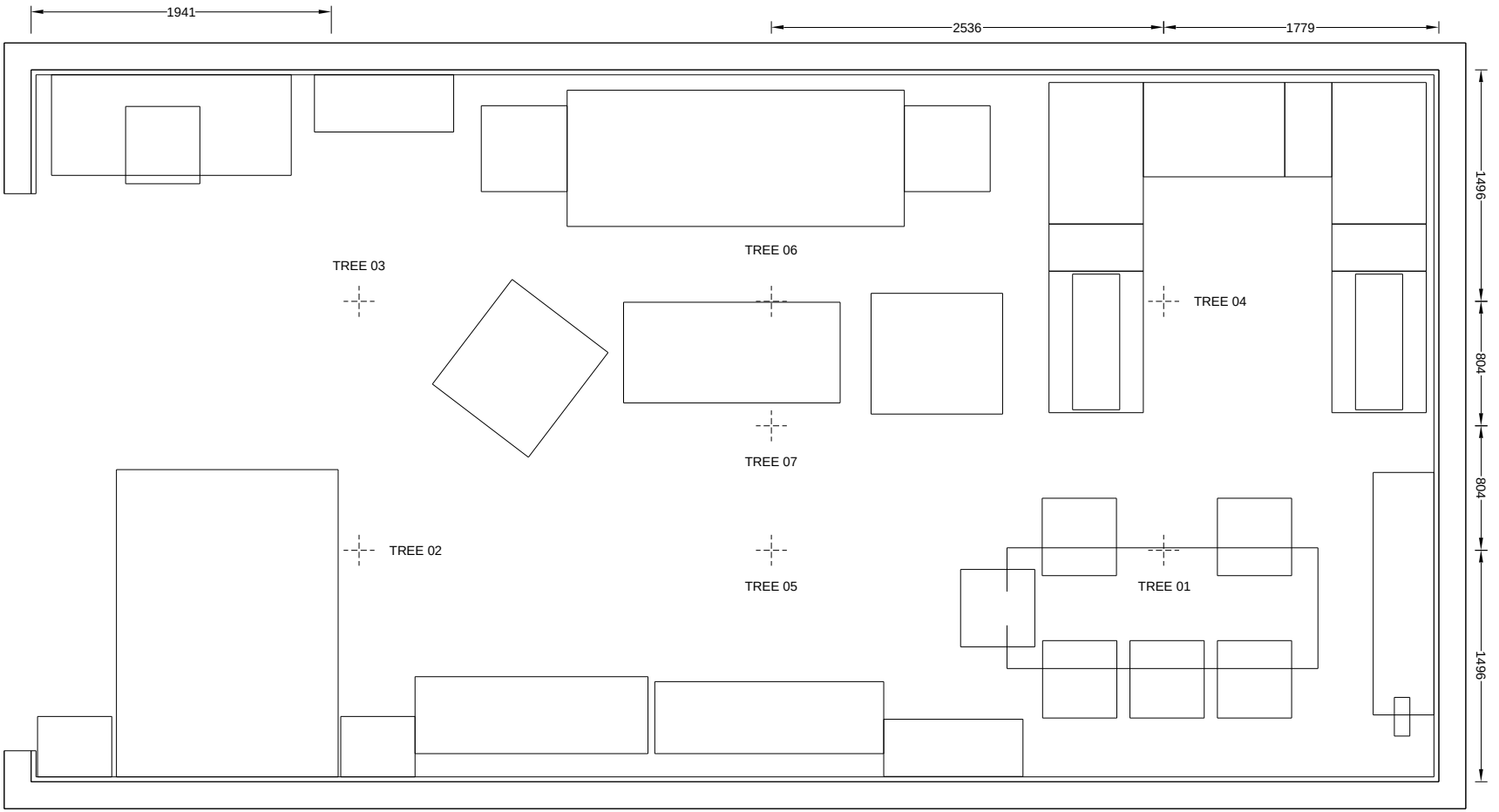

Figure A 49. Test 1-3 Large Compartment CLT - Instrumentation Tree Layout

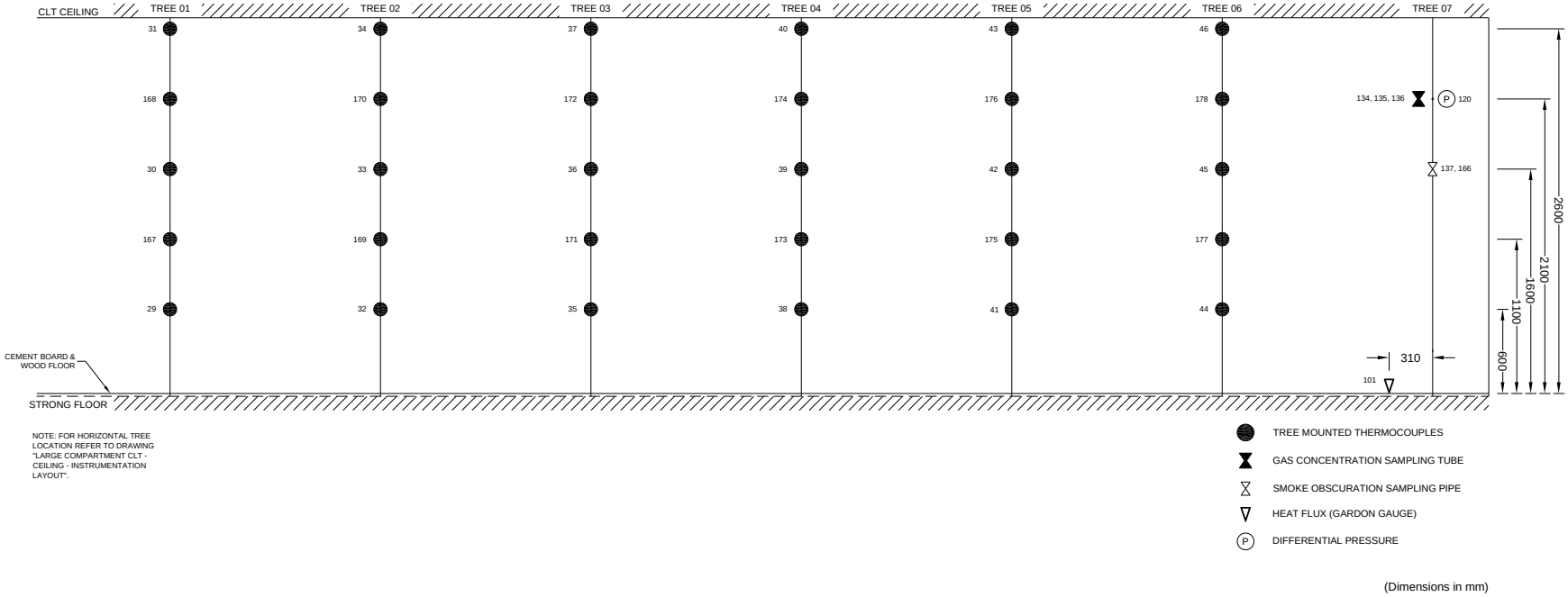

Figure A 50. Test 1-3 Large Compartment CLT - Instrumentation Tree Specifications

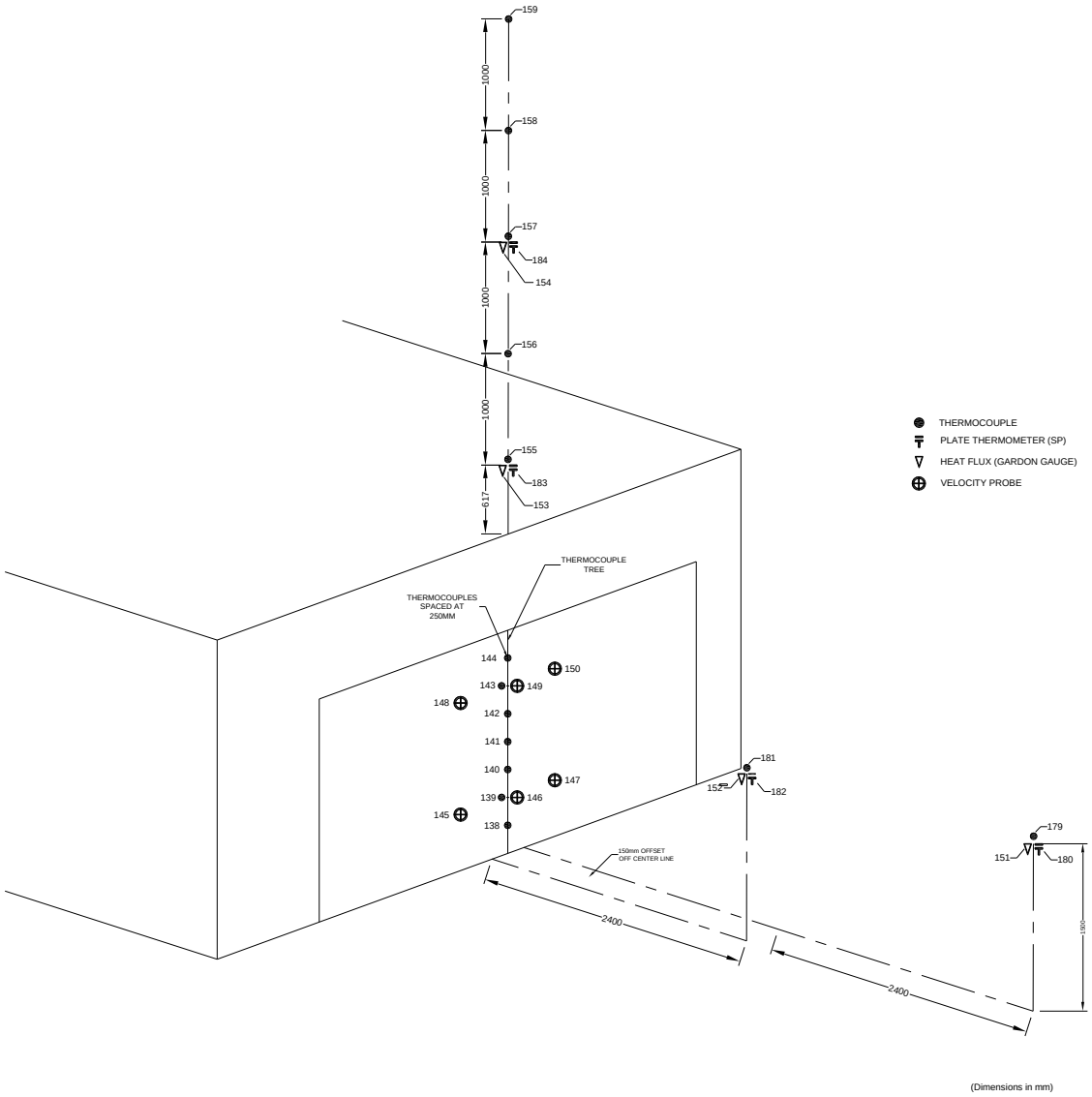

Figure A 51. Test 1-3 Large Compartment CLT - Exterior Instrumentation Layout

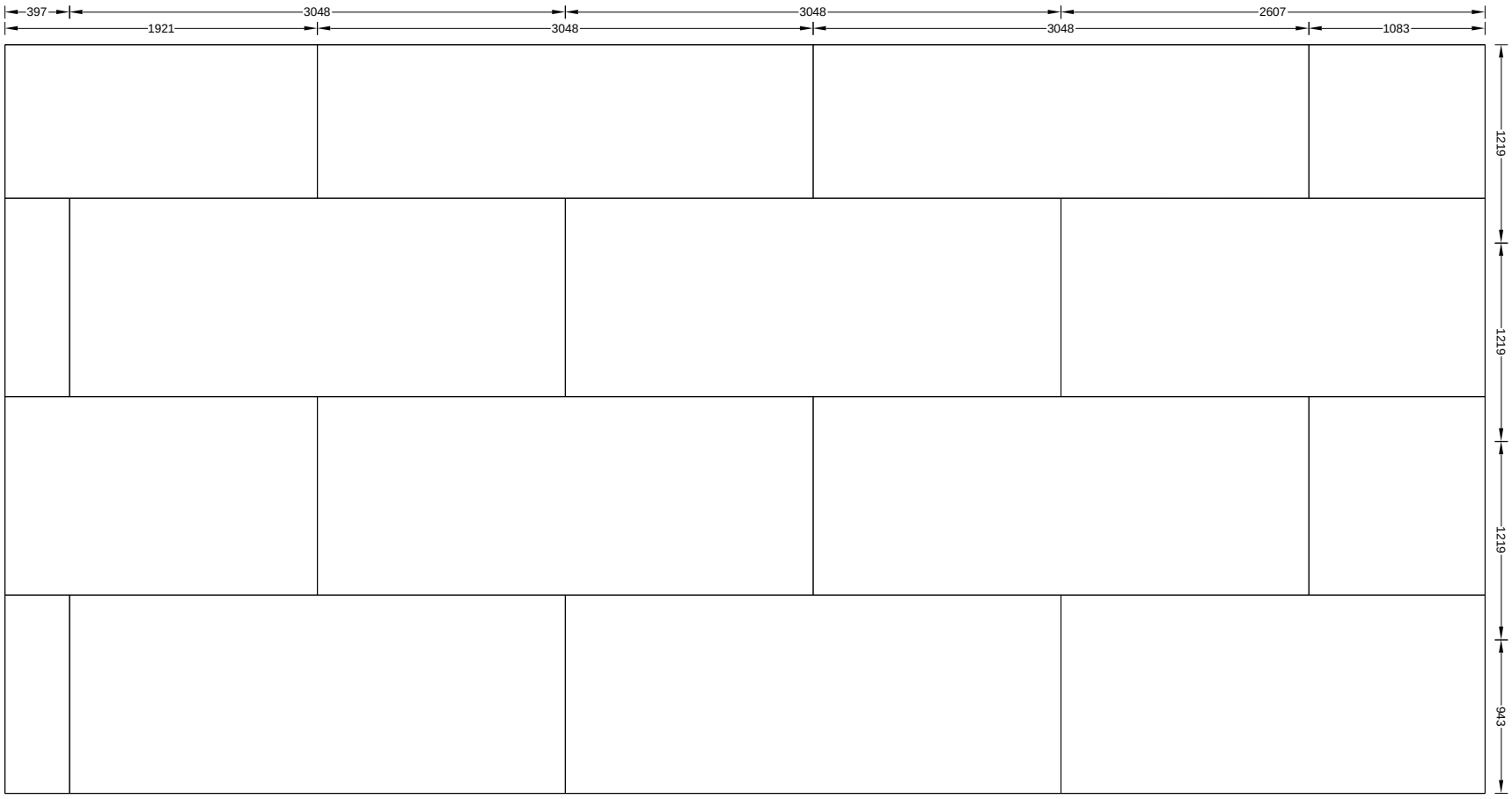

Figure A 52. Test 1-3 Large Compartment CLT - Ceiling - Gypsum Layout - Base Layer

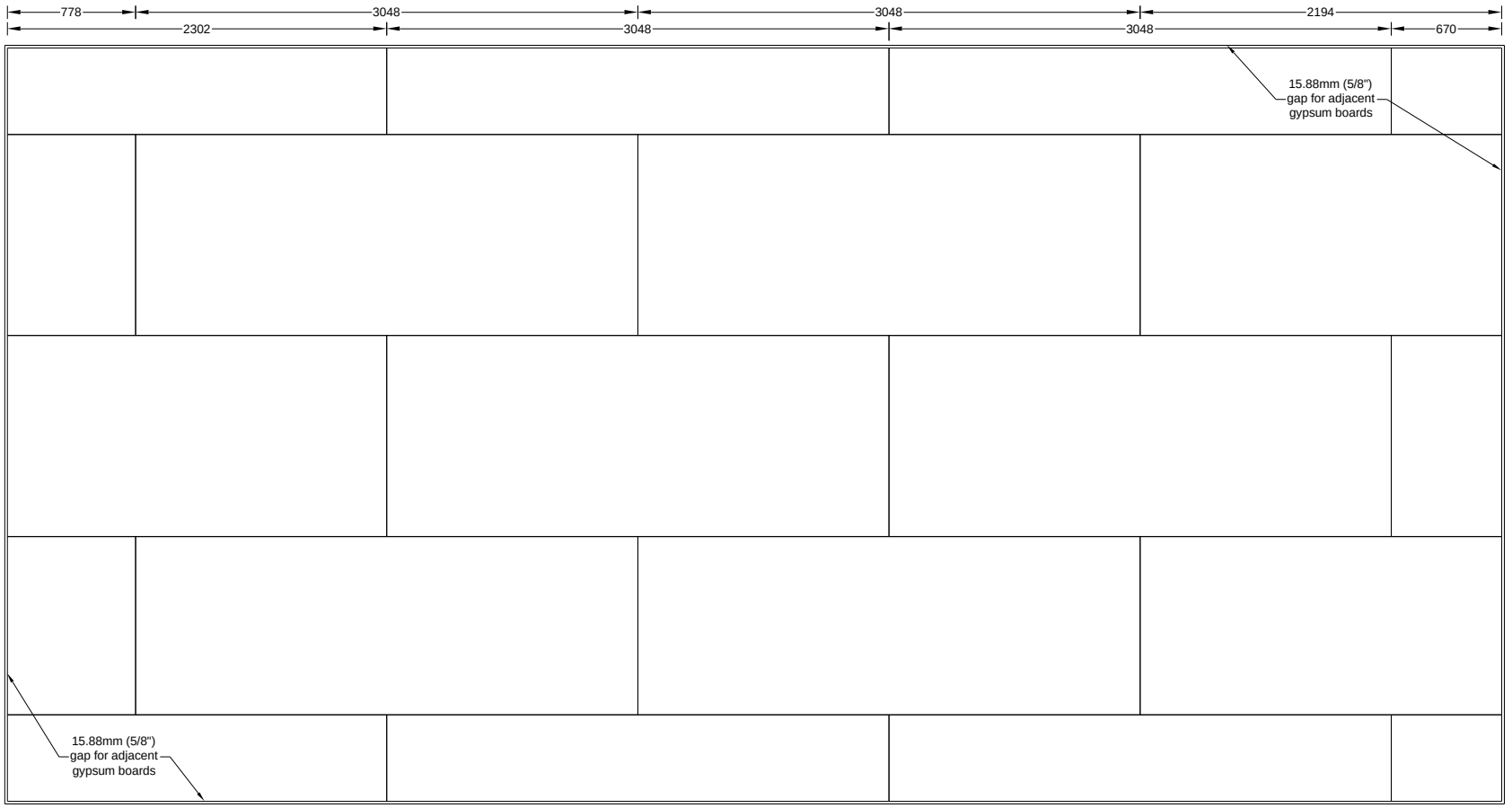

Figure A 53. Test 1-3 Large Compartment CLT - Ceiling - Gypsum Layout - Middle Layer

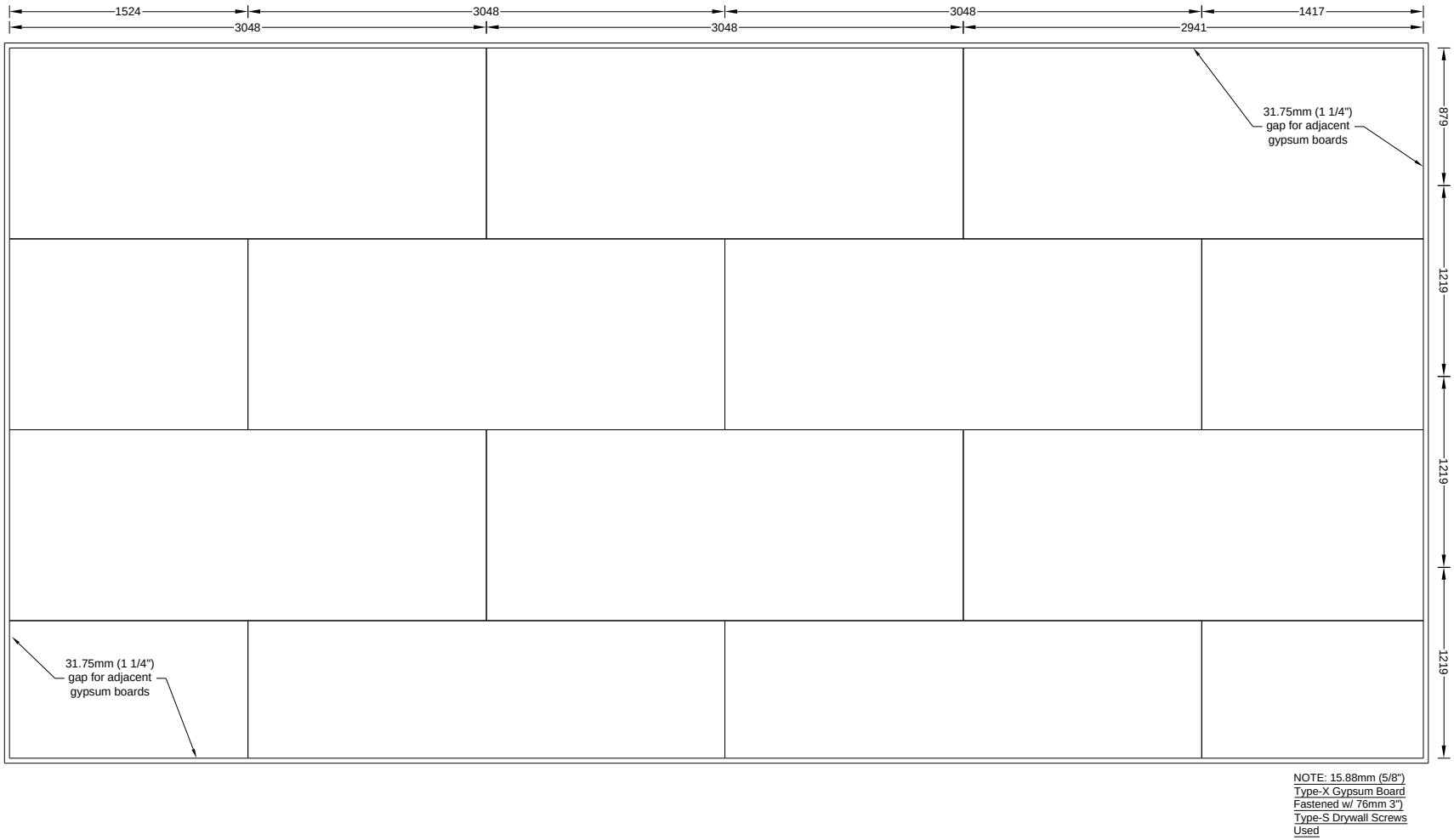

Figure A 54. Test 1-3 Large Compartment CLT - Ceiling - Gypsum Layout - Face Layer

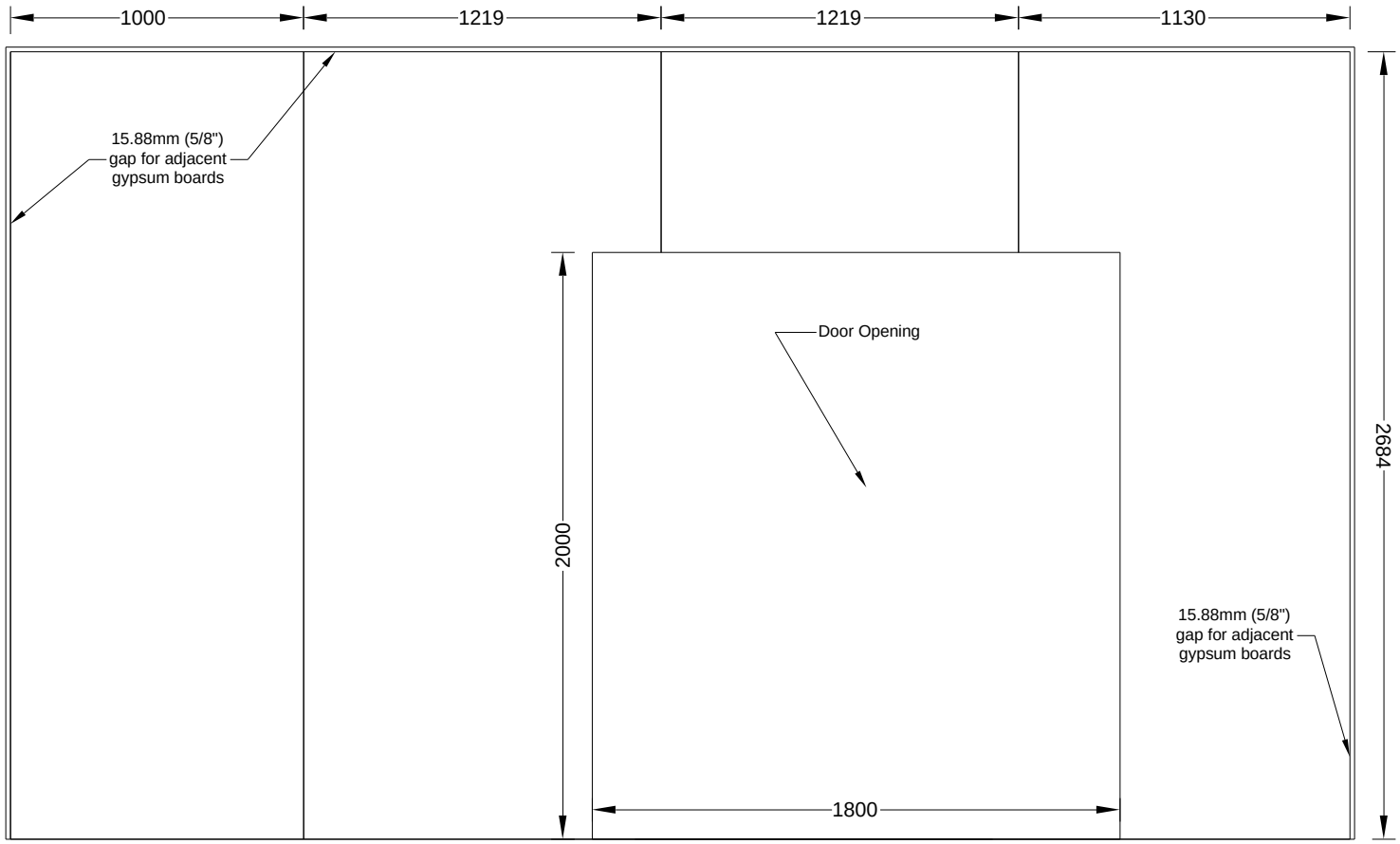

(Dimensions in mm)

Figure A 55. Test 1-3 Large Compartment CLT - W2 - Gypsum Layout - Base Layer

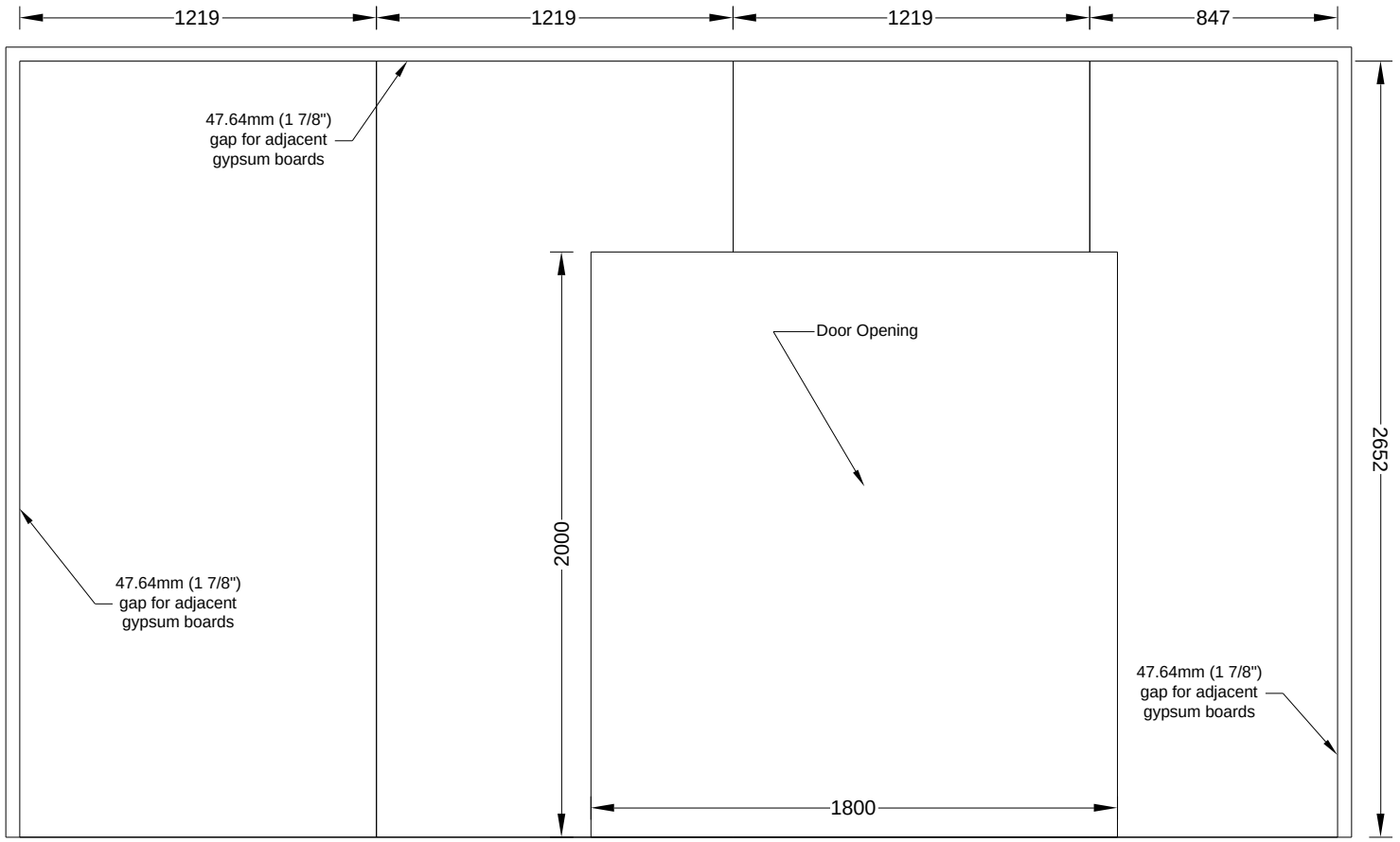

(Dimensions in mm)

Figure A 56. Test 1-3 Large Compartment CLT - W2 - Gypsum Layout - Face Layer

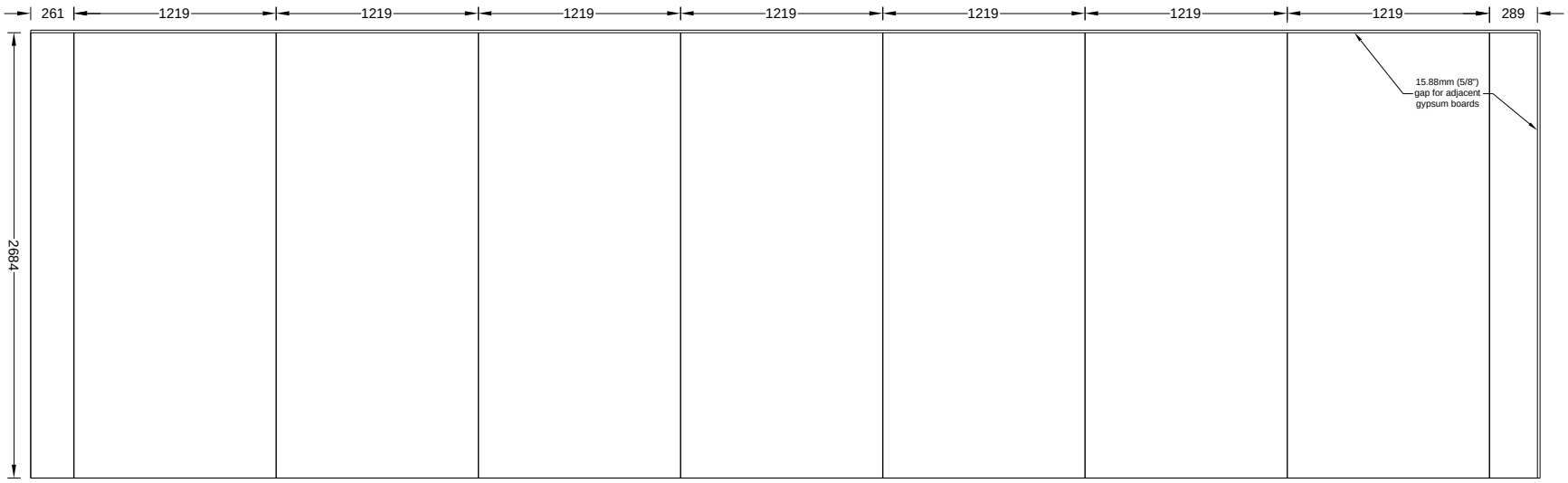

Figure A 57. Test 1-2 Large Compartment CLT - W3 - Gypsum Layout - Base Layer

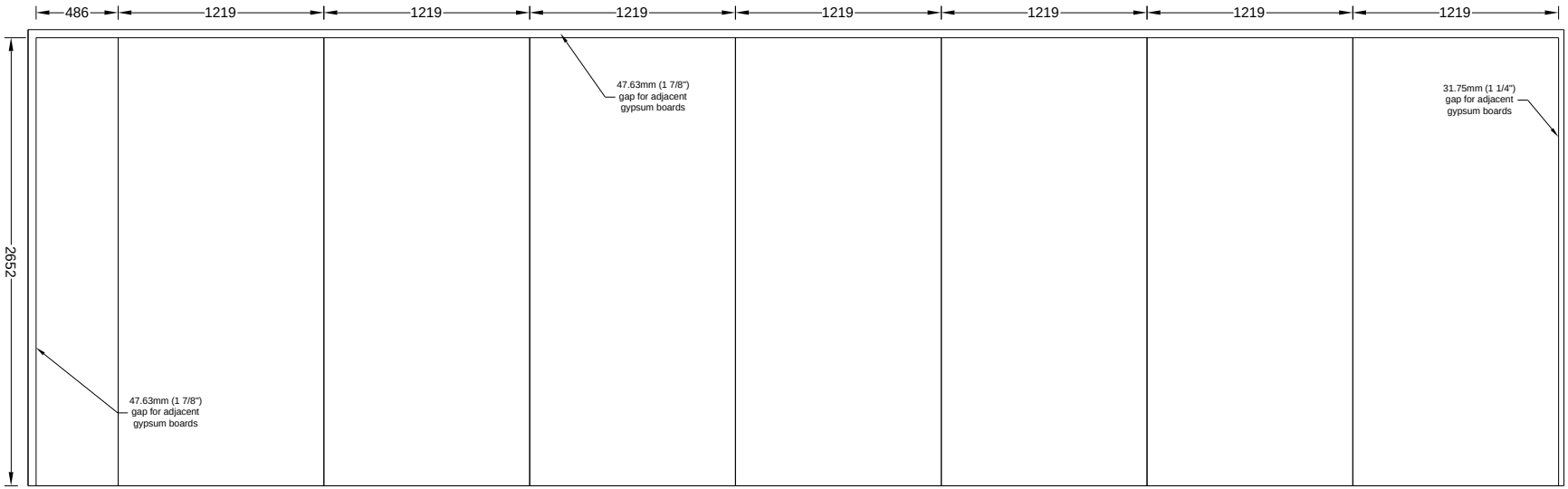

(Dimensions in mm)

Figure A 58. Test 1-3 Large Compartment CLT - W3 - Gypsum Layout - Face Layer

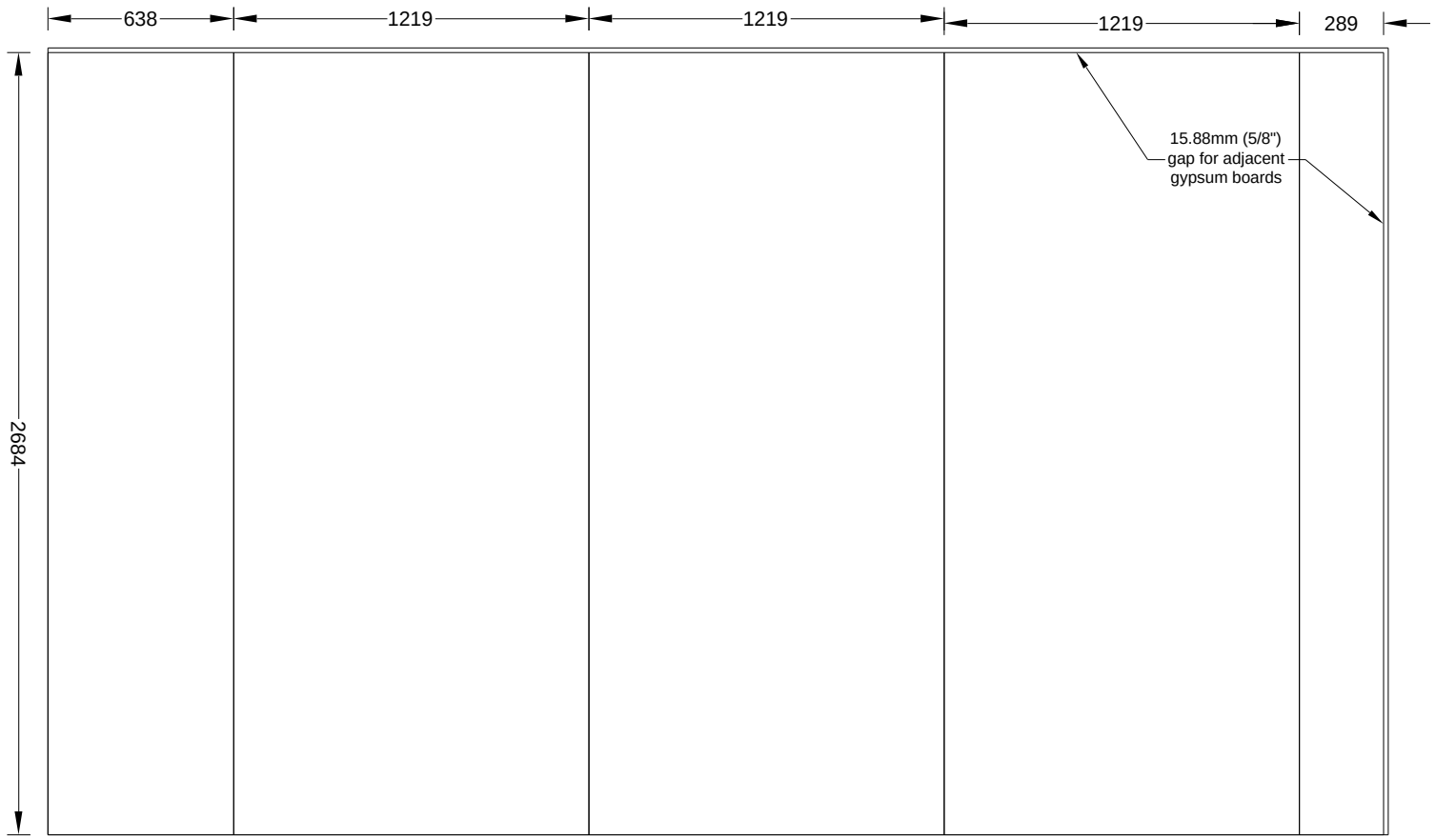

(Dimensions in mm)

Figure A 59. Test 1-3 Large Compartment CLT - W4 - Gypsum Layout - Base Layer

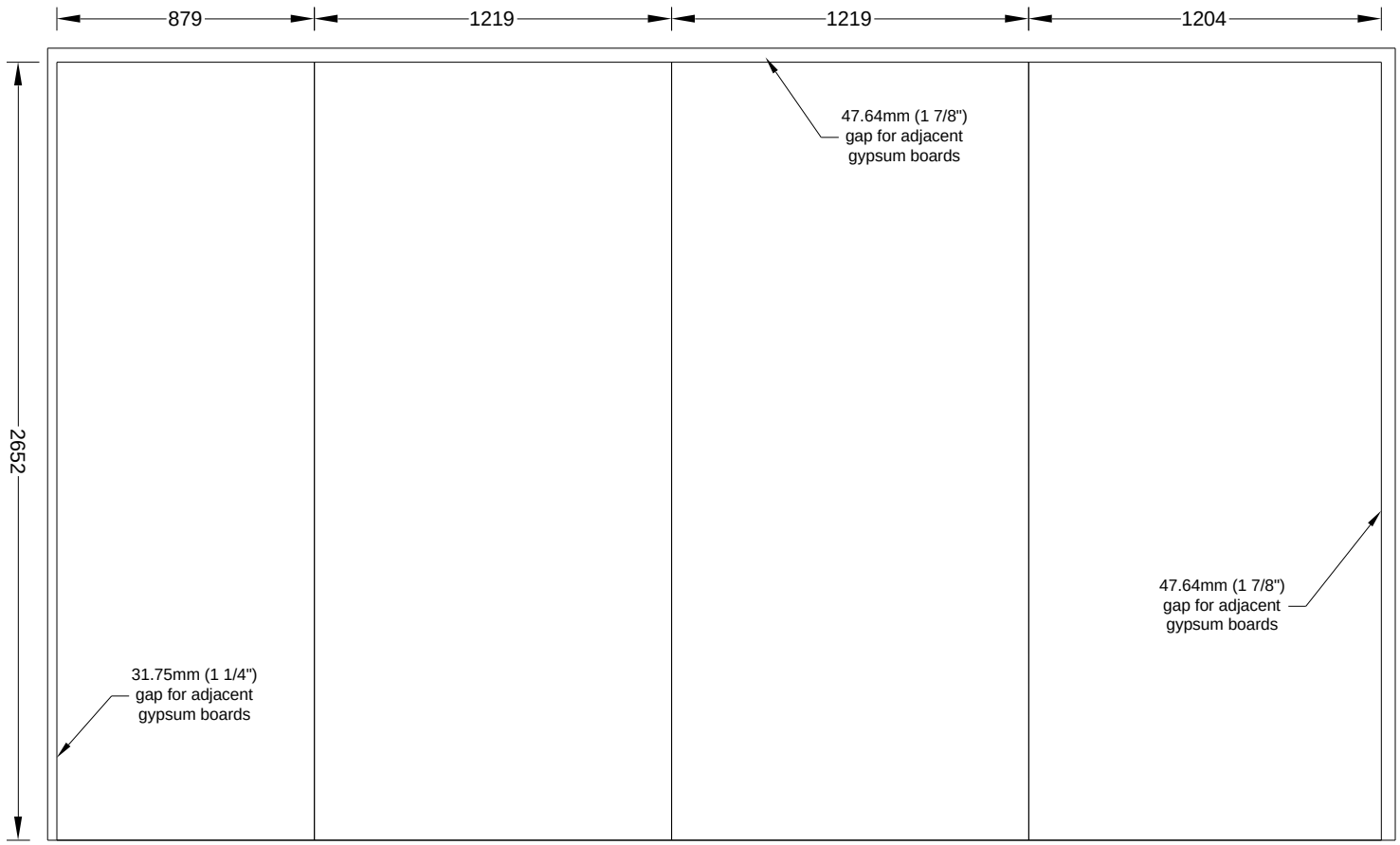

Figure A 60. Test 1-3 Large Compartment CLT - W4 - Gypsum Layout - Face Layer

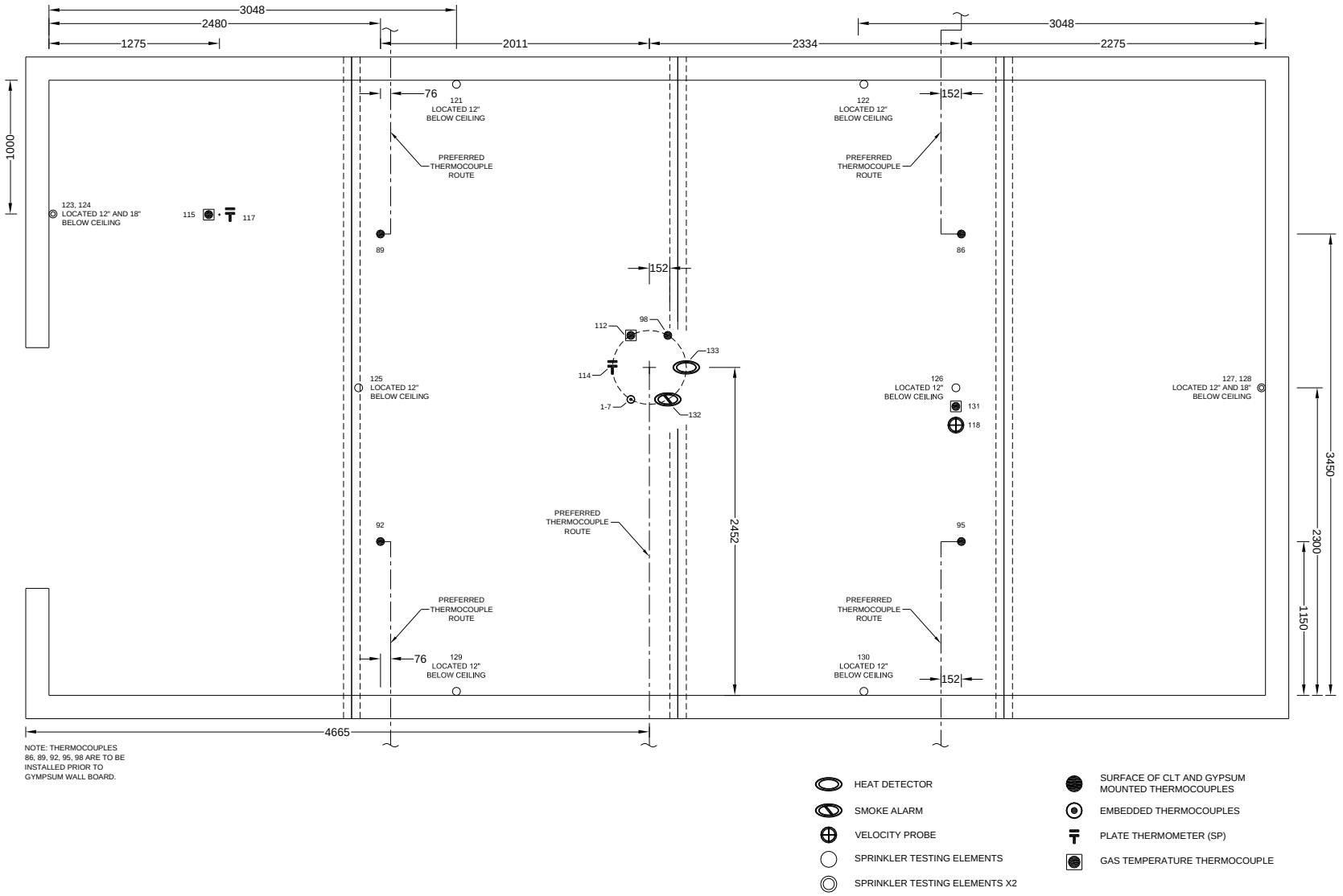

(Dimensions in mm)

Figure A 61. Test 1-4 Large Compartment CLT - Ceiling - Instrumentation Layout

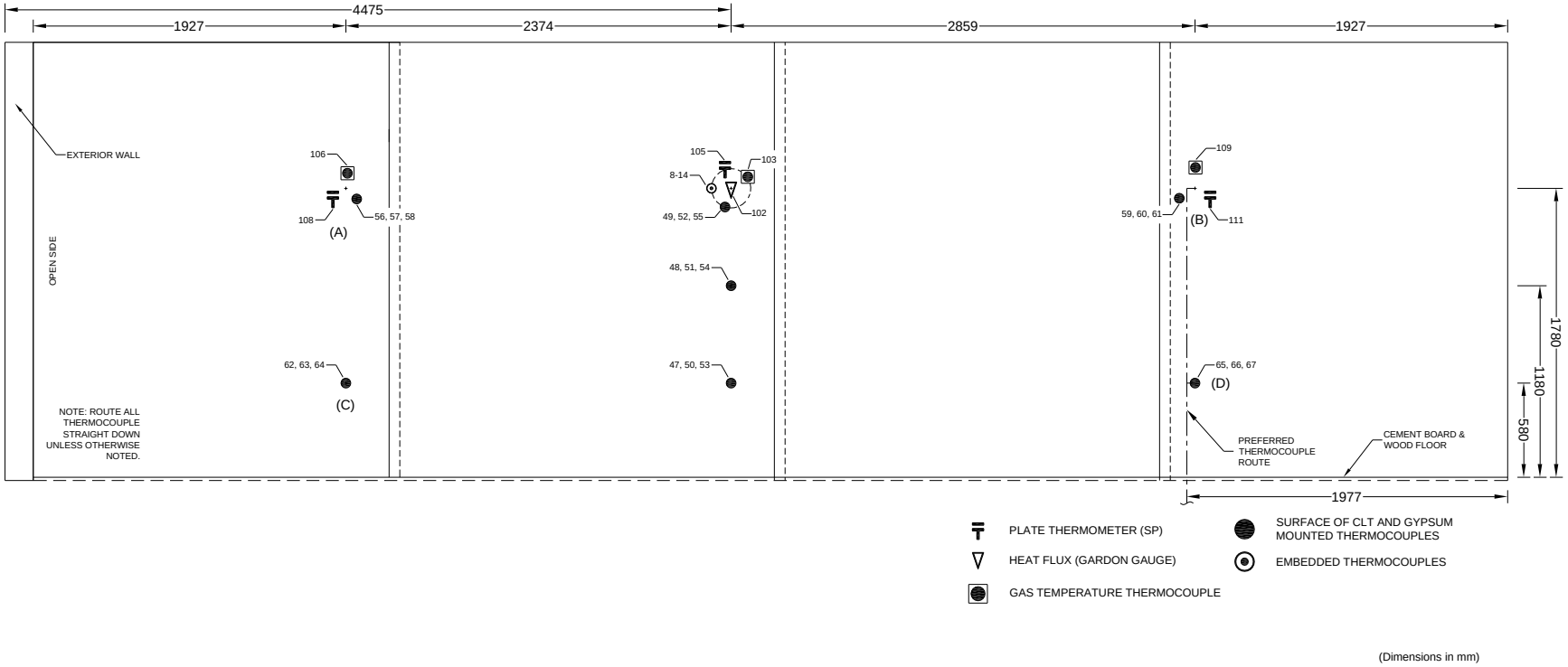

Figure A 62. Test 1-4 Large Compartment CLT - W1 - Instrumentation Layout

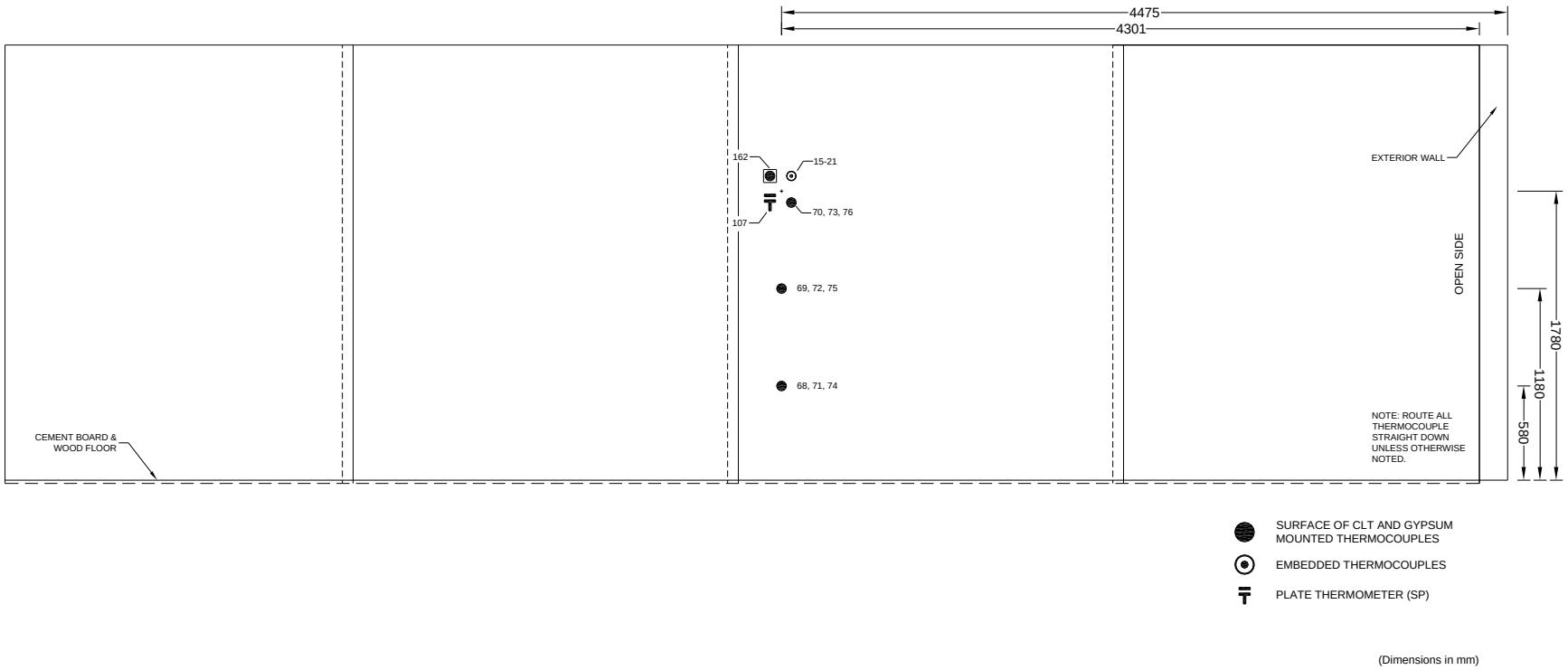

Figure A 63. Test 1-4 Large Compartment CLT - W3 - Instrumentation Layout

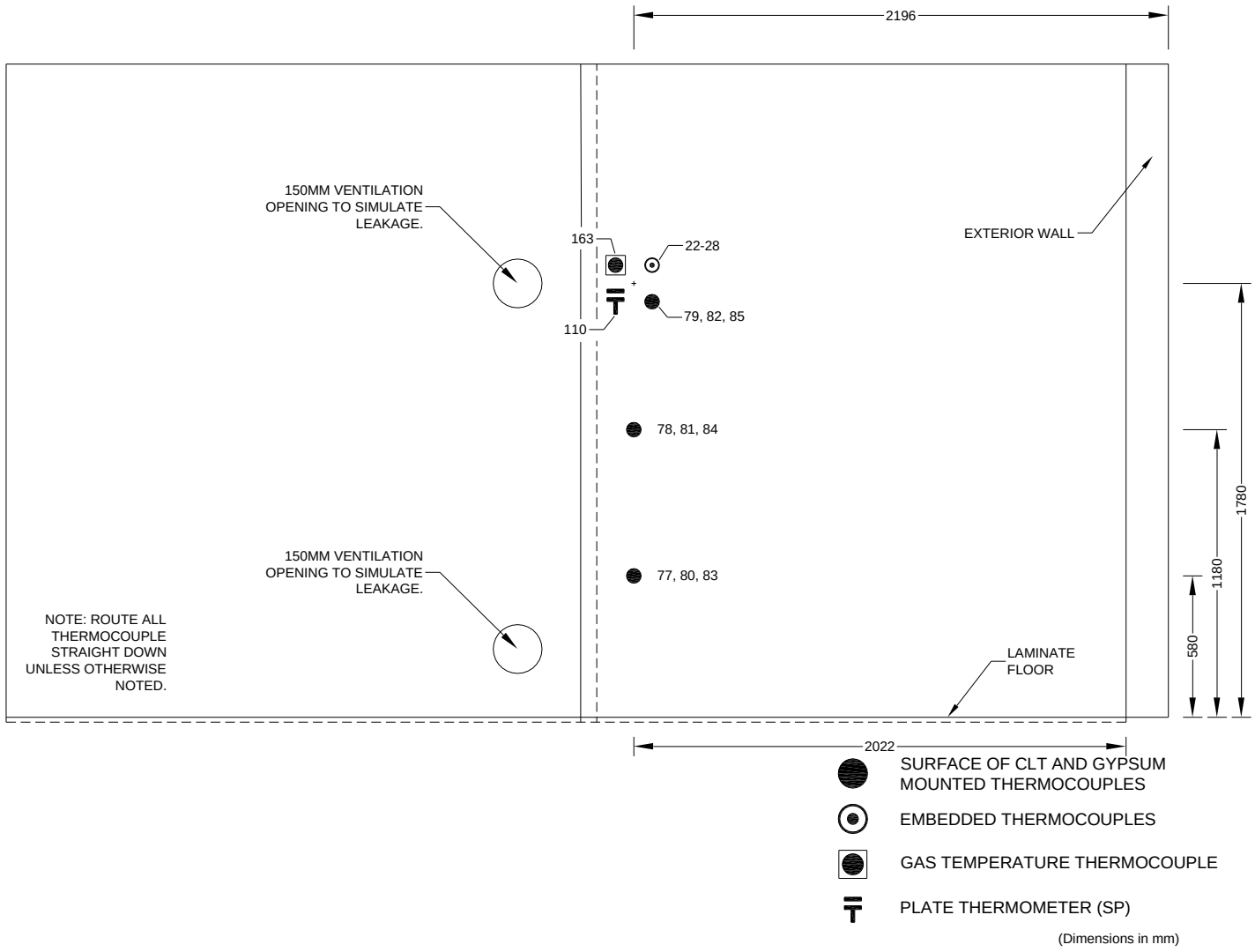

Figure A 64. Test 1-4 Large Compartment CLT - W4 - Instrumentation Layout

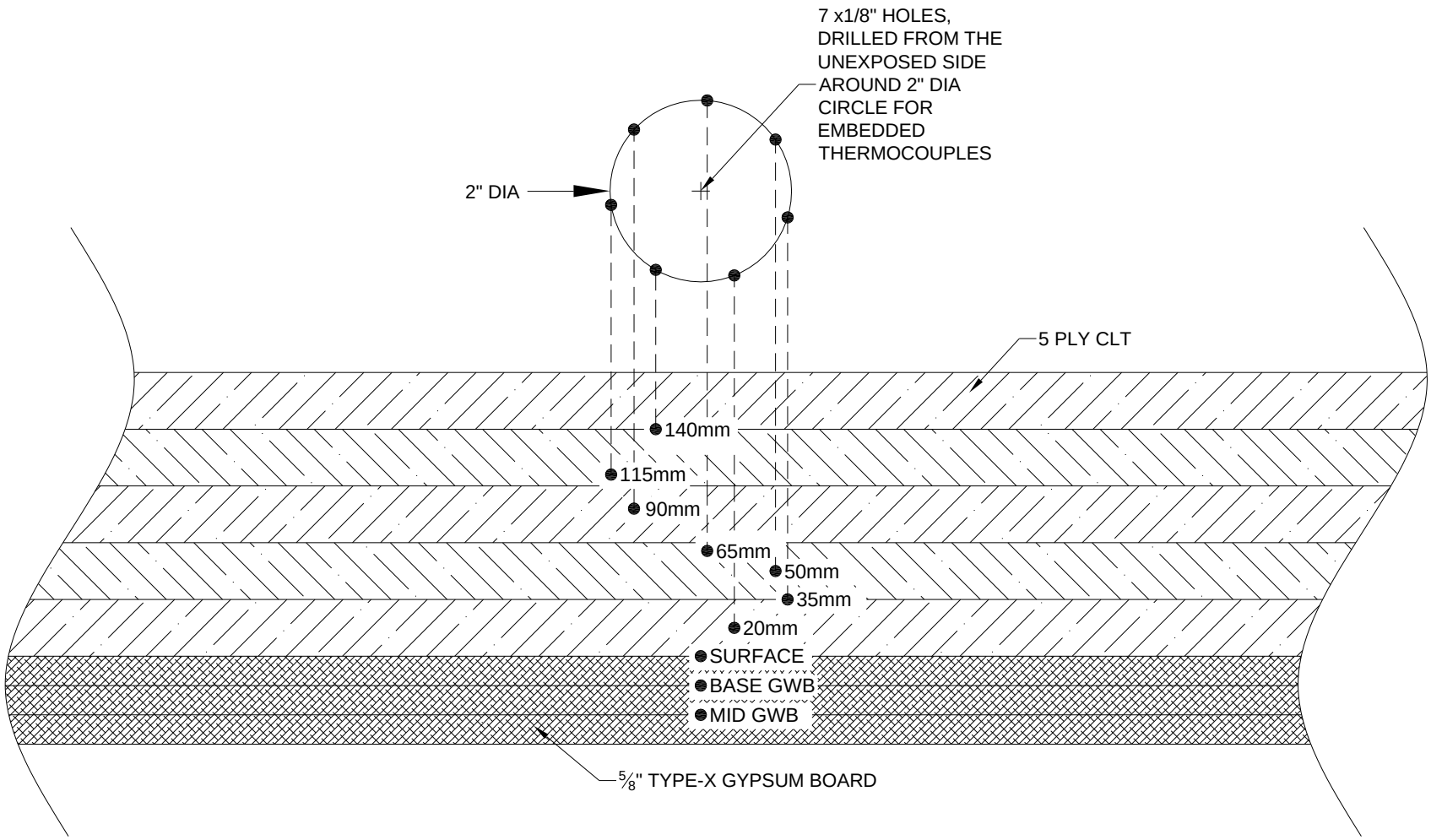

Figure A 65. Test 1-4 Large Compartment CLT - Embedded Thermocouple Detail

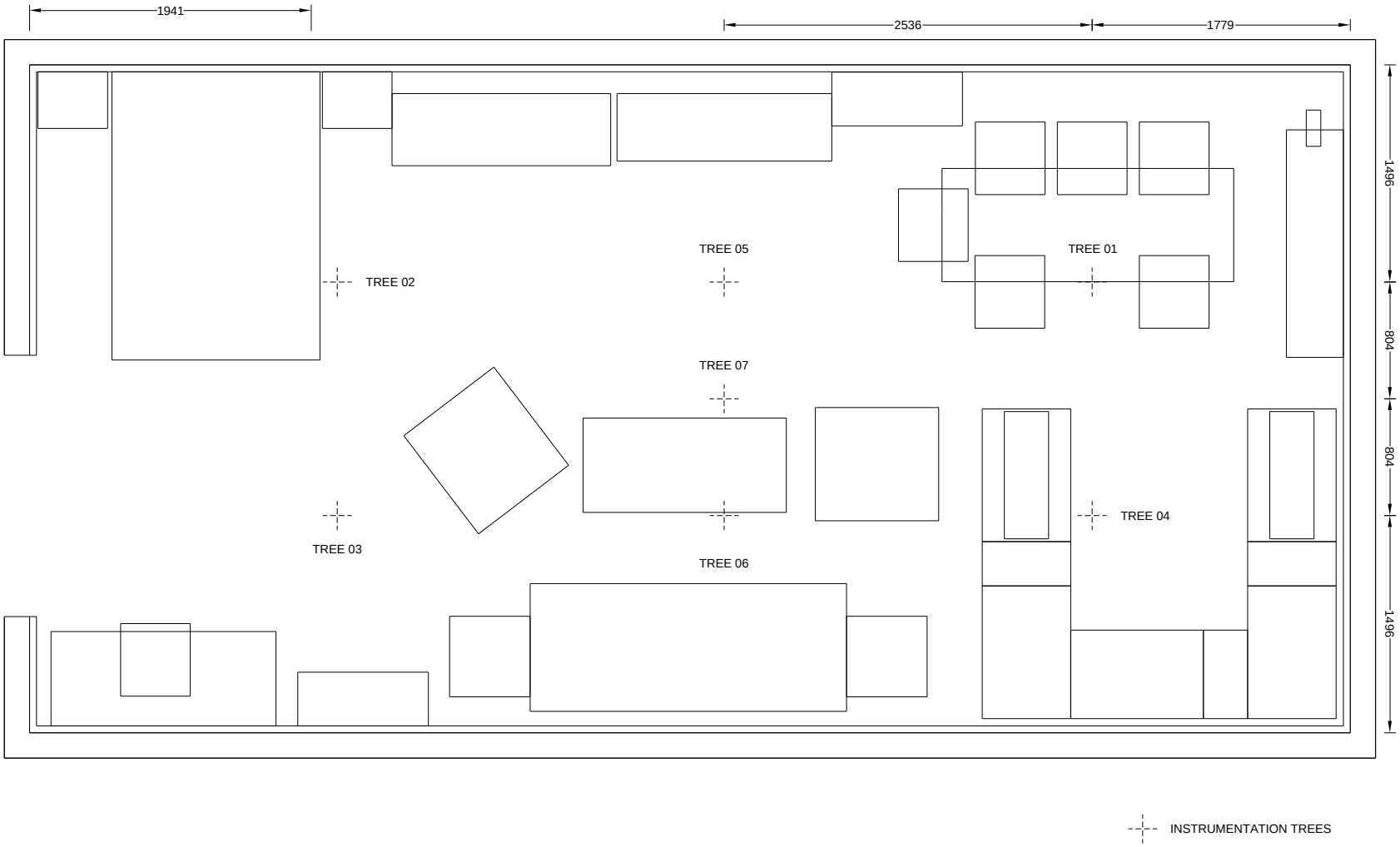

Figure A 66. Test 1-4 Large Compartment CLT - Instrumentation Tree Layout

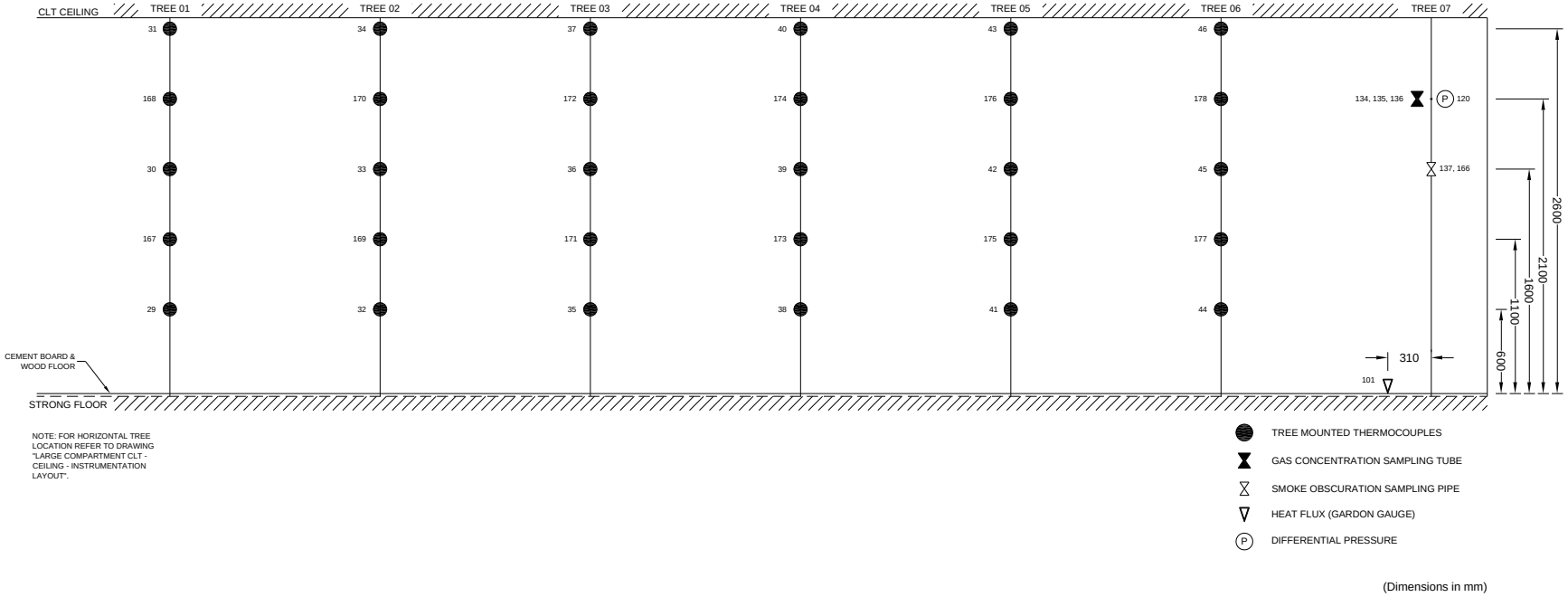

Figure A 67. Test 1-4 Large Compartment CLT - Instrumentation Tree Specifications

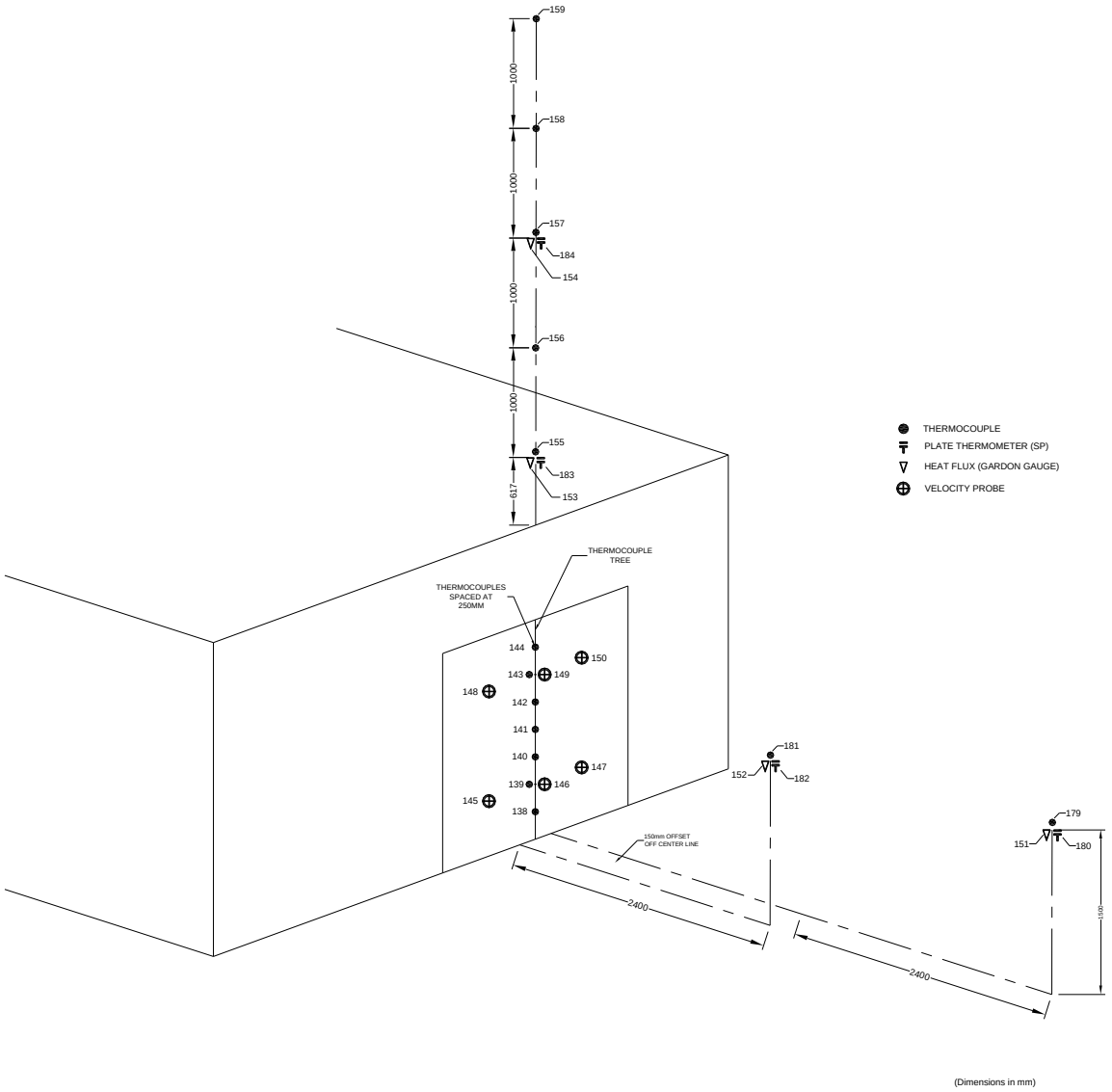

Figure A 68. Test 1-4 Large Compartment CLT - Exterior Instrumentation Layout

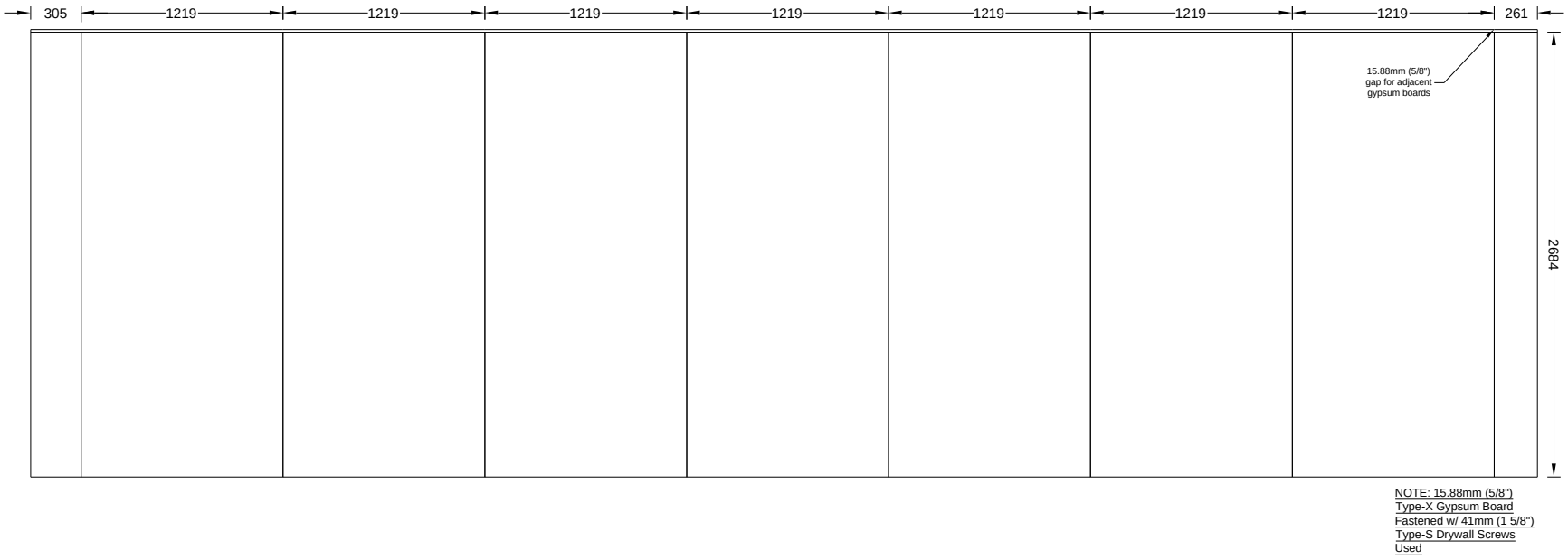

Figure A 69. Test 1-4 Large Compartment CLT - W1 - Gypsum Layout - Base Layer

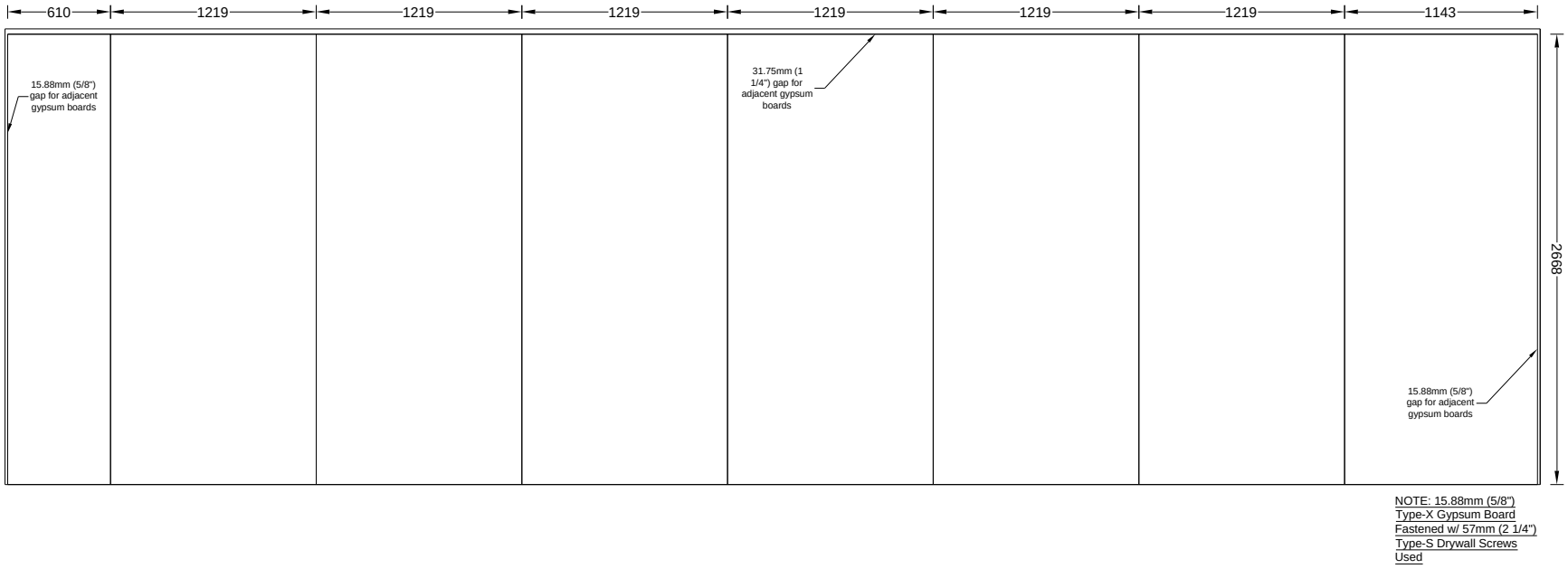

Figure A 70. Test 1-4 Large Compartment CLT - W1 - Gypsum Layout - Middle Layer

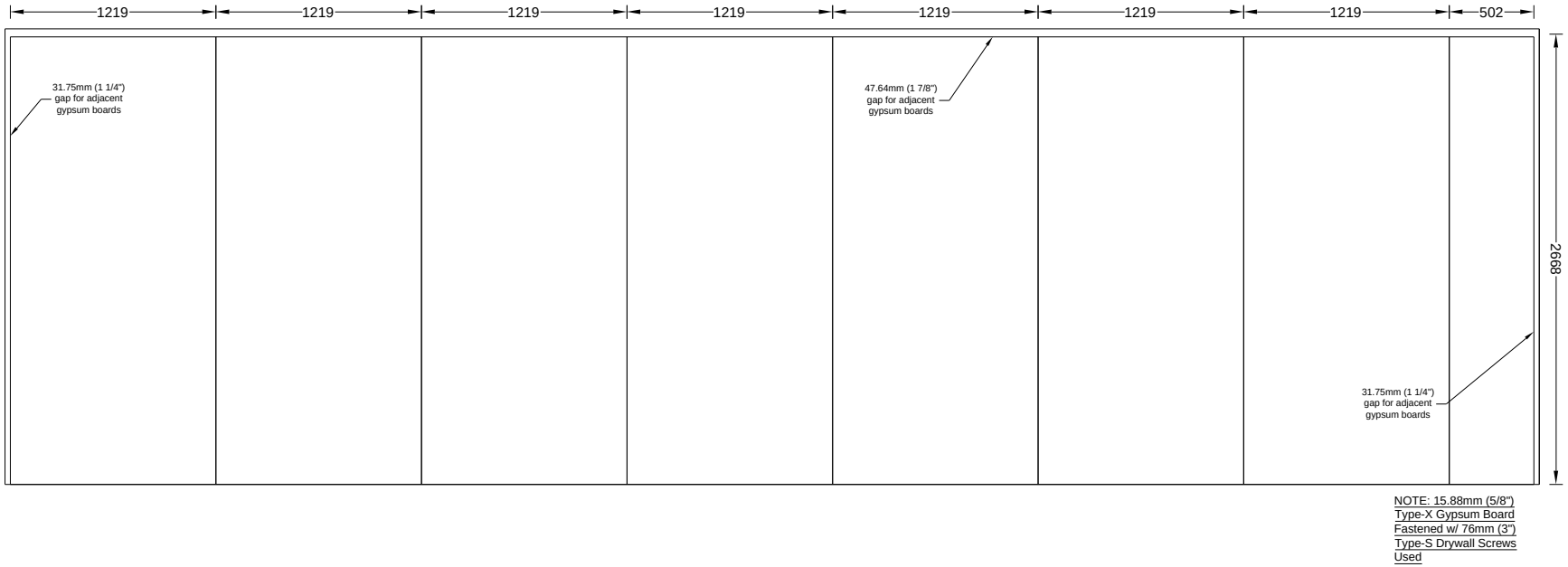

Figure A 71. Test 1-4 Large Compartment CLT - W1 - Gypsum Layout - Face Layer

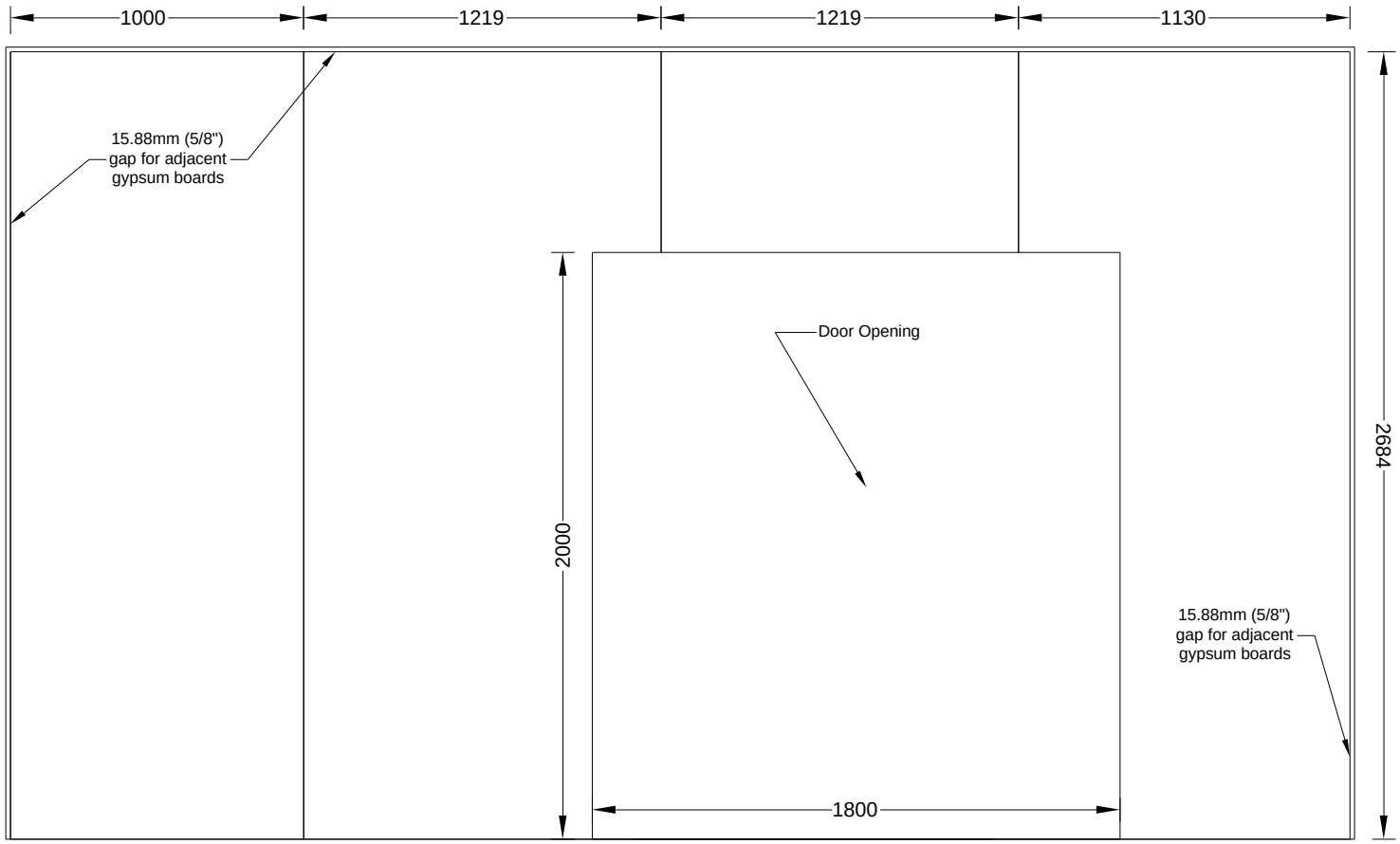

(Dimensions in mm)

Figure A 72. Test 1-4 Large Compartment CLT - W2 - Gypsum Layout - Base Layer

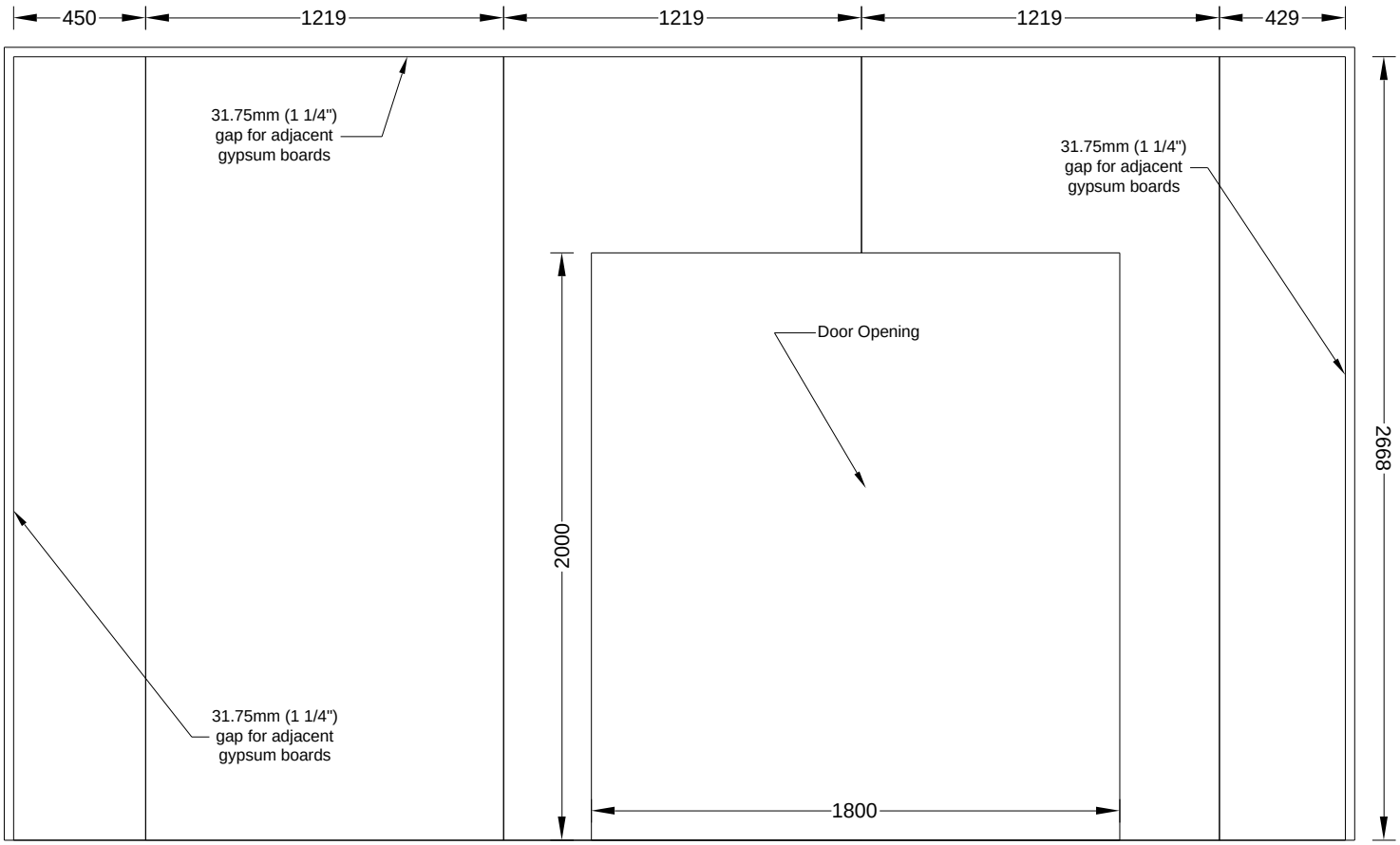

Figure A 73. Test 1-4 Large Compartment CLT - W2 - Gypsum Layout - Middle Layer

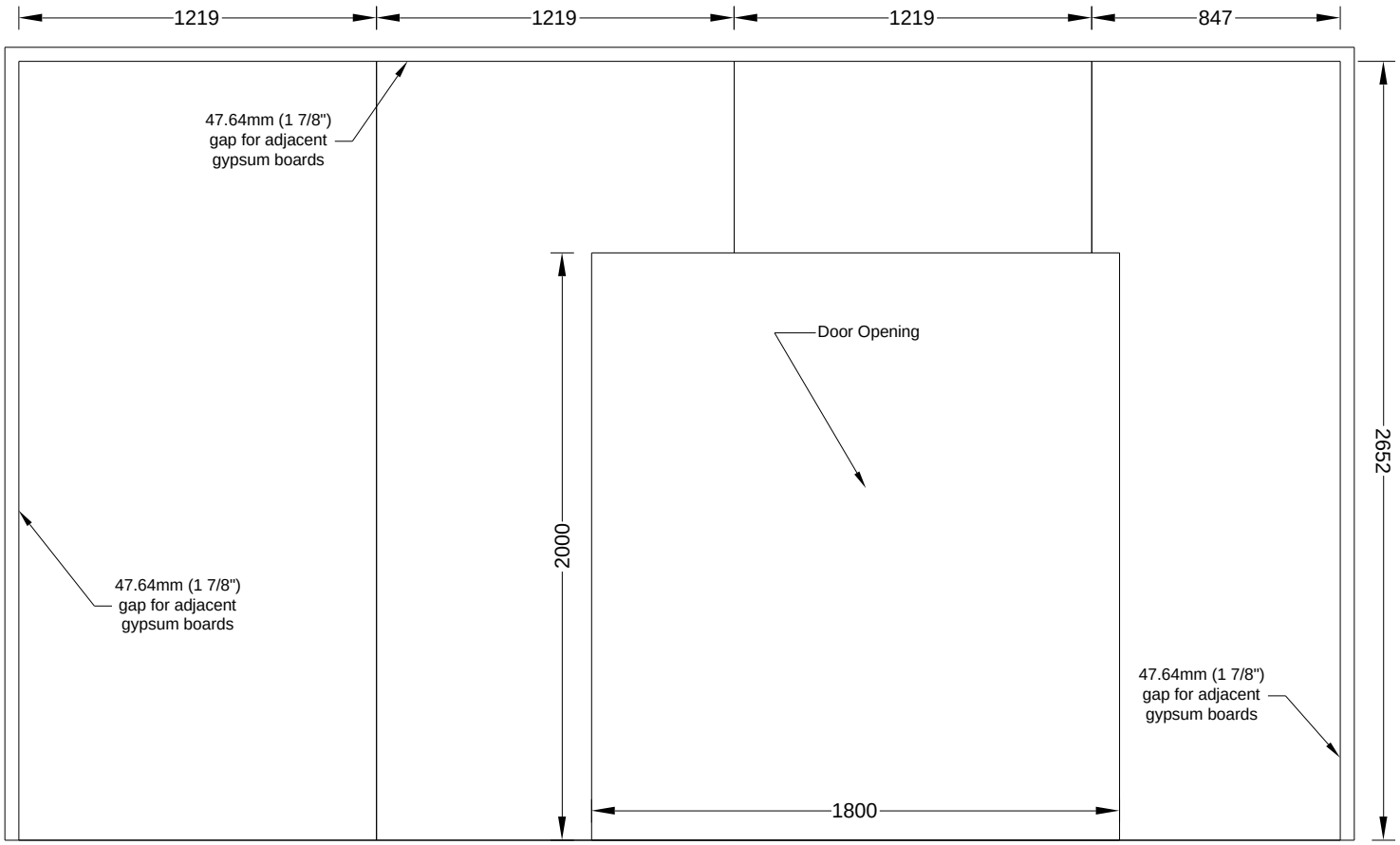

(Dimensions in mm)

Figure A 74. Test 1-4 Large Compartment CLT - W2 - Gypsum Layout - Face Layer

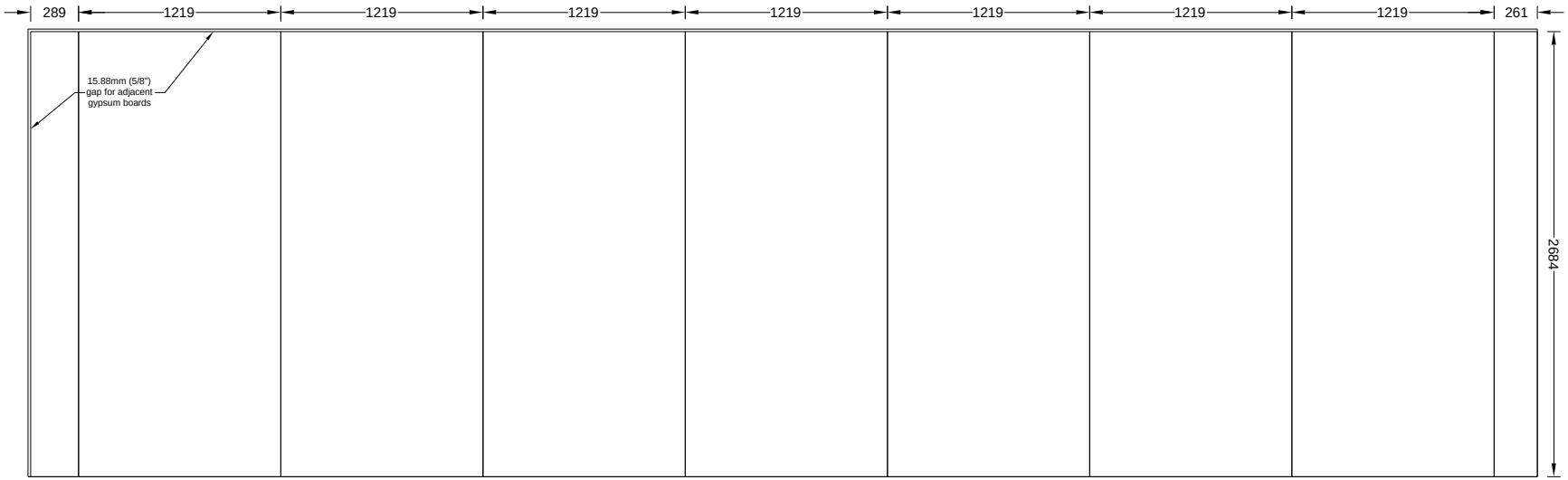

Figure A 75. Test 1-4 Large Compartment CLT - W3 - Gypsum Layout - Base Layer

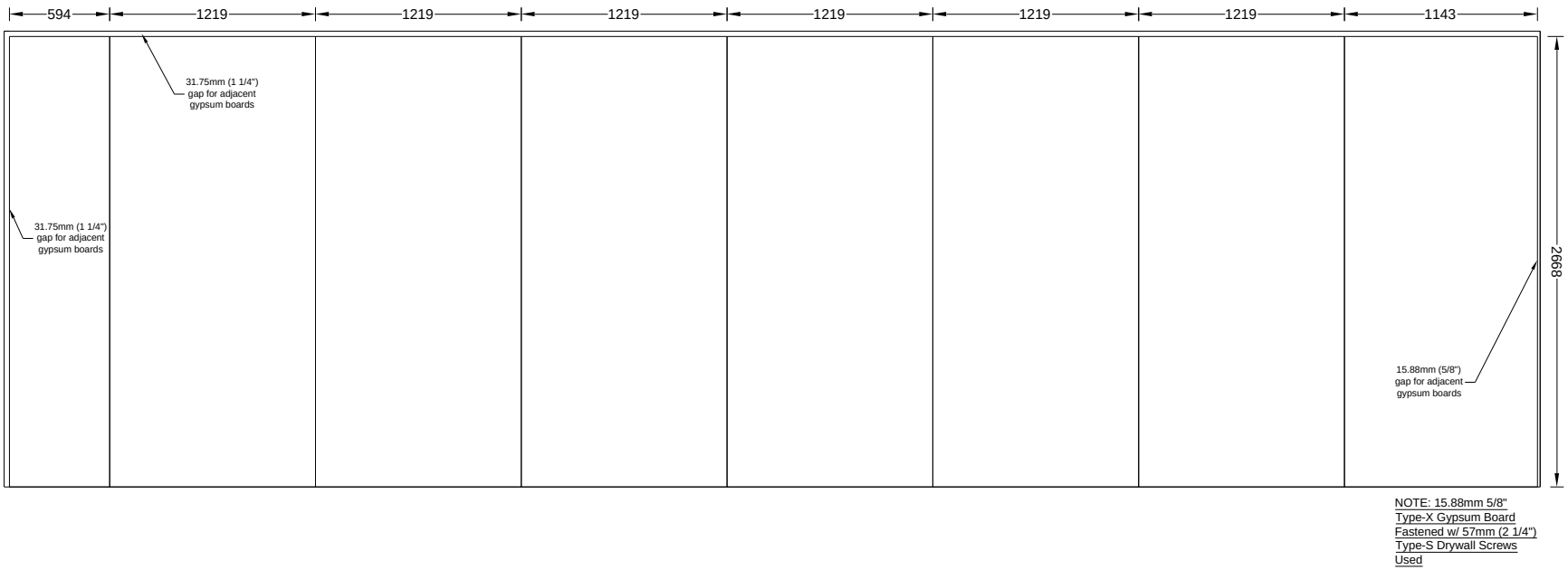

Figure A 76. Test 1-4 Large Compartment CLT - W3 - Gypsum Layout - Middle Layer

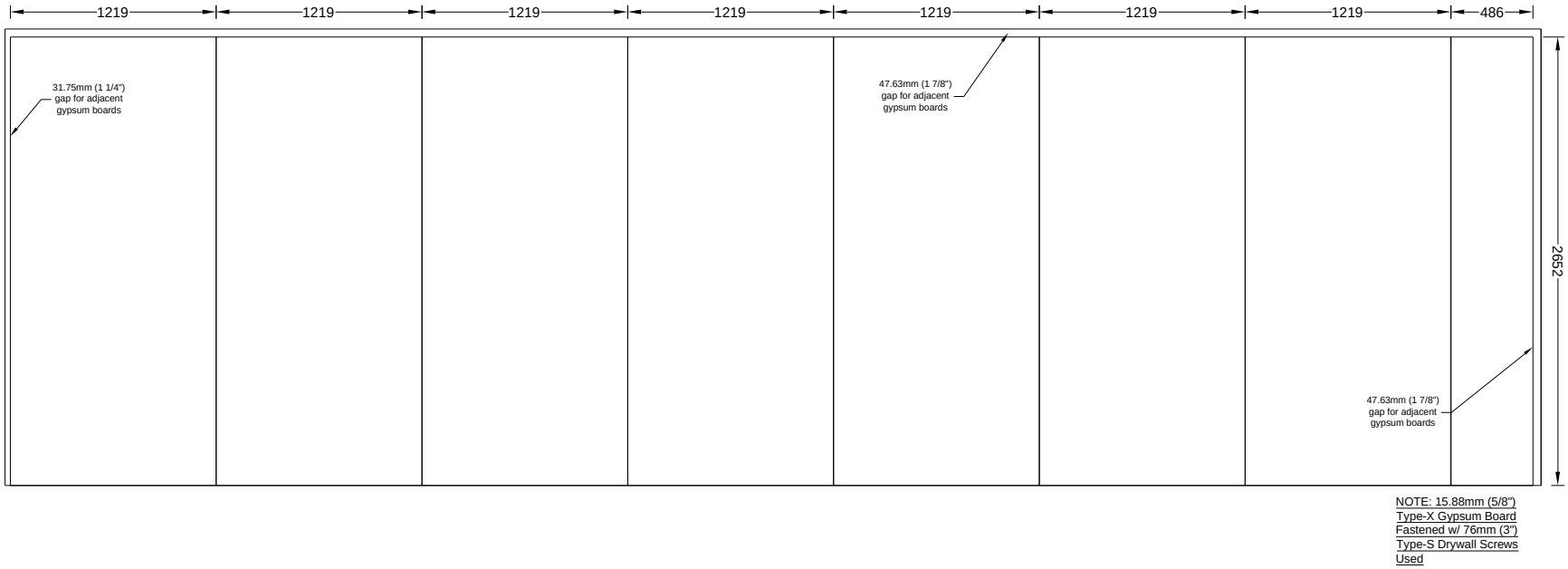

Figure A 77. Test 1-4 Large Compartment CLT - W3 - Gypsum Layout - Face Layer

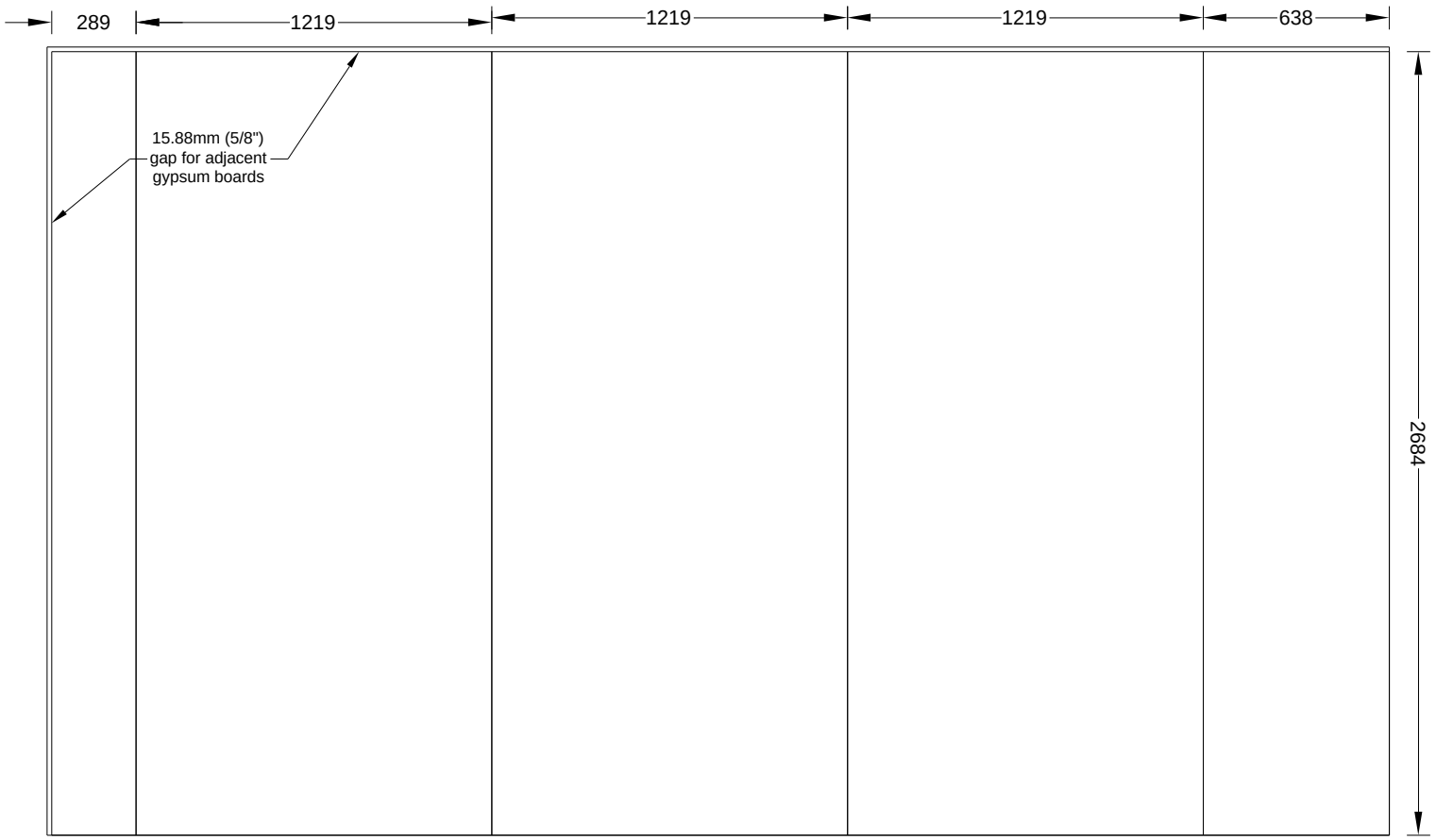

Figure A 78. Test 1-4 Large Compartment CLT - W4 - Gypsum Layout - Base Layer

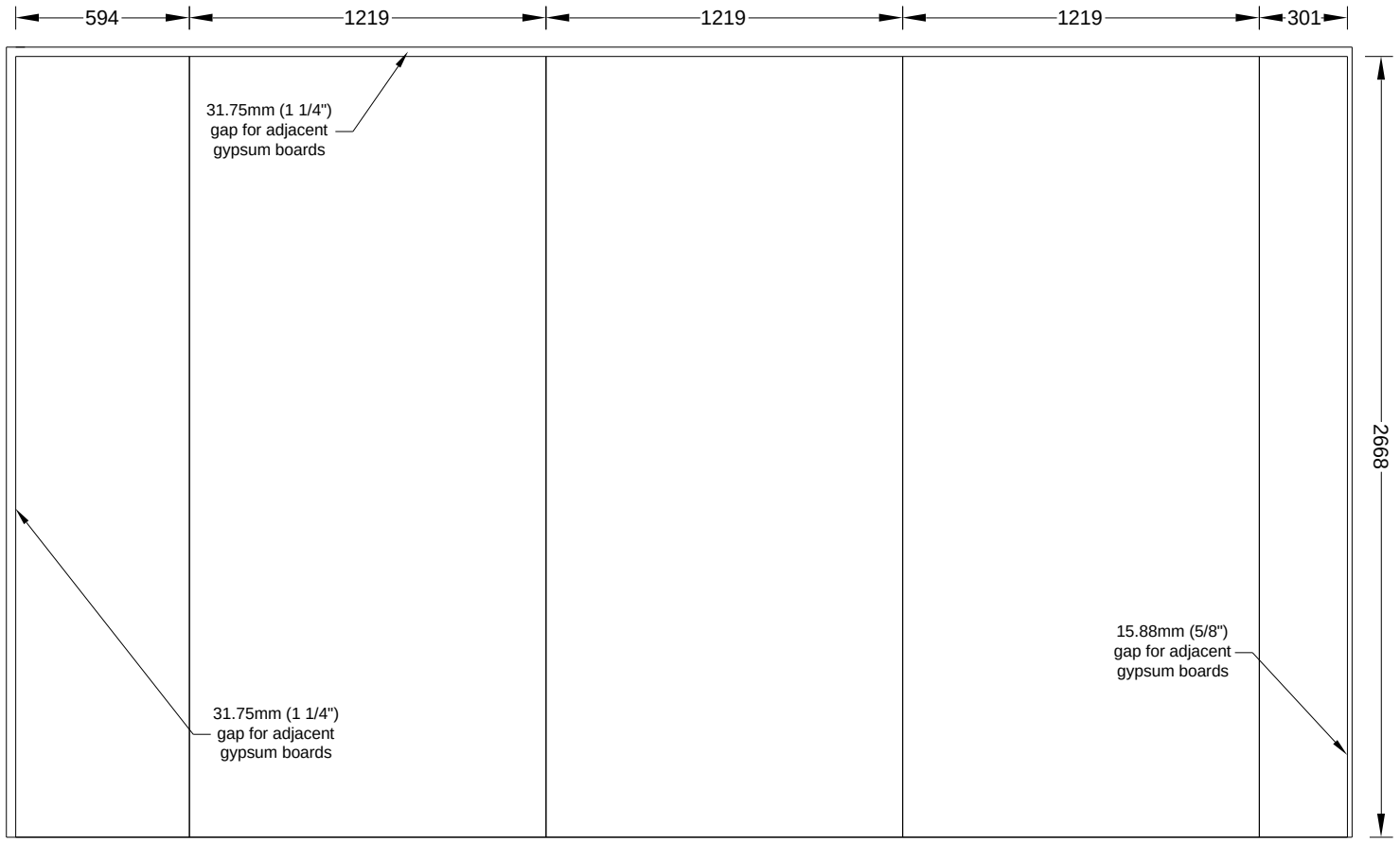

Figure A 79. Test 1-4 Large Compartment CLT - W4 - Gypsum Layout - Middle Layer

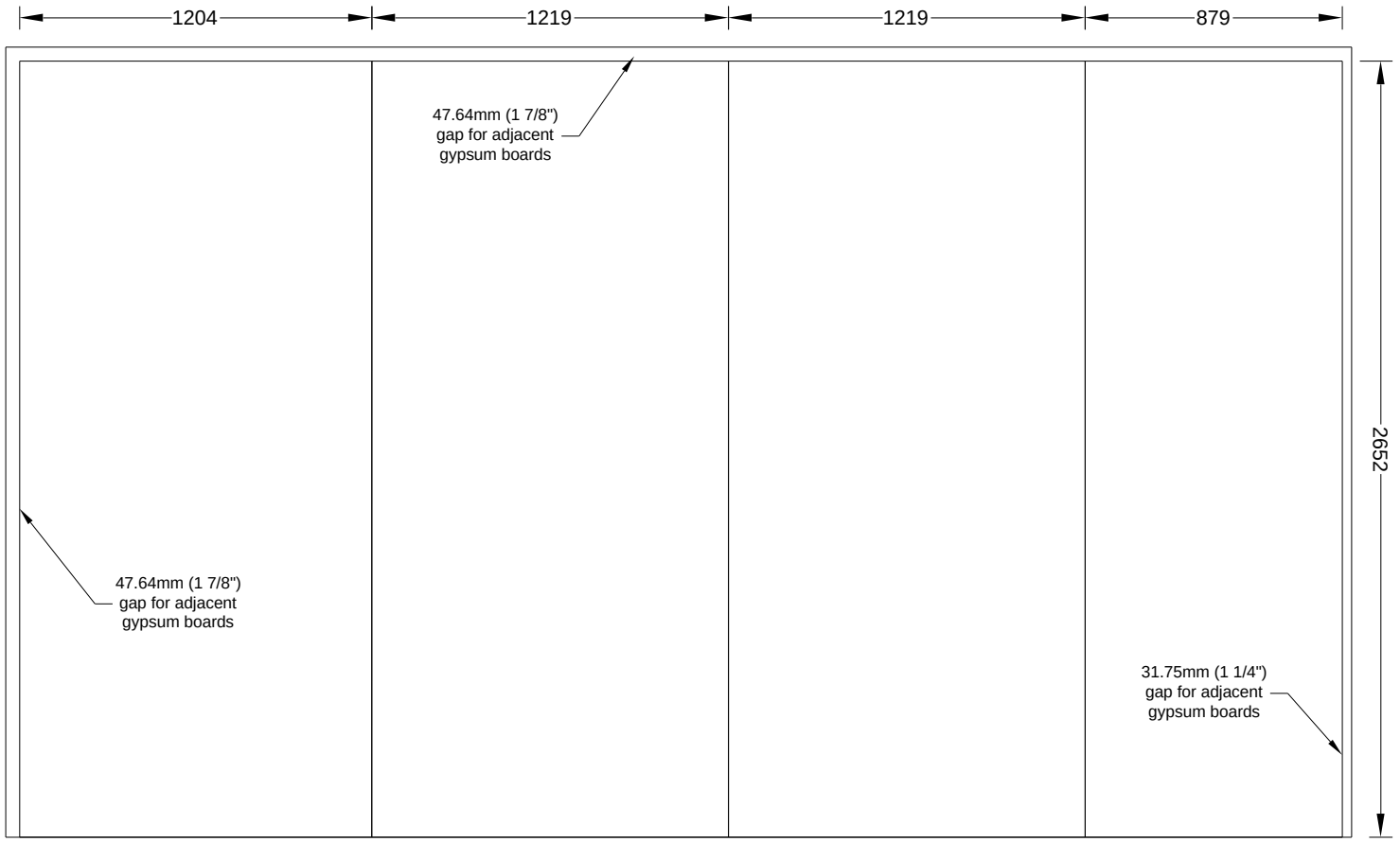

Figure A 80. Test 1-4 Large Compartment CLT - W4 - Gypsum Layout - Face Layer

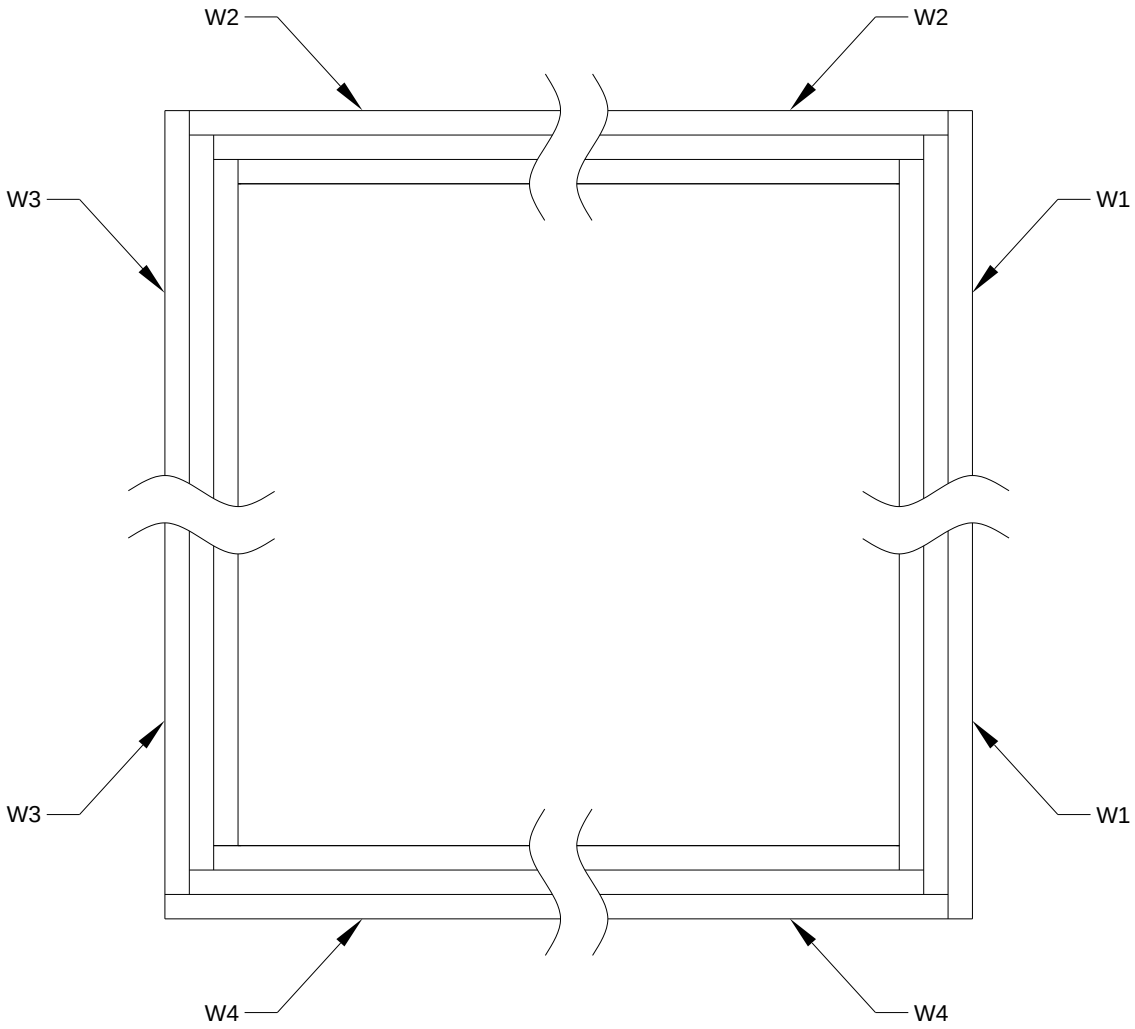

Figure A 81. Test 1-4 Large Compartment CLT - Wall - Gypsum Stagger in Corners

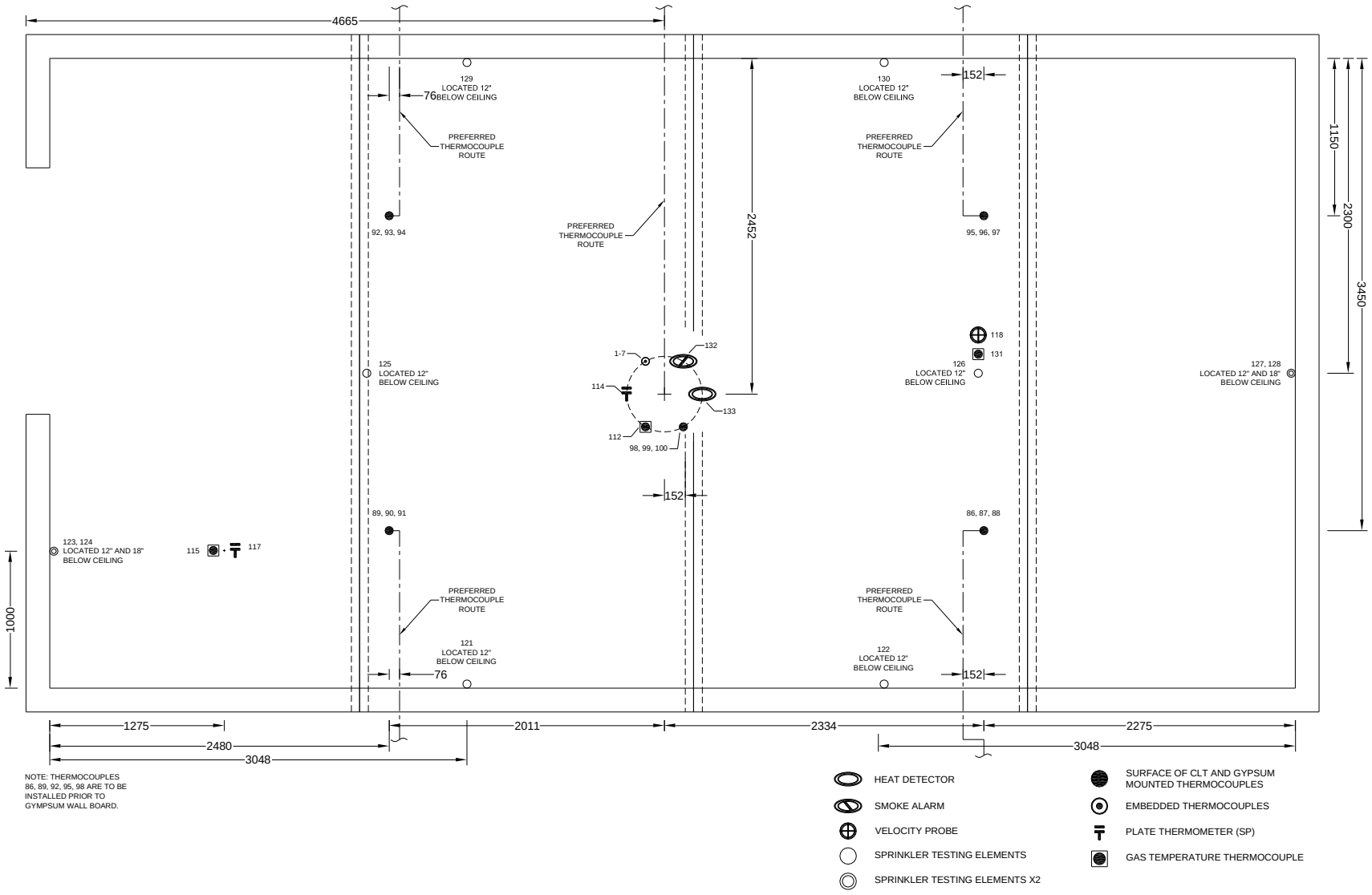

(Dimensions in mm)

Figure A 82. Test 1-5 Large Compartment CLT - Ceiling - Instrumentation Layout

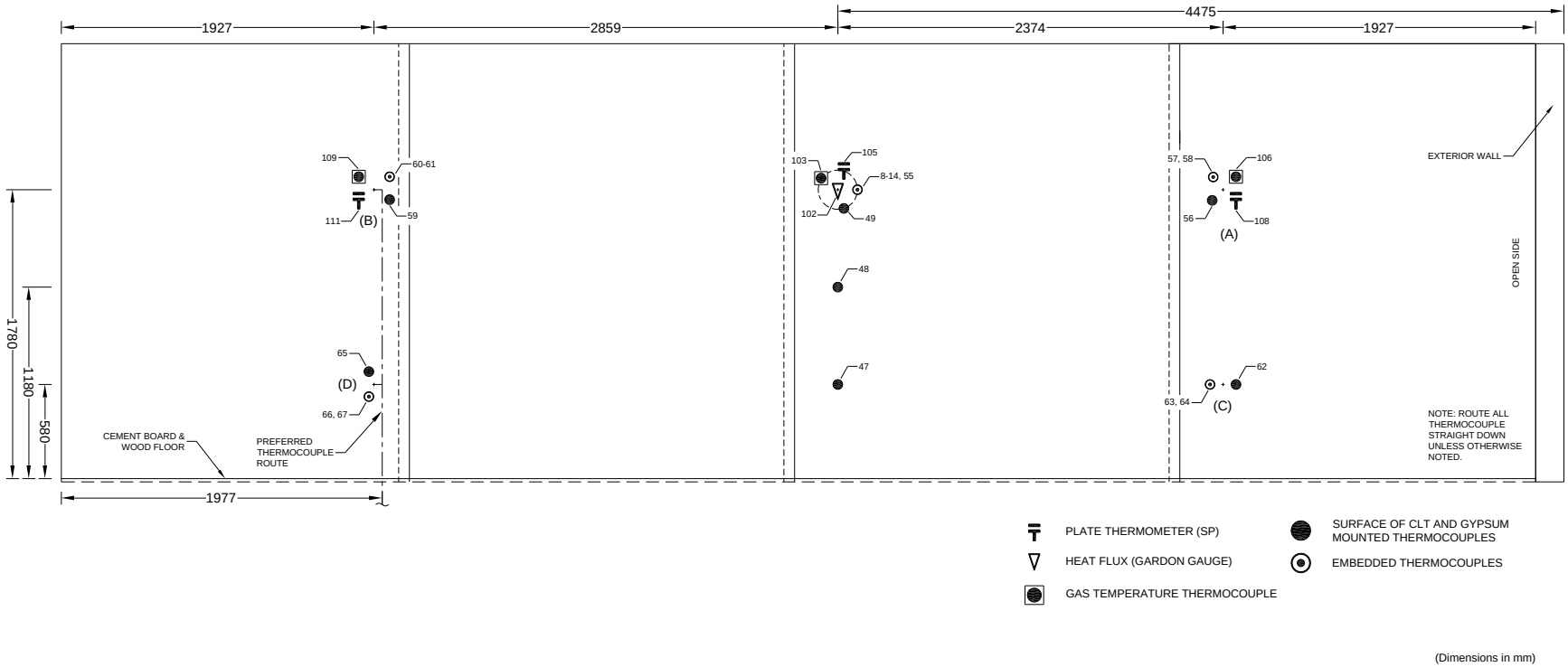

Figure A 83. Test 1-5 Large Compartment CLT - W1 - Instrumentation Layout

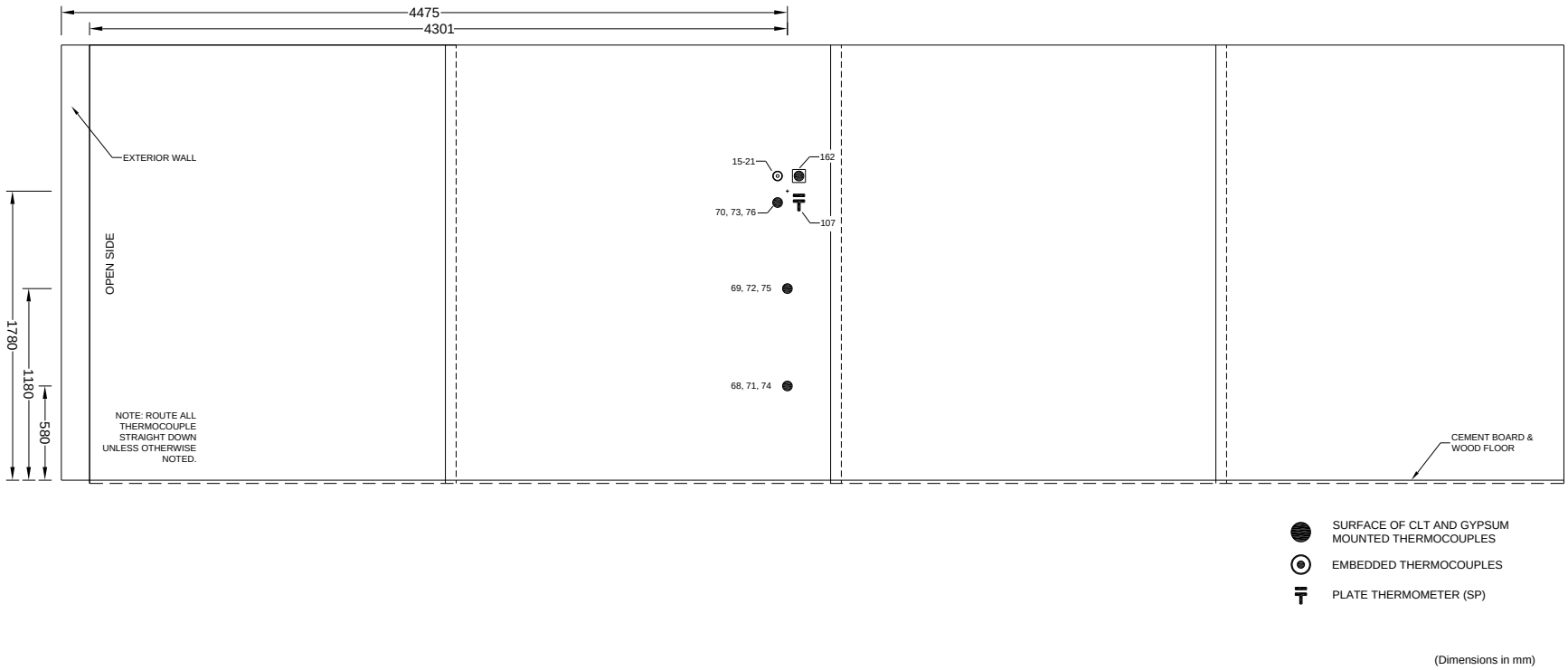

Figure A 84. Test 1-5 Large Compartment CLT - W3 - Instrumentation Layout

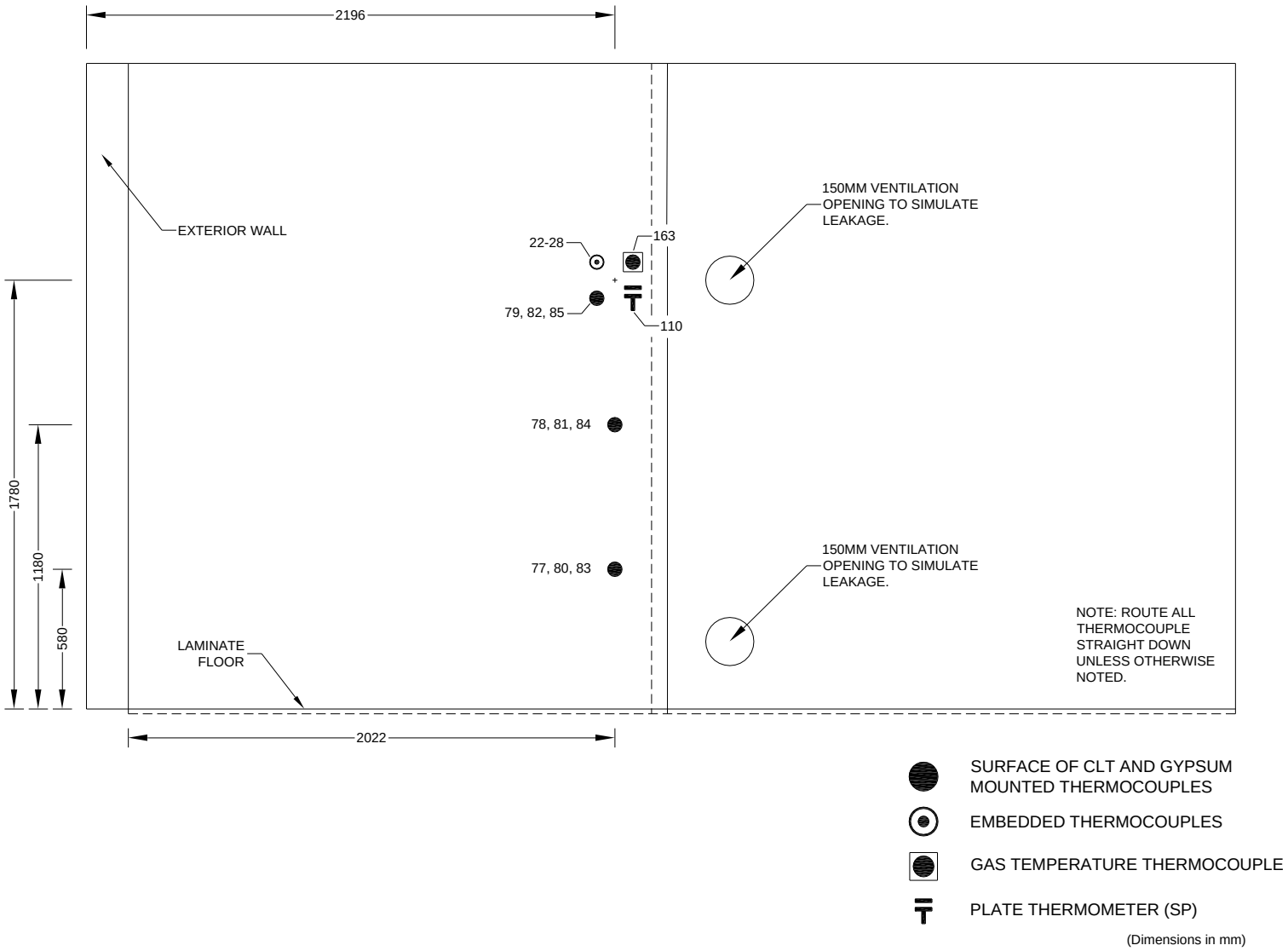

Figure A 85. Test 1-5 Large Compartment CLT - W4 - Instrumentation Layout

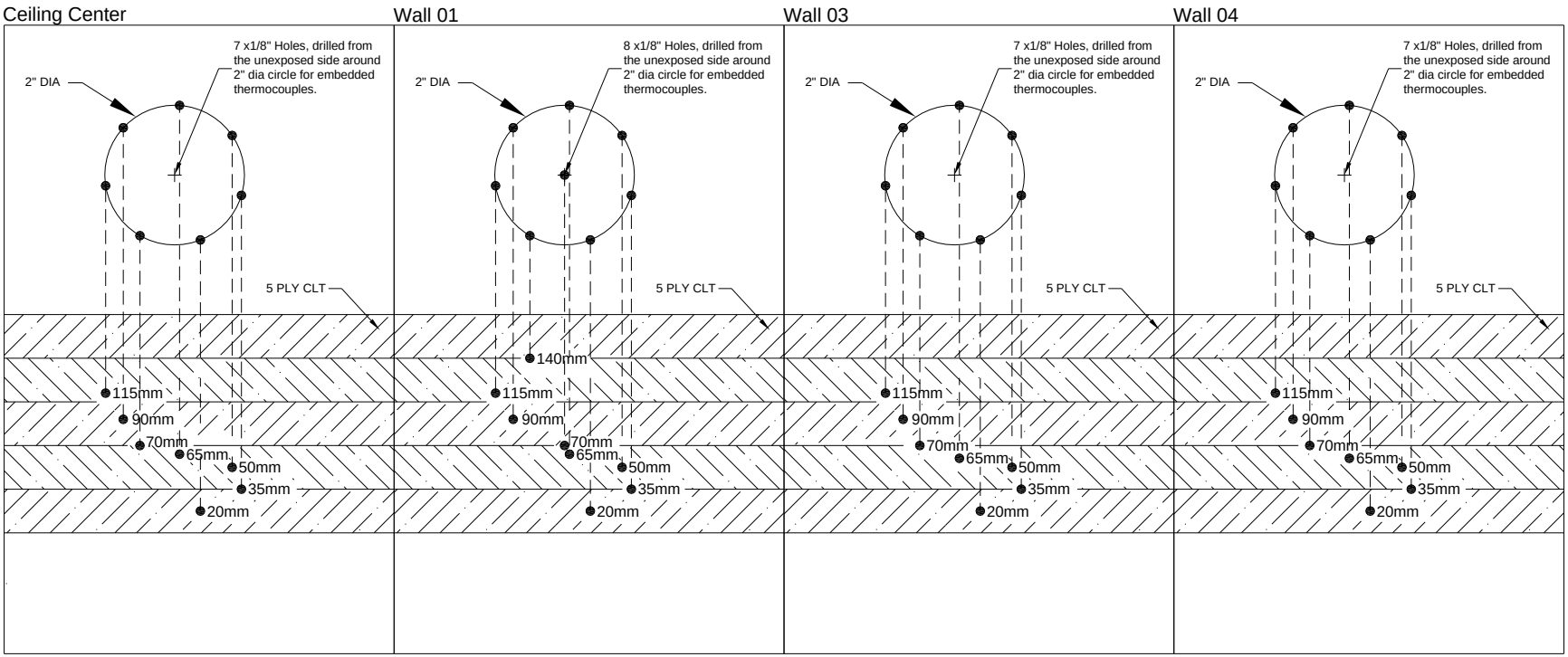

Figure A 86. Test 1-5 Large Compartment CLT - Embedded Thermocouple Detail

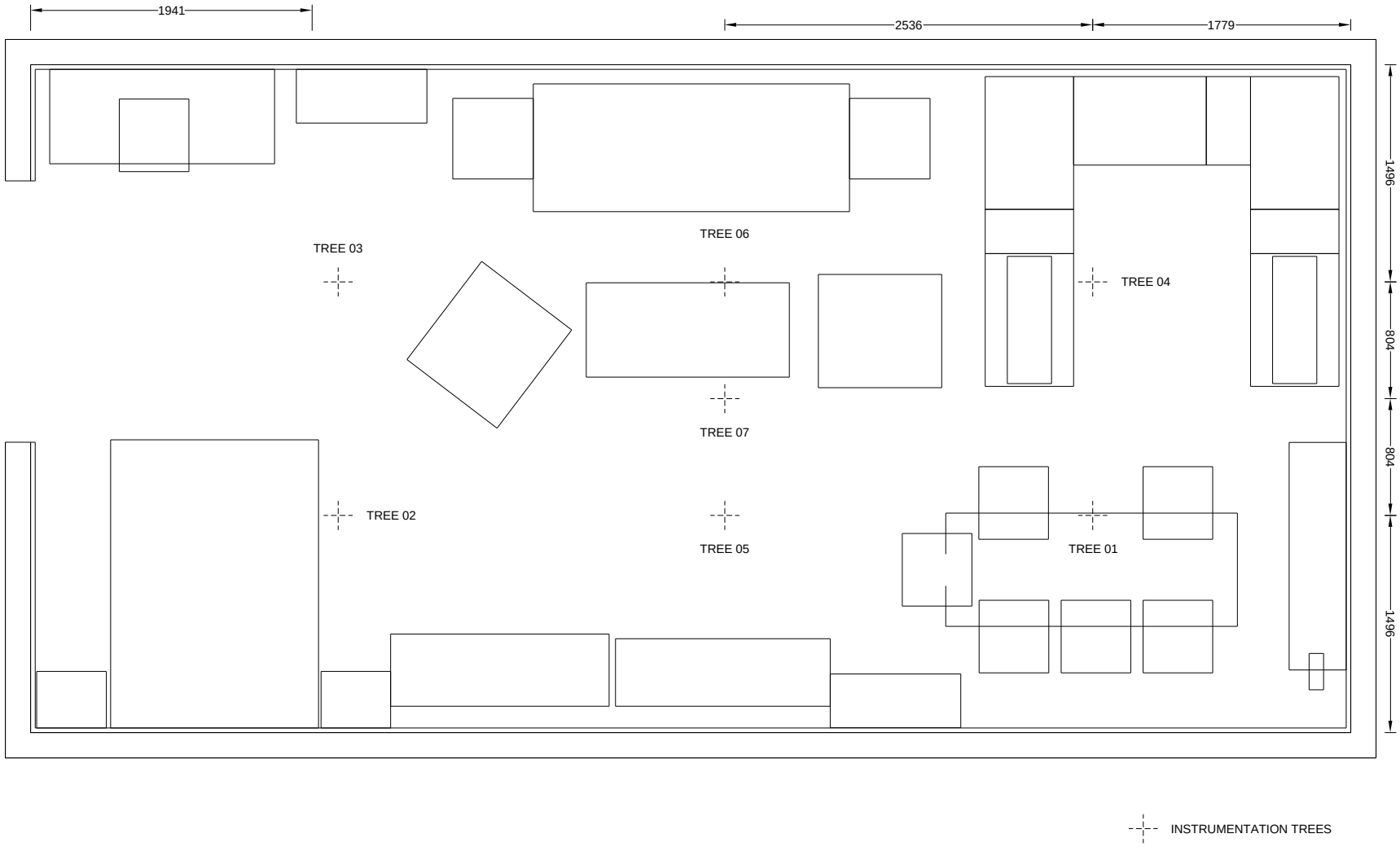

Figure A 87. Test 1-5 Large Compartment CLT - Instrumentation Tree Layout

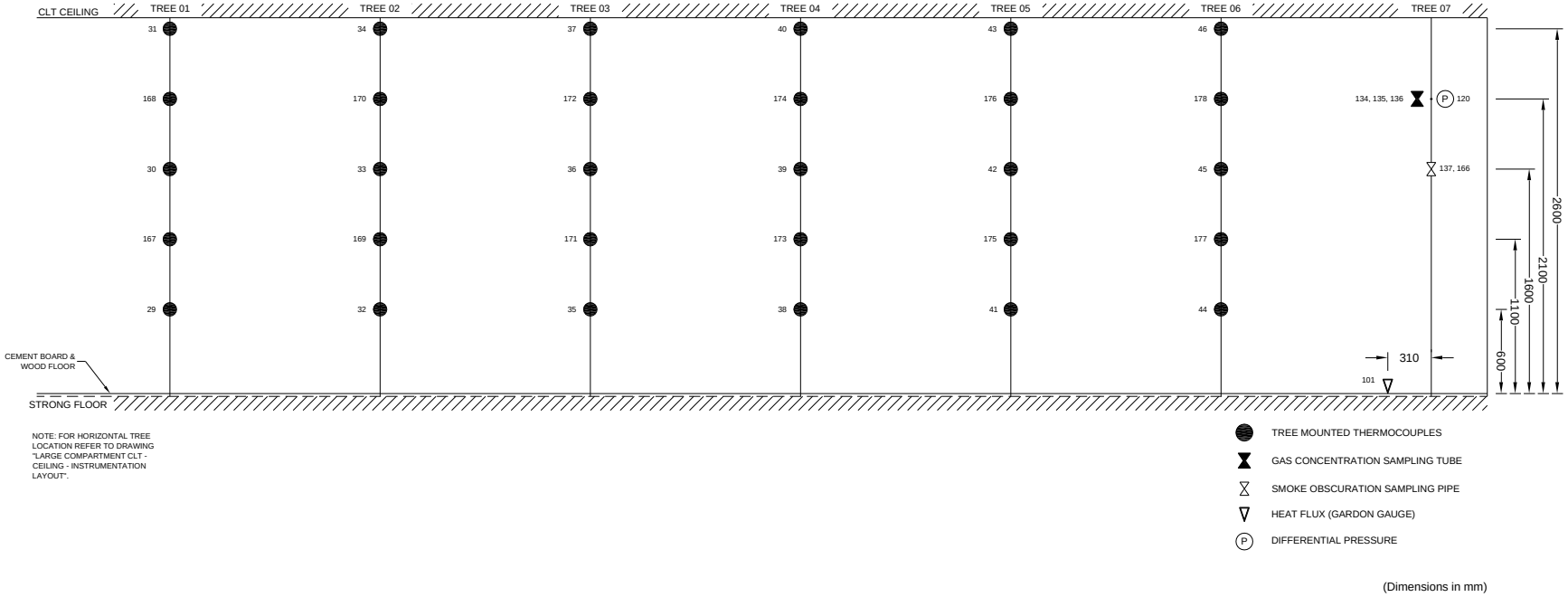

Figure A 88. Test 1-5 Large Compartment CLT - Instrumentation Tree Specifications

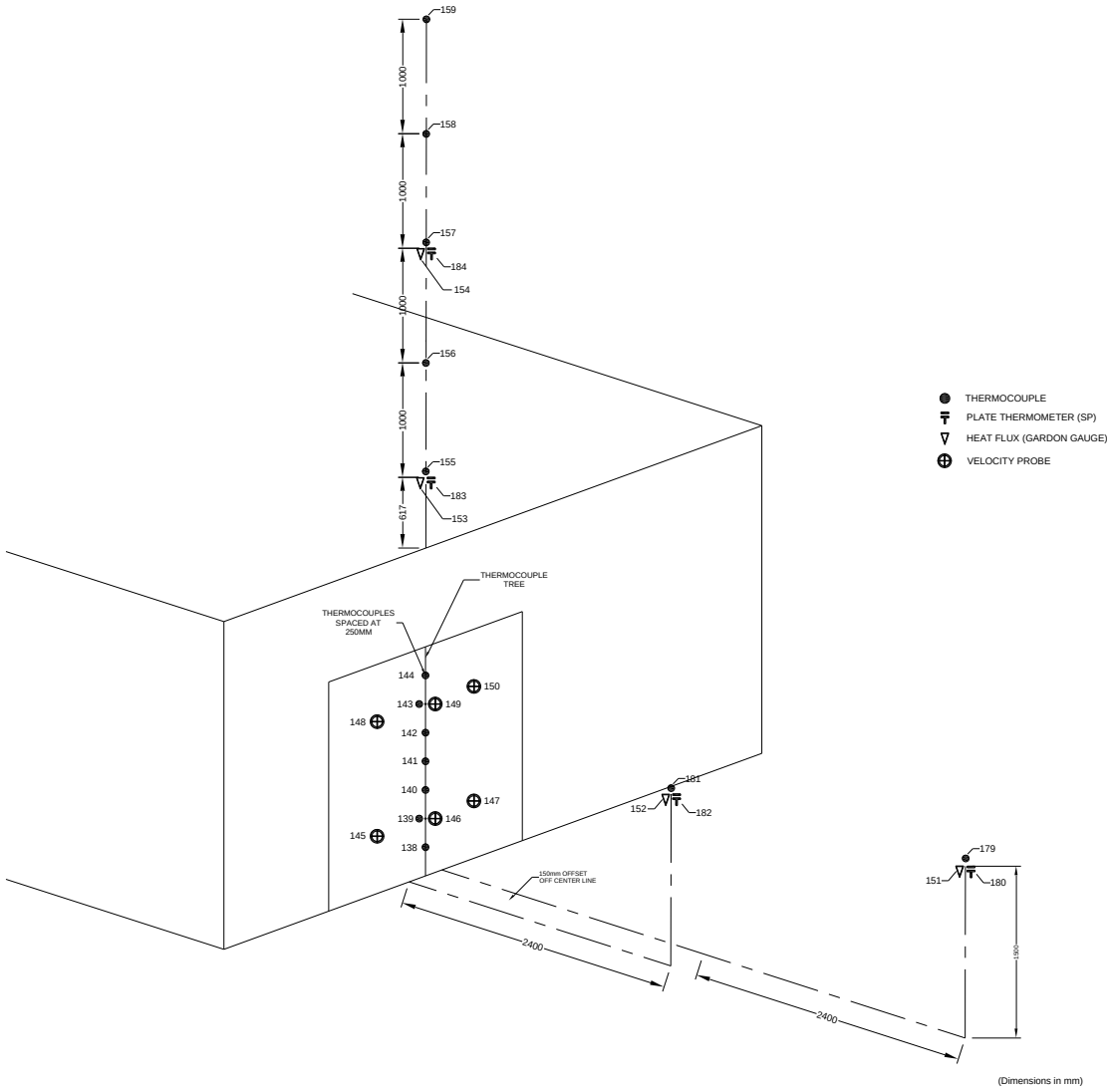

Figure A 89. Test 1-5 Large Compartment CLT - Exterior Instrumentation Layout

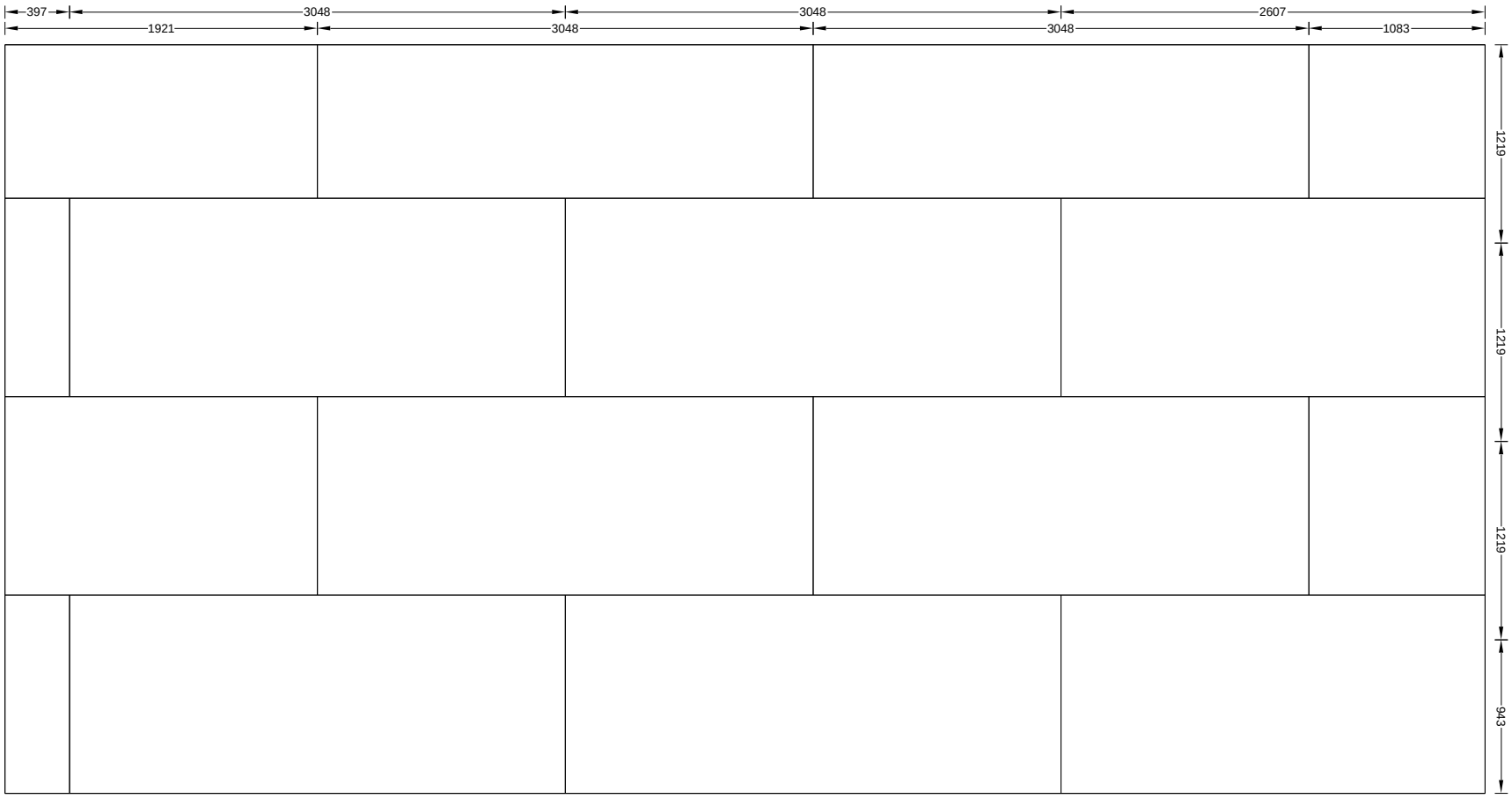

Figure A 90. Test 1-5 Large Compartment CLT - Ceiling - Gypsum Layout - Base Layer

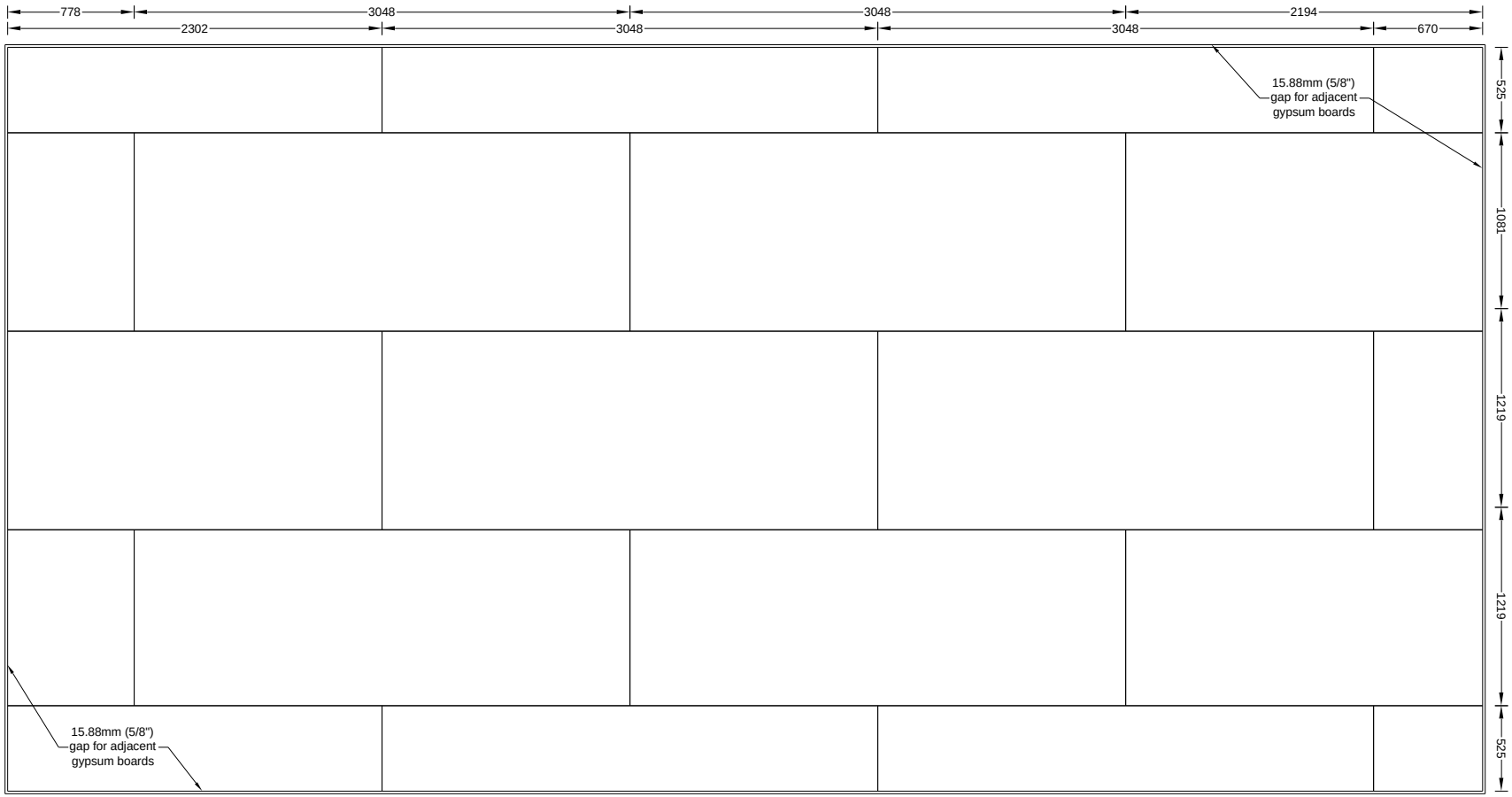

Figure A 91. Test 1-5 Large Compartment CLT - Ceiling - Gypsum Layout - Middle Layer

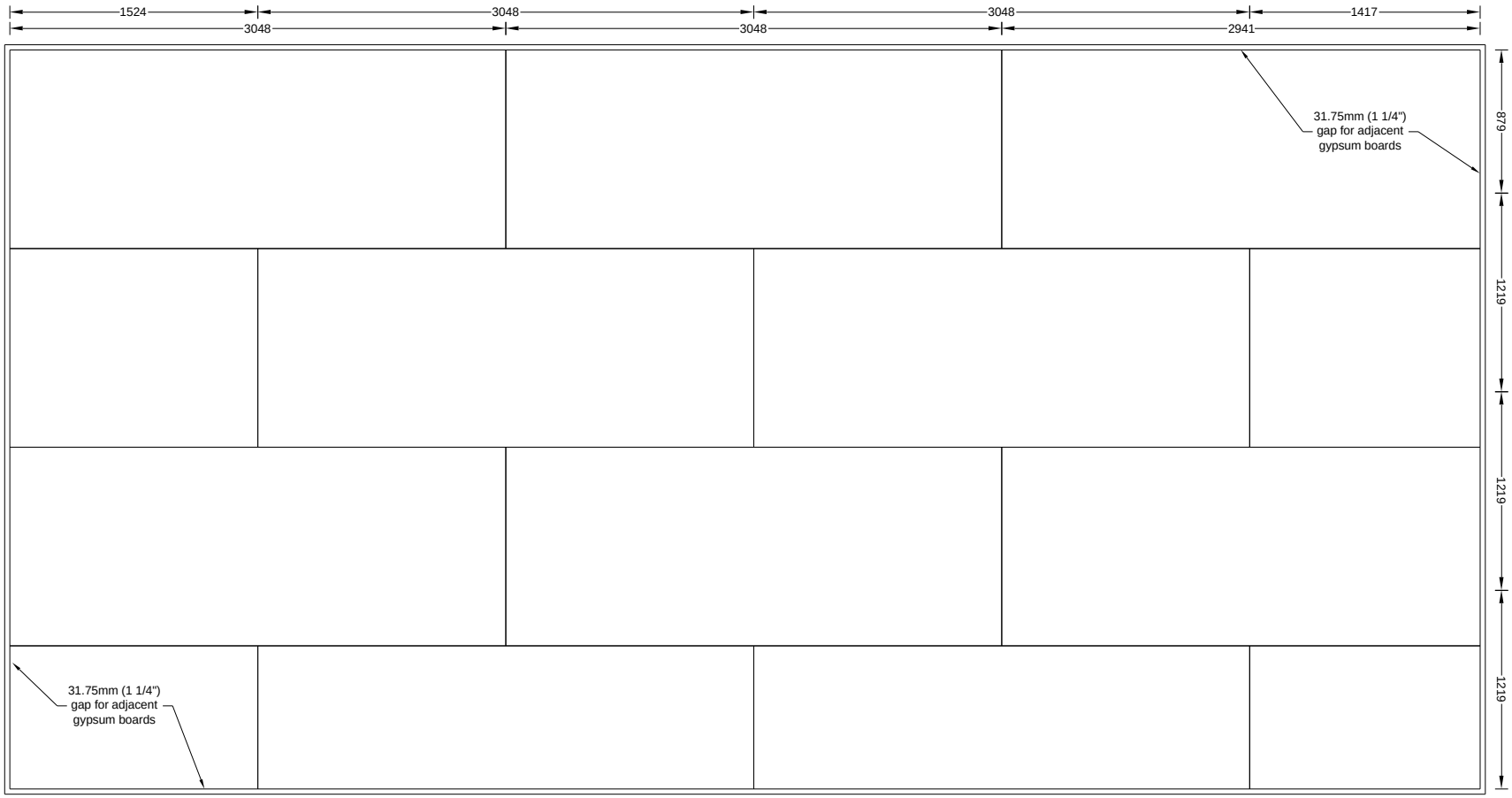

(Dimensions in mm)

Figure A 92. Test 1-5 Large Compartment CLT - Ceiling - Gypsum Layout - Face Layer

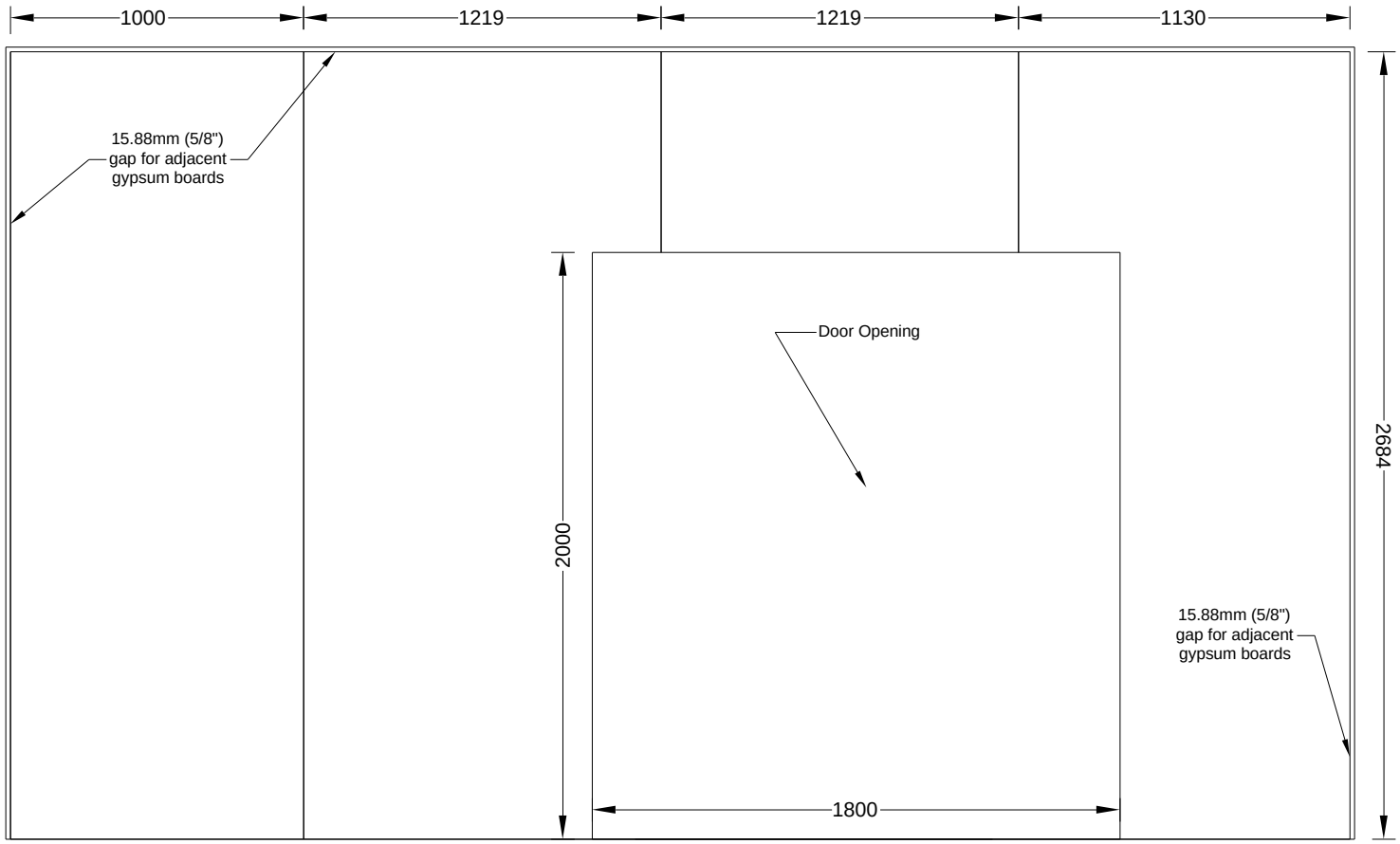

(Dimensions in mm)

Figure A 93. Test 1-5 Large Compartment CLT - W2 - Gypsum Layout - Base Layer

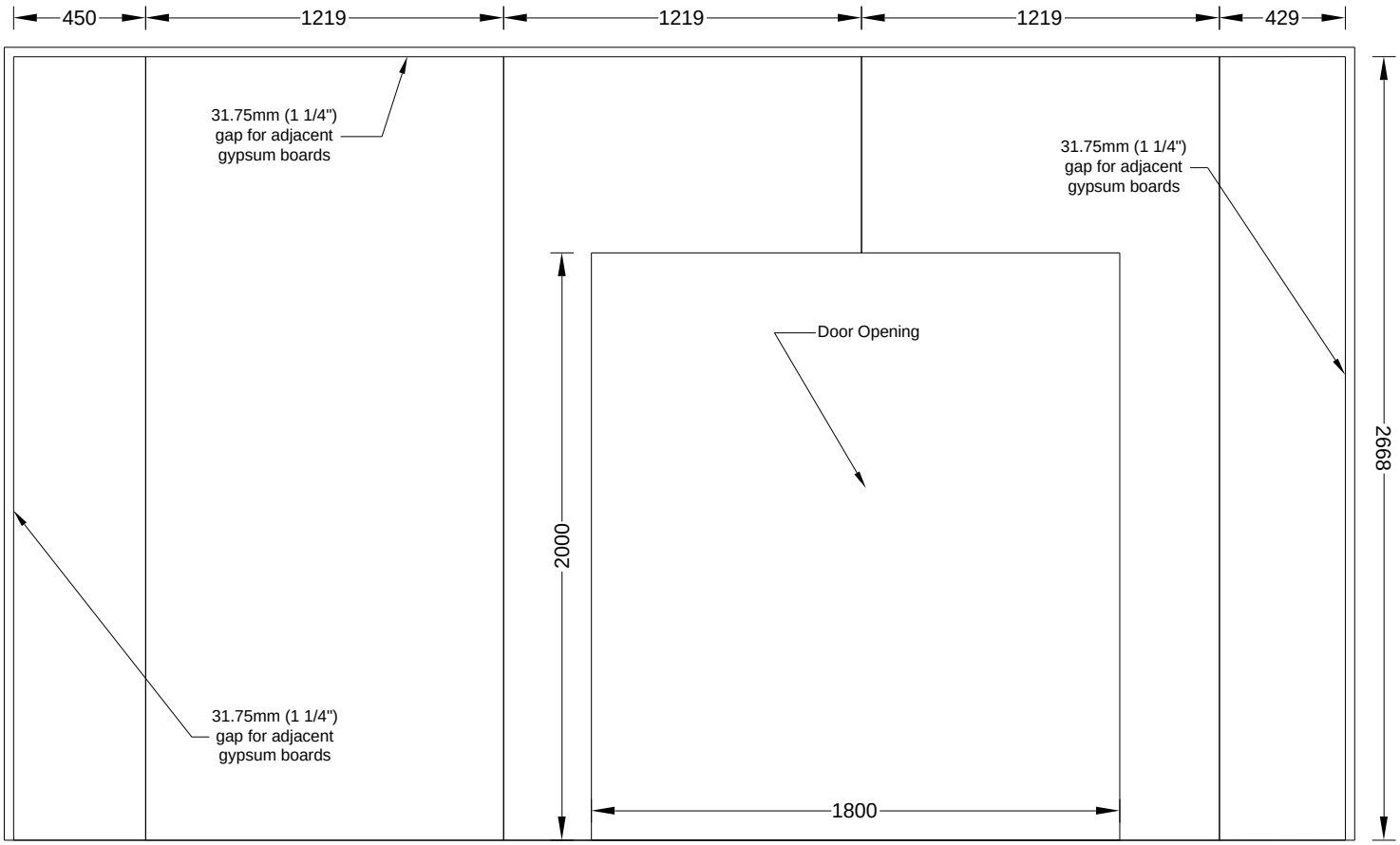

Figure A 94. Test 1-5 Large Compartment CLT - W2 - Gypsum Layout - Middle Layer

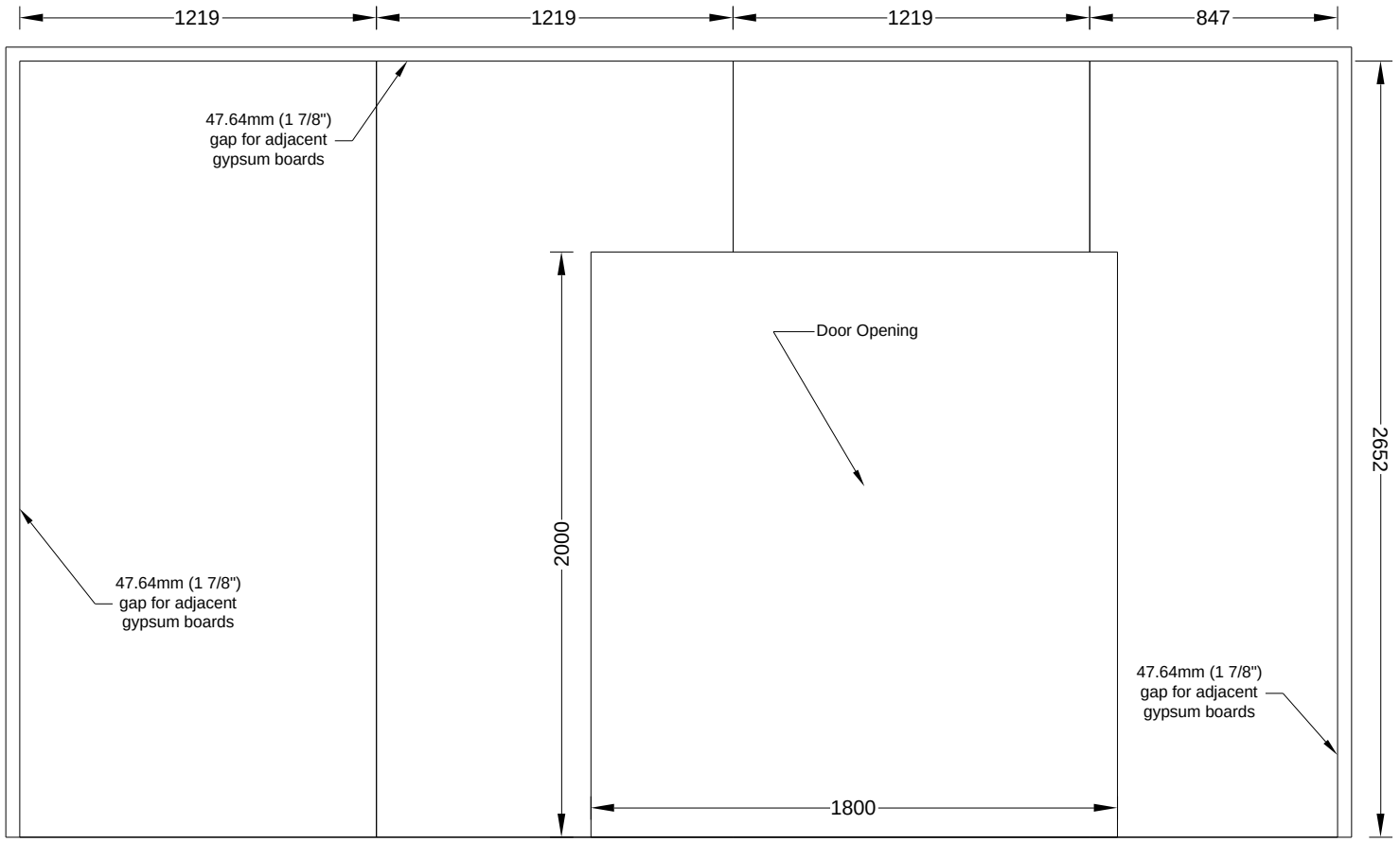

(Dimensions in mm)

Figure A 95. Test 1-5 Large Compartment CLT - W2 - Gypsum Layout - Face Layer

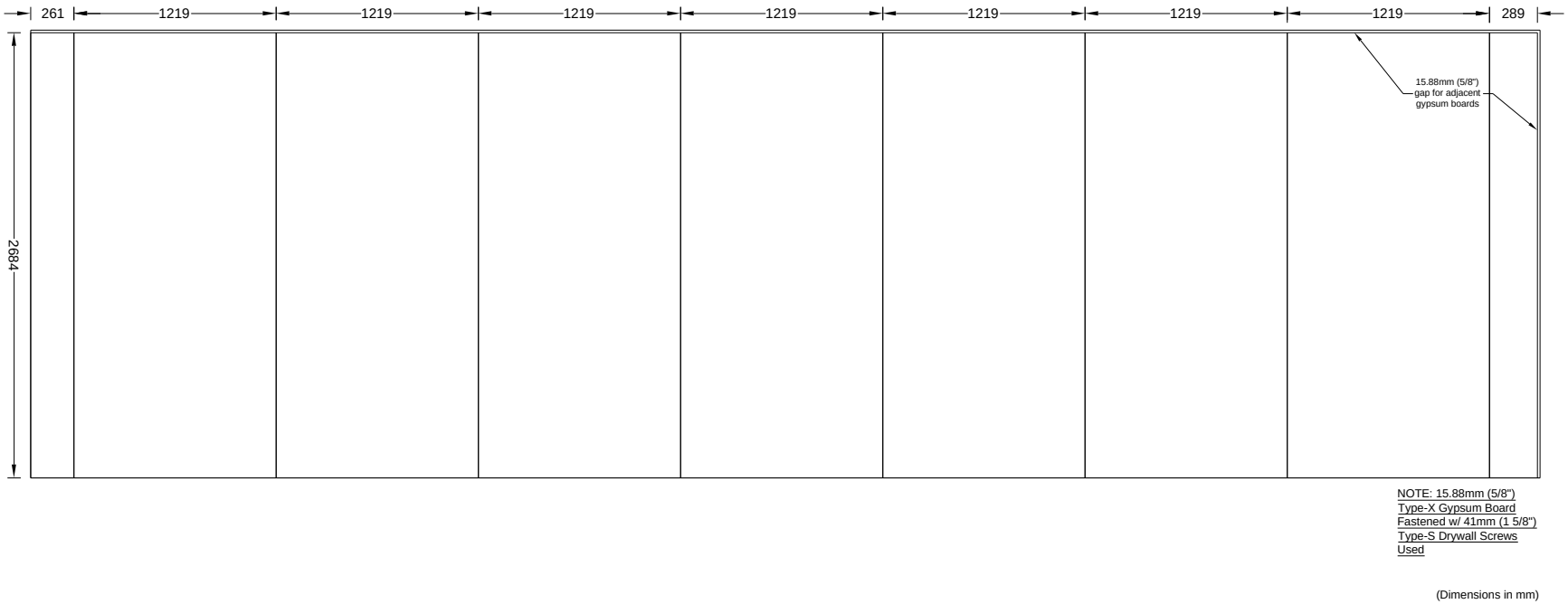

Figure A 96. Test 1-5 Large Compartment CLT - W3 - Gypsum Layout - Base Layer

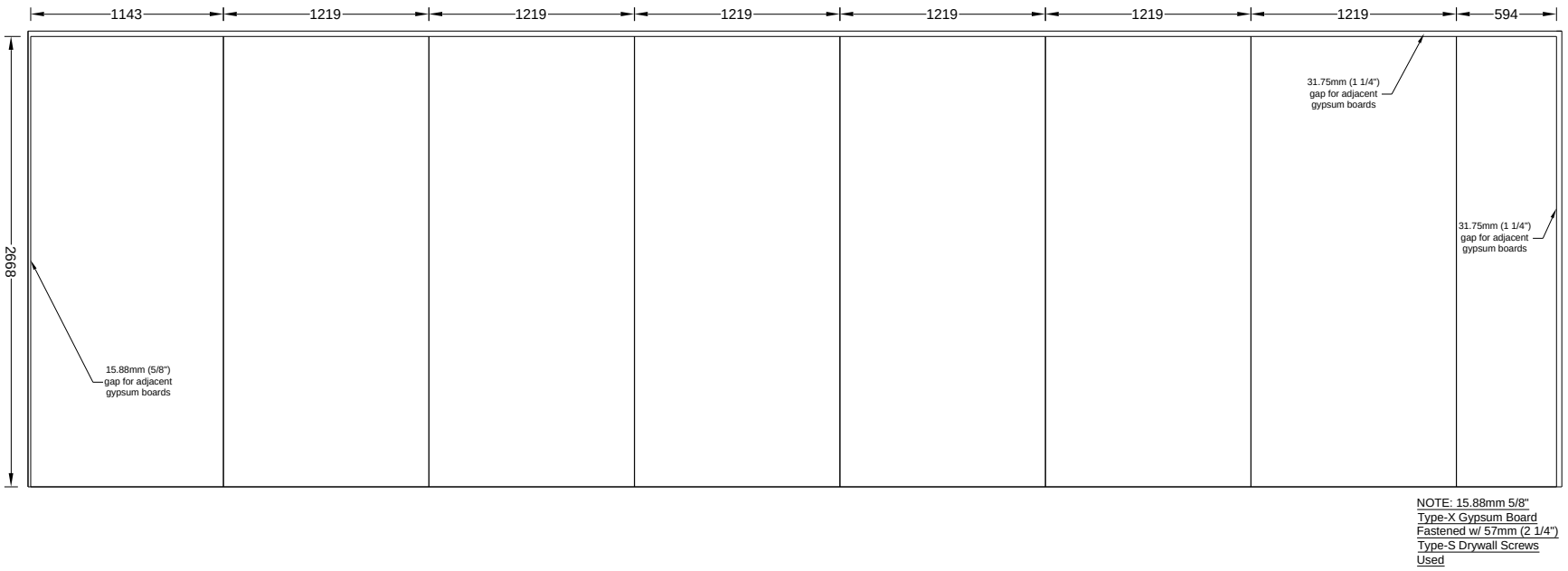

Figure A 97. Test 1-5 Large Compartment CLT - W3 - Gypsum Layout - Middle Layer

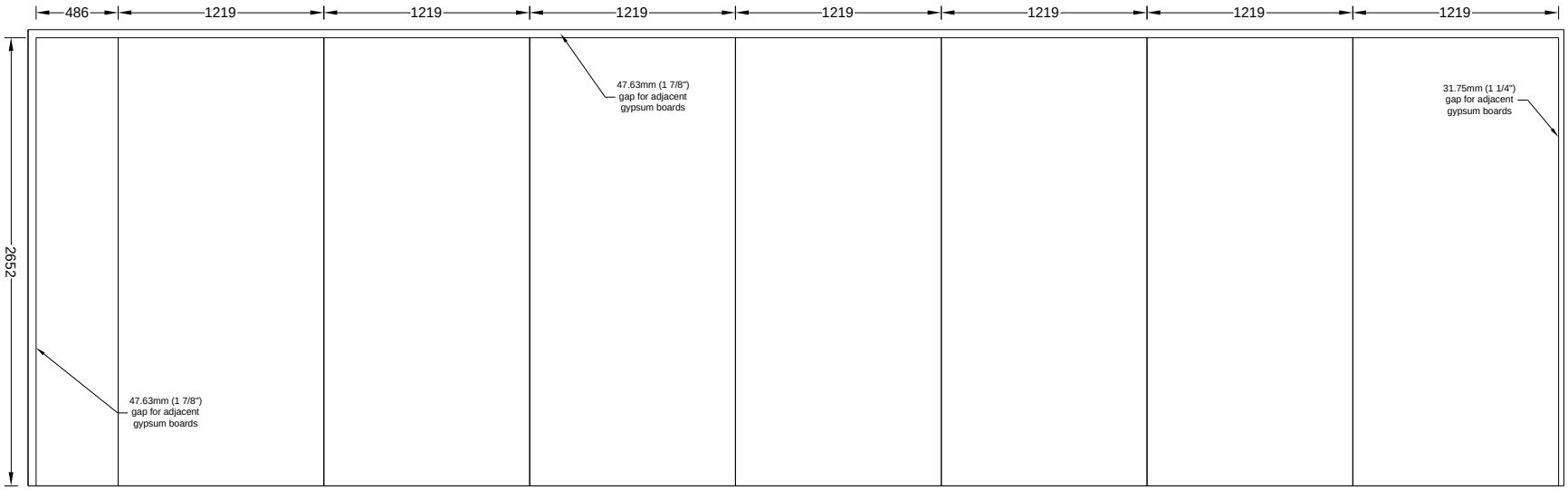

Figure A 98. Test 1-5 Large Compartment CLT - W3 - Gypsum Layout - Face Layer

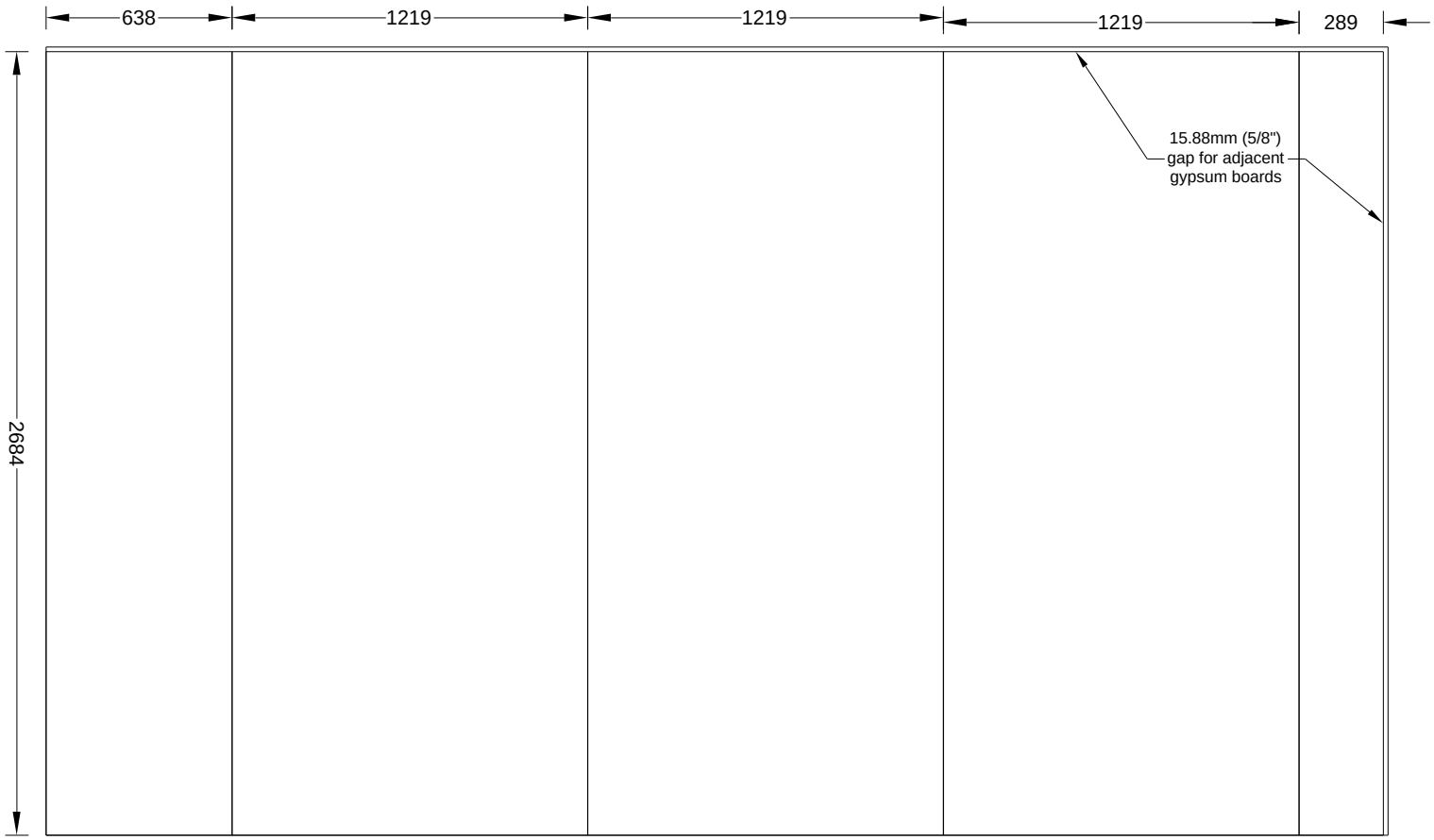

(Dimensions in mm)

Figure A 99. Test 1-5 Large Compartment CLT - W4 - Gypsum Layout - Base Layer

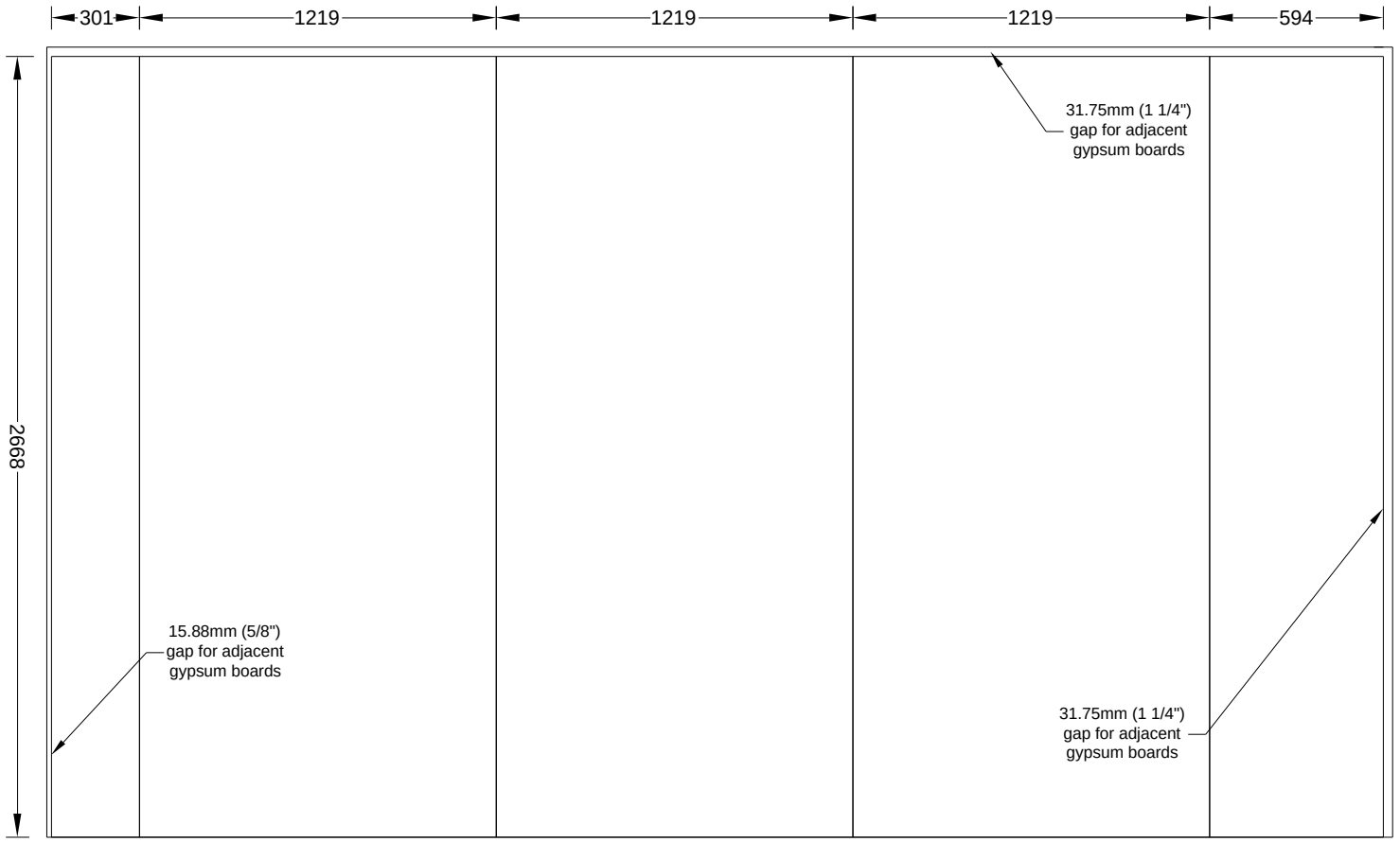

Figure A 100. Test 1-5 Large Compartment CLT - W4 - Gypsum Layout - Middle Layer

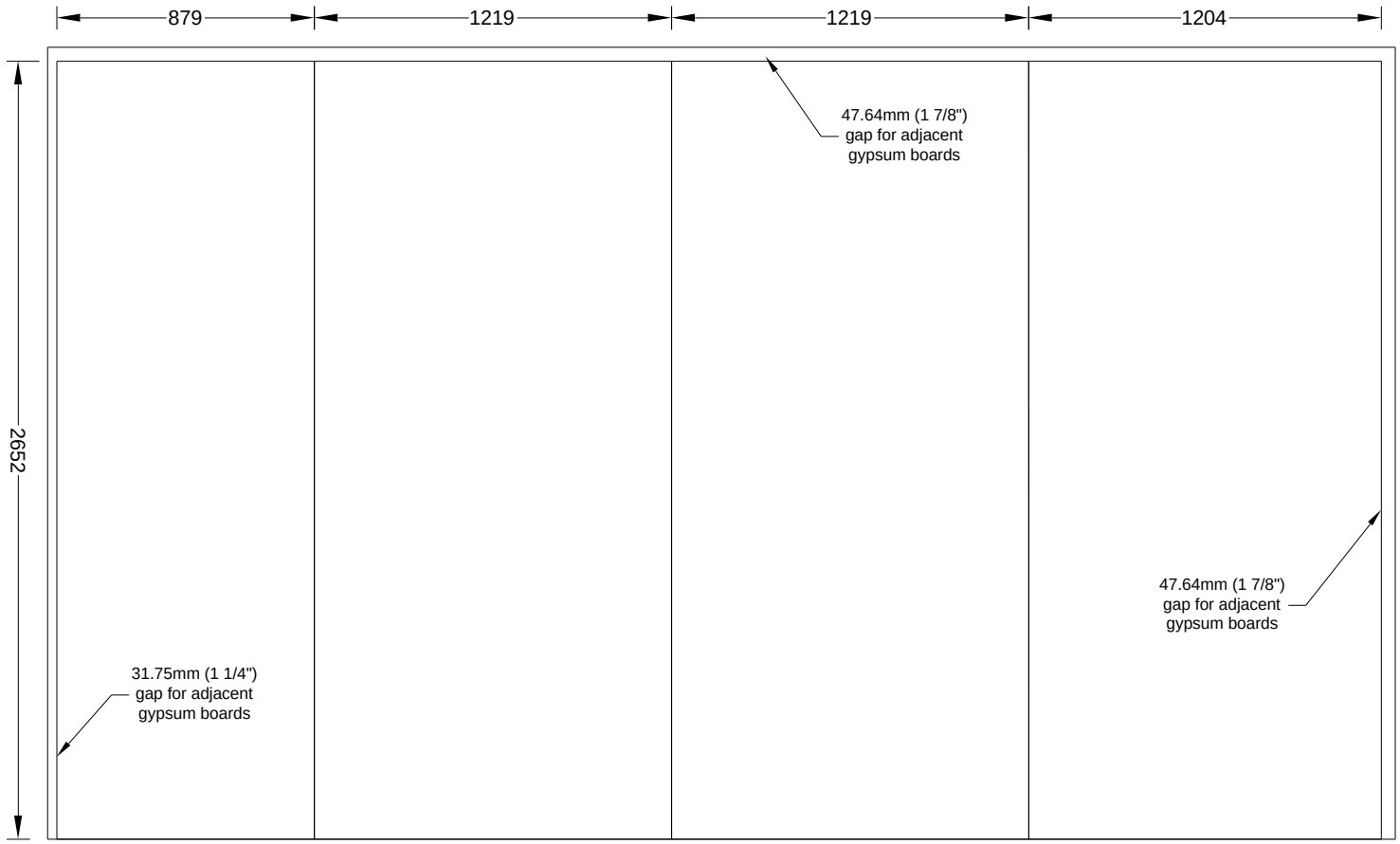

(Dimensions in mm)

Figure A 101. Test 1-5 Large Compartment CLT - W4 - Gypsum Layout - Face Layer

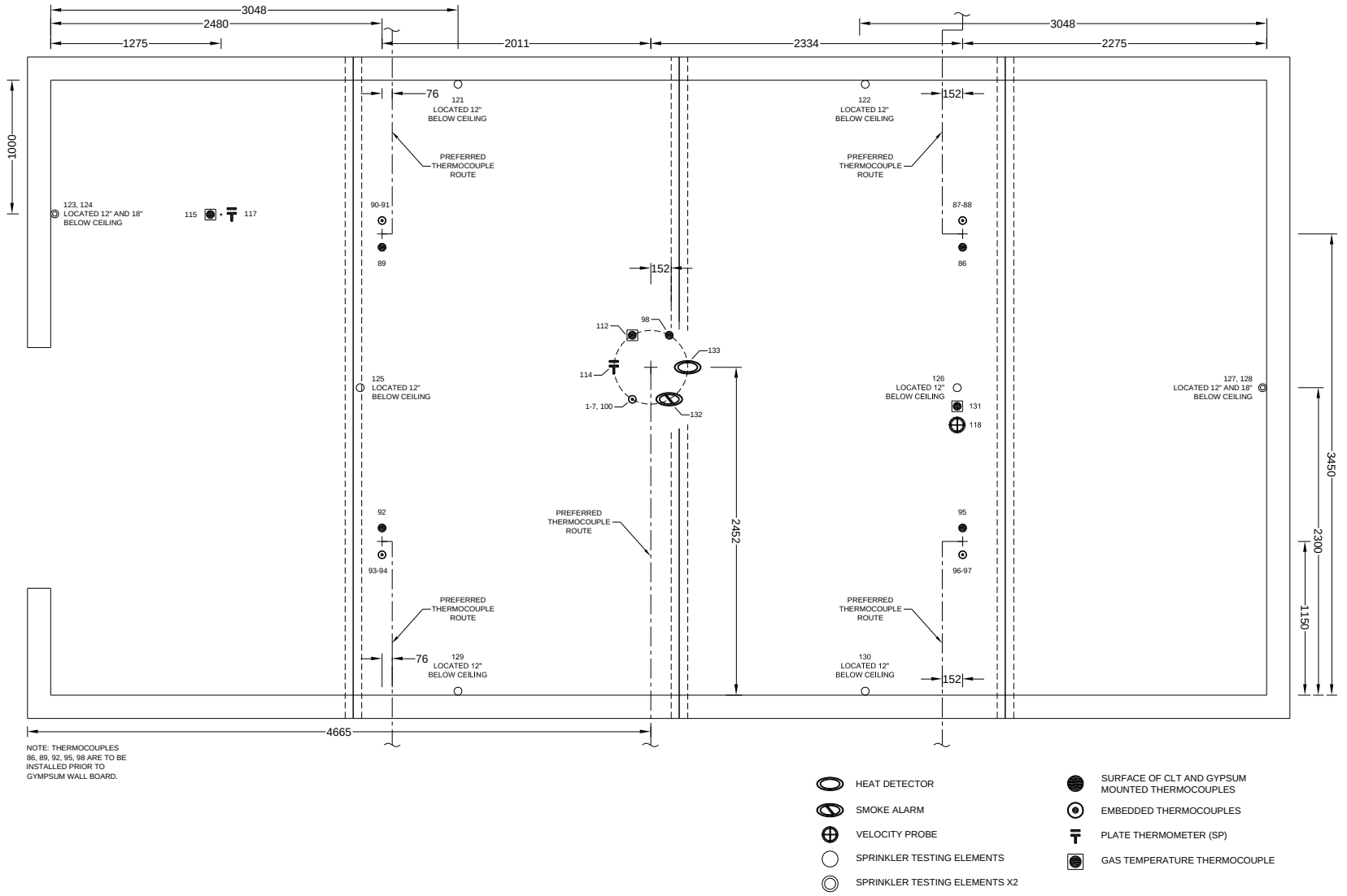

Figure A 102. Test 1-6 Large Compartment CLT - Ceiling - Instrumentation Layout

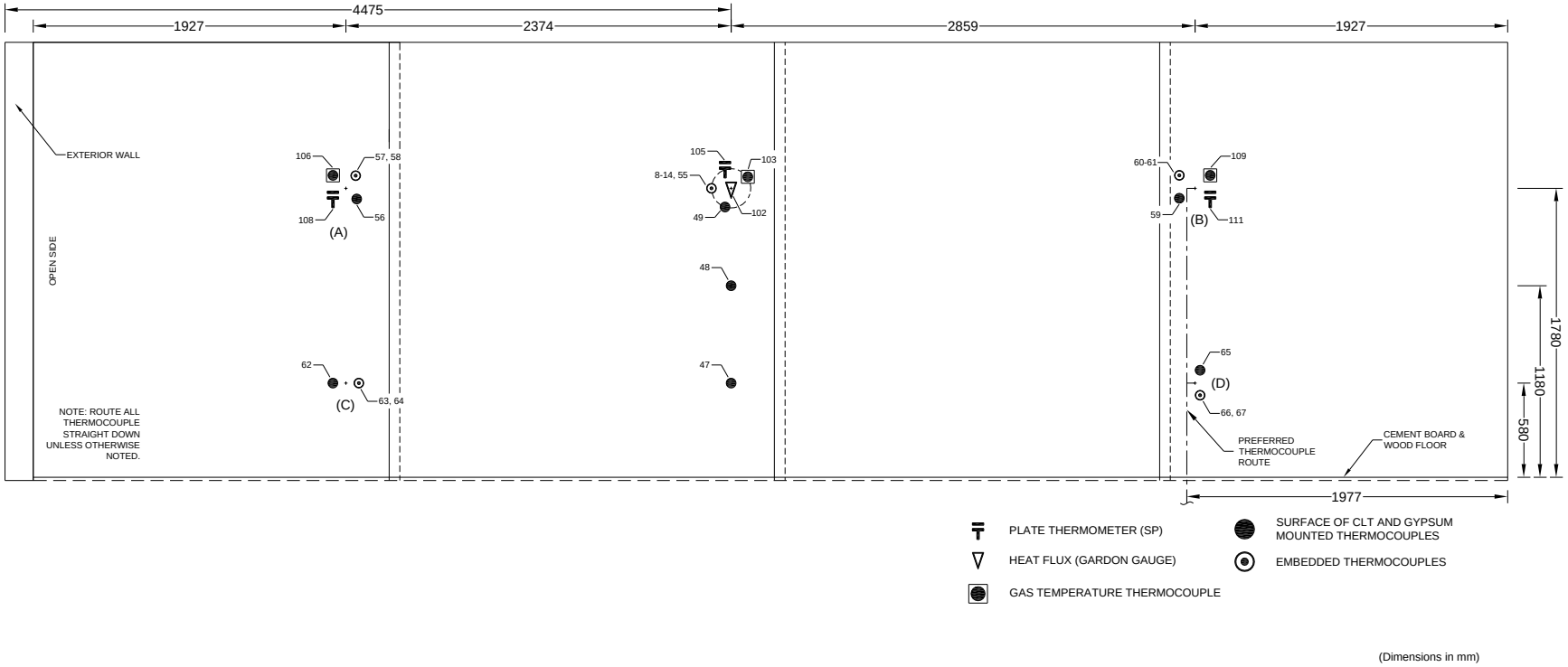

Figure A 103. Test 1-6 Large Compartment CLT - W1 - Instrumentation Layout

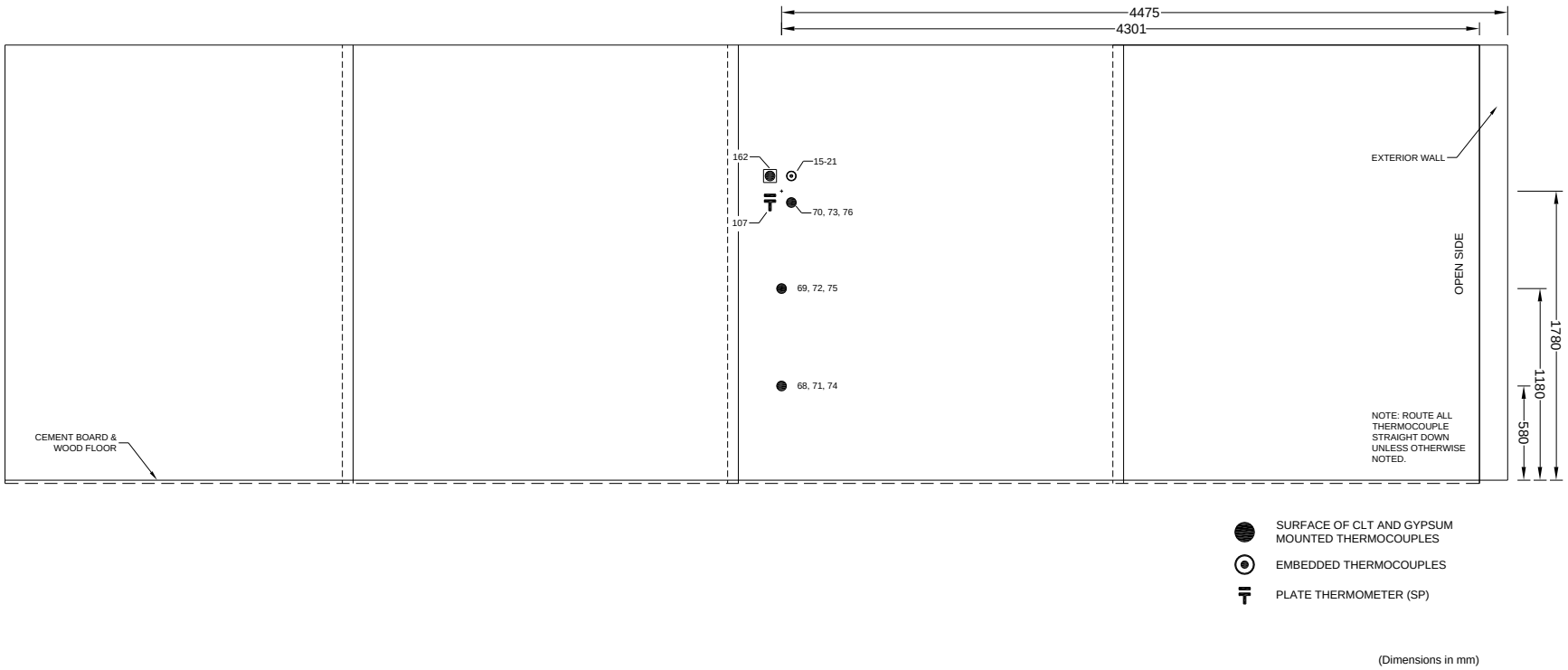

Figure A 104. Test 1-6 Large Compartment CLT - W3 - Instrumentation Layout

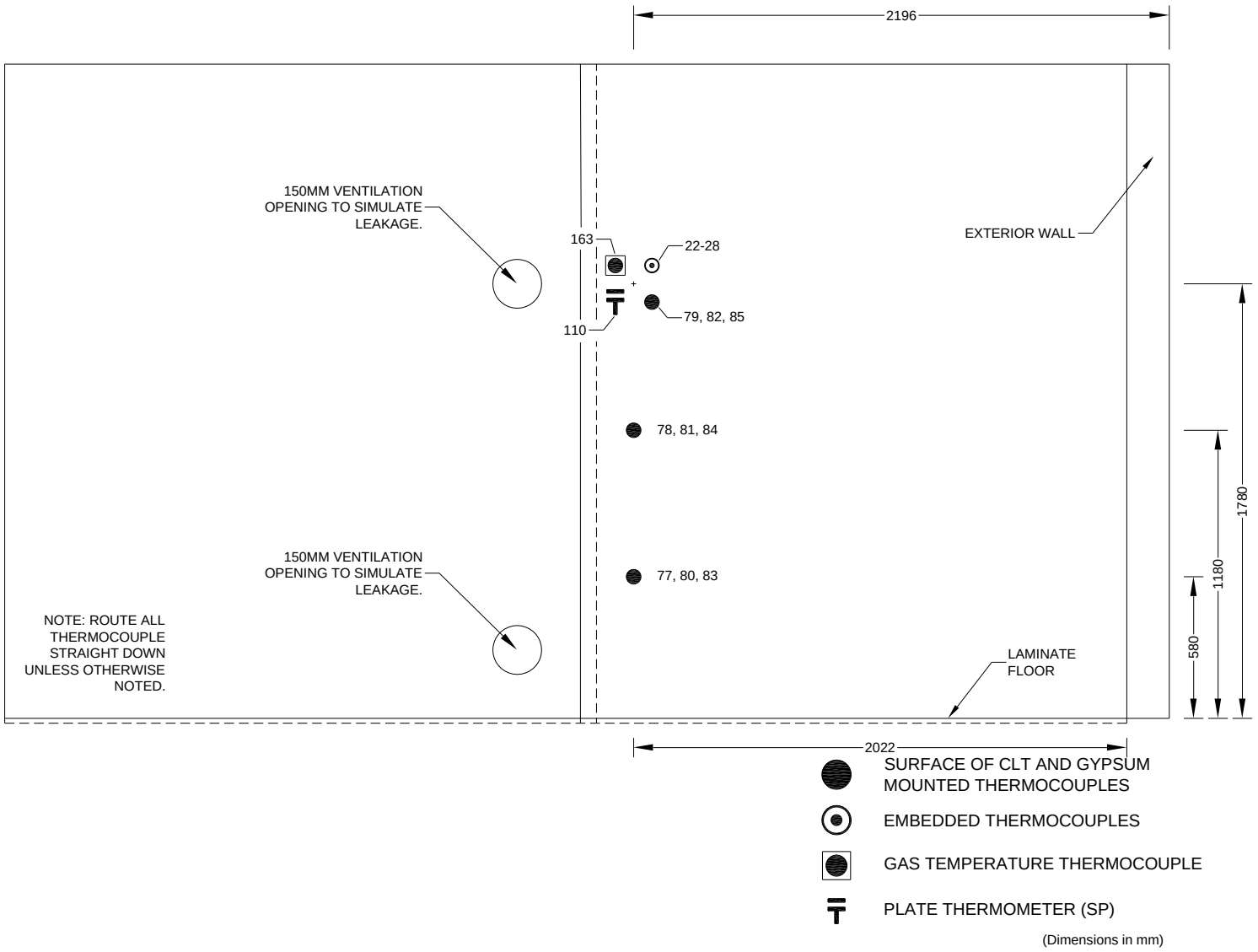

Figure A 105. Test 1-6 Large Compartment CLT - W4 - Instrumentation Layout

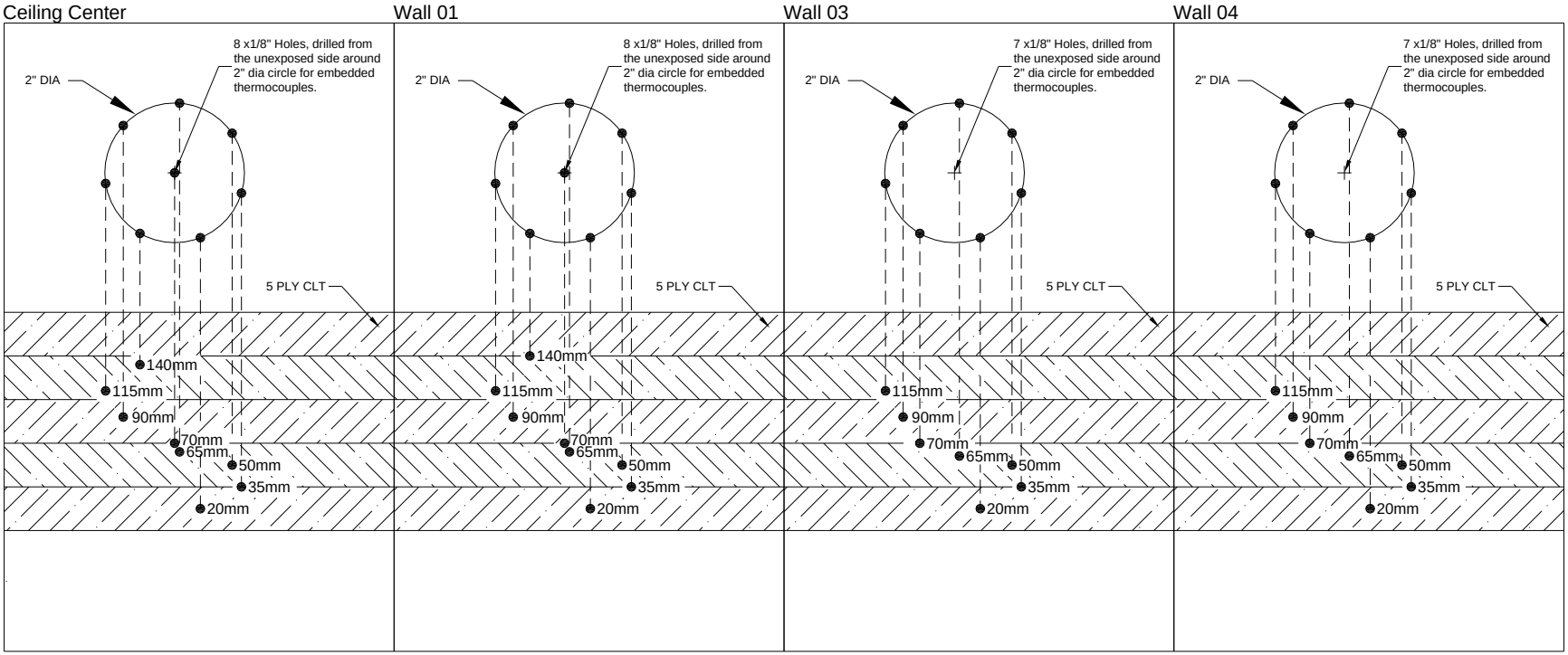

Figure A 106. Test 1-6 Large Compartment CLT - Embedded Thermocouple Detail

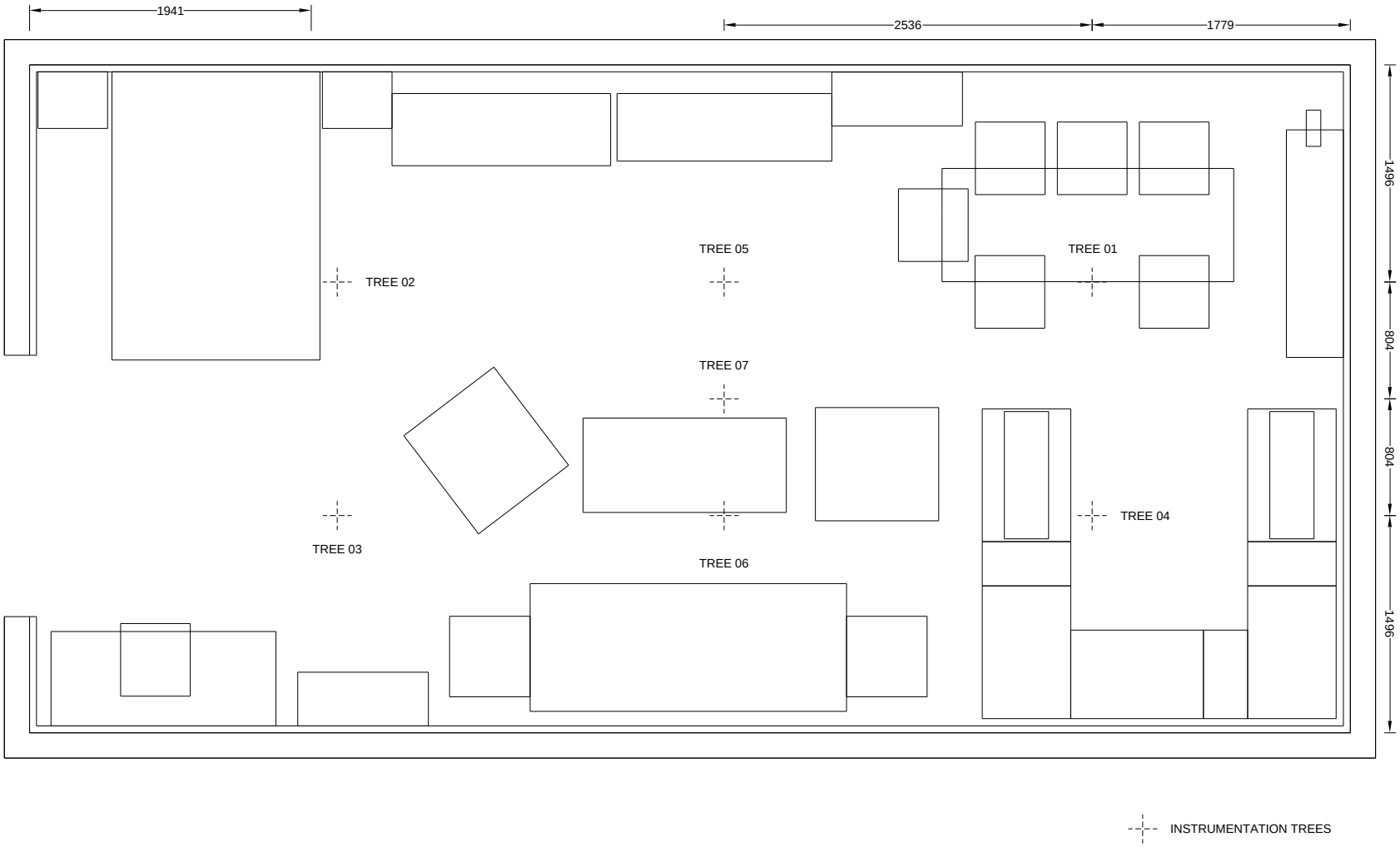

Figure A 107. Test 1-6 Large Compartment CLT - Instrumentation Tree Layout

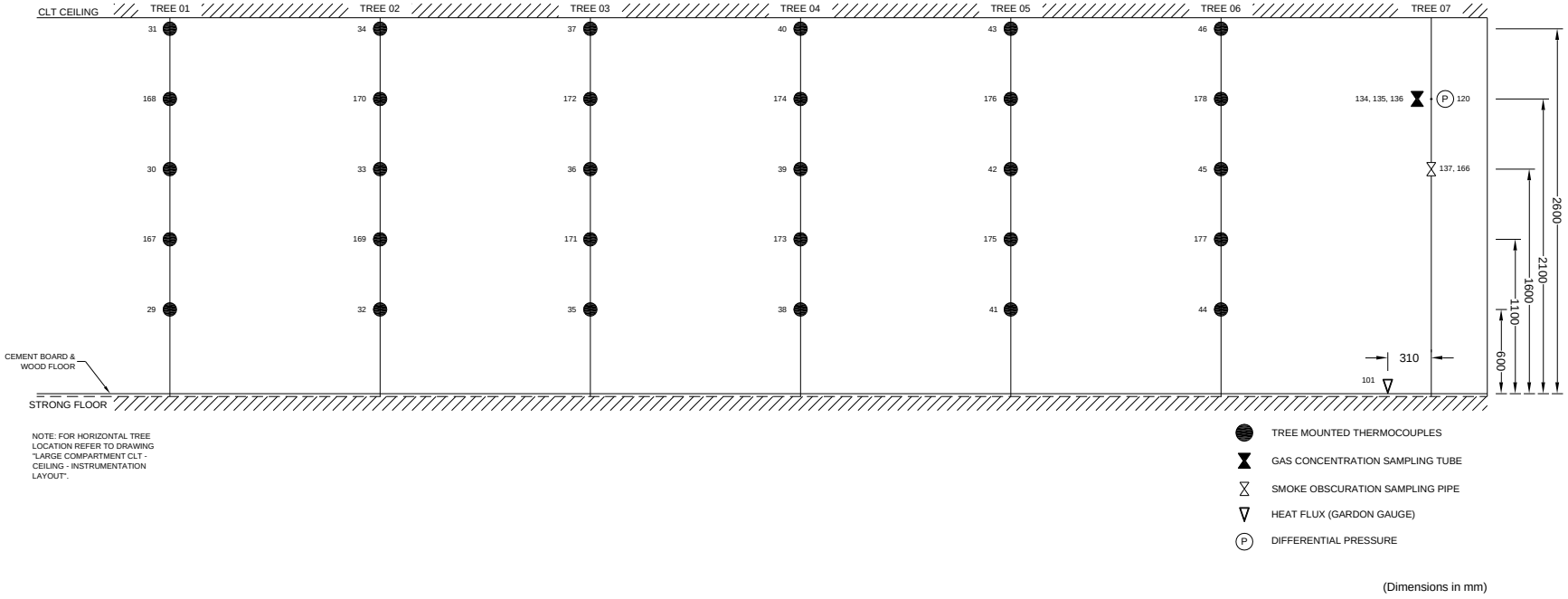

Figure A 108. Test 1-6 Large Compartment CLT - Instrumentation Tree Specifications

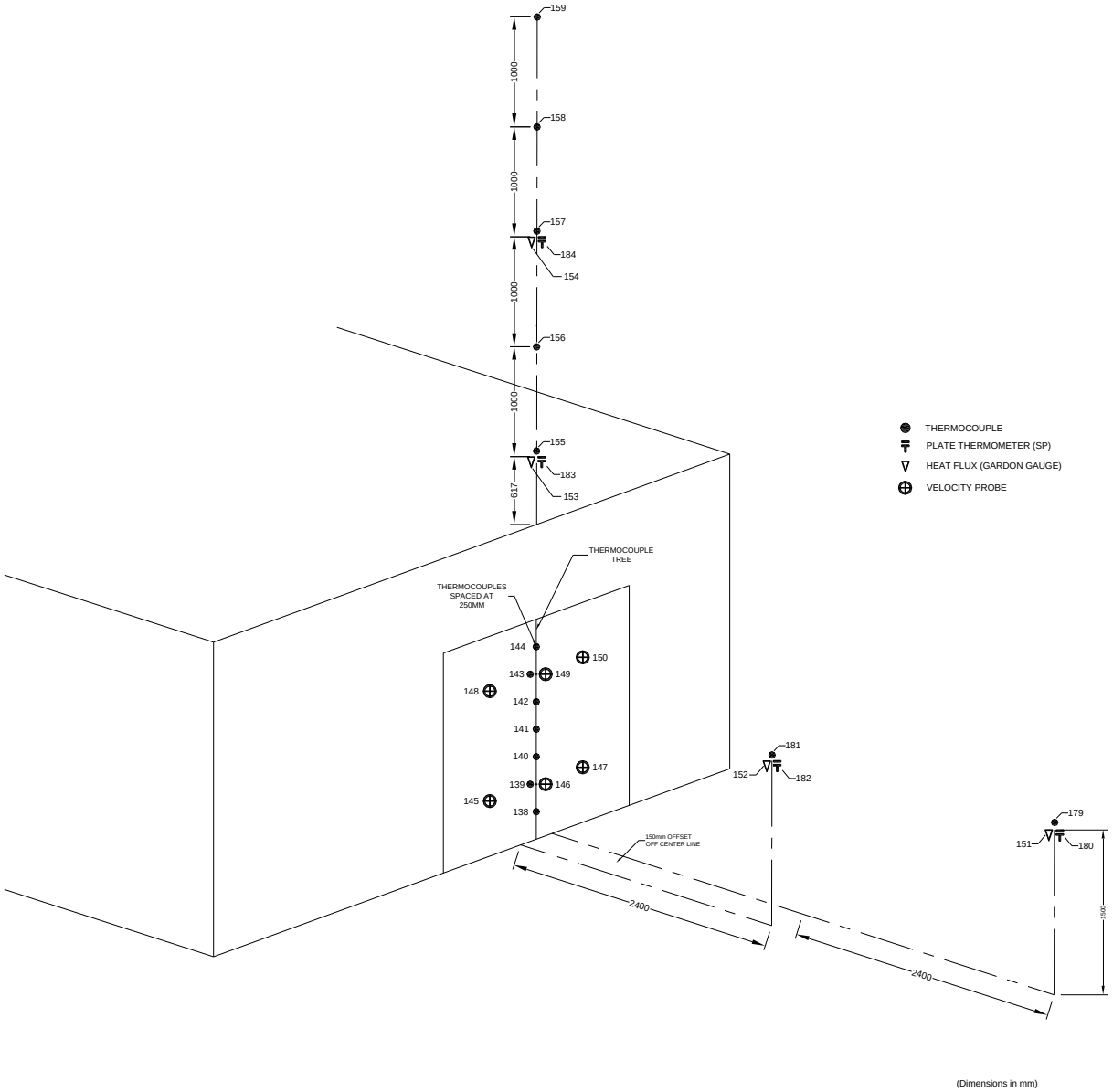

Figure A 109. Test 1-6 Large Compartment CLT - Exterior Instrumentation Layout

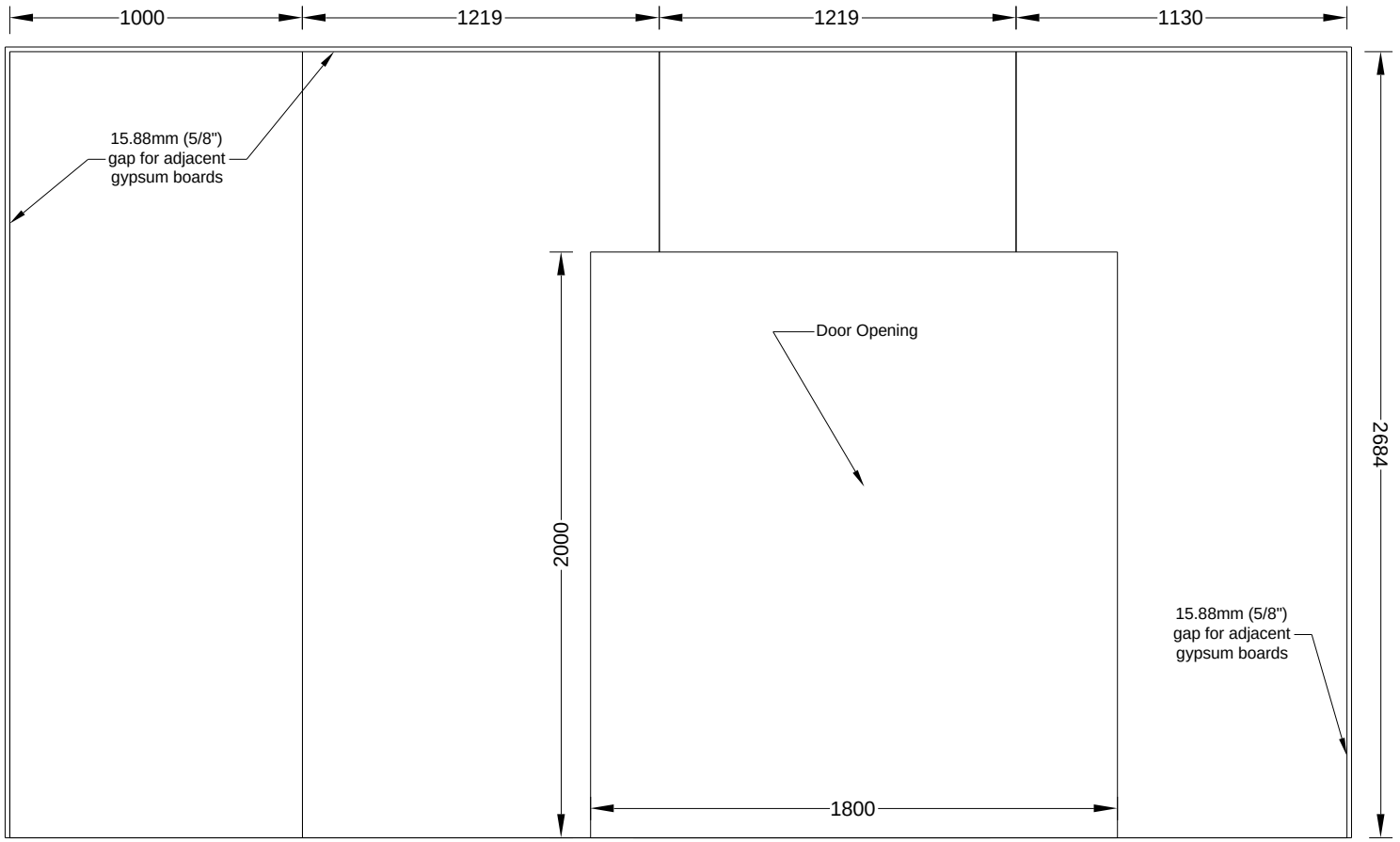

Figure A 110. Test 1-6 Large Compartment CLT - W2 - Gypsum Layout - Base Layer

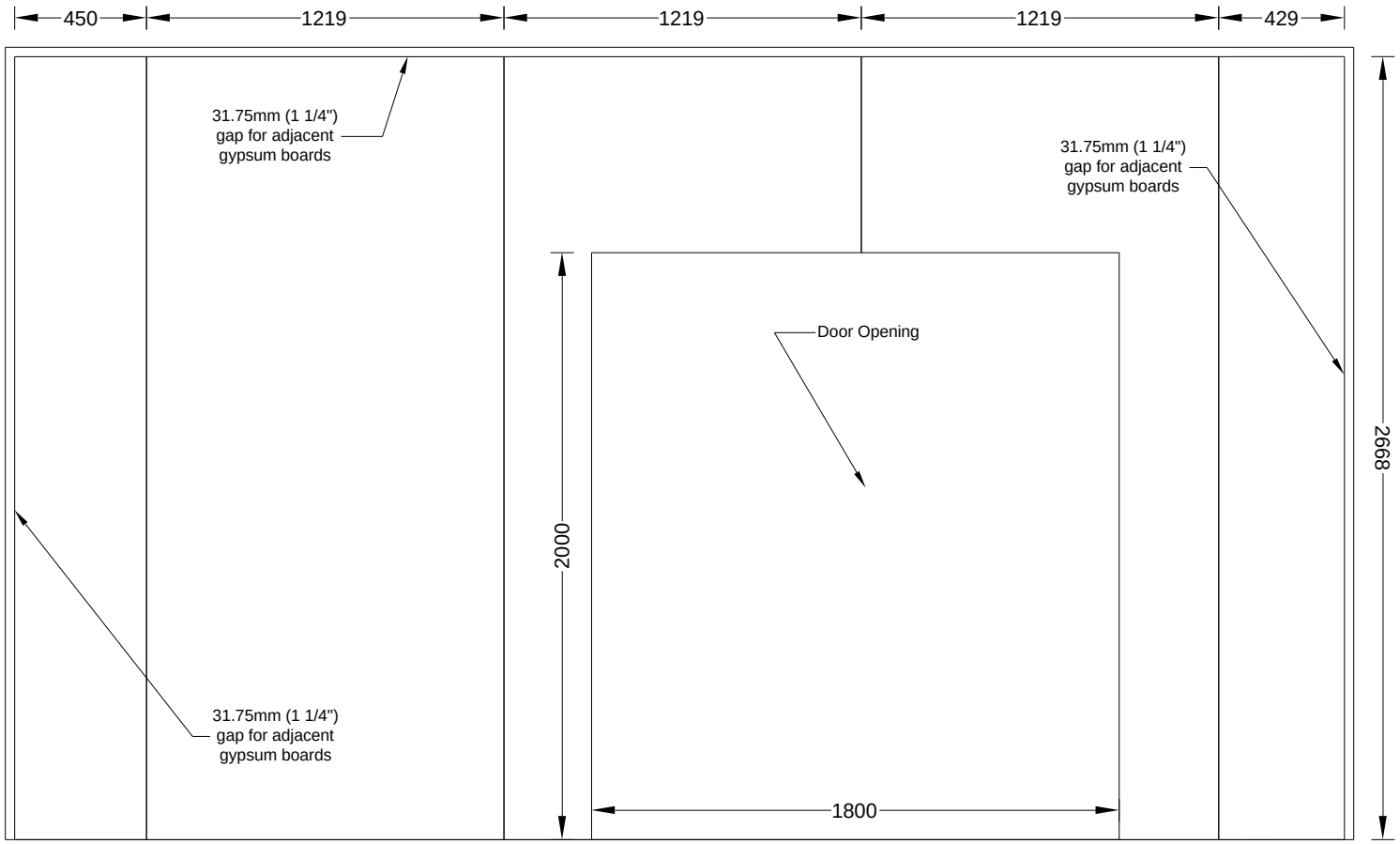

(Dimensions in mm)

Figure A 111. Test 1-6 Large Compartment CLT - W2 - Gypsum Layout - Middle Layer

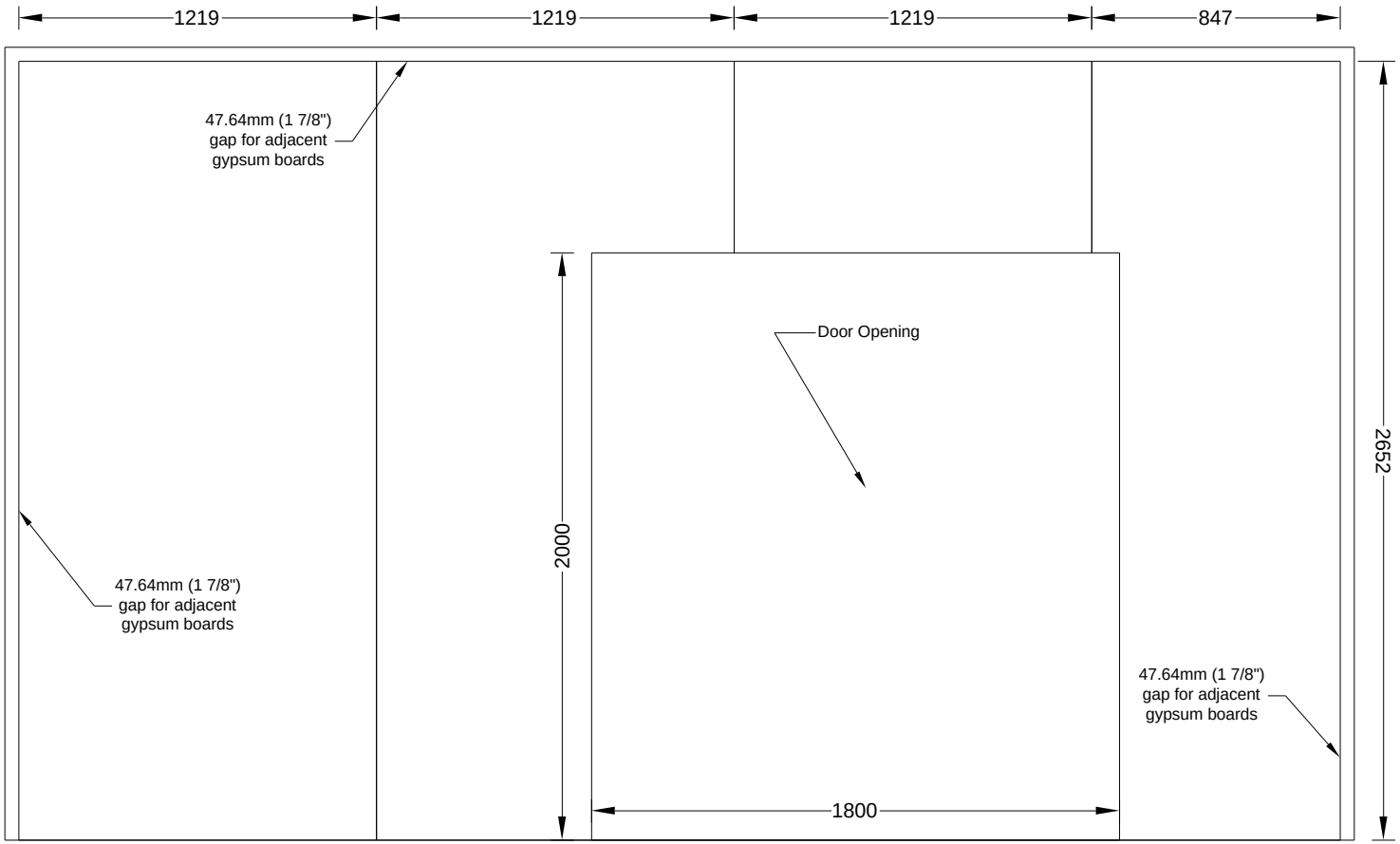

(Dimensions in mm)

Figure A 112. Test 1-6 Large Compartment CLT - W2 - Gypsum Layout - Face Layer

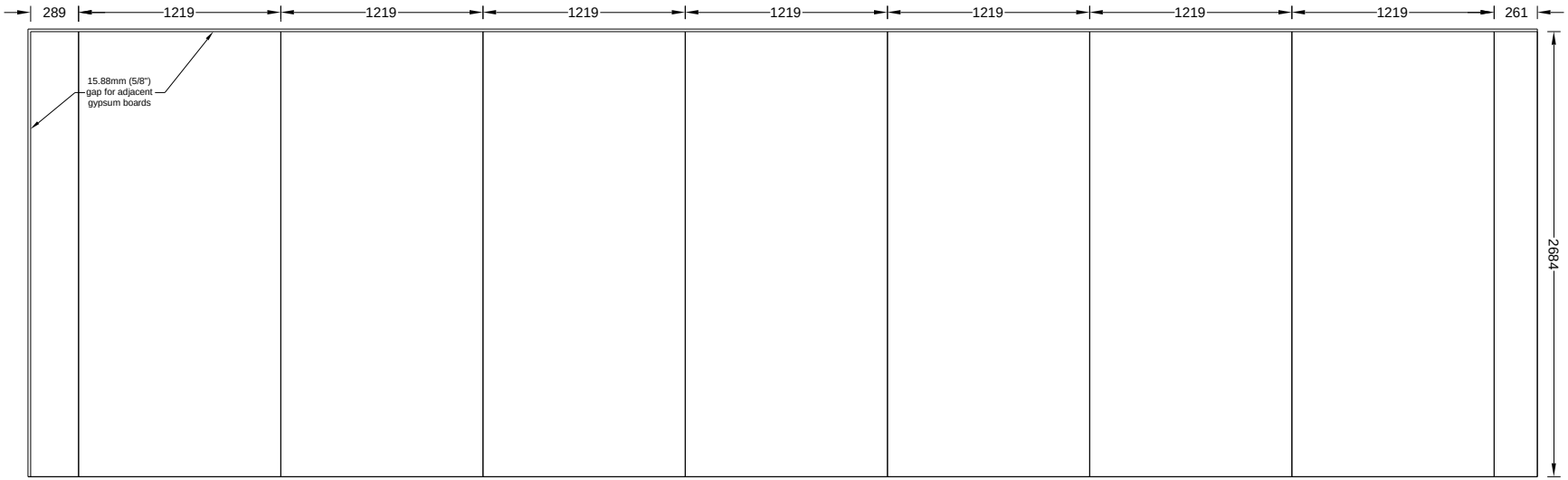

Figure A 113. Test 1-6 Large Compartment CLT - W3 - Gypsum Layout - Base Layer

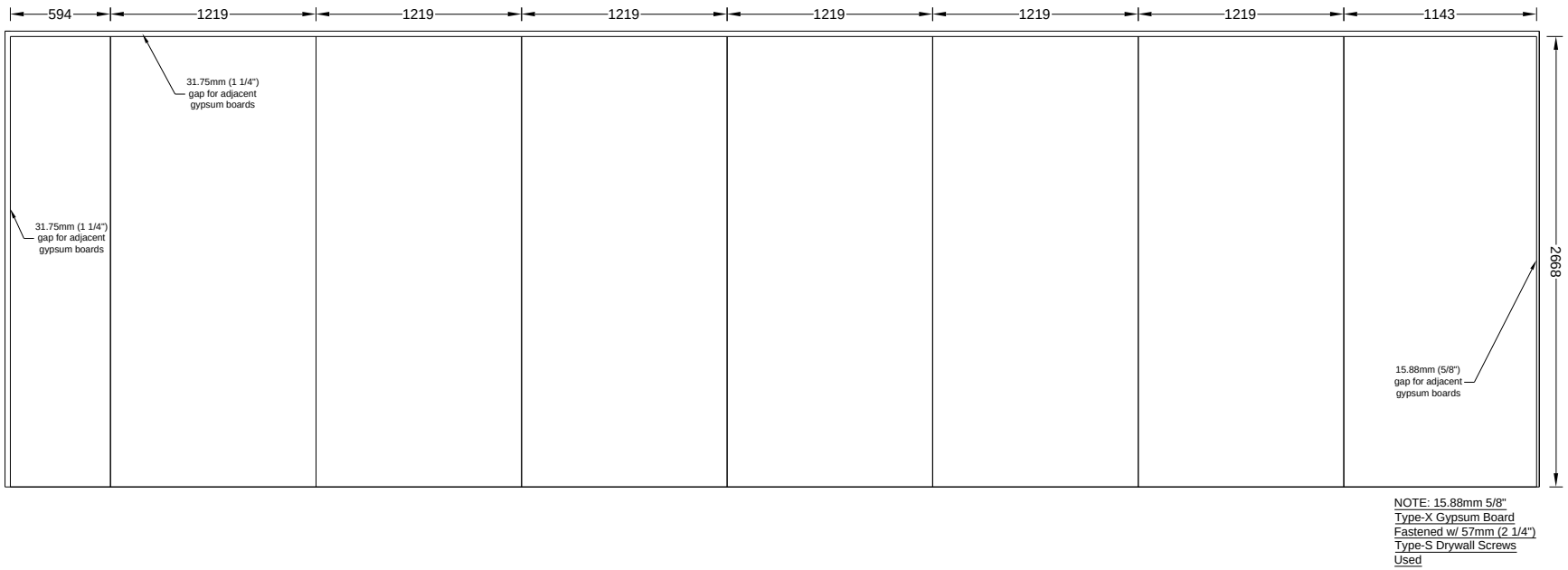

Figure A 114. Test 1-6 Large Compartment CLT - W3 - Gypsum Layout - Middle Layer

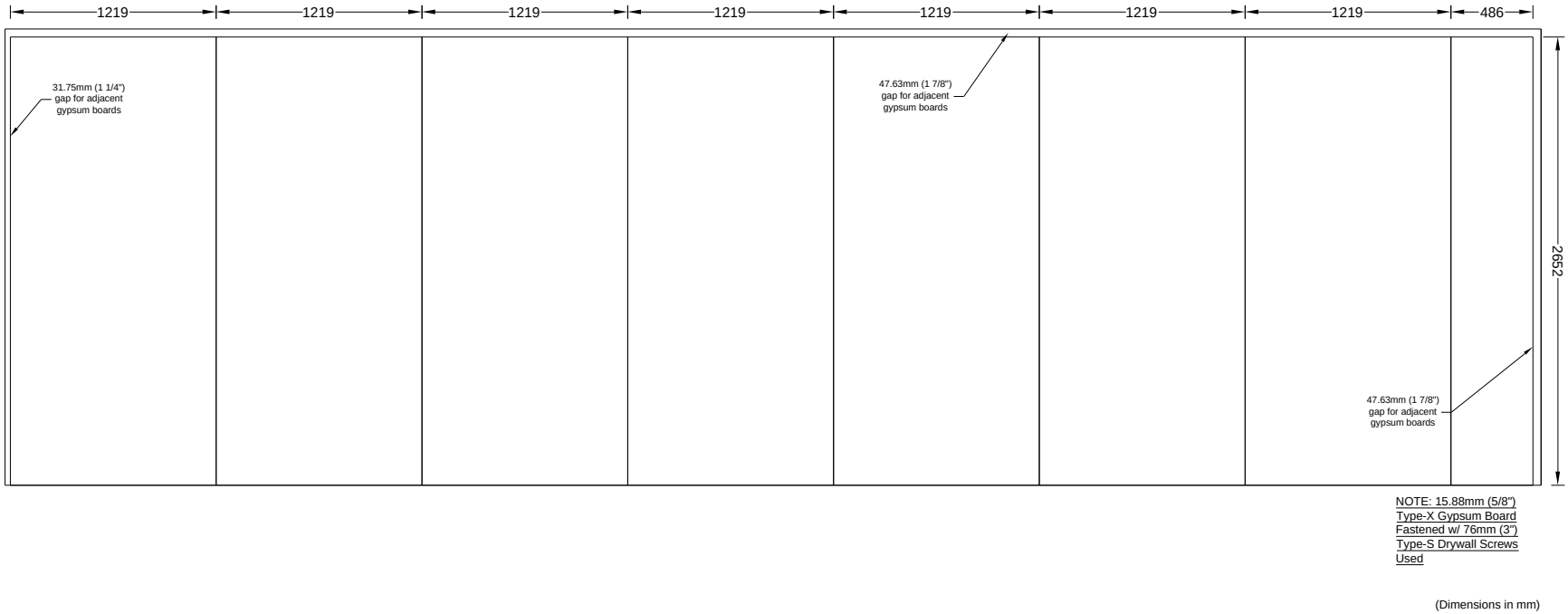

Figure A 115. Test 1-6 Large Compartment CLT - W3 - Gypsum Layout - Face Layer

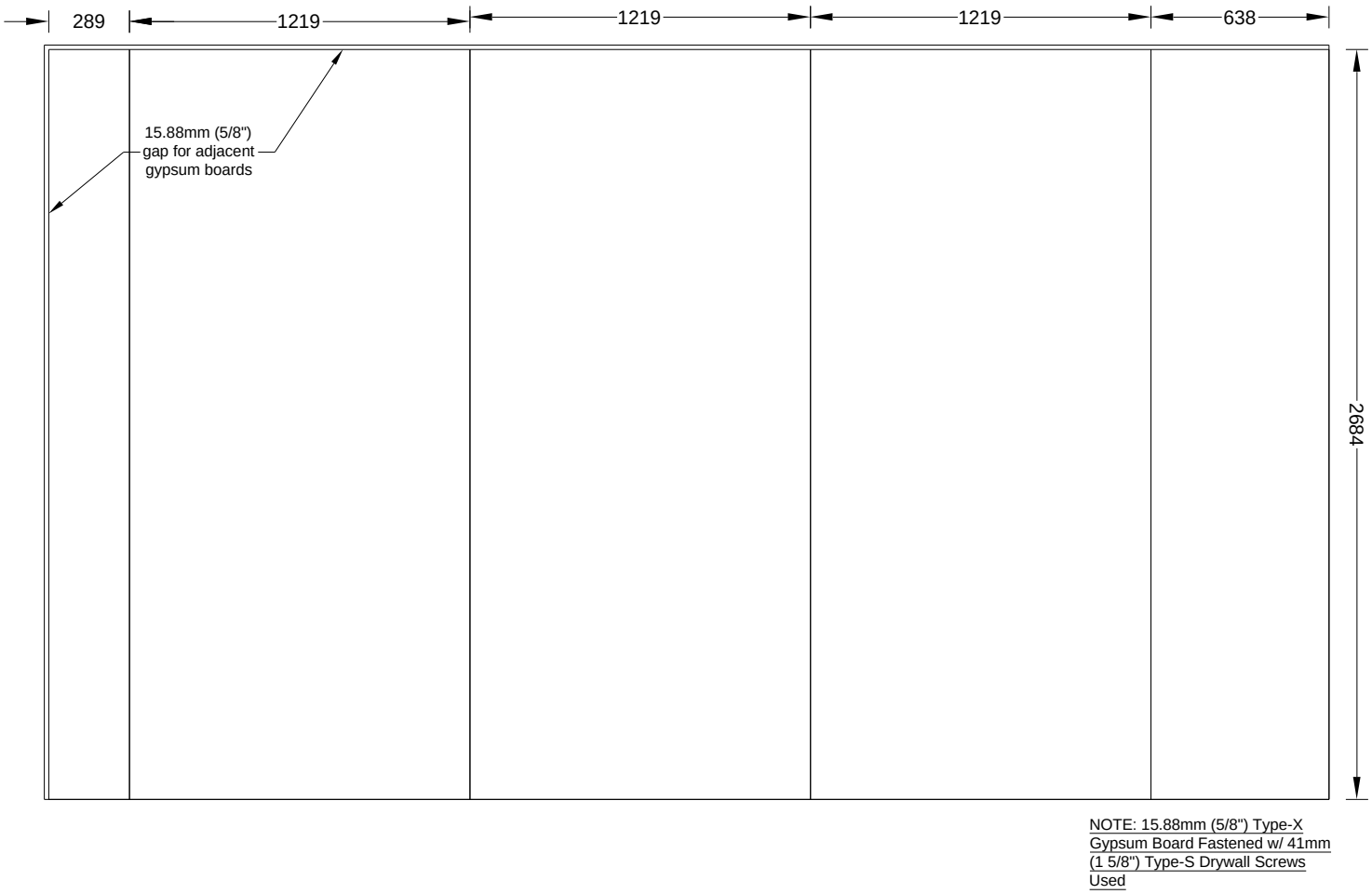

(Dimensions in mm)

Figure A 116. Test 1-6 Large Compartment CLT - W4 - Gypsum Layout - Base Layer

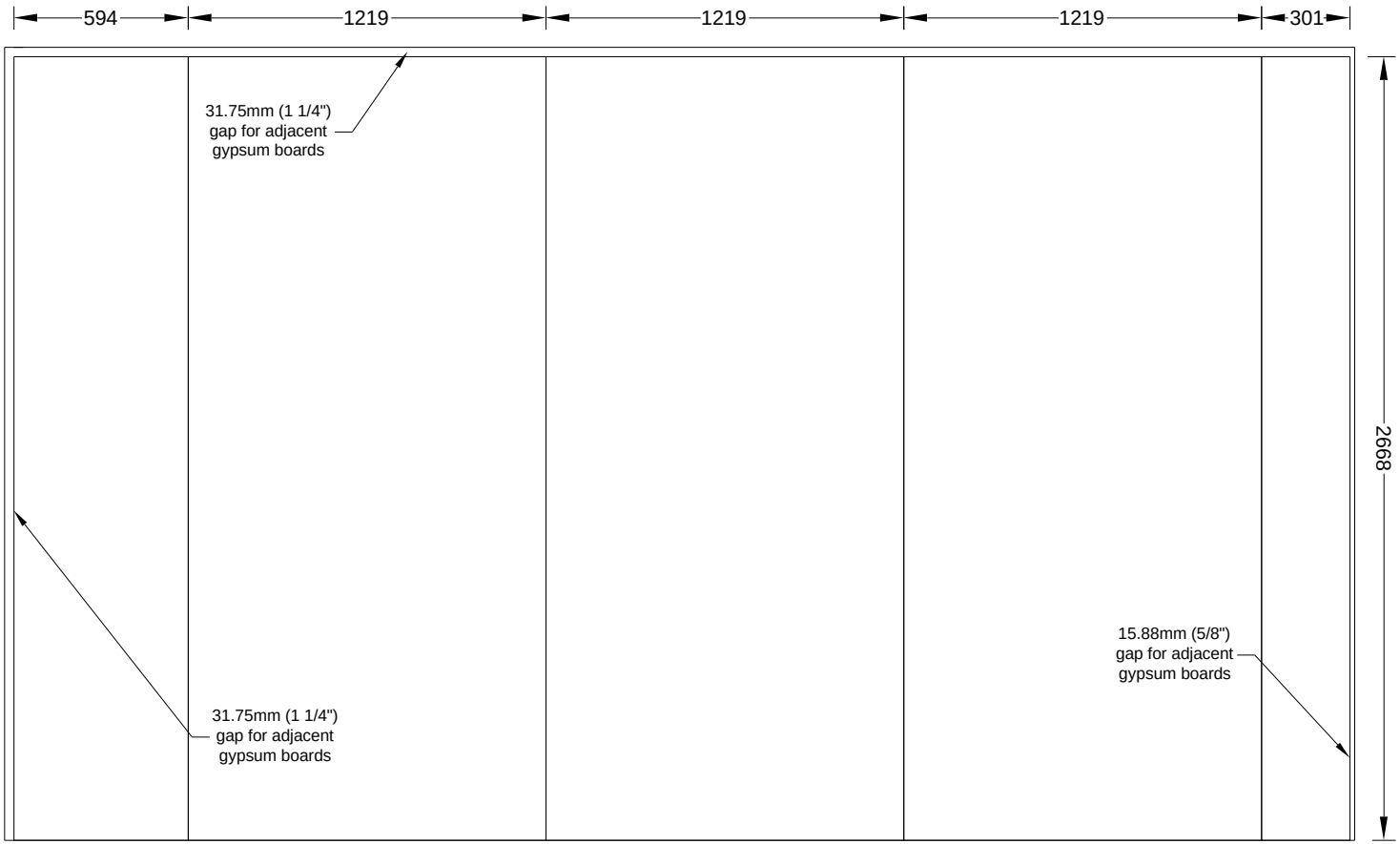

(Dimensions in mm)

Figure A 117. Test 1-6 Large Compartment CLT - W4 - Gypsum Layout - Middle Layer

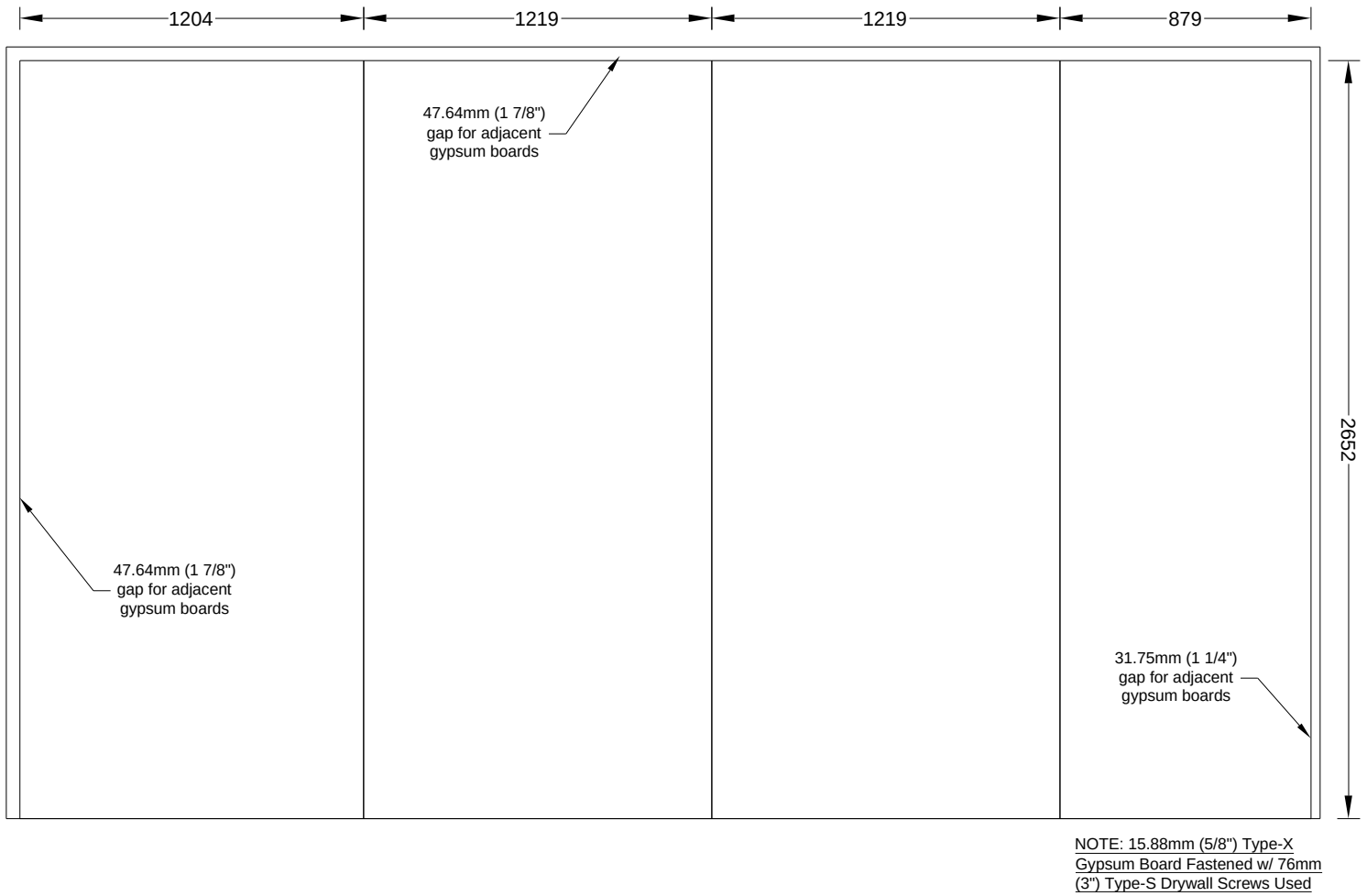

Figure A 118. Test 1-6 Large Compartment CLT - W4 - Gypsum Layout - Face Layer

Appendix B - Pretest moisture content of the CLT panels

Table B 1. Test 1-1 pretest panel moisture content.

Location	Percent moisture content, %					Remarks*
	1	2	3	Mean	SD	* Measurement taken on outside of compartment.
W1	7.6	6.6	7.5	**7.2**	**0.6**	
W2	-	-	-	**-**	**-**	Not accessible
W3	7.1	8.4	9.1	**8.2**	**1.0**	
W4	8.0	8.1	7.5	**7.9**	**0.3**	
Roof	5.8	5.8	6.9	**6.2**	**0.6**	Measured on panel ends
				7.4	**1.0**	

Table B 2. Test 1-2 pretest panel moisture content.

Location	Percent moisture content, %					Remarks*
	1	2	3	Mean	SD	* Measurement taken on outside of compartment.
W1	7.9	8.2	8.0	**8.0**	**0.2**	
W2	-	-	-	**-**	**-**	Not accessible
W3	6.1	8.4	8.4	**7.6**	**1.3**	
W4	8.9	8.0	7.5	**8.1**	**0.7**	
Roof	7.2	5.9	7.5	**6.9**	**0.9**	Measured on panel ends
				7.7	**0.9**	

Table B 3. Test 1-3 pretest panel moisture content.

Location	Percent moisture content, %					Remarks
	1	2	3	Mean	SD	
W1	8.2	8.5	7.8	**8.2**	**0.4**	
W2	8.2	7.1	7.1	**7.5**	**0.6**	
W3	9.1	8.1	8.7	**8.6**	**0.5**	
W4	6.0	7.5	7.0	**6.8**	**0.8**	
Roof	7.1	6.1	6.0	**6.4**	**0.6**	
				7.5	**1.0**	

Table B 4. Test 1-4 pretest panel moisture content.

Location	Percent moisture content, %					Remarks
	1	2	3	Mean	SD	
W1	10.0	10.4	9.2	**9.9**	**0.6**	
W2	9.4	7.7	8.9	**8.7**	**0.9**	
W3	8.6	8.4	9.5	**8.8**	**0.6**	
W4	7.9	9.1	9.3	**8.8**	**0.8**	
Roof	6.9	6.4	8.4	**7.2**	**1.0**	
				8.7	**1.1**	

Table B 5. Test 1-5 pretest panel moisture content.

Location	Percent moisture content, %					Remarks
	1	2	3	Mean	SD	
W1	8.6	7.9	6.9	**7.8**	**0.9**	
W2	8.1	8.0	7.0	**7.7**	**0.6**	
W3	7.6	6.5	8.7	**7.6**	**1.1**	
W4	8.7	8.0	6.9	**7.9**	**0.9**	
Roof	8.1	7.5	8.0	**7.9**	**0.3**	
				7.8	**0.7**	

Table B 6. Test 1-6 pretest panel moisture content.

Location	Percent moisture content, %					Remarks
	1	2	3	Mean	SD	
W1	7.6	7.1	7.0	**7.2**	**0.3**	
W2	8.4	7.4	7.2	**7.7**	**0.6**	
W3	6.9	6.1	6.1	**6.4**	**0.5**	
W4	6.5	6.5	7.1	**6.7**	**0.3**	
Roof	8.0	7.6	8.0	**7.9**	**0.2**	
				7.2	**0.7**	

Appendix C - Moveable fuel load data

Table C 1. Test 1-1 compartment content mass and fuel load calculation.

Item	Manufacturer / Supplier	Product name	Article / Model / Description	Dimensions, mm X	Y	Z	Material	Mass, kg 1	2	3	4	5	6	Mean	SD	Total mass, kg	Heat value,	Energy, MJ
Gypsum paper	US Gypsum	FireCore Type X	-	9100	2700	0.25	Paper	-	-	-	-	-	-	-	-	9.4	17	159
				4600	2700	0.25	Paper	-	-	-	-	-	-	-	-	4.7	17	80
				9100	4600	0.25	Paper	-	-	-	-	-	-	-	-	8.0	17	136
																22	-	**375**
Flooring	trafficMASTER	-	38701	1290	194	7	Hardboard	1.478	1.484	1.492	1.500	1.500	1.484	1.5	0.0	241.1	19.9	4797
Console table	IKEA	HEMNES	502.821.39	390	1570	740	White pine	25.934	-	-	-	-	-	25.9	-	25.9	19.2	498
12" cabinets	Home Depot	Base	B120HD	610	305	876	White pine	17.988	18.378	18.384	18.432	18.498	-	18.3	0.2	91.7	19.2	1760
36" cabinets	Home Depot	Sink Base	B360HD	610	914	876	White pine	26.426	25.982	26.264	26.240	26.856	-	26.4	0.3	131.8	19.2	2530
Table	IKEA	GAMLEBY	602.470.27	2010	780	740	White pine	29.540	-	-	-	-	-	29.5	-	29.5	19.2	567
Chairs	IKEA	HARRY	201.058.31	450	490	960	White pine	5.064	4.926	5.230	5.276	5.368	5.640	5.3	0.2	31.5	19.2	605
Bookcases	IKEA	HEMNES	402.821.30	890	370	1970	White pine	27.770	27.676	-	-	-	-	27.7	0.1	55.4	19.2	1065
TV unit	IKEA	HEMNES	202.421.02	1480	465	570	White pine	30.656	-	-	-	-	-	30.7	-	30.7	19.2	589
8-Dresser dresser	IKEA	HEMNES	003.185.98	1600	500	950	White pine	54.258	-	-	-	-	-	54.3	-	54.3	19.2	1042
Armchair frame	IKEA	JENNYLUND	300.475.48	730	760	850	White pine	18.326	18.406	-	-	-	-	18.4	0.1	36.7	19.2	705
Armchair cushions	IKEA	JENNYLUND	-	510	460	120	PU Foam	1.524	1.550	-	-	-	-	1.5	0.0	3.1	29	89
Sofa frame	IKEA	EKTROP	401.850.30	2180	860	900	White pine	43.700	-	-	-	-	-	43.7	-	43.7	19.2	839
Sofa cushions	IKEA	EKTROP	-	1670	700	120	PU Foam	13.996	-	-	-	-	-	14.0	-	14.0	29	406
Side table	IKEA	HEMNES	802.821.52	550	550	500	White pine	8.028	8.370	-	-	-	-	8.2	0.2	16.4	19.2	315
Coffee table	IKEA	ARKELSTROP	302.608.07	1380	650	520	White pine	16.342	-	-	-	-	-	16.3	-	16.3	19.2	314
Night stands	IKEA	TARVA	502.196.09	480	390	620	White pine	9.254	9.168	-	-	-	-	9.2	0.1	18.4	19.2	354
Bed frame	IKEA	HEMNES	202.421.02	1470	2000	400	White pine	32.058	-	-	-	-	-	32.1	-	32.1	19.2	616
Bed drawers	IKEA	HEMNES	103.262.96	1470	2000	200	White pine	7.812	8.084	4.286	4.246	-	-	6.1	2.1	24.4	19.2	469
Bed frame slats	Home Depot	Whitewood	569062	1331	102	51	White pine	9.254	-	-	-	-	-	9.3	-	9.3	19.2	178
Mattress	IKEA	MOREDAL	802.773.82	1340	1870	170	PU Foam	17.938	-	-	-	-	-	17.9	-	17.9	29	520
Desk	IKEA	HEMNES	502.821.44	1550	650	740	White pine	36.474	-	-	-	-	-	36.5	-	36.5	19.2	700
Desk hutch	IKEA	HEMNES	202.821.26	1520	250	630	White pine	20.868	-	-	-	-	-	20.9	-	20.9	19.2	401
Desk Chair	IKEA	HARRY	201.058.31	450	490	960	White pine	4.886	-	-	-	-	-	4.9	-	4.9	19.2	94
Wood cribs	Lowes*	HT 591	28 pcs 2 in. x 2 in x 12 in.	305	305	305	White pine	4.454	4.482	4.444	4.570	-	-	4.5	0.1	18.0	19.2	345
Counter top	Home Depot	-	2 in. x 12 in. & 2 in. x 4 in.	660	2210	38	Douglas fir	32.436	30.572	-	-	-	-	31.5	1.3	63.0	21	1323
Counter top	Home Depot	-	2 in. x 12 in. & 2 in. x 4 in.	660	1210	38	Douglas fir	17.292	-	-	-	-	-	-	-	17.3	21	363
Wood cribs	Lowes*	-	6 pcs 2 in. x 4 in x 12 in. 6 pcs 2 in. x 4 in x 30 in.	762	305	152	White pine	10.316	9.868	10.222	9.732	9.394	9.822	9.9	0.3	59.4	19.2	1140
* Unspecified																**Without drywall paper**	**1144**	-	**22622**
																With drywall paper	**1166**		**22997**

Area	**41.86**	**m2**
Load density (w/o paper)	**540**	**MJ/m2**
Load density (w/ paper)	**549**	**MJ/m2**

Table C 2. Test 1-2 compartment content mass and fuel load calculation.

Item	Manufacturer / Supplier	Product name	Article / Model / Description	Dimensions, mm X	Y	Z	Material	Mass, kg 1	2	3	4	5	6	Mean	SD	Total mass, kg	Heat value,	Energy, MJ	
Gypsum paper	US Gypsum	FireCore Type X	-	9100	2700	0.25	Paper	-	-	-	-	-	-	-	-	9.4	17	159	
				4600	2700	0.25	Paper	-	-	-	-	-	-	-	-	4.7	17	80	
				9100	4600	0.25	Paper	-	-	-	-	-	-	-	-	8.0	17	136	
																22	-	**375**	1.6%
Flooring	trafficMASTER	-	38701	1290	194	7	Hardboard	1.478	1.484	1.492	1.500	1.500	1.484	1.5	0.0	241.1	19.9	4797	
Console table	IKEA	HEMNES	502.821.39	390	1570	740	White pine	25.584	-	-	-	-	-	25.6	-	25.6	19.2	491	
12" cabinets	Home Depot	Base	B120HD	610	305	876	White pine	18.380	18.096	18.488	18.430	18.336	-	18.3	0.2	91.7	19.2	1761	
36" cabinets	Home Depot	Sink Base	B360HD	610	914	876	White pine	26.712	26.482	26.060	26.346	26.458	-	26.4	0.2	132.1	19.2	2536	
Table	IKEA	GAMLEBY	602.470.27	2010	780	740	White pine	28.908	-	-	-	-	-	28.9	-	28.9	19.2	555	
Chairs	IKEA	HARRY	201.058.31	450	490	960	White pine	5.100	5.156	5.090	5.070	5.154	5.048	5.1	0.0	30.6	19.2	588	
Bookcases	IKEA	HEMNES	402.821.30	890	370	1970	White pine	27.680	27.780	-	-	-	-	27.7	0.1	55.5	19.2	1065	
TV unit	IKEA	HEMNES	202.421.02	1480	465	570	White pine	29.810	-	-	-	-	-	29.8	-	29.8	19.2	572	
8-Dresser dresser	IKEA	HEMNES	003.185.98	1600	500	950	White pine	53.224	-	-	-	-	-	53.2	-	53.2	19.2	1022	
Armchair frame	IKEA	JENNYLUND	300.475.48	730	760	850	White pine	18.218	18.508	-	-	-	-	18.4	0.2	36.7	19.2	705	
Armchair cushions	IKEA	JENNYLUND	-	510	460	120	PU Foam	1.504	1.466	-	-	-	-	1.5	0.0	3.0	29	86	
Sofa frame	IKEA	EKTROP	401.850.30	2180	860	900	White pine	44.446	-	-	-	-	-	44.4	-	44.4	19.2	853	
Sofa cushions	IKEA	EKTROP	-	1670	700	120	PU Foam	14.084	-	-	-	-	-	14.1	-	14.1	29	408	
Side table	IKEA	HEMNES	802.821.52	550	550	500	White pine	8.294	8.148	-	-	-	-	8.2	0.1	16.4	19.2	316	
Coffee table	IKEA	ARKELSTROP	302.608.07	1380	650	520	White pine	16.194	-	-	-	-	-	16.2	-	16.2	19.2	311	
Night stands	IKEA	TARVA	502.196.09	480	390	620	White pine	9.272	9.352	-	-	-	-	9.3	0.1	18.6	19.2	358	
Bed frame	IKEA	HEMNES	202.421.02	1470	2000	400	White pine	31.954	-	-	-	-	-	32.0	-	32.0	19.2	614	
Bed drawers	IKEA	HEMNES	103.262.96	1470	2000	200	White pine	7.898	7.904	4.356	4.318	-	-	6.1	2.1	24.5	19.2	470	
Bed frame slats	Home Depot	Whitewood	569062	1331	102	51	White pine	7.988	-	-	-	-	-	8.0	-	8.0	19.2	153	
Mattress	IKEA	MOREDAL	802.773.82	1340	1870	170	PU Foam	17.864	-	-	-	-	-	17.9	-	17.9	29	518	
Desk	IKEA	HEMNES	502.821.44	1550	650	740	White pine	37.360	-	-	-	-	-	37.4	-	37.4	19.2	717	
Desk hutch	IKEA	HEMNES	202.821.26	1520	250	630	White pine	20.396	-	-	-	-	-	20.4	-	20.4	19.2	392	
Desk Chair	IKEA	HARRY	201.058.31	450	490	960	White pine	4.990	-	-	-	-	-	5.0	-	5.0	19.2	96	
Wood cribs	Lowes*	HT 591	28 pcs 2 in. x 2 in x 12 in.	305	305	305	White pine	4.660	4.802	4.560	4.642	-	-	4.7	0.1	18.7	19.2	358	
Counter top	Home Depot	-	2 in. x 12 in. & 2 in. x 4 in.	660	2210	38	Douglas fir	28.530	35.892	-	-	-	-	32.2	5.2	64.4	21	1353	
Counter top	Home Depot	-	2 in. x 12 in. & 2 in. x 4 in.	660	1210	38	Douglas fir	17.238	-	-	-	-	-	-	-	17.2	21	362	
Wood cribs	Lowes*	-	6 pcs 2 in. x 4 in x 12 in. 6 pcs 2 in. x 4 in x 30 in.	762	305	152	White pine	10.332	9.718	10.215	9.940	8.660	7.782	9.4	1.0	56.6	19.2	1088	
* Unspecified																**Without drywall paper**	**1140**	-	**22545** 98.4%
																With drywall paper	**1162**		**22920**

Area	**41.86**	**m2**
Load density (w/o paper)	**539**	**MJ/m2**
Load density (w/ paper)	**548**	**MJ/m2**

Table C 3. Test 1-3 compartment content mass and fuel load calculation.

Item	Manufacturer / Supplier	Product name	Article / Model / Description	Dimensions, mm			Material	Mass, kg								Total mass, kg	Heat value, MJ/kg	Energy, MJ
				X	Y	Z		1	2	3	4	5	6	Mean	SD			
Gypsum paper	US Gypsum	FireCore Type X	-	9100	2700	0.25	Paper	-	-	-	-	-	-	-	-	4.7	17	80
				4600	2700	0.25	Paper	-	-	-	-	-	-	-	-	4.7	17	80
				9100	4600	0.25	Paper	-	-	-	-	-	-	-	-	8.0	17	136
																17	**-**	**296**
Flooring	trafficMASTER	-	38701	1290	194	7	Hardboard	1.478	1.484	1.492	1.500	1.500	1.484	1.5	0.0	241.1	19.9	4797
Console table	IKEA	HEMNES	502.821.39	390	1570	740	White pine	25.530	-	-	-	-	-	25.5	-	25.5	19.2	490
12" cabinets	Home Depot	Base	B120HD	610	305	876	White pine	18.500	18.530	18.646	18.382	18.206	-	18.5	0.2	92.3	19.2	1771
36" cabinets	Home Depot	Sink Base	B360HD	610	914	876	White pine	27.538	26.872	27.980	26.796	26.360	-	27.1	0.6	135.5	19.2	2602
Table	IKEA	GAMLEBY	602.470.27	2010	780	740	White pine	28.920	-	-	-	-	-	28.9	-	28.9	19.2	555
Chairs	IKEA	HARRY	201.058.31	450	490	960	White pine	5.072	5.428	5.188	5.322	5.198	5.382	5.3	0.1	31.6	19.2	607
Bookcases	IKEA	HEMNES	402.821.30	890	370	1970	White pine	28.776	28.040	-	-	-	-	28.4	0.5	56.8	19.2	1091
TV unit	IKEA	HEMNES	202.421.02	1480	465	570	White pine	31.198	-	-	-	-	-	31.2	-	31.2	19.2	599
8-Dresser dresser	IKEA	HEMNES	003.185.98	1600	500	950	White pine	54.758	-	-	-	-	-	54.8	-	54.8	19.2	1051
Armchair frame	IKEA	JENNYLUND	300.475.48	730	760	850	White pine	18.740	18.632	-	-	-	-	18.7	0.1	37.4	19.2	718
Armchair cushions	IKEA	JENNYLUND	-	510	460	120	PU Foam	1.426	1.420	-	-	-	-	1.4	0.0	2.8	29	83
Sofa frame	IKEA	EKTROP	401.850.30	2180	860	900	White pine	43.234	-	-	-	-	-	43.2	-	43.2	19.2	830
Sofa cushions	IKEA	EKTROP	-	1670	700	120	PU Foam	14.090	-	-	-	-	-	14.1	-	14.1	29	409
Side table	IKEA	HEMNES	802.821.52	550	550	500	White pine	7.838	7.966	-	-	-	-	7.9	0.1	15.8	19.2	303
Coffee table	IKEA	ARKELSTROP	302.608.07	1380	650	520	White pine	16.586	-	-	-	-	-	16.6	-	16.6	19.2	318
Night stands	IKEA	TARVA	502.196.09	480	390	620	White pine	9.470	9.102	-	-	-	-	9.3	0.3	18.6	19.2	357
Bed frame	IKEA	HEMNES	202.421.02	1470	2000	400	White pine	31.960	-	-	-	-	-	32.0	-	32.0	19.2	614
Bed drawers	IKEA	HEMNES	103.262.96	1470	2000	200	White pine	8.260	8.168	4.200	4.504	-	-	6.3	2.2	25.1	19.2	483
Bed frame slats	IKEA	LUROY	601.602.17	1331	102	51	White pine	7.632	-	-	-	-	-	7.6	-	7.6	19.2	147
Mattress	IKEA	MOREDAL	802.773.82	1340	1870	170	PU Foam	17.924	-	-	-	-	-	17.9	-	17.9	29	520
Desk	IKEA	HEMNES	502.821.44	1550	650	740	White pine	37.544	-	-	-	-	-	37.5	-	37.5	19.2	721
Desk hutch	IKEA	HEMNES	202.821.26	1520	250	630	White pine	20.112	-	-	-	-	-	20.1	-	20.1	19.2	386
Desk Chair	IKEA	HARRY	201.058.31	450	490	960	White pine	5.474	-	-	-	-	-	5.5	-	5.5	19.2	105
Wood cribs	Lowes*	HT 591	28 pcs 2 in. x 2 in x 12 in.	305	305	305	White pine	6.010	6.102	5.258	4.366	-	-	5.4	0.8	21.7	19.2	417
Counter top	Home Depot	-	2 in. x 12 in. & 2 in. x 4 in.	660	2210	38	Douglas fir	32.788	36.946	-	-	-	-	34.9	2.9	69.7	21	1464
Counter top	Home Depot	-	2 in. x 12 in. & 2 in. x 4 in.	660	1210	38	Douglas fir	15.520	-	-	-	-	-	-	-	15.5	21	326
Wood cribs	Lowes*	-	6 pcs 2 in. x 4 in x 12 in. 6 pcs 2 in. x 4 in x 30 in.	762	305	152	White pine	9.940	10.236	10.852	10.854	10.674	11.258	10.6	0.5	63.8	19.2	1225
* Unspecified																**Without drywall paper**	**1163**	**-**	**22989**
																With drywall paper	**1180**		**23285**

Area	**41.86**	**m2**
Load density (w/o paper)	**549**	**MJ/m2**
Load density (w/ paper)	**556**	**MJ/m2**

Table C 4. Test 1-4 compartment content mass and fuel load calculation.

Item	Manufacturer / Supplier	Product name	Article / Model / Description	Dimensions, mm			Material	Mass, kg								Total mass, kg	Heat value, MJ/kg	Energy, MJ
				X	Y	Z		1	2	3	4	5	6	Mean	SD			
Gypsum paper	US Gypsum	FireCore Type X	-	9100	2700	0.25	Paper	-	-	-	-	-	-	-	-	9.4	17	159
				4600	2700	0.25	Paper	-	-	-	-	-	-	-	-	4.7	17	80
				9100	4600	0.25	Paper	-	-	-	-	-	-	-	-	0.0	17	0
																14	**-**	**240**
Flooring	trafficMASTER	-	38701	1290	194	7	Hardboard	1.478	1.484	1.492	1.500	1.500	1.484	1.5	0.0	241.1	19.9	4797
Console table	IKEA	HEMNES	502.821.39	390	1570	740	White pine	25.434	-	-	-	-	-	25.4	-	25.4	19.2	488
12" cabinets	Home Depot	Base	B120HD	610	305	876	White pine	18.288	18.360	18.760	18.436	18.362	-	18.4	0.2	92.2	19.2	1770
36" cabinets	Home Depot	Sink Base	B360HD	610	914	876	White pine	26.250	28.280	28.264	27.784	26.644	-	27.4	0.9	137.2	19.2	2635
Table	IKEA	GAMLEBY	602.470.27	2010	780	740	White pine	28.612	-	-	-	-	-	28.6	-	28.6	19.2	549
Chairs	IKEA	HARRY	201.058.31	450	490	960	White pine	5.082	5.422	5.290	5.082	5.280	5.416	5.3	0.2	31.6	19.2	606
Bookcases	IKEA	HEMNES	402.821.30	890	370	1970	White pine	28.516	28.078	-	-	-	-	28.3	0.3	56.6	19.2	1087
TV unit	IKEA	HEMNES	202.421.02	1480	465	570	White pine	31.142	-	-	-	-	-	31.1	-	31.1	19.2	598
8-Dresser dresser	IKEA	HEMNES	003.185.98	1600	500	950	White pine	53.948	-	-	-	-	-	53.9	-	53.9	19.2	1036
Armchair frame	IKEA	JENNYLUND	300.475.48	730	760	850	White pine	18.384	18.384	-	-	-	-	18.4	0.0	36.8	19.2	706
Armchair cushions	IKEA	JENNYLUND	-	510	460	120	PU Foam	1.446	1.452	-	-	-	-	1.4	0.0	2.9	29	84
Sofa frame	IKEA	EKTROP	401.850.30	2180	860	900	White pine	43.480	-	-	-	-	-	43.5	-	43.5	19.2	835
Sofa cushions	IKEA	EKTROP	-	1670	700	120	PU Foam	14.256	-	-	-	-	-	14.3	-	14.3	29	413
Side table	IKEA	HEMNES	802.821.52	550	550	500	White pine	8.034	7.768	-	-	-	-	7.9	0.2	15.8	19.2	303
Coffee table	IKEA	ARKELSTROP	302.608.07	1380	650	520	White pine	16.778	-	-	-	-	-	16.8	-	16.8	19.2	322
Night stands	IKEA	TARVA	502.196.09	480	390	620	White pine	9.366	9.284	-	-	-	-	9.3	0.1	18.7	19.2	358
Bed frame	IKEA	HEMNES	202.421.02	1470	2000	400	White pine	32.376	-	-	-	-	-	32.4	-	32.4	19.2	622
Bed drawers	IKEA	HEMNES	103.262.96	1470	2000	200	White pine	8.038	7.990	4.308	4.372	-	-	6.2	2.1	24.7	19.2	474
Bed frame slats	IKEA	LUROY	601.602.17	1331	102	51	White pine	7.600	-	-	-	-	-	7.6	-	7.6	19.2	146
Mattress	IKEA	MOREDAL	802.773.82	1340	1870	170	PU Foam	18.000	-	-	-	-	-	18.0	-	18.0	29	522
Desk	IKEA	HEMNES	502.821.44	1550	650	740	White pine	37.816	-	-	-	-	-	37.8	-	37.8	19.2	726
Desk hutch	IKEA	HEMNES	202.821.26	1520	250	630	White pine	20.726	-	-	-	-	-	20.7	-	20.7	19.2	398
Desk Chair	IKEA	HARRY	201.058.31	450	490	960	White pine	5.456	-	-	-	-	-	5.5	-	5.5	19.2	105
Wood cribs	Lowes*	HT 591	28 pcs 2 in. x 2 in x 12 in.	305	305	305	White pine	4.584	4.472	4.408	4.604	-	-	4.5	0.1	18.1	19.2	347
Counter top	Home Depot	-	2 in. x 12 in. & 2 in. x 4 in.	660	2210	38	Douglas fir	29.002	29.836	-	-	-	-	29.4	0.6	58.8	21	1236
Counter top	Home Depot	-	2 in. x 12 in. & 2 in. x 4 in.	660	1210	38	Douglas fir	15.532	-	-	-	-	-	-	-	15.5	21	326
Wood cribs	Lowes*	-	6 pcs 2 in. x 4 in x 12 in. 6 pcs 2 in. x 4 in x 30 in.	762	305	152	White pine	10.268	11.125	10.220	10.972	10.678	10.508	10.6	0.4	63.8	19.2	1224
* Unspecified																**Without drywall paper**	**1149**	**-**	**22714**
																With drywall paper	**1163**		**22954**

Area	**41.86**	**m2**
Load density (w/o paper)	**543**	**MJ/m2**
Load density (w/ paper)	**548**	**MJ/m2**

Table C 5. Test 1-5 compartment content mass and fuel load calculation.

Item	Manufacturer / Supplier	Product name	Article / Model / Description	Dimensions, mm			Material	Mass, kg								Total mass, kg	Heat value, MJ/kg	Energy, MJ
				X	Y	Z		1	2	3	4	5	6	Mean	SD			
Gypsum paper	US Gypsum	FireCore Type X	-	9100	2700	0.25	Paper	-	-	-	-	-	-	-	-	4.7	17	80
				4600	2700	0.25	Paper	-	-	-	-	-	-	-	-	4.7	17	80
				9100	4600	0.25	Paper	-	-	-	-	-	-	-	-	8.0	17	136
																17	-	**296**
Flooring	trafficMASTER	-	38701	1290	194	7	Hardboard	1.478	1.484	1.492	1.500	1.500	1.484	1.5	0.0	241.1	19.9	4797
Console table	IKEA	HEMNES	502.821.39	390	1570	740	White pine	25.018	-	-	-	-	-	25.0	-	25.0	19.2	480
12" cabinets	Home Depot	Base	B120HD	610	305	876	White pine	18.638	18.530	18.560	17.452	18.736	-	18.4	0.5	91.9	19.2	1765
36" cabinets	Home Depot	Sink Base	B360HD	610	914	876	White pine	26.946	26.940	26.300	26.922	26.644	-	26.8	0.3	133.8	19.2	2568
Table	IKEA	GAMLEBY	602.470.27	2010	780	740	White pine	28.824	-	-	-	-	-	28.8	-	28.8	19.2	553
Chairs	IKEA	HARRY	201.058.31	450	490	960	White pine	5.338	5.178	5.282	5.250	5.042	5.403	5.2	0.1	31.5	19.2	605
Bookcases	IKEA	HEMNES	402.821.30	890	370	1970	White pine	28.232	27.956	-	-	-	-	28.1	0.2	56.2	19.2	1079
TV unit	IKEA	HEMNES	202.421.02	1480	465	570	White pine	30.612	-	-	-	-	-	30.6	-	30.6	19.2	588
8-Dresser dresser	IKEA	HEMNES	003.185.98	1600	500	950	White pine	54.136	-	-	-	-	-	54.1	-	54.1	19.2	1039
Armchair frame	IKEA	EKTORP	801.850.52	730	760	850	White pine	28.056	28.894	-	-	-	-	28.5	0.6	57.0	19.2	1093
Armchair cushions	IKEA	EKTORP	-	510	460	120	PU Foam	5.462	5.372	-	-	-	-	5.4	0.1	10.8	29	314
Sofa frame	IKEA	EKTROP	401.850.30	2180	860	900	White pine	43.976	-	-	-	-	-	44.0	-	44.0	19.2	844
Sofa cushions	IKEA	EKTROP	-	1670	700	120	PU Foam	14.178	-	-	-	-	-	14.2	-	14.2	29	411
Side table	IKEA	HEMNES	802.821.52	550	550	500	White pine	7.540	7.884	-	-	-	-	7.7	0.2	15.4	19.2	296
Coffee table	IKEA	KRAGSTA	802.622.53	1380	650	520	White pine	13.800	-	-	-	-	-	13.8	-	13.8	19.2	265
Night stands	IKEA	TARVA	502.196.09	480	390	620	White pine	9.182	9.460	-	-	-	-	9.3	0.2	18.6	19.2	358
Bed frame	IKEA	HEMNES	202.421.02	1470	2000	400	White pine	32.140	-	-	-	-	-	32.1	-	32.1	19.2	617
Bed drawers	IKEA	HEMNES	103.262.96	1470	2000	200	White pine	4.690	4.508	8.160	8.480	-	-	6.5	2.2	25.8	19.2	496
Bed frame slats	Home Depot	Whitewood	569062	1331	102	51	White pine	7.554	-	-	-	-	-	7.6	-	7.6	19.2	145
Mattress	IKEA	MOREDAL	802.773.82	1340	1870	170	PU Foam	17.228	-	-	-	-	-	17.2	-	17.2	29	500
Desk	IKEA	HEMNES	502.821.44	1550	650	740	White pine	38.090	-	-	-	-	-	38.1	-	38.1	19.2	731
Desk hutch	IKEA	HEMNES	202.821.26	1520	250	630	White pine	19.708	-	-	-	-	-	19.7	-	19.7	19.2	378
Desk Chair	IKEA	HARRY	201.058.31	450	490	960	White pine	5.240	-	-	-	-	-	5.2	-	5.2	19.2	101
Wood cribs	Lowes*	HT 591	28 pcs 2 in. x 2 in x 12 in.	305	305	305	White pine	4.566	4.420	4.508	4.422	-	-	4.5	0.1	17.9	19.2	344
Counter top	Home Depot	-	2 in. x 12 in. & 2 in. x 4 in.	660	2210	38	Douglas fir	24.480	26.754	-	-	-	-	25.6	1.6	51.2	21	1076
Counter top	Home Depot	-	2 in. x 12 in. & 2 in. x 4 in.	660	1210	38	Douglas fir	14.426	-	-	-	-	-	-	-	14.4	21	303
Wood cribs	Lowes*	-	6 pcs 2 in. x 4 in x 12 in. 6 pcs 2 in. x 4 in x 30 in.	762	305	152	White pine	11.004	10.222	10.454	10.240	10.994	10.964	10.6	0.4	63.9	19.2	1226
* Unspecified																**Without drywall paper**	**1160**	-	**22974**
																With drywall paper	**1177**		**23270**

Area	**41.86**	**m2**
Load density (w/o paper)	**549**	**MJ/m2**
Load density (w/ paper)	**556**	**MJ/m2**

Table C 6. Test 1-6 compartment content mass and fuel load calculation.

Item	Manufacturer / Supplier	Product name	Article / Model / Description	Dimensions, mm			Material	Mass, kg								Total mass, kg	Heat value, MJ/kg	Energy, MJ
				X	Y	Z		1	2	3	4	5	6	Mean	SD			
Gypsum paper	US Gypsum	FireCore Type X	-	9100	2700	0.25	Paper	-	-	-	-	-	-	-	-	4.7	17	80
				4600	2700	0.25	Paper	-	-	-	-	-	-	-	-	4.7	17	80
				9100	4600	0.25	Paper	-	-	-	-	-	-	-	-	0.0	17	0
																9	-	**160**
Flooring	trafficMASTER	-	38701	1290	194	7	Hardboard	1.478	1.484	1.492	1.500	1.500	1.484	1.5	0.0	241.1	19.9	4797
Console table	IKEA	HEMNES	502.821.39	390	1570	740	White pine	25.650	-	-	-	-	-	25.7	-	25.7	19.2	492
12" cabinets	Home Depot	Base	B120HD	610	305	876	White pine	18.582	18.434	18.550	18.652	18.550	-	18.6	0.1	92.8	19.2	1781
36" cabinets	Home Depot	Sink Base	B360HD	610	914	876	White pine	26.730	26.774	26.416	26.890	26.006	-	26.6	0.4	132.8	19.2	2550
Table	IKEA	GAMLEBY	602.470.27	2010	780	740	White pine	28.628	-	-	-	-	-	28.6	-	28.6	19.2	550
Chairs	IKEA	HARRY	201.058.31	450	490	960	White pine	5.264	5.454	5.434	5.380	5.432	5.518	5.4	0.1	32.5	19.2	624
Bookcases	IKEA	HEMNES	402.821.30	890	370	1970	White pine	28.322	28.078	-	-	-	-	28.2	0.2	56.4	19.2	1083
TV unit	IKEA	HEMNES	202.421.02	1480	465	570	White pine	31.048	-	-	-	-	-	31.0	-	31.0	19.2	596
8-Dresser dresser	IKEA	HEMNES	003.185.98	1600	500	950	White pine	53.924	-	-	-	-	-	53.9	-	53.9	19.2	1035
Armchair frame	IKEA	EKTORP	801.850.52	730	760	850	White pine	28.840	28.852	-	-	-	-	28.8	0.0	57.7	19.2	1108
Armchair cushions	IKEA	EKTORP	-	510	460	120	PU Foam	5.398	5.402	-	-	-	-	5.4	0.0	10.8	29	313
Sofa frame	IKEA	EKTROP	401.850.30	2180	860	900	White pine	43.532	-	-	-	-	-	43.5	-	43.5	19.2	836
Sofa cushions	IKEA	EKTROP	-	1670	700	120	PU Foam	14.313	-	-	-	-	-	14.3	-	14.3	29	415
Side table	IKEA	HEMNES	802.821.52	550	550	500	White pine	7.410		-	-	-	-	7.4	#DIV/0!	7.4	19.2	142
Coffee table	IKEA	KRAGSTA	802.622.53	1380	650	520	White pine	13.952	-	-	-	-	-	14.0	-	14.0	19.2	268
Night stands	IKEA	TARVA	502.196.09	480	390	620	White pine	9.328	9.328	-	-	-	-	9.3	0.0	18.7	19.2	358
Bed frame	IKEA	HEMNES	202.421.02	1470	2000	400	White pine	32.008	-	-	-	-	-	32.0	-	32.0	19.2	615
Bed drawers	IKEA	HEMNES	103.262.96	1470	2000	200	White pine	4.486	4.350	8.134	8.152	-	-	6.3	2.2	25.1	19.2	482
Bed frame slats	Home Depot	Whitewood	569062	1331	102	51	White pine	8.759	-	-	-	-	-	8.8	-	8.8	19.2	168
Mattress	IKEA	MOREDAL	802.773.82	1340	1870	170	PU Foam	18.310	-	-	-	-	-	18.3	-	18.3	29	531
Desk	IKEA	HEMNES	502.821.44	1550	650	740	White pine	36.808	-	-	-	-	-	36.8	-	36.8	19.2	707
Desk hutch	IKEA	HEMNES	202.821.26	1520	250	630	White pine	20.048	-	-	-	-	-	20.0	-	20.0	19.2	385
Desk Chair	IKEA	HARRY	201.058.31	450	490	960	White pine	5.106	-	-	-	-	-	5.1	-	5.1	19.2	98
Wood cribs	Lowes*	HT 591	28 pcs 2 in. x 2 in x 12 in.	305	305	305	White pine	4.286	4.394	4.960	5.640	-	-	4.8	0.6	19.3	19.2	370
Counter top	Home Depot	-	2 in. x 12 in. & 2 in. x 4 in.	660	2210	38	Douglas fir	28.404	25.176	-	-	-	-	26.8	2.3	53.6	21	1125
Counter top	Home Depot	-	2 in. x 12 in. & 2 in. x 4 in.	660	1210	38	Douglas fir	12.906	-	-	-	-	-	-	-	12.9	21	271
Wood cribs	Lowes*	-	6 pcs 2 in. x 4 in x 12 in. 6 pcs 2 in. x 4 in x 30 in.	762	305	152	White pine	10.220	10.108	9.260	9.938	10.422	10.192	10.0	0.4	60.1	19.2	1155
* Unspecified																**Without drywall paper**	**1153**	-	**22856**
																With drywall paper	**1163**		**23016**

Area	**41.86**	**m2**
Load density (w/o paper)	**546**	**MJ/m2**
Load density (w/ paper)	**550**	**MJ/m2**

Table C 7. Compartment movable fuel dimensions, position and assumed mass distribution used to determine energy distribution for Test 1-1.

Item	Dimensions, mm			Position, mm			Mass distribution, %								Total	Energy,
	X	Y	Z	XX	YY	ZZ	N	E	S	W	Top	Bot	Vert	Hor	mass, kg	MJ
Flooring	9100	4600	7	0	0	0	0	0	0	0	100	0	0	0	241.1	4797
Console table	390	1570	740	0	400	0	10	0	10	0	25	25	15	15	25.9	498
12" cabinets	305	876	610	202	2416	100	0	25	25	0	25	25	0	0	18.0	345
	610	305	876	50	3330	0	25	25	25	25	0	0	0	0	18.4	353
	305	610	876	660	3940	0	25	25	25	25	0	0	0	0	18.4	353
	610	305	876	1879	3330	0	25	25	25	25	0	0	0	0	18.4	354
	305	876	610	2031	2416	100	0	25	25	0	25	25	0	0	18.5	355
36" cabinets	610	914	876	50	2416	0	25	25	25	25	0	0	0	0	26.4	507
	610	914	876	50	3635	0	25	25	25	25	0	0	0	0	26.0	499
	914	610	876	964	3940	0	25	25	25	25	0	0	0	0	26.3	504
	610	914	876	1879	3635	0	25	25	25	25	0	0	0	0	26.2	504
	610	914	876	1879	2416	0	25	25	25	25	0	0	0	0	26.9	516
Table	2010	780	740	750	700	0	0	0	0	0	100	0	0	0	29.5	567
Chairs	450	490	960	935	380	0	50	0	0	0	0	0	0	50	5.1	97
	450	490	960	1500	380	0	50	0	0	0	0	0	0	50	4.9	95
	450	490	960	2065	380	0	50	0	0	0	0	0	0	50	5.2	100
	490	450	960	2570	865	0	0	0	0	50	0	0	0	50	5.3	101
	450	490	960	935	1310	0	0	0	50	0	0	0	0	50	5.4	103
	450	490	960	2065	1310	0	0	0	50	0	0	0	0	50	5.6	108
Bookcases	890	370	1970	2660	0	0	20	20	0	20	10	0	15	15	27.8	533
	890	370	1970	6410	4145	0	0	20	20	20	10	0	15	15	27.7	531
TV unit	1480	465	570	3550	150	0	13	13	13	13	13	13	13	13	30.7	589
8-Dresser dresser	1600	500	950	5030	150	0	13	13	13	13	13	13	13	13	54.3	1042
Armchair frame	730	760	850	2788	2150	0	20	40	20	0	0	0	0	20	18.3	352
	730	760	850	5298	2150	0	20	0	20	40	0	0	0	20	18.4	353
Armchair cushions	510	460	120	3008	2300	300	13	13	13	13	13	13	13	13	1.5	44
	510	460	120	5298	2300	300	13	13	13	13	13	13	13	13	1.6	45
Sofa frame	2180	860	900	3418	3640	0	13	13	13	13	13	13	13	13	43.7	839
Sofa cushions	1670	700	120	3673	3640	300	13	13	13	13	13	13	13	13	14.0	406
Side table	550	550	500	2868	3750	0	0	0	0	0	50	0	0	50	8.0	154
	550	550	500	5598	3750	0	0	0	0	0	50	0	0	50	8.4	161
Coffee table	1380	650	520	3718	2350	0	0	0	0	0	100	0	0	0	16.3	314
Night stands	480	390	620	6630	0	0	0	20	0	20	20	0	20	20	9.3	178
	480	390	620	8580	0	0	0	20	0	20	20	0	20	20	9.2	176
Bed frame	1470	2000	400	7110	0	0	25	25	25	25	0	0	0	0	32.1	616
Bed drawers	1470	2000	200	7110	0	0	15	15	15	15	0	40	0	0	24.4	469
Bed frame slats	1470	2000	38	7110	0	400	13	13	13	13	13	13	13	13	9.3	178
Mattress	1340	1870	170	7175	65	400	13	13	13	13	13	13	13	13	17.9	520
Desk	1550	650	740	7350	3950	0	13	13	13	13	13	13	13	13	36.5	700
Desk hutch	1520	250	630	7365	4350	740	13	13	13	13	13	13	13	13	20.9	401
Desk Chair	450	490	960	7900	3850	0	50	0	0	0	0	0	0	50	4.9	94
Wood cribs	305	305	305	0	500	160	13	13	13	13	13	13	13	13	4.5	86
	305	305	305	0	855	160	13	13	13	13	13	13	13	13	4.5	86
	305	305	305	0	1210	160	13	13	13	13	13	13	13	13	4.4	85
	305	305	305	0	1565	160	13	13	13	13	13	13	13	13	4.6	88
Counter top	660	2210	38	0	2390	876	13	13	13	13	13	13	13	13	32.4	681
	660	2210	38	1870	2390	876	13	13	13	13	13	13	13	13	30.6	642
Counter top	1210	660	38	660	3940	876	13	13	13	13	13	13	13	13	17.3	363
Wood cribs	762	305	152	2724	0	160	13	13	13	13	13	13	13	13	10.3	198
	762	305	152	2724	0	490	13	13	13	13	13	13	13	13	9.9	189
	762	305	152	2724	0	810	13	13	13	13	13	13	13	13	9.4	180
	762	305	152	6474	4145	160	13	13	13	13	13	13	13	13	10.2	196
	762	305	152	6474	4145	490	13	13	13	13	13	13	13	13	9.7	187
	762	305	152	6474	4145	810	13	13	13	13	13	13	13	13	9.8	189
														Without drywall paper	**1144**	**22622**

Appendix D - Hardware configuration

Table D 1. Hardware configuration for Test 1-1.

Wire	Legend/ID	Range/Type	Slope	Units	Notes
1	TC_Ceiling_Center_020	Thermocouple	1	°C	At the centre of the ceiling in panel 20 mm from interface
2	TC_Ceiling_Center_035	Thermocouple	1	°C	At the centre of the ceiling in panel 35 mm from interface
3	TC_Ceiling_Center_050	Thermocouple	1	°C	At the centre of the ceiling in panel 50 mm from interface
4	TC_Ceiling_Center_065	Thermocouple	1	°C	At the centre of the ceiling in panel 65 mm from interface
5	TC_Ceiling_Center_090	Thermocouple	1	°C	At the centre of the ceiling in panel 90 mm from interface
6	TC_Ceiling_Center_115	Thermocouple	1	°C	At the centre of the ceiling in panel 115 mm from interface
7	TC_Ceiling_Center_140	Thermocouple	1	°C	At the centre of the ceiling in panel 140 mm from interface
8	TC_W1_Middle_180_020	Thermocouple	1	°C	W1 at the mid length at h=1.8 m in panel 20 mm from interface
9	TC_W1_Middle_180_035	Thermocouple	1	°C	W1 at the mid length at h=1.8 m in panel 35 mm from interface
10	TC_W1_Middle_180_050	Thermocouple	1	°C	W1 at the mid length at h=1.8 m in panel 50 mm from interface
11	TC_W1_Middle_180_065	Thermocouple	1	°C	W1 at the mid length at h=1.8 m in panel 65 mm from interface
12	TC_W1_Middle_180_090	Thermocouple	1	°C	W1 at the mid length at h=1.8 m in panel 90 mm from interface
13	TC_W1_Middle_180_115	Thermocouple	1	°C	W1 at the mid length at h=1.8 m in panel 115 mm from interface
14	TC_W1_Middle_180_140	Thermocouple	1	°C	W1 at the mid length at h=1.8 m in panel 140 mm from interface
15	TC_W3_Middle_180_020	Thermocouple	1	°C	W3 at the mid length at h=1.8 m in panel 20 mm from interface
16	TC_W3_Middle_180_035	Thermocouple	1	°C	W3 at the mid length at h=1.8 m in panel 35 mm from interface
17	TC_W3_Middle_180_050	Thermocouple	1	°C	W3 at the mid length at h=1.8 m in panel 50 mm from interface
18	TC_W3_Middle_180_065	Thermocouple	1	°C	W3 at the mid length at h=1.8 m in panel 65 mm from interface
19	TC_W3_Middle_180_090	Thermocouple	1	°C	W3 at the mid length at h=1.8 m in panel 90 mm from interface
20	TC_W3_Middle_180_115	Thermocouple	1	°C	W3 at the mid length at h=1.8 m in panel 115 mm from interface
21	TC_W3_Middle_180_140	Thermocouple	1	°C	W3 at the mid length at h=1.8 m in panel 140 mm from interface
22	TC_W4_Middle_180_020	Thermocouple	1	°C	W4 at the mid length at h=1.8 m in panel 20 mm from interface
23	TC_W4_Middle_180_035	Thermocouple	1	°C	W4 at the mid length at h=1.8 m in panel 35 mm from interface
24	TC_W4_Middle_180_050	Thermocouple	1	°C	W4 at the mid length at h=1.8 m in panel 50 mm from interface
25	TC_W4_Middle_180_065	Thermocouple	1	°C	W4 at the mid length at h=1.8 m in panel 65 mm from interface
26	TC_W4_Middle_180_090	Thermocouple	1	°C	W4 at the mid length at h=1.8 m in panel 90 mm from interface
27	TC_W4_Middle_180_115	Thermocouple	1	°C	W4 at the mid length at h=1.8 m in panel 115 mm from interface
28	TC_W4_Middle_180_140	Thermocouple	1	°C	W4 at the mid length at h=1.8 m in panel 140 mm from interface
29	TC_Tree_Tr1_060	Thermocouple	1	°C	Tree Tr1 at h=0.6 m
30	TC_Tree_Tr1_160	Thermocouple	1	°C	Tree Tr1 at h=1.6 m
31	TC_Tree_Tr1_260	Thermocouple	1	°C	Tree Tr1 at h=2.6 m
32	TC_Tree_Tr2_060	Thermocouple	1	°C	Tree Tr2 at h=0.6 m
33	TC_Tree_Tr2_160	Thermocouple	1	°C	Tree Tr2 at h=1.6 m
34	TC_Tree_Tr2_260	Thermocouple	1	°C	Tree Tr2 at h=2.6 m
35	TC_Tree_Tr3_060	Thermocouple	1	°C	Tree Tr3 at h=0.6 m
36	TC_Tree_Tr3_160	Thermocouple	1	°C	Tree Tr3 at h=1.6 m
37	TC_Tree_Tr3_260	Thermocouple	1	°C	Tree Tr3 at h=2.6 m
38	TC_Tree_Tr4_060	Thermocouple	1	°C	Tree Tr4 at h=0.6 m
39	TC_Tree_Tr4_160	Thermocouple	1	°C	Tree Tr4 at h=1.6 m
40	TC_Tree_Tr4_260	Thermocouple	1	°C	Tree Tr4 at h=2.6 m
41	TC_Tree_Tr5_060	Thermocouple	1	°C	Tree Tr5 at h=0.6 m
42	TC_Tree_Tr5_160	Thermocouple	1	°C	Tree Tr5 at h=1.6 m
43	TC_Tree_Tr5_260	Thermocouple	1	°C	Tree Tr5 at h=2.6 m
44	TC_Tree_Tr6_060	Thermocouple	1	°C	Tree Tr6 at h=0.6 m
45	TC_Tree_Tr6_160	Thermocouple	1	°C	Tree Tr6 at h=1.6 m
46	TC_Tree_Tr6_260	Thermocouple	1	°C	Tree Tr6 at h=2.6 m
47	TC_W1_Middle_060_CLT	Thermocouple	1	°C	W1 at the mid length at h=0.6 m on the surface of CLT
48	TC_W1_Middle_120_CLT	Thermocouple	1	°C	W1 at the mid length at h=1.2 m on the surface of CLT
49	TC_W1_Middle_180_CLT	Thermocouple	1	°C	W1 at the mid length at h=1.8 m on the surface of CLT
50	TC_W1_Middle_060_1GB	Thermocouple	1	°C	W1 at the mid length at h=0.6 m on the surface of 1st GB
51	TC_W1_Middle_120_1GB	Thermocouple	1	°C	W1 at the mid length at h=1.2 m on the surface of 1st GB
52	TC_W1_Middle_180_1GB	Thermocouple	1	°C	W1 at the mid length at h=1.8 m on the surface of 1st GB
53	TC_W1_Middle_060_2GB	Thermocouple	1	°C	W1 at the mid length at h=0.6 m on the surface of 2nd GB
54	TC_W1_Middle_120_2GB	Thermocouple	1	°C	W1 at the mid length at h=1.2 m on the surface of 2nd GB
55	TC_W1_Middle_180_2GB	Thermocouple	1	°C	W1 at the mid length at h=1.8 m on the surface of 2nd GB
56	TC_W1_Front_180_CLT	Thermocouple	1	°C	W1 at the front at h=1.8 m on the surface of CLT
57	TC_W1_Front_180_1GB	Thermocouple	1	°C	W1 at the front at h=1.8 m on the surface of 1st GB
58	TC_W1_Front_180_2GB	Thermocouple	1	°C	W1 at the front at h=1.8 m on the surface of 2st GB
59	TC_W1_Rear_180_CLT	Thermocouple	1	°C	W1 at the rear at h=1.8 m on the surface of CLT
60	TC_W1_Rear_180_1GB	Thermocouple	1	°C	W1 at the rear at h=1.8 m on the surface of 1st GB
61	TC_W1_Rear_180_2GB	Thermocouple	1	°C	W1 at the rear at h=1.8 m on the surface of 2st GB
62	TC_W1_Front_060_CLT	Thermocouple	1	°C	W1 at the front at h=0.6 m on the surface of CLT
63	TC_W1_Front_060_1GB	Thermocouple	1	°C	W1 at the front at h=0.6 m on the surface of 1st GB
64	TC_W1_Front_060_2GB	Thermocouple	1	°C	W1 at the front at h=0.6 m on the surface of 2st GB
65	TC_W1_Rear_060_CLT	Thermocouple	1	°C	W1 at the rear at h=0.6 m on the surface of CLT
66	TC_W1_Rear_060_1GB	Thermocouple	1	°C	W1 at the rear at h=0.6 m on the surface of 1st GB
67	TC_W1_Rear_060_2GB	Thermocouple	1	°C	W1 at the rear at h=0.6 m on the surface of 2st GB
68	TC_W3_Middle_060_CLT	Thermocouple	1	°C	W3 on the surface of CLT
69	TC_W3_Middle_120_CLT	Thermocouple	1	°C	W3 on the surface of CLT
70	TC_W3_Middle_180_CLT	Thermocouple	1	°C	W3 on the surface of CLT
71	TC_W3_Middle_060_1GB	Thermocouple	1	°C	W3 on the surface of 1st GB
72	TC_W3_Middle_120_1GB	Thermocouple	1	°C	W3 on the surface of 1st GB

Wire	Legend/ID	Range/Type	Slope	Units	Notes
73	TC_W3_Middle_180_1GB	Thermocouple	1	°C	W3 on the surface of 1st GB
74	TC_W3_Middle_060_2GB	Thermocouple	1	°C	W3 on the surface of 2nd GB
75	TC_W3_Middle_120_2GB	Thermocouple	1	°C	W3 on the surface of 2nd GB
76	TC_W3_Middle_180_2GB	Thermocouple	1	°C	W3 on the surface of 2nd GB
77	TC_W4_Middle_060_CLT	Thermocouple	1	°C	W4 on the surface of CLT
78	TC_W4_Middle_120_CLT	Thermocouple	1	°C	W4 on the surface of CLT
79	TC_W4_Middle_180_CLT	Thermocouple	1	°C	W4 on the surface of CLT
80	TC_W4_Middle_060_1GB	Thermocouple	1	°C	W4 on the surface of 1st GB
81	TC_W4_Middle_120_1GB	Thermocouple	1	°C	W4 on the surface of 1st GB
82	TC_W4_Middle_180_1GB	Thermocouple	1	°C	W4 on the surface of 1st GB
83	TC_W4_Middle_060_2GB	Thermocouple	1	°C	W4 on the surface of 2nd GB
84	TC_W4_Middle_120_2GB	Thermocouple	1	°C	W4 on the surface of 2nd GB
85	TC_W4_Middle_180_2GB	Thermocouple	1	°C	W4 on the surface of 2nd GB
86	TC_Ceiling_Tr1_CLT	Thermocouple	1	°C	ceiling above Tr1 on the surface of CLT
87	TC_Ceiling_Tr1_1GB	Thermocouple	1	°C	ceiling above Tr1 on the surface of 1st GB
88	TC_Ceiling_Tr1_2GB	Thermocouple	1	°C	ceiling above Tr1 on the surface of 2nd GB
89	TC_Ceiling_Tr2_CLT	Thermocouple	1	°C	ceiling above Tr2 on the surface of CLT
90	TC_Ceiling_Tr2_1GB	Thermocouple	1	°C	ceiling above Tr2 on the surface of 1st GB
91	TC_Ceiling_Tr2_2GB	Thermocouple	1	°C	ceiling above Tr2 on the surface of 2nd GB
92	TC_Ceiling_Tr3_CLT	Thermocouple	1	°C	Ceiling above Tr3 on the surface of CLT
93	TC_Ceiling_Tr3_1GB	Thermocouple	1	°C	Ceiling above Tr3 on the surface of 1st GB
94	TC_Ceiling_Tr3_2GB	Thermocouple	1	°C	Ceiling above Tr3 on the surface of 2nd GB
95	TC_Ceiling_Tr4_CLT	Thermocouple	1	°C	Ceiling above Tr4 on the surface of CLT
96	TC_Ceiling_Tr4_1GB	Thermocouple	1	°C	Ceiling above Tr4 on the surface of 1st GB
97	TC_Ceiling_Tr4_2GB	Thermocouple	1	°C	Ceiling above Tr4 on the surface of 2nd GB
98	TC_Ceiling_Center_CLT	Thermocouple	1	°C	Ceiling at the centre on the surface of CLT
99	TC_Ceiling_Center_1GB	Thermocouple	1	°C	Ceiling at the centre on the surface of 1st GB
100	TC_Ceiling_Center_2GB	Thermocouple	1	°C	Ceiling at the centre on the surface of 2nd GB
101	Gardon_Floor_Center	±0.2V default	17620	kW/m2	At the center of the floor
102	Gardon_W1_Middle_180	±0.2V default	19380	kW/m2	W1 at the mid length at h=1.8 m
103	PT_W1_Middle_180_SPy	Thermocouple	1	°C	Temperature for plate thermometer on W1 at the mid length at h=1.8 m
104	DFT_W1_Middle_180_Px	Thermocouple	1	°C	DFT on W1 at the mid length at h=1.8 m (Front plate)
105	PT_W1_Middle_180_SPx	Thermocouple	1	°C	W1 at the mid length at h=1.8 m (SP model 5928060-001)
106	PT_W1_Front_180_SPy	Thermocouple	1	°C	Temperature for plate thermometer on W1 at front
107	DFT_W3_Middle_180_Px	Thermocouple	1	°C	DFT on W3 at the mid length at h=1.8 m (Back plate)
108	PT_W1_Front_180_SPx	Thermocouple	1	°C	W1 in the front of the compartment at h=1.8 m
109	PT_W1_Rear_180_SPy	Thermocouple	1	°C	Temperature for plate thermometer on W1 in the rear of the compartment at h=1.8 m
110	DFT_W4_Middle_180_Px	Thermocouple	1	°C	DFT on W4 at the mid length at h=1.8 m (Front plate)
111	PT_W1_Rear_180_SPx	Thermocouple	1	°C	W1 in the rear of the compartment at h=1.8 m
112	PT_Ceiling_Center_SPy	Thermocouple	1	°C	Temperature for plate thermometer
113	DFT_Ceiling_Center_Px	Thermocouple	1	°C	DFT at the centre of the ceiling (Back plate)
114	PT_Ceiling_Center_SPx	Thermocouple	1	°C	At the centre of the ceiling
115	PT_Ceiling_Bed_SPy	Thermocouple	1	°C	Temperature for plate thermometer on ceiling above the bed
116	DFT_Ceiling_Bed_Px	Thermocouple	1	°C	DFT on the ceiling above the bed (Back plate)
117	PT_Ceiling_Bed_SPx	Thermocouple	1	°C	on the ceiling above the bed
118	dP_c	±10V default	400	Pa	5/8" diameter bidirectional probe on ceiling near STE 6, Direction normal to the opening
120	dP_r	±10V default	400	Pa	On smoke sample line near gas analyzer sample line at 2.1m 1/4" SS tube
121	STE_1	Thermocouple	1	°C	12" below ceiling (see "Drawings")
122	STE_2	Thermocouple	1	°C	12" below ceiling (see "Drawings")
123	STE_3	Thermocouple	1	°C	12" below ceiling (see "Drawings")
124	STE_4	Thermocouple	1	°C	18" below ceiling (see "Drawings")
125	STE_5	Thermocouple	1	°C	12" below ceiling (see "Drawings")
126	STE_6	Thermocouple	1	°C	12" below ceiling (see "Drawings")
127	STE_7	Thermocouple	1	°C	12" below ceiling (see "Drawings")
128	STE_8	Thermocouple	1	°C	18" below ceiling (see "Drawings")
129	STE_9	Thermocouple	1	°C	12" below ceiling (see "Drawings")
130	STE_10	Thermocouple	1	°C	12" below ceiling (see "Drawings")
131	TC_V_c	Thermocouple	1	°C	Temperature co-located with V_c
132	SmokeAlarm	±10V default	1	V	Smoke detector at the centre of the ceiling
133	HeatAlarm	±10V default	1	V	Heat detector at the centre of the ceiling
134	O2_room	±10V default	4.275504	%	At the centre of the room, 2.1 m high
135	CO2_room	±10V default	3.823816	%	At the centre of the room, 2.1 m high
136	CO_room	±10V default	4.412315	%	At the centre of the room, 2.1 m high
137	SMOKE	±10V default	1	V	at the centre of the room, 1.6 m high
138	Door_TC_1	Thermocouple	1	°C	At the centreline of the opening
139	Door_TC_2	Thermocouple	1	°C	At the centreline of the opening
140	Door_TC_3	Thermocouple	1	°C	At the centreline of the opening
141	Door_TC_4	Thermocouple	1	°C	At the centreline of the opening
142	Door_TC_5	Thermocouple	1	°C	At the centreline of the opening
143	Door_TC_6	Thermocouple	1	°C	At the centreline of the opening
144	Door_TC_7	Thermocouple	1	°C	At the centreline of the opening
145	dP_o1	±10V default	400	Pa	5/8" diameter bidirectional probe at the opening (low, long side)
146	dP_o2	±10V default	400	Pa	5/8" diameter bidirectional probe at the opening (low, middle)
147	dP_o3	±10V default	400	Pa	5/8" diameter bidirectional probe at the opening (low, short side)
148	dP_o4	±10V default	400	Pa	5/8" diameter bidirectional probe at the opening (high, long side)
149	dP_o5	±10V default	400	Pa	5/8" diameter bidirectional probe at the opening (high, middle)
150	dP_o6	±10V default	400	Pa	5/8" diameter bidirectional probe at the opening (high, short side)

Wire	Legend/ID	Range/Type	Slope	Units	Notes
151	Gardon_Front_a480	±0.2V default	19460	kW/m2	facing the centre of the opening
152	Gardon_Front_a240	±0.2V default	20980	kW/m2	facing the centre of the opening
153	Gardon_Front_e350	±0.2V default	20260	kW/m2	3.5 m above ground
154	Gardon_Front_e550	±0.2V default	18820	kW/m2	5.5 m above ground
155	Roof_TC_350	Thermocouple	1	°C	3.5 m above ground
156	Roof_TC_450	Thermocouple	1	°C	4.5 m above ground
157	Roof_TC_550	Thermocouple	1	°C	5.5 m above ground
158	Roof_TC_650	Thermocouple	1	°C	6.5 m above ground
159	Roof_TC_750	Thermocouple	1	°C	7.5 m above ground
161	DFT_W1_Middle_180_Py	Thermocouple	1	°C	DFT on W1 at the mid length at h=1.8 m
162	DFT_W3_Middle_180_Py	Thermocouple	1	°C	DFT on W3 at the mid length at h=1.8 m (Front plate)
163	DFT_W4_Middle_180_Py	Thermocouple	1	°C	DFT on W4 at the mid length at h=1.8 m (Back plate)
164	DFT_Ceiling_Center_Py	Thermocouple	1	°C	DFT at the centre of the ceiling (Front plate)
165	DFT_Ceiling_Bed_Py	Thermocouple	1	°C	DFT on the ceiling above the bed (Front plate)
166	DEWpt_rack	±10V default	30.1205	°C	Gas rack dew point measurement
167	TC_Tree_Tr1_110	Thermocouple	1	°C	Tree Tr1 at h=1.1 m
168	TC_Tree_Tr1_210	Thermocouple	1	°C	Tree Tr1 at h=2.1 m
169	TC_Tree_Tr2_110	Thermocouple	1	°C	Tree Tr2 at h=1.1 m
170	TC_Tree_Tr2_210	Thermocouple	1	°C	Tree Tr2 at h=2.1 m
171	TC_Tree_Tr3_110	Thermocouple	1	°C	Tree Tr3 at h=1.1 m
172	TC_Tree_Tr3_210	Thermocouple	1	°C	Tree Tr3 at h=2.1 m
173	TC_Tree_Tr4_110	Thermocouple	1	°C	Tree Tr4 at h=1.1 m
174	TC_Tree_Tr4_210	Thermocouple	1	°C	Tree Tr4 at h=2.1 m
175	TC_Tree_Tr5_110	Thermocouple	1	°C	Tree Tr5 at h=1.1 m
176	TC_Tree_Tr5_210	Thermocouple	1	°C	Tree Tr5 at h=2.1 m
177	TC_Tree_Tr6_110	Thermocouple	1	°C	Tree Tr6 at h=1.1 m
178	TC_Tree_Tr6_210	Thermocouple	1	°C	Tree Tr6 at h=2.1 m
179	PT_Front_a480_SPy	Thermocouple	1	°C	Facing the centre of the opening (offset 150 from centerline)
180	PT_Front_a480_SPx	Thermocouple	1	°C	Facing the centre of the opening (offset 150 from centerline)
181	PT_Front_a240_SPy	Thermocouple	1	°C	Facing the centre of the opening (offset 150 from centerline)
182	PT_Front_a240_SPx	Thermocouple	1	°C	Facing the centre of the opening (offset 150 from centerline)
183	PT_Front_e350_SPx	Thermocouple	1	°C	3.5 m above ground
184	PT_Front_e550_SPx	Thermocouple	1	°C	5.5 m above the top of the opening
185	TC_Smoke	Thermocouple	1	°C	Gas temperature at SMOKE2 outflow (for shutoff)
186	TC_HFGtower	Thermocouple	1	°C	H2O outflow temperatures of heat flux gages on roof tower
187	TC_HFGfloor	Thermocouple	1	°C	H2O outflow temperatures of heat flux gages on floor
188	TC_HFGw1	Thermocouple	1	°C	H2O outflow temperatures of heat flux gages on W1
189	TC_GoPro	Thermocouple	1	°C	H2O outflow temperatures of GoPro water bath
190	TC_TreeSteel	Thermocouple	1	°C	Temperature of steel behind thermal insulation in Tree 03 at 2.1 m height
191	TC_TBD	Thermocouple	1	°C	Extra TC location TBD
	VI	±10V default	1	V	Internal heartbeat
	HRR	N/A	1	kW	Calculated channel
	HRRburner	N/A	1	kW	Calculated channel
	VelCeiling	N/A	-	m/s	Calculated channel
	VelDoor1	N/A	-	m/s	Calculated channel
	VelDoor2	N/A	-	m/s	Calculated channel
	VelDoor3	N/A	-	m/s	Calculated channel
	VelDoor4	N/A	-	m/s	Calculated channel
	VelDoor5	N/A	-	m/s	Calculated channel
	VelDoor6	N/A	-	m/s	Calculated channel

Table D 2. Hardware configuration for Test 1-2.

Wire	Legend/ID	Range/Type	Slope	Units	Notes
1	TC_Ceiling_Center_020	Thermocouple	1	°C	At the centre of the ceiling in panel 20 mm from interface
2	TC_Ceiling_Center_035	Thermocouple	1	°C	At the centre of the ceiling in panel 35 mm from interface
3	TC_Ceiling_Center_050	Thermocouple	1	°C	At the centre of the ceiling in panel 50 mm from interface
4	TC_Ceiling_Center_065	Thermocouple	1	°C	At the centre of the ceiling in panel 65 mm from interface
5	TC_Ceiling_Center_090	Thermocouple	1	°C	At the centre of the ceiling in panel 90 mm from interface
6	TC_Ceiling_Center_115	Thermocouple	1	°C	At the centre of the ceiling in panel 115 mm from interface
7	TC_Ceiling_Center_140	Thermocouple	1	°C	At the centre of the ceiling in panel 140 mm from interface
8	TC_W1_Middle_180_020	Thermocouple	1	°C	W1 at the mid length at h=1.8 m in panel 20 mm from interface
9	TC_W1_Middle_180_035	Thermocouple	1	°C	W1 at the mid length at h=1.8 m in panel 35 mm from interface
10	TC_W1_Middle_180_050	Thermocouple	1	°C	W1 at the mid length at h=1.8 m in panel 50 mm from interface
11	TC_W1_Middle_180_065	Thermocouple	1	°C	W1 at the mid length at h=1.8 m in panel 65 mm from interface
12	TC_W1_Middle_180_090	Thermocouple	1	°C	W1 at the mid length at h=1.8 m in panel 90 mm from interface
13	TC_W1_Middle_180_115	Thermocouple	1	°C	W1 at the mid length at h=1.8 m in panel 115 mm from interface
14	TC_W1_Middle_180_140	Thermocouple	1	°C	W1 at the mid length at h=1.8 m in panel 140 mm from interface
15	TC_W3_Middle_180_020	Thermocouple	1	°C	W3 at the mid length at h=1.8 m in panel 20 mm from interface
16	TC_W3_Middle_180_035	Thermocouple	1	°C	W3 at the mid length at h=1.8 m in panel 35 mm from interface
17	TC_W3_Middle_180_050	Thermocouple	1	°C	W3 at the mid length at h=1.8 m in panel 50 mm from interface
18	TC_W3_Middle_180_065	Thermocouple	1	°C	W3 at the mid length at h=1.8 m in panel 65 mm from interface
19	TC_W3_Middle_180_090	Thermocouple	1	°C	W3 at the mid length at h=1.8 m in panel 90 mm from interface
20	TC_W3_Middle_180_115	Thermocouple	1	°C	W3 at the mid length at h=1.8 m in panel 115 mm from interface
21	TC_W3_Middle_180_140	Thermocouple	1	°C	W3 at the mid length at h=1.8 m in panel 140 mm from interface

Wire	Legend/ID	Range/Type	Slope	Units	Notes
22	TC_W4_Middle_180_020	Thermocouple	1	°C	W4 at the mid length at h=1.8 m in panel 20 mm from interface
23	TC_W4_Middle_180_035	Thermocouple	1	°C	W4 at the mid length at h=1.8 m in panel 35 mm from interface
24	TC_W4_Middle_180_050	Thermocouple	1	°C	W4 at the mid length at h=1.8 m in panel 50 mm from interface
25	TC_W4_Middle_180_065	Thermocouple	1	°C	W4 at the mid length at h=1.8 m in panel 65 mm from interface
26	TC_W4_Middle_180_090	Thermocouple	1	°C	W4 at the mid length at h=1.8 m in panel 90 mm from interface
27	TC_W4_Middle_180_115	Thermocouple	1	°C	W4 at the mid length at h=1.8 m in panel 115 mm from interface
28	TC_W4_Middle_180_140	Thermocouple	1	°C	W4 at the mid length at h=1.8 m in panel 140 mm from interface
29	TC_Tree_Tr1_060	Thermocouple	1	°C	Tree Tr1 at h=0.6 m
30	TC_Tree_Tr1_160	Thermocouple	1	°C	Tree Tr1 at h=1.6 m
31	TC_Tree_Tr1_260	Thermocouple	1	°C	Tree Tr1 at h=2.6 m
32	TC_Tree_Tr2_060	Thermocouple	1	°C	Tree Tr2 at h=0.6 m
33	TC_Tree_Tr2_160	Thermocouple	1	°C	Tree Tr2 at h=1.6 m
34	TC_Tree_Tr2_260	Thermocouple	1	°C	Tree Tr2 at h=2.6 m
35	TC_Tree_Tr3_060	Thermocouple	1	°C	Tree Tr3 at h=0.6 m
36	TC_Tree_Tr3_160	Thermocouple	1	°C	Tree Tr3 at h=1.6 m
37	TC_Tree_Tr3_260	Thermocouple	1	°C	Tree Tr3 at h=2.6 m
38	TC_Tree_Tr4_060	Thermocouple	1	°C	Tree Tr4 at h=0.6 m
39	TC_Tree_Tr4_160	Thermocouple	1	°C	Tree Tr4 at h=1.6 m
40	TC_Tree_Tr4_260	Thermocouple	1	°C	Tree Tr4 at h=2.6 m
41	TC_Tree_Tr5_060	Thermocouple	1	°C	Tree Tr5 at h=0.6 m
42	TC_Tree_Tr5_160	Thermocouple	1	°C	Tree Tr5 at h=1.6 m
43	TC_Tree_Tr5_260	Thermocouple	1	°C	Tree Tr5 at h=2.6 m
44	TC_Tree_Tr6_060	Thermocouple	1	°C	Tree Tr6 at h=0.6 m
45	TC_Tree_Tr6_160	Thermocouple	1	°C	Tree Tr6 at h=1.6 m
46	TC_Tree_Tr6_260	Thermocouple	1	°C	Tree Tr6 at h=2.6 m
47	TC_W1_Middle_060_CLT	Thermocouple	1	°C	W1 at the mid length at h=0.6 m on the surface of CLT
48	TC_W1_Middle_120_CLT	Thermocouple	1	°C	W1 at the mid length at h=1.2 m on the surface of CLT
49	TC_W1_Middle_180_CLT	Thermocouple	1	°C	W1 at the mid length at h=1.8 m on the surface of CLT
50	TC_W1_Middle_060_1GB	Thermocouple	1	°C	W1 at the mid length at h=0.6 m on the surface of 1st GB
51	TC_W1_Middle_120_1GB	Thermocouple	1	°C	W1 at the mid length at h=1.2 m on the surface of 1st GB
52	TC_W1_Middle_180_1GB	Thermocouple	1	°C	W1 at the mid length at h=1.8 m on the surface of 1st GB
53	TC_W1_Middle_060_2GB	Thermocouple	1	°C	W1 at the mid length at h=0.6 m on the surface of 2nd GB
54	TC_W1_Middle_120_2GB	Thermocouple	1	°C	W1 at the mid length at h=1.2 m on the surface of 2nd GB
55	TC_W1_Middle_180_2GB	Thermocouple	1	°C	W1 at the mid length at h=1.8 m on the surface of 2nd GB
56	TC_W1_Front_180_CLT	Thermocouple	1	°C	W1 at the front at h=1.8 m on the surface of CLT
57	TC_W1_Front_180_1GB	Thermocouple	1	°C	W1 at the front at h=1.8 m on the surface of 1st GB
58	TC_W1_Front_180_2GB	Thermocouple	1	°C	W1 at the front at h=1.8 m on the surface of 2st GB
59	TC_W1_Rear_180_CLT	Thermocouple	1	°C	W1 at the rear at h=1.8 m on the surface of CLT
60	TC_W1_Rear_180_1GB	Thermocouple	1	°C	W1 at the rear at h=1.8 m on the surface of 1st GB
61	TC_W1_Rear_180_2GB	Thermocouple	1	°C	W1 at the rear at h=1.8 m on the surface of 2st GB
62	TC_W1_Front_060_CLT	Thermocouple	1	°C	W1 at the front at h=0.6 m on the surface of CLT
63	TC_W1_Front_060_1GB	Thermocouple	1	°C	W1 at the front at h=0.6 m on the surface of 1st GB
64	TC_W1_Front_060_2GB	Thermocouple	1	°C	W1 at the front at h=0.6 m on the surface of 2st GB
65	TC_W1_Rear_060_CLT	Thermocouple	1	°C	W1 at the rear at h=0.6 m on the surface of CLT
66	TC_W1_Rear_060_1GB	Thermocouple	1	°C	W1 at the rear at h=0.6 m on the surface of 1st GB
67	TC_W1_Rear_060_2GB	Thermocouple	1	°C	W1 at the rear at h=0.6 m on the surface of 2st GB
68	TC_W3_Middle_060_CLT	Thermocouple	1	°C	W3 on the surface of CLT
69	TC_W3_Middle_120_CLT	Thermocouple	1	°C	W3 on the surface of CLT
70	TC_W3_Middle_180_CLT	Thermocouple	1	°C	W3 on the surface of CLT
71	TC_W3_Middle_060_1GB	Thermocouple	1	°C	W3 on the surface of 1st GB
72	TC_W3_Middle_120_1GB	Thermocouple	1	°C	W3 on the surface of 1st GB
73	TC_W3_Middle_180_1GB	Thermocouple	1	°C	W3 on the surface of 1st GB
74	TC_W3_Middle_060_2GB	Thermocouple	1	°C	W3 on the surface of 2nd GB
75	TC_W3_Middle_120_2GB	Thermocouple	1	°C	W3 on the surface of 2nd GB
76	TC_W3_Middle_180_2GB	Thermocouple	1	°C	W3 on the surface of 2nd GB
77	TC_W4_Middle_060_CLT	Thermocouple	1	°C	W4 on the surface of CLT
78	TC_W4_Middle_120_CLT	Thermocouple	1	°C	W4 on the surface of CLT
79	TC_W4_Middle_180_CLT	Thermocouple	1	°C	W4 on the surface of CLT
80	TC_W4_Middle_060_1GB	Thermocouple	1	°C	W4 on the surface of 1st GB
81	TC_W4_Middle_120_1GB	Thermocouple	1	°C	W4 on the surface of 1st GB
82	TC_W4_Middle_180_1GB	Thermocouple	1	°C	W4 on the surface of 1st GB
83	TC_W4_Middle_060_2GB	Thermocouple	1	°C	W4 on the surface of 2nd GB
84	TC_W4_Middle_120_2GB	Thermocouple	1	°C	W4 on the surface of 2nd GB
85	TC_W4_Middle_180_2GB	Thermocouple	1	°C	W4 on the surface of 2nd GB
86	TC_Ceiling_Tr1_CLT	Thermocouple	1	°C	ceiling above Tr1 on the surface of CLT
87	TC_Ceiling_Tr1_1GB	Thermocouple	1	°C	ceiling above Tr1 on the surface of 1st GB
88	TC_Ceiling_Tr1_2GB	Thermocouple	1	°C	ceiling above Tr1 on the surface of 2nd GB
89	TC_Ceiling_Tr2_CLT	Thermocouple	1	°C	ceiling above Tr2 on the surface of CLT
90	TC_Ceiling_Tr2_1GB	Thermocouple	1	°C	ceiling above Tr2 on the surface of 1st GB
91	TC_Ceiling_Tr2_2GB	Thermocouple	1	°C	ceiling above Tr2 on the surface of 2nd GB
92	TC_Ceiling_Tr3_CLT	Thermocouple	1	°C	Ceiling above Tr3 on the surface of CLT
93	TC_Ceiling_Tr3_1GB	Thermocouple	1	°C	Ceiling above Tr3 on the surface of 1st GB
94	TC_Ceiling_Tr3_2GB	Thermocouple	1	°C	Ceiling above Tr3 on the surface of 2nd GB
95	TC_Ceiling_Tr4_CLT	Thermocouple	1	°C	Ceiling above Tr4 on the surface of CLT
96	TC_Ceiling_Tr4_1GB	Thermocouple	1	°C	Ceiling above Tr4 on the surface of 1st GB
97	TC_Ceiling_Tr4_2GB	Thermocouple	1	°C	Ceiling above Tr4 on the surface of 2nd GB
98	TC_Ceiling_Center_CLT	Thermocouple	1	°C	Ceiling at the centre on the surface of CLT

Wire	Legend/ID	Range/Type	Slope	Units	Notes
99	TC_Ceiling_Center_1GB	Thermocouple	1	°C	Ceiling at the centre on the surface of 1st GB
100	TC_Ceiling_Center_2GB	Thermocouple	1	°C	Ceiling at the centre on the surface of 2nd GB
101	Gardon_Floor_Center	±0.2V default	19870	kW/m2	At the center of the floor
102	Gardon_W1_Middle_180	±0.2V default	19260	kW/m2	W1 at the mid length at h=1.8 m
103	PT_W1_Middle_180_SPy	Thermocouple	1	°C	Temperature for plate thermometer on W1 at the mid length at h=1.8 m
104	DFT_W1_Middle_180_Px	Thermocouple	1	°C	DFT on W1 at the mid length at h=1.8 m (Front plate)
105	PT_W1_Middle_180_SPx	Thermocouple	1	°C	W1 at the mid length at h=1.8 m (SP model 5928060-001)
106	PT_W1_Front_180_SPy	Thermocouple	1	°C	Temperature for plate thermometer on W1 at front
107	DFT_W3_Middle_180_Px	Thermocouple	1	°C	DFT on W3 at the mid length at h=1.8 m (Back plate)
108	PT_W1_Front_180_SPx	Thermocouple	1	°C	W1 in the front of the compartment at h=1.8 m
109	PT_W1_Rear_180_SPy	Thermocouple	1	°C	Temperature for plate thermometer on W1 in the rear of the compartment at h=1.8 m
110	DFT_W4_Middle_180_Px	Thermocouple	1	°C	DFT on W4 at the mid length at h=1.8 m (Front plate)
111	PT_W1_Rear_180_SPx	Thermocouple	1	°C	W1 in the rear of the compartment at h=1.8 m
112	PT_Ceiling_Center_SPy	Thermocouple	1	°C	Temperature for plate thermometer
113	DFT_Ceiling_Center_Px	Thermocouple	1	°C	DFT at the centre of the ceiling (Back plate)
114	PT_Ceiling_Center_SPx	Thermocouple	1	°C	At the centre of the ceiling
115	PT_Ceiling_Bed_SPy	Thermocouple	1	°C	Temperature for plate thermometer on ceiling above the bed
116	DFT_Ceiling_Bed_Px	Thermocouple	1	°C	DFT on the ceiling above the bed (Back plate)
117	PT_Ceiling_Bed_SPx	Thermocouple	1	°C	on the ceiling above the bed
118	dP_c	±10V default	400	Pa	5/8" diameter bidirectional probe on ceiling near STE 6, Direction normal to the opening
120	dP_r	±10V default	400	Pa	On smoke sample line near gas analyzer sample line at 2.1m 1/4" SS tube
121	STE_1	Thermocouple	1	°C	12" below ceiling (see "Drawings")
122	STE_2	Thermocouple	1	°C	12" below ceiling (see "Drawings")
123	STE_3	Thermocouple	1	°C	12" below ceiling (see "Drawings")
124	STE_4	Thermocouple	1	°C	18" below ceiling (see "Drawings")
125	STE_5	Thermocouple	1	°C	12" below ceiling (see "Drawings")
126	STE_6	Thermocouple	1	°C	12" below ceiling (see "Drawings")
127	STE_7	Thermocouple	1	°C	12" below ceiling (see "Drawings")
128	STE_8	Thermocouple	1	°C	18" below ceiling (see "Drawings")
129	STE_9	Thermocouple	1	°C	12" below ceiling (see "Drawings")
130	STE_10	Thermocouple	1	°C	12" below ceiling (see "Drawings")
131	TC_V_c	Thermocouple	1	°C	Temperature co-located with V_c
132	SmokeAlarm	±10V default	1	V	Smoke detector at the centre of the ceiling
133	HeatAlarm	±10V default	1	V	Heat detector at the centre of the ceiling
134	O2_room	±10V default	4.275504	%	At the centre of the room, 2.1 m high
135	CO2_room	±10V default	3.823816	%	At the centre of the room, 2.1 m high
136	CO_room	±10V default	4.412315	%	At the centre of the room, 2.1 m high
137	SMOKE	±10V default	1	V	at the centre of the room, 1.6 m high
138	Door_TC_1	Thermocouple	1	°C	At the centreline of the opening
139	Door_TC_2	Thermocouple	1	°C	At the centreline of the opening
140	Door_TC_3	Thermocouple	1	°C	At the centreline of the opening
141	Door_TC_4	Thermocouple	1	°C	At the centreline of the opening
142	Door_TC_5	Thermocouple	1	°C	At the centreline of the opening
143	Door_TC_6	Thermocouple	1	°C	At the centreline of the opening
144	Door_TC_7	Thermocouple	1	°C	At the centreline of the opening
145	dP_o1	±10V default	400	Pa	5/8" diameter bidirectional probe at the opening (low, long side)
146	dP_o2	±10V default	400	Pa	5/8" diameter bidirectional probe at the opening (low, middle)
147	dP_o3	±10V default	400	Pa	5/8" diameter bidirectional probe at the opening (low, short side)
148	dP_o4	±10V default	400	Pa	5/8" diameter bidirectional probe at the opening (high, long side)
149	dP_o5	±10V default	400	Pa	5/8" diameter bidirectional probe at the opening (high, middle)
150	dP_o6	±10V default	400	Pa	5/8" diameter bidirectional probe at the opening (high, short side)
151	Gardon_Front_a480	±0.2V default	19460	kW/m2	facing the centre of the opening
152	Gardon_Front_a240	±0.2V default	20980	kW/m2	facing the centre of the opening
153	Gardon_Front_e350	±0.2V default	20260	kW/m2	3.5 m above ground
154	Gardon_Front_e550	±0.2V default	18820	kW/m2	5.5 m above ground
155	Roof_TC_350	Thermocouple	1	°C	3.5 m above ground
156	Roof_TC_450	Thermocouple	1	°C	4.5 m above ground
157	Roof_TC_550	Thermocouple	1	°C	5.5 m above ground
158	Roof_TC_650	Thermocouple	1	°C	6.5 m above ground
159	Roof_TC_750	Thermocouple	1	°C	7.5 m above ground
161	DFT_W1_Middle_180_Py	Thermocouple	1	°C	DFT on W1 at the mid length at h=1.8 m
162	DFT_W3_Middle_180_Py	Thermocouple	1	°C	DFT on W3 at the mid length at h=1.8 m (Front plate)
163	DFT_W4_Middle_180_Py	Thermocouple	1	°C	DFT on W4 at the mid length at h=1.8 m (Back plate)
164	DFT_Ceiling_Center_Py	Thermocouple	1	°C	DFT at the centre of the ceiling (Front plate)
165	DFT_Ceiling_Bed_Py	Thermocouple	1	°C	DFT on the ceiling above the bed (Front plate)
166	DEWpt_rack	±10V default	30.1205	°C	Gas rack dew point measurement
167	TC_Tree_Tr1_110	Thermocouple	1	°C	Tree Tr1 at h=1.1 m
168	TC_Tree_Tr1_210	Thermocouple	1	°C	Tree Tr1 at h=2.1 m
169	TC_Tree_Tr2_110	Thermocouple	1	°C	Tree Tr2 at h=1.1 m
170	TC_Tree_Tr2_210	Thermocouple	1	°C	Tree Tr2 at h=2.1 m
171	TC_Tree_Tr3_110	Thermocouple	1	°C	Tree Tr3 at h=1.1 m
172	TC_Tree_Tr3_210	Thermocouple	1	°C	Tree Tr3 at h=2.1 m
173	TC_Tree_Tr4_110	Thermocouple	1	°C	Tree Tr4 at h=1.1 m
174	TC_Tree_Tr4_210	Thermocouple	1	°C	Tree Tr4 at h=2.1 m
175	TC_Tree_Tr5_110	Thermocouple	1	°C	Tree Tr5 at h=1.1 m
176	TC_Tree_Tr5_210	Thermocouple	1	°C	Tree Tr5 at h=2.1 m
177	TC_Tree_Tr6_110	Thermocouple	1	°C	Tree Tr6 at h=1.1 m

Wire	Legend/ID	Range/Type	Slope	Units	Notes
178	TC_Tree_Tr6_210	Thermocouple	1	°C	Tree Tr6 at h=2.1 m
179	PT_Front_a480_SPy	Thermocouple	1	°C	Facing the centre of the opening (offset 150 from centerline)
180	PT_Front_a480_SPx	Thermocouple	1	°C	Facing the centre of the opening (offset 150 from centerline)
181	PT_Front_a240_SPy	Thermocouple	1	°C	Facing the centre of the opening (offset 150 from centerline)
182	PT_Front_a240_SPx	Thermocouple	1	°C	Facing the centre of the opening (offset 150 from centerline)
183	PT_Front_e350_SPx	Thermocouple	1	°C	3.5 m above ground
184	PT_Front_e550_SPx	Thermocouple	1	°C	5.5 m above the top of the opening
185	TC_Smoke	Thermocouple	1	°C	Gas temperature at SMOKE2 outflow (for shutoff)
186	TC_HFGtower	Thermocouple	1	°C	H2O outflow temperatures of heat flux gages on roof tower
187	TC_HFGfloor	Thermocouple	1	°C	H2O outflow temperatures of heat flux gages on floor
188	TC_HFGw1	Thermocouple	1	°C	H2O outflow temperatures of heat flux gages on W1
189	TC_GoPro	Thermocouple	1	°C	H2O outflow temperatures of GoPro water bath
190	TC_TreeSteel	Thermocouple	1	°C	Temperature of steel behind thermal insulation in Tree 03 at 2.1 m height
191	TC_TBD	Thermocouple	1	°C	Extra TC location TBD
	VI	±10V default	1	V	Internal heartbeat
	HRR	N/A	1	kW	Calculated channel
	HRRburner	N/A	1	kW	Calculated channel
	VelCeiling	N/A	-	m/s	Calculated channel
	VelDoor1	N/A	-	m/s	Calculated channel
	VelDoor2	N/A	-	m/s	Calculated channel
	VelDoor3	N/A	-	m/s	Calculated channel
	VelDoor4	N/A	-	m/s	Calculated channel
	VelDoor5	N/A	-	m/s	Calculated channel
	VelDoor6	N/A	-	m/s	Calculated channel

Table D 3. Hardware configuration for Test 1-3.

Wire	Legend/ID	Manufacturer	Model	Slope	Units	Notes
1	TC_Ceiling_Center_020	Omega.com	GG-K-24-SLE-1000	1	°C	At the centre of the ceiling in panel 20 mm from interface
2	TC_Ceiling_Center_035	Omega.com	GG-K-24-SLE-1000	1	°C	At the centre of the ceiling in panel 35 mm from interface
3	TC_Ceiling_Center_050	Omega.com	GG-K-24-SLE-1000	1	°C	At the centre of the ceiling in panel 50 mm from interface
4	TC_Ceiling_Center_065	Omega.com	GG-K-24-SLE-1000	1	°C	At the centre of the ceiling in panel 65 mm from interface
5	TC_Ceiling_Center_090	Omega.com	GG-K-24-SLE-1000	1	°C	At the centre of the ceiling in panel 90 mm from interface
6	TC_Ceiling_Center_115	Omega.com	GG-K-24-SLE-1000	1	°C	At the centre of the ceiling in panel 115 mm from interface
7	TC_Ceiling_Center_140	Omega.com	GG-K-24-SLE-1000	1	°C	At the centre of the ceiling in panel 140 mm from interface
8	TC_W1_Middle_180_020	Omega.com	GG-K-24-SLE-1000	1	°C	W1 at the mid length at h=1.8 m in panel 20 mm from interface
9	TC_W1_Middle_180_035	Omega.com	GG-K-24-SLE-1000	1	°C	W1 at the mid length at h=1.8 m in panel 35 mm from interface
10	TC_W1_Middle_180_050	Omega.com	GG-K-24-SLE-1000	1	°C	W1 at the mid length at h=1.8 m in panel 50 mm from interface
11	TC_W1_Middle_180_065	Omega.com	GG-K-24-SLE-1000	1	°C	W1 at the mid length at h=1.8 m in panel 65 mm from interface
12	TC_W1_Middle_180_090	Omega.com	GG-K-24-SLE-1000	1	°C	W1 at the mid length at h=1.8 m in panel 90 mm from interface
13	TC_W1_Middle_180_115	Omega.com	GG-K-24-SLE-1000	1	°C	W1 at the mid length at h=1.8 m in panel 115 mm from interface
14	TC_W1_Middle_180_140	Omega.com	GG-K-24-SLE-1000	1	°C	W1 at the mid length at h=1.8 m in panel 140 mm from interface
15	TC_W3_Middle_180_020	Omega.com	GG-K-24-SLE-1000	1	°C	W3 at the mid length at h=1.8 m in panel 20 mm from interface
16	TC_W3_Middle_180_035	Omega.com	GG-K-24-SLE-1000	1	°C	W3 at the mid length at h=1.8 m in panel 35 mm from interface
17	TC_W3_Middle_180_050	Omega.com	GG-K-24-SLE-1000	1	°C	W3 at the mid length at h=1.8 m in panel 50 mm from interface
18	TC_W3_Middle_180_065	Omega.com	GG-K-24-SLE-1000	1	°C	W3 at the mid length at h=1.8 m in panel 65 mm from interface
19	TC_W3_Middle_180_090	Omega.com	GG-K-24-SLE-1000	1	°C	W3 at the mid length at h=1.8 m in panel 90 mm from interface
20	TC_W3_Middle_180_115	Omega.com	GG-K-24-SLE-1000	1	°C	W3 at the mid length at h=1.8 m in panel 115 mm from interface
21	TC_W3_Middle_180_140	Omega.com	GG-K-24-SLE-1000	1	°C	W3 at the mid length at h=1.8 m in panel 140 mm from interface
22	TC_W4_Middle_180_020	Omega.com	GG-K-24-SLE-1000	1	°C	W4 at the mid length at h=1.8 m in panel 20 mm from interface
23	TC_W4_Middle_180_035	Omega.com	GG-K-24-SLE-1000	1	°C	W4 at the mid length at h=1.8 m in panel 35 mm from interface
24	TC_W4_Middle_180_050	Omega.com	GG-K-24-SLE-1000	1	°C	W4 at the mid length at h=1.8 m in panel 50 mm from interface
25	TC_W4_Middle_180_065	Omega.com	GG-K-24-SLE-1000	1	°C	W4 at the mid length at h=1.8 m in panel 65 mm from interface
26	TC_W4_Middle_180_090	Omega.com	GG-K-24-SLE-1000	1	°C	W4 at the mid length at h=1.8 m in panel 90 mm from interface
27	TC_W4_Middle_180_115	Omega.com	GG-K-24-SLE-1000	1	°C	W4 at the mid length at h=1.8 m in panel 115 mm from interface
28	TC_W4_Middle_180_140	Omega.com	GG-K-24-SLE-1000	1	°C	W4 at the mid length at h=1.8 m in panel 140 mm from interface
29	TC_Tree_Tr1_060	Omega.com	HKQSS-18G-XXX	1	°C	Tree Tr1 at h=0.6 m
30	TC_Tree_Tr1_160	Omega.com	HKQSS-18G-XXX	1	°C	Tree Tr1 at h=1.6 m
31	TC_Tree_Tr1_260	Omega.com	HKQSS-18G-XXX	1	°C	Tree Tr1 at h=2.6 m
32	TC_Tree_Tr2_060	Omega.com	HKQSS-18G-XXX	1	°C	Tree Tr2 at h=0.6 m
33	TC_Tree_Tr2_160	Omega.com	HKQSS-18G-XXX	1	°C	Tree Tr2 at h=1.6 m
34	TC_Tree_Tr2_260	Omega.com	HKQSS-18G-XXX	1	°C	Tree Tr2 at h=2.6 m
35	TC_Tree_Tr3_060	Omega.com	HKQSS-18G-XXX	1	°C	Tree Tr3 at h=0.6 m
36	TC_Tree_Tr3_160	Omega.com	HKQSS-18G-XXX	1	°C	Tree Tr3 at h=1.6 m
37	TC_Tree_Tr3_260	Omega.com	HKQSS-18G-XXX	1	°C	Tree Tr3 at h=2.6 m
38	TC_Tree_Tr4_060	Omega.com	HKQSS-18G-XXX	1	°C	Tree Tr4 at h=0.6 m
39	TC_Tree_Tr4_160	Omega.com	HKQSS-18G-XXX	1	°C	Tree Tr4 at h=1.6 m
40	TC_Tree_Tr4_260	Omega.com	HKQSS-18G-XXX	1	°C	Tree Tr4 at h=2.6 m
41	TC_Tree_Tr5_060	Omega.com	HKQSS-18G-XXX	1	°C	Tree Tr5 at h=0.6 m
42	TC_Tree_Tr5_160	Omega.com	HKQSS-18G-XXX	1	°C	Tree Tr5 at h=1.6 m
43	TC_Tree_Tr5_260	Omega.com	HKQSS-18G-XXX	1	°C	Tree Tr5 at h=2.6 m
44	TC_Tree_Tr6_060	Omega.com	HKQSS-18G-XXX	1	°C	Tree Tr6 at h=0.6 m
45	TC_Tree_Tr6_160	Omega.com	HKQSS-18G-XXX	1	°C	Tree Tr6 at h=1.6 m
46	TC_Tree_Tr6_260	Omega.com	HKQSS-18G-XXX	1	°C	Tree Tr6 at h=2.6 m
47	TC_W1_Middle_060_CLT	Omega.com	GG-K-24-SLE-1000	1	°C	W1 at the mid length at h=0.6 m on the surface of CLT

Wire	Legend/ID	Manufacturer	Model	Slope	Units	Notes
48	TC_W1_Middle_120_CLT	Omega.com	GG-K-24-SLE-1000	1	°C	W1 at the mid length at h=1.2 m on the surface of CLT
49	TC_W1_Middle_180_CLT	Omega.com	GG-K-24-SLE-1000	1	°C	W1 at the mid length at h=1.8 m on the surface of CLT
50	TC_W1_Middle_060_1GB	Omega.com	GG-K-24-SLE-1000	1	°C	W1 at the mid length at h=0.6 m on the surface of 1st GB
51	TC_W1_Middle_120_1GB	Omega.com	GG-K-24-SLE-1000	1	°C	W1 at the mid length at h=1.2 m on the surface of 1st GB
52	TC_W1_Middle_180_1GB	Omega.com	GG-K-24-SLE-1000	1	°C	W1 at the mid length at h=1.8 m on the surface of 1st GB
53	TC_W1_Middle_060_2GB	Omega.com	GG-K-24-SLE-1000	1	°C	W1 at the mid length at h=0.6 m on the surface of 2nd GB
54	TC_W1_Middle_120_2GB	Omega.com	GG-K-24-SLE-1000	1	°C	W1 at the mid length at h=1.2 m on the surface of 2nd GB
55	TC_W1_Middle_180_2GB	Omega.com	GG-K-24-SLE-1000	1	°C	W1 at the mid length at h=1.8 m on the surface of 2nd GB
56	TC_W1_Front_180_CLT	Omega.com	GG-K-24-SLE-1000	1	°C	W1 at the front at h=1.8 m on the surface of CLT
57	TC_W1_Front_180_1GB	Omega.com	GG-K-24-SLE-1000	1	°C	W1 at the front at h=1.8 m on the surface of 1st GB
58	TC_W1_Front_180_2GB	Omega.com	GG-K-24-SLE-1000	1	°C	W1 at the front at h=1.8 m on the surface of 2st GB
59	TC_W1_Rear_180_CLT	Omega.com	GG-K-24-SLE-1000	1	°C	W1 at the rear at h=1.8 m on the surface of CLT
60	TC_W1_Rear_180_1GB	Omega.com	GG-K-24-SLE-1000	1	°C	W1 at the rear at h=1.8 m on the surface of 1st GB
61	TC_W1_Rear_180_2GB	Omega.com	GG-K-24-SLE-1000	1	°C	W1 at the rear at h=1.8 m on the surface of 2st GB
62	TC_W1_Front_060_CLT	Omega.com	GG-K-24-SLE-1000	1	°C	W1 at the front at h=0.6 m on the surface of CLT
63	TC_W1_Front_060_1GB	Omega.com	GG-K-24-SLE-1000	1	°C	W1 at the front at h=0.6 m on the surface of 1st GB
64	TC_W1_Front_060_2GB	Omega.com	GG-K-24-SLE-1000	1	°C	W1 at the front at h=0.6 m on the surface of 2st GB
65	TC_W1_Rear_060_CLT	Omega.com	GG-K-24-SLE-1000	1	°C	W1 at the rear at h=0.6 m on the surface of CLT
66	TC_W1_Rear_060_1GB	Omega.com	GG-K-24-SLE-1000	1	°C	W1 at the rear at h=0.6 m on the surface of 1st GB
67	TC_W1_Rear_060_2GB	Omega.com	GG-K-24-SLE-1000	1	°C	W1 at the rear at h=0.6 m on the surface of 2st GB
68	TC_W3_Middle_060_CLT	Omega.com	GG-K-24-SLE-1000	1	°C	W3 on the surface of CLT
69	TC_W3_Middle_120_CLT	Omega.com	GG-K-24-SLE-1000	1	°C	W3 on the surface of CLT
70	TC_W3_Middle_180_CLT	Omega.com	GG-K-24-SLE-1000	1	°C	W3 on the surface of CLT
71	TC_W3_Middle_060_1GB	Omega.com	GG-K-24-SLE-1000	1	°C	W3 on the surface of 1st GB
72	TC_W3_Middle_120_1GB	Omega.com	GG-K-24-SLE-1000	1	°C	W3 on the surface of 1st GB
73	TC_W3_Middle_180_1GB	Omega.com	GG-K-24-SLE-1000	1	°C	W3 on the surface of 1st GB
74	TC_W3_Middle_060_2GB	Omega.com	GG-K-24-SLE-1000	1	°C	W3 on the surface of 2nd GB
75	TC_W3_Middle_120_2GB	Omega.com	GG-K-24-SLE-1000	1	°C	W3 on the surface of 2nd GB
76	TC_W3_Middle_180_2GB	Omega.com	GG-K-24-SLE-1000	1	°C	W3 on the surface of 2nd GB
77	TC_W4_Middle_060_CLT	Omega.com	GG-K-24-SLE-1000	1	°C	W4 on the surface of CLT
78	TC_W4_Middle_120_CLT	Omega.com	GG-K-24-SLE-1000	1	°C	W4 on the surface of CLT
79	TC_W4_Middle_180_CLT	Omega.com	GG-K-24-SLE-1000	1	°C	W4 on the surface of CLT
80	TC_W4_Middle_060_1GB	Omega.com	GG-K-24-SLE-1000	1	°C	W4 on the surface of 1st GB
81	TC_W4_Middle_120_1GB	Omega.com	GG-K-24-SLE-1000	1	°C	W4 on the surface of 1st GB
82	TC_W4_Middle_180_1GB	Omega.com	GG-K-24-SLE-1000	1	°C	W4 on the surface of 1st GB
83	TC_W4_Middle_060_2GB	Omega.com	GG-K-24-SLE-1000	1	°C	W4 on the surface of 2nd GB
84	TC_W4_Middle_120_2GB	Omega.com	GG-K-24-SLE-1000	1	°C	W4 on the surface of 2nd GB
85	TC_W4_Middle_180_2GB	Omega.com	GG-K-24-SLE-1000	1	°C	W4 on the surface of 2nd GB
86	TC_Ceiling_Tr1_CLT	Omega.com	GG-K-24-SLE-1000	1	°C	ceiling above Tr1 on the surface of CLT
87	TC_Ceiling_Tr1_1GB	Omega.com	GG-K-24-SLE-1000	1	°C	ceiling above Tr1 on the surface of 1st GB
88	TC_Ceiling_Tr1_2GB	Omega.com	GG-K-24-SLE-1000	1	°C	ceiling above Tr1 on the surface of 2nd GB
89	TC_Ceiling_Tr2_CLT	Omega.com	GG-K-24-SLE-1000	1	°C	ceiling above Tr2 on the surface of CLT
90	TC_Ceiling_Tr2_1GB	Omega.com	GG-K-24-SLE-1000	1	°C	ceiling above Tr2 on the surface of 1st GB
91	TC_Ceiling_Tr2_2GB	Omega.com	GG-K-24-SLE-1000	1	°C	ceiling above Tr2 on the surface of 2nd GB
92	TC_Ceiling_Tr3_CLT	Omega.com	GG-K-24-SLE-1000	1	°C	Ceiling above Tr3 on the surface of CLT
93	TC_Ceiling_Tr3_1GB	Omega.com	GG-K-24-SLE-1000	1	°C	Ceiling above Tr3 on the surface of 1st GB
94	TC_Ceiling_Tr3_2GB	Omega.com	GG-K-24-SLE-1000	1	°C	Ceiling above Tr3 on the surface of 2nd GB
95	TC_Ceiling_Tr4_CLT	Omega.com	GG-K-24-SLE-1000	1	°C	Ceiling above Tr4 on the surface of CLT
96	TC_Ceiling_Tr4_1GB	Omega.com	GG-K-24-SLE-1000	1	°C	Ceiling above Tr4 on the surface of 1st GB
97	TC_Ceiling_Tr4_2GB	Omega.com	GG-K-24-SLE-1000	1	°C	Ceiling above Tr4 on the surface of 2nd GB
98	TC_Ceiling_Center_CLT	Omega.com	GG-K-24-SLE-1000	1	°C	Ceiling at the centre on the surface of CLT
99	TC_Ceiling_Center_1GB	Omega.com	GG-K-24-SLE-1000	1	°C	Ceiling at the centre on the surface of 1st GB
100	TC_Ceiling_Center_2GB	Omega.com	GG-K-24-SLE-1000	1	°C	Ceiling at the centre on the surface of 2nd GB
101	Gardon_Floor_Center	Medtherm	64-20-18	19870	kW/m2	At the center of the floor
102	Gardon_W1_Middle_180	Medtherm	64-20-18	19260	kW/m2	W1 at the mid length at h=1.8 m
103	PT_W1_Middle_180_SPy	Omega.com	GG-K-24-SLE-1000	1	°C	Temperature for plate thermometer on W1 at the mid length at h=1.8 m
104	DFT_W1_Middle_180_Px	Sandia	TN-TN-K	1	°C	DFT on W1 at the mid length at h=1.8 m (Front plate)
105	PT_W1_Middle_180_SPx	Pentronic	5928060-001	1	°C	Plate thermometer on W1 at the mid length at h=1.8 m
106	PT_W1_Front_180_SPy	Omega.com	GG-K-24-SLE-1000	1	°C	Temperature for plate thermometer on W1 at front
107	PT_W3_Middle_180_SPx	Pentronic	TN-TN-K	1	°C	Plate thermometer on W3 at the mid length at h=1.8 m
108	PT_W1_Front_180_SPx	Pentronic	5928060-001	1	°C	Plate thermometer on W1 in the front of the compartment at h=1.8 m
109	PT_W1_Rear_180_SPy	Omega.com	GG-K-24-SLE-1000	1	°C	Temperature for plate thermometer on W1 in the rear of the compartment at h=1.8 m
110	PT_W4_Middle_180_SPx	Pentronic	TN-TN-K	1	°C	Plate thermometer on W4 at the mid length at h=1.8 m
111	PT_W1_Rear_180_SPx	Pentronic	5928060-001	1	°C	plate thermometer on W1 in the rear of the compartment at h=1.8 m
112	PT_Ceiling_Center_SPy	Omega.com	GG-K-24-SLE-1000	1	°C	Temperature for plate thermometer at the centre of the ceiling
113	DFT_Ceiling_Center_Px	Sandia	TN-TN-K	1	°C	DFT at the centre of the ceiling (Back plate)
114	PT_Ceiling_Center_SPx	Pentronic	5928060-001	1	°C	Plate thermometer at the centre of the ceiling
115	PT_Ceiling_Bed_SPy	Omega.com	GG-K-24-SLE-1000	1	°C	Temperature for plate thermometer on ceiling above the bed
116	DFT_Ceiling_Bed_Px	Sandia	TN-TN-K	1	°C	DFT on the ceiling above the bed (Back plate)
117	PT_Ceiling_Bed_SPx	Pentronic	5928060-001	1	°C	Plate thermometer on the ceiling above the bed
118	dP_c	Greisinger	GMH 3181-01	400	Pa	5/8" diameter bidirectional probe on ceiling near STE 6, Direction normal to the opening
120	dP_r	Greisinger	GMH 3181-01	400	Pa	On smoke sample line near gas analyzer sample line at 2.1m 1/4" SS tube
121	STE_1	FM Global	See "Drawings"	1	°C	12" below ceiling (see "Drawings")
122	STE_2	FM Global	See "Drawings"	1	°C	12" below ceiling (see "Drawings")
123	STE_3	FM Global	See "Drawings"	1	°C	12" below ceiling (see "Drawings")
124	STE_4	FM Global	See "Drawings"	1	°C	18" below ceiling (see "Drawings")
125	STE_5	FM Global	See "Drawings"	1	°C	12" below ceiling (see "Drawings")

Wire	Legend/ID	Manufacturer	Model	Slope	Units	Notes
126	STE_6	FM Global	See "Drawings"	1	°C	12" below ceiling (see "Drawings")
127	STE_7	FM Global	See "Drawings"	1	°C	12" below ceiling (see "Drawings")
128	STE_8	FM Global	See "Drawings"	1	°C	18" below ceiling (see "Drawings")
129	STE_9	FM Global	See "Drawings"	1	°C	12" below ceiling (see "Drawings")
130	STE_10	FM Global	See "Drawings"	1	°C	12" below ceiling (see "Drawings")
131	TC_V_c	Omega.com	GG-K-24-SLE-1000	1	°C	Temperature co-located with V_c
132	SmokeAlarm	Kidde	PE120	1	V	Smoke detector at the centre of the ceiling
133	HeatAlarm	Kidde	HD135F	1	V	Heat detector at the centre of the ceiling
134	O2_room	-	-	4.274	%	At the centre of the room, 2.1 m high
135	CO2_room	-	-	3.497	%	At the centre of the room, 2.1 m high
136	CO_room	-	-	4.410	%	At the centre of the room, 2.1 m high
137	SMOKE	NRC	Photo Diode Meter	1	V	at the centre of the room, 1.6 m high
138	Door_TC_1	Omega.com	HKQSS-18G-XXX	1	°C	At the centreline of the opening
139	Door_TC_2	Omega.com	HKQSS-18G-XXX	1	°C	At the centreline of the opening
140	Door_TC_3	Omega.com	HKQSS-18G-XXX	1	°C	At the centreline of the opening
141	Door_TC_4	Omega.com	HKQSS-18G-XXX	1	°C	At the centreline of the opening
142	Door_TC_5	Omega.com	HKQSS-18G-XXX	1	°C	At the centreline of the opening
143	Door_TC_6	Omega.com	HKQSS-18G-XXX	1	°C	At the centreline of the opening
144	Door_TC_7	Omega.com	HKQSS-18G-XXX	1	°C	At the centreline of the opening
145	dP_o1	Greisinger	GMH 3181-01	400	Pa	5/8" diameter bidirectional probe at the opening (low, long side)
146	dP_o2	Greisinger	GMH 3181-01	400	Pa	5/8" diameter bidirectional probe at the opening (low, middle)
147	dP_o3	Greisinger	GMH 3181-01	400	Pa	5/8" diameter bidirectional probe at the opening (low, short side)
148	dP_o4	Greisinger	GMH 3181-01	400	Pa	5/8" diameter bidirectional probe at the opening (high, long side)
149	dP_o5	Greisinger	GMH 3181-01	400	Pa	5/8" diameter bidirectional probe at the opening (high, middle)
150	dP_o6	Greisinger	GMH 3181-01	400	Pa	5/8" diameter bidirectional probe at the opening (high, short side)
151	Gardon_Front_a480	Medtherm	64-20-18	19460	kW/m2	facing the centre of the opening
152	Gardon_Front_a240	Medtherm	64-20-18	20980	kW/m2	facing the centre of the opening
153	Gardon_Front_e350	Medtherm	64-20-18	20260	kW/m2	3.5 m above ground
154	Gardon_Front_e550	Medtherm	64-20-18	18820	kW/m2	5.5 m above ground
155	Roof_TC_350	Omega.com	GG-K-24-SLE-1000	1	°C	3.5 m above ground
156	Roof_TC_450	Omega.com	GG-K-24-SLE-1000	1	°C	4.5 m above ground
157	Roof_TC_550	Omega.com	GG-K-24-SLE-1000	1	°C	5.5 m above ground
158	Roof_TC_650	Omega.com	GG-K-24-SLE-1000	1	°C	6.5 m above ground
159	Roof_TC_750	Omega.com	GG-K-24-SLE-1000	1	°C	7.5 m above ground
161	DFT_W1_Middle_180_Py	Sandia	TN-TN-K	1	°C	DFT on W1 at the mid length at h=1.8 m
162	PT_W3_Middle_180_SPy	Omega.com	GG-K-24-SLE-1000	1	°C	Temperature for plate thermometer on W3 at the mid length at h=1.8 m
163	PT_W4_Middle_180_SPy	Omega.com	GG-K-24-SLE-1000	1	°C	Temperature for plate thermometer on W4 at the mid length at h=1.8 m
164	DFT_Ceiling_Center_Py	Sandia	TN-TN-K	1	°C	DFT at the centre of the ceiling (Front plate)
165	DFT_Ceiling_Bed_Py	Sandia	TN-TN-K	1	°C	DFT on the ceiling above the bed (Front plate)
166	DEWpt_rack	-	-	30.121	°C	Gas rack dew point measurement
167	TC_Tree_Tr1_110	Omega.com	HKQSS-18G-XXX	1	°C	Tree Tr1 at h=1.1 m
168	TC_Tree_Tr1_210	Omega.com	HKQSS-18G-XXX	1	°C	Tree Tr1 at h=2.1 m
169	TC_Tree_Tr2_110	Omega.com	HKQSS-18G-XXX	1	°C	Tree Tr2 at h=1.1 m
170	TC_Tree_Tr2_210	Omega.com	HKQSS-18G-XXX	1	°C	Tree Tr2 at h=2.1 m
171	TC_Tree_Tr3_110	Omega.com	HKQSS-18G-XXX	1	°C	Tree Tr3 at h=1.1 m
172	TC_Tree_Tr3_210	Omega.com	HKQSS-18G-XXX	1	°C	Tree Tr3 at h=2.1 m
173	TC_Tree_Tr4_110	Omega.com	HKQSS-18G-XXX	1	°C	Tree Tr4 at h=1.1 m
174	TC_Tree_Tr4_210	Omega.com	HKQSS-18G-XXX	1	°C	Tree Tr4 at h=2.1 m
175	TC_Tree_Tr5_110	Omega.com	HKQSS-18G-XXX	1	°C	Tree Tr5 at h=1.1 m
176	TC_Tree_Tr5_210	Omega.com	HKQSS-18G-XXX	1	°C	Tree Tr5 at h=2.1 m
177	TC_Tree_Tr6_110	Omega.com	HKQSS-18G-XXX	1	°C	Tree Tr6 at h=1.1 m
178	TC_Tree_Tr6_210	Omega.com	HKQSS-18G-XXX	1	°C	Tree Tr6 at h=2.1 m
179	PT_Front_a480_SPy	Omega.com	GG-K-24-SLE-1000	1	°C	Facing the centre of the opening (offset 150 from centerline)
180	PT_Front_a480_SPx	Pentronic	5928060-001	1	°C	Facing the centre of the opening (offset 150 from centerline)
181	PT_Front_a240_SPy	Omega.com	GG-K-24-SLE-1000	1	°C	Facing the centre of the opening (offset 150 from centerline)
182	PT_Front_a240_SPx	Pentronic	5928060-001	1	°C	Facing the centre of the opening (offset 150 from centerline)
183	PT_Front_e350_SPx	Pentronic	5928060-001	1	°C	3.5 m above ground
184	PT_Front_e550_SPx	Pentronic	5928060-001	1	°C	5.5 m above the top of the opening
185	TC_Smoke	Omega.com	GG-K-24-SLE-1000	1	°C	Gas temperature at SMOKE2 outflow (for shutoff)
186	TC_HFGtower	Omega.com	EXPP-K-24-SLE-1000	1	°C	H2O outflow temperatures of heat flux gages on roof tower
187	TC_HFGfloor	Omega.com	KMQSS-040	1	°C	H2O outflow temperatures of heat flux gages on floor
188	TC_HFGw1	Omega.com	KMQSS-040	1	°C	H2O outflow temperatures of heat flux gages on W1
189	TC_GoPro	Omega.com	KMQSS-040	1	°C	H2O outflow temperatures of GoPro water bath
190	TC_TreeSteel	Omega.com	GG-K-24-SLE-1000	1	°C	Temperature of steel behind thermal insulation in Tree 03 at 2.1 m height
191	TC_TBD	Omega.com	GG-K-24-SLE-1000	1	°C	Extra TC location TBD
	VI	-	-	1	V	Internal heartbeat
	HRR	-	-	1	kW	Calculated channel
	HRRburner	-	-	1	kW	Calculated channel
	VelCeiling	-	-	-	m/s	Calculated channel
	VelDoor1	-	-	-	m/s	Calculated channel
	VelDoor2	-	-	-	m/s	Calculated channel
	VelDoor3	-	-	-	m/s	Calculated channel
	VelDoor4	-	-	-	m/s	Calculated channel
	VelDoor5	-	-	-	m/s	Calculated channel
	VelDoor6	-	-	-	m/s	Calculated channel

Table D 4. Hardware configuration for Test 1-4.

Wire	Legend/ID	Manufacturer	Model	Slope	Units	Notes
1	TC_Ceiling_Center_020	Omega.com	GG-K-24-SLE-1000	1	°C	At the centre of the ceiling in panel 20 mm from interface
2	TC_Ceiling_Center_035	Omega.com	GG-K-24-SLE-1000	1	°C	At the centre of the ceiling in panel 35 mm from interface
3	TC_Ceiling_Center_050	Omega.com	GG-K-24-SLE-1000	1	°C	At the centre of the ceiling in panel 50 mm from interface
4	TC_Ceiling_Center_065	Omega.com	GG-K-24-SLE-1000	1	°C	At the centre of the ceiling in panel 65 mm from interface
5	TC_Ceiling_Center_090	Omega.com	GG-K-24-SLE-1000	1	°C	At the centre of the ceiling in panel 90 mm from interface
6	TC_Ceiling_Center_115	Omega.com	GG-K-24-SLE-1000	1	°C	At the centre of the ceiling in panel 115 mm from interface
7	TC_Ceiling_Center_140	Omega.com	GG-K-24-SLE-1000	1	°C	At the centre of the ceiling in panel 140 mm from interface
8	TC_W1_Middle_180_020	Omega.com	GG-K-24-SLE-1000	1	°C	W1 at the mid length at h=1.8 m in panel 20 mm from interface
9	TC_W1_Middle_180_035	Omega.com	GG-K-24-SLE-1000	1	°C	W1 at the mid length at h=1.8 m in panel 35 mm from interface
10	TC_W1_Middle_180_050	Omega.com	GG-K-24-SLE-1000	1	°C	W1 at the mid length at h=1.8 m in panel 50 mm from interface
11	TC_W1_Middle_180_065	Omega.com	GG-K-24-SLE-1000	1	°C	W1 at the mid length at h=1.8 m in panel 65 mm from interface
12	TC_W1_Middle_180_090	Omega.com	GG-K-24-SLE-1000	1	°C	W1 at the mid length at h=1.8 m in panel 90 mm from interface
13	TC_W1_Middle_180_115	Omega.com	GG-K-24-SLE-1000	1	°C	W1 at the mid length at h=1.8 m in panel 115 mm from interface
14	TC_W1_Middle_180_140	Omega.com	GG-K-24-SLE-1000	1	°C	W1 at the mid length at h=1.8 m in panel 140 mm from interface
15	TC_W3_Middle_180_020	Omega.com	GG-K-24-SLE-1000	1	°C	W3 at the mid length at h=1.8 m in panel 20 mm from interface
16	TC_W3_Middle_180_035	Omega.com	GG-K-24-SLE-1000	1	°C	W3 at the mid length at h=1.8 m in panel 35 mm from interface
17	TC_W3_Middle_180_050	Omega.com	GG-K-24-SLE-1000	1	°C	W3 at the mid length at h=1.8 m in panel 50 mm from interface
18	TC_W3_Middle_180_065	Omega.com	GG-K-24-SLE-1000	1	°C	W3 at the mid length at h=1.8 m in panel 65 mm from interface
19	TC_W3_Middle_180_090	Omega.com	GG-K-24-SLE-1000	1	°C	W3 at the mid length at h=1.8 m in panel 90 mm from interface
20	TC_W3_Middle_180_115	Omega.com	GG-K-24-SLE-1000	1	°C	W3 at the mid length at h=1.8 m in panel 115 mm from interface
21	TC_W3_Middle_180_140	Omega.com	GG-K-24-SLE-1000	1	°C	W3 at the mid length at h=1.8 m in panel 140 mm from interface
22	TC_W4_Middle_180_020	Omega.com	GG-K-24-SLE-1000	1	°C	W4 at the mid length at h=1.8 m in panel 20 mm from interface
23	TC_W4_Middle_180_035	Omega.com	GG-K-24-SLE-1000	1	°C	W4 at the mid length at h=1.8 m in panel 35 mm from interface
24	TC_W4_Middle_180_050	Omega.com	GG-K-24-SLE-1000	1	°C	W4 at the mid length at h=1.8 m in panel 50 mm from interface
25	TC_W4_Middle_180_065	Omega.com	GG-K-24-SLE-1000	1	°C	W4 at the mid length at h=1.8 m in panel 65 mm from interface
26	TC_W4_Middle_180_090	Omega.com	GG-K-24-SLE-1000	1	°C	W4 at the mid length at h=1.8 m in panel 90 mm from interface
27	TC_W4_Middle_180_115	Omega.com	GG-K-24-SLE-1000	1	°C	W4 at the mid length at h=1.8 m in panel 115 mm from interface
28	TC_W4_Middle_180_140	Omega.com	GG-K-24-SLE-1000	1	°C	W4 at the mid length at h=1.8 m in panel 140 mm from interface
29	TC_Tree_Tr1_060	Omega.com	HKQSS-18G-XXX	1	°C	Tree Tr1 at h=0.6 m
30	TC_Tree_Tr1_160	Omega.com	HKQSS-18G-XXX	1	°C	Tree Tr1 at h=1.6 m
31	TC_Tree_Tr1_260	Omega.com	HKQSS-18G-XXX	1	°C	Tree Tr1 at h=2.6 m
32	TC_Tree_Tr2_060	Omega.com	HKQSS-18G-XXX	1	°C	Tree Tr2 at h=0.6 m
33	TC_Tree_Tr2_160	Omega.com	HKQSS-18G-XXX	1	°C	Tree Tr2 at h=1.6 m
34	TC_Tree_Tr2_260	Omega.com	HKQSS-18G-XXX	1	°C	Tree Tr2 at h=2.6 m
35	TC_Tree_Tr3_060	Omega.com	HKQSS-18G-XXX	1	°C	Tree Tr3 at h=0.6 m
36	TC_Tree_Tr3_160	Omega.com	HKQSS-18G-XXX	1	°C	Tree Tr3 at h=1.6 m
37	TC_Tree_Tr3_260	Omega.com	HKQSS-18G-XXX	1	°C	Tree Tr3 at h=2.6 m
38	TC_Tree_Tr4_060	Omega.com	HKQSS-18G-XXX	1	°C	Tree Tr4 at h=0.6 m
39	TC_Tree_Tr4_160	Omega.com	HKQSS-18G-XXX	1	°C	Tree Tr4 at h=1.6 m
40	TC_Tree_Tr4_260	Omega.com	HKQSS-18G-XXX	1	°C	Tree Tr4 at h=2.6 m
41	TC_Tree_Tr5_060	Omega.com	HKQSS-18G-XXX	1	°C	Tree Tr5 at h=0.6 m
42	TC_Tree_Tr5_160	Omega.com	HKQSS-18G-XXX	1	°C	Tree Tr5 at h=1.6 m
43	TC_Tree_Tr5_260	Omega.com	HKQSS-18G-XXX	1	°C	Tree Tr5 at h=2.6 m
44	TC_Tree_Tr6_060	Omega.com	HKQSS-18G-XXX	1	°C	Tree Tr6 at h=0.6 m
45	TC_Tree_Tr6_160	Omega.com	HKQSS-18G-XXX	1	°C	Tree Tr6 at h=1.6 m
46	TC_Tree_Tr6_260	Omega.com	HKQSS-18G-XXX	1	°C	Tree Tr6 at h=2.6 m
47	TC_W1_Middle_060_CLT	Omega.com	GG-K-24-SLE-1000	1	°C	W1 at the mid length at h=0.6 m on the surface of CLT
48	TC_W1_Middle_120_CLT	Omega.com	GG-K-24-SLE-1000	1	°C	W1 at the mid length at h=1.2 m on the surface of CLT
49	TC_W1_Middle_180_CLT	Omega.com	GG-K-24-SLE-1000	1	°C	W1 at the mid length at h=1.8 m on the surface of CLT
50	TC_W1_Middle_060_1GB	Omega.com	GG-K-24-SLE-1000	1	°C	W1 at the mid length at h=0.6 m on the surface of 1st GB
51	TC_W1_Middle_120_1GB	Omega.com	GG-K-24-SLE-1000	1	°C	W1 at the mid length at h=1.2 m on the surface of 1st GB
52	TC_W1_Middle_180_1GB	Omega.com	GG-K-24-SLE-1000	1	°C	W1 at the mid length at h=1.8 m on the surface of 1st GB
53	TC_W1_Middle_060_2GB	Omega.com	GG-K-24-SLE-1000	1	°C	W1 at the mid length at h=0.6 m on the surface of 2nd GB
54	TC_W1_Middle_120_2GB	Omega.com	GG-K-24-SLE-1000	1	°C	W1 at the mid length at h=1.2 m on the surface of 2nd GB
55	TC_W1_Middle_180_2GB	Omega.com	GG-K-24-SLE-1000	1	°C	W1 at the mid length at h=1.8 m on the surface of 2nd GB
56	TC_W1_Front_180_CLT	Omega.com	GG-K-24-SLE-1000	1	°C	W1 at the front at h=1.8 m on the surface of CLT
57	TC_W1_Front_180_1GB	Omega.com	GG-K-24-SLE-1000	1	°C	W1 at the front at h=1.8 m on the surface of 1st GB
58	TC_W1_Front_180_2GB	Omega.com	GG-K-24-SLE-1000	1	°C	W1 at the front at h=1.8 m on the surface of 2st GB
59	TC_W1_Rear_180_CLT	Omega.com	GG-K-24-SLE-1000	1	°C	W1 at the rear at h=1.8 m on the surface of CLT
60	TC_W1_Rear_180_1GB	Omega.com	GG-K-24-SLE-1000	1	°C	W1 at the rear at h=1.8 m on the surface of 1st GB
61	TC_W1_Rear_180_2GB	Omega.com	GG-K-24-SLE-1000	1	°C	W1 at the rear at h=1.8 m on the surface of 2st GB
62	TC_W1_Front_060_CLT	Omega.com	GG-K-24-SLE-1000	1	°C	W1 at the front at h=0.6 m on the surface of CLT
63	TC_W1_Front_060_1GB	Omega.com	GG-K-24-SLE-1000	1	°C	W1 at the front at h=0.6 m on the surface of 1st GB
64	TC_W1_Front_060_2GB	Omega.com	GG-K-24-SLE-1000	1	°C	W1 at the front at h=0.6 m on the surface of 2st GB
65	TC_W1_Rear_060_CLT	Omega.com	GG-K-24-SLE-1000	1	°C	W1 at the rear at h=0.6 m on the surface of CLT
66	TC_W1_Rear_060_1GB	Omega.com	GG-K-24-SLE-1000	1	°C	W1 at the rear at h=0.6 m on the surface of 1st GB
67	TC_W1_Rear_060_2GB	Omega.com	GG-K-24-SLE-1000	1	°C	W1 at the rear at h=0.6 m on the surface of 2st GB
68	TC_W3_Middle_060_CLT	Omega.com	GG-K-24-SLE-1000	1	°C	W3 on the surface of CLT
69	TC_W3_Middle_120_CLT	Omega.com	GG-K-24-SLE-1000	1	°C	W3 on the surface of CLT
70	TC_W3_Middle_180_CLT	Omega.com	GG-K-24-SLE-1000	1	°C	W3 on the surface of CLT
71	TC_W3_Middle_060_1GB	Omega.com	GG-K-24-SLE-1000	1	°C	W3 on the surface of 1st GB
72	TC_W3_Middle_120_1GB	Omega.com	GG-K-24-SLE-1000	1	°C	W3 on the surface of 1st GB
73	TC_W3_Middle_180_1GB	Omega.com	GG-K-24-SLE-1000	1	°C	W3 on the surface of 1st GB
74	TC_W3_Middle_060_2GB	Omega.com	GG-K-24-SLE-1000	1	°C	W3 on the surface of 2nd GB
75	TC_W3_Middle_120_2GB	Omega.com	GG-K-24-SLE-1000	1	°C	W3 on the surface of 2nd GB

Wire	Legend/ID	Manufacturer	Model	Slope	Units	Notes
76	TC_W3_Middle_180_2GB	Omega.com	GG-K-24-SLE-1000	1	°C	W3 on the surface of 2nd GB
77	TC_W4_Middle_060_CLT	Omega.com	GG-K-24-SLE-1000	1	°C	W4 on the surface of CLT
78	TC_W4_Middle_120_CLT	Omega.com	GG-K-24-SLE-1000	1	°C	W4 on the surface of CLT
79	TC_W4_Middle_180_CLT	Omega.com	GG-K-24-SLE-1000	1	°C	W4 on the surface of CLT
80	TC_W4_Middle_060_1GB	Omega.com	GG-K-24-SLE-1000	1	°C	W4 on the surface of 1st GB
81	TC_W4_Middle_120_1GB	Omega.com	GG-K-24-SLE-1000	1	°C	W4 on the surface of 1st GB
82	TC_W4_Middle_180_1GB	Omega.com	GG-K-24-SLE-1000	1	°C	W4 on the surface of 1st GB
83	TC_W4_Middle_060_2GB	Omega.com	GG-K-24-SLE-1000	1	°C	W4 on the surface of 2nd GB
84	TC_W4_Middle_120_2GB	Omega.com	GG-K-24-SLE-1000	1	°C	W4 on the surface of 2nd GB
85	TC_W4_Middle_180_2GB	Omega.com	GG-K-24-SLE-1000	1	°C	W4 on the surface of 2nd GB
86	TC_Ceiling_Tr1_CLT	Omega.com	GG-K-24-SLE-1000	1	°C	ceiling above Tr1 on the surface of CLT
87	TC_Ceiling_Tr1_1GB	Omega.com	GG-K-24-SLE-1000	1	°C	ceiling above Tr1 on the surface of 1st GB
88	TC_Ceiling_Tr1_2GB	Omega.com	GG-K-24-SLE-1000	1	°C	ceiling above Tr1 on the surface of 2nd GB
89	TC_Ceiling_Tr2_CLT	Omega.com	GG-K-24-SLE-1000	1	°C	ceiling above Tr2 on the surface of CLT
90	TC_Ceiling_Tr2_1GB	Omega.com	GG-K-24-SLE-1000	1	°C	ceiling above Tr2 on the surface of 1st GB
91	TC_Ceiling_Tr2_2GB	Omega.com	GG-K-24-SLE-1000	1	°C	ceiling above Tr2 on the surface of 2nd GB
92	TC_Ceiling_Tr3_CLT	Omega.com	GG-K-24-SLE-1000	1	°C	Ceiling above Tr3 on the surface of CLT
93	TC_Ceiling_Tr3_1GB	Omega.com	GG-K-24-SLE-1000	1	°C	Ceiling above Tr3 on the surface of 1st GB
94	TC_Ceiling_Tr3_2GB	Omega.com	GG-K-24-SLE-1000	1	°C	Ceiling above Tr3 on the surface of 2nd GB
95	TC_Ceiling_Tr4_CLT	Omega.com	GG-K-24-SLE-1000	1	°C	Ceiling above Tr4 on the surface of CLT
96	TC_Ceiling_Tr4_1GB	Omega.com	GG-K-24-SLE-1000	1	°C	Ceiling above Tr4 on the surface of 1st GB
97	TC_Ceiling_Tr4_2GB	Omega.com	GG-K-24-SLE-1000	1	°C	Ceiling above Tr4 on the surface of 2nd GB
98	TC_Ceiling_Center_CLT	Omega.com	GG-K-24-SLE-1000	1	°C	Ceiling at the centre on the surface of CLT
99	TC_Ceiling_Center_1GB	Omega.com	GG-K-24-SLE-1000	1	°C	Ceiling at the centre on the surface of 1st GB
100	TC_Ceiling_Center_2GB	Omega.com	GG-K-24-SLE-1000	1	°C	Ceiling at the centre on the surface of 2nd GB
101	Gardon_Floor_Center	Medtherm	64-20-18	19870	kW/m2	At the center of the floor
102	Gardon_W1_Middle_180	Medtherm	64-20-18	19260	kW/m2	W1 at the mid length at h=1.8 m
103	PT_W1_Middle_180_SPy	Omega.com	GG-K-24-SLE-1000	1	°C	Temperature for plate thermometer on W1 at the mid length at h=1.8 m
104	DFT_W1_Middle_180_Px	Sandia	TN-TN-K	1	°C	DFT on W1 at the mid length at h=1.8 m (Front plate)
105	PT_W1_Middle_180_SPx	Pentronic	5928060-001	1	°C	Plate thermometer on W1 at the mid length at h=1.8 m
106	PT_W1_Front_180_SPy	Omega.com	GG-K-24-SLE-1000	1	°C	Temperature for plate thermometer on W1 at front
107	PT_W3_Middle_180_SPx	Pentronic	TN-TN-K	1	°C	Plate thermometer on W3 at the mid length at h=1.8 m
108	PT_W1_Front_180_SPx	Pentronic	5928060-001	1	°C	Plate thermometer on W1 in the front of the compartment at h=1.8 m
109	PT_W1_Rear_180_SPy	Omega.com	GG-K-24-SLE-1000	1	°C	Temperature for plate thermometer on W1 in the rear of the compartment at h=1.8 m
110	PT_W4_Middle_180_SPx	Pentronic	TN-TN-K	1	°C	Plate thermometer on W4 at the mid length at h=1.8 m
111	PT_W1_Rear_180_SPx	Pentronic	5928060-001	1	°C	plate thermometer on W1 in the rear of the compartment at h=1.8 m
112	PT_Ceiling_Center_SPy	Omega.com	GG-K-24-SLE-1000	1	°C	Temperature for plate thermometer at the centre of the ceiling
113	DFT_Ceiling_Center_Px	Sandia	TN-TN-K	1	°C	DFT at the centre of the ceiling (Back plate)
114	PT_Ceiling_Center_SPx	Pentronic	5928060-001	1	°C	Plate thermometer at the centre of the ceiling
115	PT_Ceiling_Bed_SPy	Omega.com	GG-K-24-SLE-1000	1	°C	Temperature for plate thermometer on ceiling above the bed
116	DFT_Ceiling_Bed_Px	Sandia	TN-TN-K	1	°C	DFT on the ceiling above the bed (Back plate)
117	PT_Ceiling_Bed_SPx	Pentronic	5928060-001	1	°C	Plate thermometer on the ceiling above the bed
118	dP_c	Greisinger	GMH 3181-01	400	Pa	5/8" diameter bidirectional probe on ceiling near STE 6, Direction normal to the opening
120	dP_r	Greisinger	GMH 3181-01	400	Pa	On smoke sample line near gas analyzer sample line at 2.1m 1/4" SS tube
121	STE_1	FM Global	See "Drawings"	1	°C	12" below ceiling (see "Drawings")
122	STE_2	FM Global	See "Drawings"	1	°C	12" below ceiling (see "Drawings")
123	STE_3	FM Global	See "Drawings"	1	°C	12" below ceiling (see "Drawings")
124	STE_4	FM Global	See "Drawings"	1	°C	18" below ceiling (see "Drawings")
125	STE_5	FM Global	See "Drawings"	1	°C	12" below ceiling (see "Drawings")
126	STE_6	FM Global	See "Drawings"	1	°C	12" below ceiling (see "Drawings")
127	STE_7	FM Global	See "Drawings"	1	°C	12" below ceiling (see "Drawings")
128	STE_8	FM Global	See "Drawings"	1	°C	18" below ceiling (see "Drawings")
129	STE_9	FM Global	See "Drawings"	1	°C	12" below ceiling (see "Drawings")
130	STE_10	FM Global	See "Drawings"	1	°C	12" below ceiling (see "Drawings")
131	TC_V_c	Omega.com	GG-K-24-SLE-1000	1	°C	Temperature co-located with V_c
132	SmokeAlarm	Kidde	PE120	1	V	Smoke detector at the centre of the ceiling
133	HeatAlarm	Kidde	HD135F	1	V	Heat detector at the centre of the ceiling
134	O2_room	-	-	4.272	%	At the centre of the room, 2.1 m high
135	CO2_room	-	-	3.400	%	At the centre of the room, 2.1 m high
136	CO_room	-	-	4.402	%	At the centre of the room, 2.1 m high
137	SMOKE	NRC	Photo Diode Meter	1	V	at the centre of the room, 1.6 m high
138	Door_TC_1	Omega.com	HKQSS-18G-XXX	1	°C	At the centreline of the opening
139	Door_TC_2	Omega.com	HKQSS-18G-XXX	1	°C	At the centreline of the opening
140	Door_TC_3	Omega.com	HKQSS-18G-XXX	1	°C	At the centreline of the opening
141	Door_TC_4	Omega.com	HKQSS-18G-XXX	1	°C	At the centreline of the opening
142	Door_TC_5	Omega.com	HKQSS-18G-XXX	1	°C	At the centreline of the opening
143	Door_TC_6	Omega.com	HKQSS-18G-XXX	1	°C	At the centreline of the opening
144	Door_TC_7	Omega.com	HKQSS-18G-XXX	1	°C	At the centreline of the opening
145	dP_o1	Greisinger	GMH 3181-01	400	Pa	5/8" diameter bidirectional probe at the opening (low, long side)
146	dP_o2	Greisinger	GMH 3181-01	400	Pa	5/8" diameter bidirectional probe at the opening (low, middle)
147	dP_o3	Greisinger	GMH 3181-01	400	Pa	5/8" diameter bidirectional probe at the opening (low, short side)
148	dP_o4	Greisinger	GMH 3181-01	400	Pa	5/8" diameter bidirectional probe at the opening (high, long side)
149	dP_o5	Greisinger	GMH 3181-01	400	Pa	5/8" diameter bidirectional probe at the opening (high, middle)
150	dP_o6	Greisinger	GMH 3181-01	400	Pa	5/8" diameter bidirectional probe at the opening (high, short side)
151	Gardon_Front_a480	Medtherm	64-20-18	19460	kW/m2	facing the centre of the opening
152	Gardon_Front_a240	Medtherm	64-20-18	20980	kW/m2	facing the centre of the opening
153	Gardon_Front_e350	Medtherm	64-20-18	20260	kW/m2	3.5 m above ground

Wire	Legend/ID	Manufacturer	Model	Slope	Units	Notes
154	Gardon_Front_e550	Medtherm	64-20-18	18820	kW/m2	5.5 m above ground
155	Roof_TC_350	Omega.com	GG-K-24-SLE-1000	1	°C	3.5 m above ground
156	Roof_TC_450	Omega.com	GG-K-24-SLE-1000	1	°C	4.5 m above ground
157	Roof_TC_550	Omega.com	GG-K-24-SLE-1000	1	°C	5.5 m above ground
158	Roof_TC_650	Omega.com	GG-K-24-SLE-1000	1	°C	6.5 m above ground
159	Roof_TC_750	Omega.com	GG-K-24-SLE-1000	1	°C	7.5 m above ground
161	DFT_W1_Middle_180_Py	Sandia	TN-TN-K	1	°C	DFT on W1 at the mid length at h=1.8 m
162	PT_W3_Middle_180_SPy	Omega.com	GG-K-24-SLE-1000	1	°C	Temperature for plate thermometer on W3 at the mid length at h=1.8 m
163	PT_W4_Middle_180_SPy	Omega.com	GG-K-24-SLE-1000	1	°C	Temperature for plate thermometer on W4 at the mid length at h=1.8 m
164	DFT_Ceiling_Center_Py	Sandia	TN-TN-K	1	°C	DFT at the centre of the ceiling (Front plate)
165	DFT_Ceiling_Bed_Py	Sandia	TN-TN-K	1	°C	DFT on the ceiling above the bed (Front plate)
166	DEWpt_rack	-	-	30.121	°C	Gas rack dew point measurement
167	TC_Tree_Tr1_110	Omega.com	HKQSS-18G-XXX	1	°C	Tree Tr1 at h=1.1 m
168	TC_Tree_Tr1_210	Omega.com	HKQSS-18G-XXX	1	°C	Tree Tr1 at h=2.1 m
169	TC_Tree_Tr2_110	Omega.com	HKQSS-18G-XXX	1	°C	Tree Tr2 at h=1.1 m
170	TC_Tree_Tr2_210	Omega.com	HKQSS-18G-XXX	1	°C	Tree Tr2 at h=2.1 m
171	TC_Tree_Tr3_110	Omega.com	HKQSS-18G-XXX	1	°C	Tree Tr3 at h=1.1 m
172	TC_Tree_Tr3_210	Omega.com	HKQSS-18G-XXX	1	°C	Tree Tr3 at h=2.1 m
173	TC_Tree_Tr4_110	Omega.com	HKQSS-18G-XXX	1	°C	Tree Tr4 at h=1.1 m
174	TC_Tree_Tr4_210	Omega.com	HKQSS-18G-XXX	1	°C	Tree Tr4 at h=2.1 m
175	TC_Tree_Tr5_110	Omega.com	HKQSS-18G-XXX	1	°C	Tree Tr5 at h=1.1 m
176	TC_Tree_Tr5_210	Omega.com	HKQSS-18G-XXX	1	°C	Tree Tr5 at h=2.1 m
177	TC_Tree_Tr6_110	Omega.com	HKQSS-18G-XXX	1	°C	Tree Tr6 at h=1.1 m
178	TC_Tree_Tr6_210	Omega.com	HKQSS-18G-XXX	1	°C	Tree Tr6 at h=2.1 m
179	PT_Front_a480_SPy	Omega.com	GG-K-24-SLE-1000	1	°C	Facing the centre of the opening (offset 150 from centerline)
180	PT_Front_a480_SPx	Pentronic	5928060-001	1	°C	Facing the centre of the opening (offset 150 from centerline)
181	PT_Front_a240_SPy	Omega.com	GG-K-24-SLE-1000	1	°C	Facing the centre of the opening (offset 150 from centerline)
182	PT_Front_a240_SPx	Pentronic	5928060-001	1	°C	Facing the centre of the opening (offset 150 from centerline)
183	PT_Front_e350_SPx	Pentronic	5928060-001	1	°C	3.5 m above ground
184	PT_Front_e550_SPx	Pentronic	5928060-001	1	°C	5.5 m above the top of the opening
185	TC_Smoke	Omega.com	GG-K-24-SLE-1000	1	°C	Gas temperature at SMOKE2 outflow (for shutoff)
186	TC_HFGtower	Omega.com	EXPP-K-24-SLE-1000	1	°C	H2O outflow temperatures of heat flux gages on roof tower
187	TC_HFGfloor	Omega.com	KMQSS-040	1	°C	H2O outflow temperatures of heat flux gages on floor
188	TC_HFGw1	Omega.com	KMQSS-040	1	°C	H2O outflow temperatures of heat flux gages on W1
189	TC_GoPro	Omega.com	KMQSS-040	1	°C	H2O outflow temperatures of GoPro water bath
190	TC_TreeSteel	Omega.com	GG-K-24-SLE-1000	1	°C	Temperature of steel behind thermal insulation in Tree 03 at 2.1 m height
191	TC_TBD	Omega.com	GG-K-24-SLE-1000	1	°C	Extra TC location TBD
	VI	-	-	1	V	Internal heartbeat
	HRR	-	-	1	kW	calculated channel
	HRRburner	-	-	1	kW	calculated channel
	VelCeiling	-	-	-	m/s	calculated channel
	VelDoor1	-	-	-	m/s	calculated channel
	VelDoor2	-	-	-	m/s	calculated channel
	VelDoor3	-	-	-	m/s	calculated channel
	VelDoor4	-	-	-	m/s	calculated channel
	VelDoor5	-	-	-	m/s	calculated channel
	VelDoor6	-	-	-	m/s	calculated channel

Table D 5. Hardware configuration for Test 1-5.

Wire	Legend/ID	Manufacturer	Model	Slope	Units	Notes
1	TC_Ceiling_Center_020	Omega.com	GG-K-24-SLE-1000	1	°C	At the centre of the ceiling in panel 20 mm from interface
2	TC_Ceiling_Center_035	Omega.com	GG-K-24-SLE-1000	1	°C	At the centre of the ceiling in panel 35 mm from interface
3	TC_Ceiling_Center_050	Omega.com	GG-K-24-SLE-1000	1	°C	At the centre of the ceiling in panel 50 mm from interface
4	TC_Ceiling_Center_065	Omega.com	GG-K-24-SLE-1000	1	°C	At the centre of the ceiling in panel 65 mm from interface
5	TC_Ceiling_Center_090	Omega.com	GG-K-24-SLE-1000	1	°C	At the centre of the ceiling in panel 90 mm from interface
6	TC_Ceiling_Center_115	Omega.com	GG-K-24-SLE-1000	1	°C	At the centre of the ceiling in panel 115 mm from interface
7	TC_Ceiling_Center_070	Omega.com	GG-K-24-SLE-1000	1	°C	At the centre of the ceiling in panel 70 mm from interface
8	TC_W1_Middle_180_020	Omega.com	GG-K-24-SLE-1000	1	°C	W1 at the mid length at h=1.8 m in panel 20 mm from interface
9	TC_W1_Middle_180_035	Omega.com	GG-K-24-SLE-1000	1	°C	W1 at the mid length at h=1.8 m in panel 35 mm from interface
10	TC_W1_Middle_180_050	Omega.com	GG-K-24-SLE-1000	1	°C	W1 at the mid length at h=1.8 m in panel 50 mm from interface
11	TC_W1_Middle_180_065	Omega.com	GG-K-24-SLE-1000	1	°C	W1 at the mid length at h=1.8 m in panel 65 mm from interface
12	TC_W1_Middle_180_090	Omega.com	GG-K-24-SLE-1000	1	°C	W1 at the mid length at h=1.8 m in panel 90 mm from interface
13	TC_W1_Middle_180_115	Omega.com	GG-K-24-SLE-1000	1	°C	W1 at the mid length at h=1.8 m in panel 115 mm from interface
14	TC_W1_Middle_180_140	Omega.com	GG-K-24-SLE-1000	1	°C	W1 at the mid length at h=1.8 m in panel 140 mm from interface
15	TC_W3_Middle_180_020	Omega.com	GG-K-24-SLE-1000	1	°C	W3 at the mid length at h=1.8 m in panel 20 mm from interface
16	TC_W3_Middle_180_035	Omega.com	GG-K-24-SLE-1000	1	°C	W3 at the mid length at h=1.8 m in panel 35 mm from interface
17	TC_W3_Middle_180_050	Omega.com	GG-K-24-SLE-1000	1	°C	W3 at the mid length at h=1.8 m in panel 50 mm from interface
18	TC_W3_Middle_180_065	Omega.com	GG-K-24-SLE-1000	1	°C	W3 at the mid length at h=1.8 m in panel 65 mm from interface
19	TC_W3_Middle_180_090	Omega.com	GG-K-24-SLE-1000	1	°C	W3 at the mid length at h=1.8 m in panel 90 mm from interface
20	TC_W3_Middle_180_115	Omega.com	GG-K-24-SLE-1000	1	°C	W3 at the mid length at h=1.8 m in panel 115 mm from interface
21	TC_W3_Middle_180_070	Omega.com	GG-K-24-SLE-1000	1	°C	W3 at the mid length at h=1.8 m in panel 70 mm from interface
22	TC_W4_Middle_180_020	Omega.com	GG-K-24-SLE-1000	1	°C	W4 at the mid length at h=1.8 m in panel 20 mm from interface
23	TC_W4_Middle_180_035	Omega.com	GG-K-24-SLE-1000	1	°C	W4 at the mid length at h=1.8 m in panel 35 mm from interface
24	TC_W4_Middle_180_050	Omega.com	GG-K-24-SLE-1000	1	°C	W4 at the mid length at h=1.8 m in panel 50 mm from interface

Wire	Legend/ID	Manufacturer	Model	Slope	Units	Notes
25	TC_W4_Middle_180_065	Omega.com	GG-K-24-SLE-1000	1	°C	W4 at the mid length at h=1.8 m in panel 65 mm from interface
26	TC_W4_Middle_180_090	Omega.com	GG-K-24-SLE-1000	1	°C	W4 at the mid length at h=1.8 m in panel 90 mm from interface
27	TC_W4_Middle_180_115	Omega.com	GG-K-24-SLE-1000	1	°C	W4 at the mid length at h=1.8 m in panel 115 mm from interface
28	TC_W4_Middle_180_070	Omega.com	GG-K-24-SLE-1000	1	°C	W4 at the mid length at h=1.8 m in panel 70 mm from interface
29	TC_Tree_Tr1_060	Omega.com	HKQSS-18G-XXX	1	°C	Tree Tr1 at h=0.6 m
30	TC_Tree_Tr1_160	Omega.com	HKQSS-18G-XXX	1	°C	Tree Tr1 at h=1.6 m
31	TC_Tree_Tr1_260	Omega.com	HKQSS-18G-XXX	1	°C	Tree Tr1 at h=2.6 m
32	TC_Tree_Tr2_060	Omega.com	HKQSS-18G-XXX	1	°C	Tree Tr2 at h=0.6 m
33	TC_Tree_Tr2_160	Omega.com	HKQSS-18G-XXX	1	°C	Tree Tr2 at h=1.6 m
34	TC_Tree_Tr2_260	Omega.com	HKQSS-18G-XXX	1	°C	Tree Tr2 at h=2.6 m
35	TC_Tree_Tr3_060	Omega.com	HKQSS-18G-XXX	1	°C	Tree Tr3 at h=0.6 m
36	TC_Tree_Tr3_160	Omega.com	HKQSS-18G-XXX	1	°C	Tree Tr3 at h=1.6 m
37	TC_Tree_Tr3_260	Omega.com	HKQSS-18G-XXX	1	°C	Tree Tr3 at h=2.6 m
38	TC_Tree_Tr4_060	Omega.com	HKQSS-18G-XXX	1	°C	Tree Tr4 at h=0.6 m
39	TC_Tree_Tr4_160	Omega.com	HKQSS-18G-XXX	1	°C	Tree Tr4 at h=1.6 m
40	TC_Tree_Tr4_260	Omega.com	HKQSS-18G-XXX	1	°C	Tree Tr4 at h=2.6 m
41	TC_Tree_Tr5_060	Omega.com	HKQSS-18G-XXX	1	°C	Tree Tr5 at h=0.6 m
42	TC_Tree_Tr5_160	Omega.com	HKQSS-18G-XXX	1	°C	Tree Tr5 at h=1.6 m
43	TC_Tree_Tr5_260	Omega.com	HKQSS-18G-XXX	1	°C	Tree Tr5 at h=2.6 m
44	TC_Tree_Tr6_060	Omega.com	HKQSS-18G-XXX	1	°C	Tree Tr6 at h=0.6 m
45	TC_Tree_Tr6_160	Omega.com	HKQSS-18G-XXX	1	°C	Tree Tr6 at h=1.6 m
46	TC_Tree_Tr6_260	Omega.com	HKQSS-18G-XXX	1	°C	Tree Tr6 at h=2.6 m
47	TC_W1_Middle_060_CLT	Omega.com	GG-K-24-SLE-1000	1	°C	W1 at the mid length at h=0.6 m on the surface of CLT
48	TC_W1_Middle_120_CLT	Omega.com	GG-K-24-SLE-1000	1	°C	W1 at the mid length at h=1.2 m on the surface of CLT
49	TC_W1_Middle_180_CLT	Omega.com	GG-K-24-SLE-1000	1	°C	W1 at the mid length at h=1.8 m on the surface of CLT
50	TC_W1_Middle_060_1GB	Omega.com	GG-K-24-SLE-1000	1	°C	W1 at the mid length at h=0.6 m on the surface of 1st GB
51	TC_W1_Middle_120_1GB	Omega.com	GG-K-24-SLE-1000	1	°C	W1 at the mid length at h=1.2 m on the surface of 1st GB
52	TC_W1_Middle_180_1GB	Omega.com	GG-K-24-SLE-1000	1	°C	W1 at the mid length at h=1.8 m on the surface of 1st GB
53	TC_W1_Middle_060_2GB	Omega.com	GG-K-24-SLE-1000	1	°C	W1 at the mid length at h=0.6 m on the surface of 2nd GB
54	TC_W1_Middle_120_2GB	Omega.com	GG-K-24-SLE-1000	1	°C	W1 at the mid length at h=1.2 m on the surface of 2nd GB
55	TC_W1_Middle_180_070	Omega.com	GG-K-24-SLE-1000	1	°C	W1 at the mid length at h=1.8 m in panel 70 mm from interface
56	TC_W1_Front_180_CLT	Omega.com	GG-K-24-SLE-1000	1	°C	W1 at the front at h=1.8 m on the surface of CLT
57	TC_W1_Front_180_035	Omega.com	GG-K-24-SLE-1000	1	°C	W1 at the front at h=1.8 m in panel 35 mm from interface
58	TC_W1_Front_180_070	Omega.com	GG-K-24-SLE-1000	1	°C	W1 at the front at h=1.8 m in panel 70 mm from interface
59	TC_W1_Rear_180_CLT	Omega.com	GG-K-24-SLE-1000	1	°C	W1 at the rear at h=1.8 m on the surface of CLT
60	TC_W1_Rear_180_035	Omega.com	GG-K-24-SLE-1000	1	°C	W1 at the rear at h=1.8 m in panel 35 mm from interface
61	TC_W1_Rear_180_070	Omega.com	GG-K-24-SLE-1000	1	°C	W1 at the rear at h=1.8 m in panel 70 mm from interface
62	TC_W1_Front_060_CLT	Omega.com	GG-K-24-SLE-1000	1	°C	W1 at the front at h=0.6 m on the surface of CLT
63	TC_W1_Front_060_035	Omega.com	GG-K-24-SLE-1000	1	°C	W1 at the front at h=0.6 m in panel 35 mm from interface
64	TC_W1_Front_060_070	Omega.com	GG-K-24-SLE-1000	1	°C	W1 at the front at h=0.6 m in panel 70 mm from interface
65	TC_W1_Rear_060_CLT	Omega.com	GG-K-24-SLE-1000	1	°C	W1 at the rear at h=0.6 m on the surface of CLT
66	TC_W1_Rear_060_035	Omega.com	GG-K-24-SLE-1000	1	°C	W1 at the rear at h=0.6 m in panel 35 mm from interface
67	TC_W1_Rear_060_070	Omega.com	GG-K-24-SLE-1000	1	°C	W1 at the rear at h=0.6 m in panel 70 mm from interface
68	TC_W3_Middle_060_CLT	Omega.com	GG-K-24-SLE-1000	1	°C	W3 on the surface of CLT
69	TC_W3_Middle_120_CLT	Omega.com	GG-K-24-SLE-1000	1	°C	W3 on the surface of CLT
70	TC_W3_Middle_180_CLT	Omega.com	GG-K-24-SLE-1000	1	°C	W3 on the surface of CLT
71	TC_W3_Middle_060_1GB	Omega.com	GG-K-24-SLE-1000	1	°C	W3 on the surface of 1st GB
72	TC_W3_Middle_120_1GB	Omega.com	GG-K-24-SLE-1000	1	°C	W3 on the surface of 1st GB
73	TC_W3_Middle_180_1GB	Omega.com	GG-K-24-SLE-1000	1	°C	W3 on the surface of 1st GB
74	TC_W3_Middle_060_2GB	Omega.com	GG-K-24-SLE-1000	1	°C	W3 on the surface of 2nd GB
75	TC_W3_Middle_120_2GB	Omega.com	GG-K-24-SLE-1000	1	°C	W3 on the surface of 2nd GB
76	TC_W3_Middle_180_2GB	Omega.com	GG-K-24-SLE-1000	1	°C	W3 on the surface of 2nd GB
77	TC_W4_Middle_060_CLT	Omega.com	GG-K-24-SLE-1000	1	°C	W4 on the surface of CLT
78	TC_W4_Middle_120_CLT	Omega.com	GG-K-24-SLE-1000	1	°C	W4 on the surface of CLT
79	TC_W4_Middle_180_CLT	Omega.com	GG-K-24-SLE-1000	1	°C	W4 on the surface of CLT
80	TC_W4_Middle_060_1GB	Omega.com	GG-K-24-SLE-1000	1	°C	W4 on the surface of 1st GB
81	TC_W4_Middle_120_1GB	Omega.com	GG-K-24-SLE-1000	1	°C	W4 on the surface of 1st GB
82	TC_W4_Middle_180_1GB	Omega.com	GG-K-24-SLE-1000	1	°C	W4 on the surface of 1st GB
83	TC_W4_Middle_060_2GB	Omega.com	GG-K-24-SLE-1000	1	°C	W4 on the surface of 2nd GB
84	TC_W4_Middle_120_2GB	Omega.com	GG-K-24-SLE-1000	1	°C	W4 on the surface of 2nd GB
85	TC_W4_Middle_180_2GB	Omega.com	GG-K-24-SLE-1000	1	°C	W4 on the surface of 2nd GB
86	TC_Ceiling_Tr1_CLT	Omega.com	GG-K-24-SLE-1000	1	°C	ceiling above Tr1 on the surface of CLT
87	TC_Ceiling_Tr1_1GB	Omega.com	GG-K-24-SLE-1000	1	°C	ceiling above Tr1 on the surface of 1st GB
88	TC_Ceiling_Tr1_2GB	Omega.com	GG-K-24-SLE-1000	1	°C	ceiling above Tr1 on the surface of 2nd GB
89	TC_Ceiling_Tr2_CLT	Omega.com	GG-K-24-SLE-1000	1	°C	ceiling above Tr2 on the surface of CLT
90	TC_Ceiling_Tr2_1GB	Omega.com	GG-K-24-SLE-1000	1	°C	ceiling above Tr2 on the surface of 1st GB
91	TC_Ceiling_Tr2_2GB	Omega.com	GG-K-24-SLE-1000	1	°C	ceiling above Tr2 on the surface of 2nd GB
92	TC_Ceiling_Tr3_CLT	Omega.com	GG-K-24-SLE-1000	1	°C	Ceiling above Tr3 on the surface of CLT
93	TC_Ceiling_Tr3_1GB	Omega.com	GG-K-24-SLE-1000	1	°C	Ceiling above Tr3 on the surface of 1st GB
94	TC_Ceiling_Tr3_2GB	Omega.com	GG-K-24-SLE-1000	1	°C	Ceiling above Tr3 on the surface of 2nd GB
95	TC_Ceiling_Tr4_CLT	Omega.com	GG-K-24-SLE-1000	1	°C	Ceiling above Tr4 on the surface of CLT
96	TC_Ceiling_Tr4_1GB	Omega.com	GG-K-24-SLE-1000	1	°C	Ceiling above Tr4 on the surface of 1st GB
97	TC_Ceiling_Tr4_2GB	Omega.com	GG-K-24-SLE-1000	1	°C	Ceiling above Tr4 on the surface of 2nd GB
98	TC_Ceiling_Center_CLT	Omega.com	GG-K-24-SLE-1000	1	°C	Ceiling at the centre on the surface of CLT
99	TC_Ceiling_Center_1GB	Omega.com	GG-K-24-SLE-1000	1	°C	Ceiling at the centre on the surface of 1st GB
100	TC_Ceiling_Center_2GB	Omega.com	GG-K-24-SLE-1000	1	°C	Ceiling at the centre on the surface of 2nd GB
101	Gardon_Floor_Center	Medtherm	64-20-18	17360	kW/m2	At the center of the floor

Wire	Legend/ID	Manufacturer	Model	Slope	Units	Notes
102	Gardon_W1_Middle_180	Medtherm	64-20-18	18550	kW/m2	W1 at the mid length at h=1.8 m
103	PT_W1_Middle_180_SPy	Omega.com	GG-K-24-SLE-1000	1	°C	Temperature for plate thermometer on W1 at the mid length at h=1.8 m
104	DFT_W1_Middle_180_Px	Sandia	TN-TN-K	1	°C	DFT on W1 at the mid length at h=1.8 m (Front plate)
105	PT_W1_Middle_180_SPx	Pentronic	5928060-001	1	°C	Plate thermometer on W1 at the mid length at h=1.8 m
106	PT_W1_Front_180_SPy	Omega.com	GG-K-24-SLE-1000	1	°C	Temperature for plate thermometer on W1 at front
107	PT_W3_Middle_180_SPx	Pentronic	TN-TN-K	1	°C	Plate thermometer on W3 at the mid length at h=1.8 m
108	PT_W1_Front_180_SPx	Pentronic	5928060-001	1	°C	Plate thermometer on W1 in the front of the compartment at h=1.8 m
109	PT_W1_Rear_180_SPy	Omega.com	GG-K-24-SLE-1000	1	°C	Temperature for plate thermometer on W1 in the rear of the compartment at h=1.8 m
110	PT_W4_Middle_180_SPx	Pentronic	TN-TN-K	1	°C	Plate thermometer on W4 at the mid length at h=1.8 m
111	PT_W1_Rear_180_SPx	Pentronic	5928060-001	1	°C	plate thermometer on W1 in the rear of the compartment at h=1.8 m
112	PT_Ceiling_Center_SPy	Omega.com	GG-K-24-SLE-1000	1	°C	Temperature for plate thermometer at the centre of the ceiling
113	DFT_Ceiling_Center_Px	Sandia	TN-TN-K	1	°C	DFT at the centre of the ceiling (Back plate)
114	PT_Ceiling_Center_SPx	Pentronic	5928060-001	1	°C	Plate thermometer at the centre of the ceiling
115	PT_Ceiling_Bed_SPy	Omega.com	GG-K-24-SLE-1000	1	°C	Temperature for plate thermometer on ceiling above the bed
116	DFT_Ceiling_Bed_Px	Sandia	TN-TN-K	1	°C	DFT on the ceiling above the bed (Back plate)
117	PT_Ceiling_Bed_SPx	Pentronic	5928060-001	1	°C	Plate thermometer on the ceiling above the bed
118	dP_c	Greisinger	GMH 3181-01	400	Pa	5/8" diameter bidirectional probe on ceiling near STE 6, Direction normal to the opening
120	dP_r	Greisinger	GMH 3181-01	400	Pa	On smoke sample line near gas analyzer sample line at 2.1m 1/4" SS tube
121	STE_1	FM Global	See "Drawings"	1	°C	12" below ceiling (see "Drawings")
122	STE_2	FM Global	See "Drawings"	1	°C	12" below ceiling (see "Drawings")
123	STE_3	FM Global	See "Drawings"	1	°C	12" below ceiling (see "Drawings")
124	STE_4	FM Global	See "Drawings"	1	°C	18" below ceiling (see "Drawings")
125	STE_5	FM Global	See "Drawings"	1	°C	12" below ceiling (see "Drawings")
126	STE_6	FM Global	See "Drawings"	1	°C	12" below ceiling (see "Drawings")
127	STE_7	FM Global	See "Drawings"	1	°C	12" below ceiling (see "Drawings")
128	STE_8	FM Global	See "Drawings"	1	°C	18" below ceiling (see "Drawings")
129	STE_9	FM Global	See "Drawings"	1	°C	12" below ceiling (see "Drawings")
130	STE_10	FM Global	See "Drawings"	1	°C	12" below ceiling (see "Drawings")
131	TC_V_c	Omega.com	GG-K-24-SLE-1000	1	°C	Temperature co-located with V_c
132	SmokeAlarm	Kidde	PE120	1	V	Smoke detector at the centre of the ceiling
133	HeatAlarm	Kidde	HD135F	1	V	Heat detector at the centre of the ceiling
134	O2_room	-	-	4.278	%	At the centre of the room, 2.1 m high
135	CO2_room	-	-	3.744	%	At the centre of the room, 2.1 m high
136	CO_room	-	-	4.423	%	At the centre of the room, 2.1 m high
137	SMOKE	NRC	Photo Diode Meter	1	V	at the centre of the room, 1.6 m high
138	Door_TC_1	Omega.com	HKQSS-18G-XXX	1	°C	At the centreline of the opening
139	Door_TC_2	Omega.com	HKQSS-18G-XXX	1	°C	At the centreline of the opening
140	Door_TC_3	Omega.com	HKQSS-18G-XXX	1	°C	At the centreline of the opening
141	Door_TC_4	Omega.com	HKQSS-18G-XXX	1	°C	At the centreline of the opening
142	Door_TC_5	Omega.com	HKQSS-18G-XXX	1	°C	At the centreline of the opening
143	Door_TC_6	Omega.com	HKQSS-18G-XXX	1	°C	At the centreline of the opening
144	Door_TC_7	Omega.com	HKQSS-18G-XXX	1	°C	At the centreline of the opening
145	dP_o1	Greisinger	GMH 3181-01	400	Pa	5/8" diameter bidirectional probe at the opening (low, long side)
146	dP_o2	Greisinger	GMH 3181-01	400	Pa	5/8" diameter bidirectional probe at the opening (low, middle)
147	dP_o3	Greisinger	GMH 3181-01	400	Pa	5/8" diameter bidirectional probe at the opening (low, short side)
148	dP_o4	Greisinger	GMH 3181-01	400	Pa	5/8" diameter bidirectional probe at the opening (high, long side)
149	dP_o5	Greisinger	GMH 3181-01	400	Pa	5/8" diameter bidirectional probe at the opening (high, middle)
150	dP_o6	Greisinger	GMH 3181-01	400	Pa	5/8" diameter bidirectional probe at the opening (high, short side)
151	Gardon_Front_a480	Medtherm	64-20-18	19460	kW/m2	facing the centre of the opening
152	Gardon_Front_a240	Medtherm	64-20-18	20980	kW/m2	facing the centre of the opening
153	Gardon_Front_e350	Medtherm	64-20-18	19660	kW/m2	3.5 m above ground
154	Gardon_Front_e550	Medtherm	64-20-18	19020	kW/m2	5.5 m above ground
155	Roof_TC_350	Omega.com	GG-K-24-SLE-1000	1	°C	3.5 m above ground
156	Roof_TC_450	Omega.com	GG-K-24-SLE-1000	1	°C	4.5 m above ground
157	Roof_TC_550	Omega.com	GG-K-24-SLE-1000	1	°C	5.5 m above ground
158	Roof_TC_650	Omega.com	GG-K-24-SLE-1000	1	°C	6.5 m above ground
159	Roof_TC_750	Omega.com	GG-K-24-SLE-1000	1	°C	7.5 m above ground
161	DFT_W1_Middle_180_Py	Sandia	TN-TN-K	1	°C	DFT on W1 at the mid length at h=1.8 m
162	PT_W3_Middle_180_SPy	Omega.com	GG-K-24-SLE-1000	1	°C	Temperature for plate thermometer on W3 at the mid length at h=1.8 m
163	PT_W4_Middle_180_SPy	Omega.com	GG-K-24-SLE-1000	1	°C	Temperature for plate thermometer on W4 at the mid length at h=1.8 m
164	DFT_Ceiling_Center_Py	Sandia	TN-TN-K	1	°C	DFT at the centre of the ceiling (Front plate)
165	DFT_Ceiling_Bed_Py	Sandia	TN-TN-K	1	°C	DFT on the ceiling above the bed (Front plate)
166	DEWpt_rack	-	-	30.121	°C	Gas rack dew point measurement
167	TC_Tree_Tr1_110	Omega.com	HKQSS-18G-XXX	1	°C	Tree Tr1 at h=1.1 m
168	TC_Tree_Tr1_210	Omega.com	HKQSS-18G-XXX	1	°C	Tree Tr1 at h=2.1 m
169	TC_Tree_Tr2_110	Omega.com	HKQSS-18G-XXX	1	°C	Tree Tr2 at h=1.1 m
170	TC_Tree_Tr2_210	Omega.com	HKQSS-18G-XXX	1	°C	Tree Tr2 at h=2.1 m
171	TC_Tree_Tr3_110	Omega.com	HKQSS-18G-XXX	1	°C	Tree Tr3 at h=1.1 m
172	TC_Tree_Tr3_210	Omega.com	HKQSS-18G-XXX	1	°C	Tree Tr3 at h=2.1 m
173	TC_Tree_Tr4_110	Omega.com	HKQSS-18G-XXX	1	°C	Tree Tr4 at h=1.1 m
174	TC_Tree_Tr4_210	Omega.com	HKQSS-18G-XXX	1	°C	Tree Tr4 at h=2.1 m
175	TC_Tree_Tr5_110	Omega.com	HKQSS-18G-XXX	1	°C	Tree Tr5 at h=1.1 m
176	TC_Tree_Tr5_210	Omega.com	HKQSS-18G-XXX	1	°C	Tree Tr5 at h=2.1 m
177	TC_Tree_Tr6_110	Omega.com	HKQSS-18G-XXX	1	°C	Tree Tr6 at h=1.1 m
178	TC_Tree_Tr6_210	Omega.com	HKQSS-18G-XXX	1	°C	Tree Tr6 at h=2.1 m
179	PT_Front_a480_SPy	Omega.com	GG-K-24-SLE-1000	1	°C	Facing the centre of the opening (offset 150 from centerline)
180	PT_Front_a480_SPx	Pentronic	5928060-001	1	°C	Facing the centre of the opening (offset 150 from centerline)

Wire	Legend/ID	Manufacturer	Model	Slope	Units	Notes
181	PT_Front_a240_SPy	Omega.com	GG-K-24-SLE-1000	1	°C	Facing the centre of the opening (offset 150 from centerline)
182	PT_Front_a240_SPx	Pentronic	5928060-001	1	°C	Facing the centre of the opening (offset 150 from centerline)
183	PT_Front_e350_SPx	Pentronic	5928060-001	1	°C	3.5 m above ground
184	PT_Front_e550_SPx	Pentronic	5928060-001	1	°C	5.5 m above the top of the opening
185	TC_Smoke	Omega.com	GG-K-24-SLE-1000	1	°C	Gas temperature at SMOKE2 outflow (for shutoff)
186	TC_HFGtower	Omega.com	EXPP-K-24-SLE-1000	1	°C	H2O outflow temperatures of heat flux gages on roof tower
187	TC_HFGfloor	Omega.com	KMQSS-040	1	°C	H2O outflow temperatures of heat flux gages on floor
188	TC_HFGw1	Omega.com	KMQSS-040	1	°C	H2O outflow temperatures of heat flux gages on W1
189	TC_GoPro	Omega.com	KMQSS-040	1	°C	H2O outflow temperatures of GoPro water bath
190	TC_TreeSteel	Omega.com	GG-K-24-SLE-1000	1	°C	Temperature of steel behind thermal insulation in Tree 03 at 2.1 m height
191	TC_TBD	Omega.com	GG-K-24-SLE-1000	1	°C	Extra TC location TBD
	VI	-	-	1	V	Internal heartbeat
	HRR	-	-	1	kW	calculated channel
	HRRburner	-	-	1	kW	calculated channel
	VelCeiling	-	-	-	m/s	calculated channel
	VelDoor1	-	-	-	m/s	calculated channel
	VelDoor2	-	-	-	m/s	calculated channel
	VelDoor3	-	-	-	m/s	calculated channel
	VelDoor4	-	-	-	m/s	calculated channel
	VelDoor5	-	-	-	m/s	calculated channel
	VelDoor6	-	-	-	m/s	calculated channel

Table D 6. Hardware configuration for Test 1-6.

Wire	Legend/ID	Manufacturer	Model	Slope	Units	Notes
1	TC_Ceiling_Center_020	Omega.com	GG-K-24-SLE-1000	1	°C	At the centre of the ceiling in panel 20 mm from interface
2	TC_Ceiling_Center_035	Omega.com	GG-K-24-SLE-1000	1	°C	At the centre of the ceiling in panel 35 mm from interface
3	TC_Ceiling_Center_050	Omega.com	GG-K-24-SLE-1000	1	°C	At the centre of the ceiling in panel 50 mm from interface
4	TC_Ceiling_Center_065	Omega.com	GG-K-24-SLE-1000	1	°C	At the centre of the ceiling in panel 65 mm from interface
5	TC_Ceiling_Center_090	Omega.com	GG-K-24-SLE-1000	1	°C	At the centre of the ceiling in panel 90 mm from interface
6	TC_Ceiling_Center_115	Omega.com	GG-K-24-SLE-1000	1	°C	At the centre of the ceiling in panel 115 mm from interface
7	TC_Ceiling_Center_140	Omega.com	GG-K-24-SLE-1000	1	°C	At the centre of the ceiling in panel 140 mm from interface
8	TC_W1_Middle_180_020	Omega.com	GG-K-24-SLE-1000	1	°C	W1 at the mid length at h=1.8 m in panel 20 mm from interface
9	TC_W1_Middle_180_035	Omega.com	GG-K-24-SLE-1000	1	°C	W1 at the mid length at h=1.8 m in panel 35 mm from interface
10	TC_W1_Middle_180_050	Omega.com	GG-K-24-SLE-1000	1	°C	W1 at the mid length at h=1.8 m in panel 50 mm from interface
11	TC_W1_Middle_180_065	Omega.com	GG-K-24-SLE-1000	1	°C	W1 at the mid length at h=1.8 m in panel 65 mm from interface
12	TC_W1_Middle_180_090	Omega.com	GG-K-24-SLE-1000	1	°C	W1 at the mid length at h=1.8 m in panel 90 mm from interface
13	TC_W1_Middle_180_115	Omega.com	GG-K-24-SLE-1000	1	°C	W1 at the mid length at h=1.8 m in panel 115 mm from interface
14	TC_W1_Middle_180_140	Omega.com	GG-K-24-SLE-1000	1	°C	W1 at the mid length at h=1.8 m in panel 140 mm from interface
15	TC_W3_Middle_180_020	Omega.com	GG-K-24-SLE-1000	1	°C	W3 at the mid length at h=1.8 m in panel 20 mm from interface
16	TC_W3_Middle_180_035	Omega.com	GG-K-24-SLE-1000	1	°C	W3 at the mid length at h=1.8 m in panel 35 mm from interface
17	TC_W3_Middle_180_050	Omega.com	GG-K-24-SLE-1000	1	°C	W3 at the mid length at h=1.8 m in panel 50 mm from interface
18	TC_W3_Middle_180_065	Omega.com	GG-K-24-SLE-1000	1	°C	W3 at the mid length at h=1.8 m in panel 65 mm from interface
19	TC_W3_Middle_180_090	Omega.com	GG-K-24-SLE-1000	1	°C	W3 at the mid length at h=1.8 m in panel 90 mm from interface
20	TC_W3_Middle_180_115	Omega.com	GG-K-24-SLE-1000	1	°C	W3 at the mid length at h=1.8 m in panel 115 mm from interface
21	TC_W3_Middle_180_070	Omega.com	GG-K-24-SLE-1000	1	°C	W3 at the mid length at h=1.8 m in panel 70 mm from interface
22	TC_W4_Middle_180_020	Omega.com	GG-K-24-SLE-1000	1	°C	W4 at the mid length at h=1.8 m in panel 20 mm from interface
23	TC_W4_Middle_180_035	Omega.com	GG-K-24-SLE-1000	1	°C	W4 at the mid length at h=1.8 m in panel 35 mm from interface
24	TC_W4_Middle_180_050	Omega.com	GG-K-24-SLE-1000	1	°C	W4 at the mid length at h=1.8 m in panel 50 mm from interface
25	TC_W4_Middle_180_065	Omega.com	GG-K-24-SLE-1000	1	°C	W4 at the mid length at h=1.8 m in panel 65 mm from interface
26	TC_W4_Middle_180_090	Omega.com	GG-K-24-SLE-1000	1	°C	W4 at the mid length at h=1.8 m in panel 90 mm from interface
27	TC_W4_Middle_180_115	Omega.com	GG-K-24-SLE-1000	1	°C	W4 at the mid length at h=1.8 m in panel 115 mm from interface
28	TC_W4_Middle_180_070	Omega.com	GG-K-24-SLE-1000	1	°C	W4 at the mid length at h=1.8 m in panel 70 mm from interface
29	TC_Tree_Tr1_060	Omega.com	HKQSS-18G-XXX	1	°C	Tree Tr1 at h=0.6 m
30	TC_Tree_Tr1_160	Omega.com	HKQSS-18G-XXX	1	°C	Tree Tr1 at h=1.6 m
31	TC_Tree_Tr1_260	Omega.com	HKQSS-18G-XXX	1	°C	Tree Tr1 at h=2.6 m
32	TC_Tree_Tr2_060	Omega.com	HKQSS-18G-XXX	1	°C	Tree Tr2 at h=0.6 m
33	TC_Tree_Tr2_160	Omega.com	HKQSS-18G-XXX	1	°C	Tree Tr2 at h=1.6 m
34	TC_Tree_Tr2_260	Omega.com	HKQSS-18G-XXX	1	°C	Tree Tr2 at h=2.6 m
35	TC_Tree_Tr3_060	Omega.com	HKQSS-18G-XXX	1	°C	Tree Tr3 at h=0.6 m
36	TC_Tree_Tr3_160	Omega.com	HKQSS-18G-XXX	1	°C	Tree Tr3 at h=1.6 m
37	TC_Tree_Tr3_260	Omega.com	HKQSS-18G-XXX	1	°C	Tree Tr3 at h=2.6 m
38	TC_Tree_Tr4_060	Omega.com	HKQSS-18G-XXX	1	°C	Tree Tr4 at h=0.6 m
39	TC_Tree_Tr4_160	Omega.com	HKQSS-18G-XXX	1	°C	Tree Tr4 at h=1.6 m
40	TC_Tree_Tr4_260	Omega.com	HKQSS-18G-XXX	1	°C	Tree Tr4 at h=2.6 m
41	TC_Tree_Tr5_060	Omega.com	HKQSS-18G-XXX	1	°C	Tree Tr5 at h=0.6 m
42	TC_Tree_Tr5_160	Omega.com	HKQSS-18G-XXX	1	°C	Tree Tr5 at h=1.6 m
43	TC_Tree_Tr5_260	Omega.com	HKQSS-18G-XXX	1	°C	Tree Tr5 at h=2.6 m
44	TC_Tree_Tr6_060	Omega.com	HKQSS-18G-XXX	1	°C	Tree Tr6 at h=0.6 m
45	TC_Tree_Tr6_160	Omega.com	HKQSS-18G-XXX	1	°C	Tree Tr6 at h=1.6 m
46	TC_Tree_Tr6_260	Omega.com	HKQSS-18G-XXX	1	°C	Tree Tr6 at h=2.6 m
47	TC_W1_Middle_060_CLT	Omega.com	GG-K-24-SLE-1000	1	°C	W1 at the mid length at h=0.6 m on the surface of CLT
48	TC_W1_Middle_120_CLT	Omega.com	GG-K-24-SLE-1000	1	°C	W1 at the mid length at h=1.2 m on the surface of CLT
49	TC_W1_Middle_180_CLT	Omega.com	GG-K-24-SLE-1000	1	°C	W1 at the mid length at h=1.8 m on the surface of CLT
50	TC_W1_Middle_060_1GB	Omega.com	GG-K-24-SLE-1000	1	°C	W1 at the mid length at h=0.6 m on the surface of 1st GB

Wire	Legend/ID	Manufacturer	Model	Slope	Units	Notes
51	TC_W1_Middle_120_1GB	Omega.com	GG-K-24-SLE-1000	1	°C	W1 at the mid length at h=1.2 m on the surface of 1st GB
52	TC_W1_Middle_180_1GB	Omega.com	GG-K-24-SLE-1000	1	°C	W1 at the mid length at h=1.8 m on the surface of 1st GB
53	TC_W1_Middle_060_2GB	Omega.com	GG-K-24-SLE-1000	1	°C	W1 at the mid length at h=0.6 m on the surface of 2nd GB
54	TC_W1_Middle_120_2GB	Omega.com	GG-K-24-SLE-1000	1	°C	W1 at the mid length at h=1.2 m on the surface of 2nd GB
55	TC_W1_Middle_180_070	Omega.com	GG-K-24-SLE-1000	1	°C	W1 at the mid length at h=1.8 m in panel 70 mm from interface
56	TC_W1_Front_180_CLT	Omega.com	GG-K-24-SLE-1000	1	°C	W1 at the front at h=1.8 m on the surface of CLT
57	TC_W1_Front_180_035	Omega.com	GG-K-24-SLE-1000	1	°C	W1 at the front at h=1.8 m in panel 35 mm from interface
58	TC_W1_Front_180_070	Omega.com	GG-K-24-SLE-1000	1	°C	W1 at the front at h=1.8 m in panel 70 mm from interface
59	TC_W1_Rear_180_CLT	Omega.com	GG-K-24-SLE-1000	1	°C	W1 at the rear at h=1.8 m on the surface of CLT
60	TC_W1_Rear_180_035	Omega.com	GG-K-24-SLE-1000	1	°C	W1 at the rear at h=1.8 m in panel 35 mm from interface
61	TC_W1_Rear_180_070	Omega.com	GG-K-24-SLE-1000	1	°C	W1 at the rear at h=1.8 m in panel 70 mm from interface
62	TC_W1_Front_060_CLT	Omega.com	GG-K-24-SLE-1000	1	°C	W1 at the front at h=0.6 m on the surface of CLT
63	TC_W1_Front_060_035	Omega.com	GG-K-24-SLE-1000	1	°C	W1 at the front at h=0.6 m in panel 35 mm from interface
64	TC_W1_Front_060_070	Omega.com	GG-K-24-SLE-1000	1	°C	W1 at the front at h=0.6 m in panel 70 mm from interface
65	TC_W1_Rear_060_CLT	Omega.com	GG-K-24-SLE-1000	1	°C	W1 at the rear at h=0.6 m on the surface of CLT
66	TC_W1_Rear_060_035	Omega.com	GG-K-24-SLE-1000	1	°C	W1 at the rear at h=0.6 m in panel 35 mm from interface
67	TC_W1_Rear_060_070	Omega.com	GG-K-24-SLE-1000	1	°C	W1 at the rear at h=0.6 m in panel 70 mm from interface
68	TC_W3_Middle_060_CLT	Omega.com	GG-K-24-SLE-1000	1	°C	W3 on the surface of CLT
69	TC_W3_Middle_120_CLT	Omega.com	GG-K-24-SLE-1000	1	°C	W3 on the surface of CLT
70	TC_W3_Middle_180_CLT	Omega.com	GG-K-24-SLE-1000	1	°C	W3 on the surface of CLT
71	TC_W3_Middle_060_1GB	Omega.com	GG-K-24-SLE-1000	1	°C	W3 on the surface of 1st GB
72	TC_W3_Middle_120_1GB	Omega.com	GG-K-24-SLE-1000	1	°C	W3 on the surface of 1st GB
73	TC_W3_Middle_180_1GB	Omega.com	GG-K-24-SLE-1000	1	°C	W3 on the surface of 1st GB
74	TC_W3_Middle_060_2GB	Omega.com	GG-K-24-SLE-1000	1	°C	W3 on the surface of 2nd GB
75	TC_W3_Middle_120_2GB	Omega.com	GG-K-24-SLE-1000	1	°C	W3 on the surface of 2nd GB
76	TC_W3_Middle_180_2GB	Omega.com	GG-K-24-SLE-1000	1	°C	W3 on the surface of 2nd GB
77	TC_W4_Middle_060_CLT	Omega.com	GG-K-24-SLE-1000	1	°C	W4 on the surface of CLT
78	TC_W4_Middle_120_CLT	Omega.com	GG-K-24-SLE-1000	1	°C	W4 on the surface of CLT
79	TC_W4_Middle_180_CLT	Omega.com	GG-K-24-SLE-1000	1	°C	W4 on the surface of CLT
80	TC_W4_Middle_060_1GB	Omega.com	GG-K-24-SLE-1000	1	°C	W4 on the surface of 1st GB
81	TC_W4_Middle_120_1GB	Omega.com	GG-K-24-SLE-1000	1	°C	W4 on the surface of 1st GB
82	TC_W4_Middle_180_1GB	Omega.com	GG-K-24-SLE-1000	1	°C	W4 on the surface of 1st GB
83	TC_W4_Middle_060_2GB	Omega.com	GG-K-24-SLE-1000	1	°C	W4 on the surface of 2nd GB
84	TC_W4_Middle_120_2GB	Omega.com	GG-K-24-SLE-1000	1	°C	W4 on the surface of 2nd GB
85	TC_W4_Middle_180_2GB	Omega.com	GG-K-24-SLE-1000	1	°C	W4 on the surface of 2nd GB
86	TC_Ceiling_Tr1_CLT	Omega.com	GG-K-24-SLE-1000	1	°C	ceiling above Tr1 on the surface of CLT
87	TC_Ceiling_Tr1_035	Omega.com	GG-K-24-SLE-1000	1	°C	ceiling above Tr1 in panel 35 mm from interface
88	TC_Ceiling_Tr1_070	Omega.com	GG-K-24-SLE-1000	1	°C	ceiling above Tr1 in panel 70 mm from interface
89	TC_Ceiling_Tr2_CLT	Omega.com	GG-K-24-SLE-1000	1	°C	ceiling above Tr2 on the surface of CLT
90	TC_Ceiling_Tr2_035	Omega.com	GG-K-24-SLE-1000	1	°C	ceiling above Tr2 in panel 35 mm from interface
91	TC_Ceiling_Tr2_070	Omega.com	GG-K-24-SLE-1000	1	°C	ceiling above Tr2 in panel 70 mm from interface
92	TC_Ceiling_Tr3_CLT	Omega.com	GG-K-24-SLE-1000	1	°C	Ceiling above Tr3 on the surface of CLT
93	TC_Ceiling_Tr3_035	Omega.com	GG-K-24-SLE-1000	1	°C	Ceiling above Tr3 in panel 35 mm from interface
94	TC_Ceiling_Tr3_070	Omega.com	GG-K-24-SLE-1000	1	°C	Ceiling above Tr3 in panel 70 mm from interface
95	TC_Ceiling_Tr4_CLT	Omega.com	GG-K-24-SLE-1000	1	°C	Ceiling above Tr4 on the surface of CLT
96	TC_Ceiling_Tr4_035	Omega.com	GG-K-24-SLE-1000	1	°C	Ceiling above Tr4 in panel 35 mm from interface
97	TC_Ceiling_Tr4_070	Omega.com	GG-K-24-SLE-1000	1	°C	Ceiling above Tr4 in panel 70 mm from interface
98	TC_Ceiling_Center_CLT	Omega.com	GG-K-24-SLE-1000	1	°C	Ceiling at the centre on the surface of CLT
99	TC_Ceiling_Center_1GB	Omega.com	GG-K-24-SLE-1000	1	°C	Ceiling at the centre on the surface of 1st GB
100	TC_Ceiling_Center_070	Omega.com	GG-K-24-SLE-1000	1	°C	Ceiling at the centre in panel 70 mm from interface
101	Gardon_Floor_Center	Medtherm	64-20-18	17360	kW/m2	At the center of the floor
102	Gardon_W1_Middle_180	Medtherm	64-20-18	18550	kW/m2	W1 at the mid length at h=1.8 m
103	PT_W1_Middle_180_SPy	Omega.com	GG-K-24-SLE-1000	1	°C	Temperature for plate thermometer on W1 at the mid length at h=1.8 m
104	DFT_W1_Middle_180_Px	Sandia	TN-TN-K	1	°C	DFT on W1 at the mid length at h=1.8 m (Front plate)
105	PT_W1_Middle_180_SPx	Pentronic	5928060-001	1	°C	Plate thermometer on W1 at the mid length at h=1.8 m
106	PT_W1_Front_180_SPy	Omega.com	GG-K-24-SLE-1000	1	°C	Temperature for plate thermometer on W1 at front
107	PT_W3_Middle_180_SPx	Pentronic	TN-TN-K	1	°C	Plate thermometer on W3 at the mid length at h=1.8 m
108	PT_W1_Front_180_SPx	Pentronic	5928060-001	1	°C	Plate thermometer on W1 in the front of the compartment at h=1.8 m
109	PT_W1_Rear_180_SPy	Omega.com	GG-K-24-SLE-1000	1	°C	Temperature for plate thermometer on W1 in the rear of the compartment at h=1.8 m
110	PT_W4_Middle_180_SPx	Pentronic	TN-TN-K	1	°C	Plate thermometer on W4 at the mid length at h=1.8 m
111	PT_W1_Rear_180_SPx	Pentronic	5928060-001	1	°C	plate thermometer on W1 in the rear of the compartment at h=1.8 m
112	PT_Ceiling_Center_SPy	Omega.com	GG-K-24-SLE-1000	1	°C	Temperature for plate thermometer at the centre of the ceiling
113	DFT_Ceiling_Center_Px	Sandia	TN-TN-K	1	°C	DFT at the centre of the ceiling (Back plate)
114	PT_Ceiling_Center_SPx	Pentronic	5928060-001	1	°C	Plate thermometer at the centre of the ceiling
115	PT_Ceiling_Bed_SPy	Omega.com	GG-K-24-SLE-1000	1	°C	Temperature for plate thermometer on ceiling above the bed
116	DFT_Ceiling_Bed_Px	Sandia	TN-TN-K	1	°C	DFT on the ceiling above the bed (Back plate)
117	PT_Ceiling_Bed_SPx	Pentronic	5928060-001	1	°C	Plate thermometer on the ceiling above the bed
118	dP_c	Greisinger	GMH 3181-01	400	Pa	5/8" diameter bidirectional probe on ceiling near STE 6, Direction normal to the opening
120	dP_r	Greisinger	GMH 3181-01	400	Pa	On smoke sample line near gas analyzer sample line at 2.1m 1/4" SS tube
121	STE_1	FM Global	See "Drawings"	1	°C	12" below ceiling (see "Drawings")
122	STE_2	FM Global	See "Drawings"	1	°C	12" below ceiling (see "Drawings")
123	STE_3	FM Global	See "Drawings"	1	°C	12" below ceiling (see "Drawings")
124	STE_4	FM Global	See "Drawings"	1	°C	18" below ceiling (see "Drawings")
125	STE_5	FM Global	See "Drawings"	1	°C	12" below ceiling (see "Drawings")
126	STE_6	FM Global	See "Drawings"	1	°C	12" below ceiling (see "Drawings")
127	STE_7	FM Global	See "Drawings"	1	°C	12" below ceiling (see "Drawings")
128	STE_8	FM Global	See "Drawings"	1	°C	18" below ceiling (see "Drawings")

Wire	Legend/ID	Manufacturer	Model	Slope	Units	Notes
129	STE_9	FM Global	See "Drawings"	1	°C	12" below ceiling (see "Drawings")
130	STE_10	FM Global	See "Drawings"	1	°C	12" below ceiling (see "Drawings")
131	TC_V_c	Omega.com	GG-K-24-SLE-1000	1	°C	Temperature co-located with V_c
132	SmokeAlarm	Kidde	PE120	1	V	Smoke detector at the centre of the ceiling
133	HeatAlarm	Kidde	HD135F	1	V	Heat detector at the centre of the ceiling
134	O2_room	-	-	4.279	%	At the centre of the room, 2.1 m high
135	CO2_room	-	-	3.752	%	At the centre of the room, 2.1 m high
136	CO_room	-	-	4.420	%	At the centre of the room, 2.1 m high
137	SMOKE	NRC	Photo Diode Meter	1	V	at the centre of the room, 1.6 m high
138	Door_TC_1	Omega.com	HKQSS-18G-XXX	1	°C	At the centreline of the opening
139	Door_TC_2	Omega.com	HKQSS-18G-XXX	1	°C	At the centreline of the opening
140	Door_TC_3	Omega.com	HKQSS-18G-XXX	1	°C	At the centreline of the opening
141	Door_TC_4	Omega.com	HKQSS-18G-XXX	1	°C	At the centreline of the opening
142	Door_TC_5	Omega.com	HKQSS-18G-XXX	1	°C	At the centreline of the opening
143	Door_TC_6	Omega.com	HKQSS-18G-XXX	1	°C	At the centreline of the opening
144	Door_TC_7	Omega.com	HKQSS-18G-XXX	1	°C	At the centreline of the opening
145	dP_o1	Greisinger	GMH 3181-01	400	Pa	5/8" diameter bidirectional probe at the opening (low, long side)
146	dP_o2	Greisinger	GMH 3181-01	400	Pa	5/8" diameter bidirectional probe at the opening (low, middle)
147	dP_o3	Greisinger	GMH 3181-01	400	Pa	5/8" diameter bidirectional probe at the opening (low, short side)
148	dP_o4	Greisinger	GMH 3181-01	400	Pa	5/8" diameter bidirectional probe at the opening (high, long side)
149	dP_o5	Greisinger	GMH 3181-01	400	Pa	5/8" diameter bidirectional probe at the opening (high, middle)
150	dP_o6	Greisinger	GMH 3181-01	400	Pa	5/8" diameter bidirectional probe at the opening (high, short side)
151	Gardon_Front_a480	Medtherm	64-20-18	19460	kW/m2	facing the centre of the opening
152	Gardon_Front_a240	Medtherm	64-20-18	20980	kW/m2	facing the centre of the opening
153	Gardon_Front_e350	Medtherm	64-20-18	19660	kW/m2	3.5 m above ground
154	Gardon_Front_e550	Medtherm	64-20-18	19020	kW/m2	5.5 m above ground
155	Roof_TC_350	Omega.com	GG-K-24-SLE-1000	1	°C	3.5 m above ground
156	Roof_TC_450	Omega.com	GG-K-24-SLE-1000	1	°C	4.5 m above ground
157	Roof_TC_550	Omega.com	GG-K-24-SLE-1000	1	°C	5.5 m above ground
158	Roof_TC_650	Omega.com	GG-K-24-SLE-1000	1	°C	6.5 m above ground
159	Roof_TC_750	Omega.com	GG-K-24-SLE-1000	1	°C	7.5 m above ground
161	DFT_W1_Middle_180_Py	Sandia	TN-TN-K	1	°C	DFT on W1 at the mid length at h=1.8 m
162	PT_W3_Middle_180_SPy	Omega.com	GG-K-24-SLE-1000	1	°C	Temperature for plate thermometer on W3 at the mid length at h=1.8 m
163	PT_W4_Middle_180_SPy	Omega.com	GG-K-24-SLE-1000	1	°C	Temperature for plate thermometer on W4 at the mid length at h=1.8 m
164	DFT_Ceiling_Center_Py	Sandia	TN-TN-K	1	°C	DFT at the centre of the ceiling (Front plate)
165	DFT_Ceiling_Bed_Py	Sandia	TN-TN-K	1	°C	DFT on the ceiling above the bed (Front plate)
166	DEWpt_rack	-	-	30.121	°C	Gas rack dew point measurement
167	TC_Tree_Tr1_110	Omega.com	HKQSS-18G-XXX	1	°C	Tree Tr1 at h=1.1 m
168	TC_Tree_Tr1_210	Omega.com	HKQSS-18G-XXX	1	°C	Tree Tr1 at h=2.1 m
169	TC_Tree_Tr2_110	Omega.com	HKQSS-18G-XXX	1	°C	Tree Tr2 at h=1.1 m
170	TC_Tree_Tr2_210	Omega.com	HKQSS-18G-XXX	1	°C	Tree Tr2 at h=2.1 m
171	TC_Tree_Tr3_110	Omega.com	HKQSS-18G-XXX	1	°C	Tree Tr3 at h=1.1 m
172	TC_Tree_Tr3_210	Omega.com	HKQSS-18G-XXX	1	°C	Tree Tr3 at h=2.1 m
173	TC_Tree_Tr4_110	Omega.com	HKQSS-18G-XXX	1	°C	Tree Tr4 at h=1.1 m
174	TC_Tree_Tr4_210	Omega.com	HKQSS-18G-XXX	1	°C	Tree Tr4 at h=2.1 m
175	TC_Tree_Tr5_110	Omega.com	HKQSS-18G-XXX	1	°C	Tree Tr5 at h=1.1 m
176	TC_Tree_Tr5_210	Omega.com	HKQSS-18G-XXX	1	°C	Tree Tr5 at h=2.1 m
177	TC_Tree_Tr6_110	Omega.com	HKQSS-18G-XXX	1	°C	Tree Tr6 at h=1.1 m
178	TC_Tree_Tr6_210	Omega.com	HKQSS-18G-XXX	1	°C	Tree Tr6 at h=2.1 m
179	PT_Front_a480_SPy	Omega.com	GG-K-24-SLE-1000	1	°C	Facing the centre of the opening (offset 150 from centerline)
180	PT_Front_a480_SPx	Pentronic	5928060-001	1	°C	Facing the centre of the opening (offset 150 from centerline)
181	PT_Front_a240_SPy	Omega.com	GG-K-24-SLE-1000	1	°C	Facing the centre of the opening (offset 150 from centerline)
182	PT_Front_a240_SPx	Pentronic	5928060-001	1	°C	Facing the centre of the opening (offset 150 from centerline)
183	PT_Front_e350_SPx	Pentronic	5928060-001	1	°C	3.5 m above ground
184	PT_Front_e550_SPx	Pentronic	5928060-001	1	°C	5.5 m above the top of the opening
185	TC_Smoke	Omega.com	GG-K-24-SLE-1000	1	°C	Gas temperature at SMOKE2 outflow (for shutoff)
186	TC_HFGtower	Omega.com	EXPP-K-24-SLE-1000	1	°C	H2O outflow temperatures of heat flux gages on roof tower
187	TC_HFGfloor	Omega.com	KMQSS-040	1	°C	H2O outflow temperatures of heat flux gages on floor
188	TC_HFGw1	Omega.com	KMQSS-040	1	°C	H2O outflow temperatures of heat flux gages on W1
189	TC_GoPro	Omega.com	KMQSS-040	1	°C	H2O outflow temperatures of GoPro water bath
190	TC_TreeSteel	Omega.com	GG-K-24-SLE-1000	1	°C	Temperature of steel behind thermal insulation in Tree 03 at 2.1 m height
191	TC_TBD	Omega.com	GG-K-24-SLE-1000	1	°C	Extra TC location TBD
	VI	-	-	1	V	Internal heartbeat
	HRR	-	-	1	kW	calculated channel
	HRRburner	-	-	1	kW	calculated channel
	VelCeiling	-	-	-	m/s	calculated channel
	VelDoor1	-	-	-	m/s	calculated channel
	VelDoor2	-	-	-	m/s	calculated channel
	VelDoor3	-	-	-	m/s	calculated channel
	VelDoor4	-	-	-	m/s	calculated channel
	VelDoor5	-	-	-	m/s	calculated channel
	VelDoor6	-	-	-	m/s	calculated channel

Appendix E - Test 1-1 data

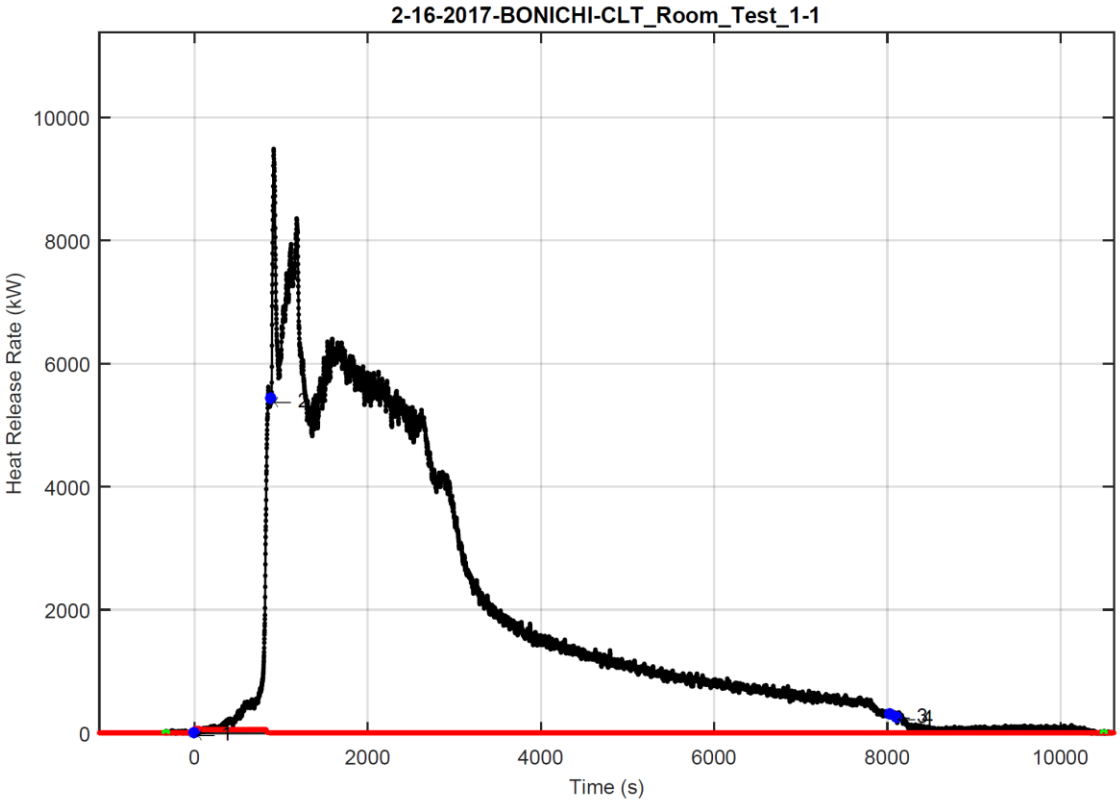

Hood Size = 15 (m)
Peak Heat Release Rate = 9487 (kW)
NG Burner Peak HRR = 74 (kW)
Exhaust Flow = 100.77 +/- 0.62 (kg/s)
O_2 Baseline = 0.2094 (Vol Fr)
O_2 Drift During Test = -14 (ppmv)
CO Generated = 50.39 (kg)

Fuel Type = PineWoodFuniture+PUF ; HOC = 19.9 (MJ/kg)
Total Heat Release = 17883 (MJ)
NG Burner Total HR = 47 (MJ)
Total Burn Time = 2.25 (Hrs)
Fuel Mass Burned = 898.64 (kg)
O_2 Consumed = 1391.79 (kg)
CO_2 Generated = 1764.93 (kg)

Test Description:
CLT Room test 1-1. Furnished room with 3 layers of type X gypsum on all walls and ceiling.

Event Count	Time (s)	Time Stamp	Event Description
1	0	2/16/2017 10:29:35 AM	Ignition
2	890	2/16/2017 10:44:30 AM	Room Flashover
3	8036	2/16/2017 12:43:31 PM	Start fire hose suppression
4	8102	2/16/2017 12:44:37 PM	Fire Out

Figure E 1. Summary report file generated by the NFRL calorimeter on the day of test.

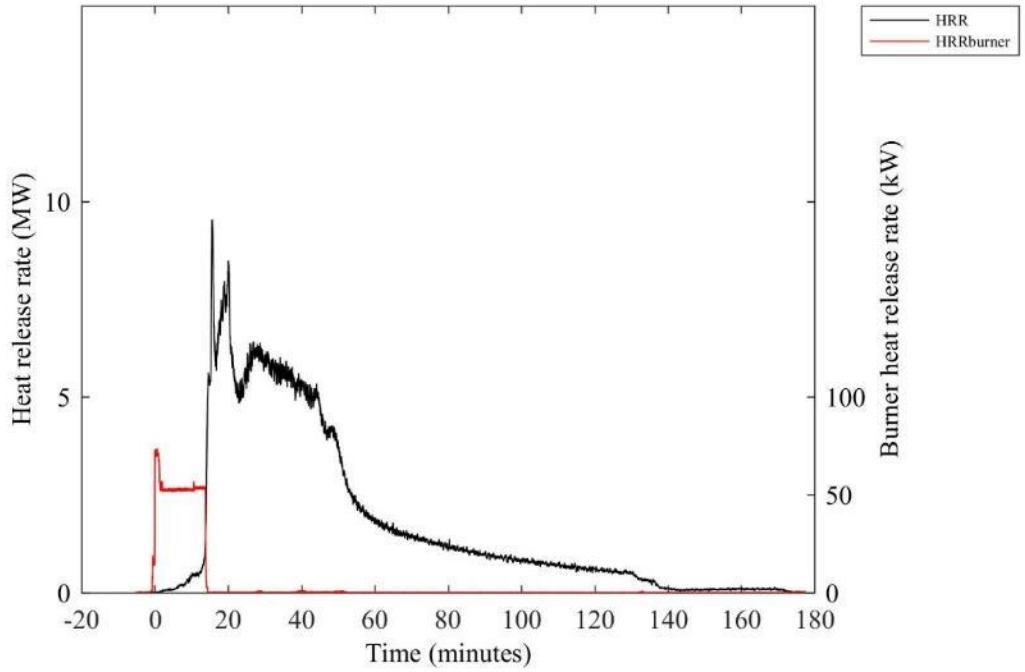

Figure E 2. Compartment (left axis) and burner (right axis) heat release rates.

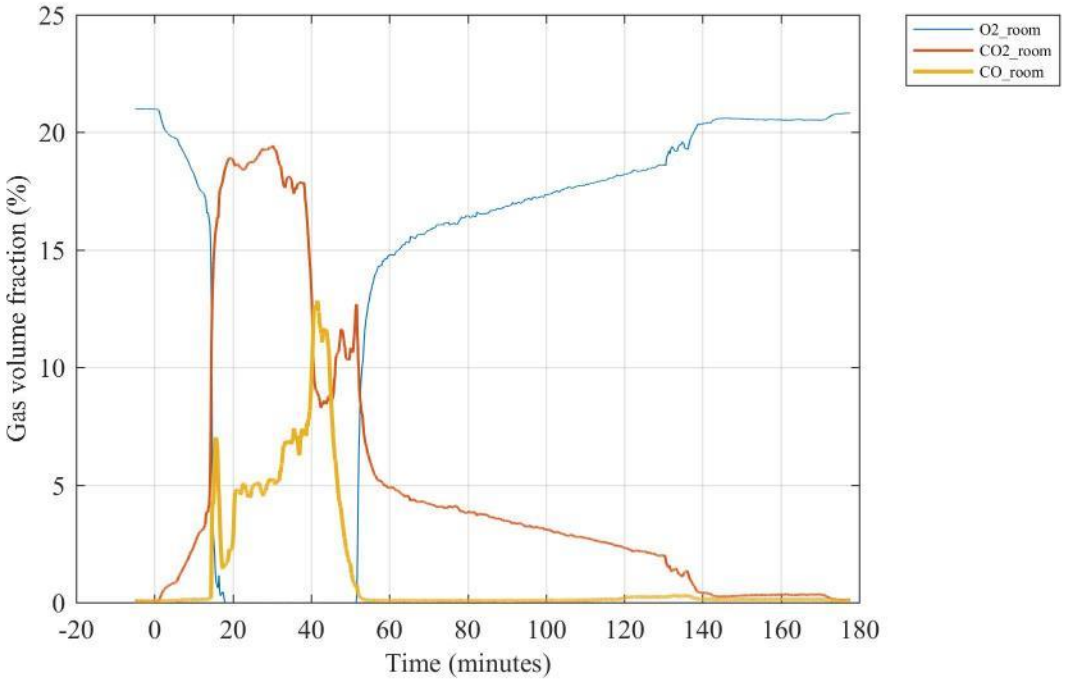

Figure E 3. Gas volume fractions for oxygen (O_2), carbon dioxide (CO_2) and carbon monoxide (CO) sampled at the center of the compartment 210 cm above the floor.

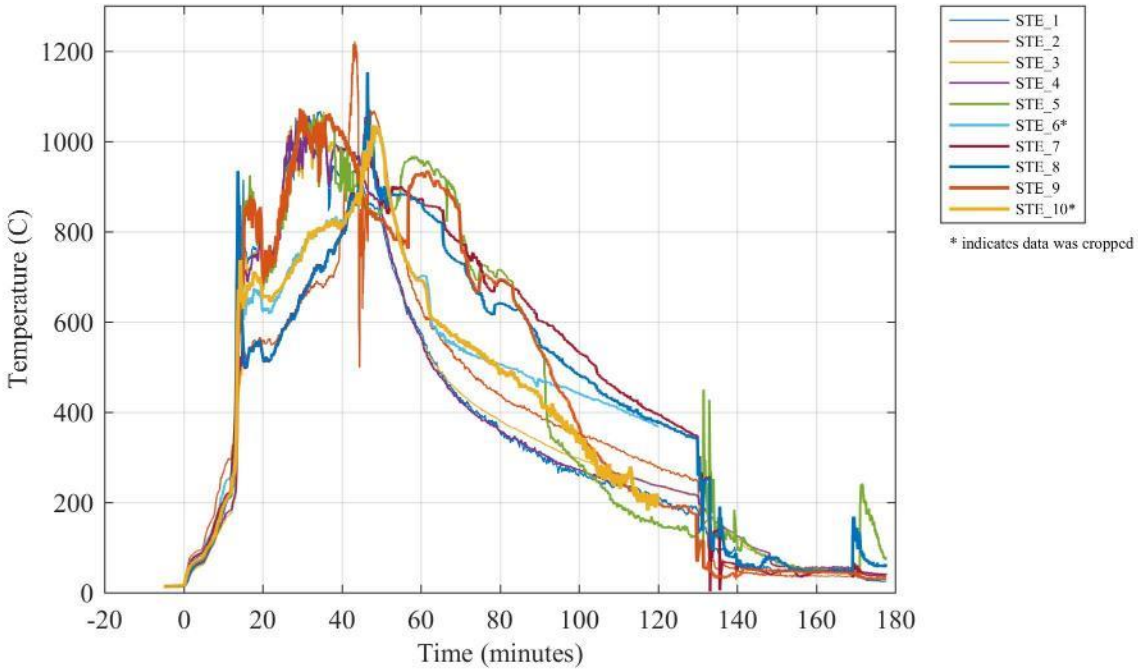

Figure E 4. Simulated thermal elements (STE) for sprinkler.

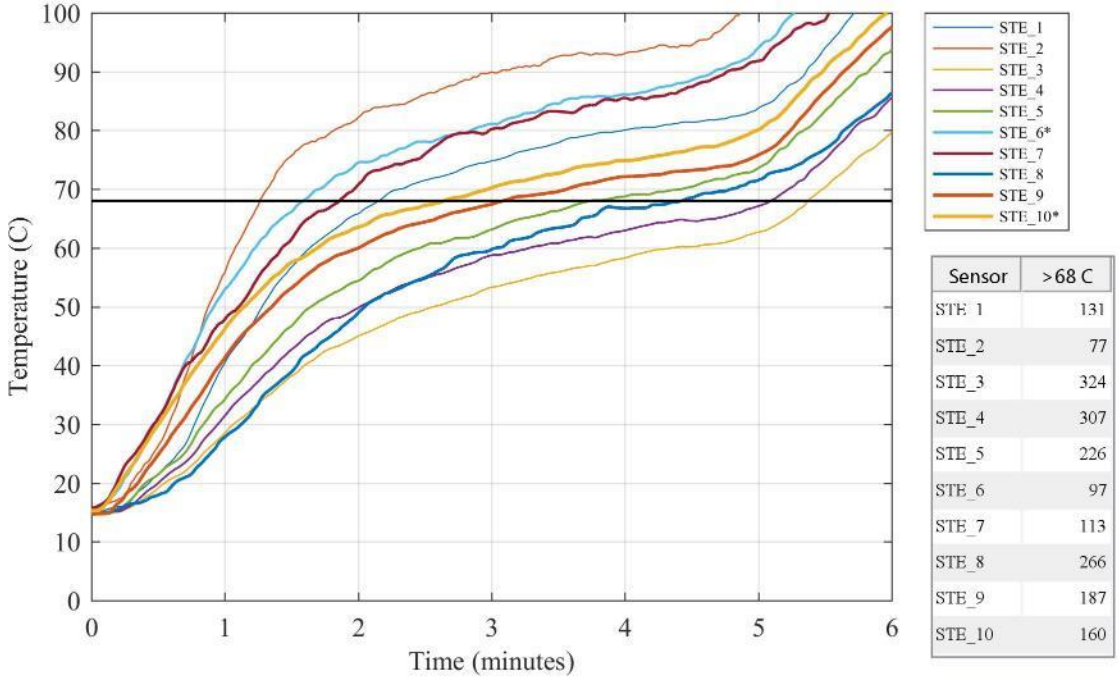

Sensor	>68 C
STE_1	131
STE_2	77
STE_3	324
STE_4	307
STE_5	226
STE_6	97
STE_7	113
STE_8	266
STE_9	187
STE_10	160

Figure E 5. Simulated thermal elements (STE) for sprinkler with table showing time after ignition (in seconds) until 68 °C is reached.

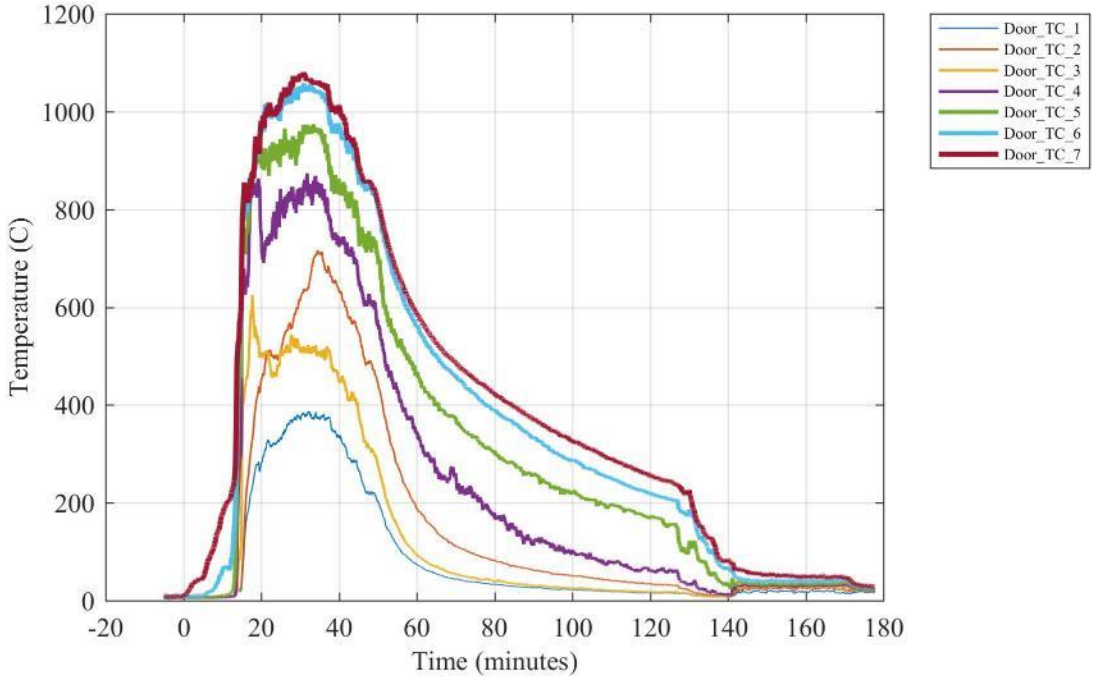

Figure E 6. Temperatures measured at various heights above the floor in the doorway.

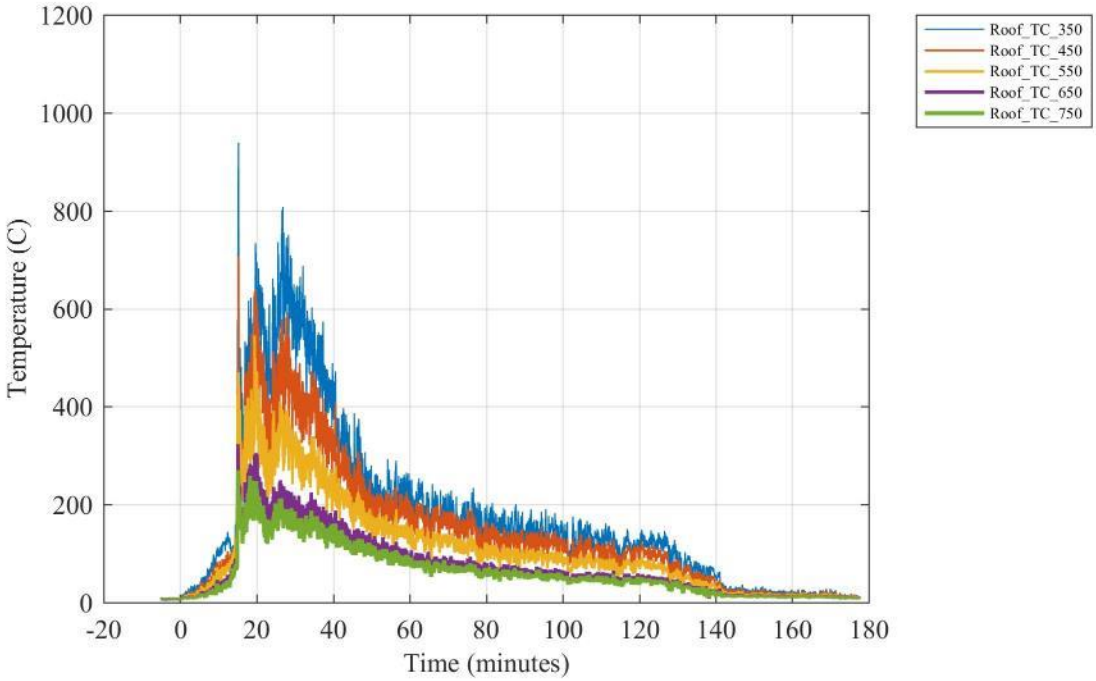

Figure E 7. Temperatures measured at various heights above the floor above the doorway.

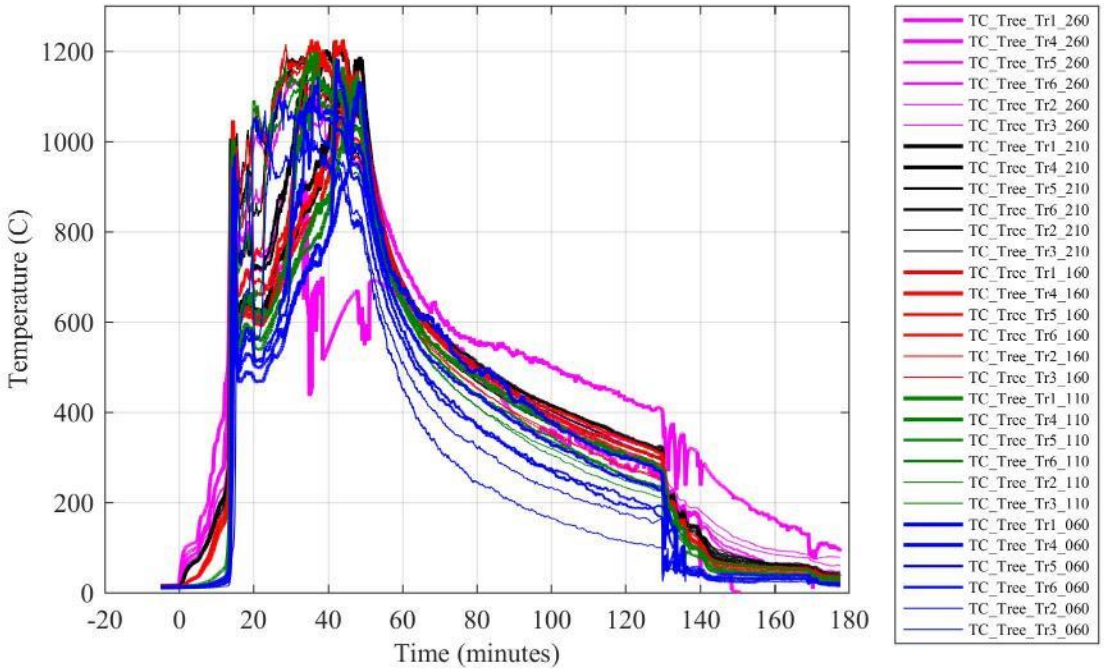

Figure E 8. Thermocouple tree temperatures at various locations inside the compartment.

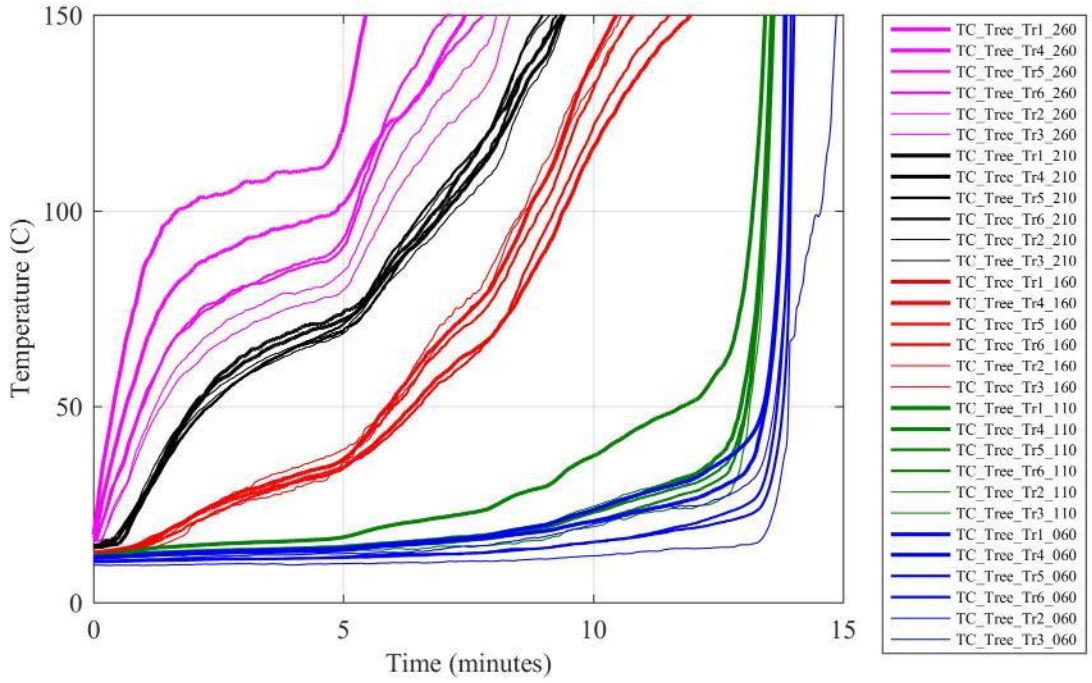

Figure E 9. Thermocouple tree temperatures at various locations inside the compartment during the first 15 min after ignition.

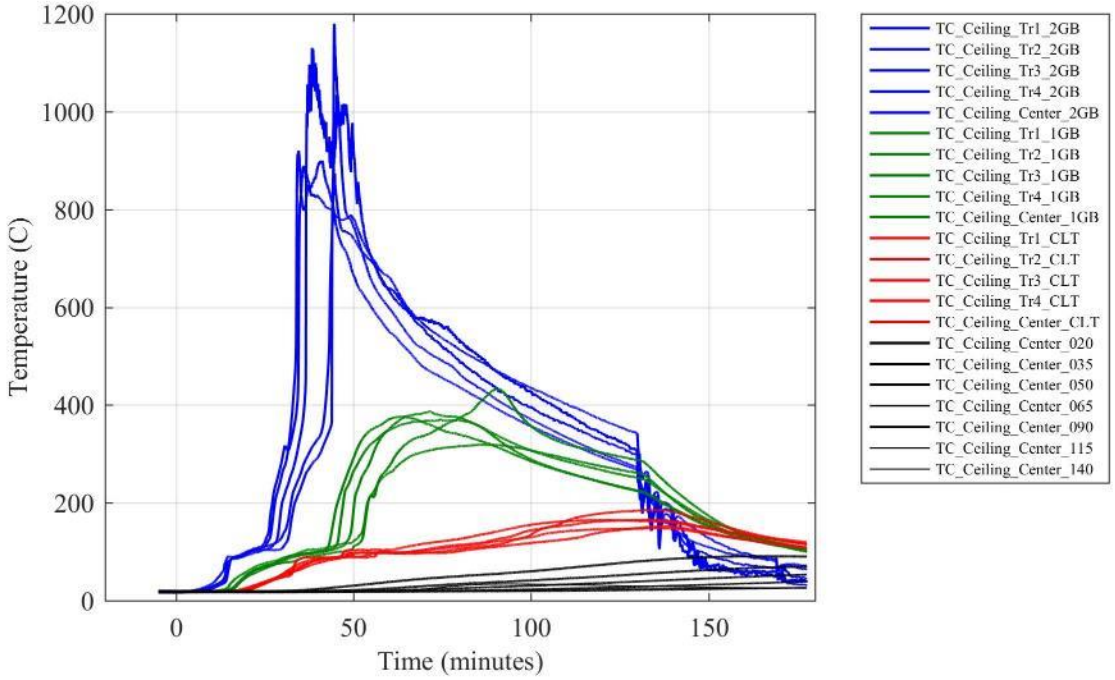

Figure E 10. Temperatures in the ceiling at various depths from the fire exposed surface.

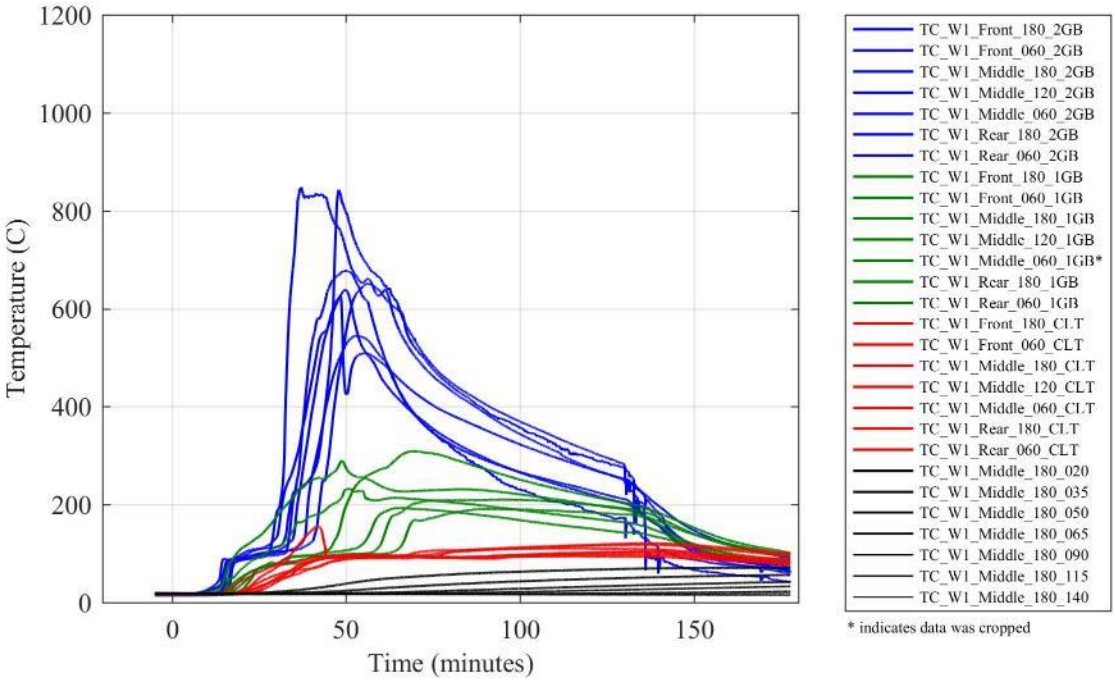

Figure E 11. Temperatures in Wall W1 at various depths from the fire exposed surface.

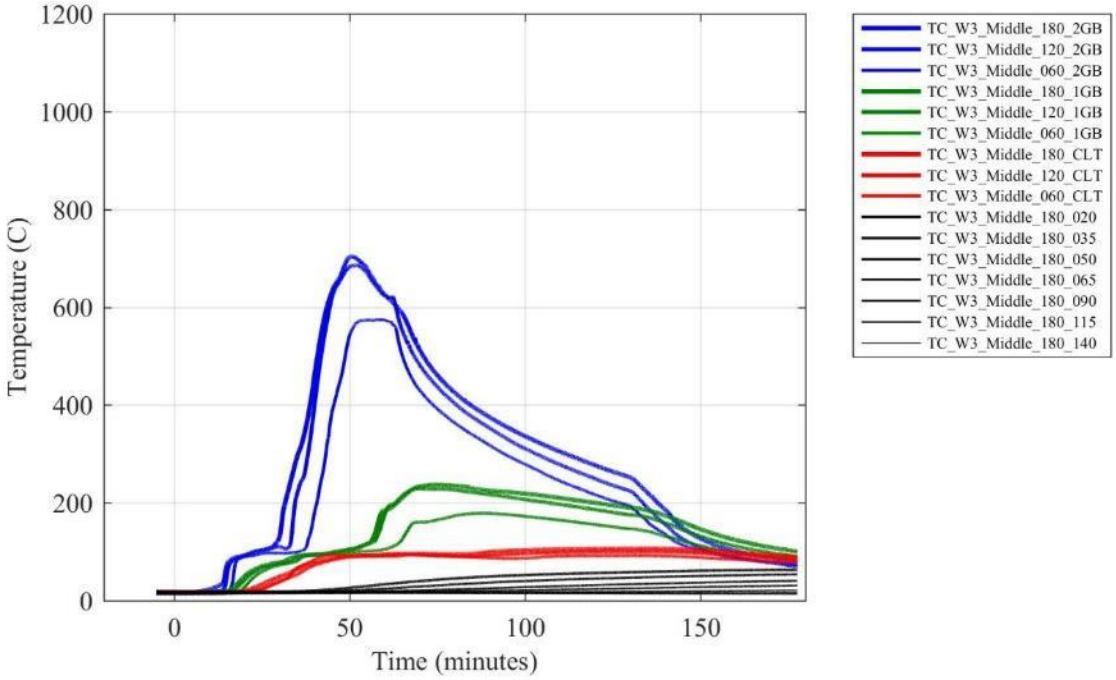

Figure E 12. Temperatures in Wall W3 at various depths from the fire exposed surface.

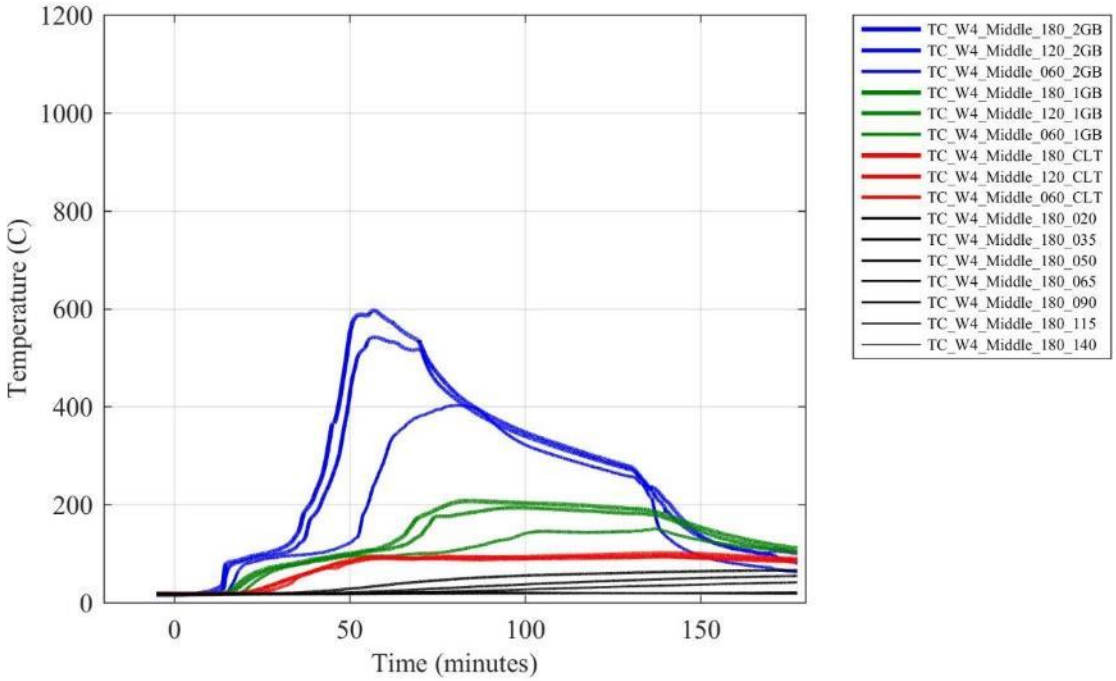

Figure E 13. Temperatures in Wall W4 at various depths from the fire exposed surface.

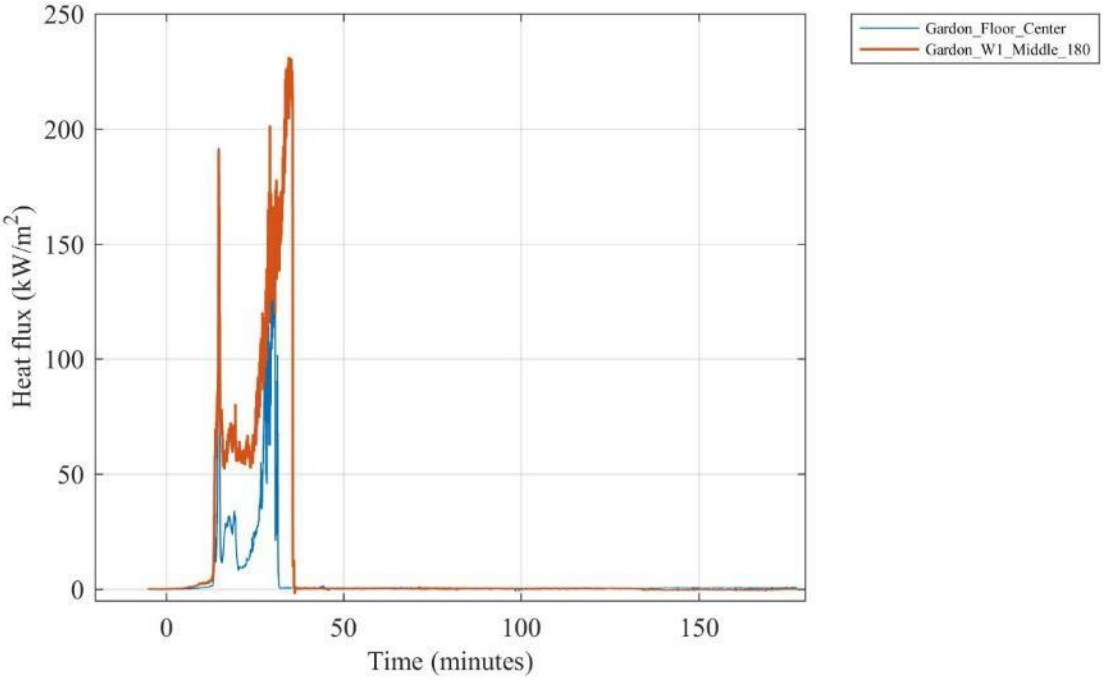

Figure E 14. Heat flux measured by Gardon gauges located inside the compartment.

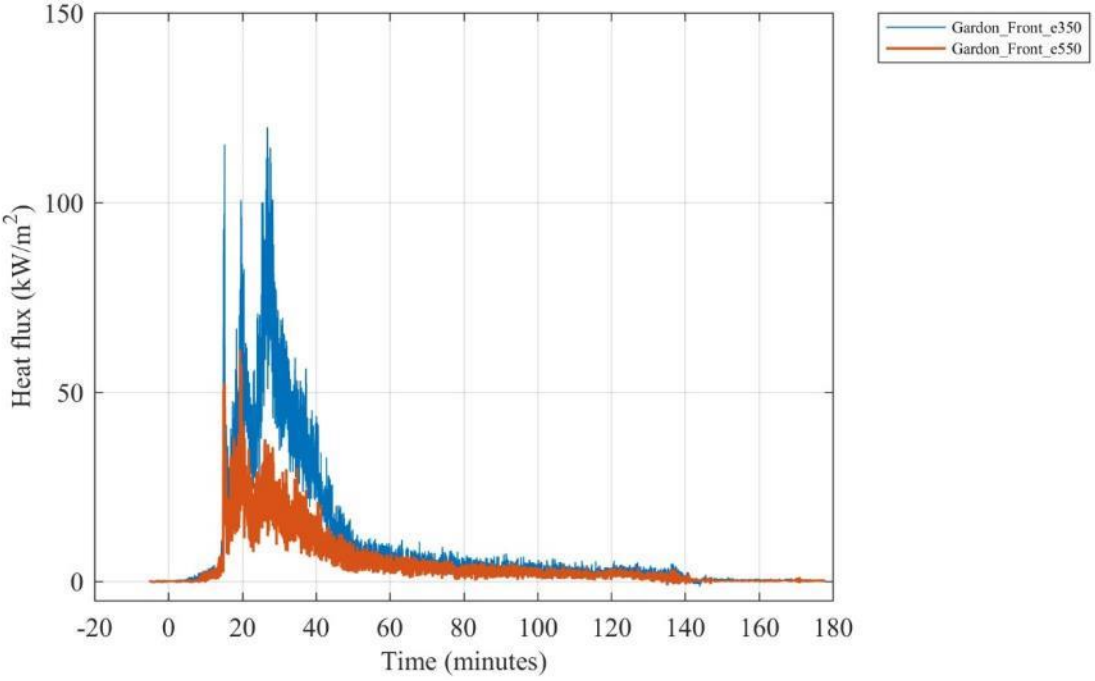

Figure E 15. Heat flux measured by Gardon gauges 350 cm and 550 cm above the floor above the doorway.

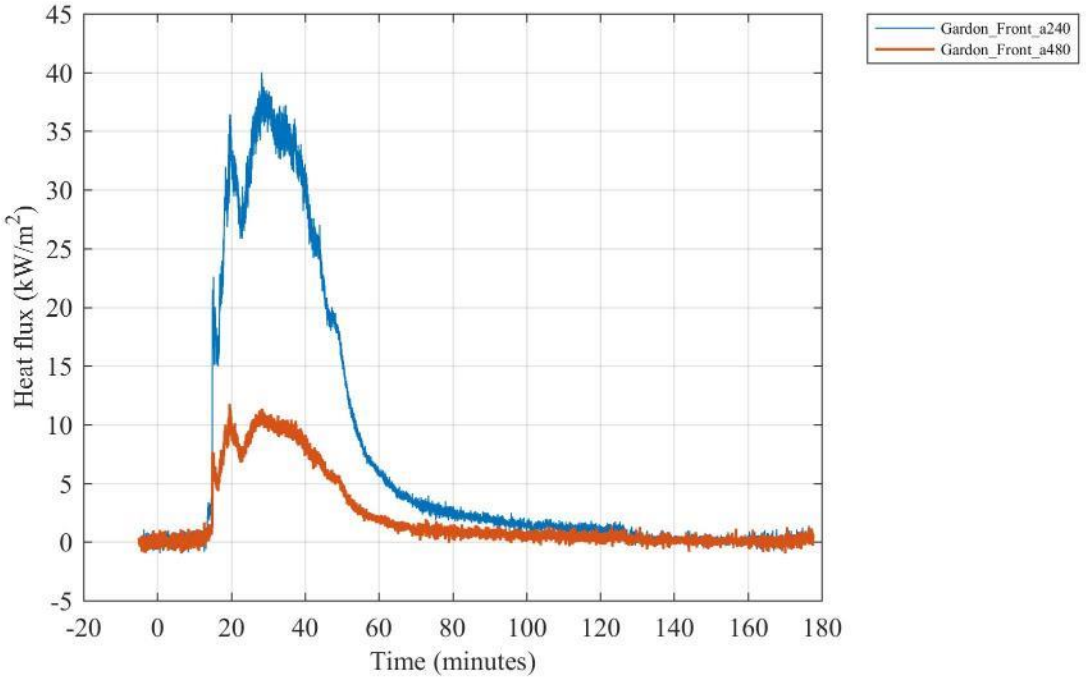

Figure E 16. Heat flux measured by Gardon gauges 240 cm and 480 cm from the doorway facing the opening.

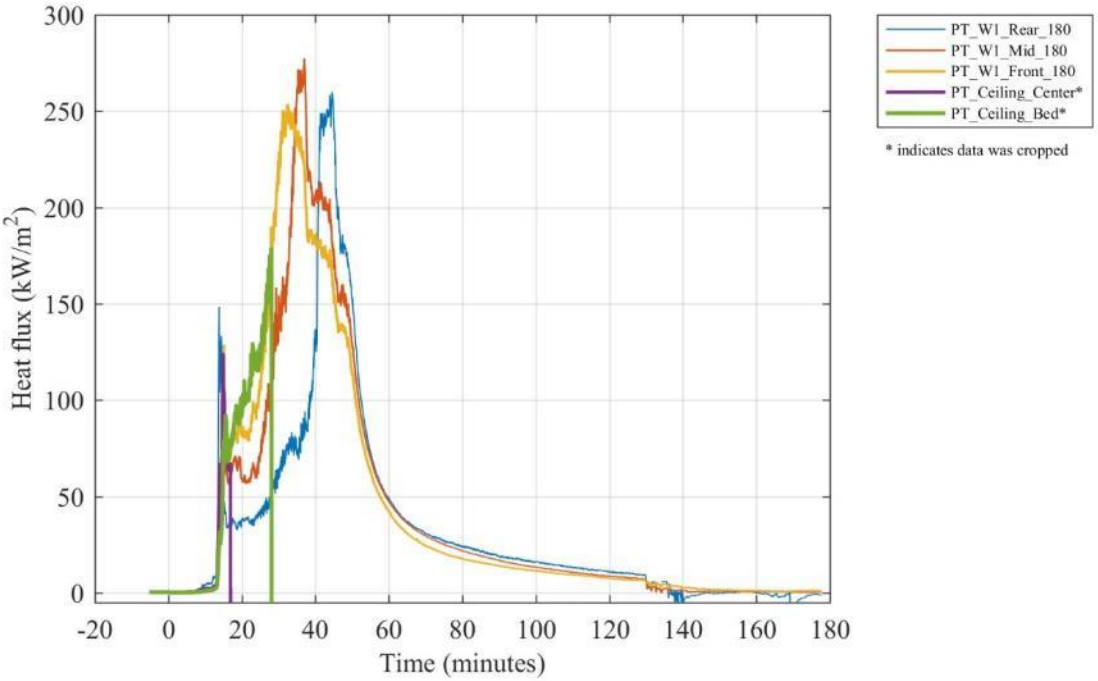

Figure E 17. Heat flux calculated from plate thermometers at various locations inside the compartment.

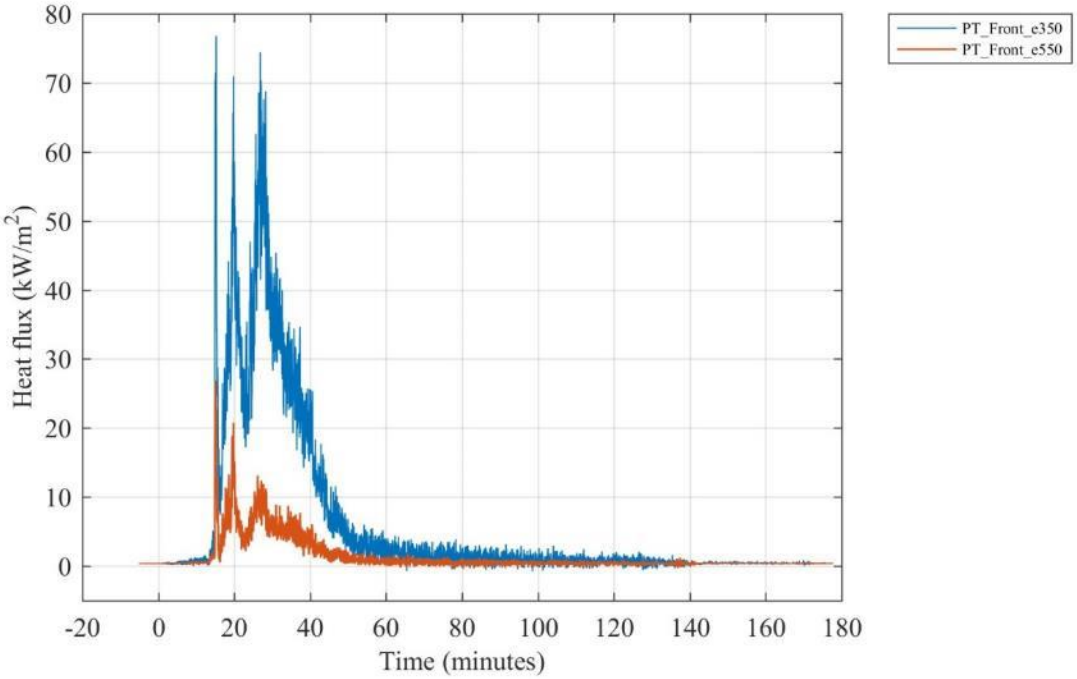

Figure E 18. Heat flux calculated from plate thermometers 350 cm and 550 cm above the floor above the doorway.

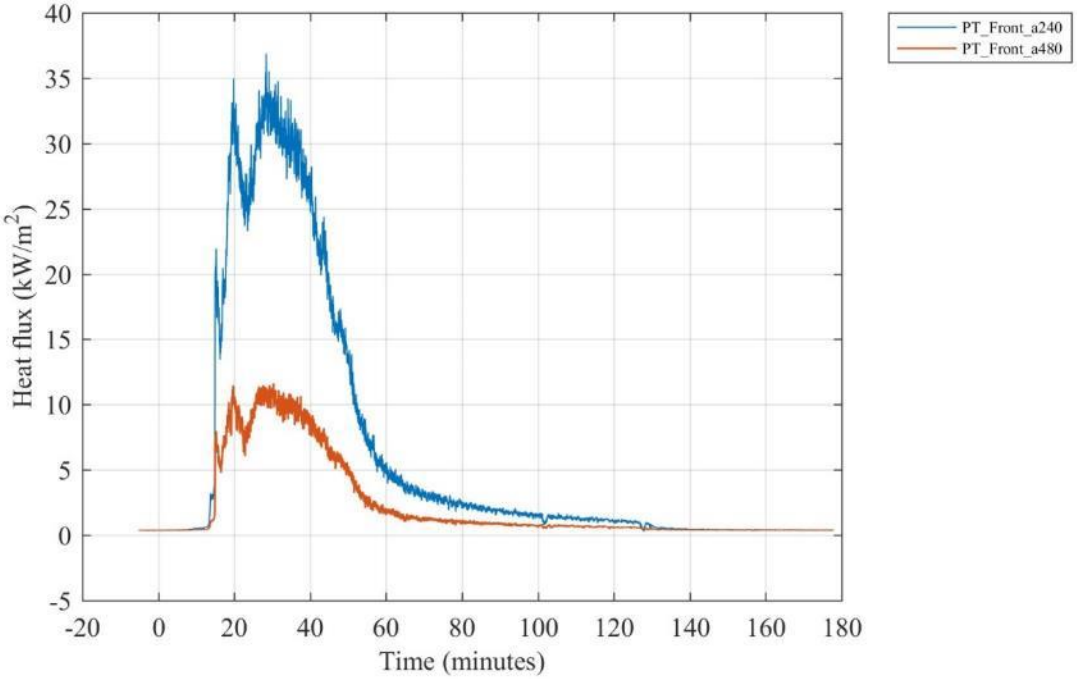

Figure E 19. Heat flux calculated from plate thermometers 240 cm and 480 cm from the doorway facing the opening.

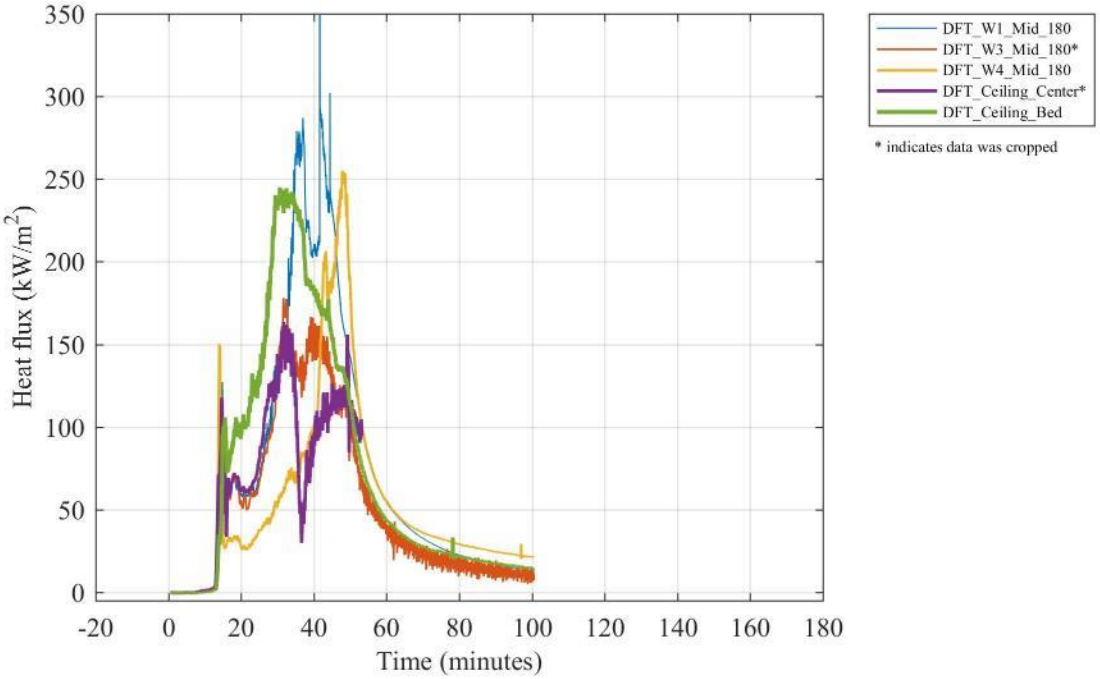

Figure E 20. Heat flux calculated from directional flame thermometers at various locations inside the compartment. [first 100 min processed]

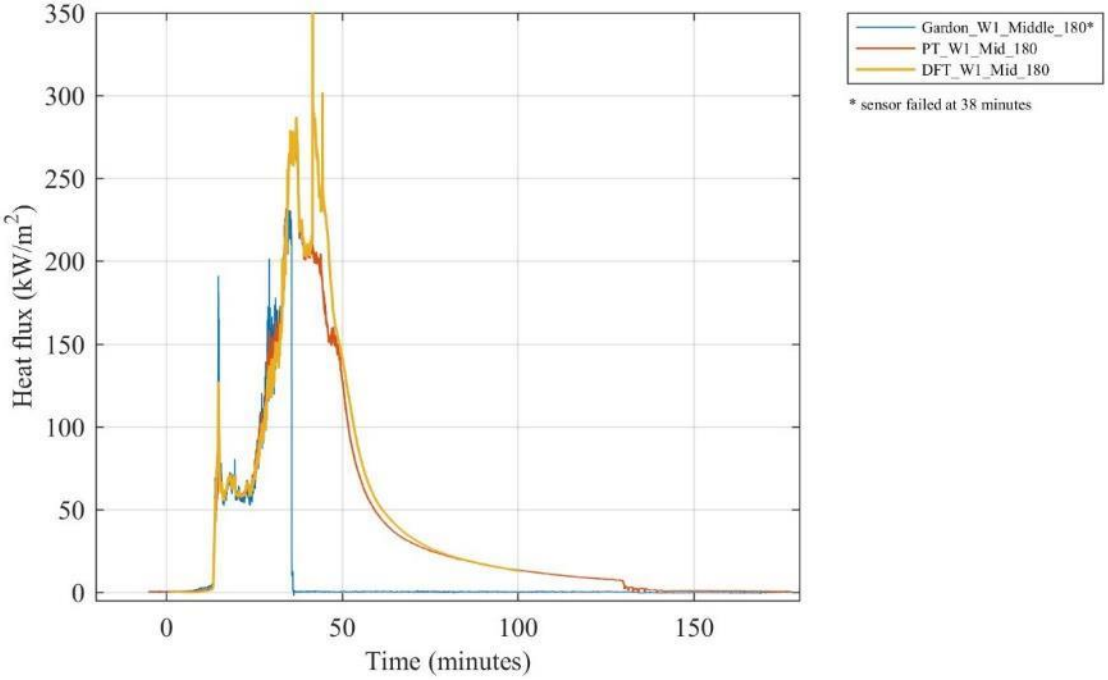

Figure E 21. Comparison of heat fluxes recorded by a collocated Gardon gauge, plate thermometer (PT) and differential flame thermometer (DFT) on Wall W1 at the middle of the compartment 1.8 m above the floor.

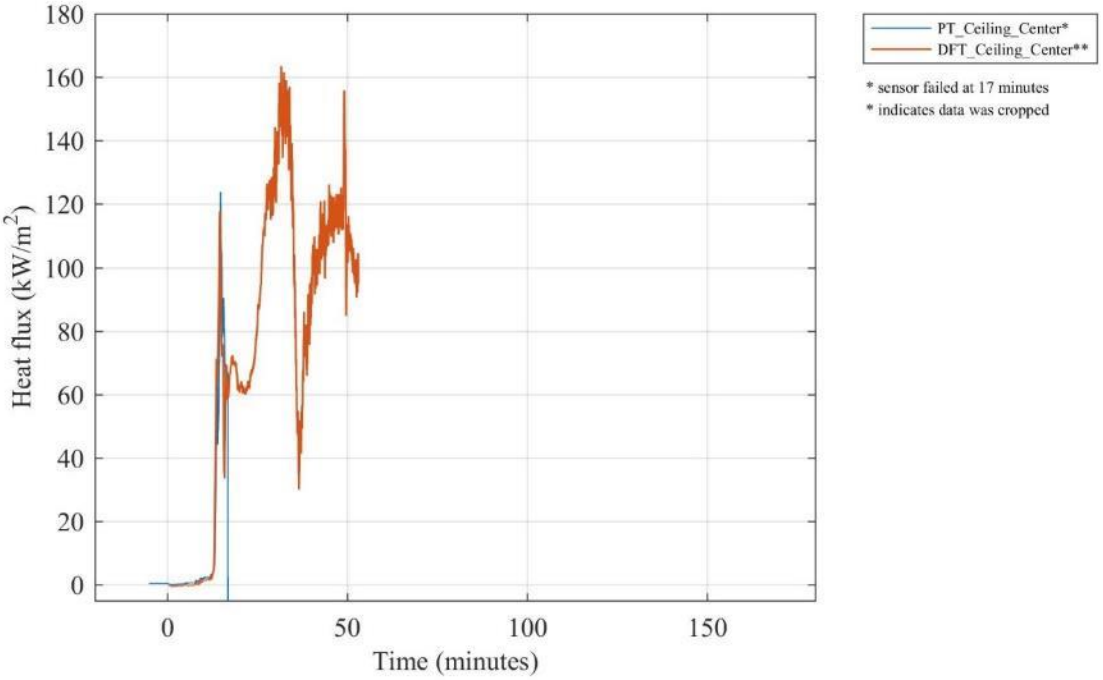

Figure E 22. Comparison of heat fluxes recorded by a collocated plate thermometer (PT) and differential flame thermometer (DFT) on the ceiling at the center of the compartment.

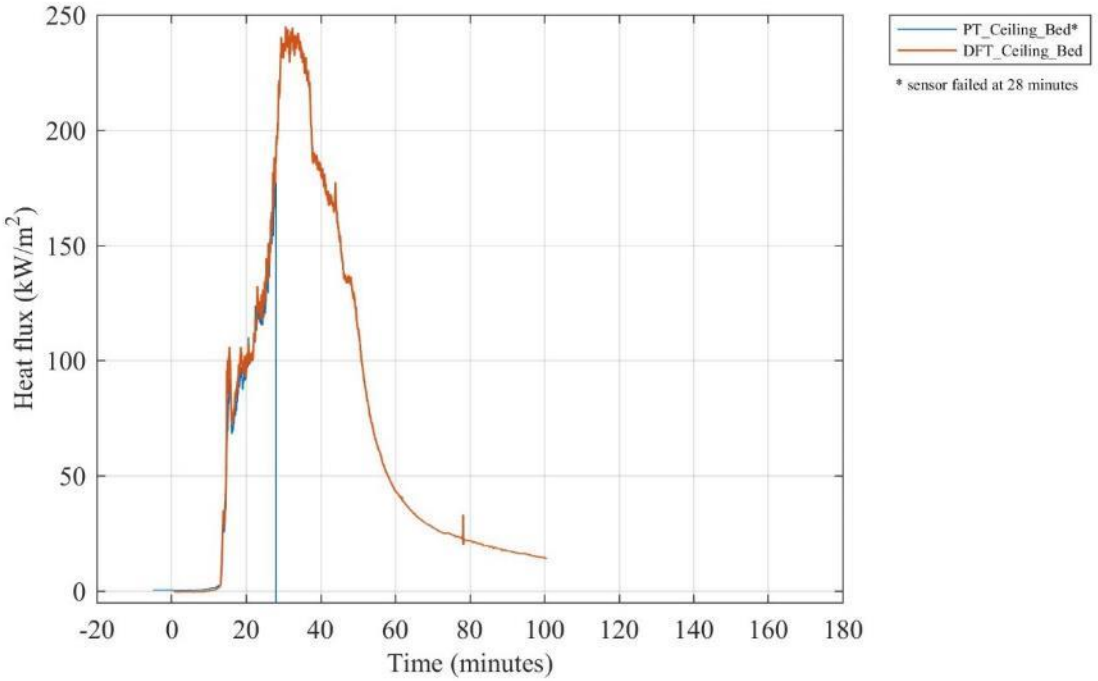

Figure E 23. Comparison of heat fluxes recorded by a collocated plate thermometer (PT) and differential flame thermometer (DFT) on the ceiling above the bed.

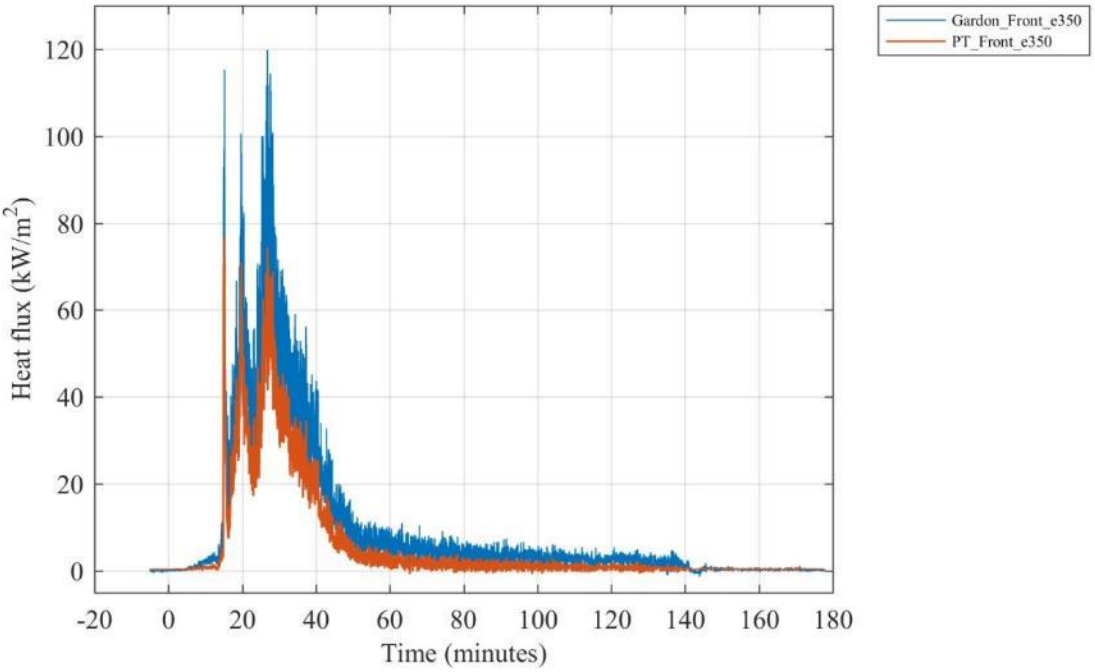

Figure E 24. Comparison of heat fluxes recorded by a collocated Gardon gauge and plate thermometer (PT) 350 cm above the floor above the doorway.

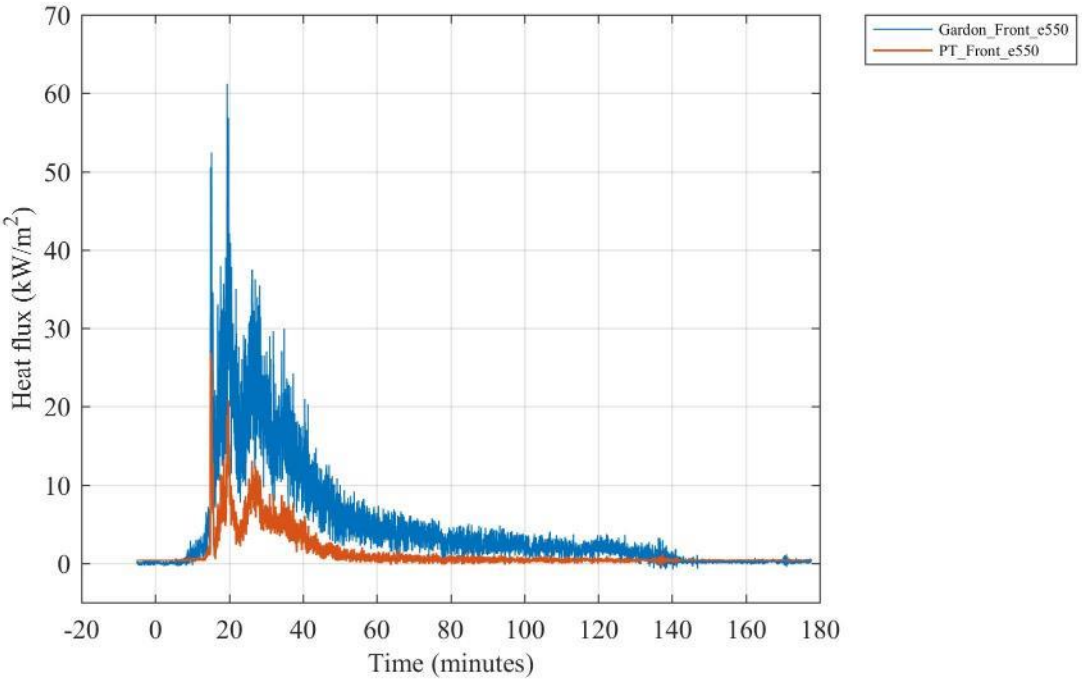

Figure E 25. Comparison of heat fluxes recorded by a collocated Gardon gauge and plate thermometer (PT) 550 cm above the floor above the doorway.

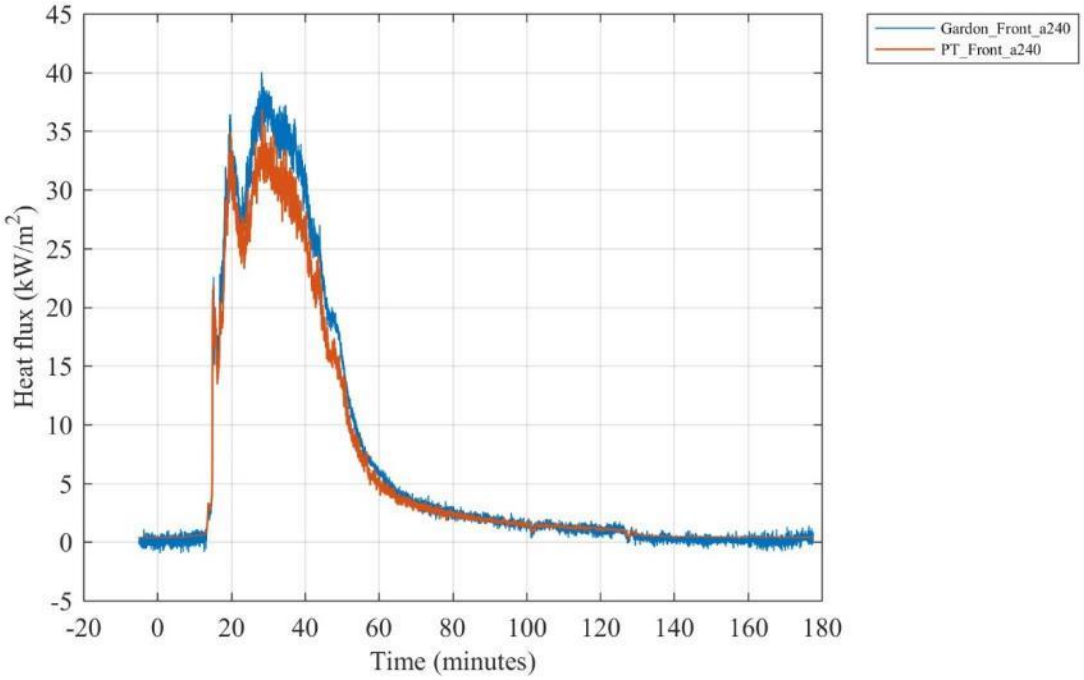

Figure E 26. Comparison of heat fluxes recorded by a collocated Gardon gauge and plate thermometer (PT) 240 cm from the doorway (facing doorway) and 150 cm above floor.

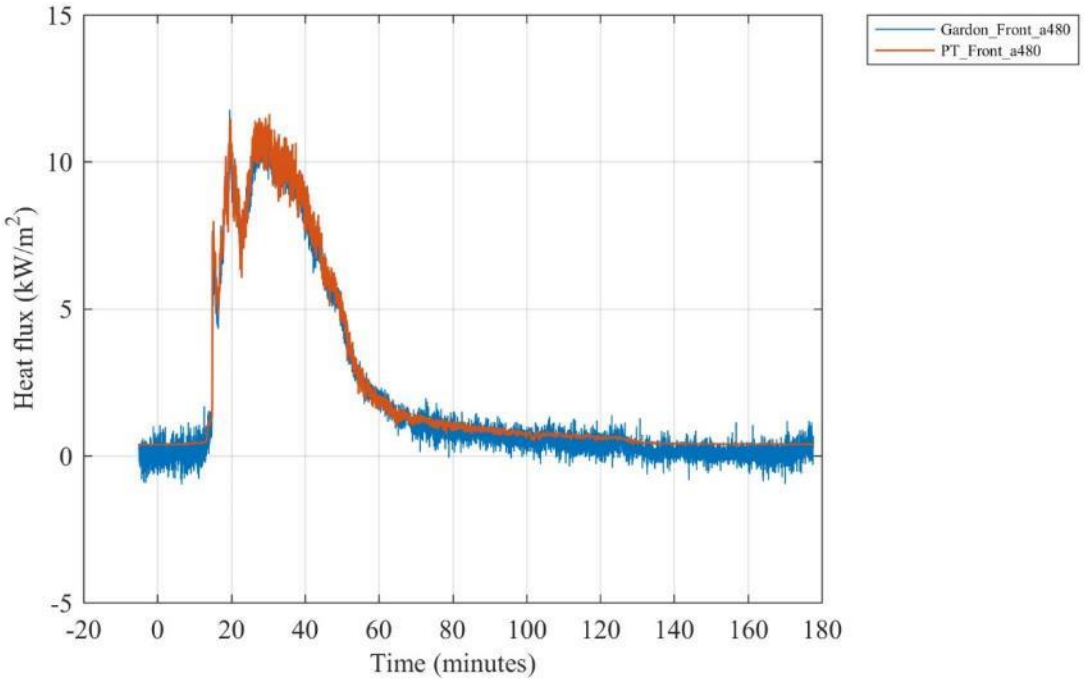

Figure E 27. Comparison of heat fluxes recorded by a collocated Gardon gauge and plate thermometer (PT) 480 cm from the doorway (facing doorway) and 150 cm above floor.

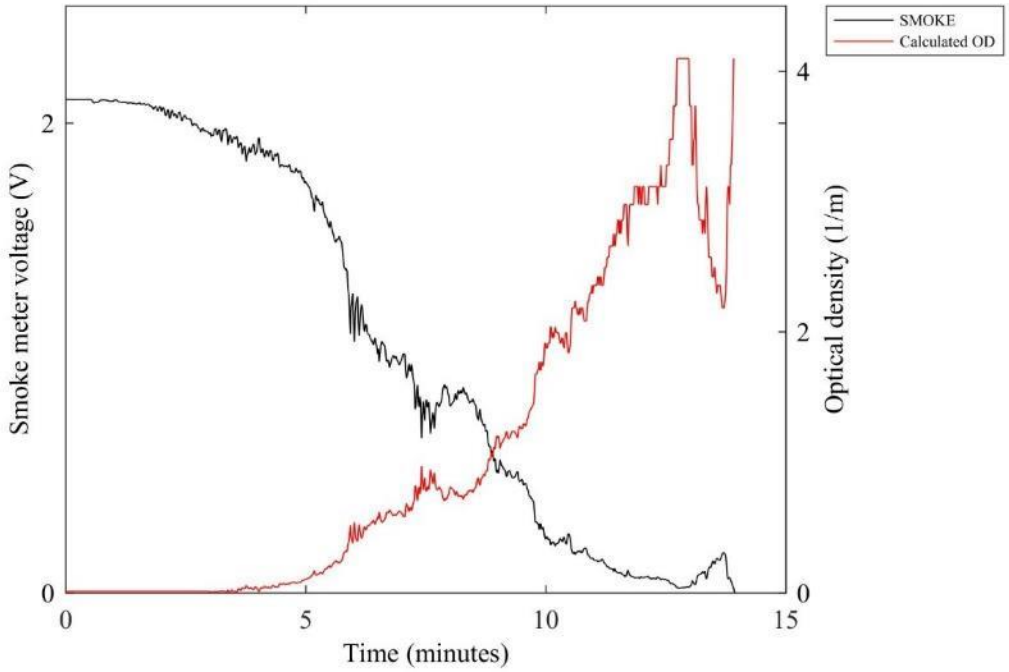

Figure E 28. Smoke meter voltage and calculated optical density (OD) from gas sampled at the center of the compartment 160 cm above the floor.

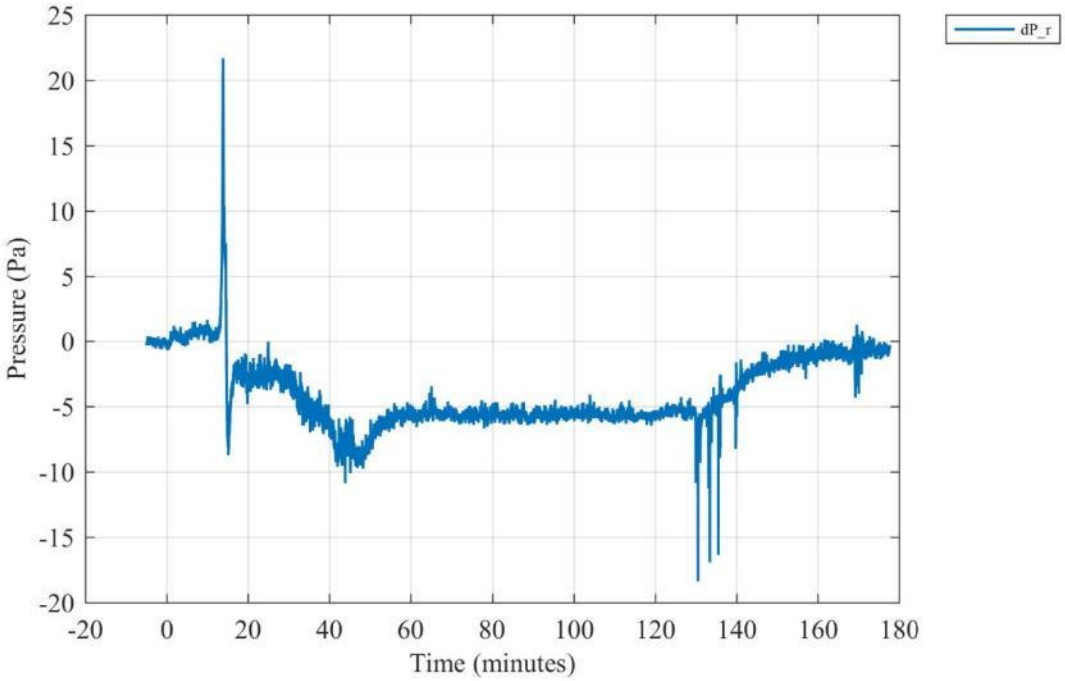

Figure E 29. Differential room pressure measured 210 cm above the floor at the center of the compartment.

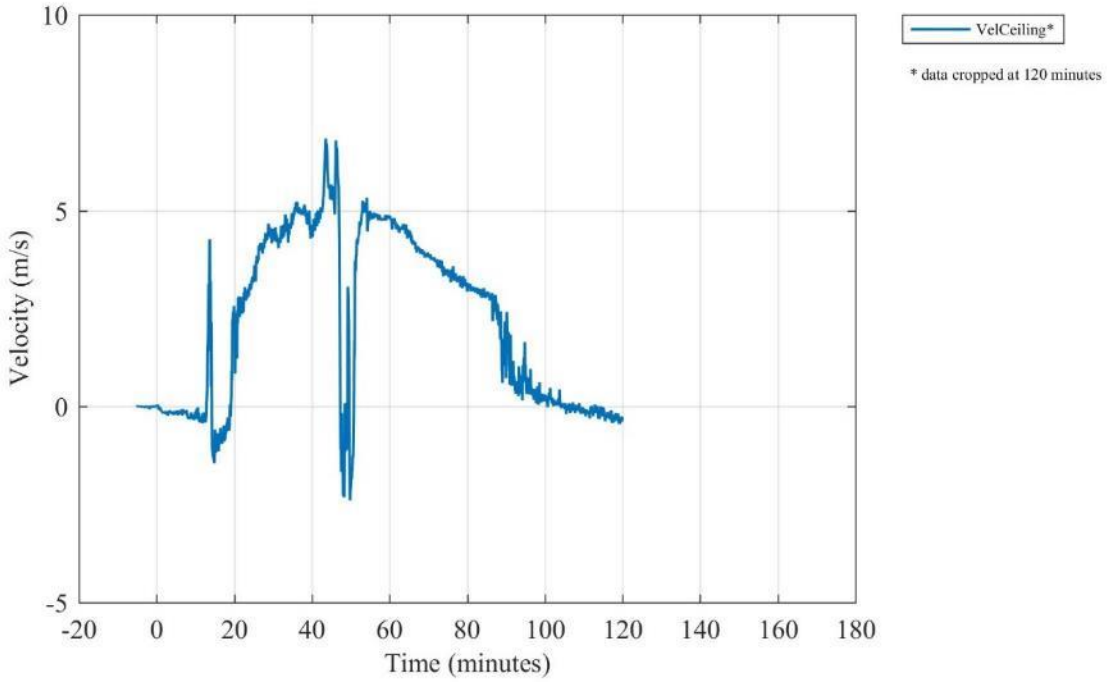

Figure E 30. Gas velocity measured 305 mm from the ceiling along the midline 227.5 cm from the back of the compartment (positive indicates flow out the door). [10 s moving average filter applied]

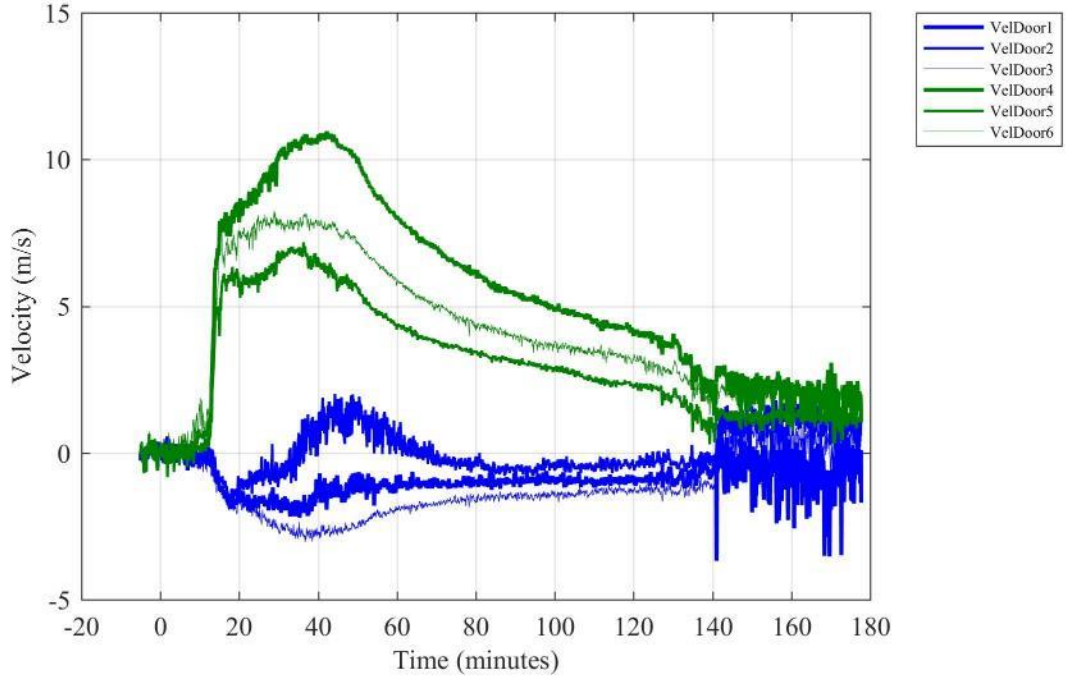

Figure E 31. Gas velocities measured in the doorway (positive indicates flow out the door). [10 s moving average filter applied]

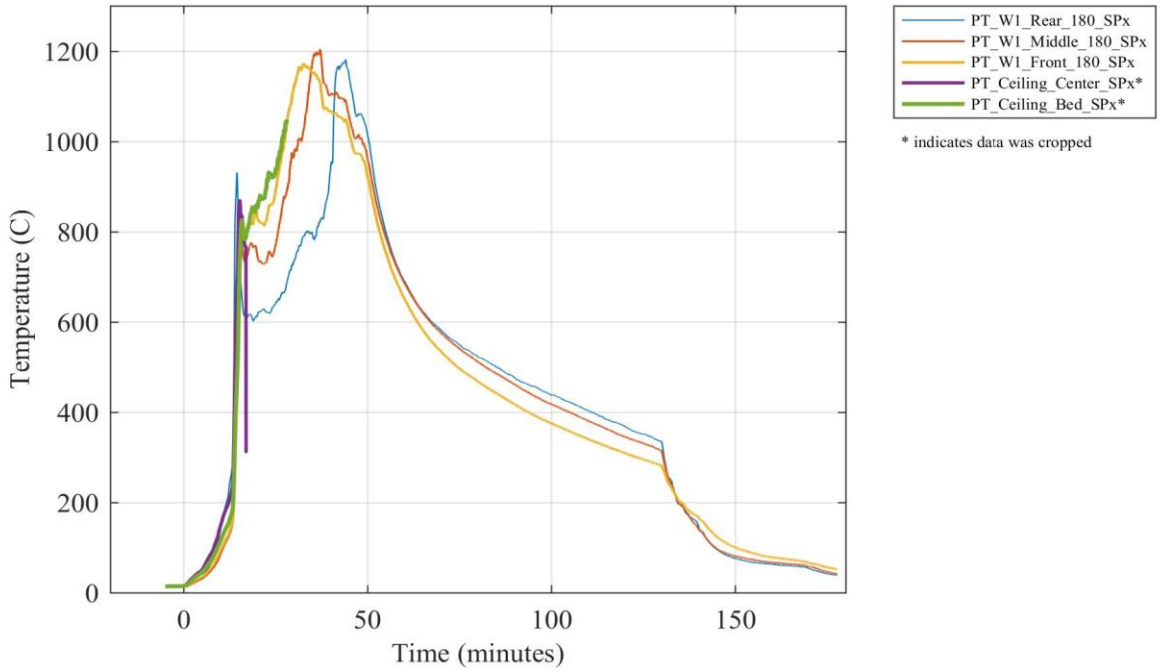

Figure E 32. Plate thermometer temperatures at various locations inside the compartment.

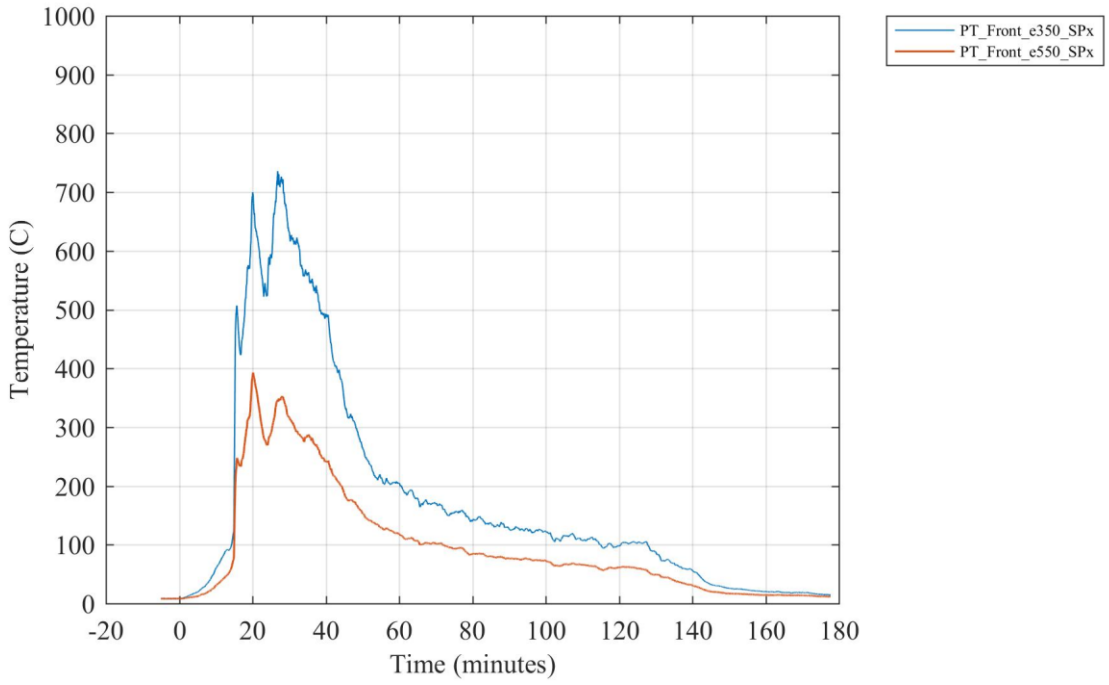

Figure E 33. Plate thermometer temperatures 350 cm and 550 cm above the floor above the doorway.

Appendix F - Test 1-2 data

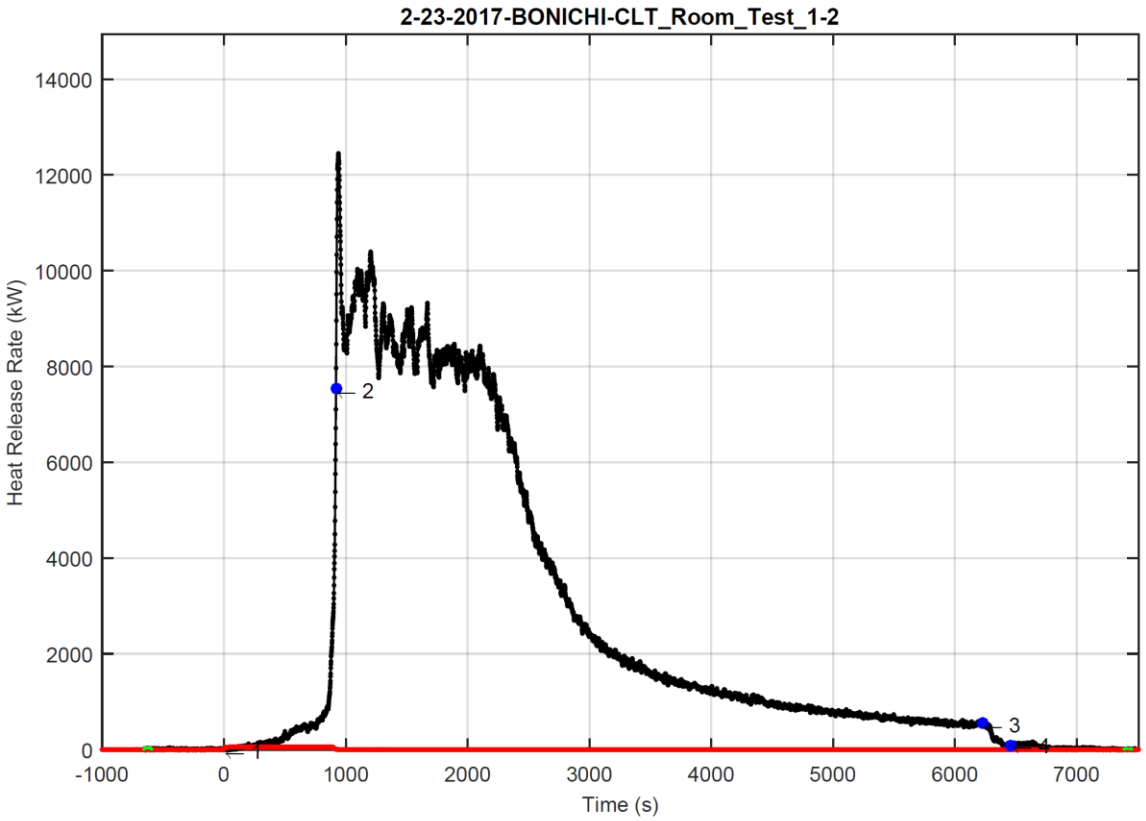

Hood Size = 15 (m)

Peak Heat Release Rate = 12451 (kW)

NG Burner Peak HRR = 58 (kW)

Exhaust Flow = 99.48 +/- 0.68 (kg/s)

O_2 Baseline = 0.20938 (Vol Fr)

O_2 Drift During Test = 59 (ppmv)

CO Generated = 31.38 (kg)

Fuel Type = WoodFurniturePUF ; HOC = 19.9 (MJ/kg)

Total Heat Release = 18541 (MJ)

NG Burner Total HR = 45 (MJ)

Total Burn Time = 1.79 (Hrs)

Fuel Mass Burned = 931.71 (kg)

O_2 Consumed = 1402.33 (kg)

CO_2 Generated = 1804.98 (kg)

Test Description:
CLT Room test 1-2. Furnished room witth 2 layers of type X gypsum on all walls and ceiling. Double wide door opening

Event Count	Time (s)	Time Stamp	Event Description
1	0	2/23/2017 10:08:39 AM	Ignition
2	920	2/23/2017 10:23:59 AM	Room Flashover
3	6228	2/23/2017 11:52:27 AM	Start fire hose suppression
4	6458	2/23/2017 11:56:17 AM	Fire Out

Figure F 1. Summary report file generated by the NFRL calorimeter on the day of test.

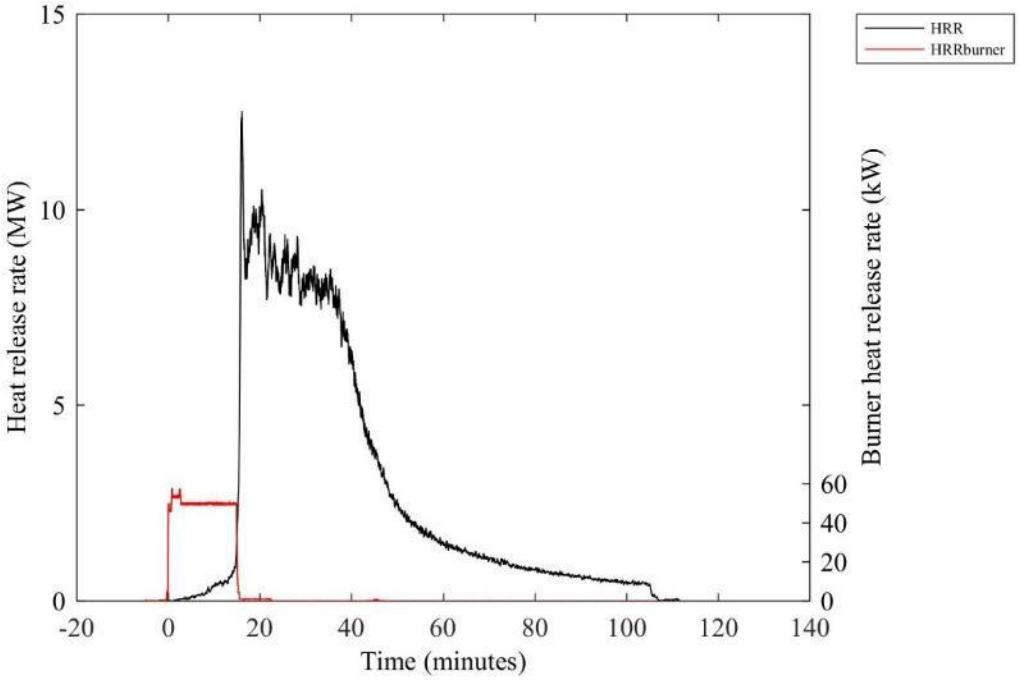

Figure F 2. Compartment (left axis) and burner (right axis) heat release rates.

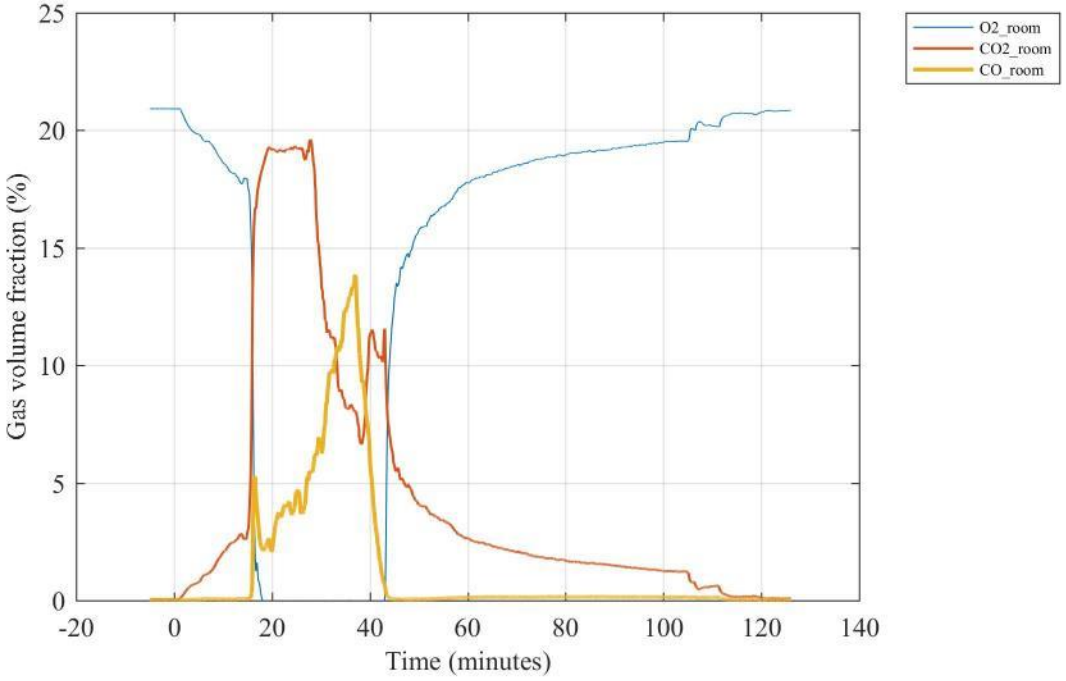

Figure F 3. Gas volume fractions for oxygen (O_2), carbon dioxide (CO_2) and carbon monoxide (CO) sampled at the center of the compartment 210 cm above the floor.

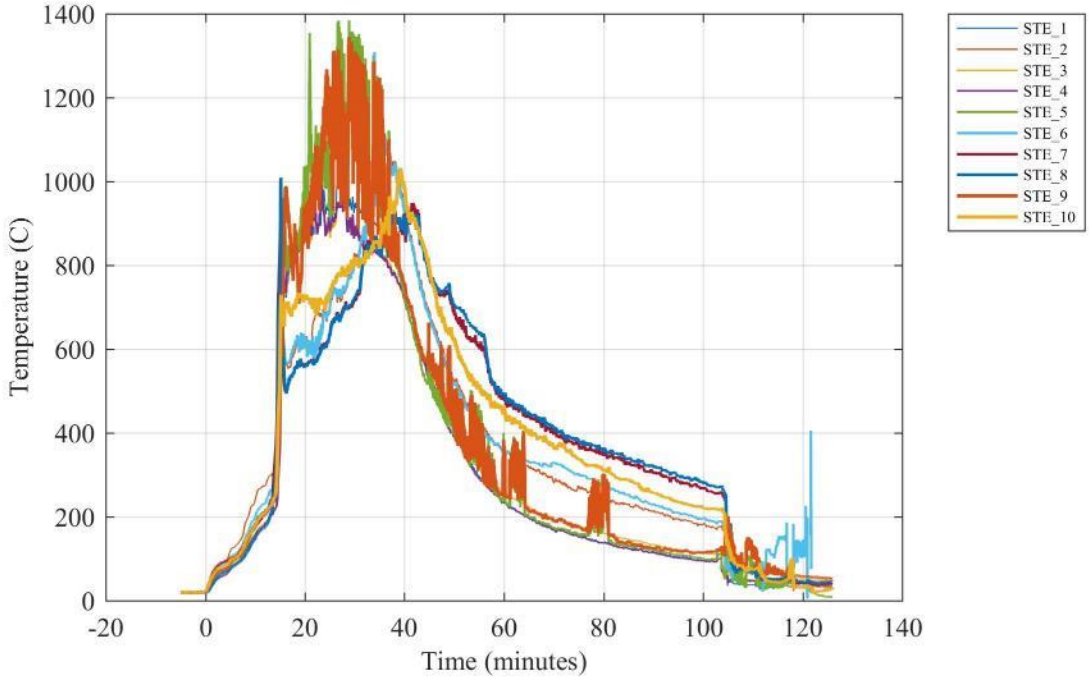

Figure F 4. Simulated thermal elements (STE) for sprinkler.

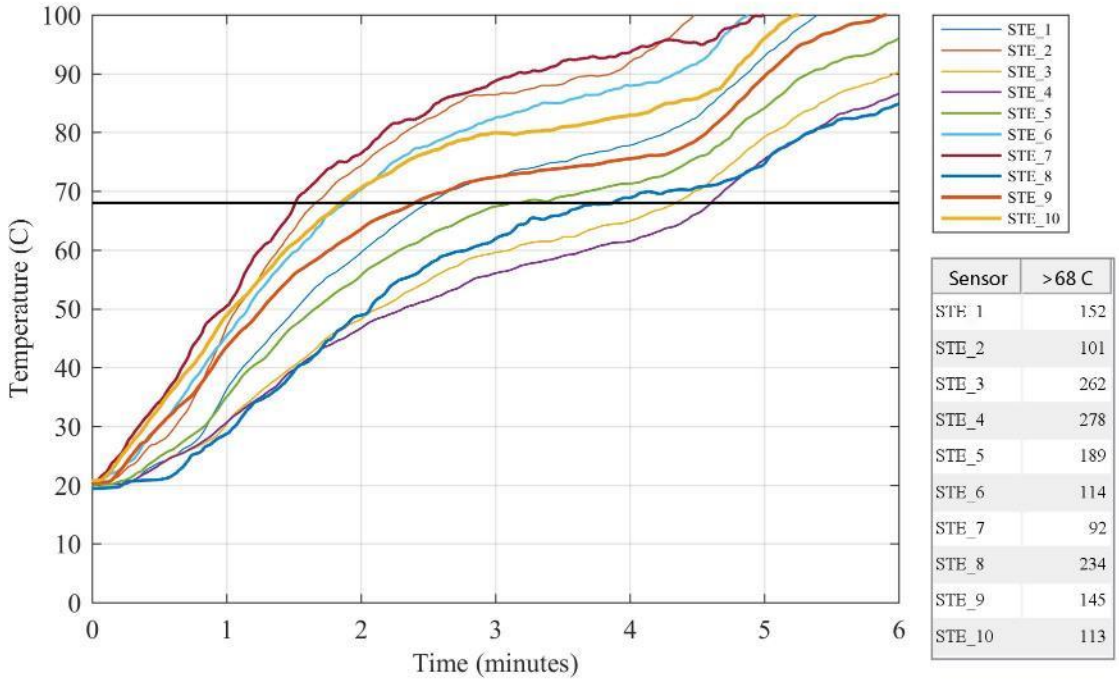

Sensor	>68 C
STE_1	152
STE_2	101
STE_3	262
STE_4	278
STE_5	189
STE_6	114
STE_7	92
STE_8	234
STE_9	145
STE_10	113

Figure F 5. Simulated thermal elements (STE) for sprinkler with table showing time after ignition (in seconds) until 68 °C is reached.

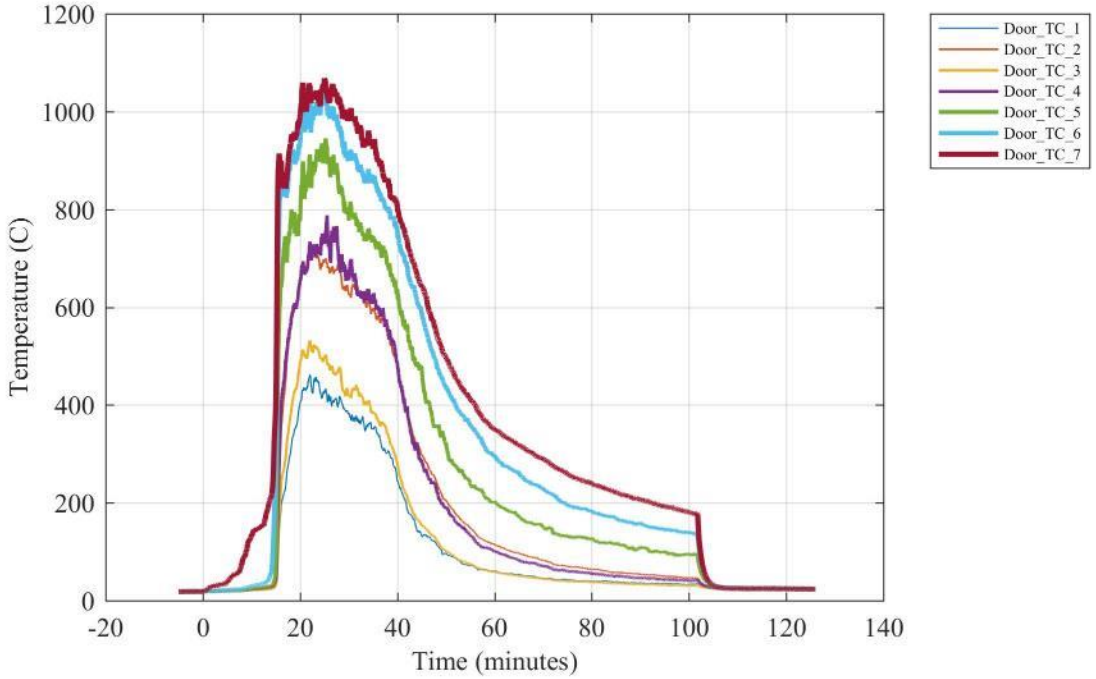

Figure F 6. Temperatures measured at various heights above the floor in the doorway.

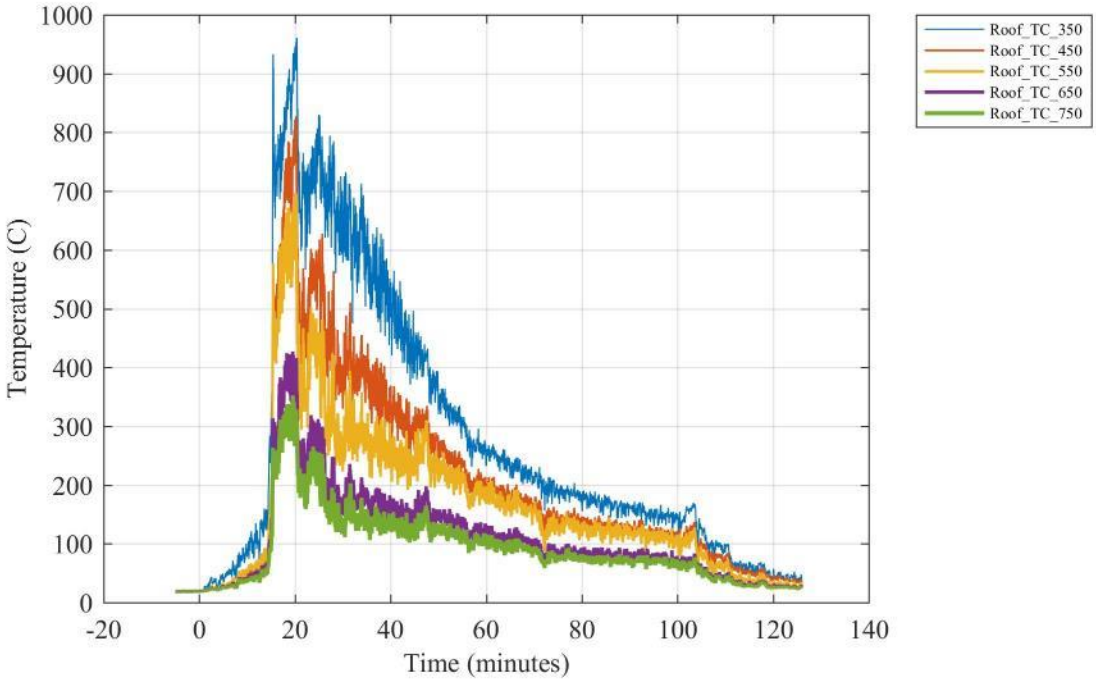

Figure F 7. Temperatures measured at various heights above the floor above the doorway.

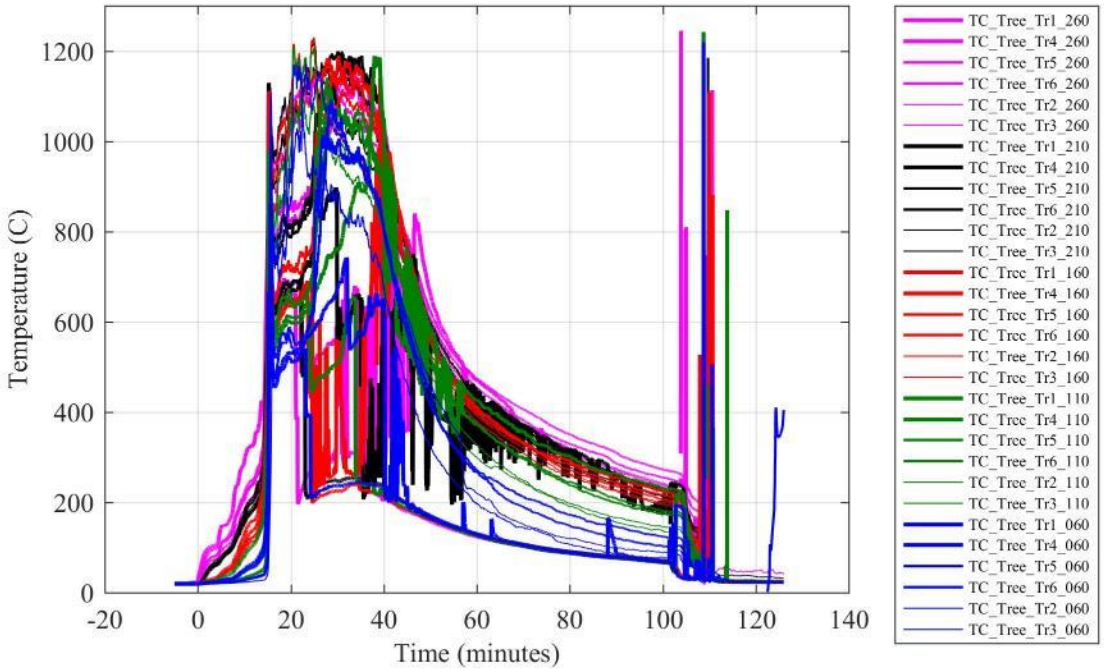

Figure F 8. Thermocouple tree temperatures at various locations inside the compartment.

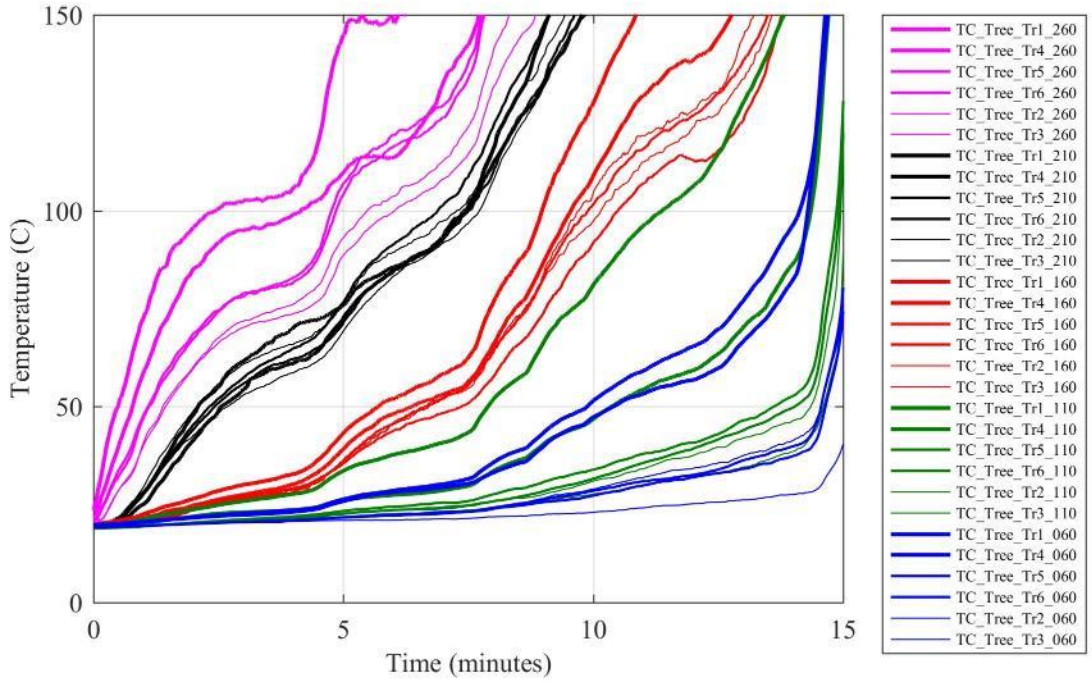

Figure F 9. Thermocouple tree temperatures at various locations inside the compartment during the first 15 min after ignition.

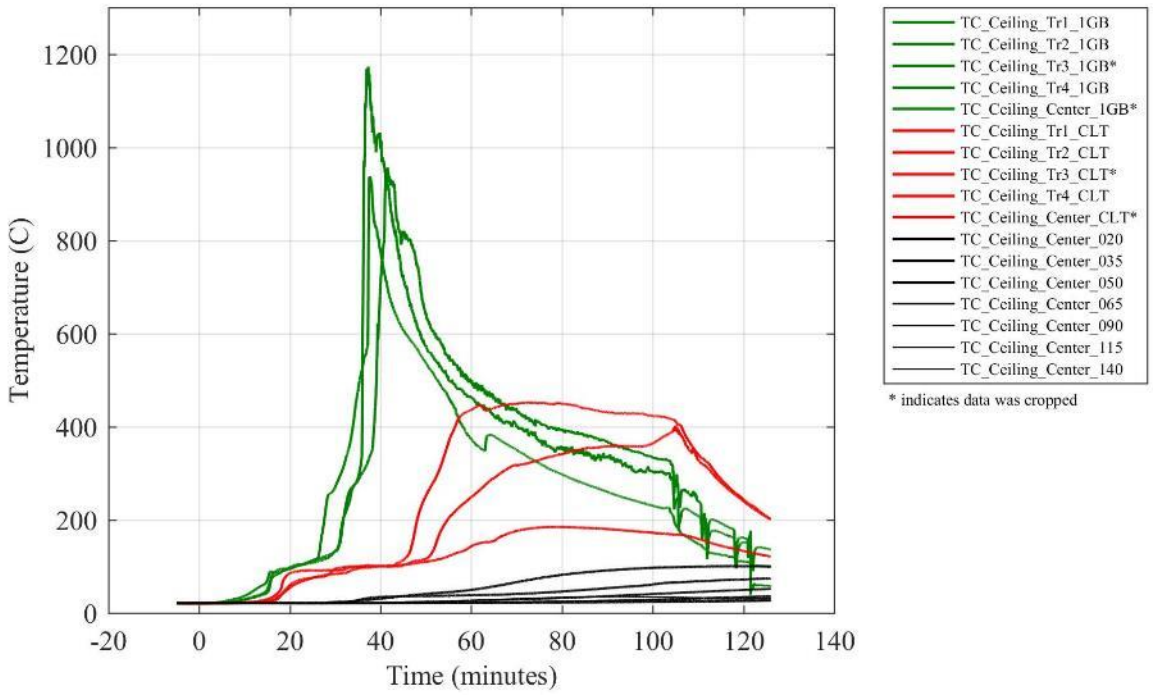

Figure F 10. Temperatures in the ceiling at various depths from the fire exposed surface.

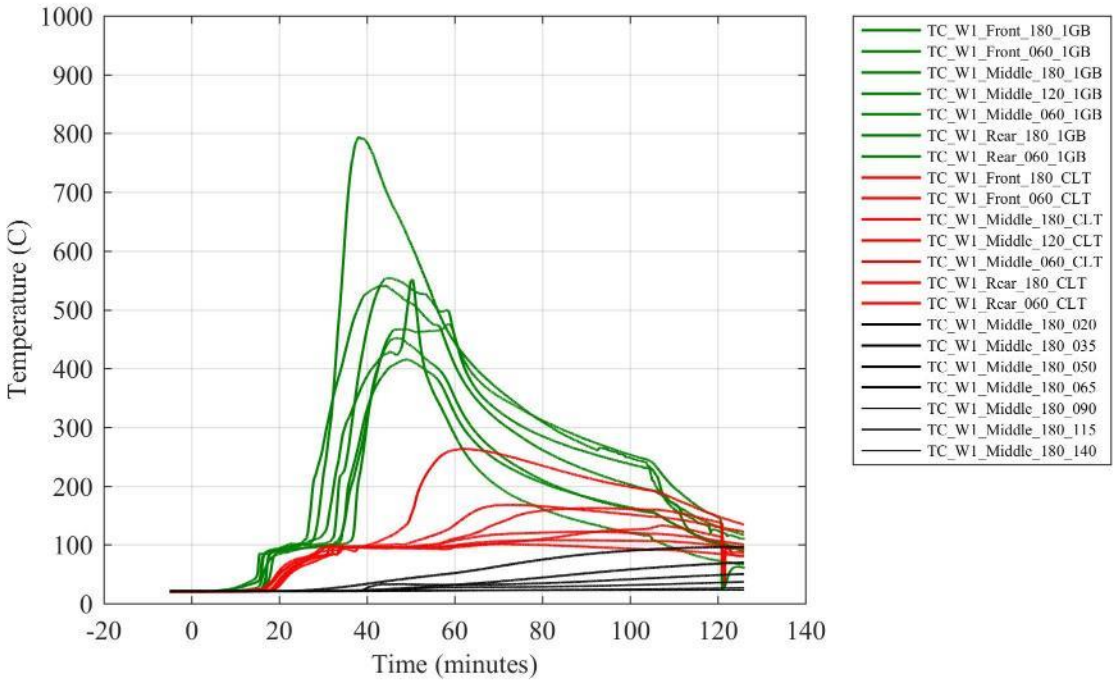

Figure F 11. Temperatures in Wall W1 at various depths from the fire exposed surface.

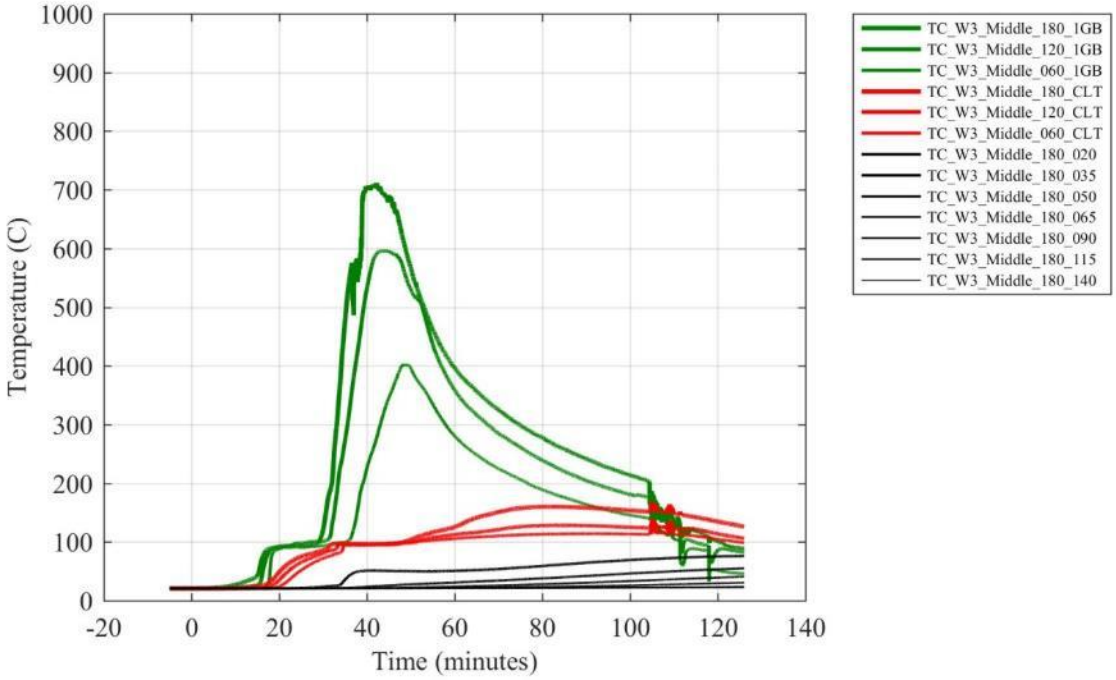

Figure F 12. Temperatures in Wall W3 at various depths from the fire exposed surface.

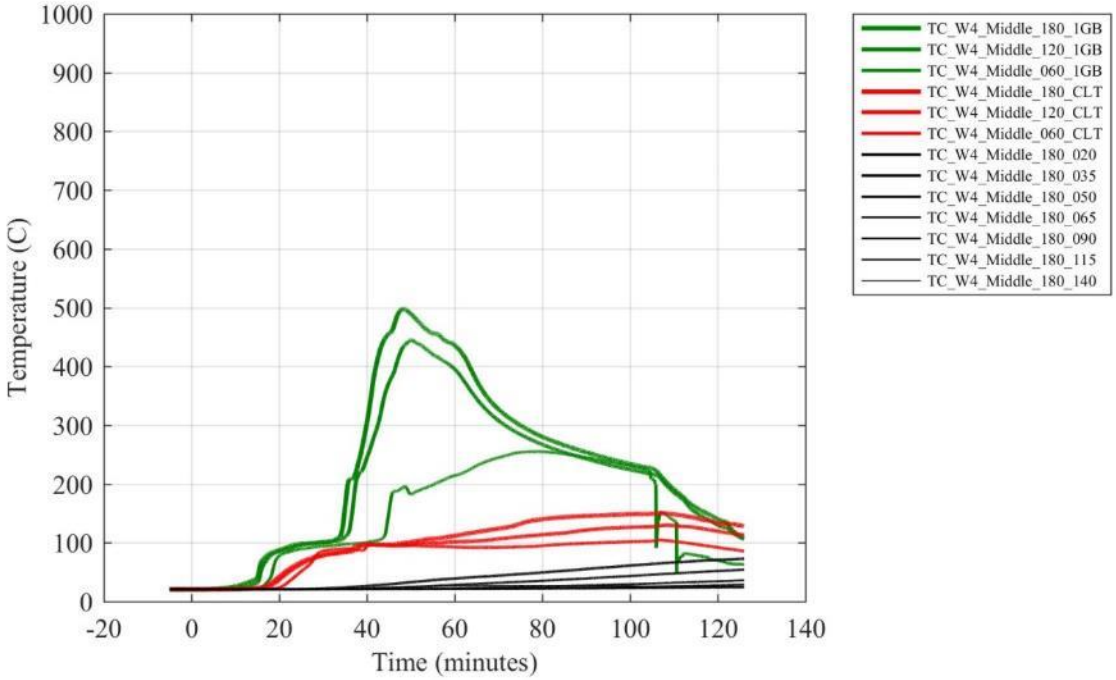

Figure F 13. Temperatures in Wall W4 at various depths from the fire exposed surface.

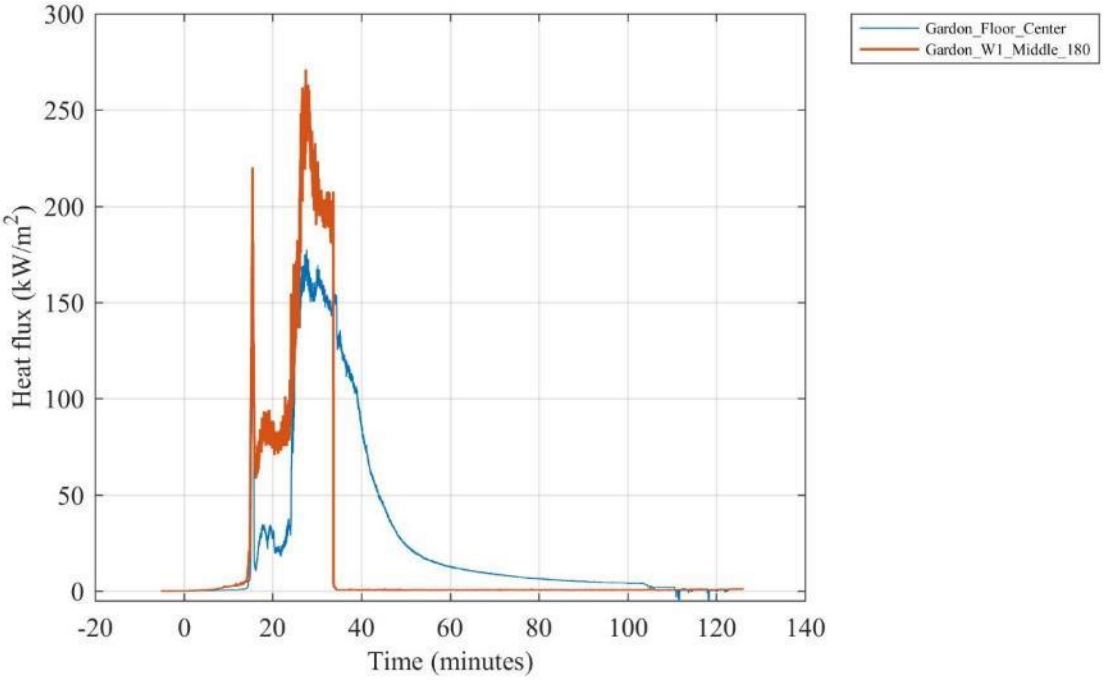

Figure F 14. Heat flux measured by Gardon gauges located inside the compartment.

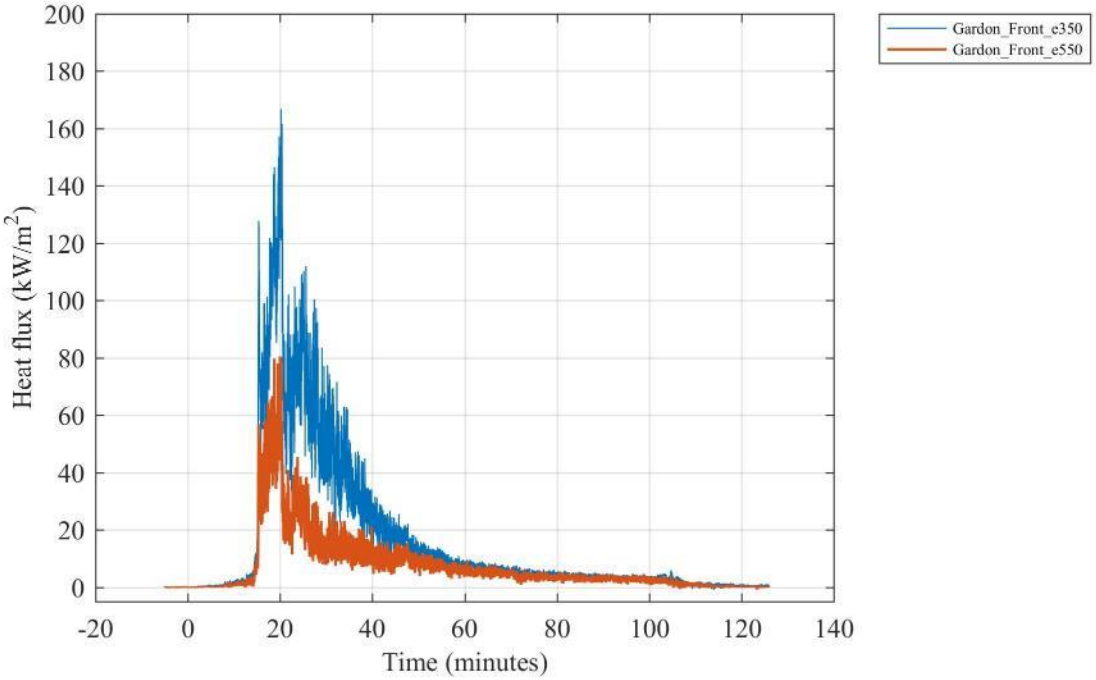

Figure F 15. Heat flux measured by Gardon gauges 350 cm and 550 cm above the floor above the doorway.

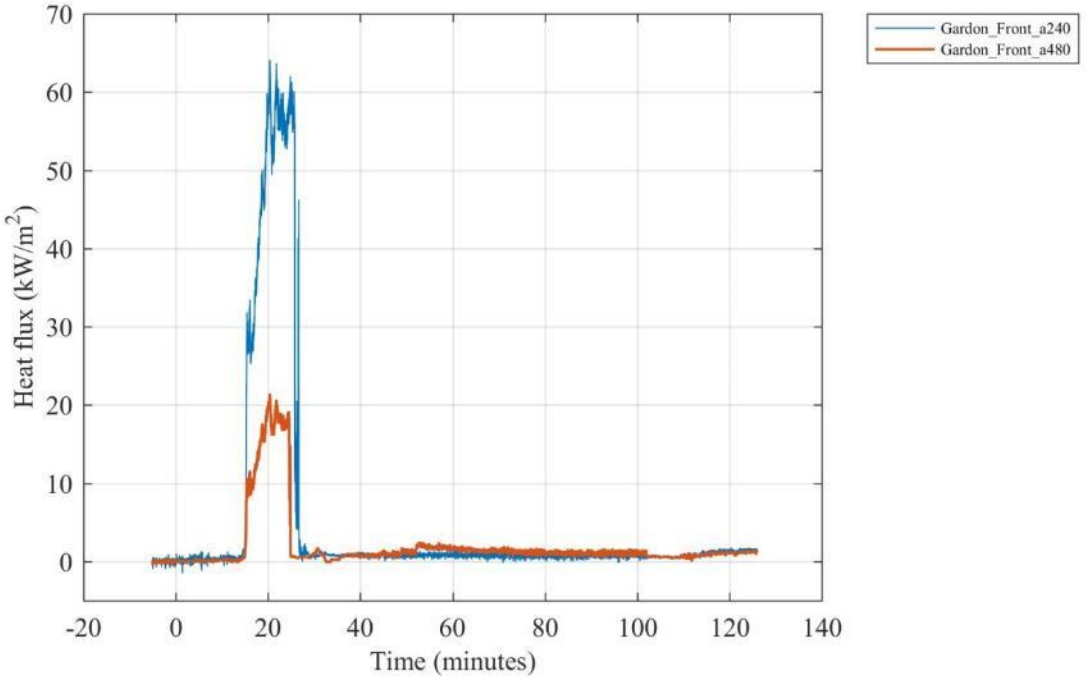

Figure F 16. Heat flux measured by Gardon gauges 240 cm and 480 cm from the doorway facing the opening.

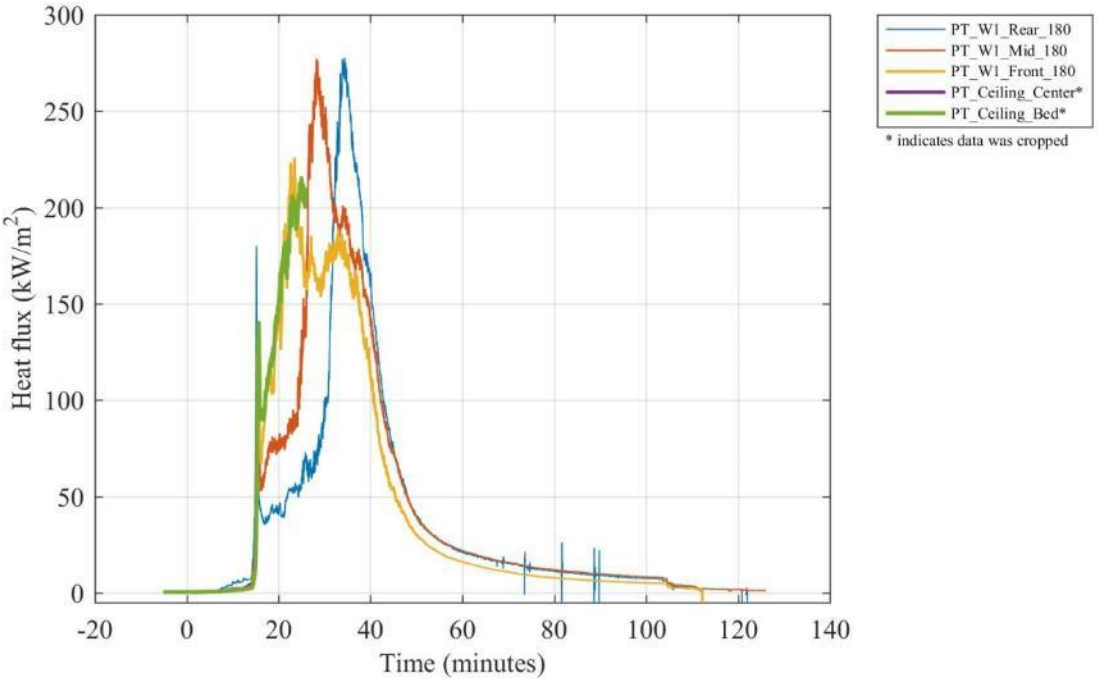

Figure F 17. Heat flux calculated from plate thermometers at various locations inside the compartment.

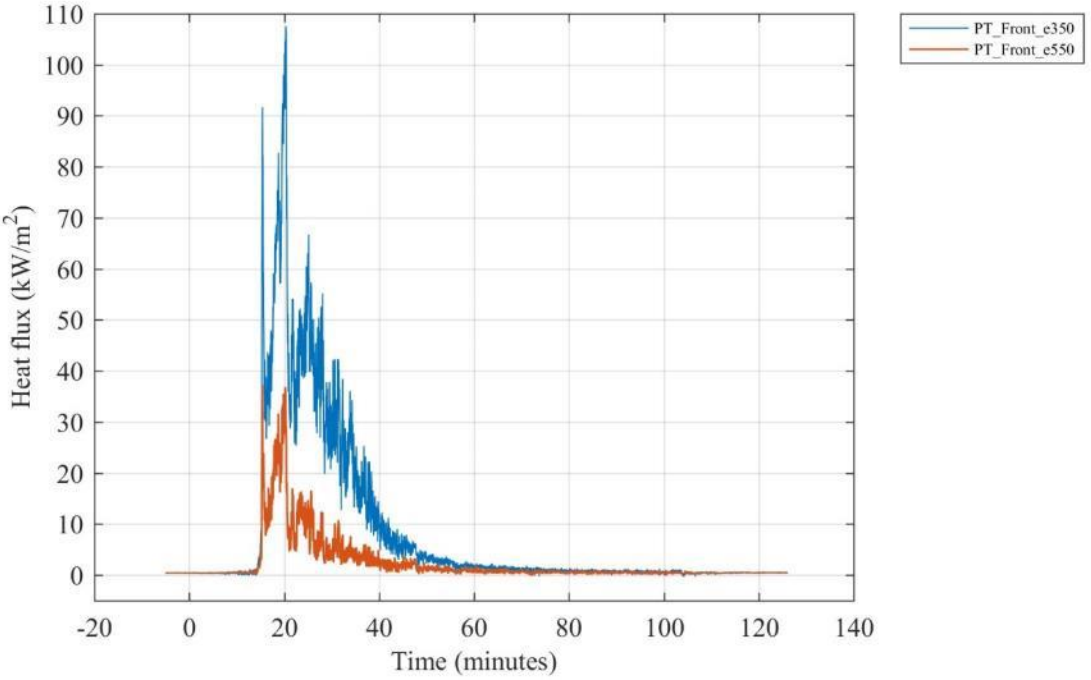

Figure F 18. Heat flux calculated from plate thermometers 350 cm and 550 cm above the floor above the doorway.

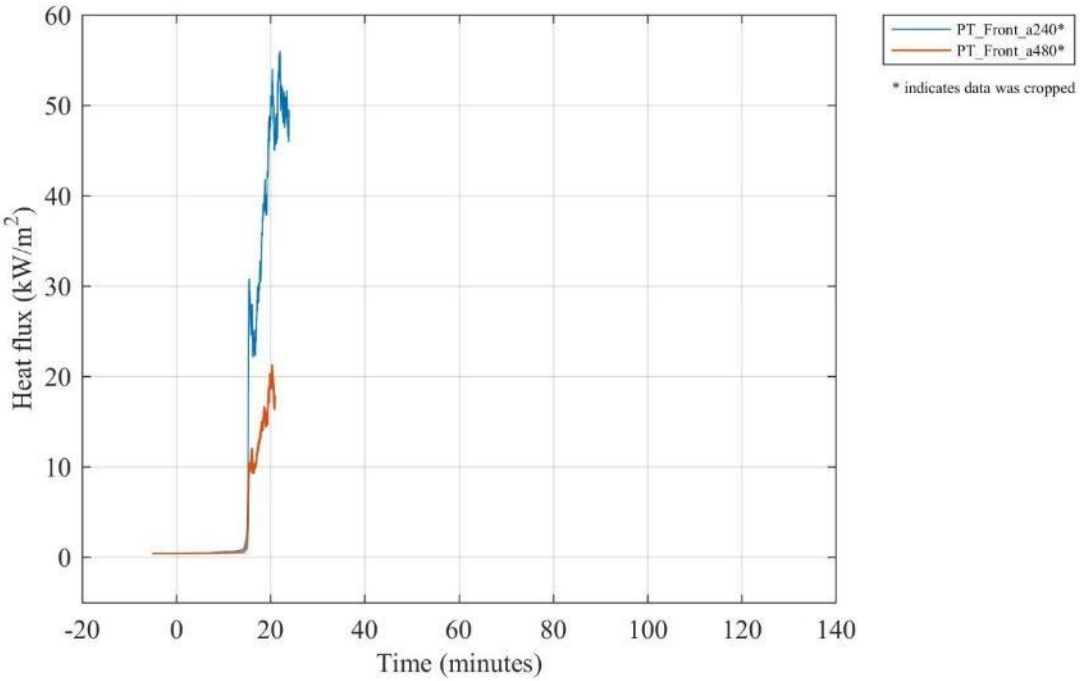

Figure F 19. Heat flux calculated from plate thermometers 240 cm and 480 cm from the doorway facing the opening.

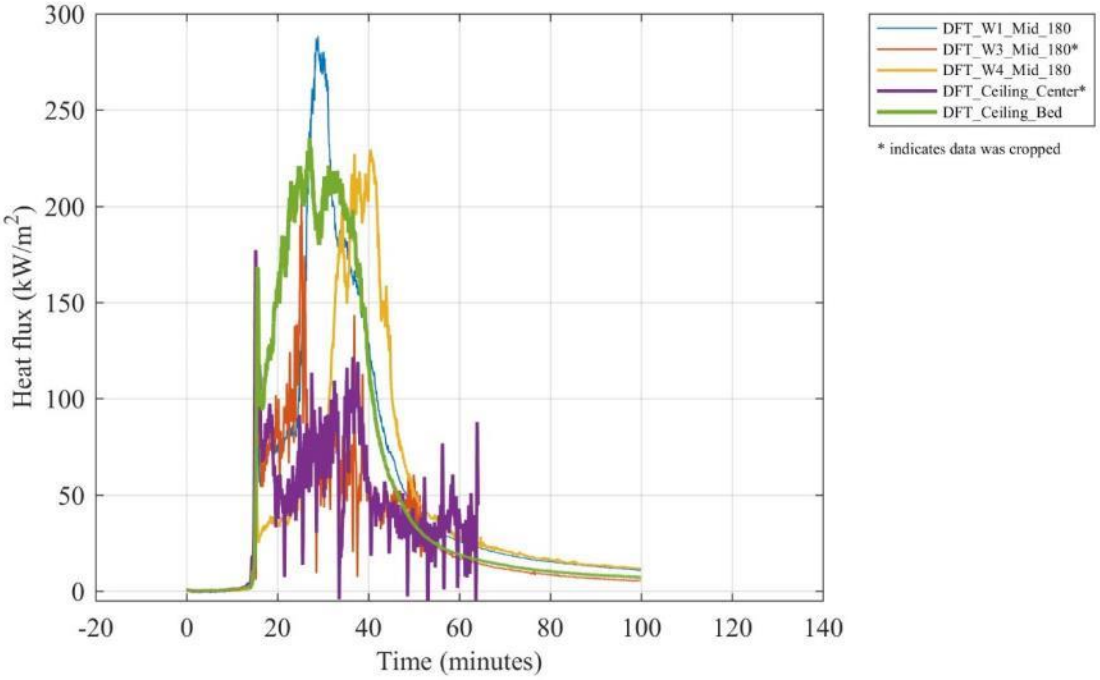

Figure F 20. Heat flux calculated from directional flame thermometers at various locations inside the compartment. [first 100 min processed]

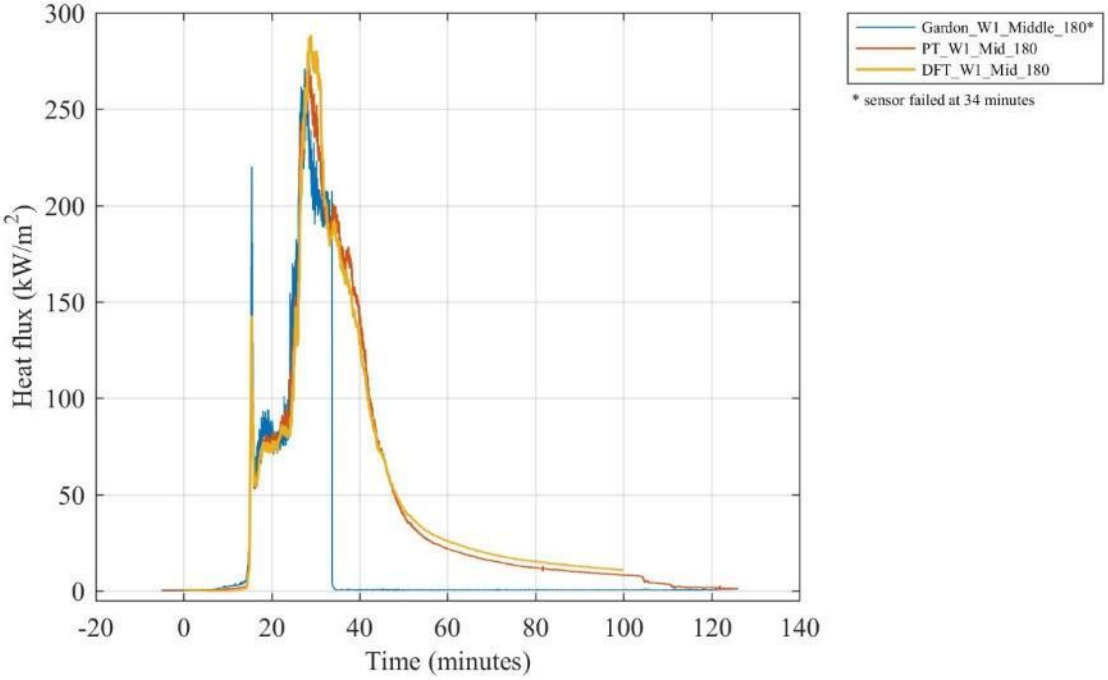

Figure F 21. Comparison of heat fluxes recorded by a collocated Gardon gauge, plate thermometer (PT) and differential flame thermometer (DFT) on Wall W1 at the middle of the compartment 1.8 m above the floor.

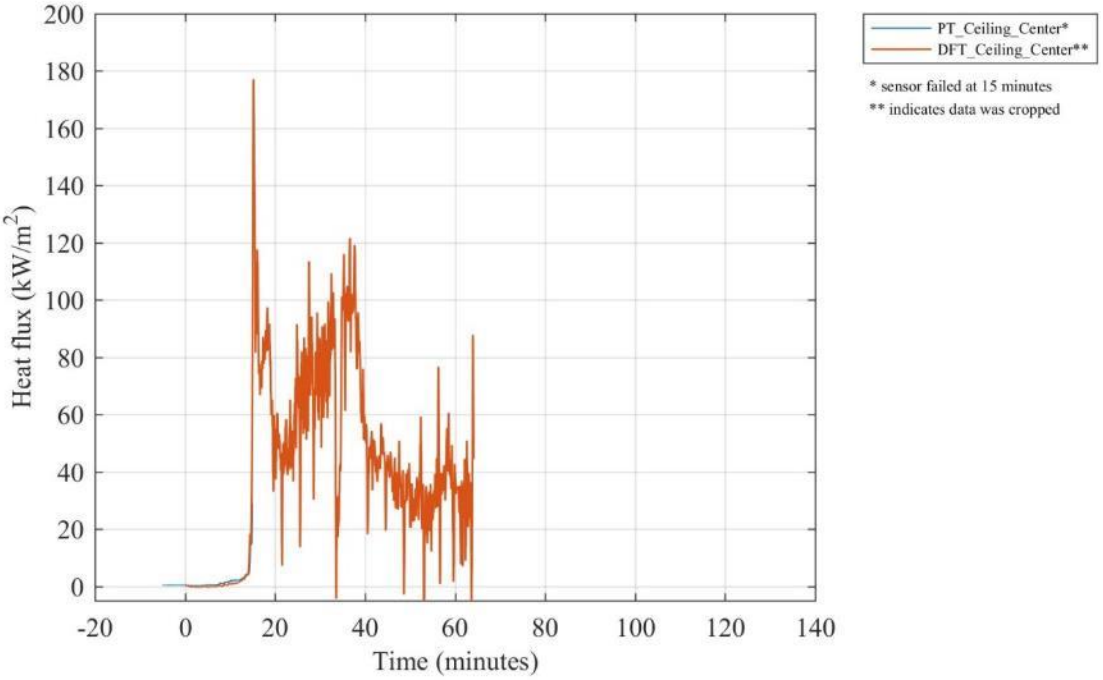

Figure F 22. Comparison of heat fluxes recorded by a collocated plate thermometer (PT) and differential flame thermometer (DFT) on the ceiling at the center of the compartment.

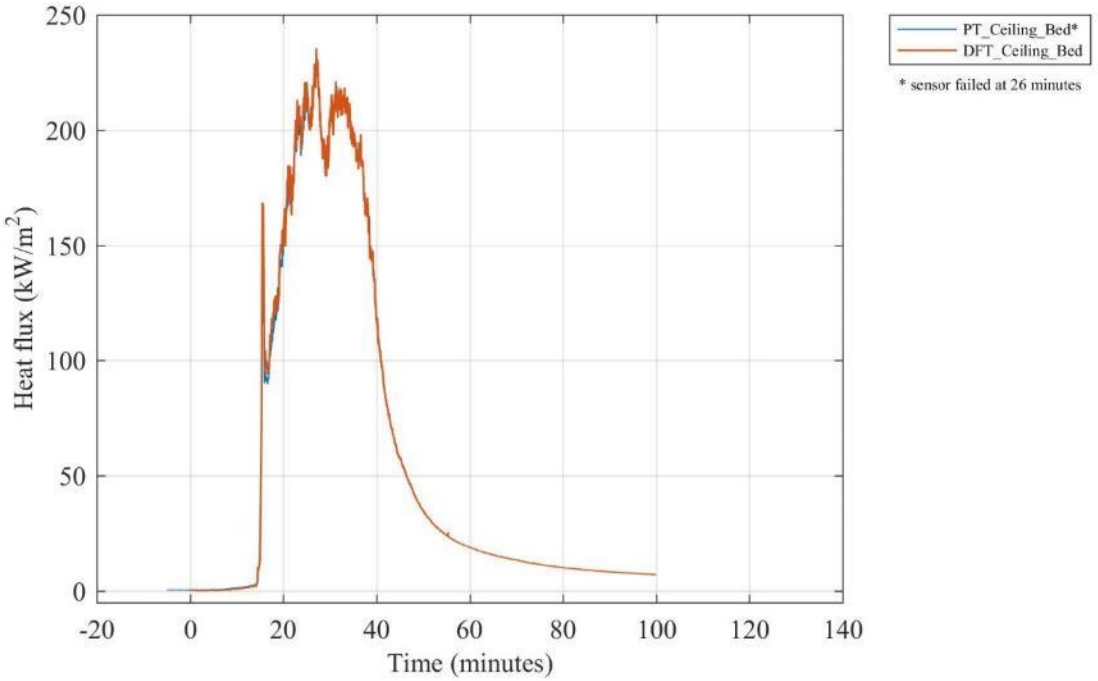

Figure F 23. Comparison of heat fluxes recorded by a collocated plate thermometer (PT) and differential flame thermometer (DFT) on the ceiling above the bed.

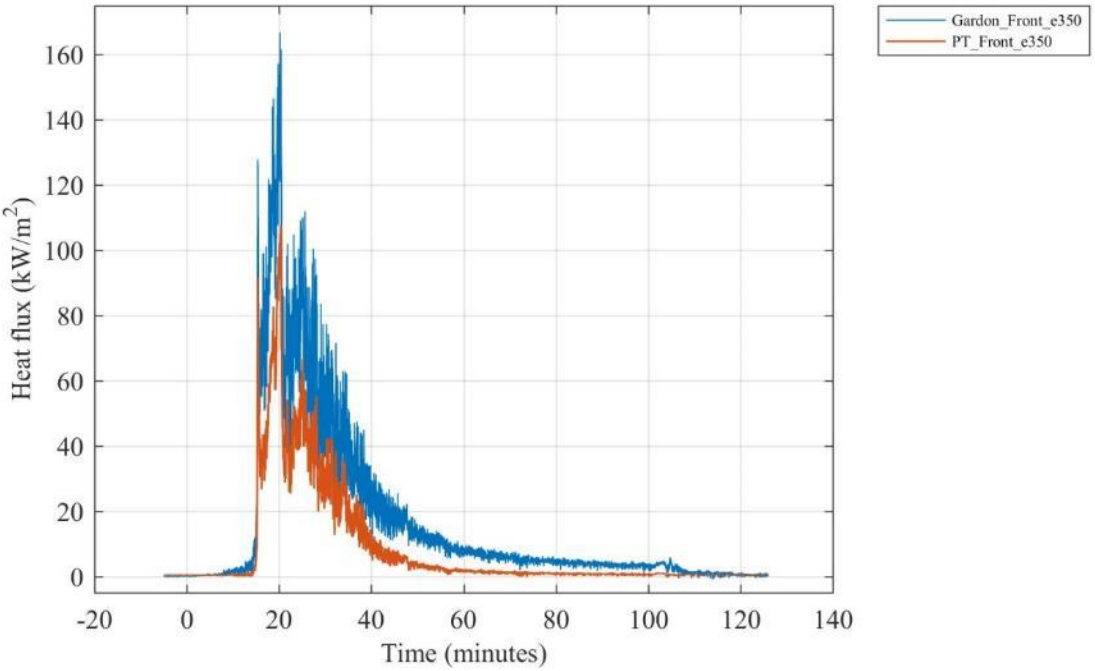

Figure F 24. Comparison of heat fluxes recorded by a collocated Gardon gauge and plate thermometer (PT) 350 cm above the floor above the doorway.

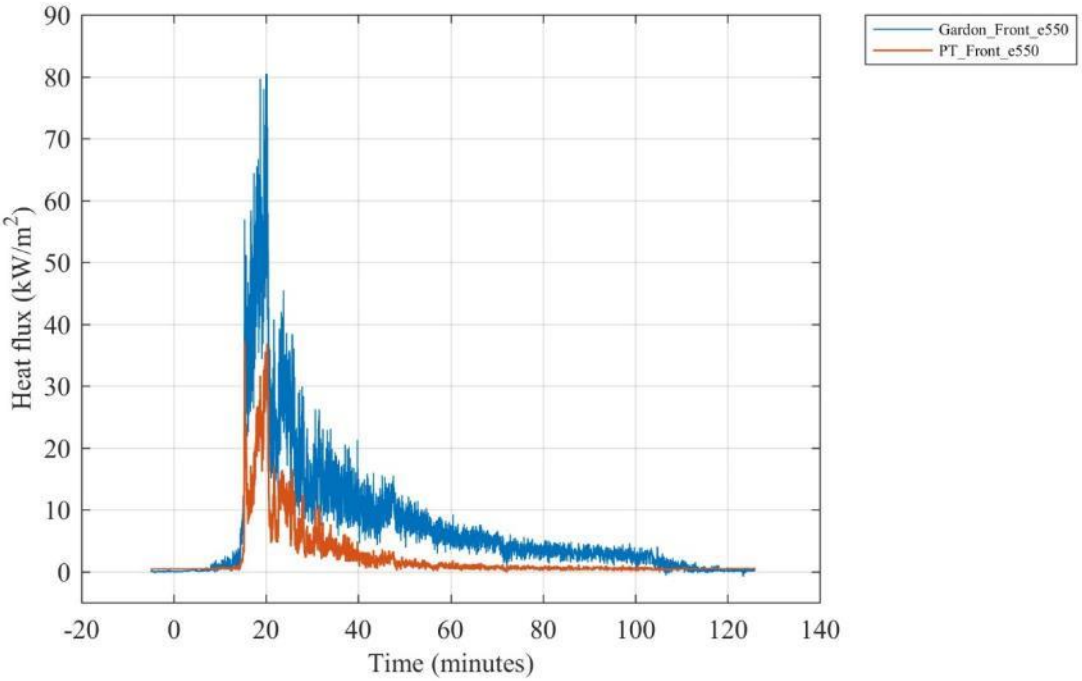

Figure F 25. Comparison of heat fluxes recorded by a collocated Gardon gauge and plate thermometer (PT) 550 cm above the floor above the doorway.

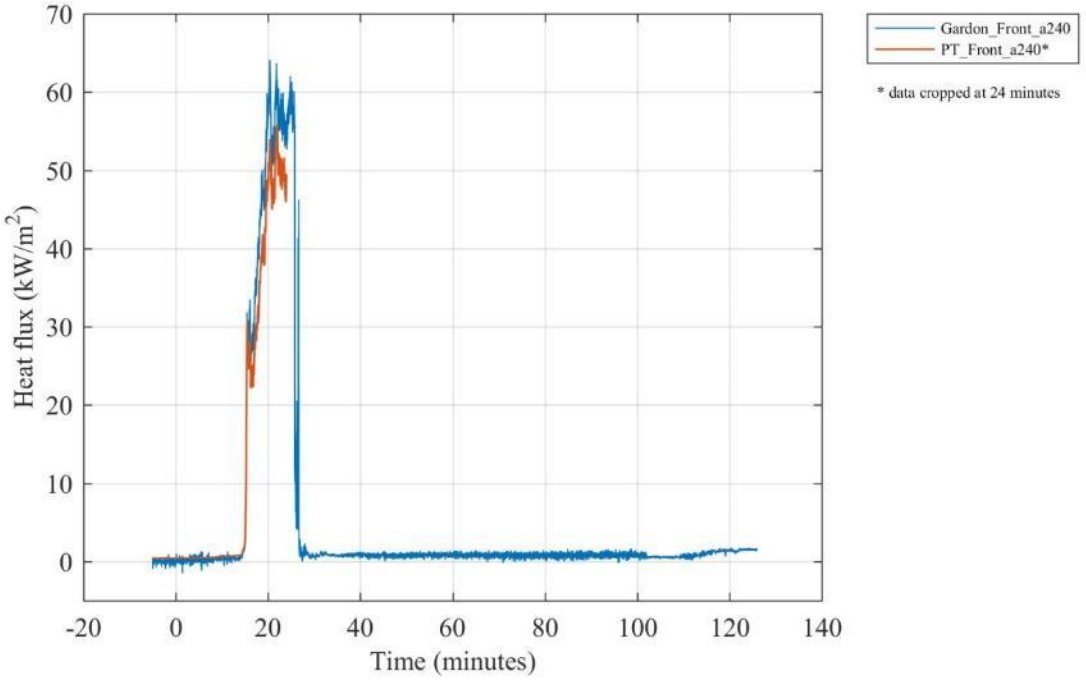

Figure F 26. Comparison of heat fluxes recorded by a collocated Gardon gauge and plate thermometer (PT) 240 cm from the doorway (facing doorway) and 150 cm above floor.

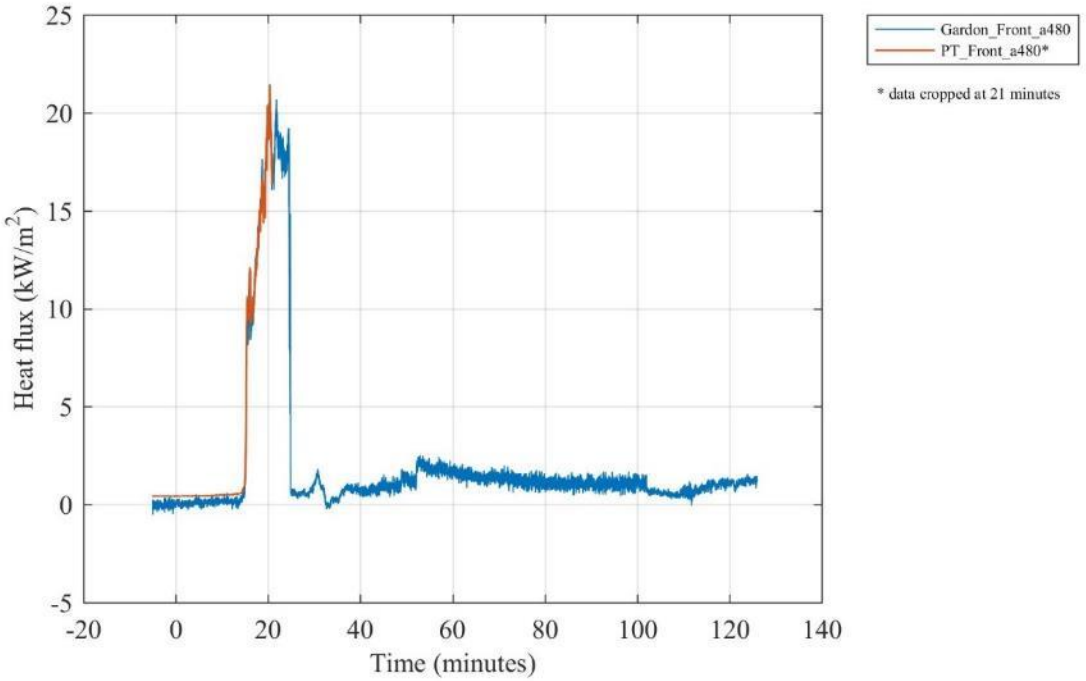

Figure F 27. Comparison of heat fluxes recorded by a collocated Gardon gauge and plate thermometer (PT) 480 cm from the doorway (facing doorway) and 150 cm above floor.

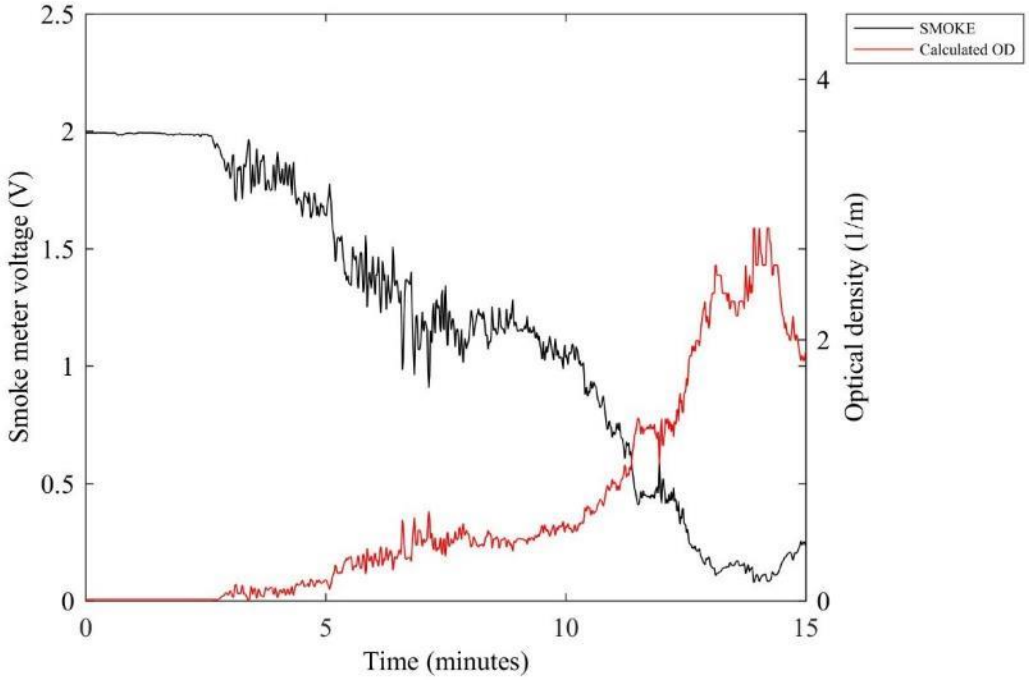

Figure F 28. Smoke meter voltage and calculated optical density (OD) from gas sampled at the center of the compartment 160 cm above the floor.

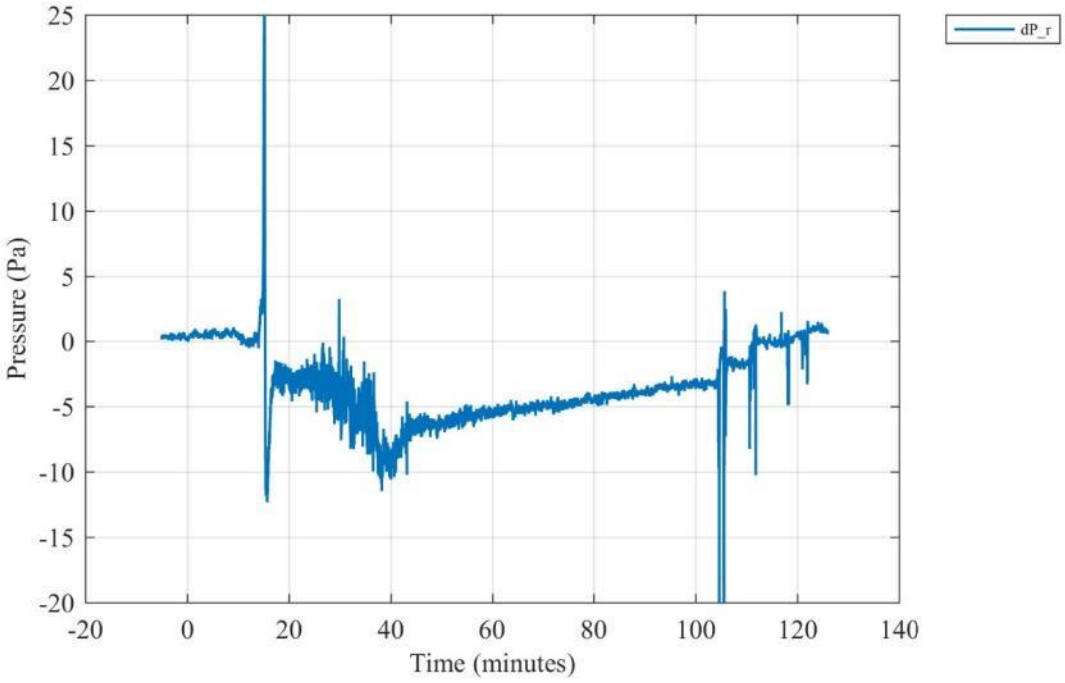

Figure F 29. Differential room pressure measured 210 cm above the floor at the center of the compartment.

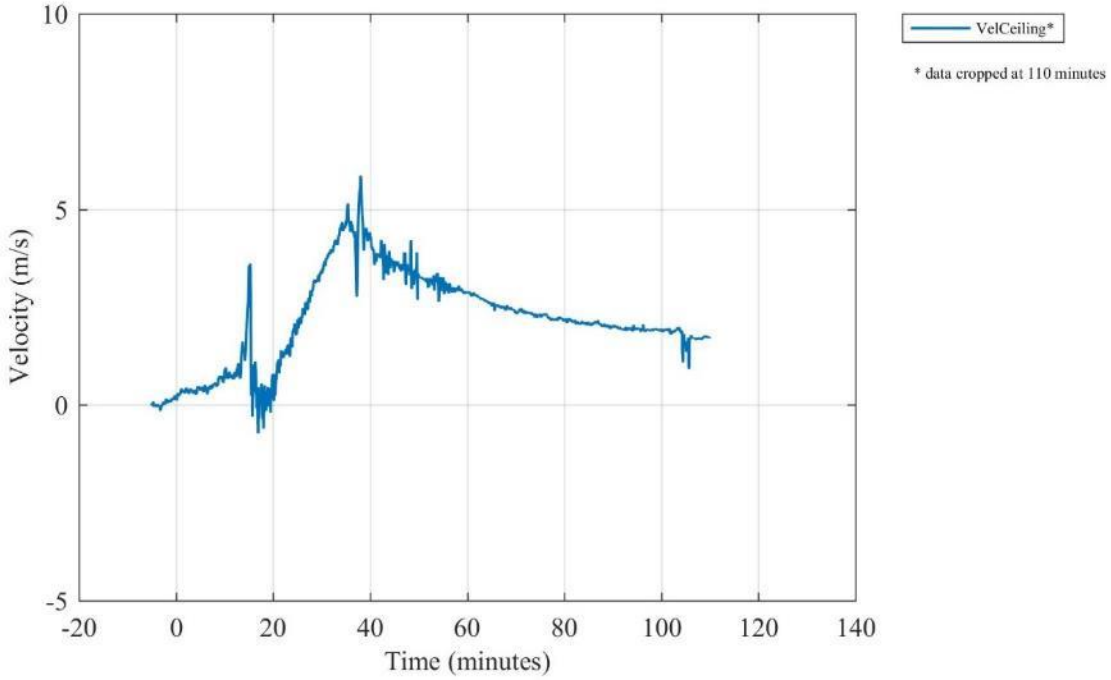

Figure F 30. Gas velocity measured 305 mm from the ceiling along the midline 227.5 cm from the back of the compartment (positive indicates flow out the door). [10 s moving average filter applied]

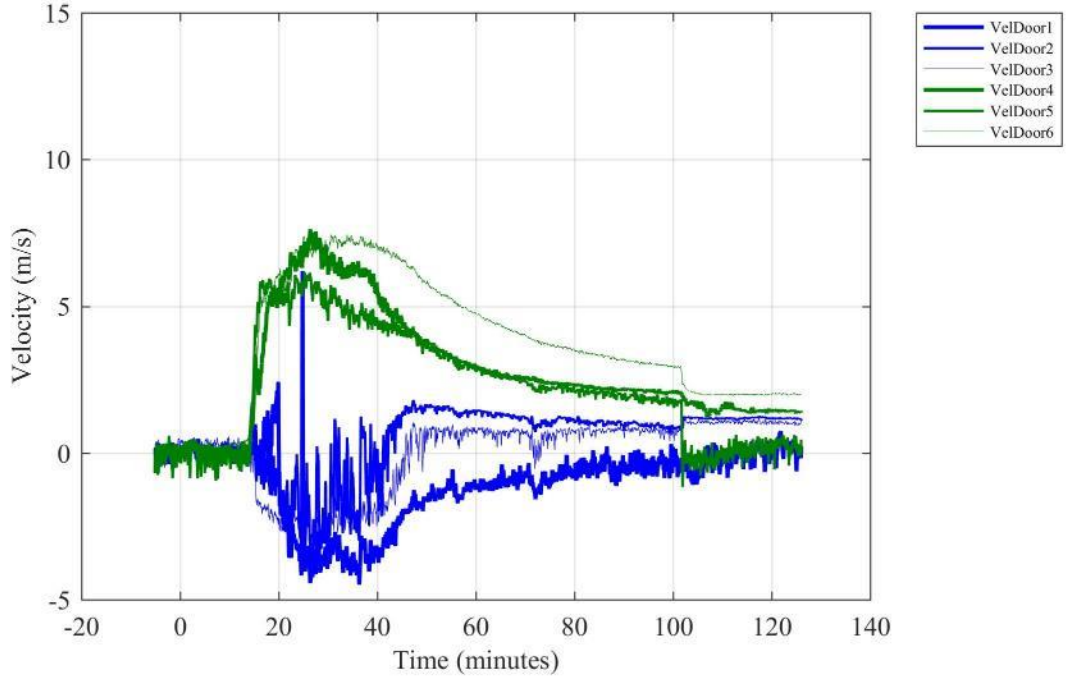

Figure F 31. Gas velocities measured in the doorway (positive indicates flow out the door). [10 s moving average filter applied]

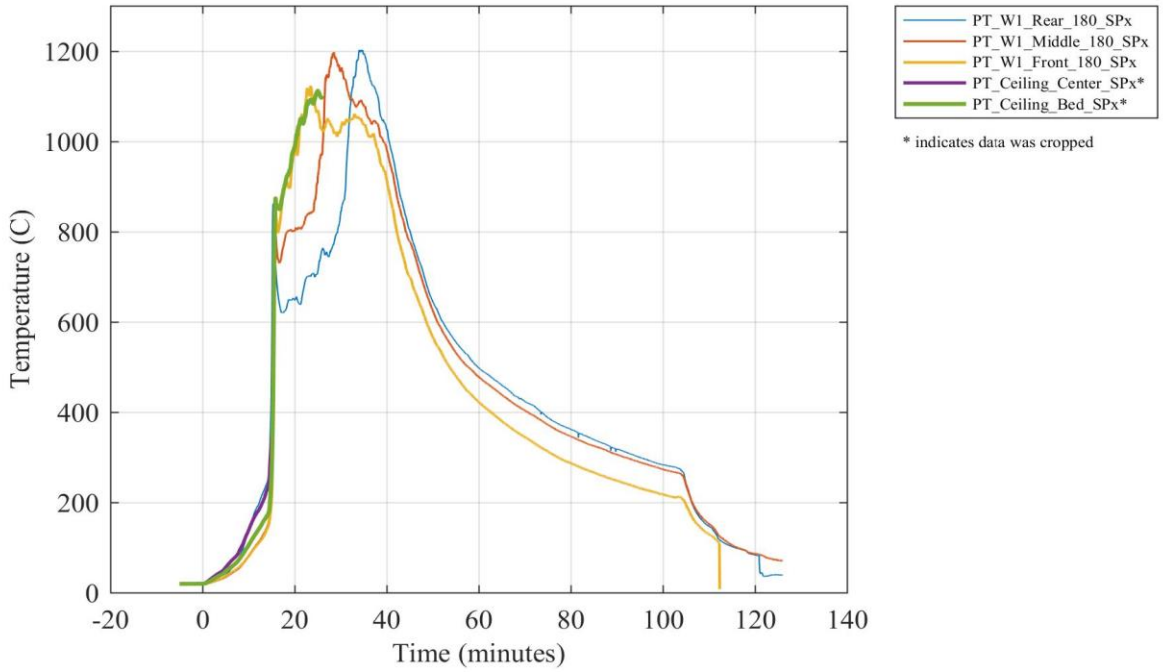

Figure F 32. Plate thermometer temperatures at various locations inside the compartment.

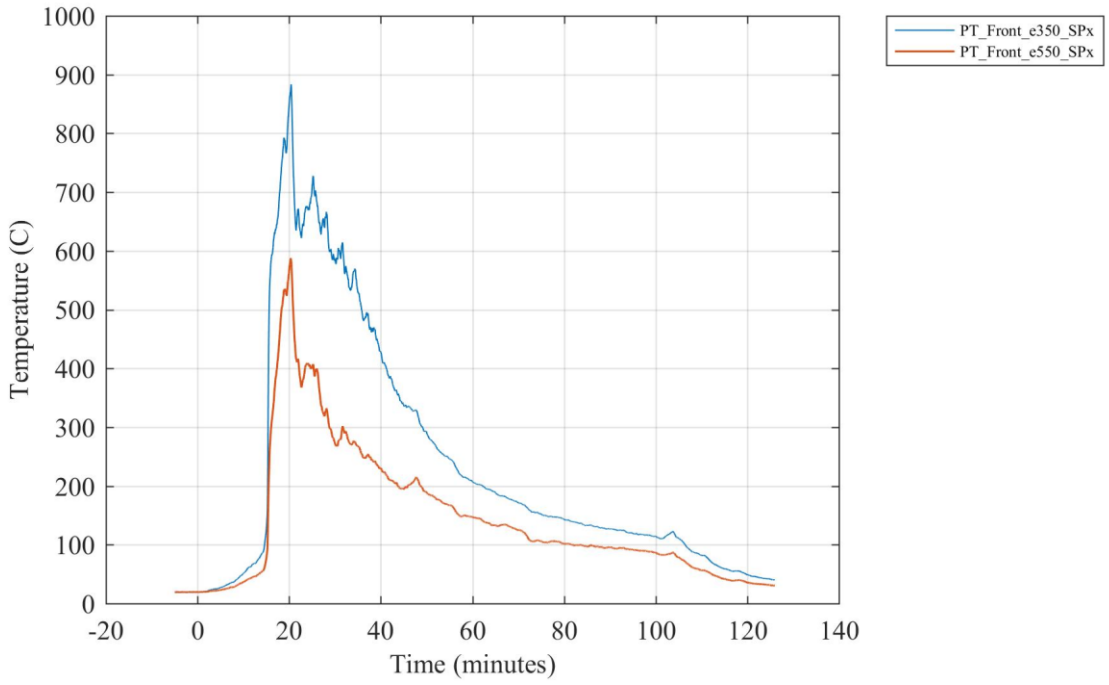

Figure F 33. Plate thermometer temperatures 350 cm and 550 cm above the floor above the doorway.

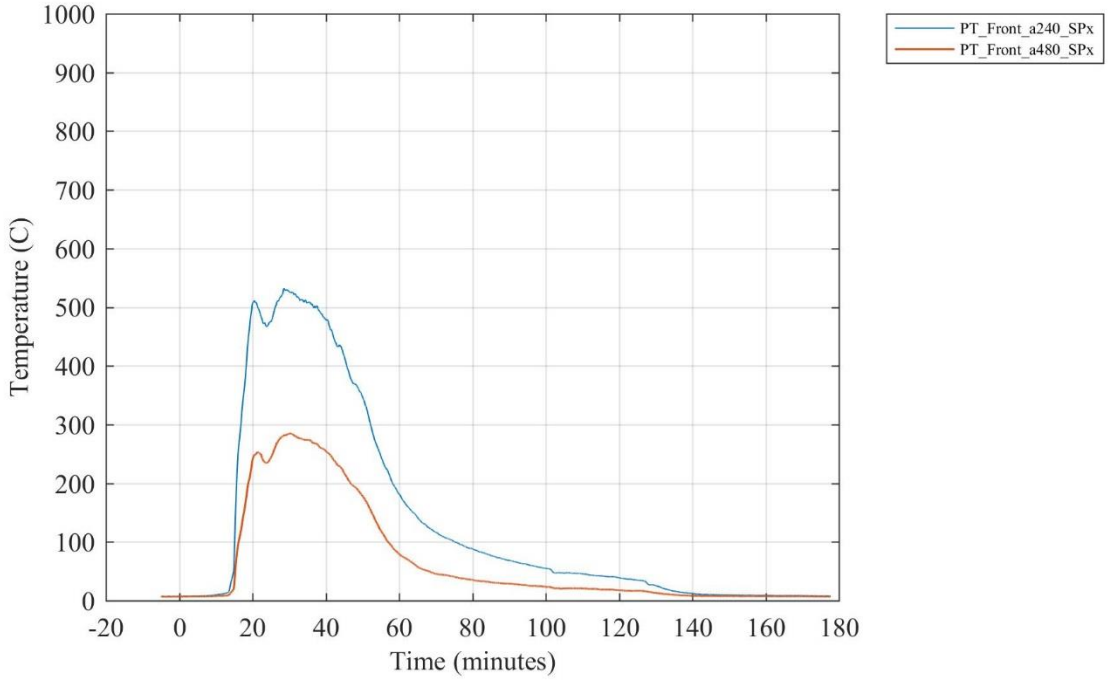

Figure F 34. Plate thermometer temperatures 240 cm and 480 cm from the doorway facing the opening.

Appendix G - Test 1-3 data

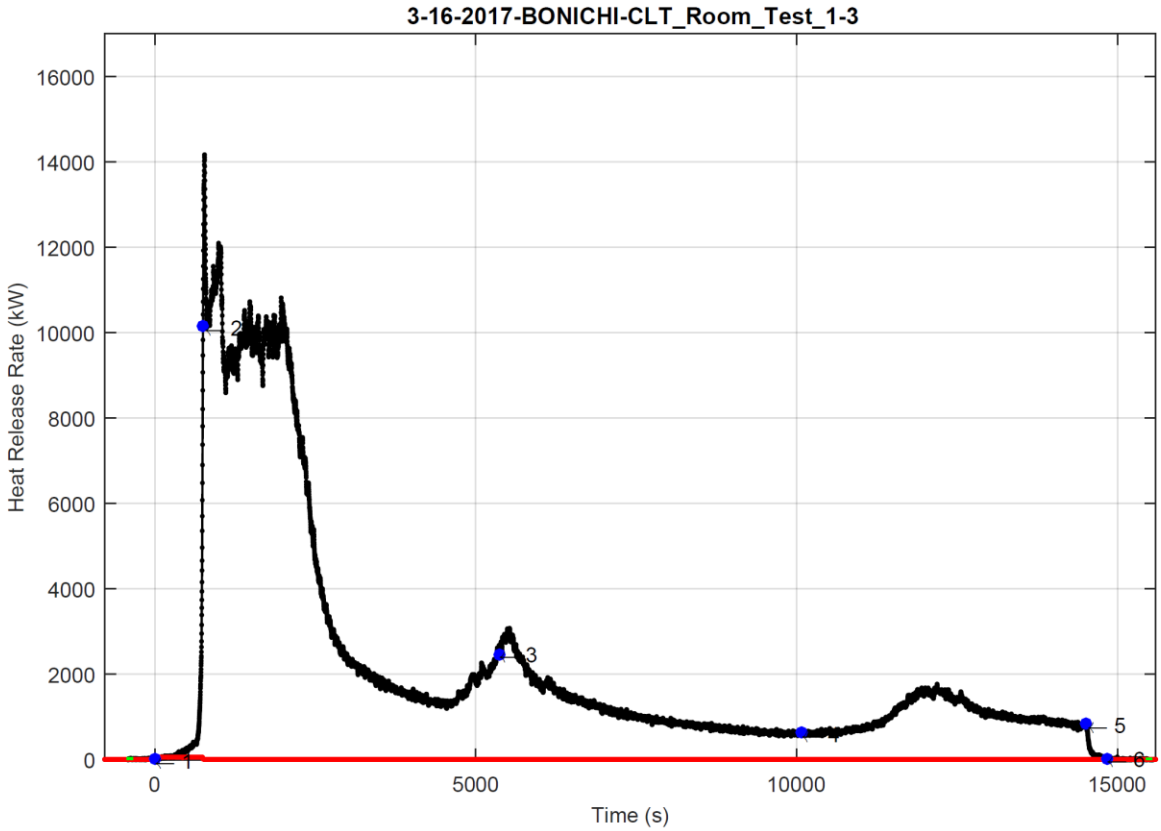

Hood Size = 15 (m)

Peak Heat Release Rate = 14171 (kW)

NG Burner Peak HRR = 51 (kW)

Exhaust Flow = 97.02 +/- 0.46 (kg/s)

O_2 Baseline = 0.20941 (Vol Fr)

O_2 Drift During Test = -25 (ppmv)

CO Generated = 112.97 (kg)

Fuel Type = WoodFurniturePUF ; HOC = 19.9 (MJ/kg)

Total Heat Release = 32448 (MJ)

NG Burner Total HR = 40 (MJ)

Total Burn Time = 4.12 (Hrs)

Fuel Mass Burned = 1630.55 (kg)

O_2 Consumed = 2526.34 (kg)

CO_2 Generated = 3251.81 (kg)

Test Description:
CLT Room test 1-3. Furnished room with 2 layers of type X gypsum on all walls and 3 layers on ceiling. Wall 1 is exposed CLT Double wide door opening

Event Count	Time (s)	Time Stamp	Event Description
1	0	3/16/2017 10:33:39 AM	Ignition
2	751	3/16/2017 10:46:11 AM	flashover
3	5358	3/16/2017 12:02:58 PM	delamination of first layer of CLT in progress
4	10071	3/16/2017 1:21:31 PM	start of delamination on second layer of CLT
5	14515	3/16/2017 2:35:35 PM	Start water suppression
6	14838	3/16/2017 2:40:58 PM	Fire Out

Figure G 1. Summary report file generated by the NFRL calorimeter on the day of test.

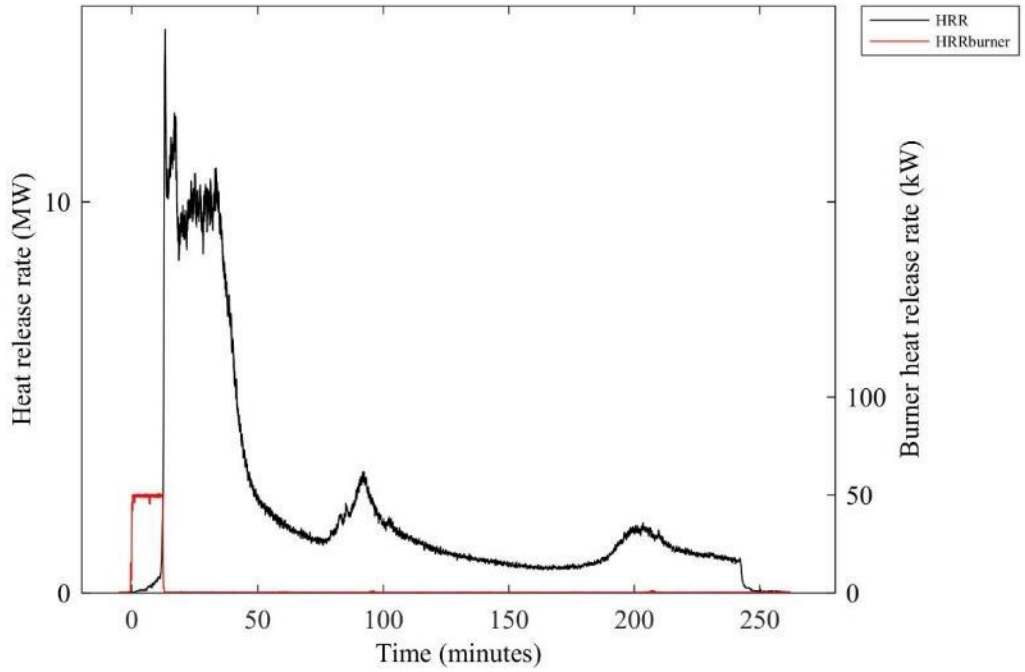

Figure G 2. Compartment (left axis) and burner (right axis) heat release rates.

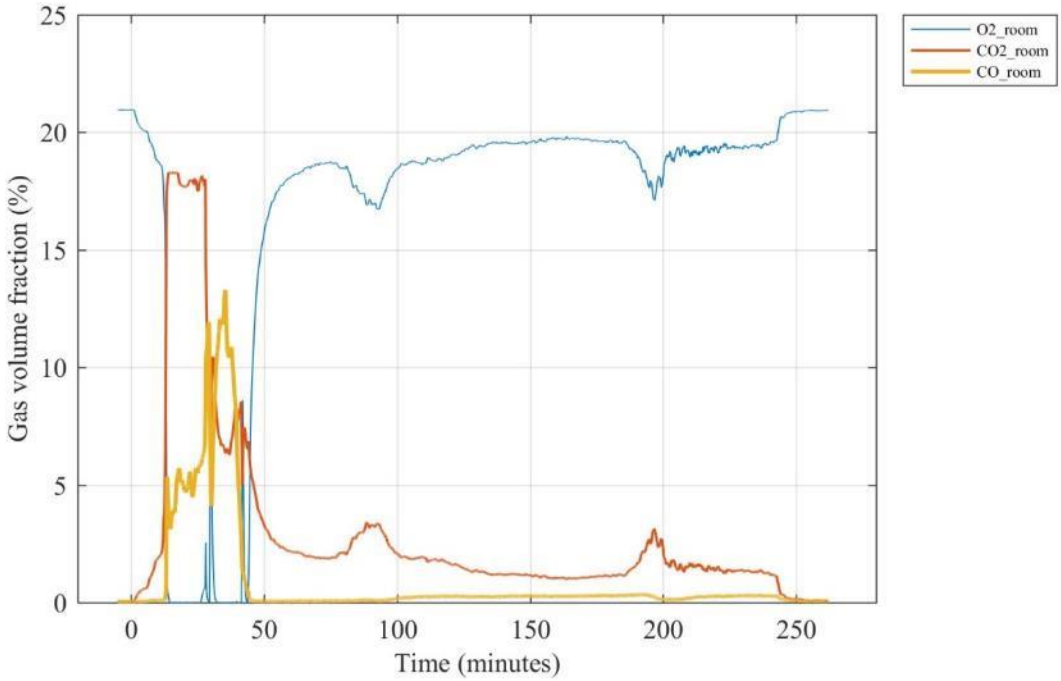

Figure G 3. Gas volume fractions for oxygen (O_2), carbon dioxide (CO_2) and carbon monoxide (CO) sampled at the center of the compartment 210 cm above the floor.

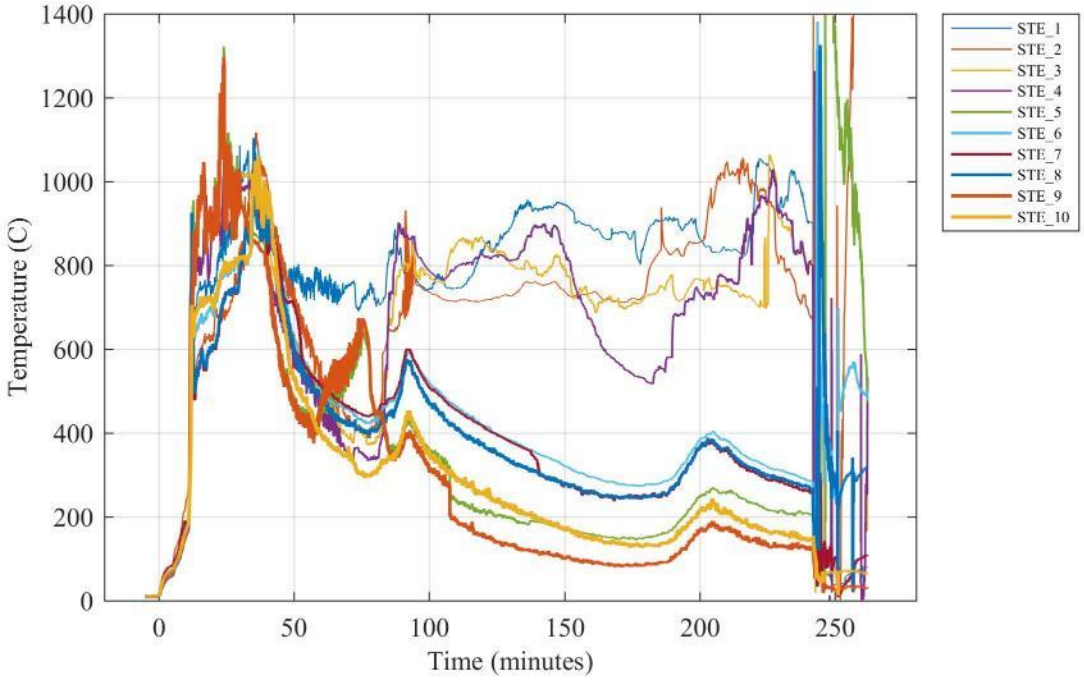

Figure G 4. Simulated thermal elements (STE) for sprinkler.

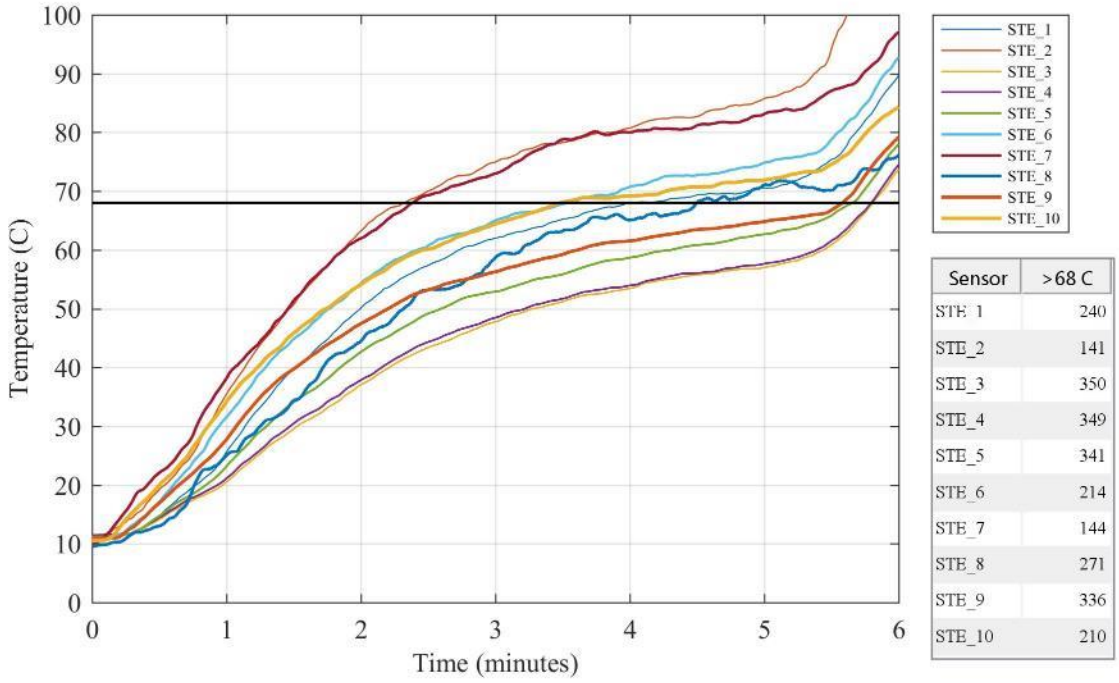

Sensor	>68 C
STE_1	240
STE_2	141
STE_3	350
STE_4	349
STE_5	341
STE_6	214
STE_7	144
STE_8	271
STE_9	336
STE_10	210

Figure G 5. Simulated thermal elements (STE) for sprinkler with table showing time after ignition (in seconds) until 68 °C is reached.

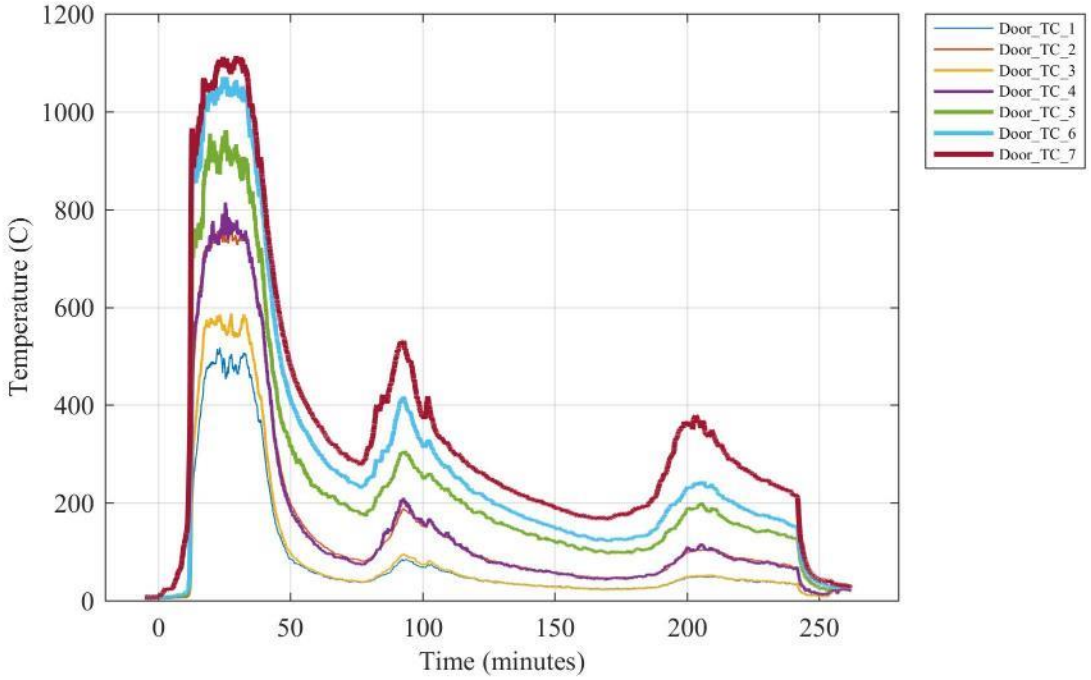

Figure G 6. Temperatures measured at various heights above the floor in the doorway.

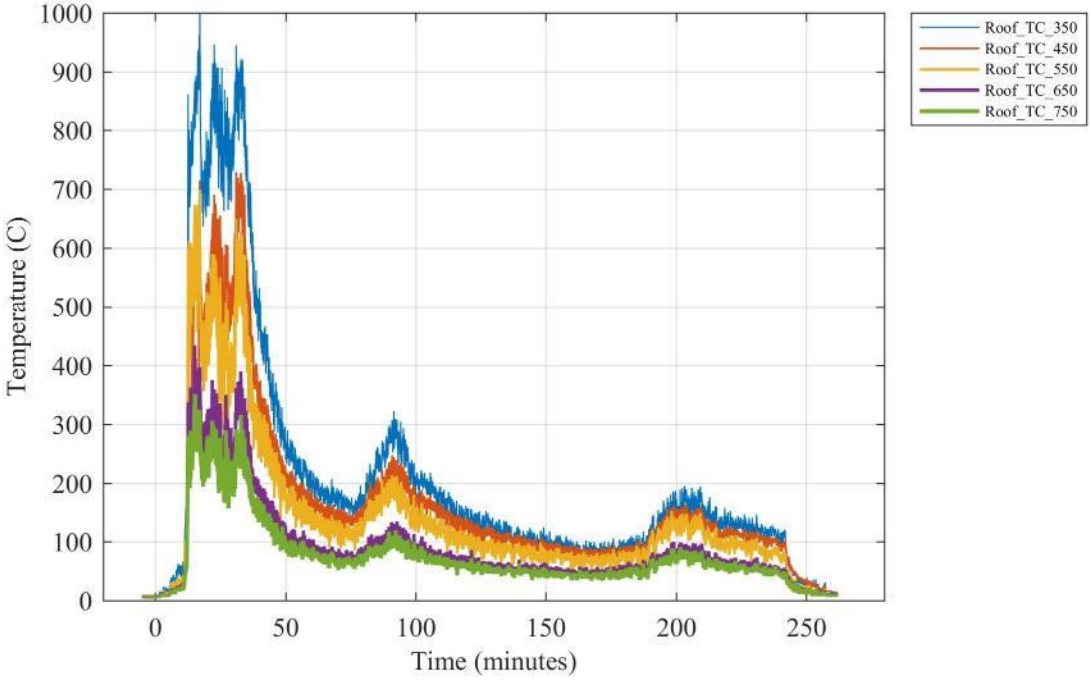

Figure G 7. Temperatures measured at various heights above the floor above the doorway.

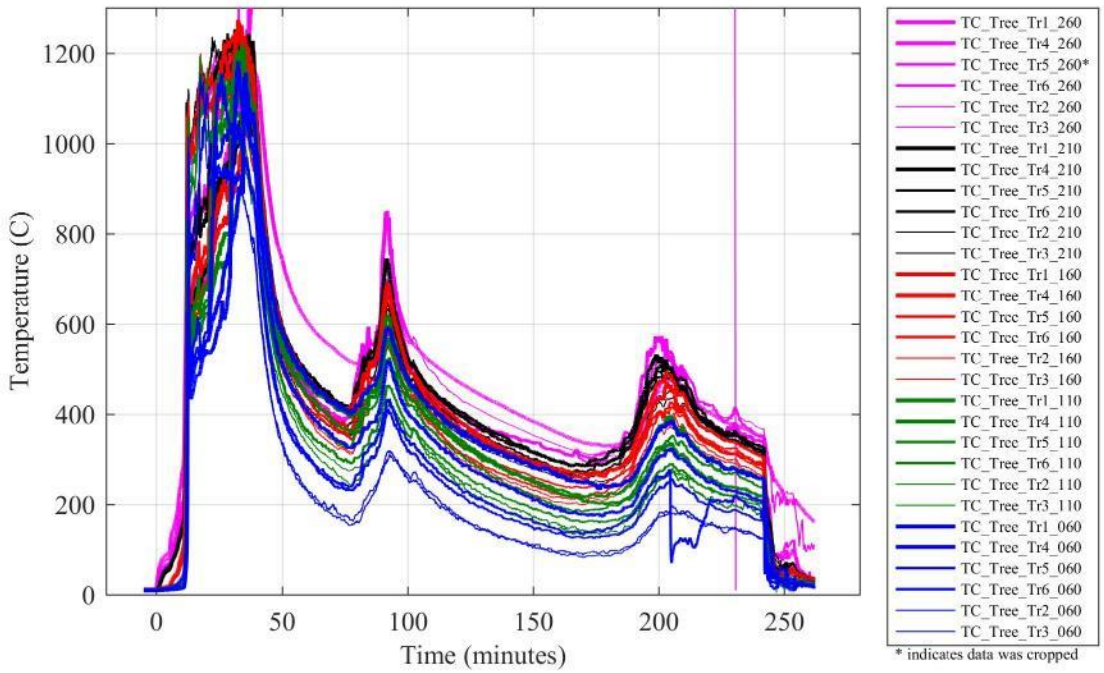

Figure G 8. Thermocouple tree temperatures at various locations inside the compartment.

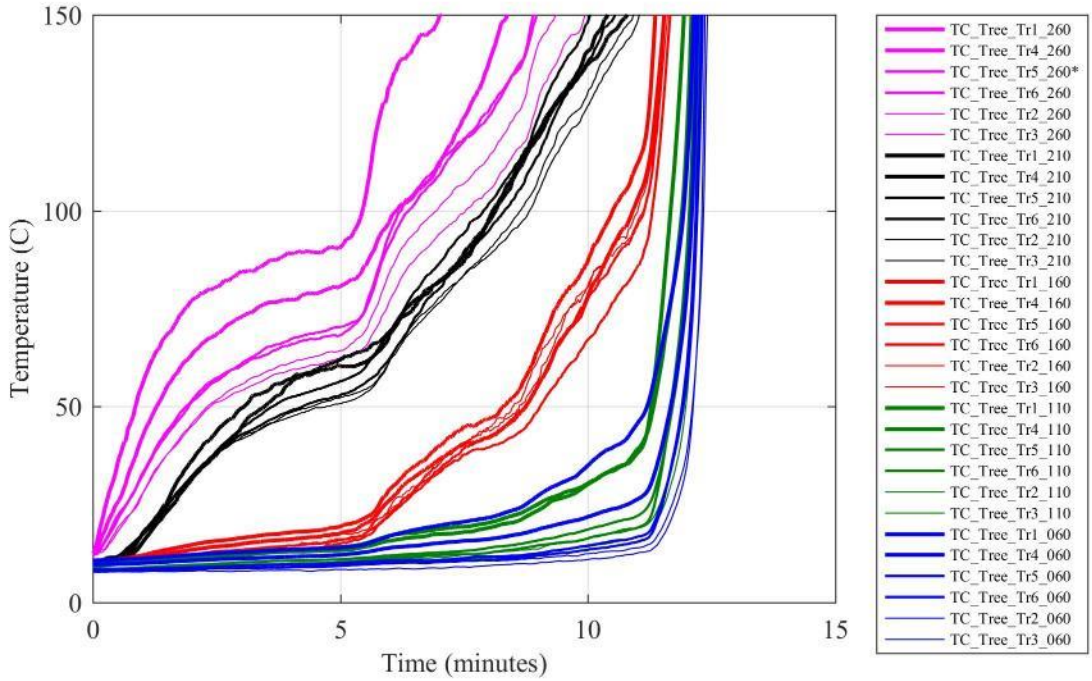

Figure G 9. Thermocouple tree temperatures at various locations inside the compartment during the first 15 min after ignition.

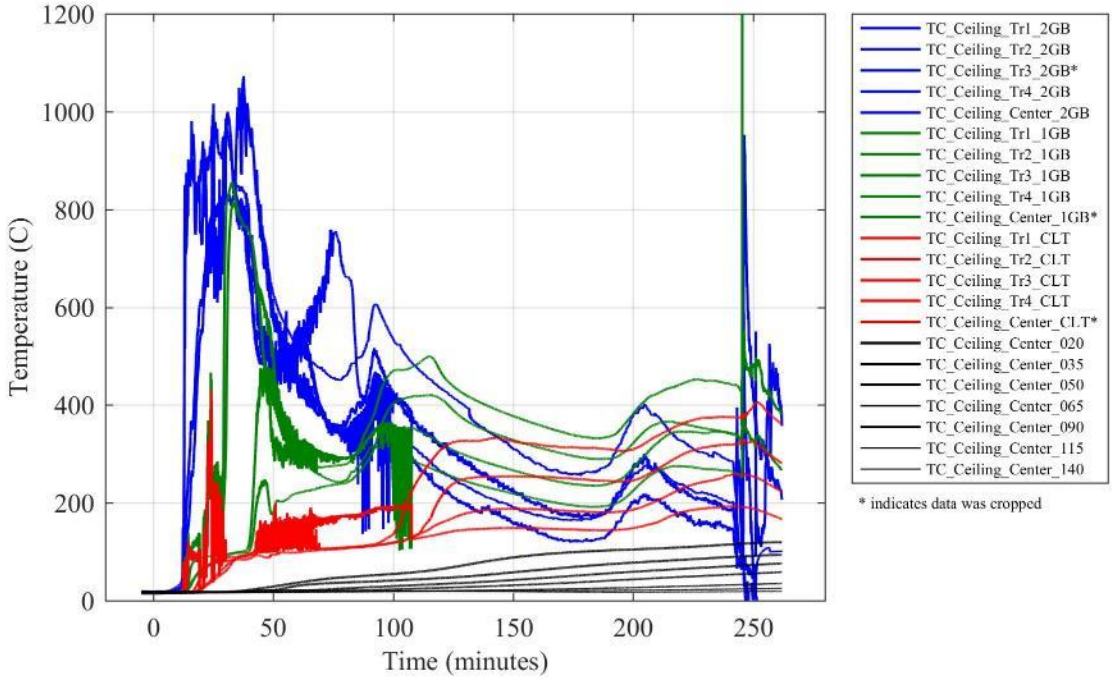

Figure G 10. Temperatures in the ceiling at various depths from the fire exposed surface.

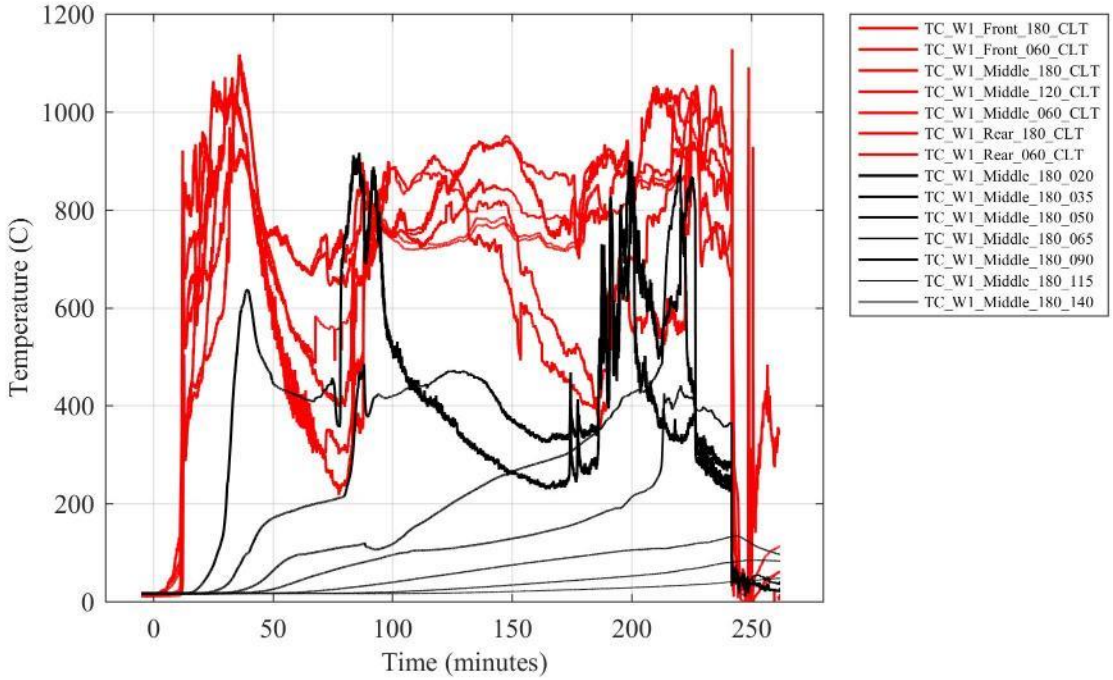

Figure G 11. Temperatures in Wall W1 at various depths from the fire exposed surface.

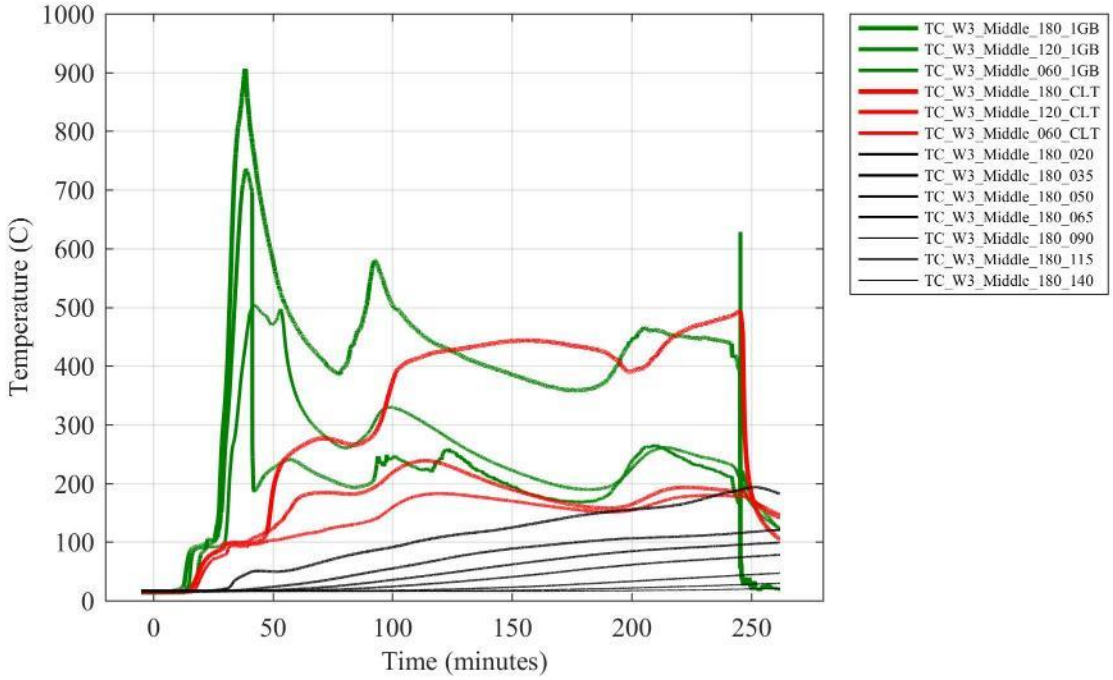

Figure G 12. Temperatures in Wall W3 at various depths from the fire exposed surface.

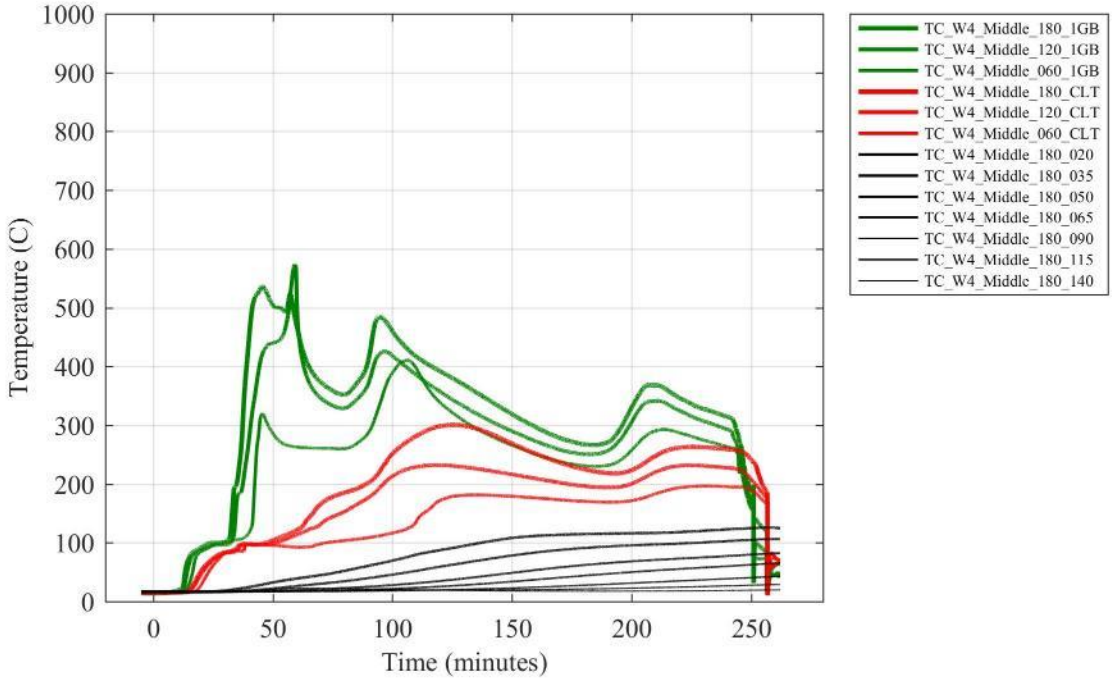

Figure G 13. Temperatures in Wall W4 at various depths from the fire exposed surface.

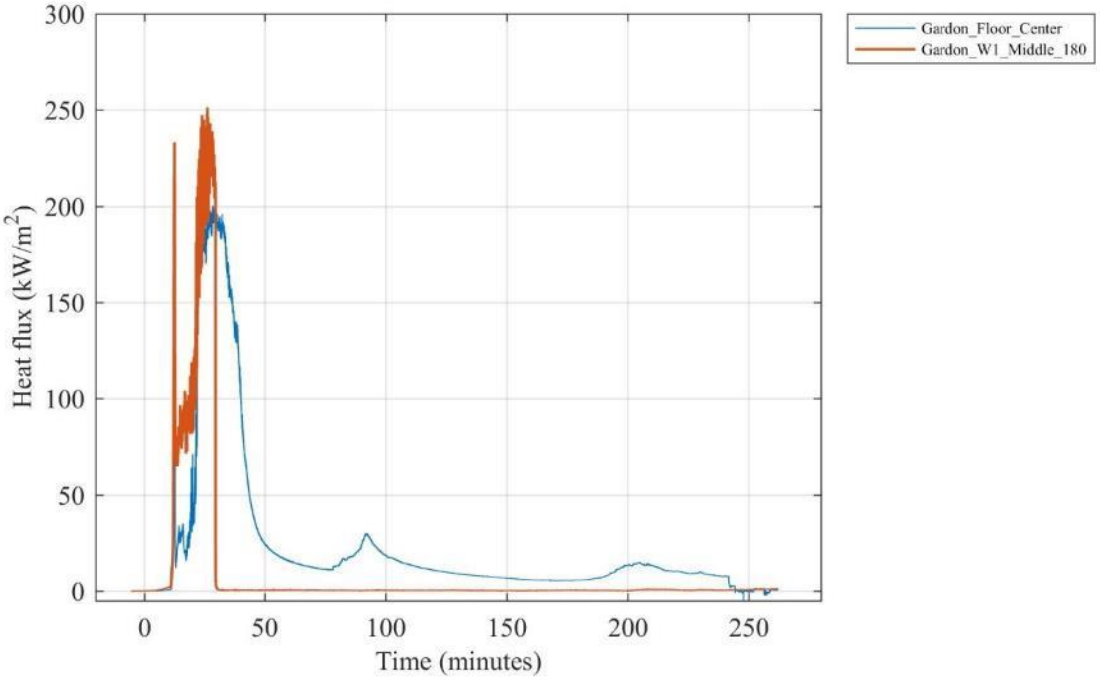

Figure G 14. Heat flux measured by Gardon gauges located inside the compartment.

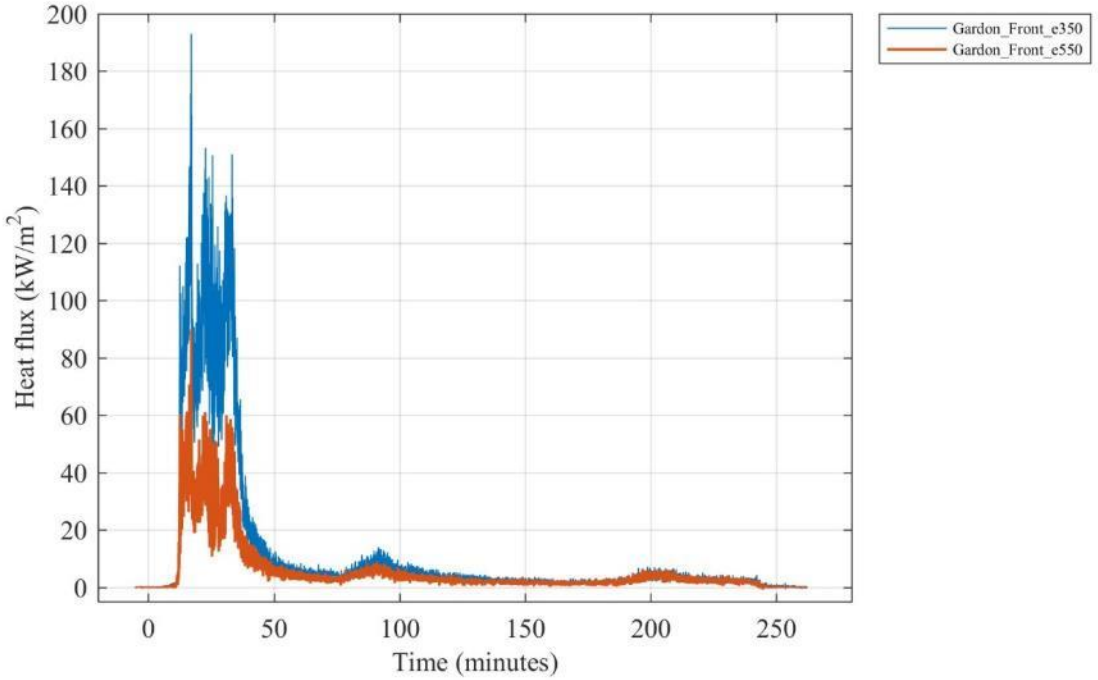

Figure G 15. Heat flux measured by Gardon gauges 350 cm and 550 cm above the floor above the doorway.

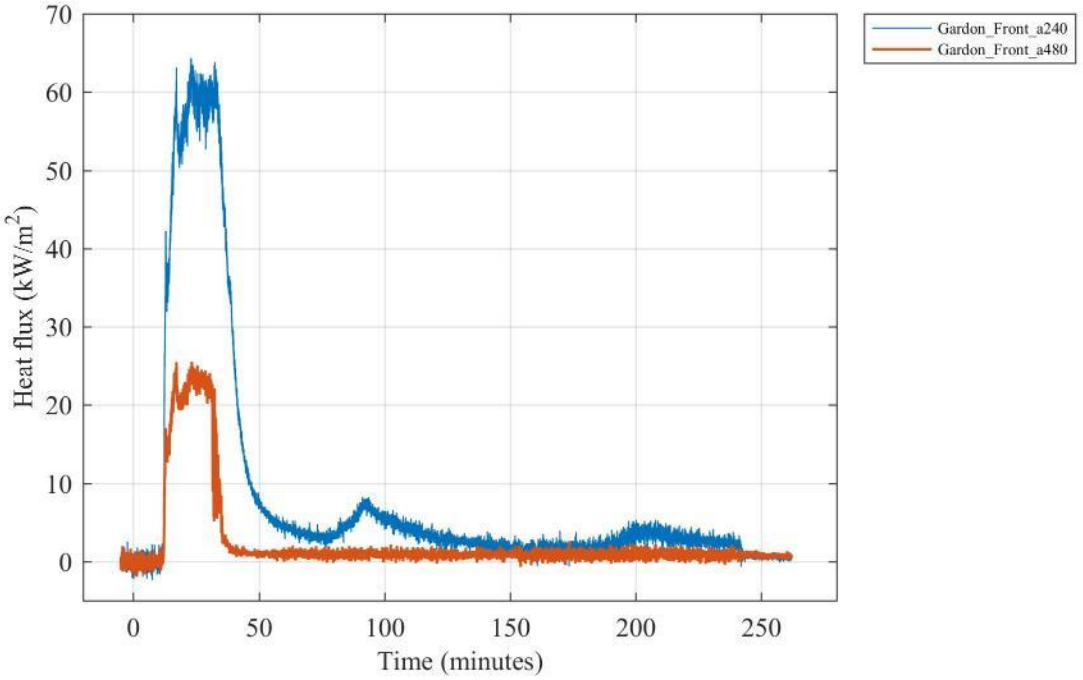

Figure G 16. Heat flux measured by Gardon gauges 240 cm and 480 cm from the doorway facing the opening.

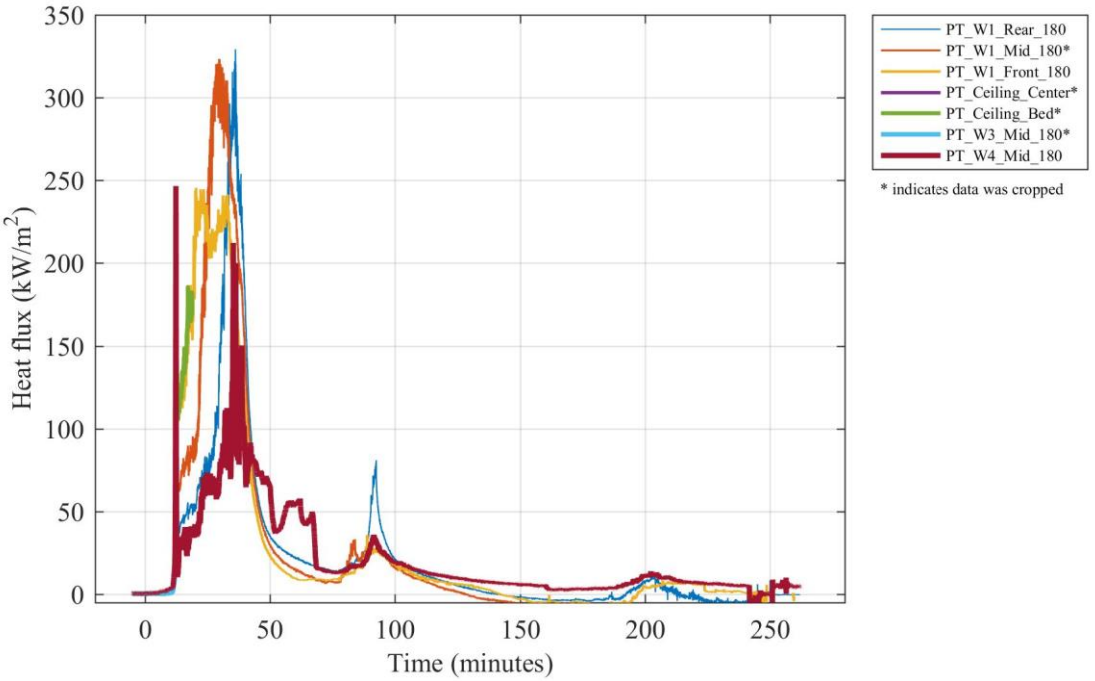

Figure G 17. Heat flux calculated from plate thermometers at various locations inside the compartment.

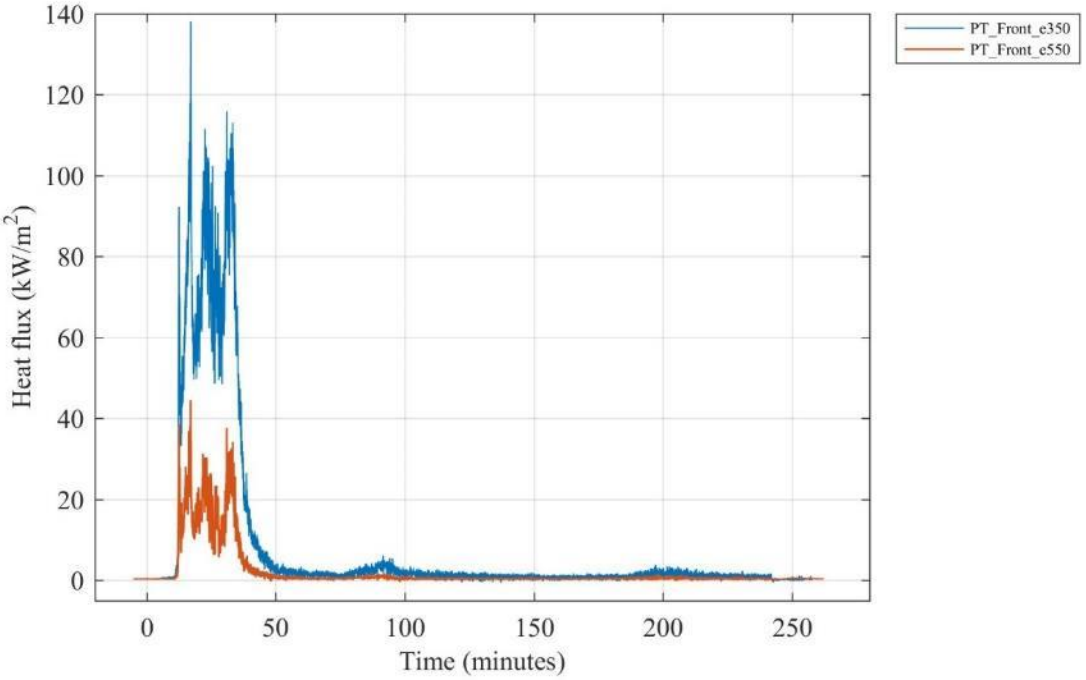

Figure G 18. Heat flux calculated from plate thermometers 350 cm and 550 cm above the floor above the doorway.

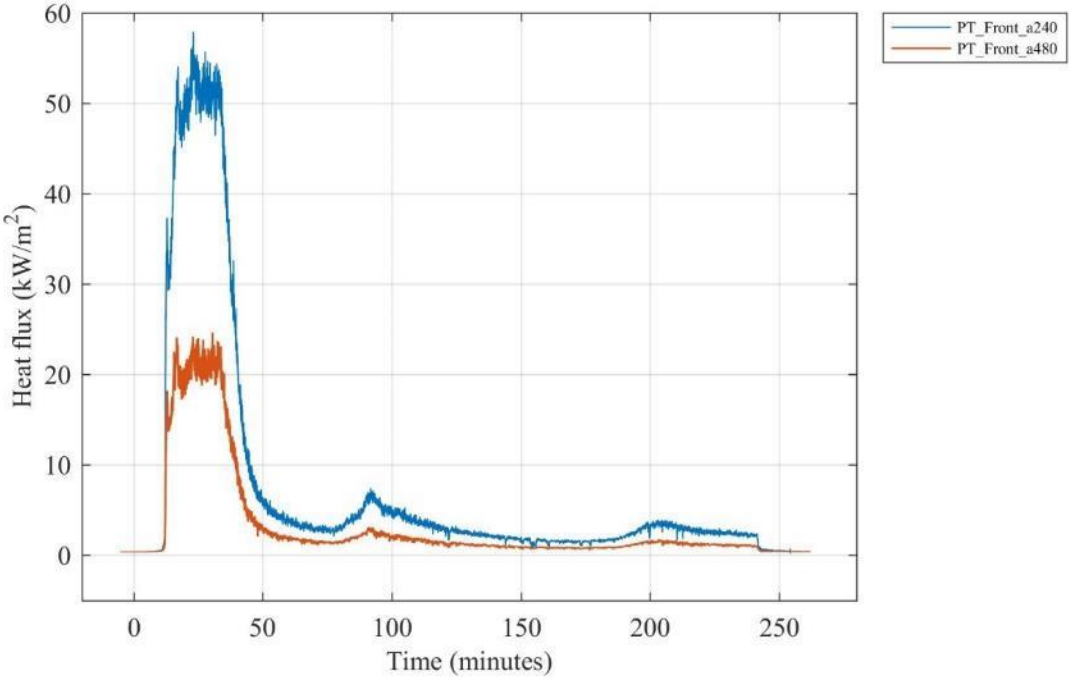

Figure G 19. Heat flux calculated from plate thermometers 240 cm and 480 cm from the doorway facing the opening.

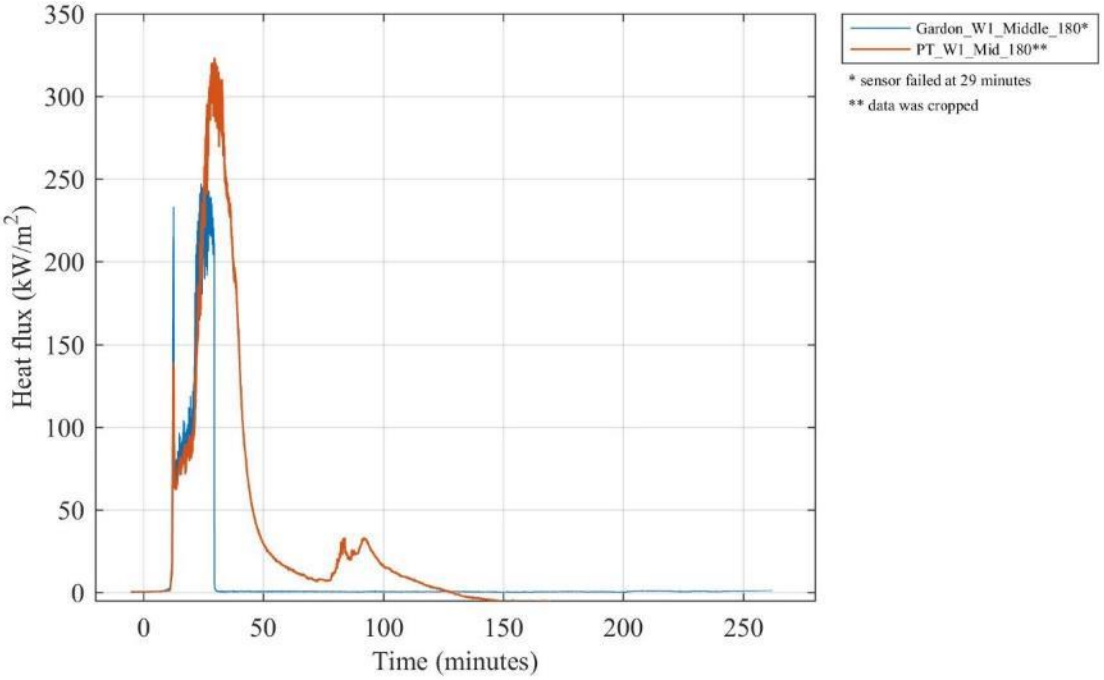

Figure G 20. Comparison of heat fluxes recorded by a collocated Gardon gauge, plate thermometer (PT) and differential flame thermometer (DFT) on Wall W1 at the middle of the compartment 1.8 m above the floor.

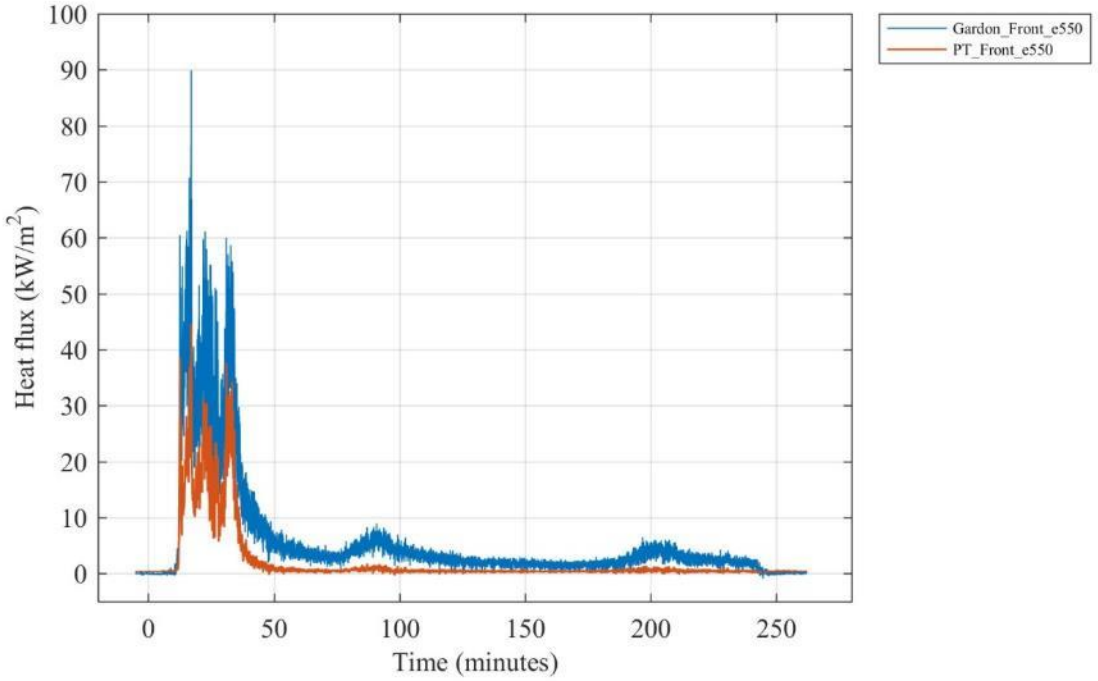

Figure G 21. Comparison of heat fluxes recorded by a collocated Gardon gauge and plate thermometer (PT) 350 cm above the floor above the doorway.

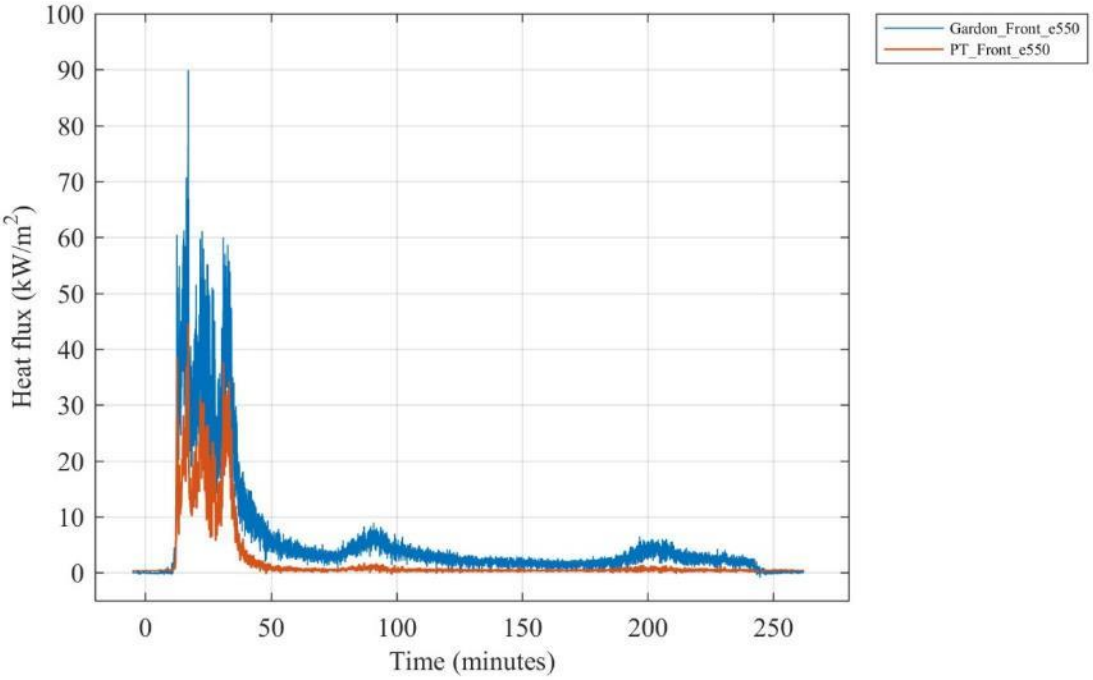

Figure G 22. Comparison of heat fluxes recorded by a collocated Gardon gauge and plate thermometer (PT) 550 cm above the floor above the doorway.

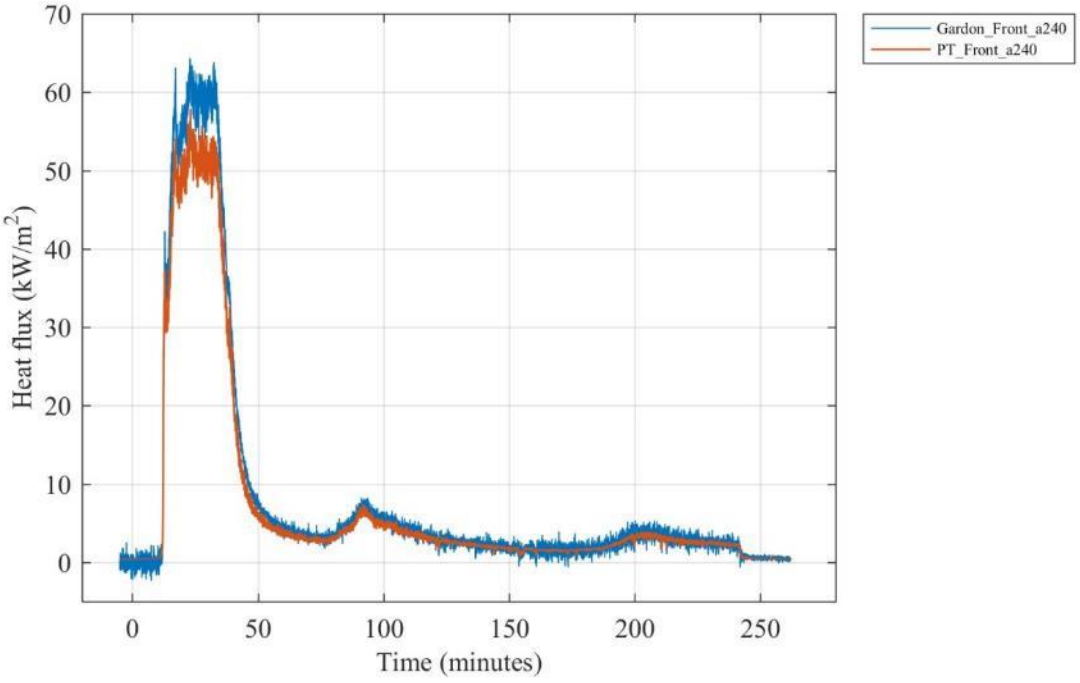

Figure G 23. Comparison of heat fluxes recorded by a collocated Gardon gauge and plate thermometer (PT) 240 cm from the doorway (facing doorway) and 150 cm above floor.

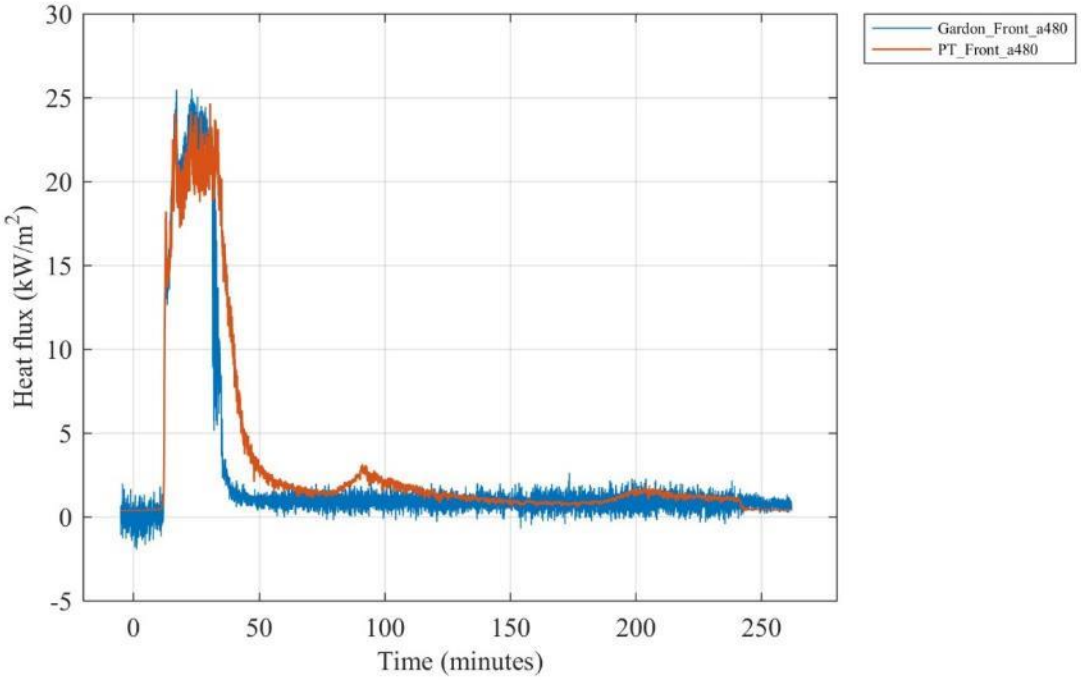

Figure G 24. Comparison of heat fluxes recorded by a collocated Gardon gauge and plate thermometer (PT) 480 cm from the doorway (facing doorway) and 150 cm above floor.

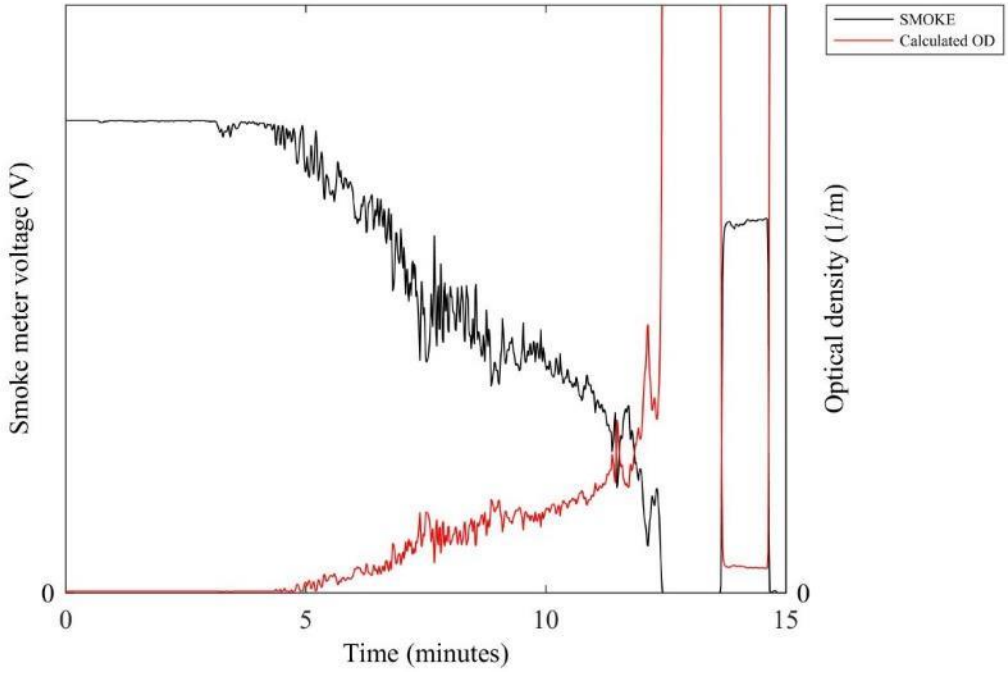

Figure G 25. Smoke meter voltage and calculated optical density (OD) from gas sampled at the center of the compartment 160 cm above the floor.

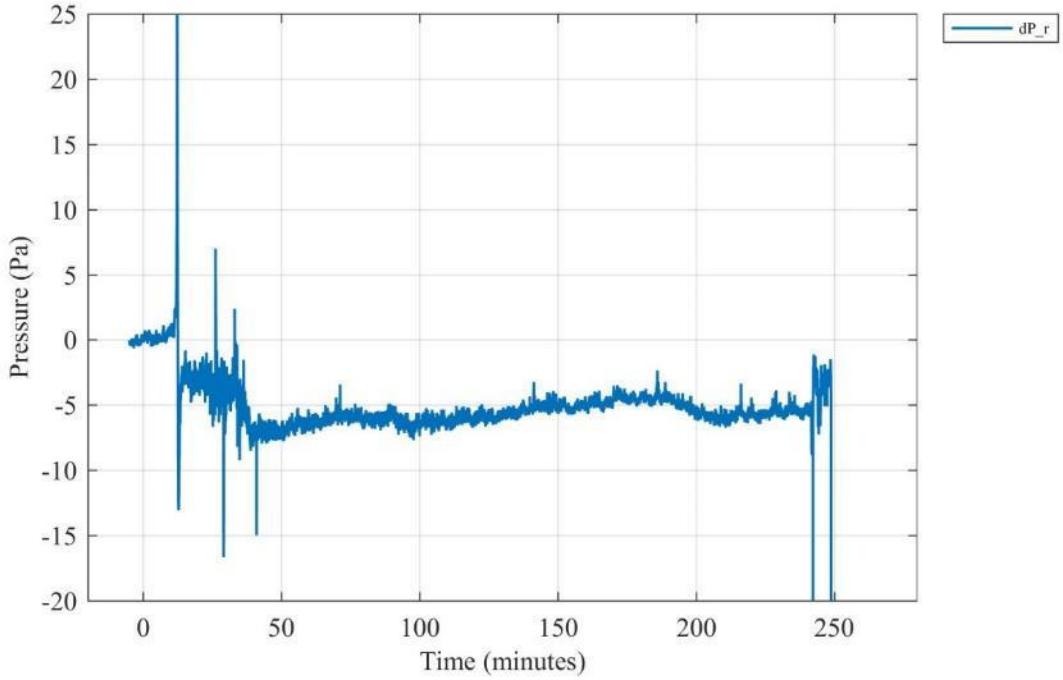

Figure G 26. Differential room pressure measured 210 cm above the floor at the center of the compartment.

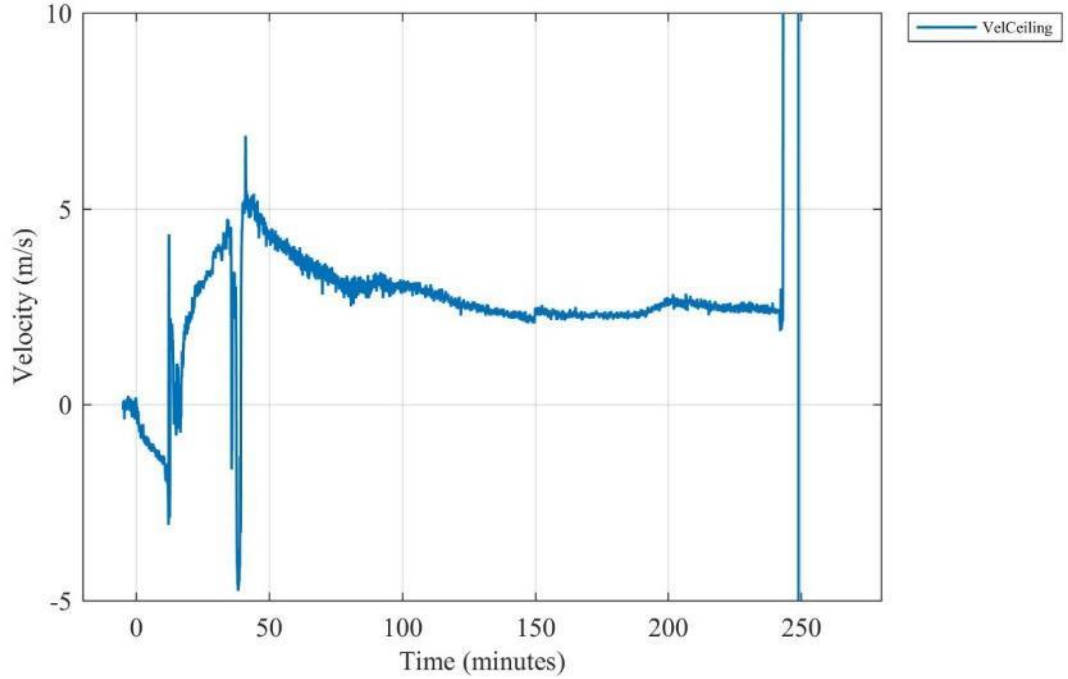

Figure G 27. Gas velocity measured 305 mm from the ceiling along the midline 227.5 cm from the back of the compartment (positive indicates flow out the door). [10 s moving average filter applied]

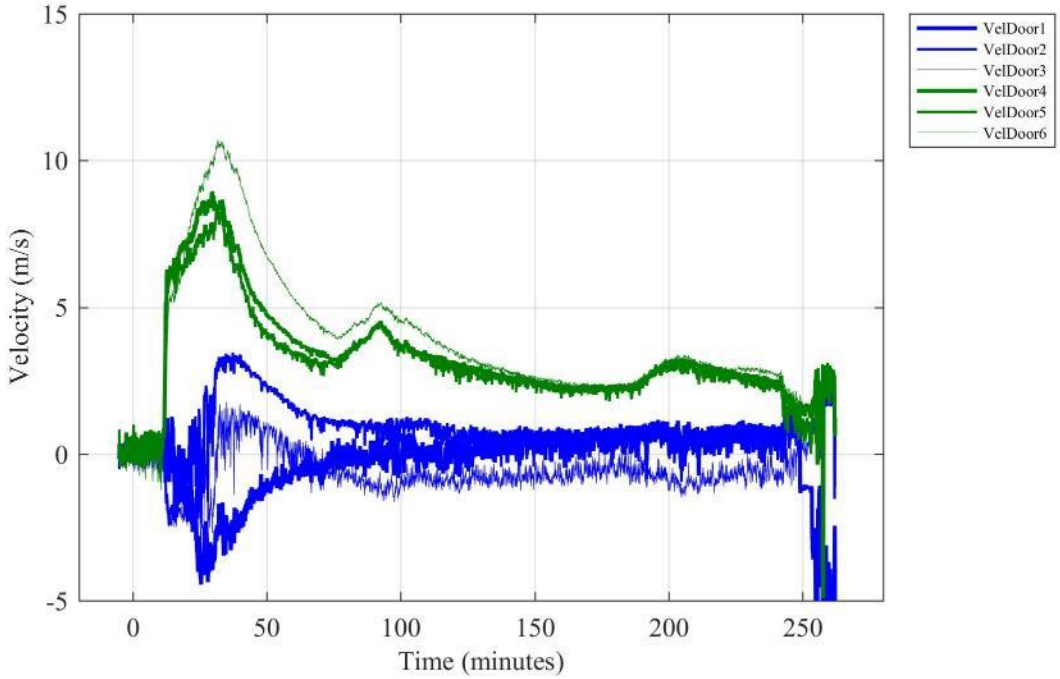

Figure G 28. Gas velocities measured in the doorway (positive indicates flow out the door). [10 s moving average filter applied]

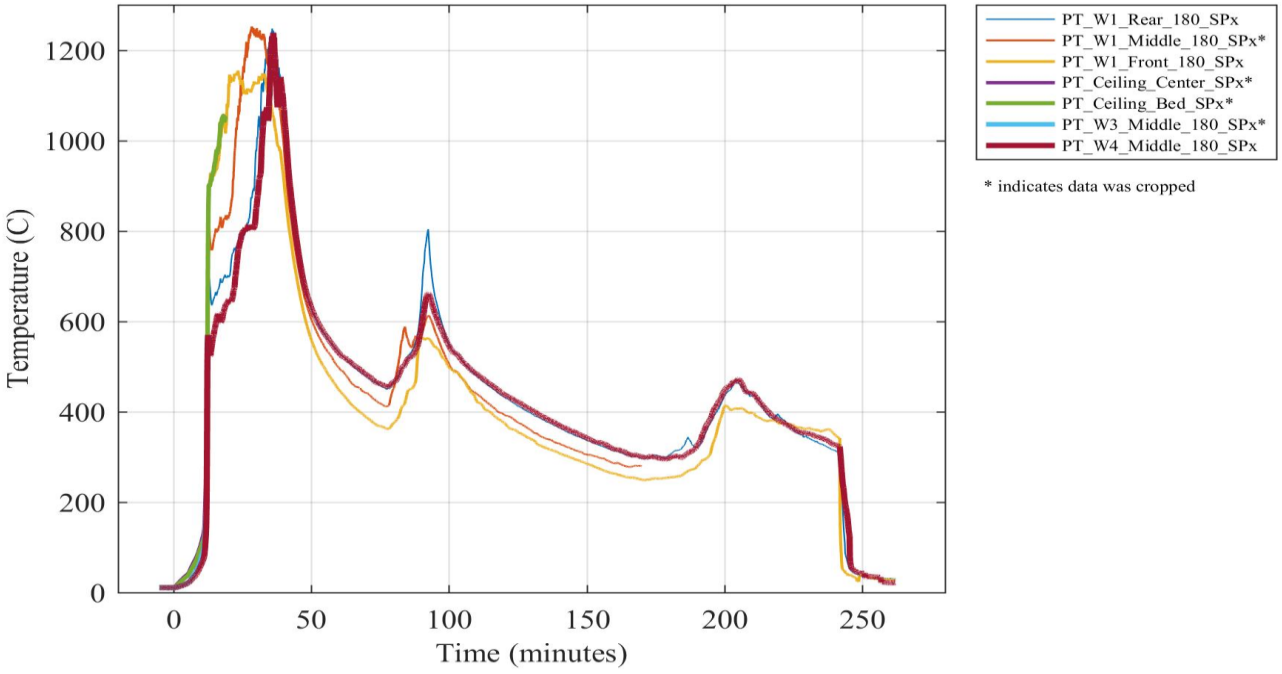

Figure G 29. Plate thermometer temperatures at various locations inside the compartment.

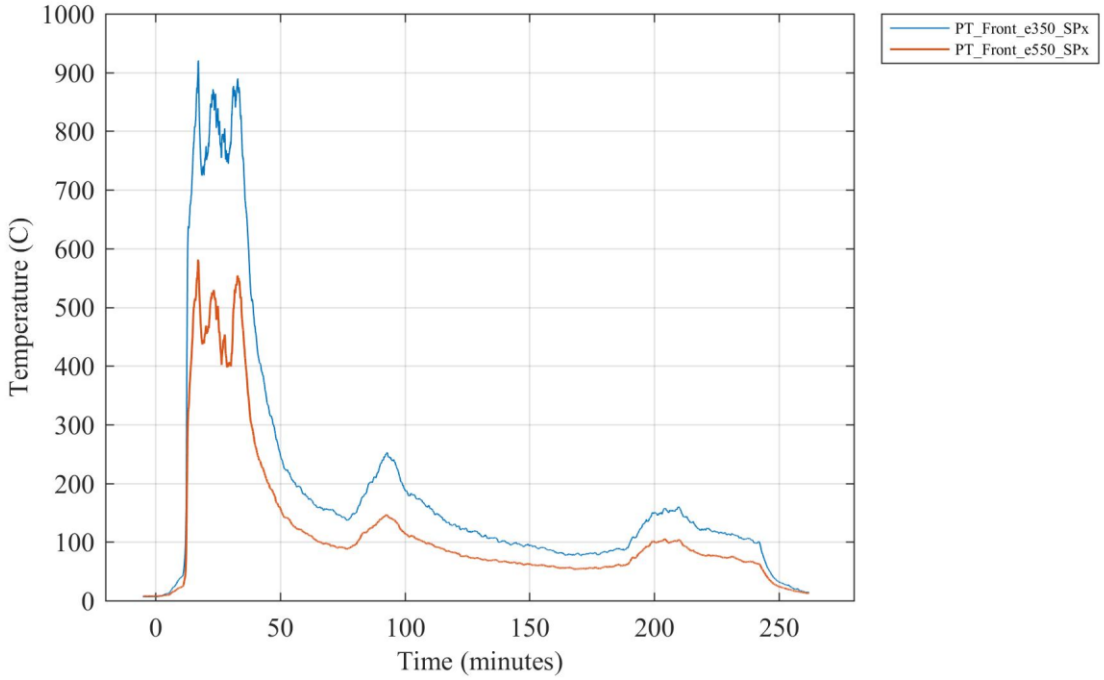

Figure G 30. Plate thermometer temperatures 350 cm and 550 cm above the floor above the doorway.

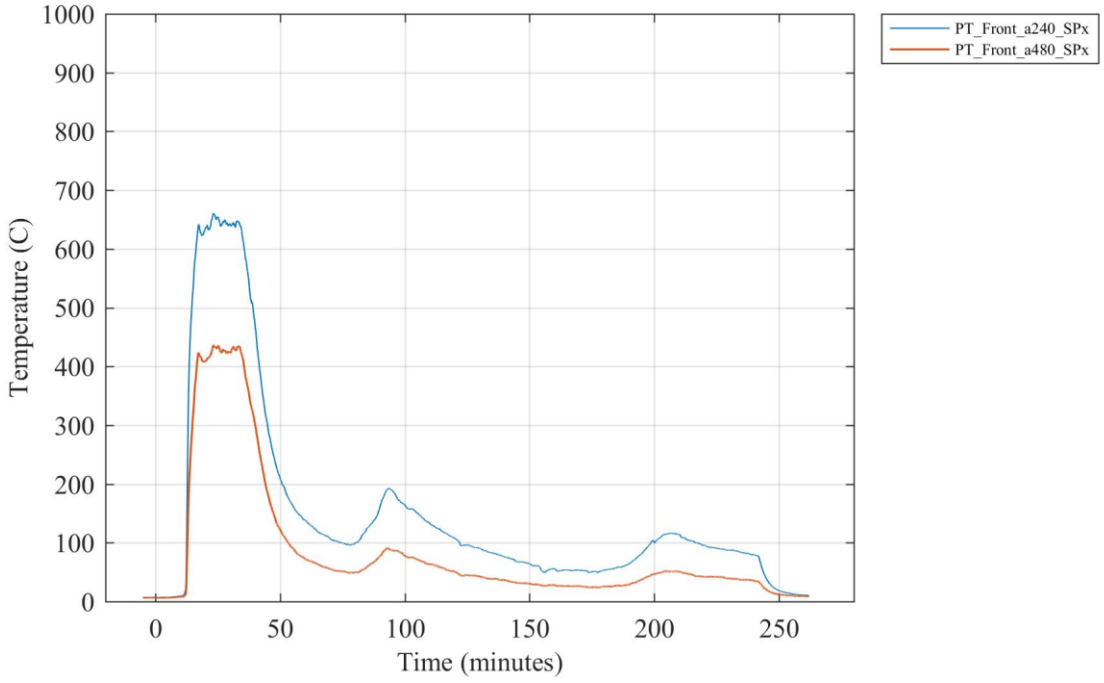

Figure G 31. Plate thermometer temperatures 240 cm and 480 cm from the doorway facing the opening.

Appendix H - Test 1-4 data

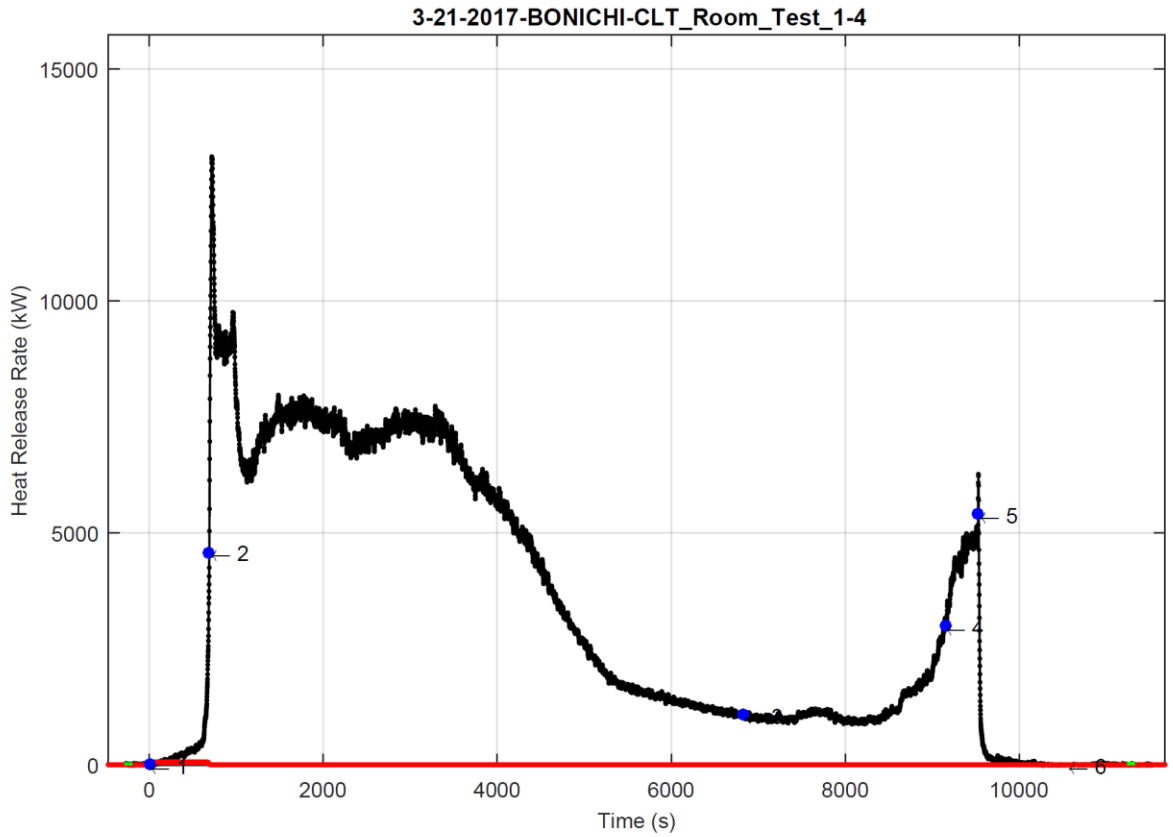

Hood Size = 15 (m)

Peak Heat Release Rate = 13114 (kW)

NG Burner Peak HRR = 78 (kW)

Exhaust Flow = 97.58 +/- 0.67 (kg/s)

O_2 Baseline = 0.20938 (Vol Fr)

O_2 Drift During Test = -27 (ppmv)

CO Generated = 63.49 (kg)

Fuel Type = WoodFurniturePUF ; HOC = 19.9 (MJ/kg)

Total Heat Release = 35941 (MJ)

NG Burner Total HR = 36 (MJ)

Total Burn Time = 2.93 (Hrs)

Fuel Mass Burned = 1806.08 (kg)

O_2 Consumed = 2779.44 (kg)

CO_2 Generated = 3629.25 (kg)

Test Description:
CLT Room test 1-4. Furnished room witth 3 layers of type X gypsum on all walls. Ceiling is exposed CLT. Narrow door opening

Event Count	Time (s)	Time Stamp	Event Description
1	0	3/21/2017 10:02:51 AM	Ignition
2	693	3/21/2017 10:14:25 AM	flashover
3	6828	3/21/2017 11:56:40 AM	flames extinguished on upper rear corner of wall 1
4	9153	3/21/2017 12:35:25 PM	flare up flames out doorway
5	9527	3/21/2017 12:41:39 PM	start fire hose water suppression
6	10544	3/21/2017 12:58:36 PM	Fire Out

Figure H 1. Summary report file generated by the NFRL calorimeter on the day of test.

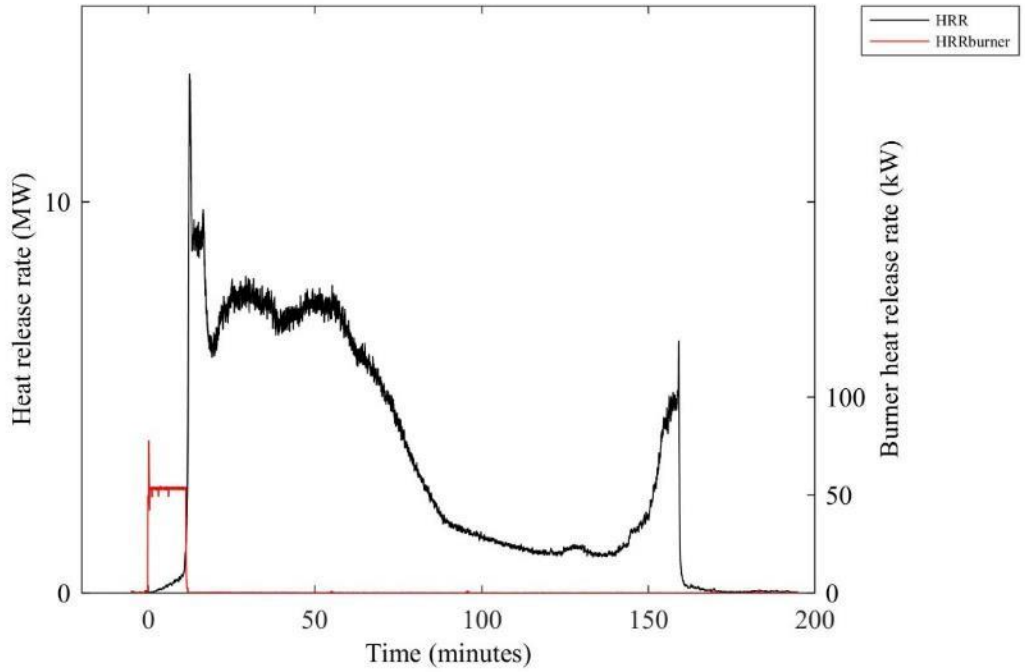

Figure H 2. Compartment (left axis) and burner (right axis) heat release rates.

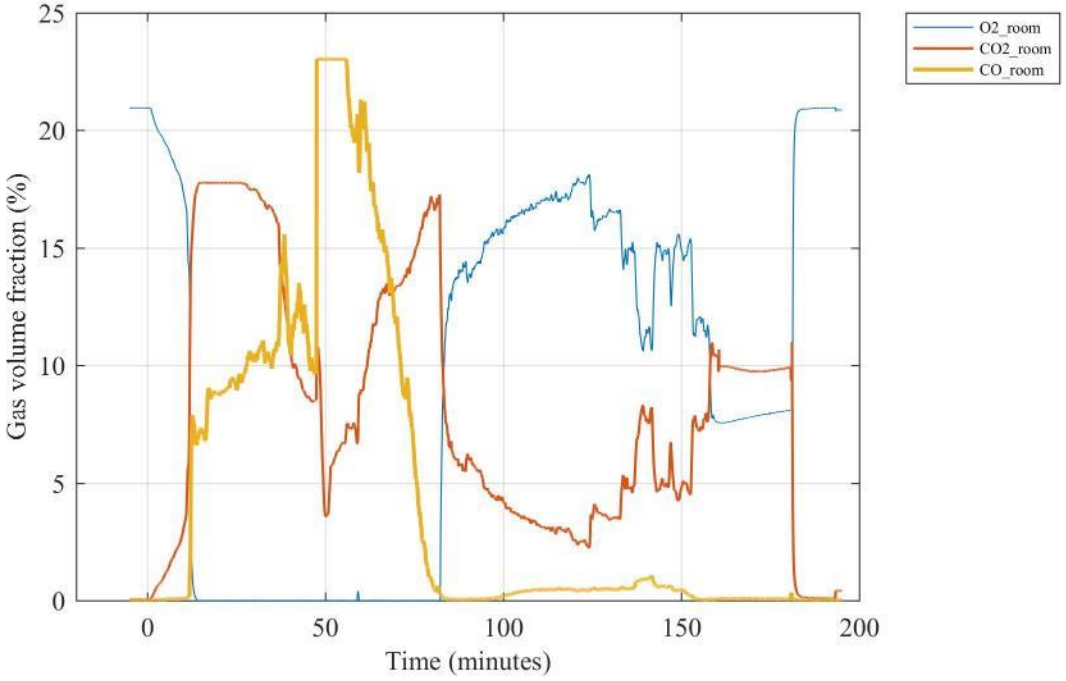

Figure H 3. Gas volume fractions for oxygen (O_2), carbon dioxide (CO_2) and carbon monoxide (CO) sampled at the center of the compartment 210 cm above the floor.

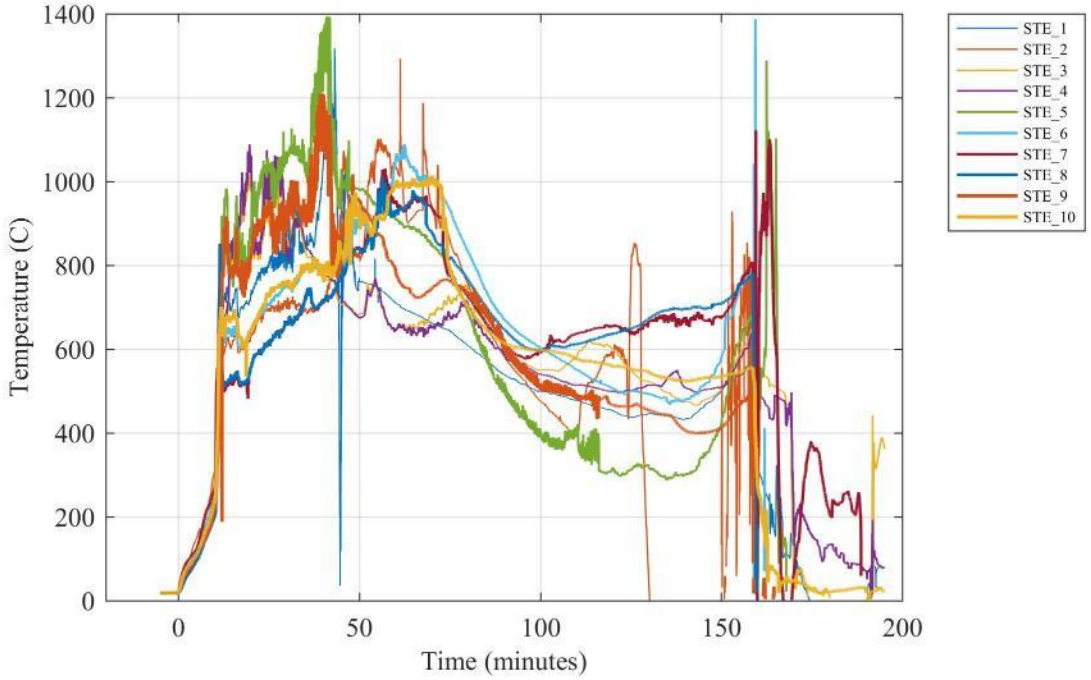

Figure H 4. Simulated thermal elements (STE) for sprinkler.

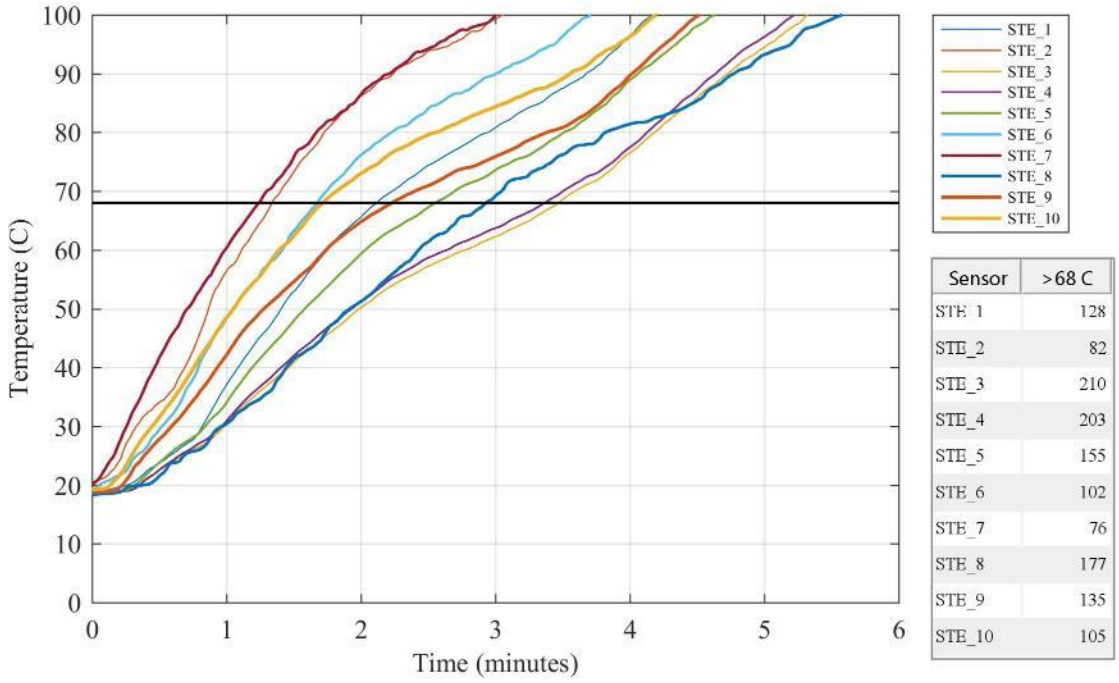

Sensor	>68 C
STE_1	128
STE_2	82
STE_3	210
STE_4	203
STE_5	155
STE_6	102
STE_7	76
STE_8	177
STE_9	135
STE_10	105

Figure H 5. Simulated thermal elements (STE) for sprinkler with table showing time after ignition (in seconds) until 68 °C is reached.

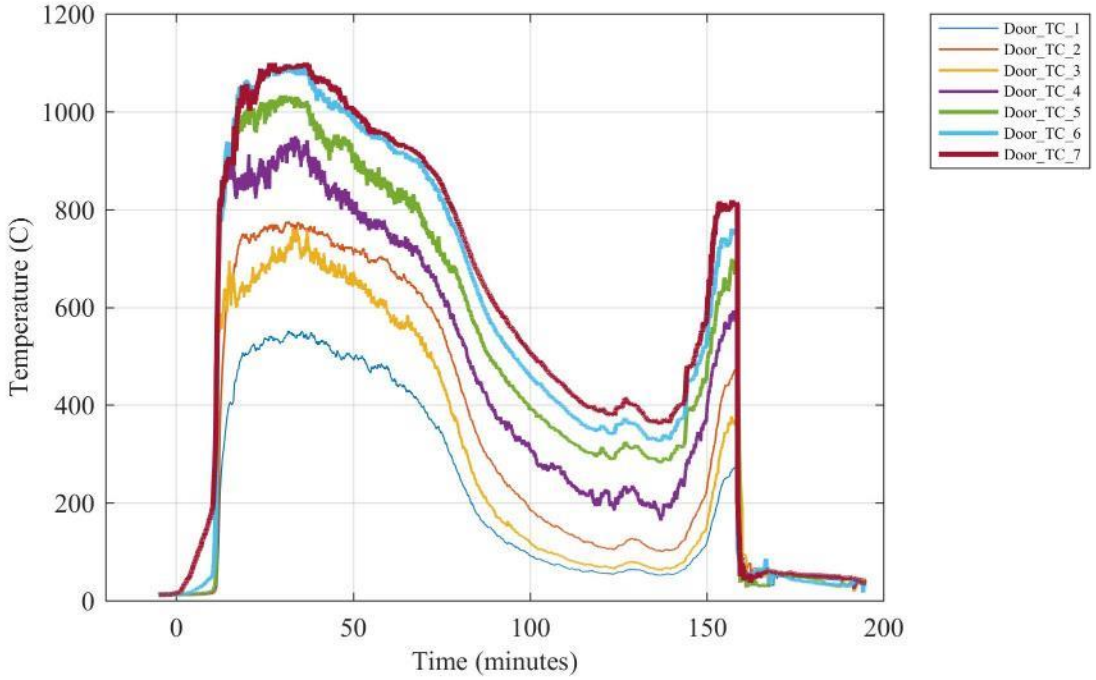

Figure H 6. Temperatures measured at various heights above the floor in the doorway.

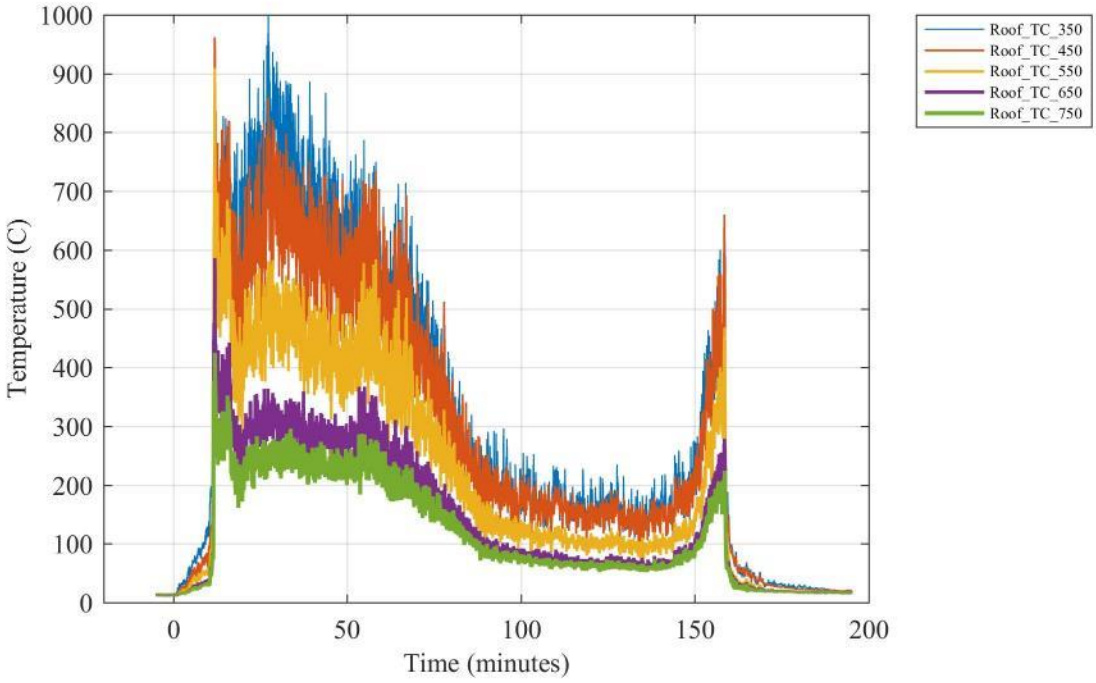

Figure H 7. Temperatures measured at various heights above the floor above the doorway.

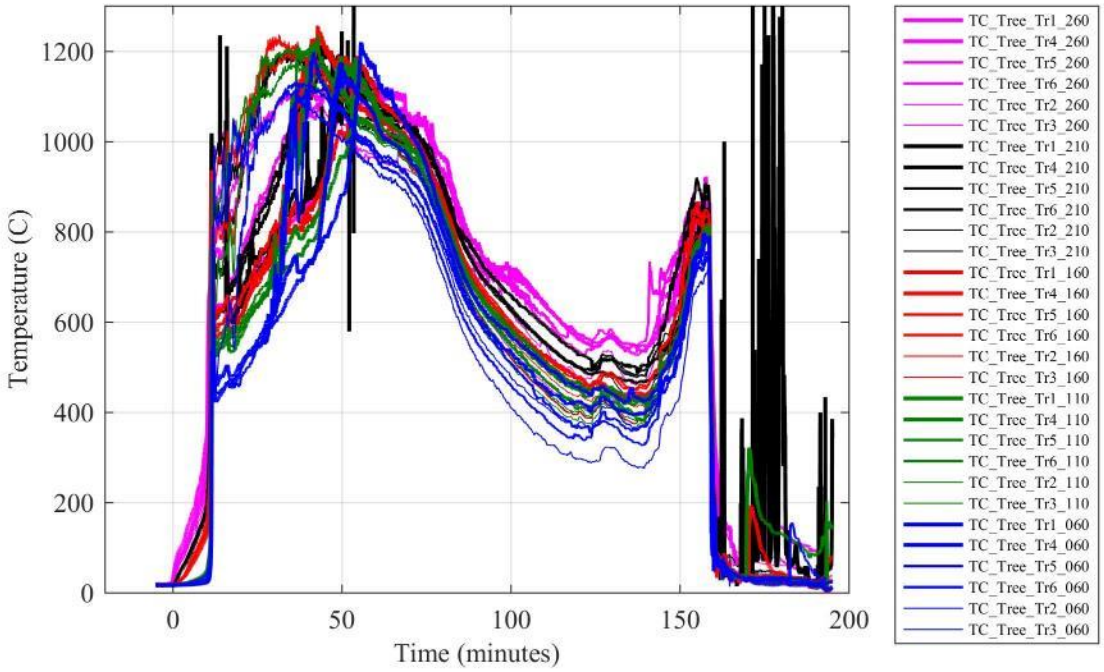

Figure H 8. Thermocouple tree temperatures at various locations inside the compartment.

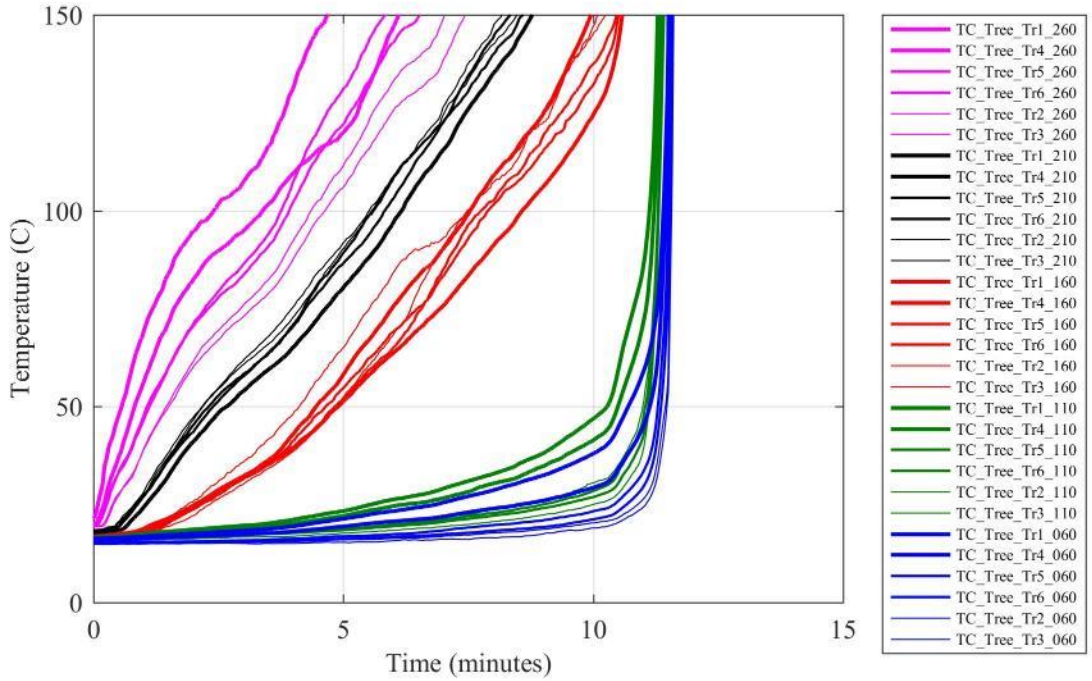

Figure H 9. Thermocouple tree temperatures at various locations inside the compartment during the first 15 min after ignition.

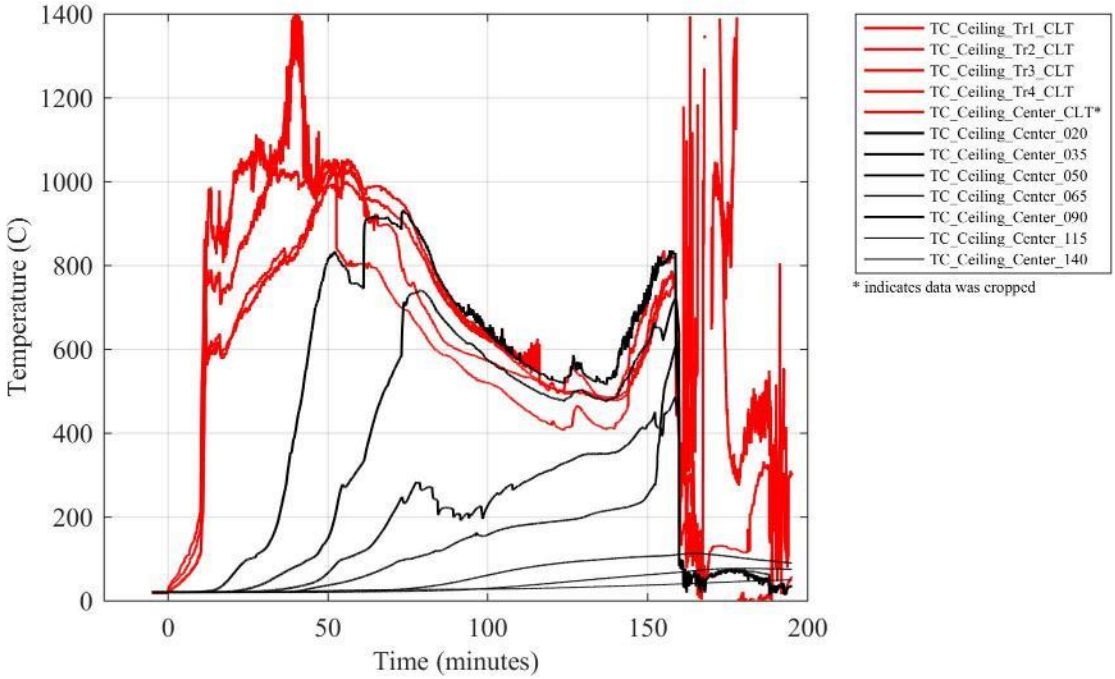

Figure H 10. Temperatures in the ceiling at various depths from the fire exposed surface.

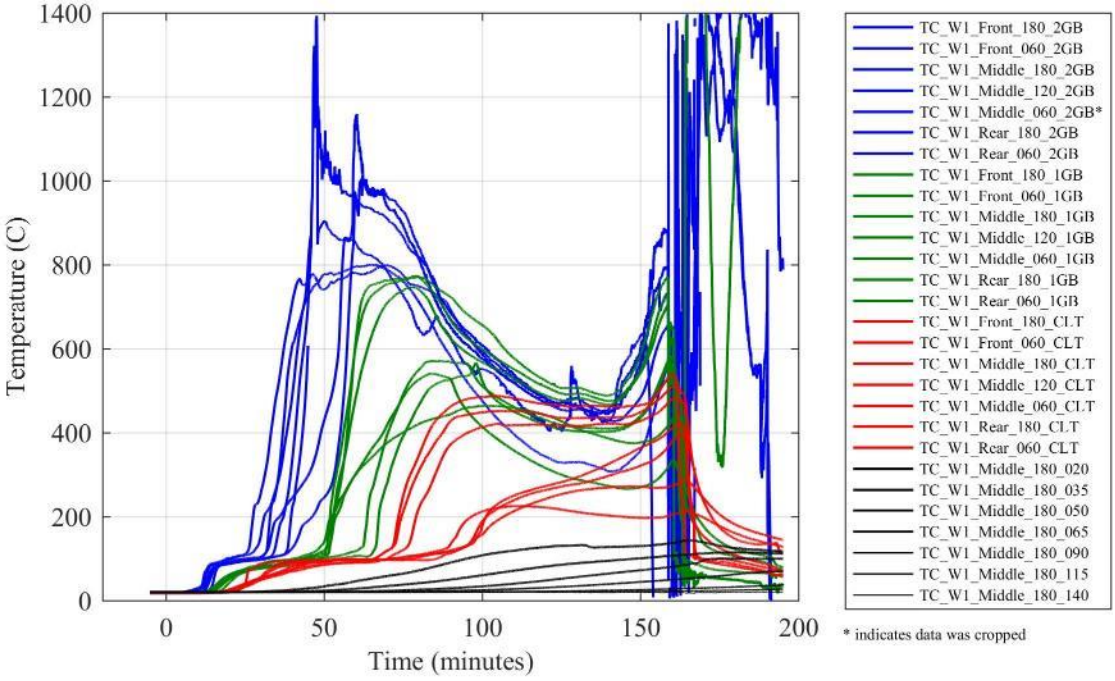

Figure H 11. Temperatures in Wall W1 at various depths from the fire exposed surface.

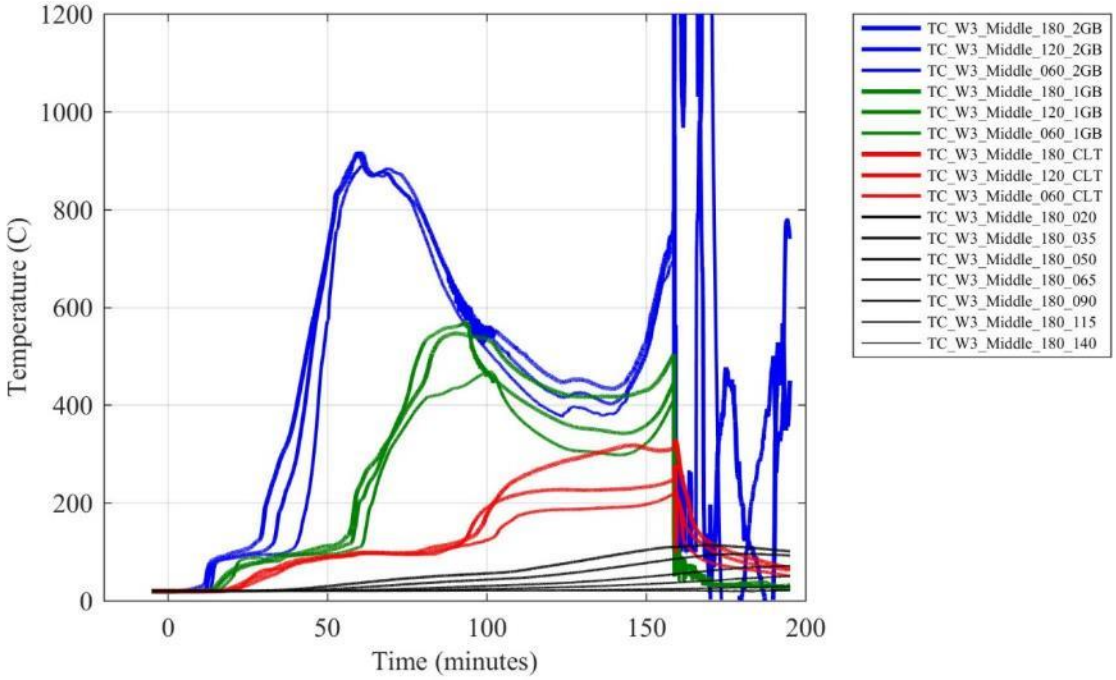

Figure H 12. Temperatures in Wall W3 at various depths from the fire exposed surface.

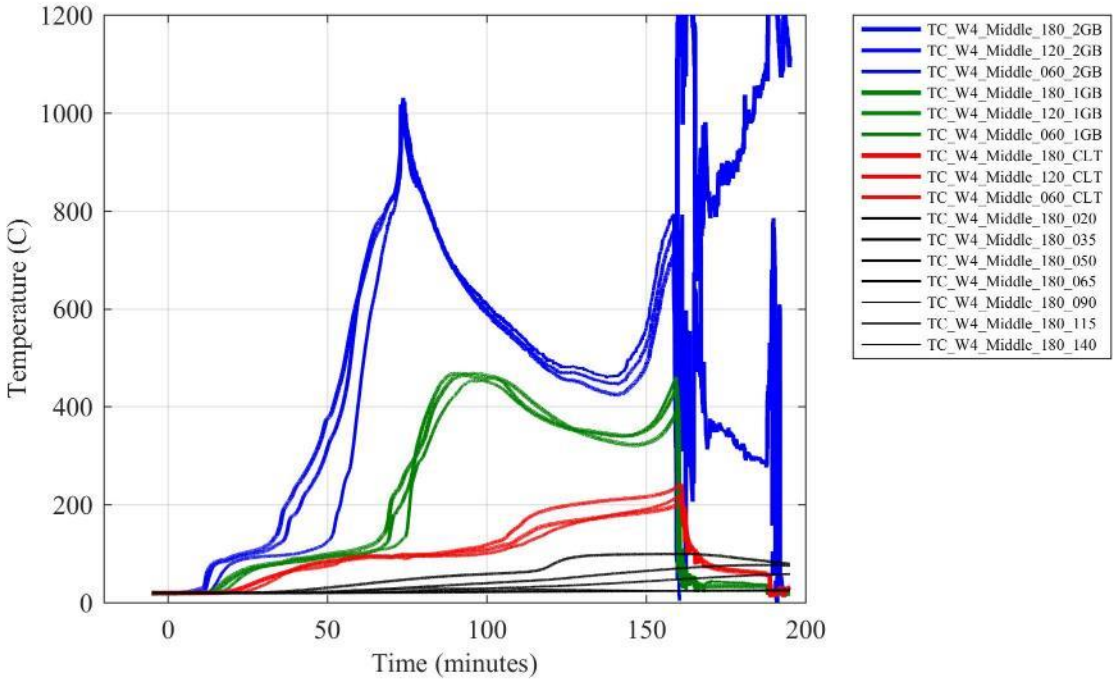

Figure H 13. Temperatures in Wall W4 at various depths from the fire exposed surface.

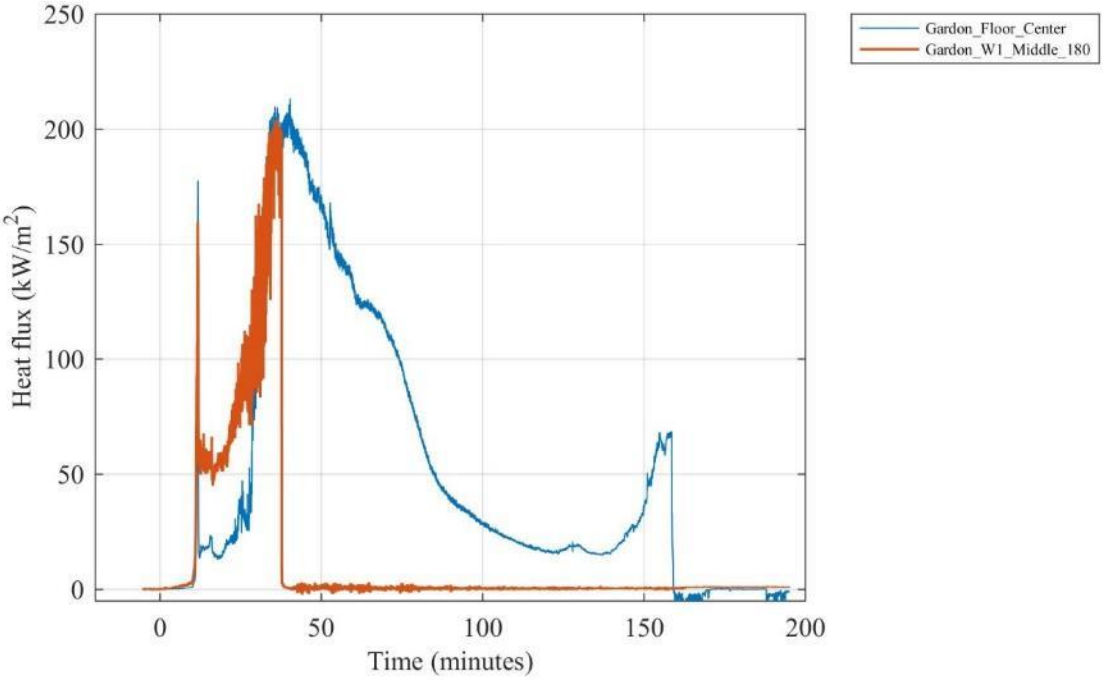

Figure H 14. Heat flux measured by Gardon gauges located inside the compartment.

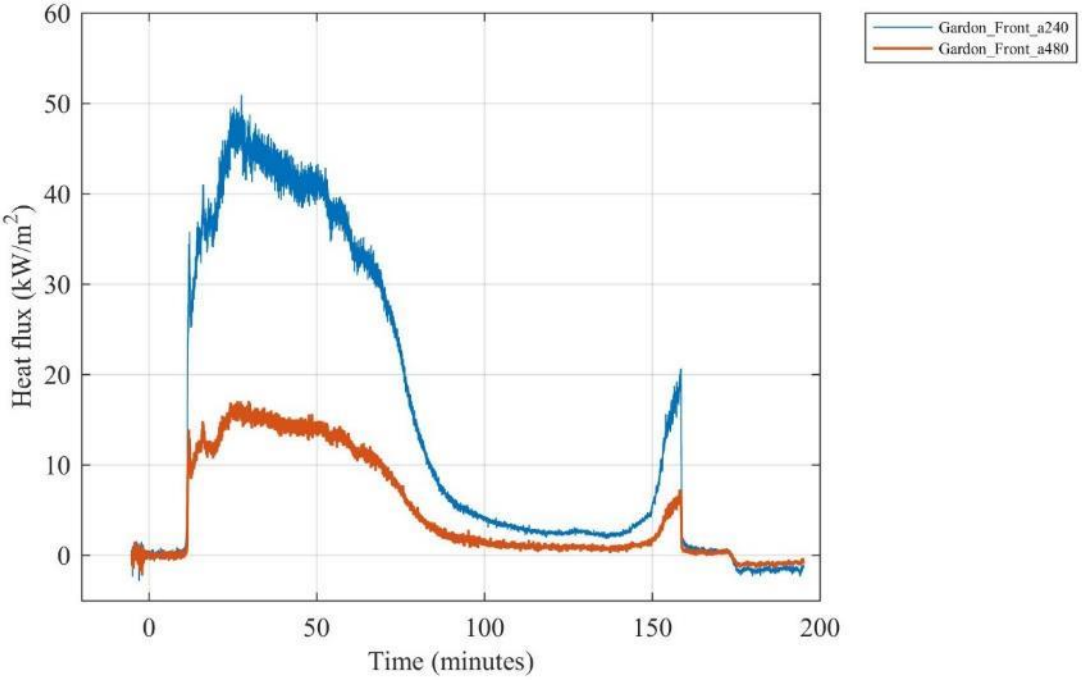

Figure H 15. Heat flux measured by Gardon gauges 350 cm and 550 cm above the floor above the doorway.

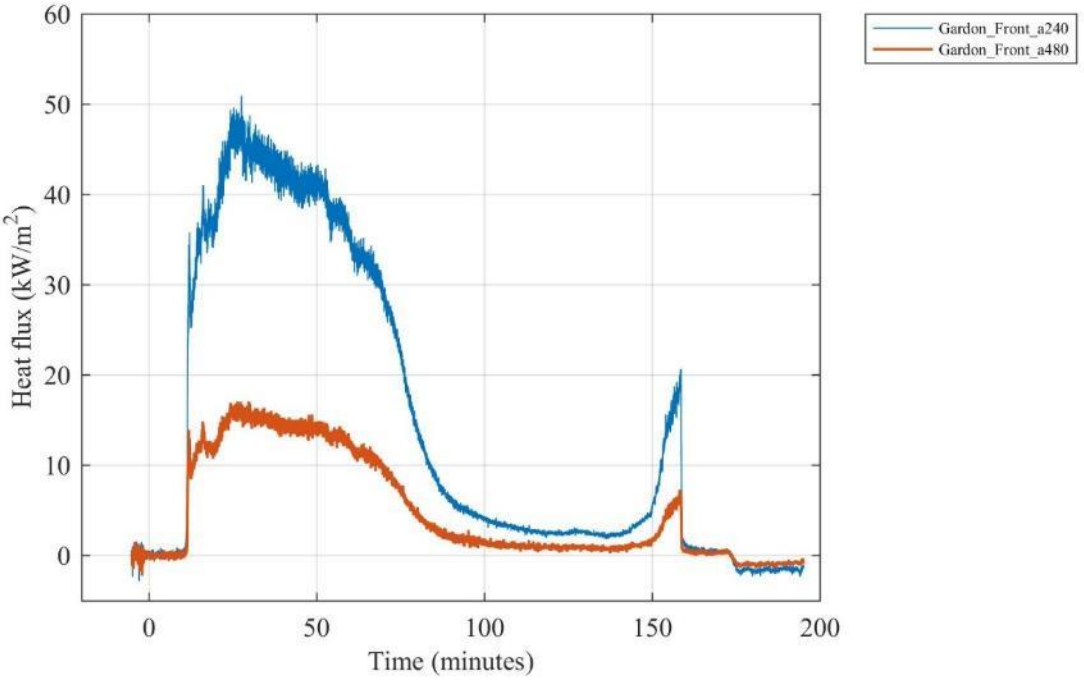

Figure H 16. Heat flux measured by Gardon gauges 240 cm and 480 cm from the doorway facing the opening.

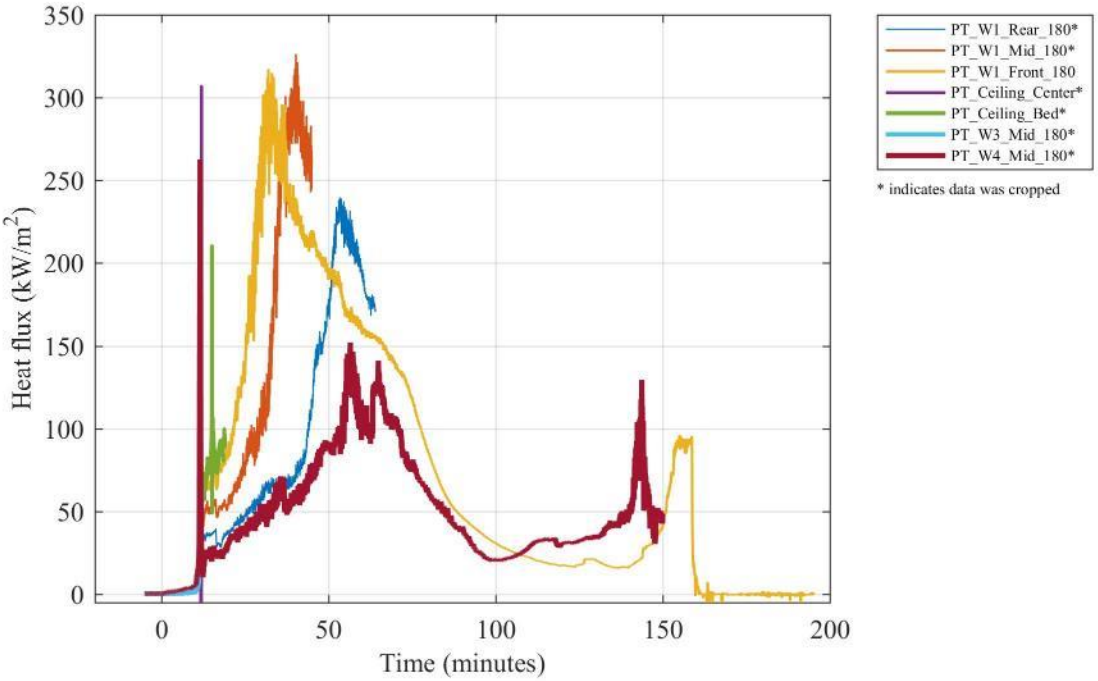

Figure H 17. Heat flux calculated from plate thermometers at various locations inside the compartment.

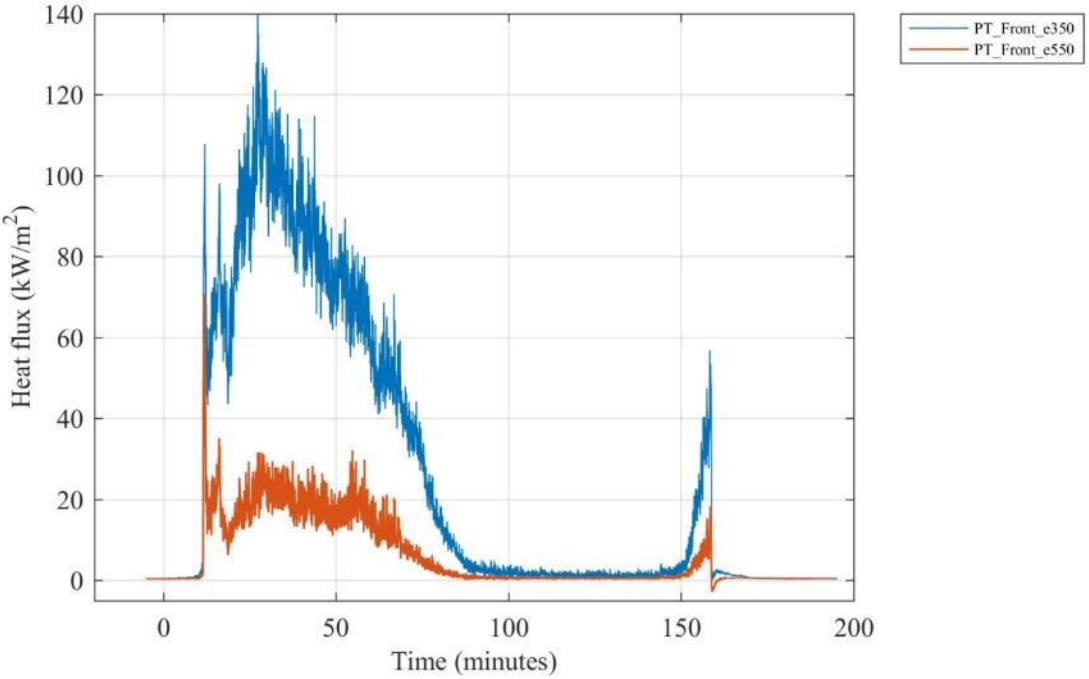

Figure H 18. Heat flux calculated from plate thermometers 350 cm and 550 cm above the floor above the doorway.

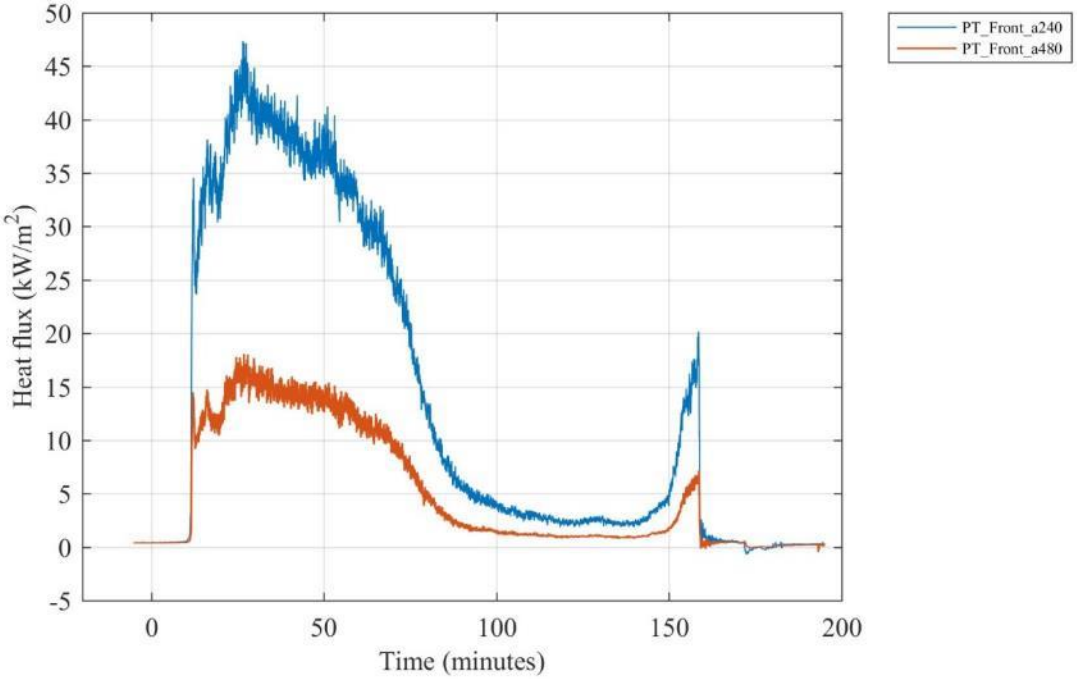

Figure H 19. Heat flux calculated from plate thermometers 240 cm and 480 cm from the doorway facing the opening.

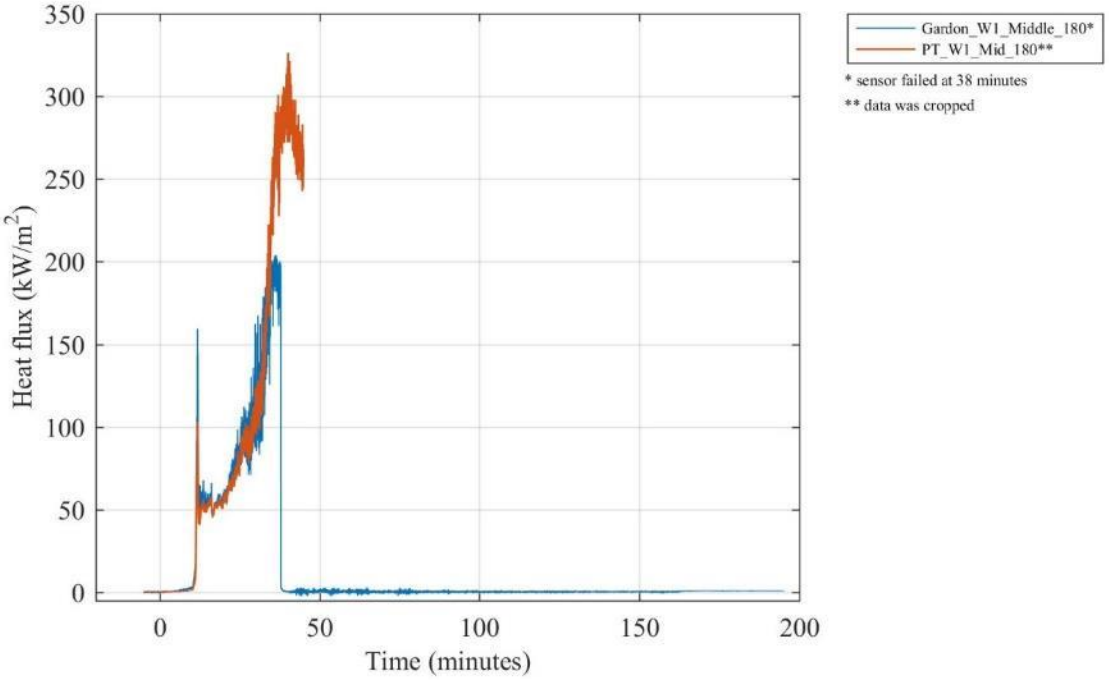

Figure H 20. Comparison of heat fluxes recorded by a collocated Gardon gauge, plate thermometer (PT) and differential flame thermometer (DFT) on Wall W1 at the middle of the compartment 1.8 m above the floor.

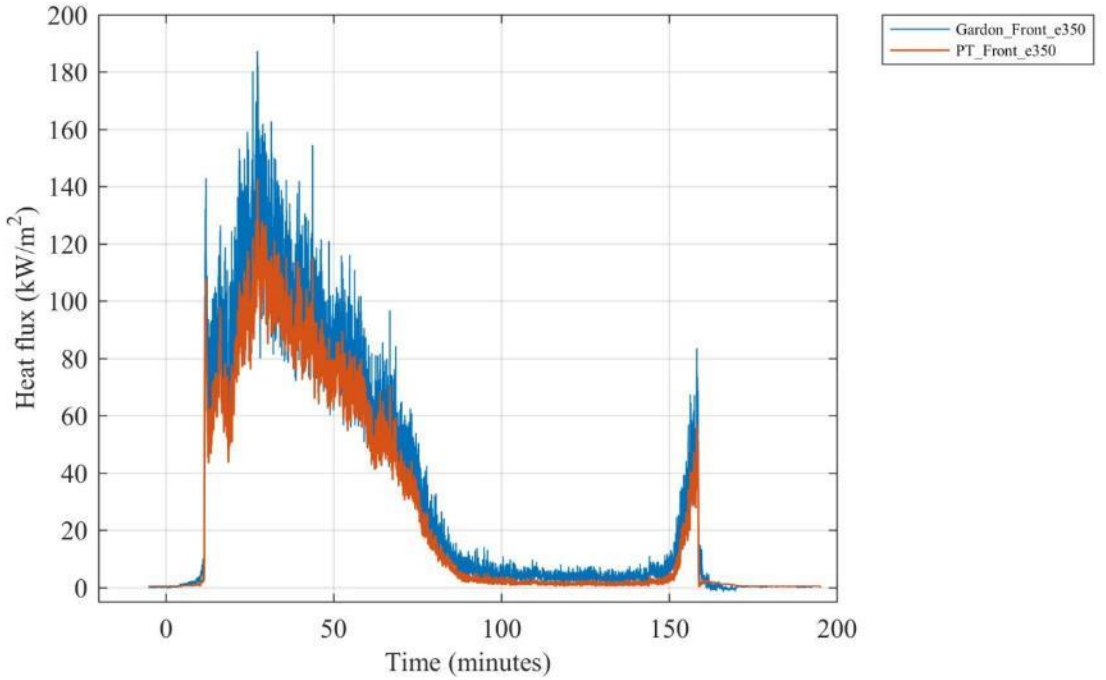

Figure H 21. Comparison of heat fluxes recorded by a collocated Gardon gauge and plate thermometer (PT) 350 cm above the floor above the doorway.

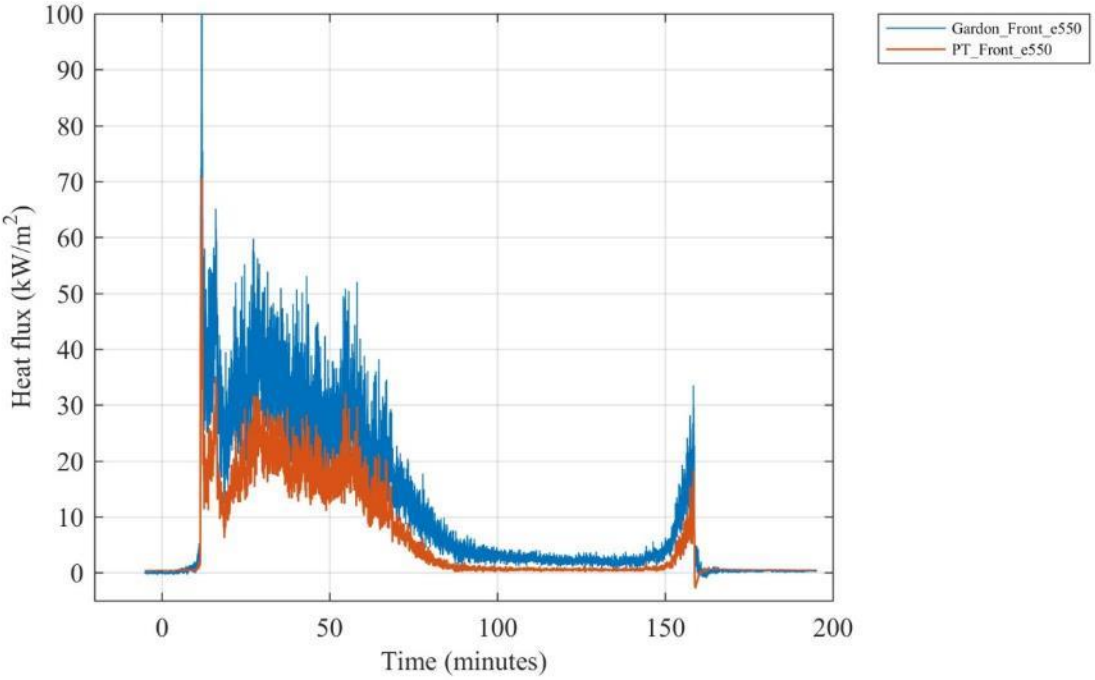

Figure H 22. Comparison of heat fluxes recorded by a collocated Gardon gauge and plate thermometer (PT) 550 cm above the floor above the doorway.

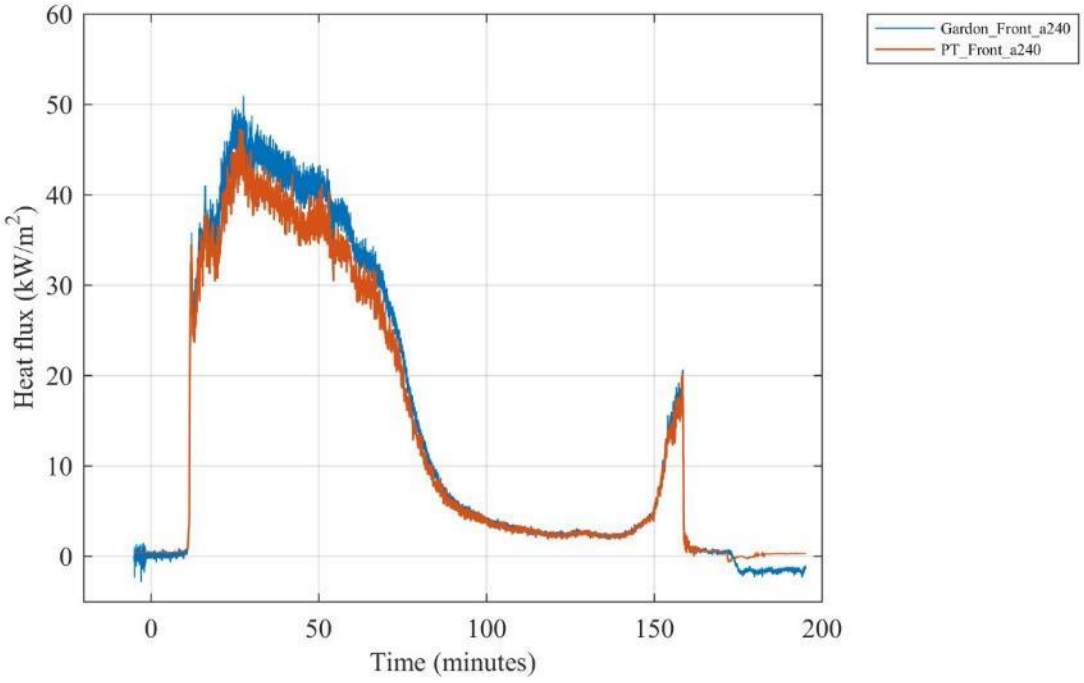

Figure H 23. Comparison of heat fluxes recorded by a collocated Gardon gauge and plate thermometer (PT) 240 cm from the doorway (facing doorway) and 150 cm above floor.

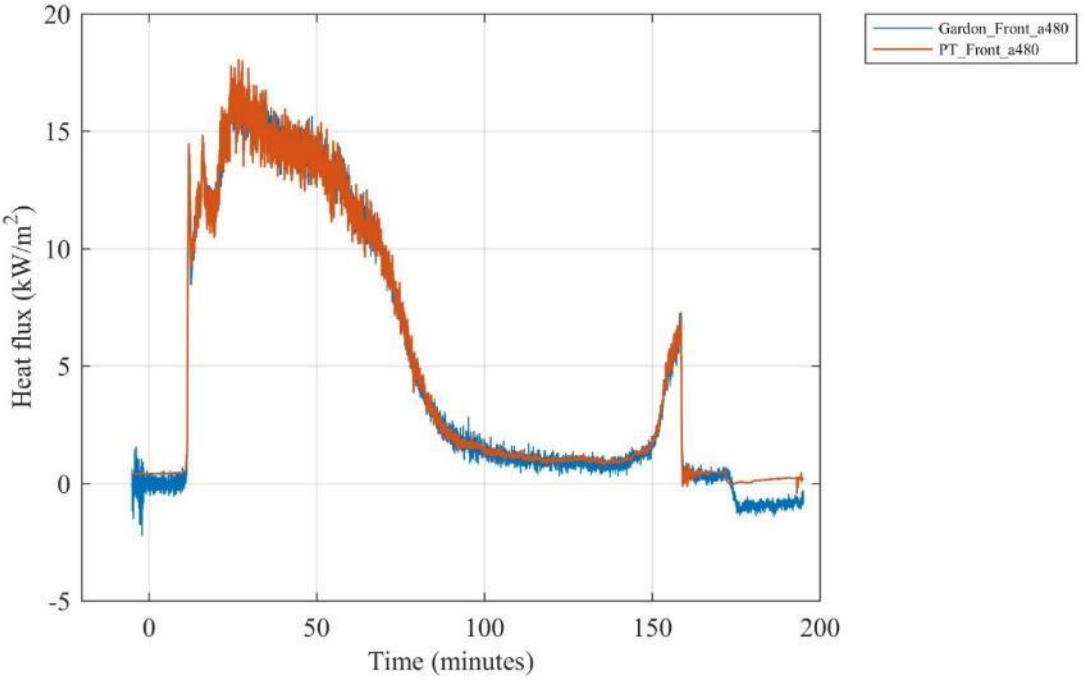

Figure H 24. Comparison of heat fluxes recorded by a collocated Gardon gauge and plate thermometer (PT) 480 cm from the doorway (facing doorway) and 150 cm above floor.

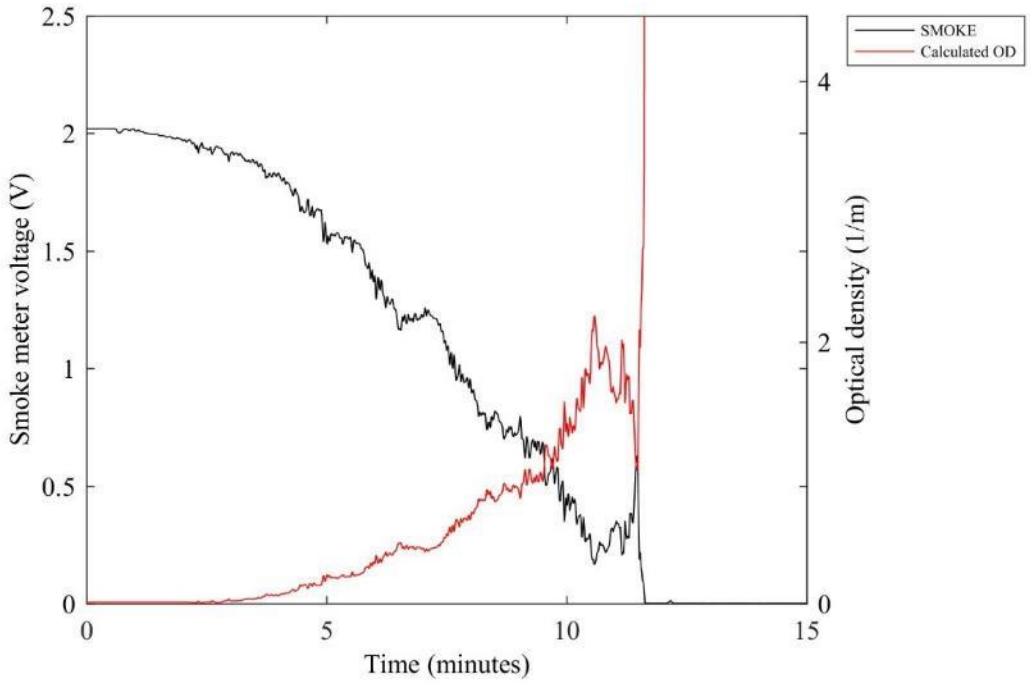

Figure H 25. Smoke meter voltage and calculated optical density (OD) from gas sampled at the center of the compartment 160 cm above the floor.

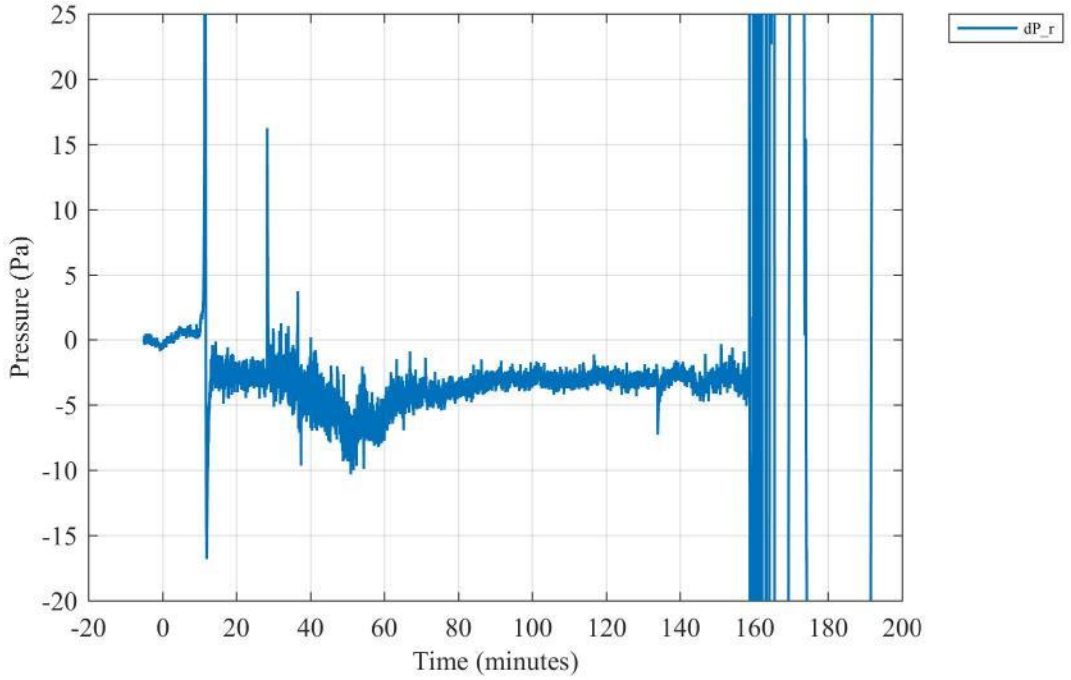

Figure H 26. Differential room pressure measured 210 cm above the floor at the center of the compartment.

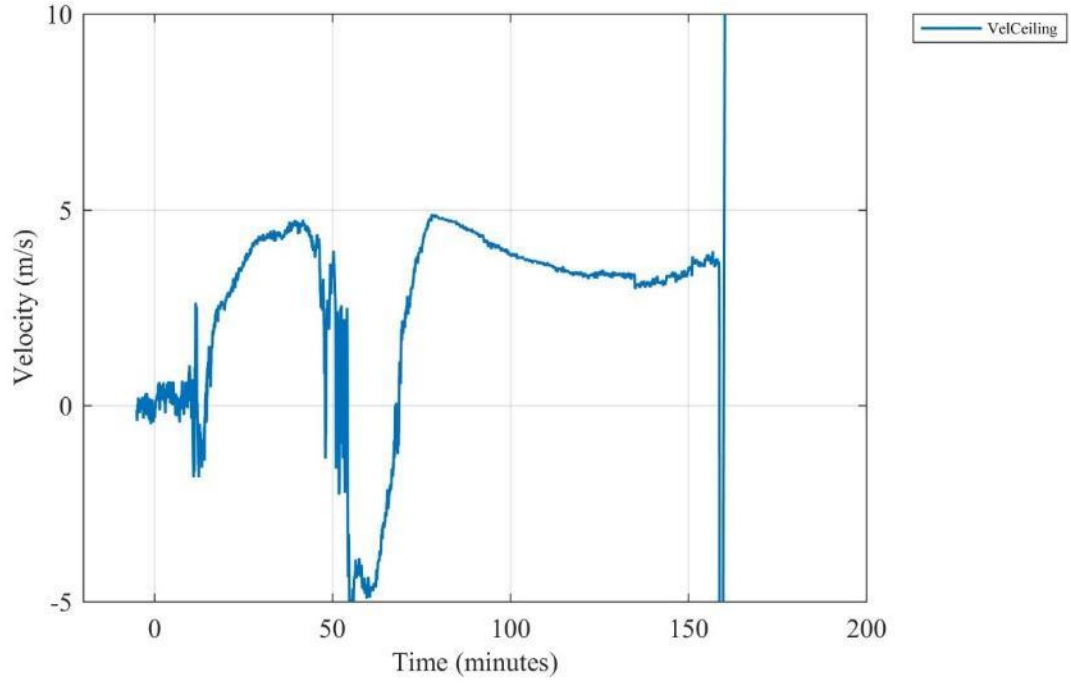

Figure H 27. Gas velocity measured 305 mm from the ceiling along the midline 227.5 cm from the back of the compartment (positive indicates flow out the door). [10 s moving average filter applied]

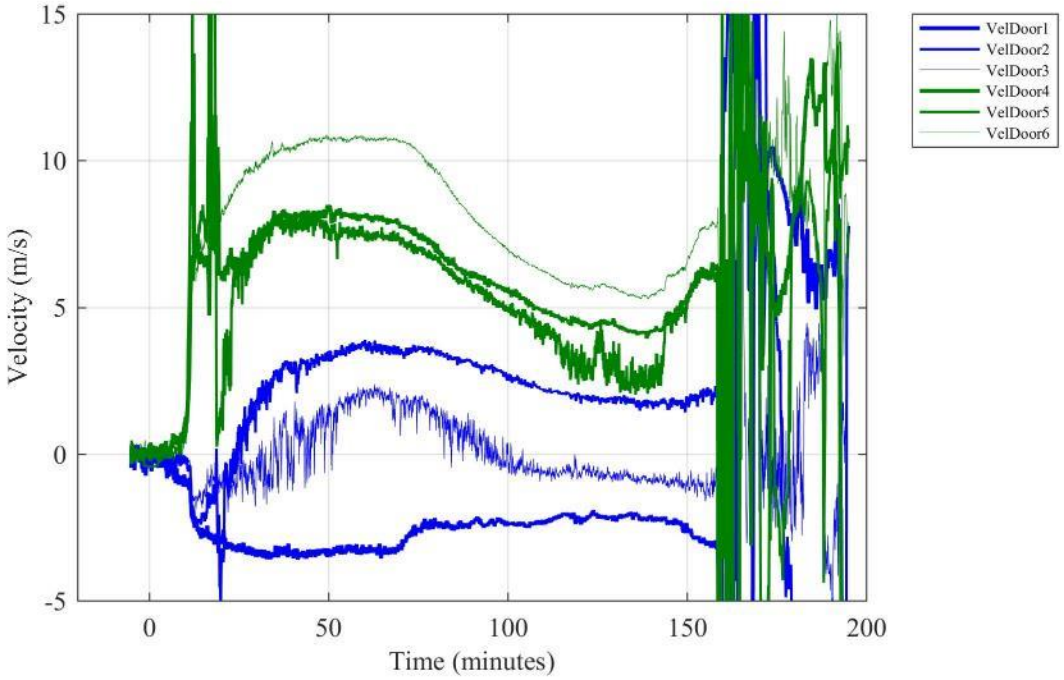

Figure H 28. Gas velocities measured in the doorway (positive indicates flow out the door). [10 s moving average filter applied]

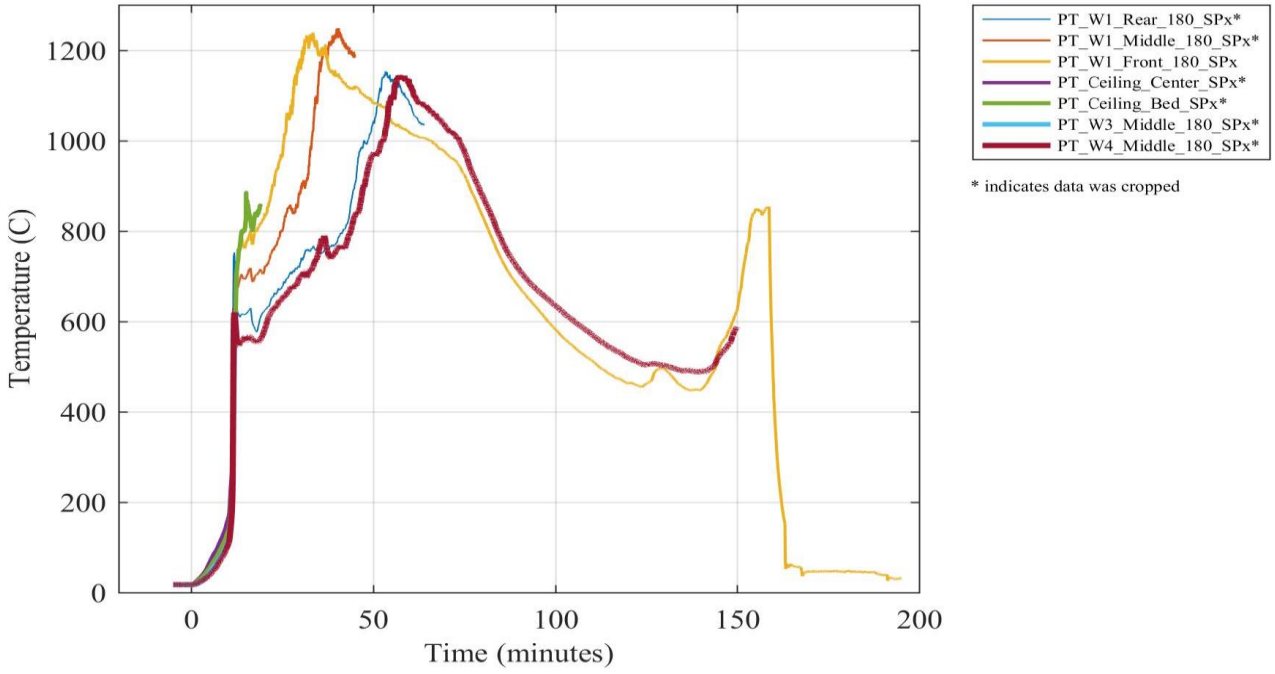

Figure H 29. Plate thermometer temperatures at various locations inside the compartment.

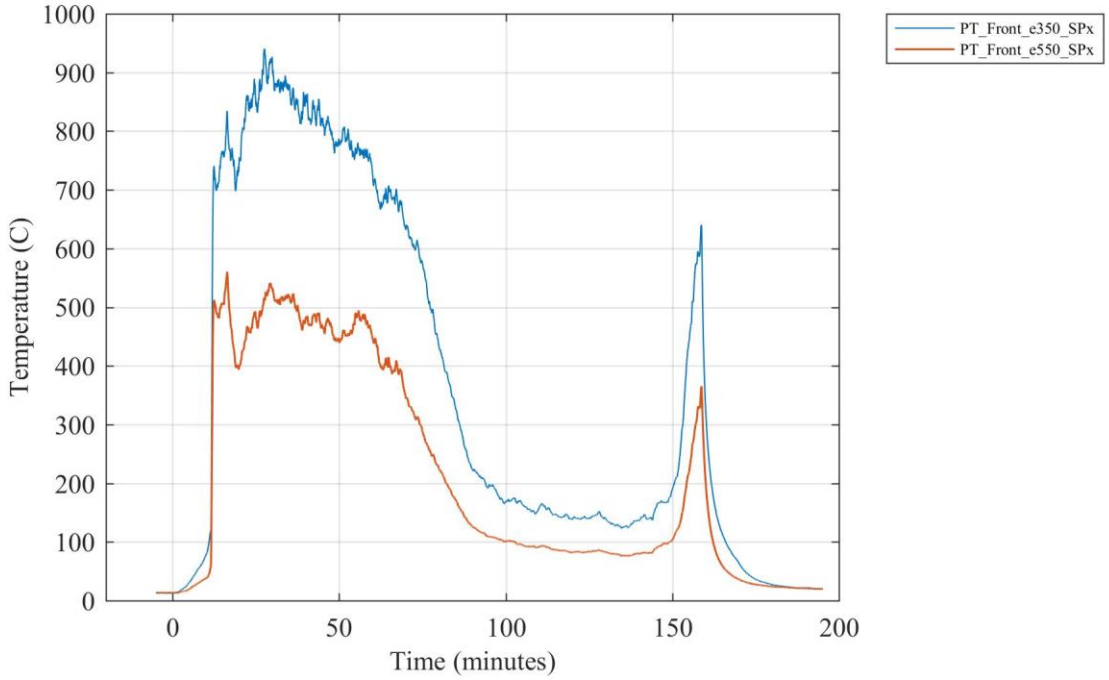

Figure H 30. Plate thermometer temperatures 350 cm and 550 cm above the floor above the doorway.

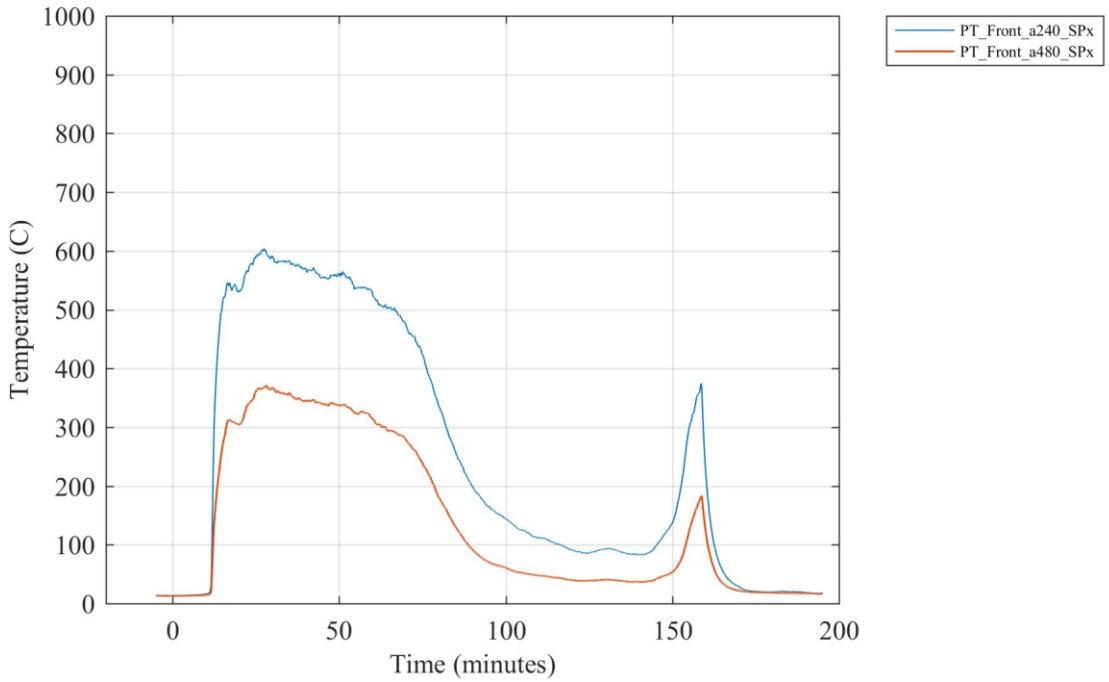

Figure H 31. Plate thermometer temperatures 240 cm and 480 cm from the doorway facing the opening.

Appendix I - Test 1-5 data

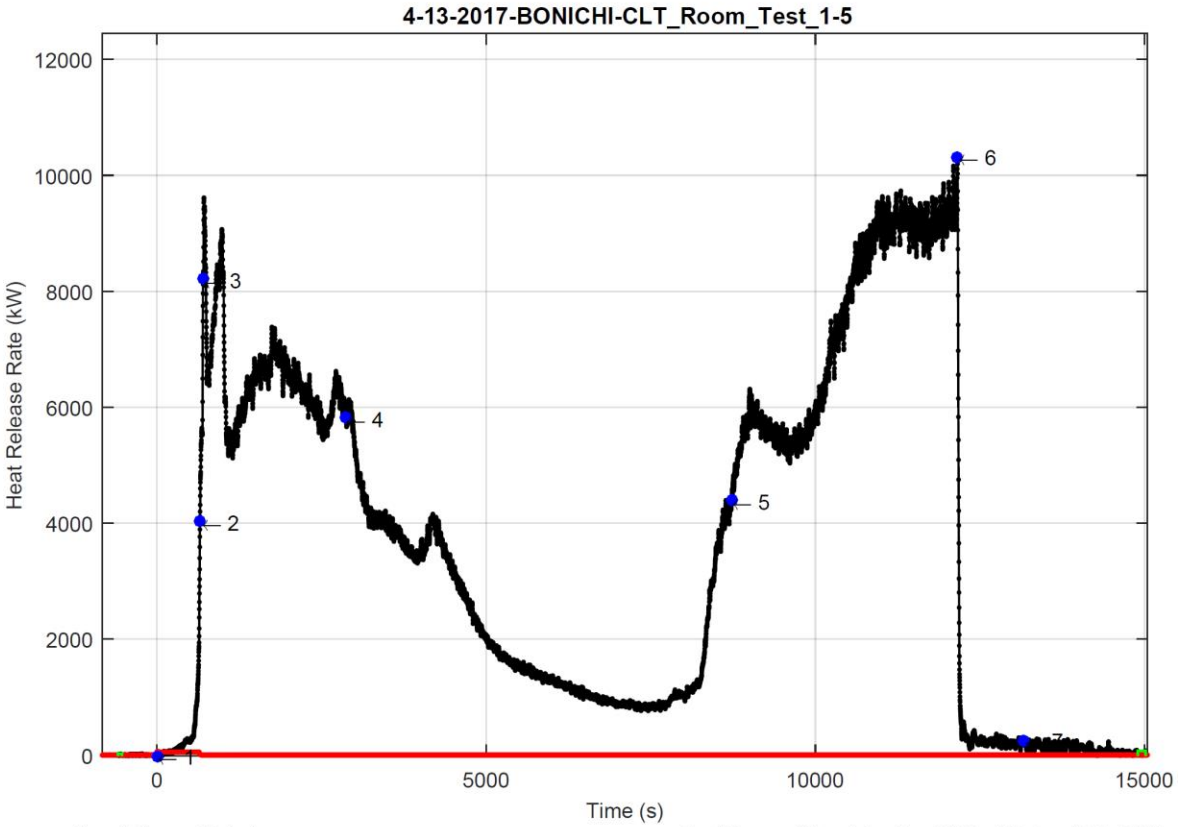

Hood Size = 15 (m)

Fuel Type = WoodFurniturePUF ; HOC = 19.9 (MJ/kg)

Peak Heat Release Rate = 10372 (kW)

Total Heat Release = 53580 (MJ)

NG Burner Peak HRR = 63 (kW)

NG Burner Total HR = 44 (MJ)

Exhaust Flow = 94.89 +/- 0.86 (kg/s)

Total Burn Time = 3.66 (Hrs)

O_2 Baseline = 0.20942 (Vol Fr)

Fuel Mass Burned = 2692.46 (kg)

O_2 Drift During Test = -137 (ppmv)

O_2 Consumed = 4282.45 (kg)

CO Generated = 88.15 (kg)

CO_2 Generated = 5804.41 (kg)

Test Description:
CLT Room test 1-5. Furnished room witth 3 layers of type X gypsum on 3 walls and ceiling. Wall 1 is exposed CLT. Narrow door opening

Event Count	Time (s)	Time Stamp	Event Description
1	0	4/13/2017 10:05:16 AM	Ignition
2	654	4/13/2017 10:16:09 AM	burner off
3	702	4/13/2017 10:16:57 AM	flashover
4	2859	4/13/2017 10:52:54 AM	room gas sample line fell -5 min
5	8729	4/13/2017 12:30:45 PM	CLT delamination in progress
6	12160	4/13/2017 1:27:56 PM	start water suppression
7	13171	4/13/2017 1:44:45 PM	Fire Out

Figure I 1. Summary report file generated by the NFRL calorimeter on the day of test.

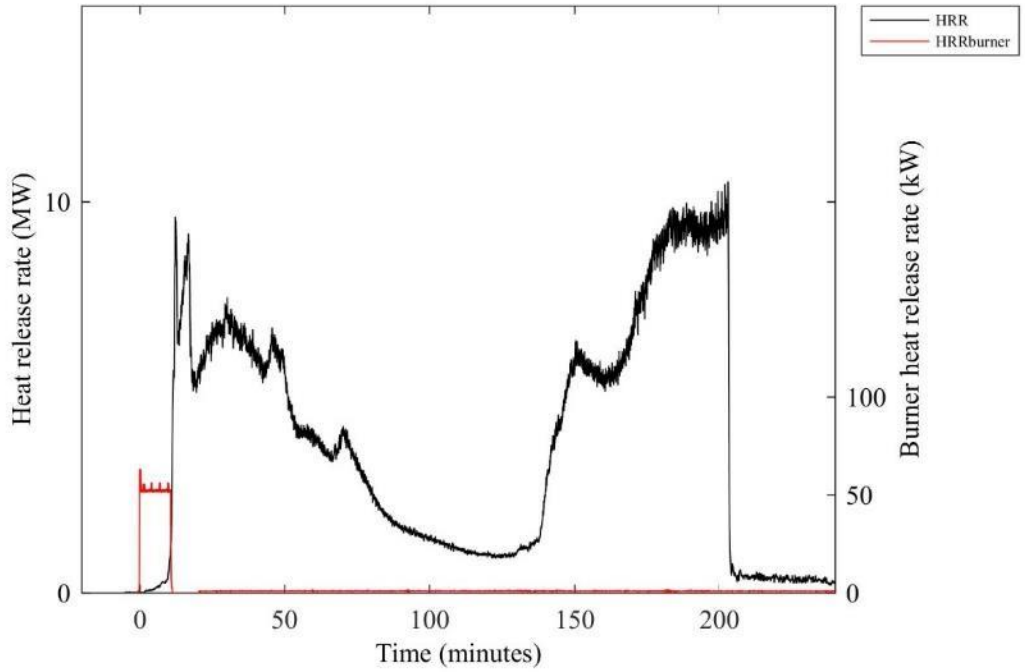

Figure I 2. Compartment (left axis) and burner (right axis) heat release rates.

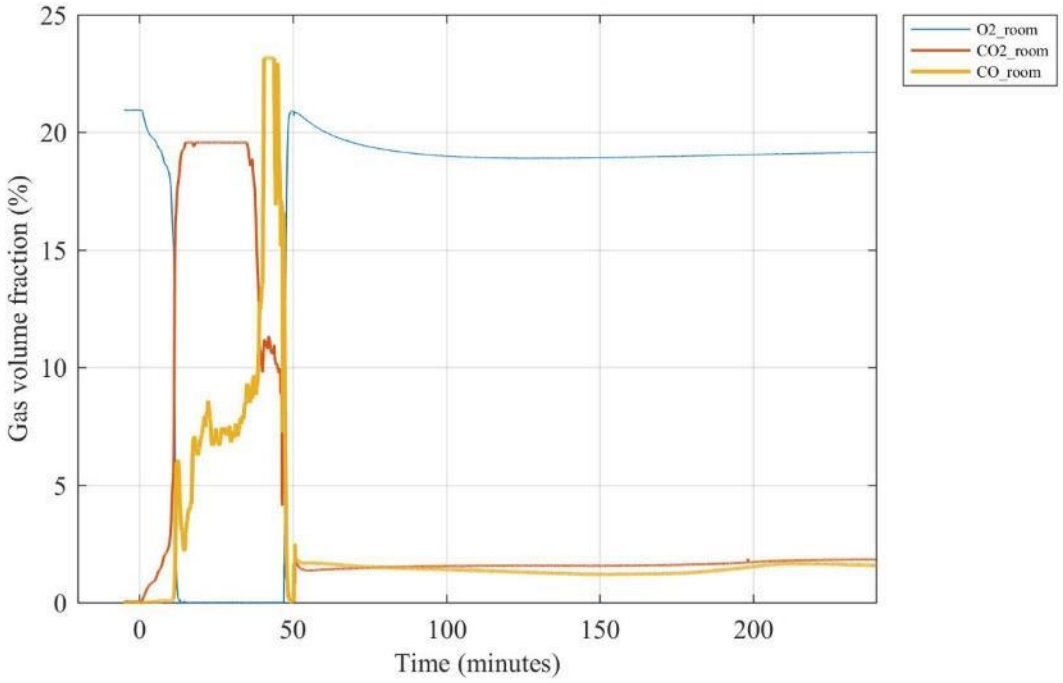

Figure I 3. Gas volume fractions for oxygen (O_2), carbon dioxide (CO_2) and carbon monoxide (CO) sampled at the center of the compartment 210 cm above the floor.

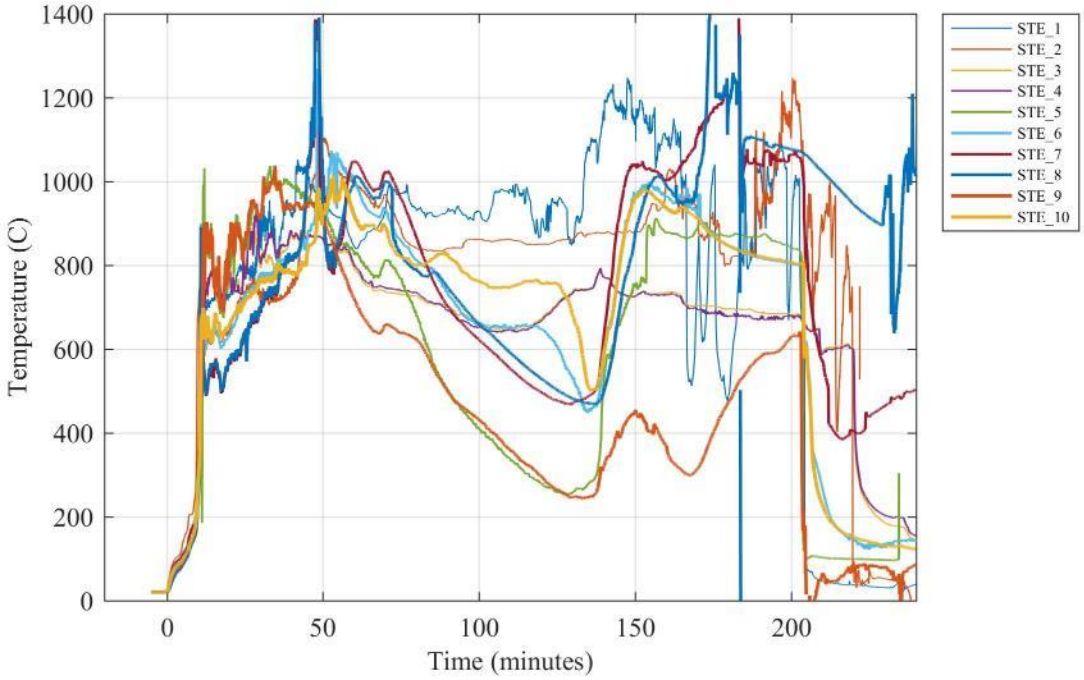

Figure I 4. Simulated thermal elements (STE) for sprinkler.

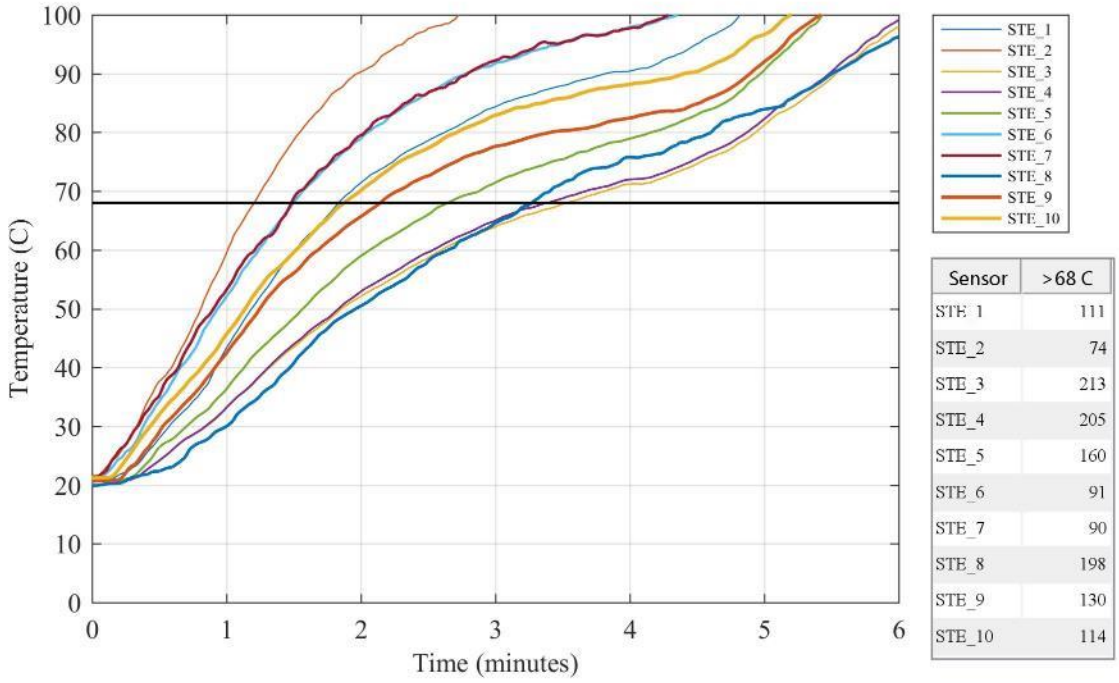

Sensor	>68 C
STE_1	111
STE_2	74
STE_3	213
STE_4	205
STE_5	160
STE_6	91
STE_7	90
STE_8	198
STE_9	130
STE_10	114

Figure I 5. Simulated thermal elements (STE) for sprinkler with table showing time after ignition (in seconds) until 68 °C is reached.

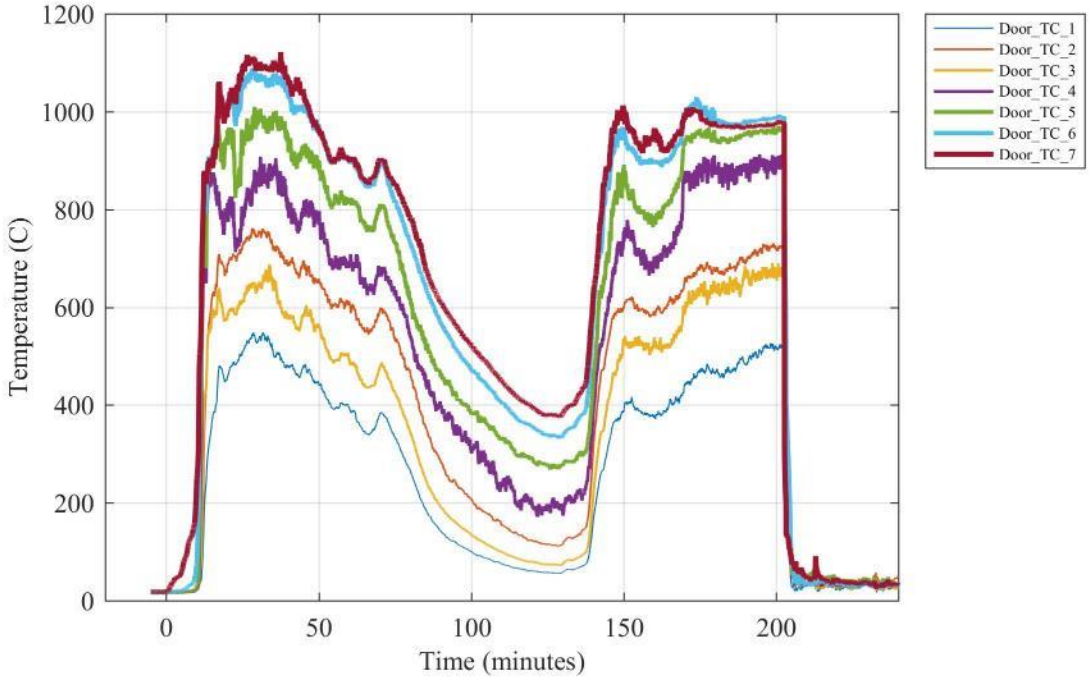

Figure I 6. Temperatures measured at various heights above the floor in the doorway.

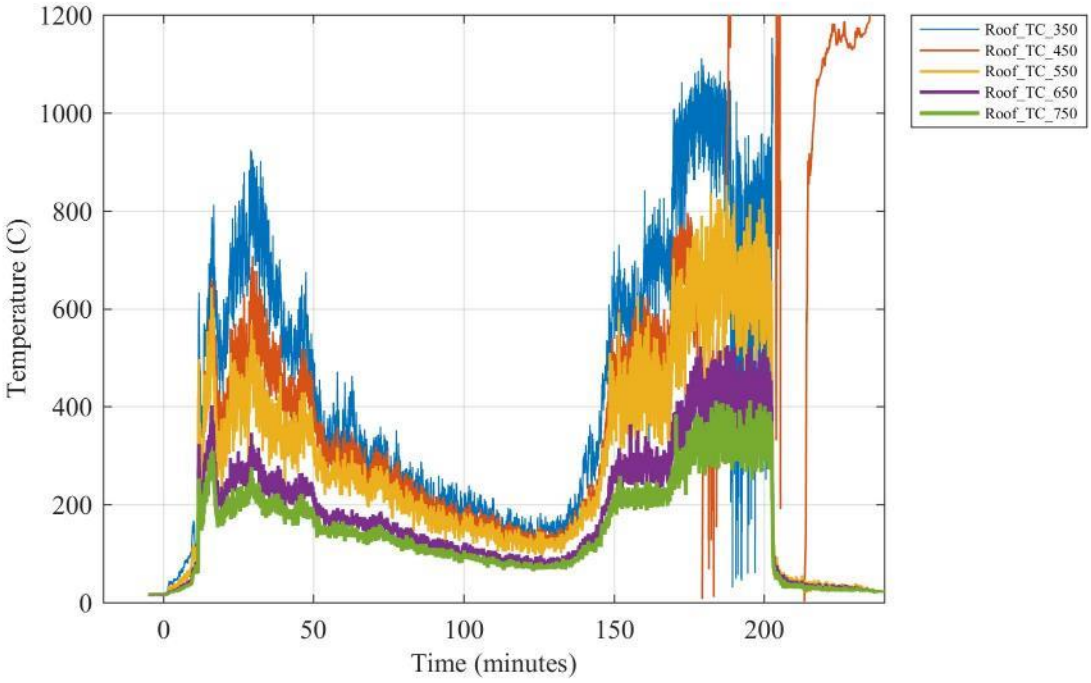

Figure I 7. Temperatures measured at various heights above the floor above the doorway.

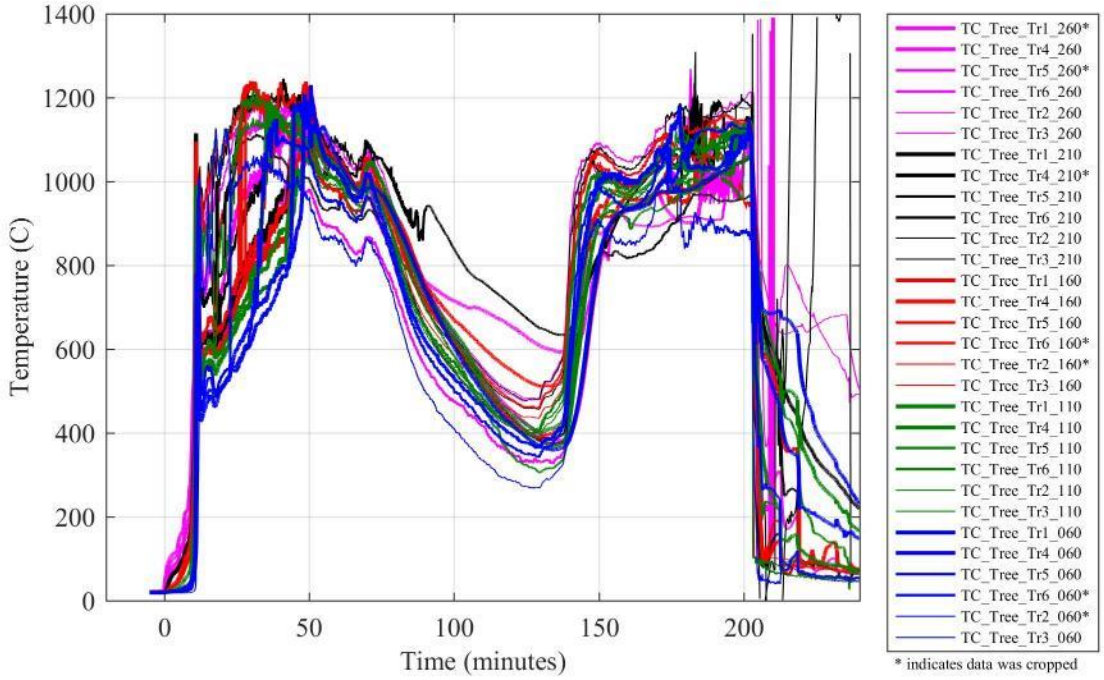

Figure I 8. Thermocouple tree temperatures at various locations inside the compartment.

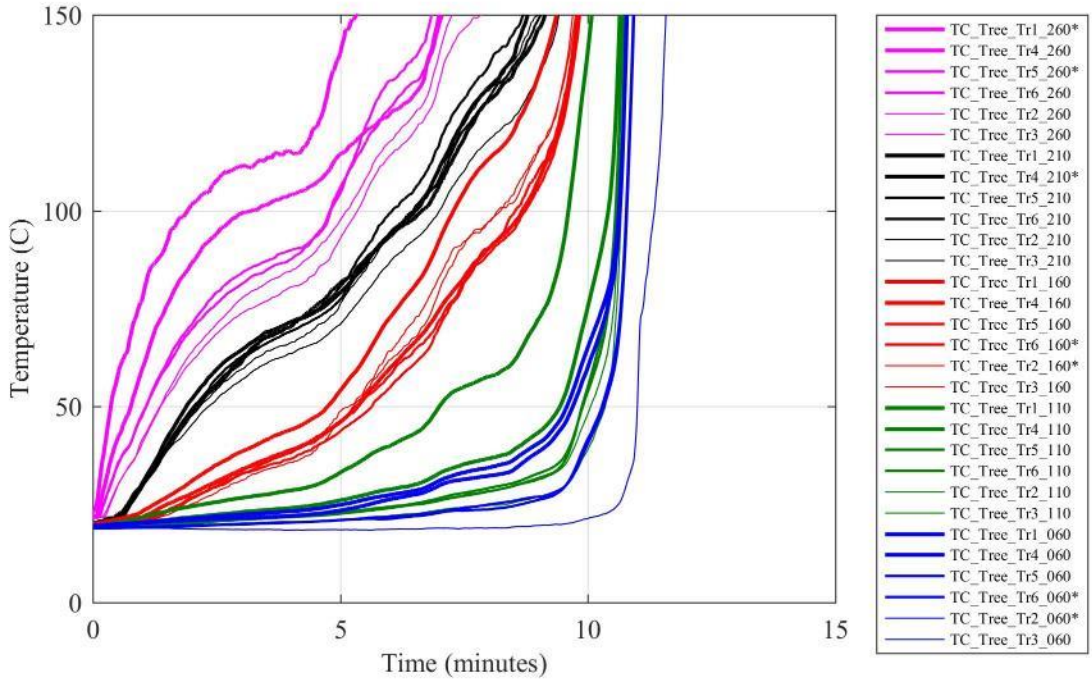

Figure I 9. Thermocouple tree temperatures at various locations inside the compartment during the first 15 min after ignition.

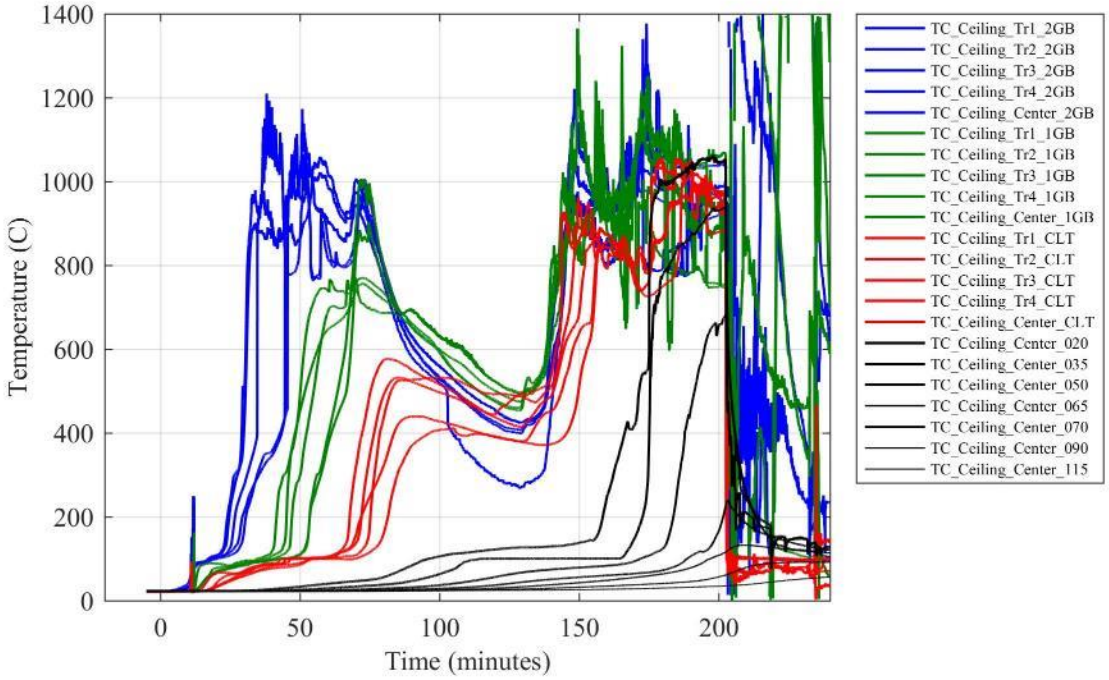

Figure I 10. Temperatures in the ceiling at various depths from the fire exposed surface.

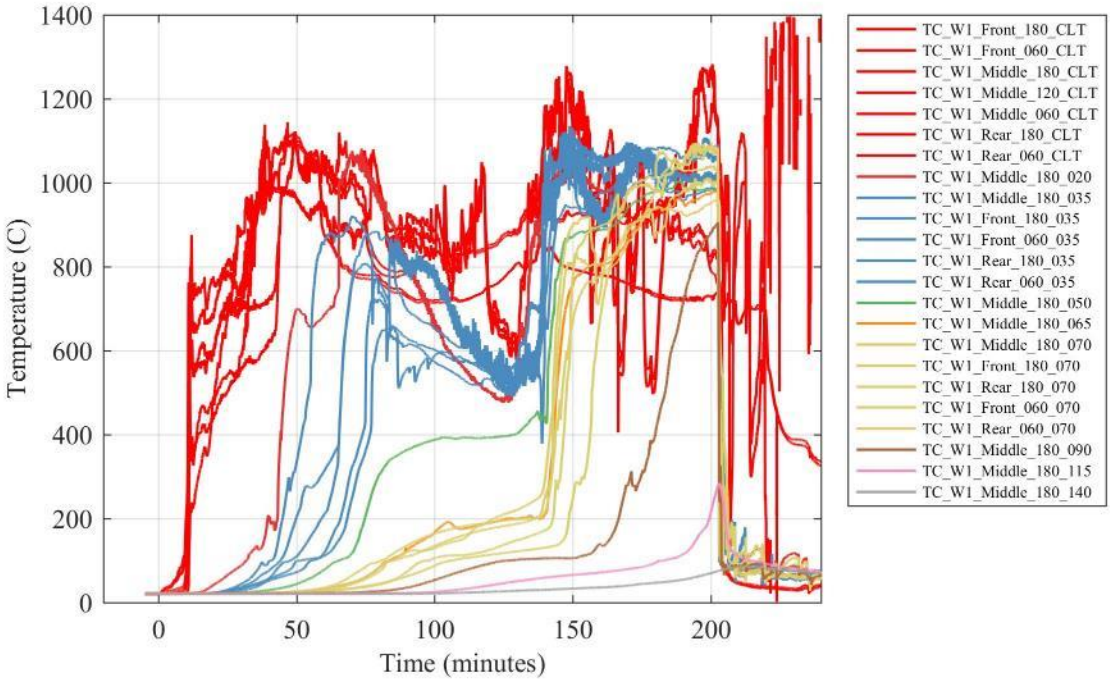

Figure I 11. Temperatures in Wall W1 at various depths from the fire exposed surface.

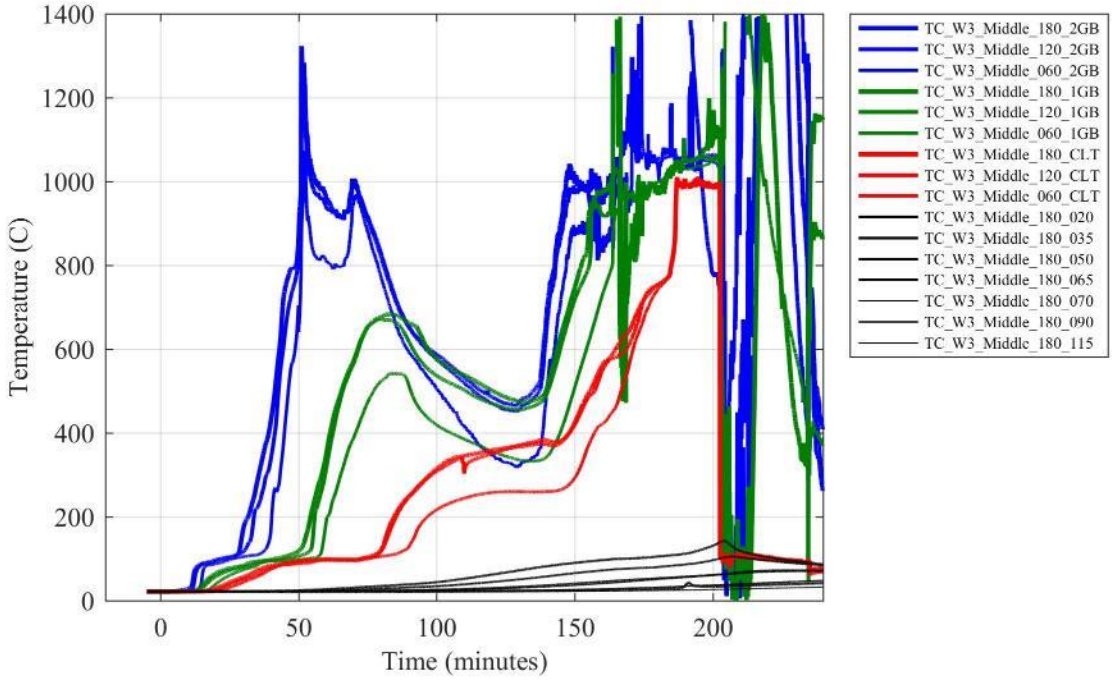

Figure I 12. Temperatures in Wall W3 at various depths from the fire exposed surface.

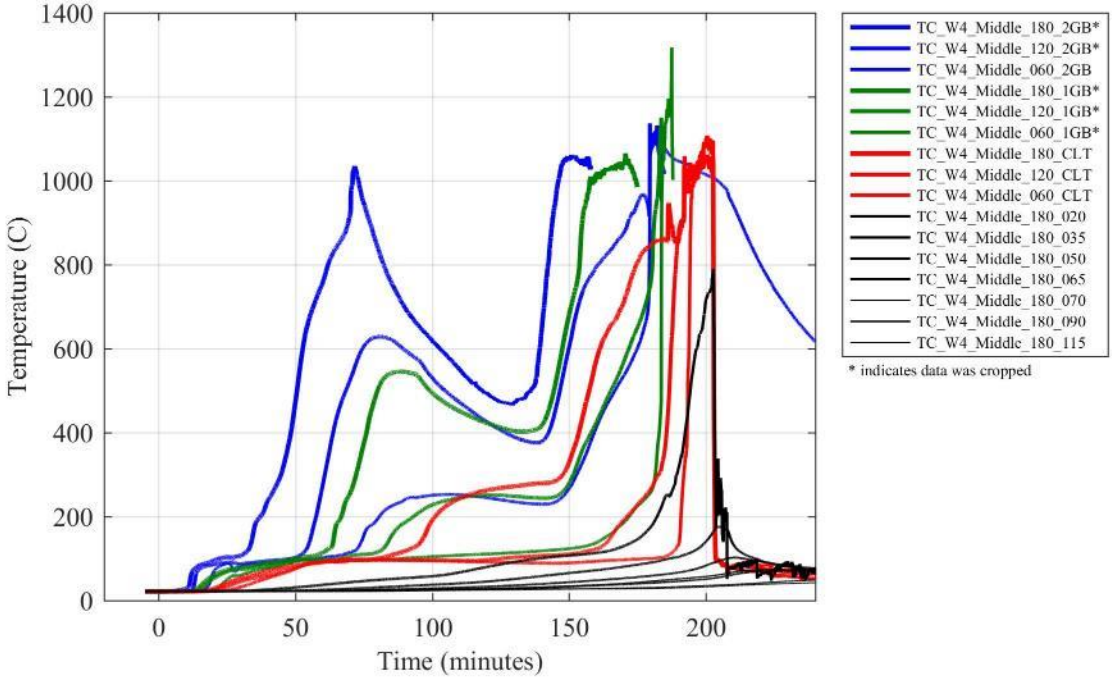

Figure I 13. Temperatures in Wall W4 at various depths from the fire exposed surface.

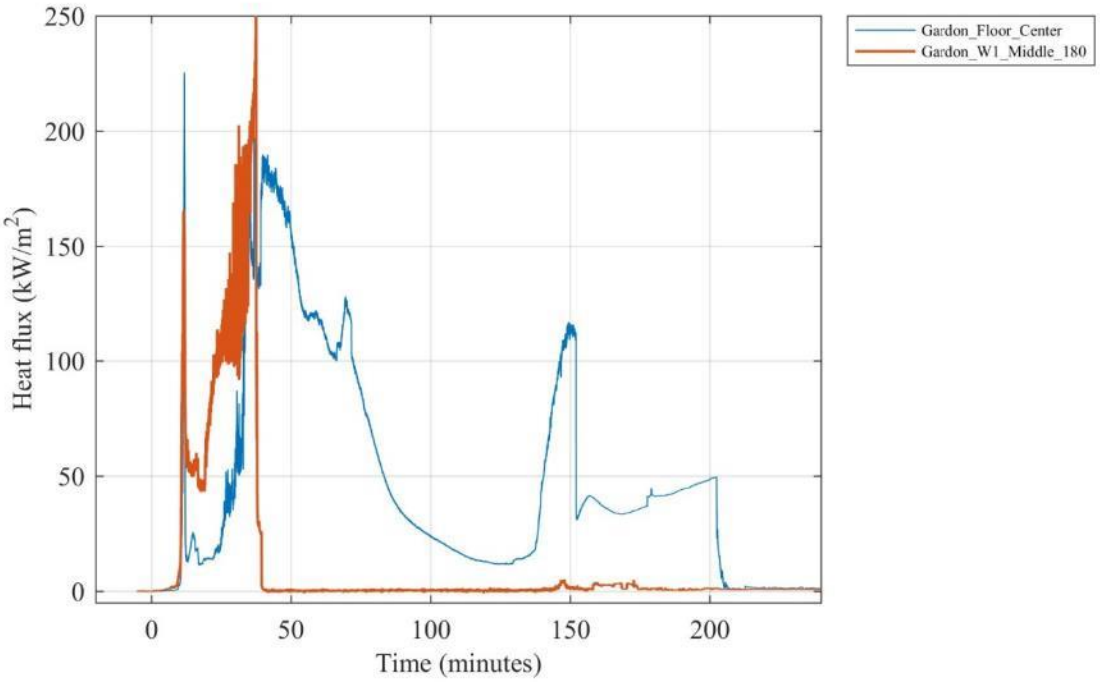

Figure I 14. Heat flux measured by Gardon gauges located inside the compartment.

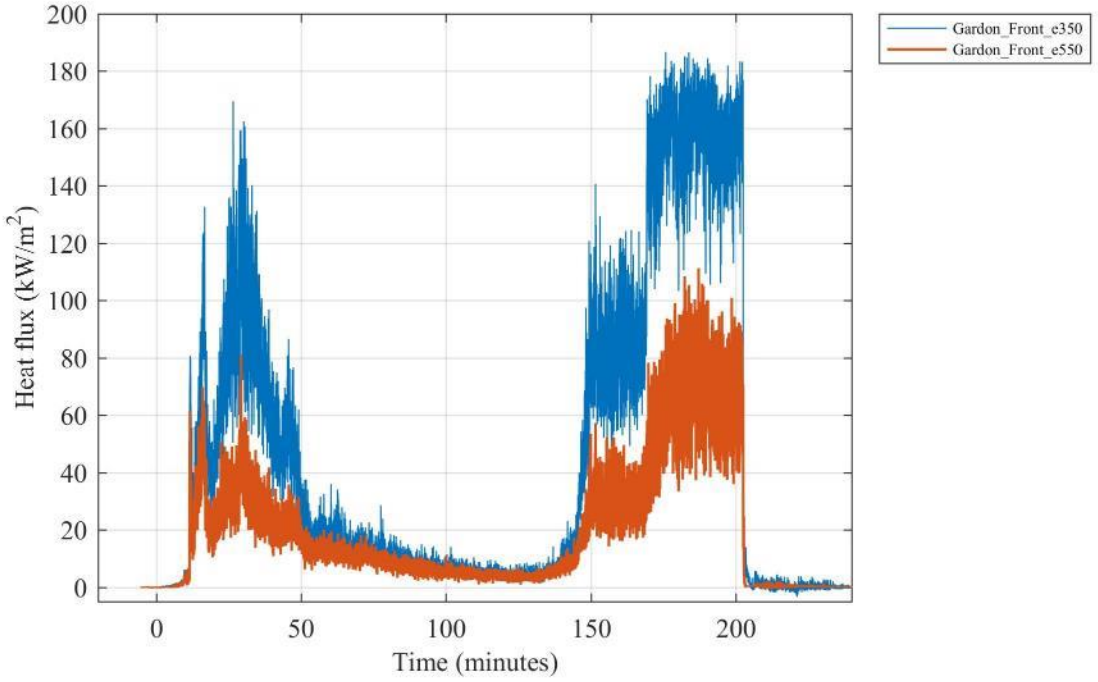

Figure I 15. Heat flux measured by Gardon gauges 350 cm and 550 cm above the floor above the doorway.

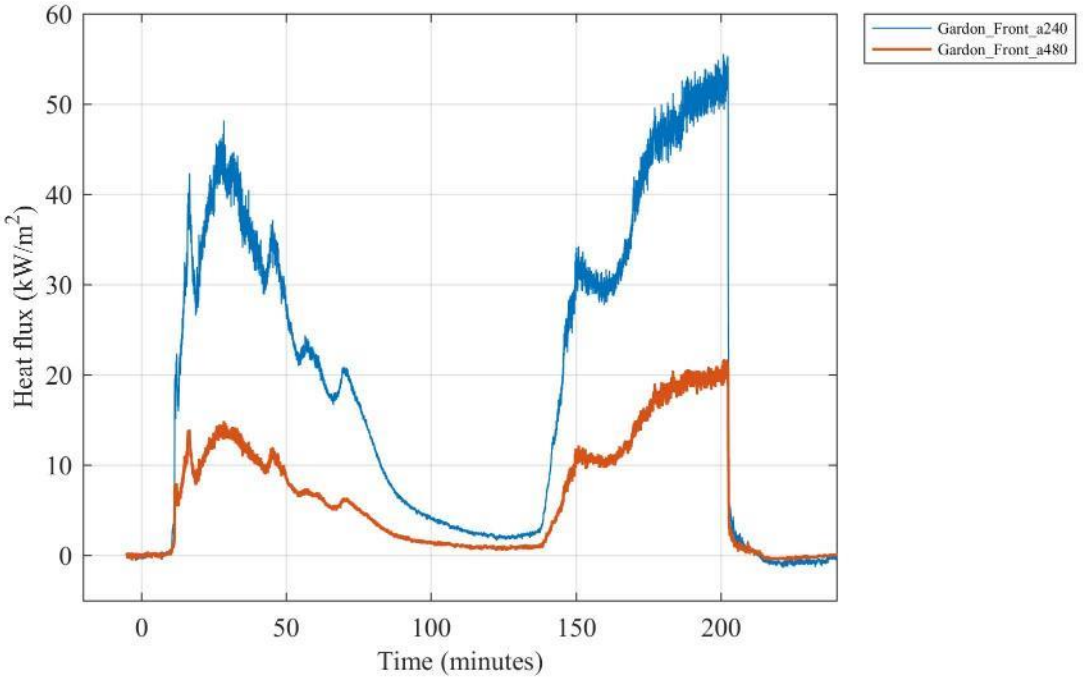

Figure I 16. Heat flux measured by Gardon gauges 240 cm and 480 cm from the doorway facing the opening.

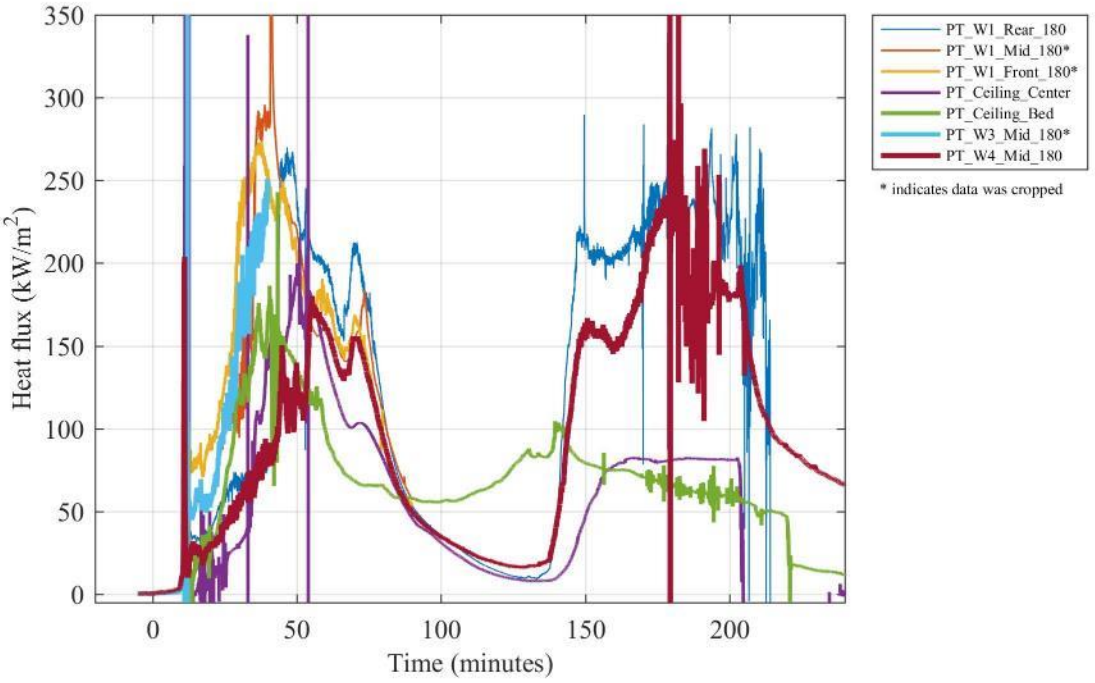

Figure I 17. Heat flux calculated from plate thermometers at various locations inside the compartment.

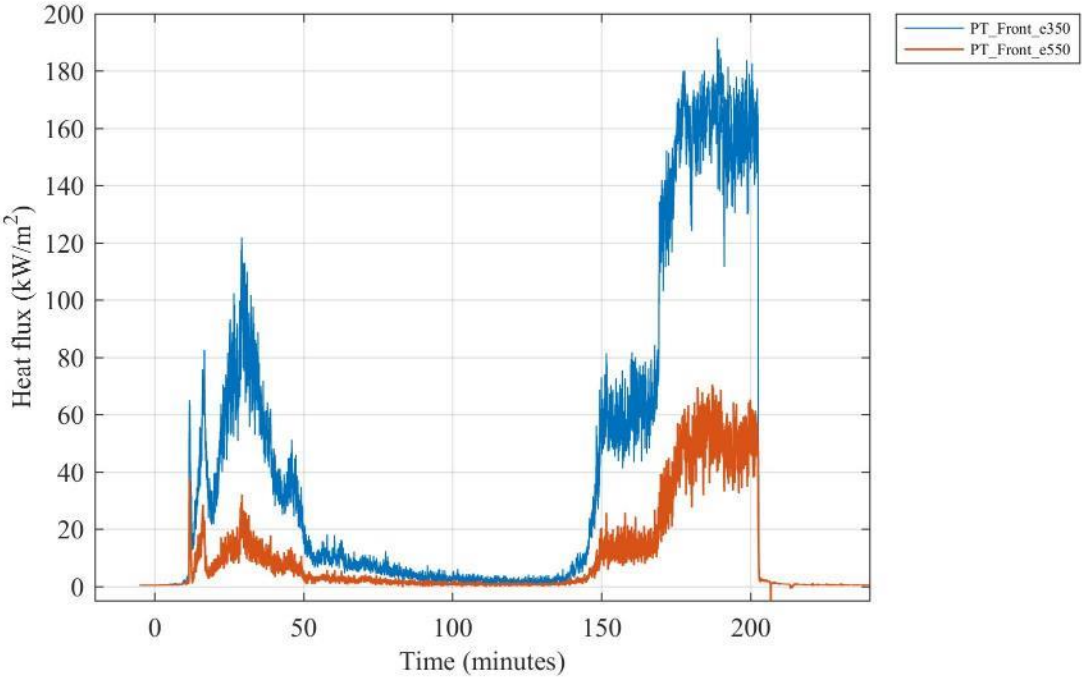

Figure I 18. Heat flux calculated from plate thermometers 350 cm and 550 cm above the floor above the doorway.

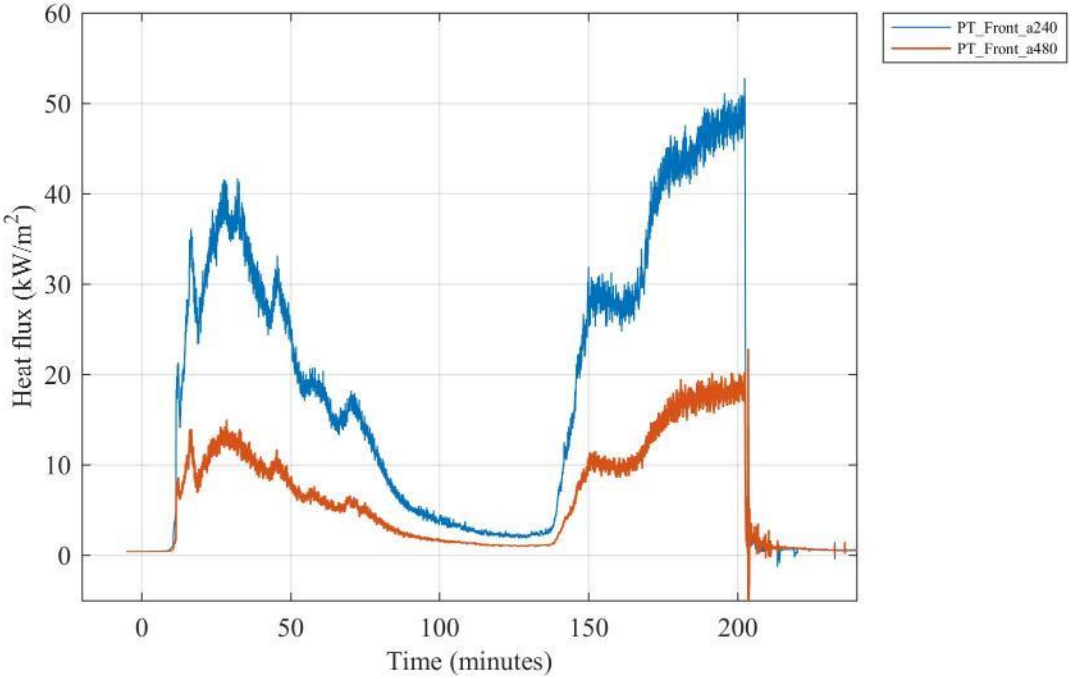

Figure I 19. Heat flux calculated from plate thermometers 240 cm and 480 cm from the doorway facing the opening.

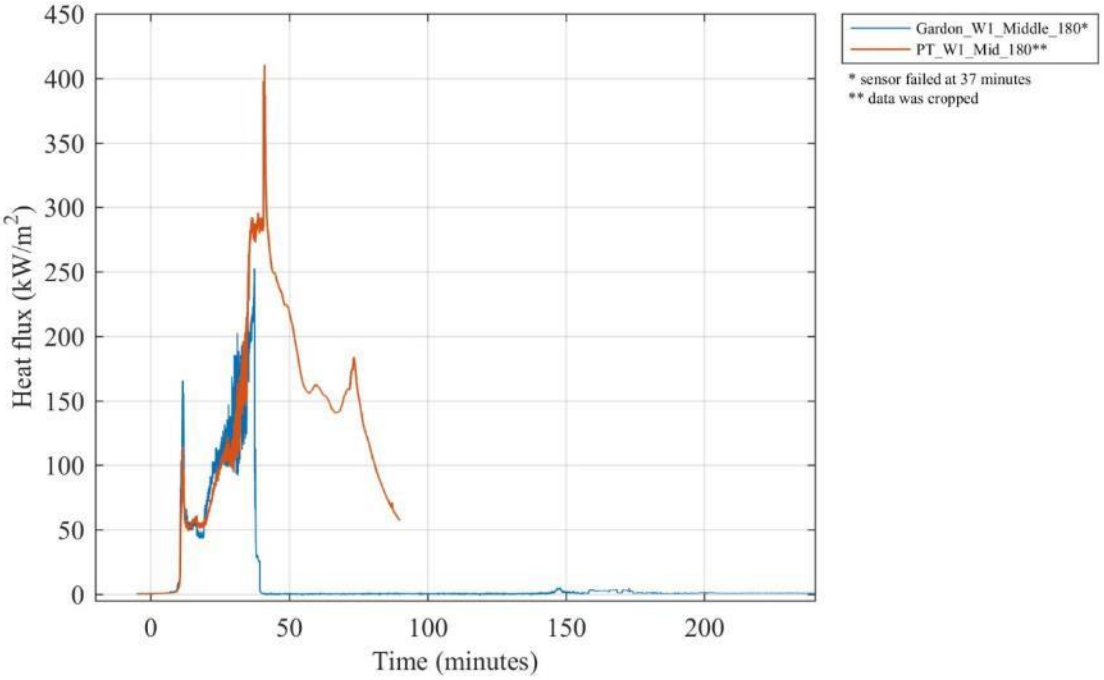

Figure I 20. Comparison of heat fluxes recorded by a collocated Gardon gauge, plate thermometer (PT) and differential flame thermometer (DFT) on Wall W1 at the middle of the compartment 1.8 m above the floor.

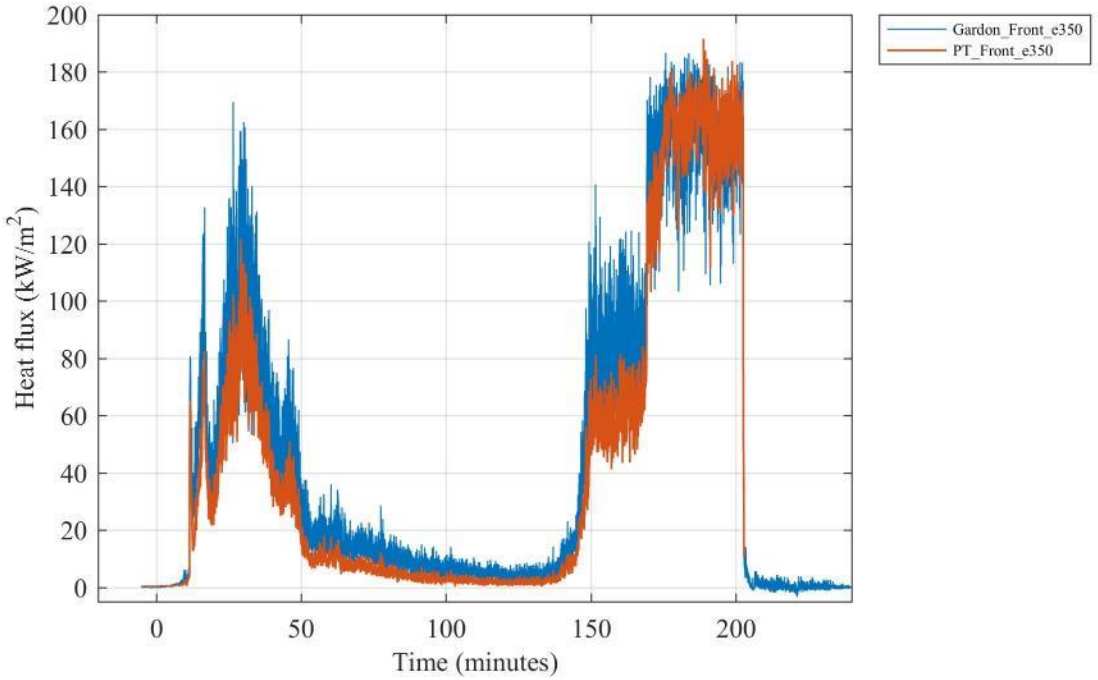

Figure I 21. Comparison of heat fluxes recorded by a collocated Gardon gauge and plate thermometer (PT) 350 cm above the floor above the doorway.

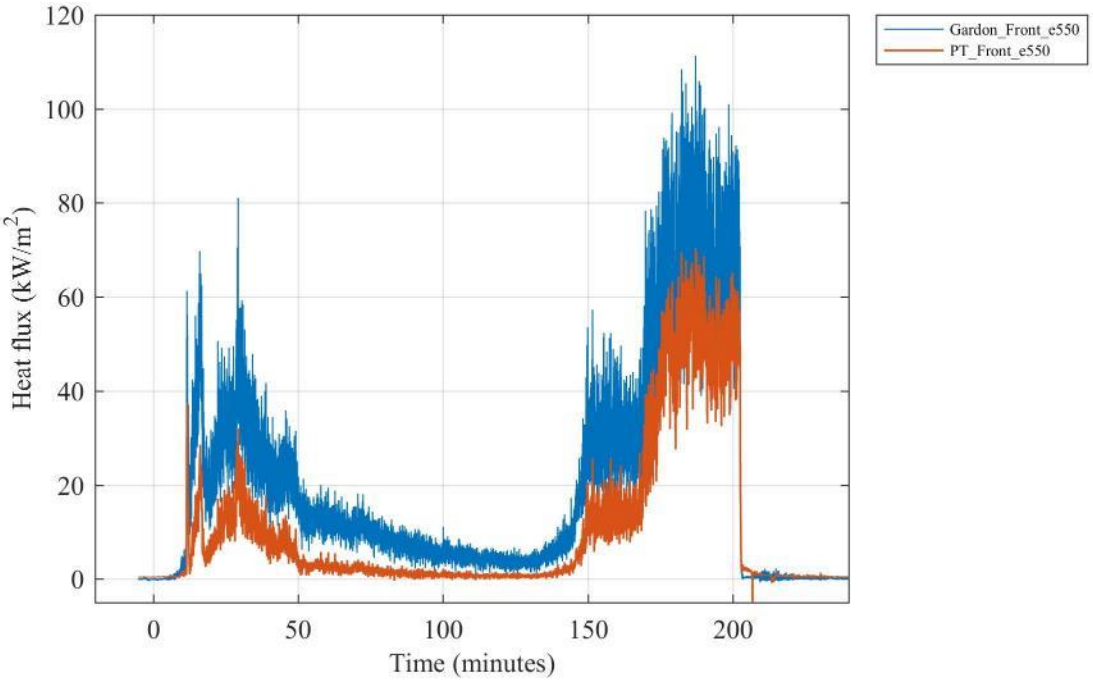

Figure I 22. Comparison of heat fluxes recorded by a collocated Gardon gauge and plate thermometer (PT) 550 cm above the floor above the doorway.

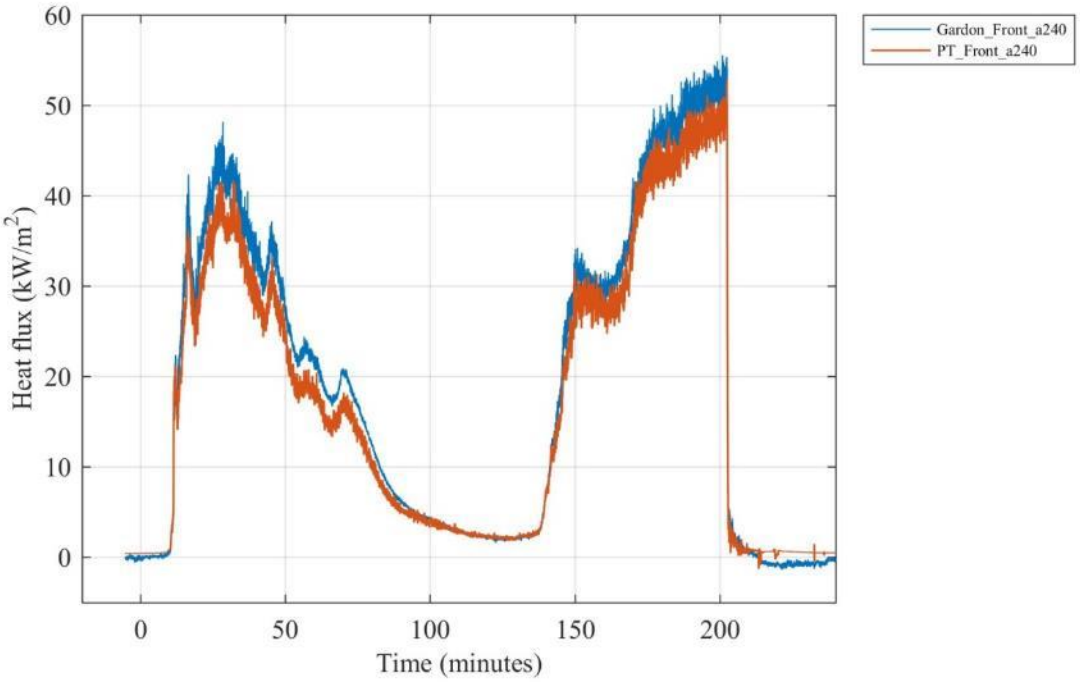

Figure I 23. Comparison of heat fluxes recorded by a collocated Gardon gauge and plate thermometer (PT) 240 cm from the doorway (facing doorway) and 150 cm above floor.

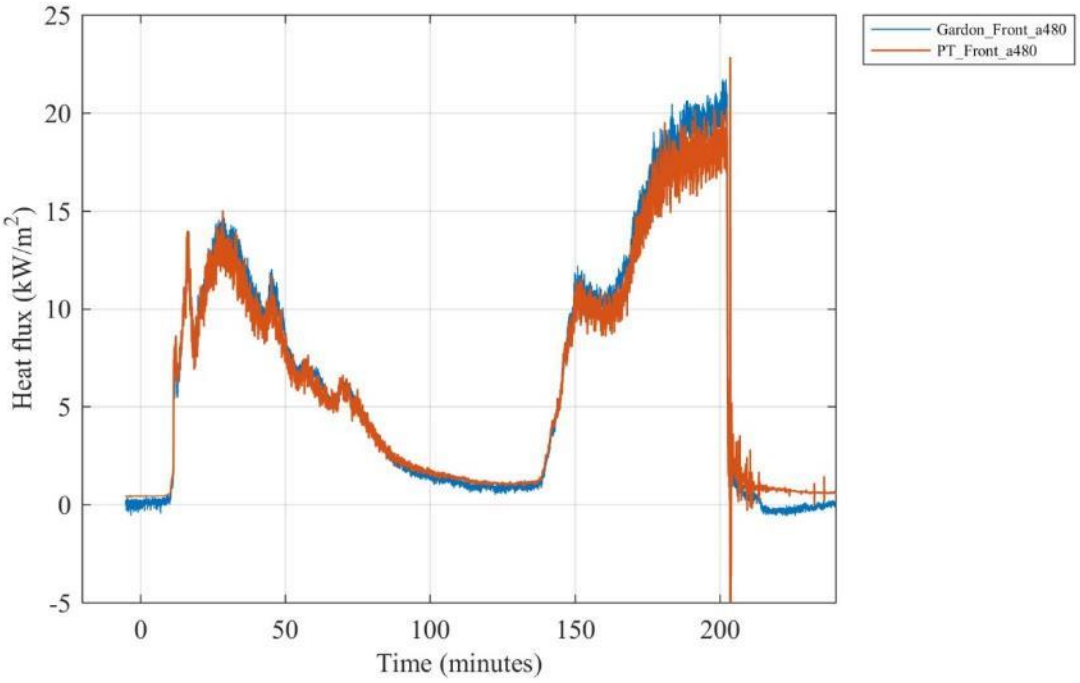

Figure I 24. Comparison of heat fluxes recorded by a collocated Gardon gauge and plate thermometer (PT) 480 cm from the doorway (facing doorway) and 150 cm above floor.

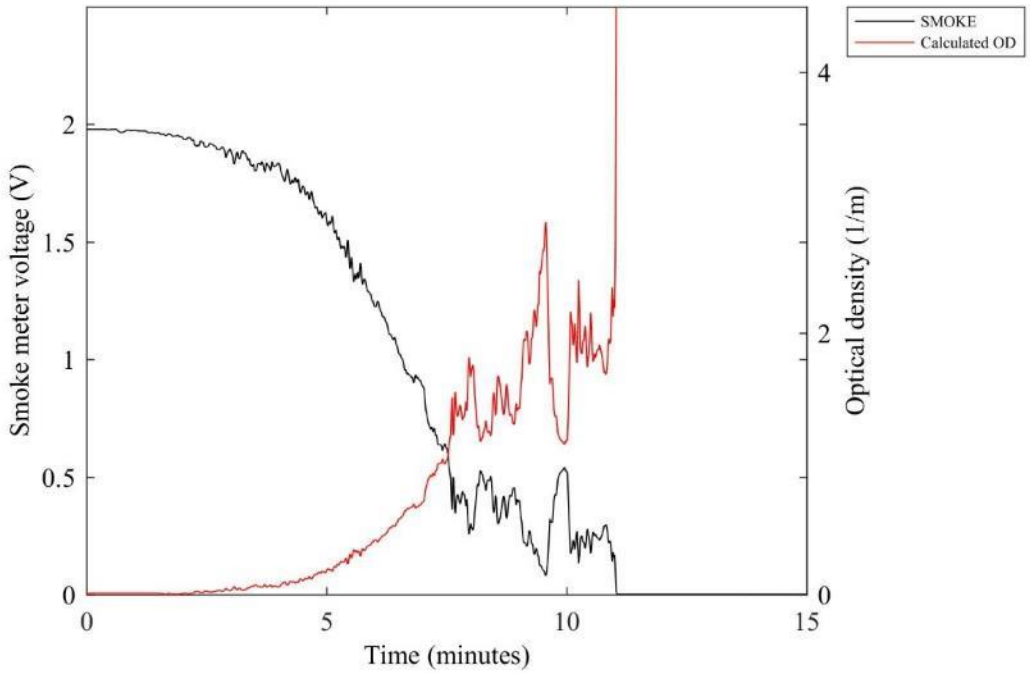

Figure I 25. Smoke meter voltage and calculated optical density (OD) from gas sampled at the center of the compartment 160 cm above the floor.

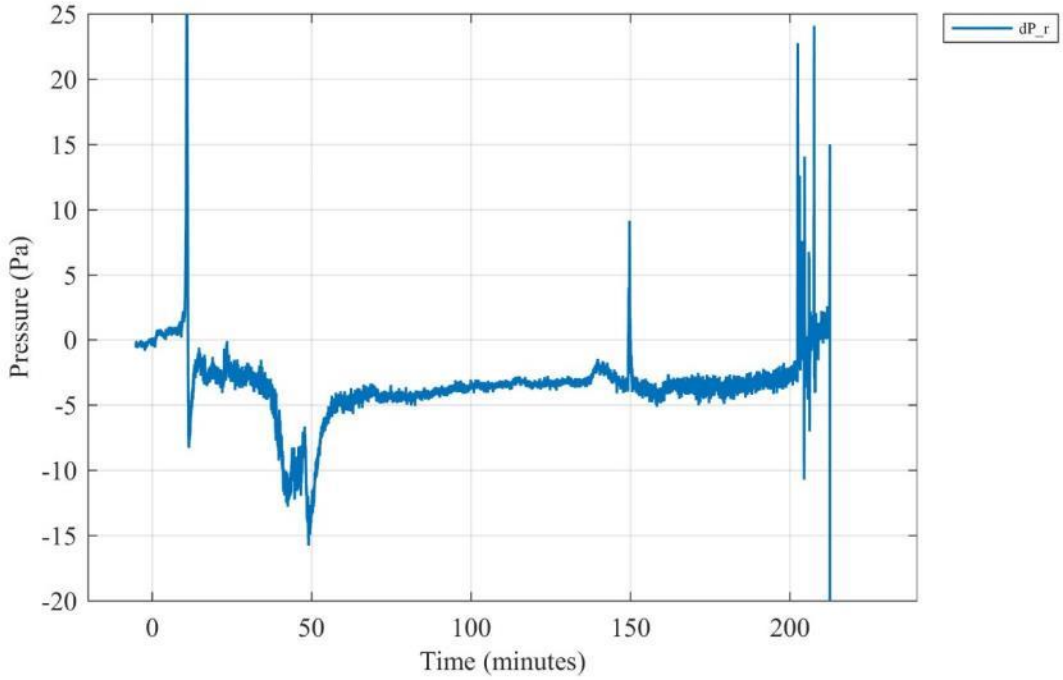

Figure I 26. Differential room pressure measured 210 cm above the floor at the center of the compartment.

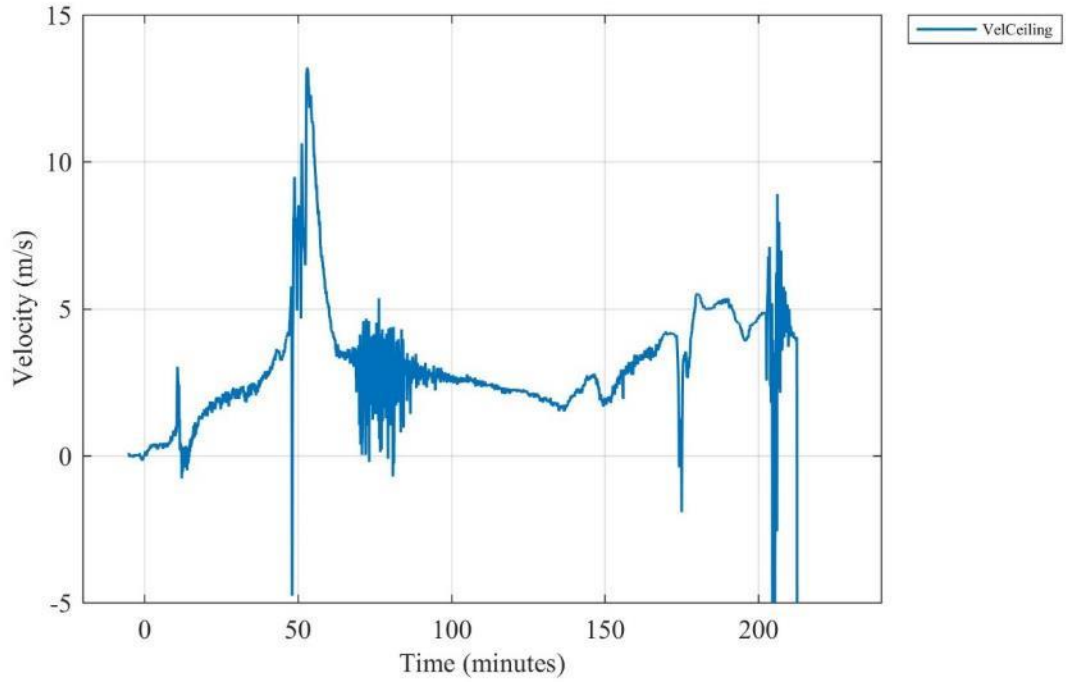

Figure I 27. Gas velocity measured 305 mm from the ceiling along the midline 227.5 cm from the back of the compartment (positive indicates flow out the door). [10 s moving average filter applied]

SENSORS DEFECTIVE

Figure I 28. Gas velocities measured in the doorway (positive indicates flow out the door). [10 s moving average filter applied]

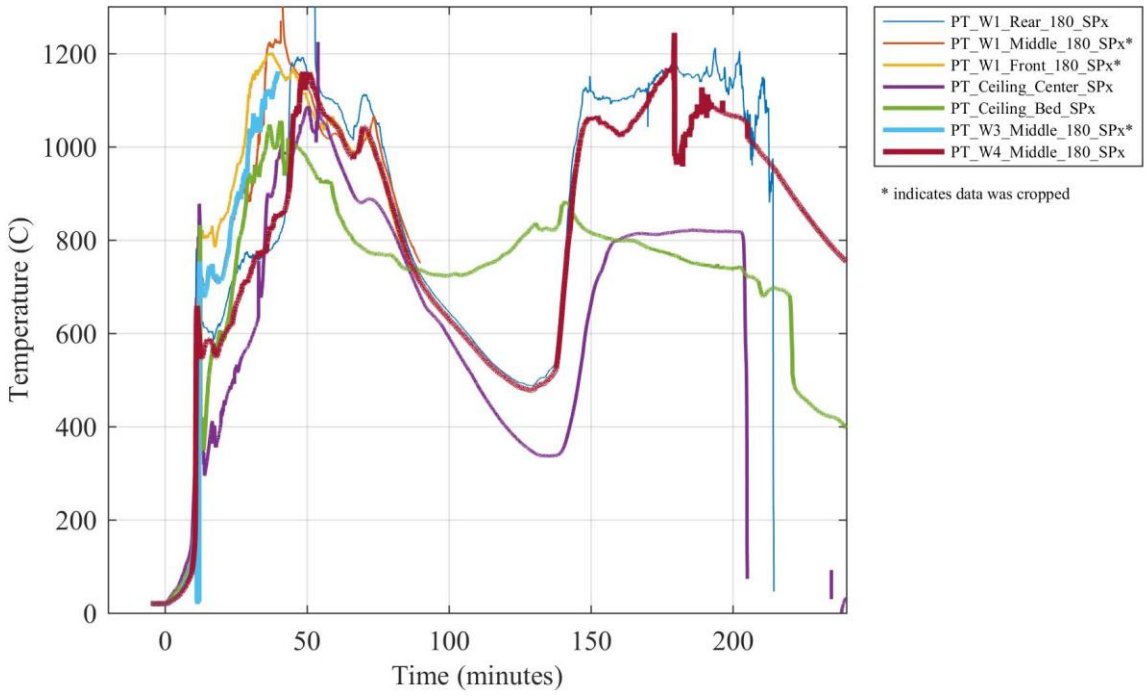

Figure I 29. Plate thermometer temperatures at various locations inside the compartment.

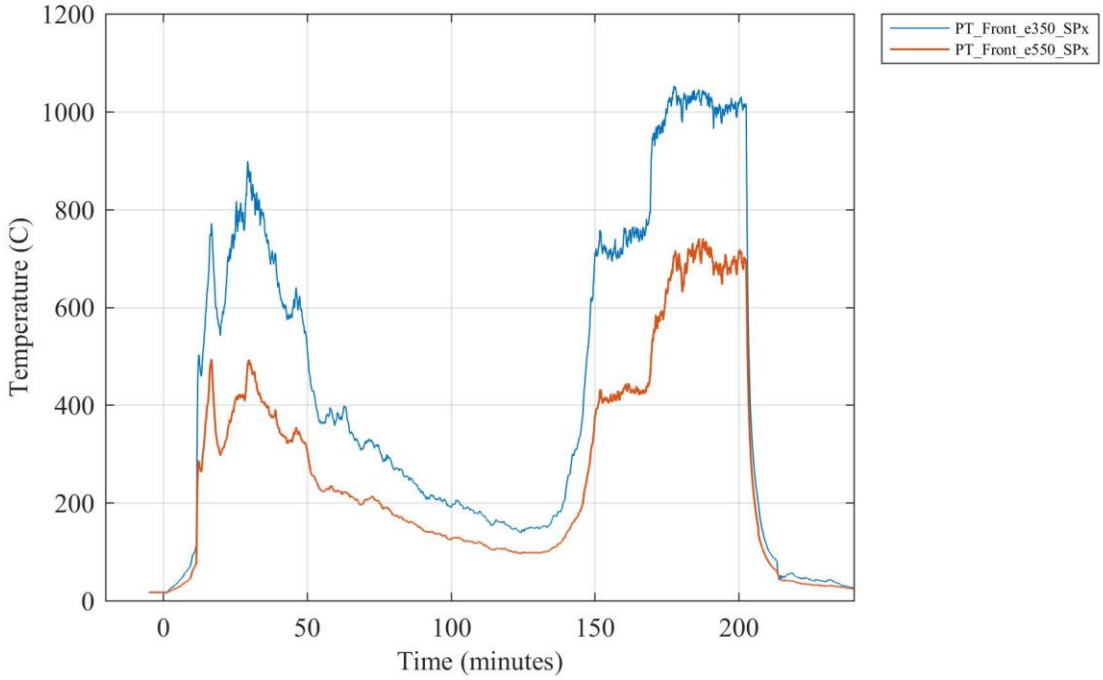

Figure I 30. Plate thermometer temperatures 350 cm and 550 cm above the floor above the doorway.

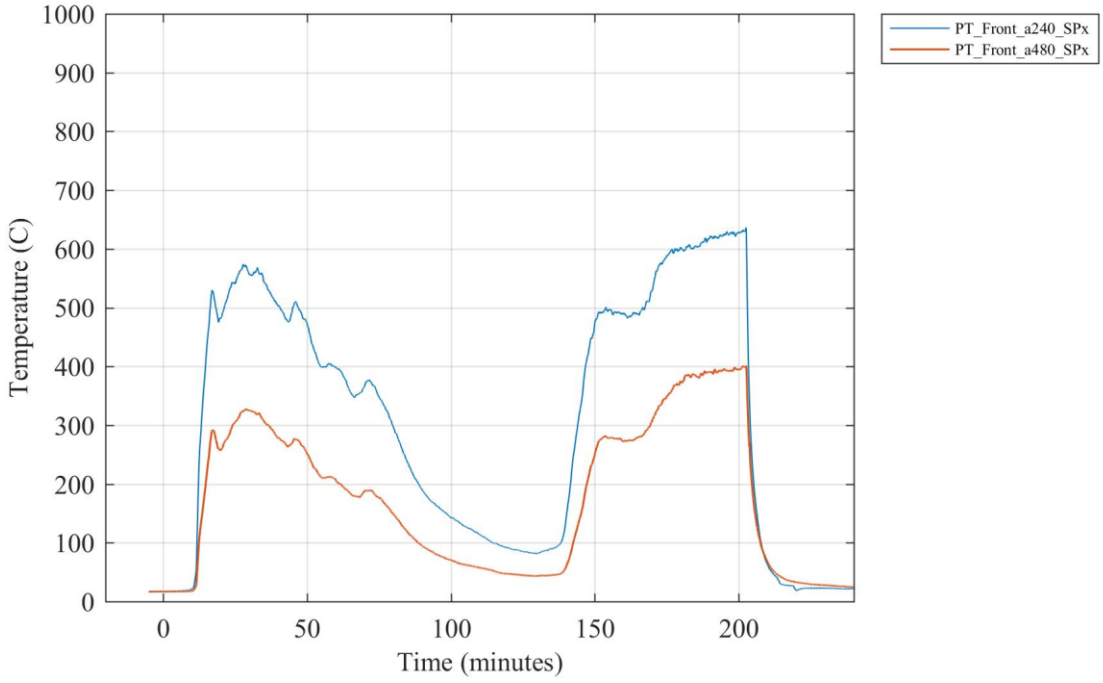

Figure I 31. Plate thermometer temperatures 240 cm and 480 cm from the doorway facing the opening.

Appendix J - Test 1-6 data

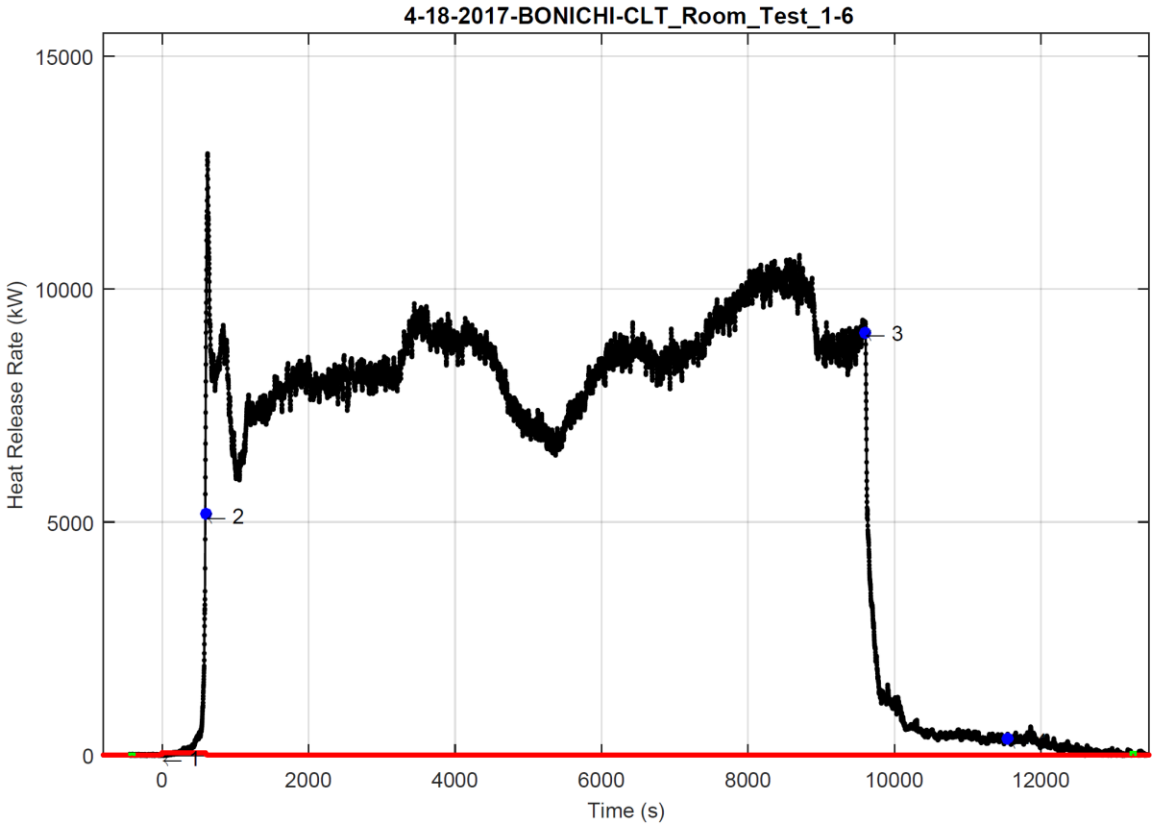

Hood Size = 15 (m)

Peak Heat Release Rate = 12910 (kW)

NG Burner Peak HRR = 52 (kW)

Exhaust Flow = 95.09 +/- 0.62 (kg/s)

O_2 Baseline = 0.2094 (Vol Fr)

O_2 Drift During Test = -122 (ppmv)

CO Generated = 63.44 (kg)

Fuel Type = WoodFurniturePUF ; HOC = 19.9 (MJ/kg)

Total Heat Release = 78200 (MJ)

NG Burner Total HR = 25 (MJ)

Total Burn Time = 3.21 (Hrs)

Fuel Mass Burned = 3929.65 (kg)

O_2 Consumed = 6132.47 (kg)

CO_2 Generated = 8229.41 (kg)

Test Description:
CLT Room test 1-6. Furnished room witth 3 layers of type X gypsum on 3 walls. Wall 1 and ceiling is exposed CLT. Narrow door opening

Event Count	Time (s)	Time Stamp	Event Description
1	0	4/18/2017 10:06:29 AM	Ignition
2	590	4/18/2017 10:16:18 AM	room flashover
3	9595	4/18/2017 12:46:25 PM	suppress
4	11552	4/18/2017 1:19:01 PM	Fire Out

Figure J 1. Summary report file generated by the NFRL calorimeter on the day of test.

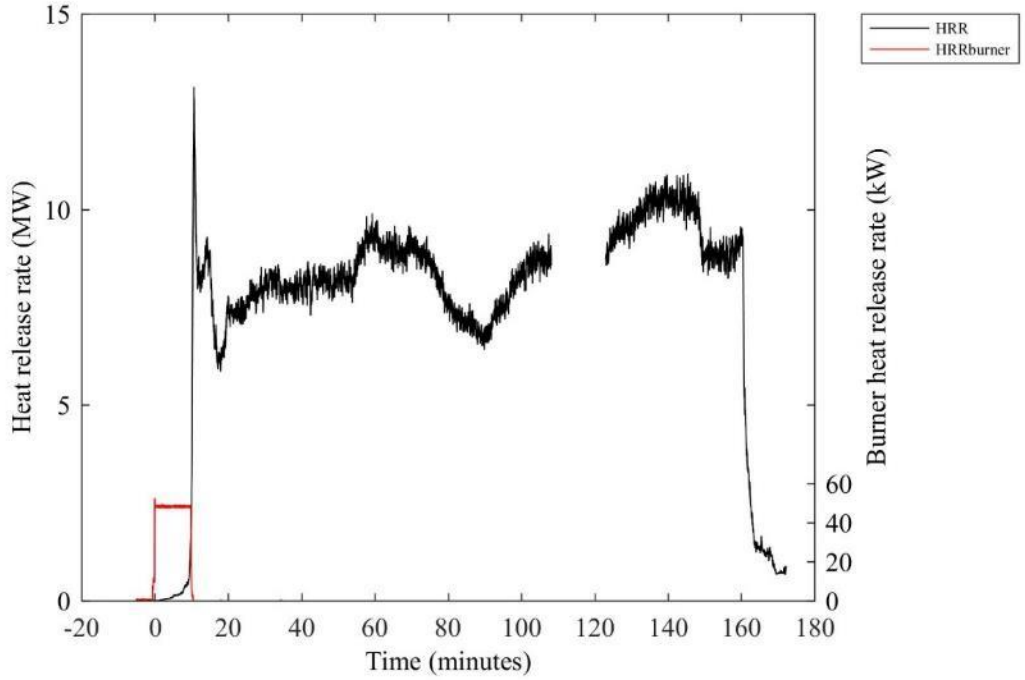

Figure J 2. Compartment (left axis) and burner (right axis) heat release rates. [lost data acquisition between 108 min and 123 min]

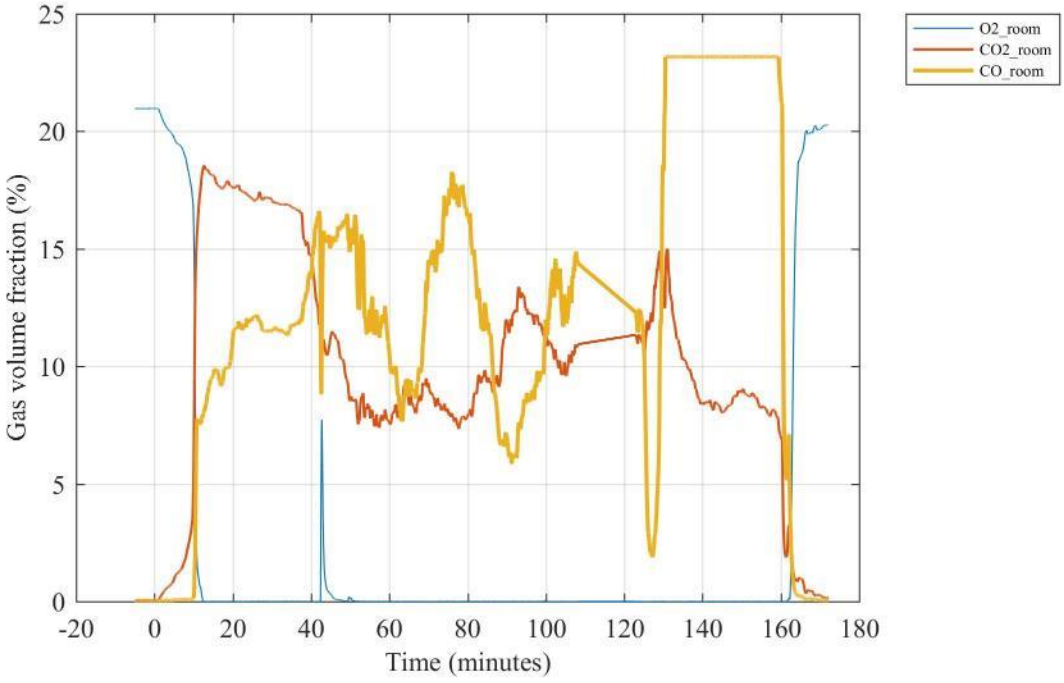

Figure J 3. Gas volume fractions for oxygen (O_2), carbon dioxide (CO_2) and carbon monoxide (CO) sampled at the center of the compartment 210 cm above the floor.

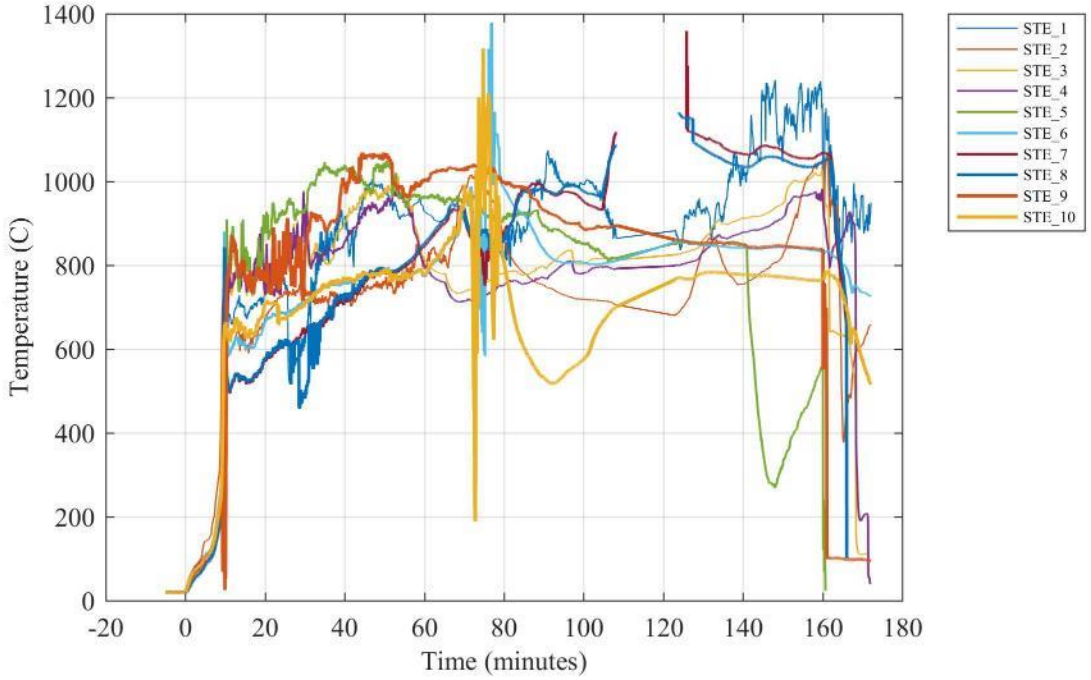

Figure J 4. Simulated thermal elements (STE) for sprinkler.

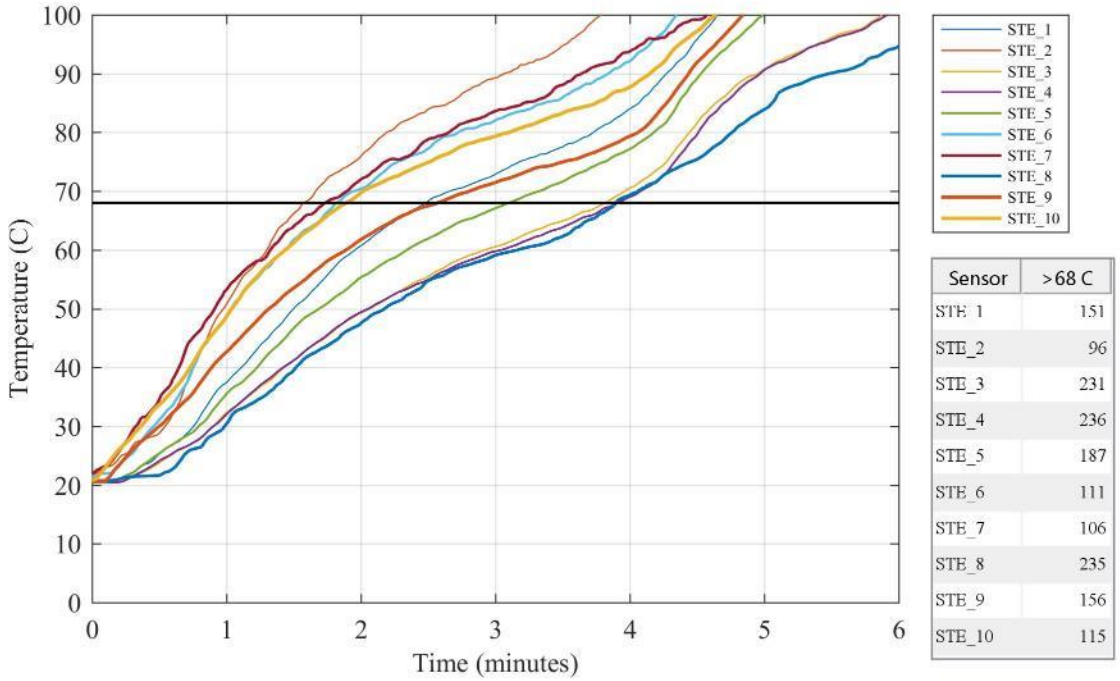

Sensor	>68 C
STE_1	151
STE_2	96
STE_3	231
STE_4	236
STE_5	187
STE_6	111
STE_7	106
STE_8	235
STE_9	156
STE_10	115

Figure J 5. Simulated thermal elements (STE) for sprinkler with table showing time after ignition (in seconds) until 68 °C is reached.

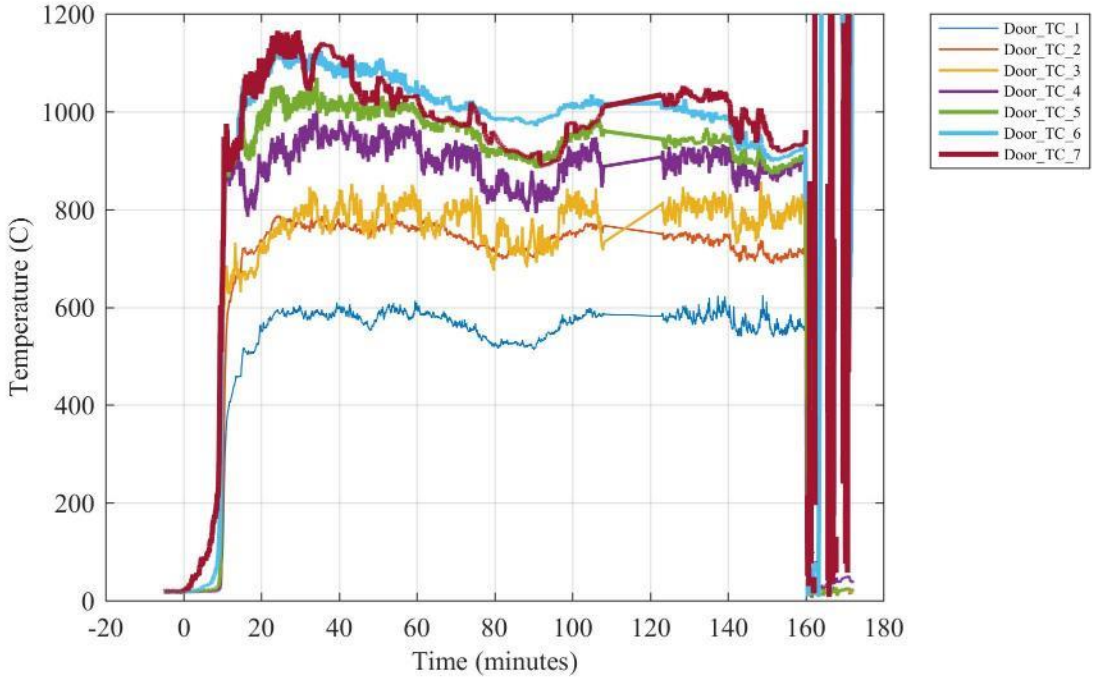

Figure J 6. Temperatures measured at various heights above the floor in the doorway.

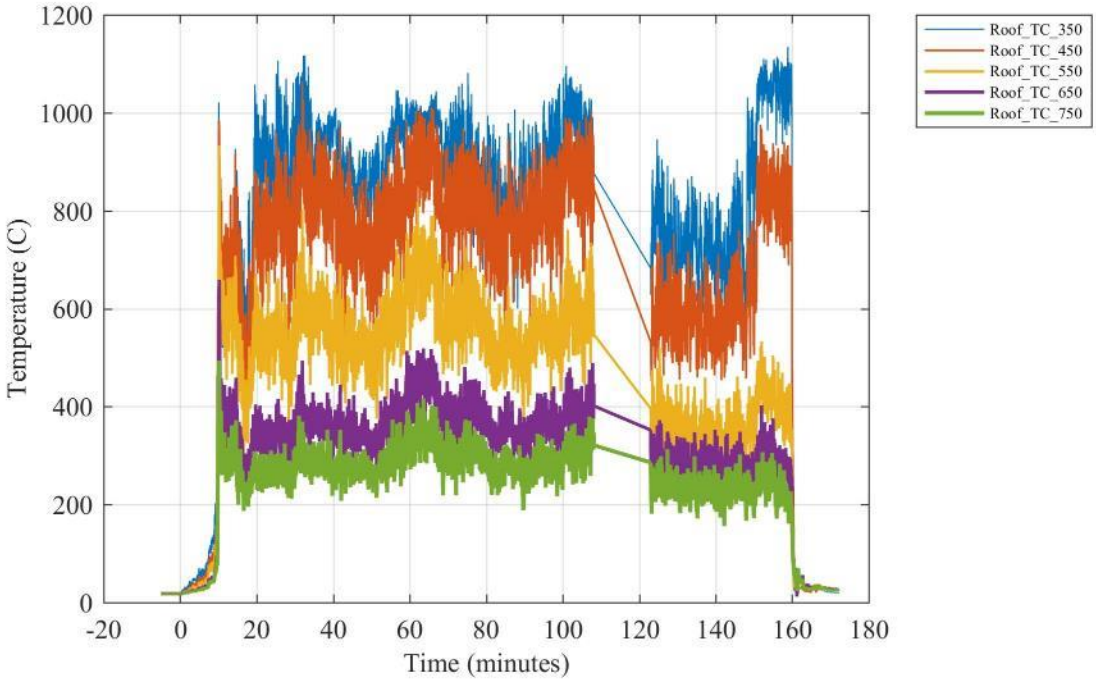

Figure J 7. Temperatures measured at various heights above the floor above the doorway.

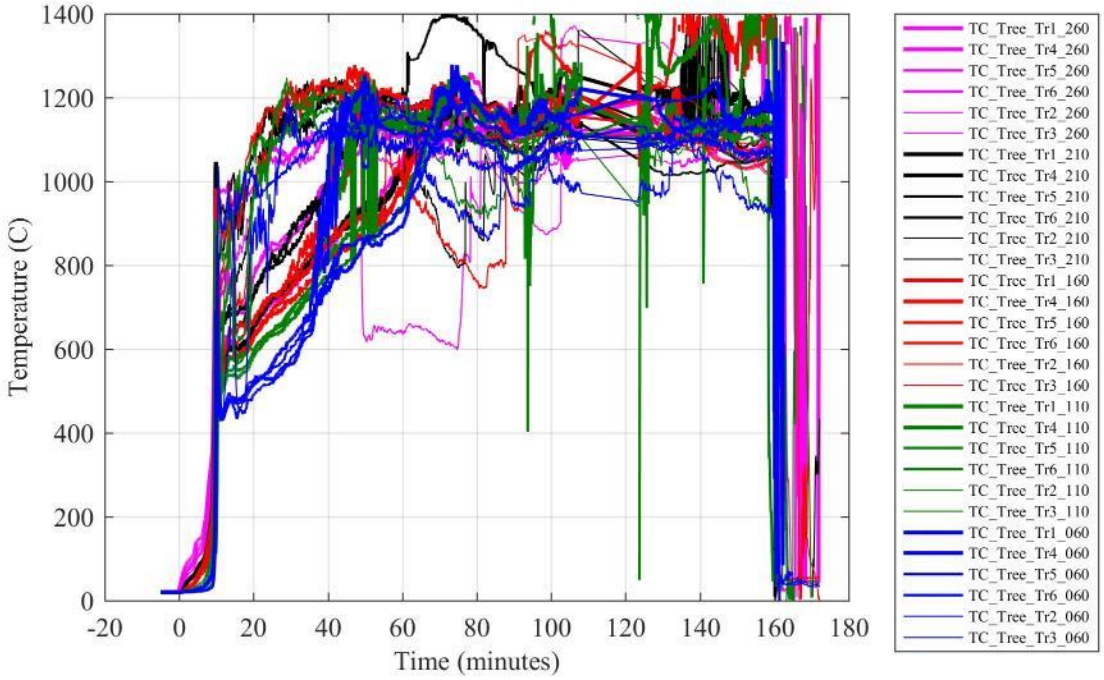

Figure J 8. Thermocouple tree temperatures at various locations inside the compartment.

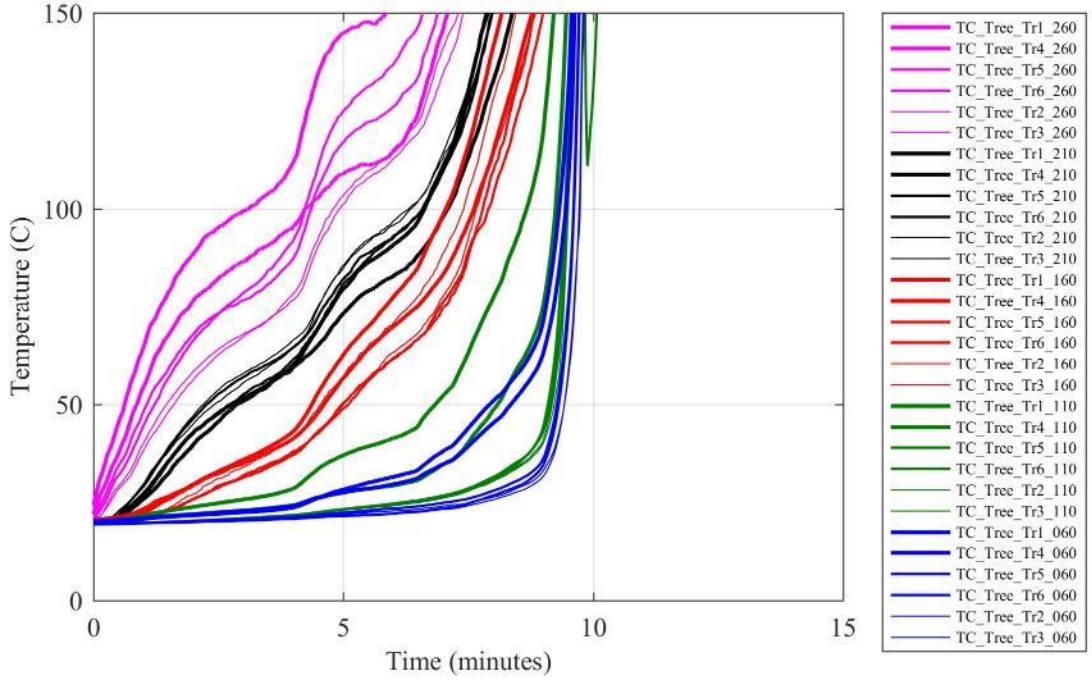

Figure J 9. Thermocouple tree temperatures at various locations inside the compartment during the first 15 min after ignition.

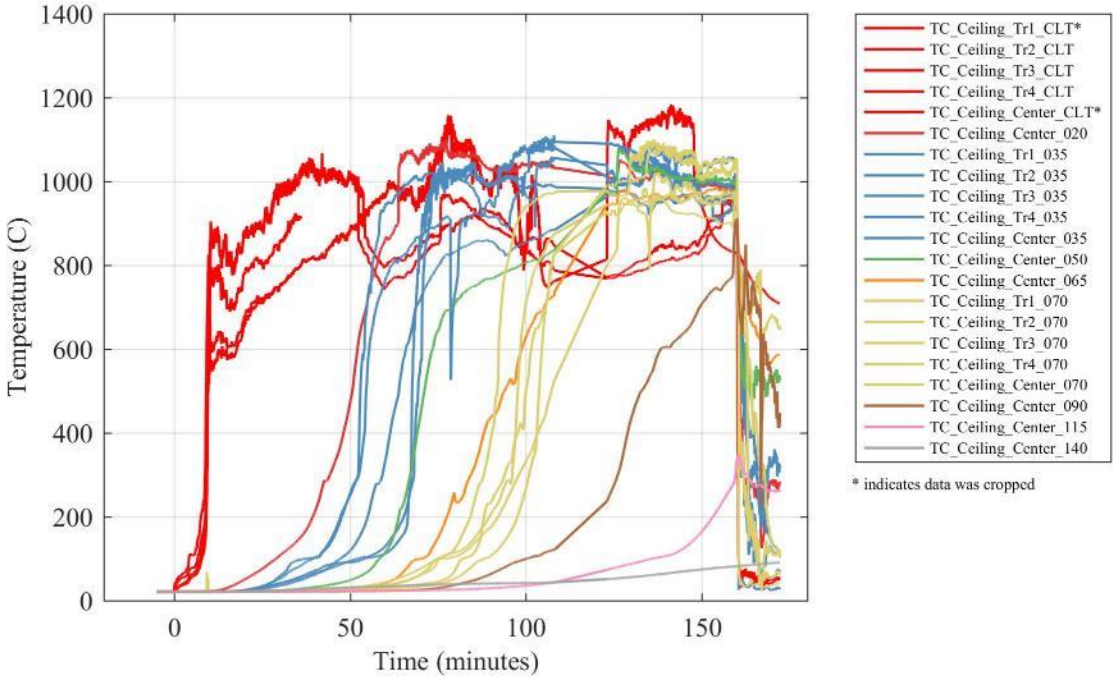

Figure J 10. Temperatures in the ceiling at various depths from the fire exposed surface.

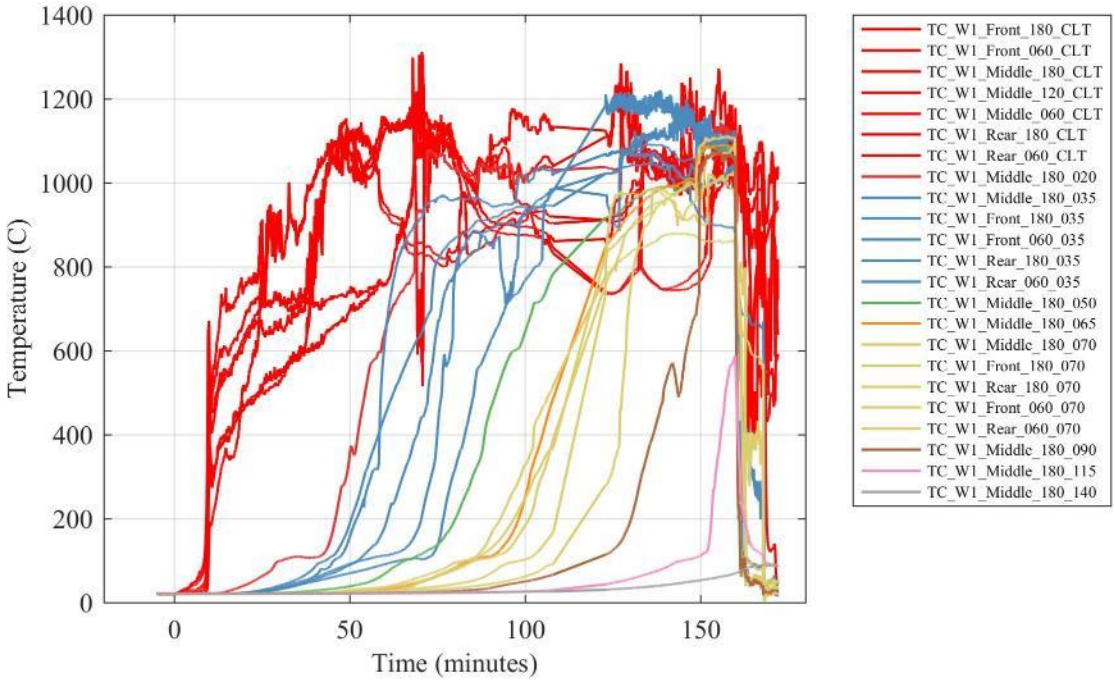

Figure J 11. Temperatures in Wall W1 at various depths from the fire exposed surface.

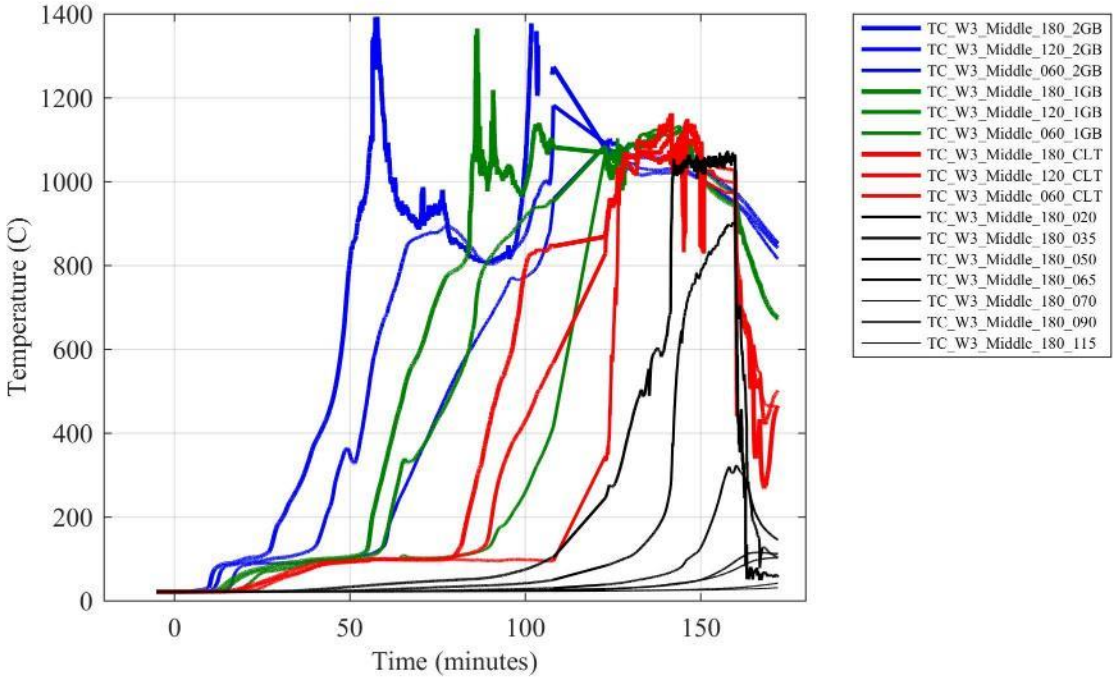

Figure J 12. Temperatures in Wall W3 at various depths from the fire exposed surface.

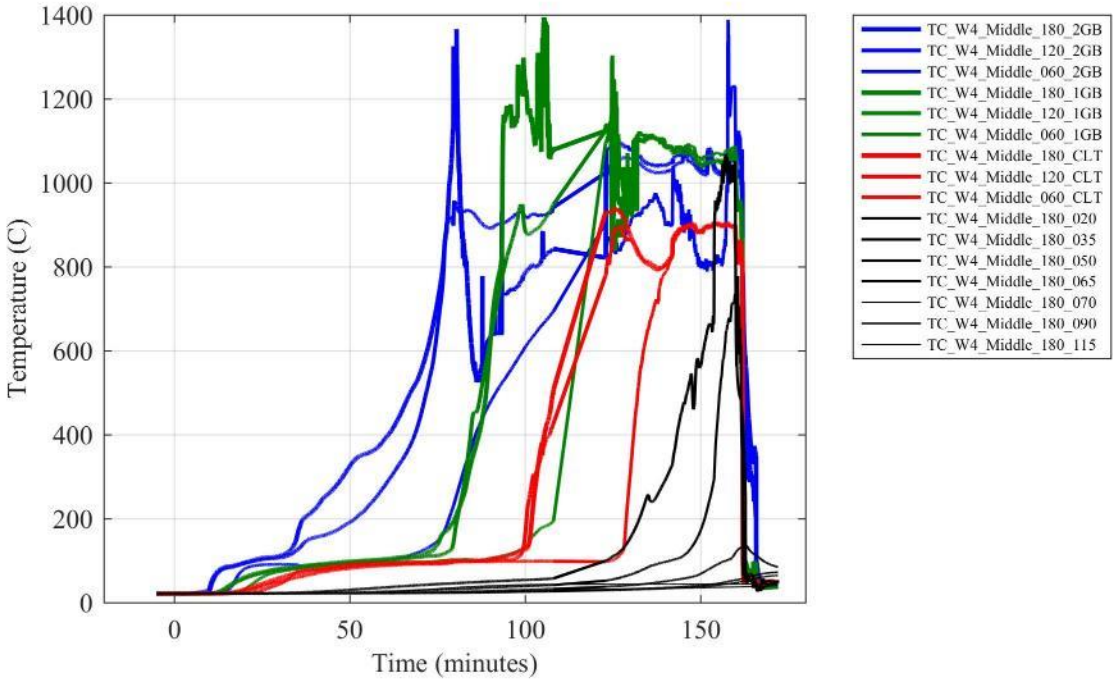

Figure J 13. Temperatures in Wall W4 at various depths from the fire exposed surface.

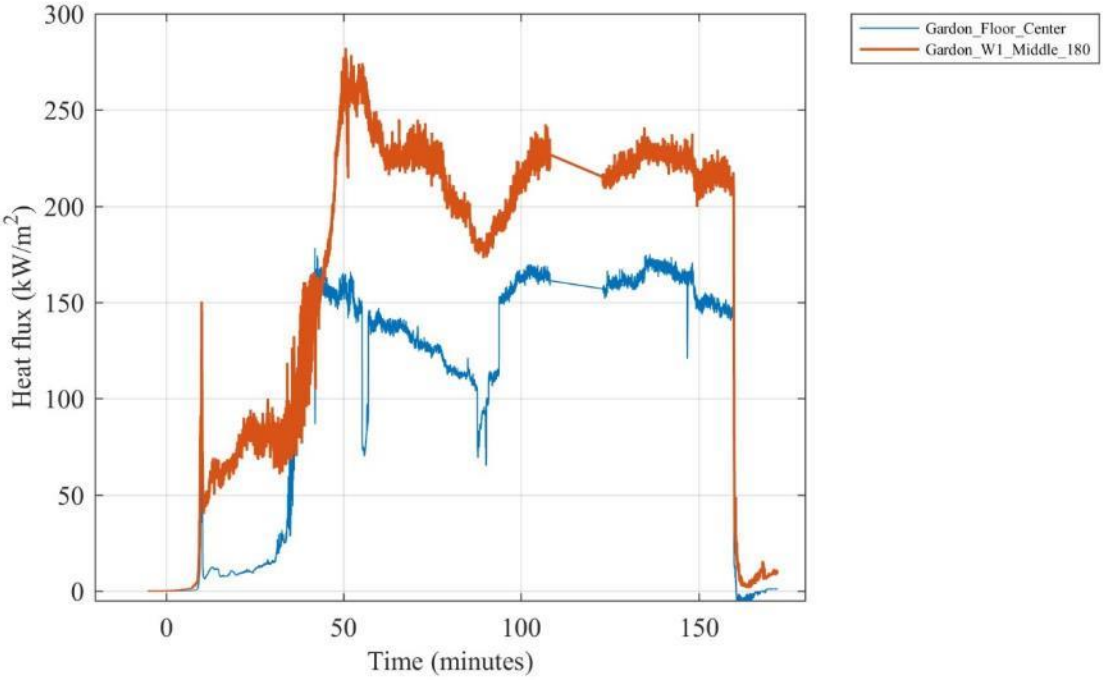

Figure J 14. Heat flux measured by Gardon gauges located inside the compartment.

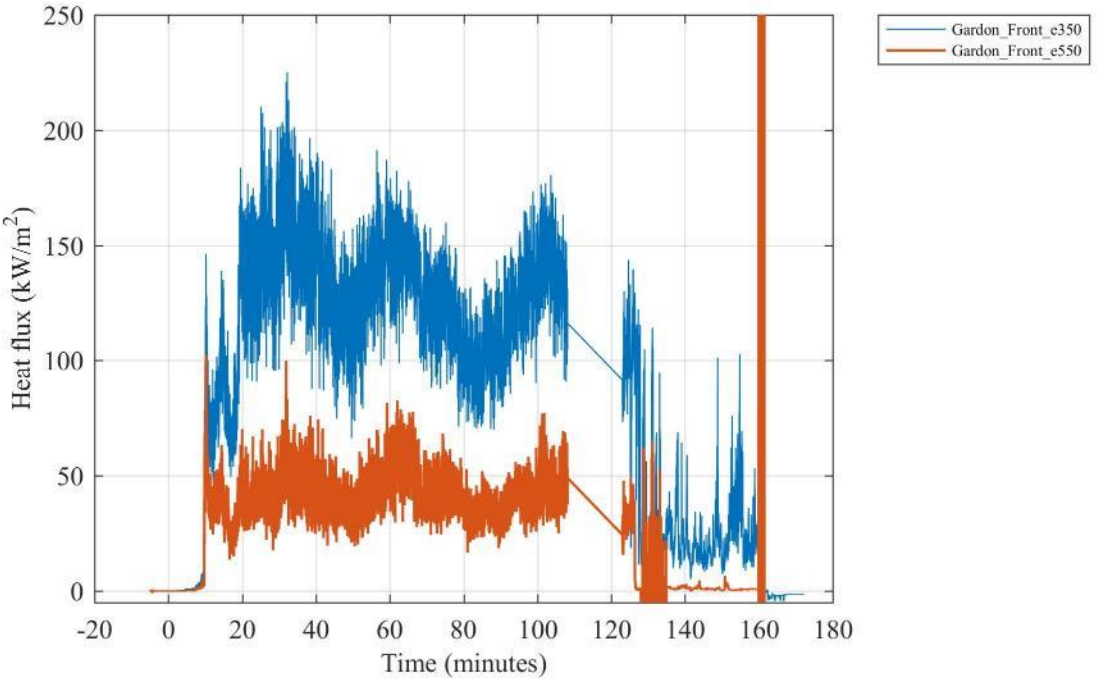

Figure J 15. Heat flux measured by Gardon gauges 350 cm and 550 cm above the floor above the doorway.

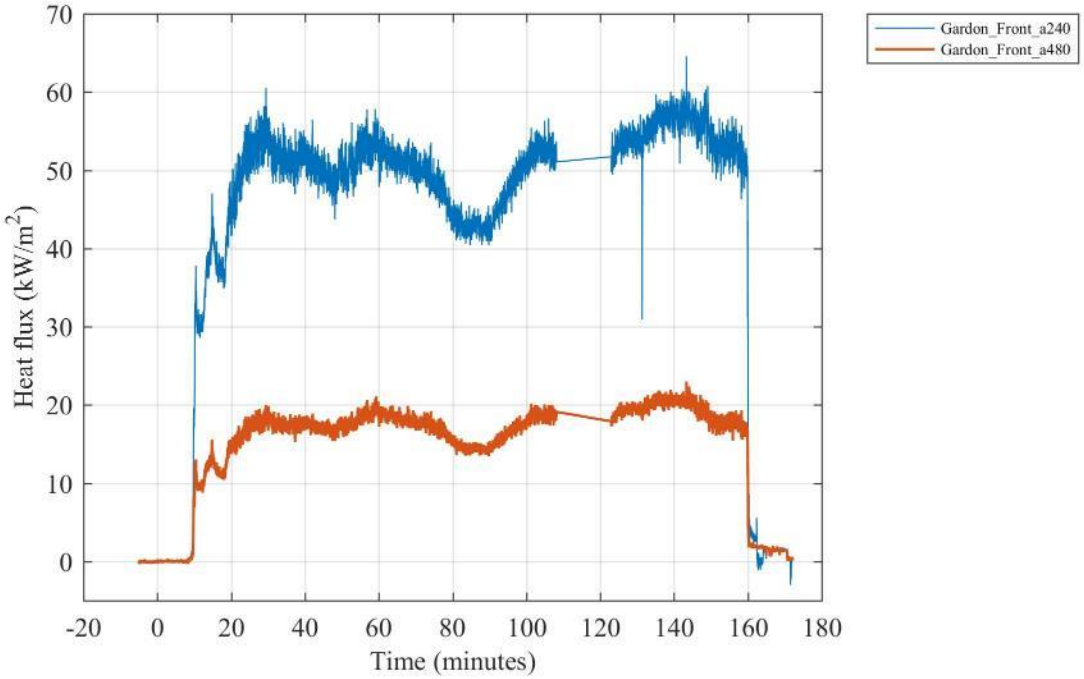

Figure J 16. Heat flux measured by Gardon gauges 240 cm and 480 cm from the doorway facing the opening.

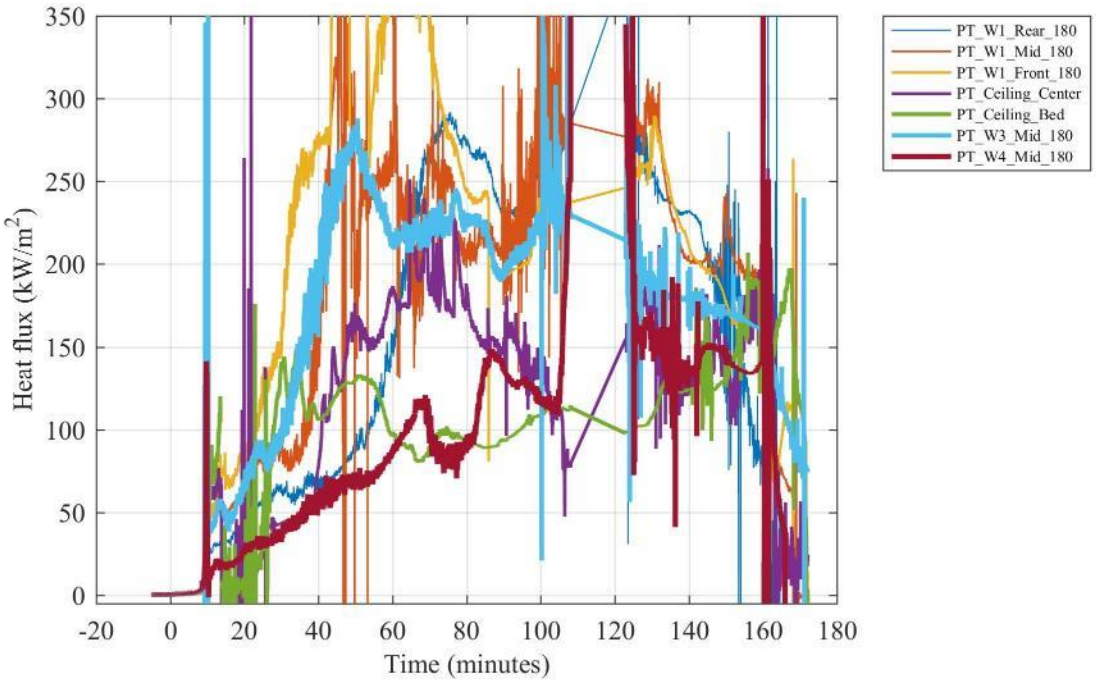

Figure J 17. Heat flux calculated from plate thermometers at various locations inside the compartment.

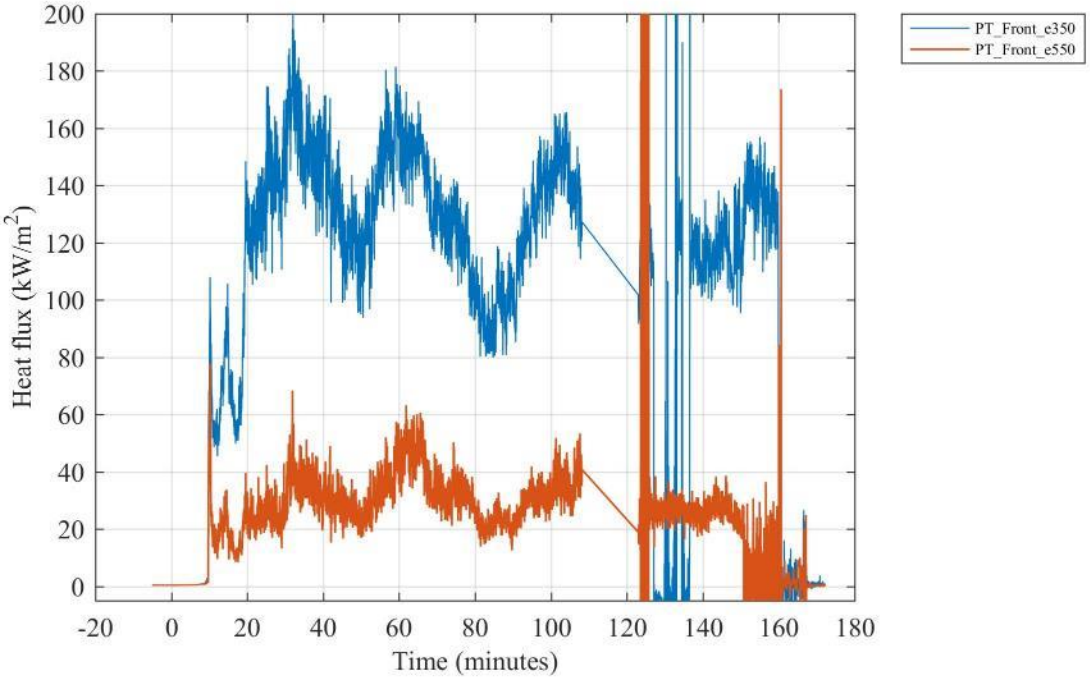

Figure J 18. Heat flux calculated from plate thermometers 350 cm and 550 cm above the floor above the doorway.

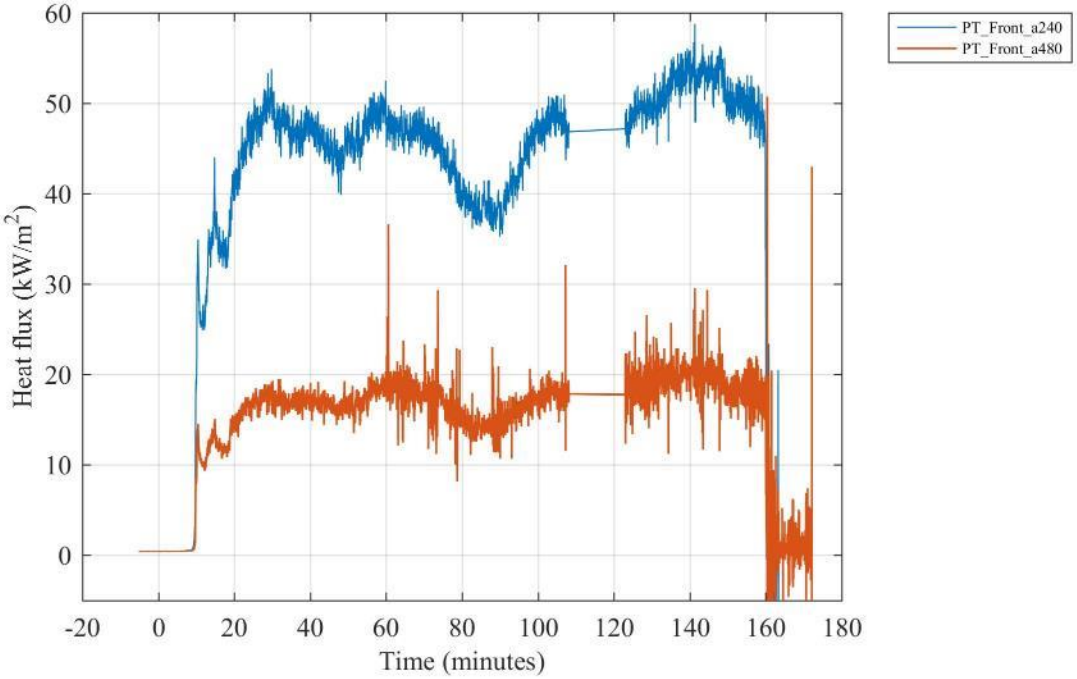

Figure J 19. Heat flux calculated from plate thermometers 240 cm and 480 cm from the doorway facing the opening.

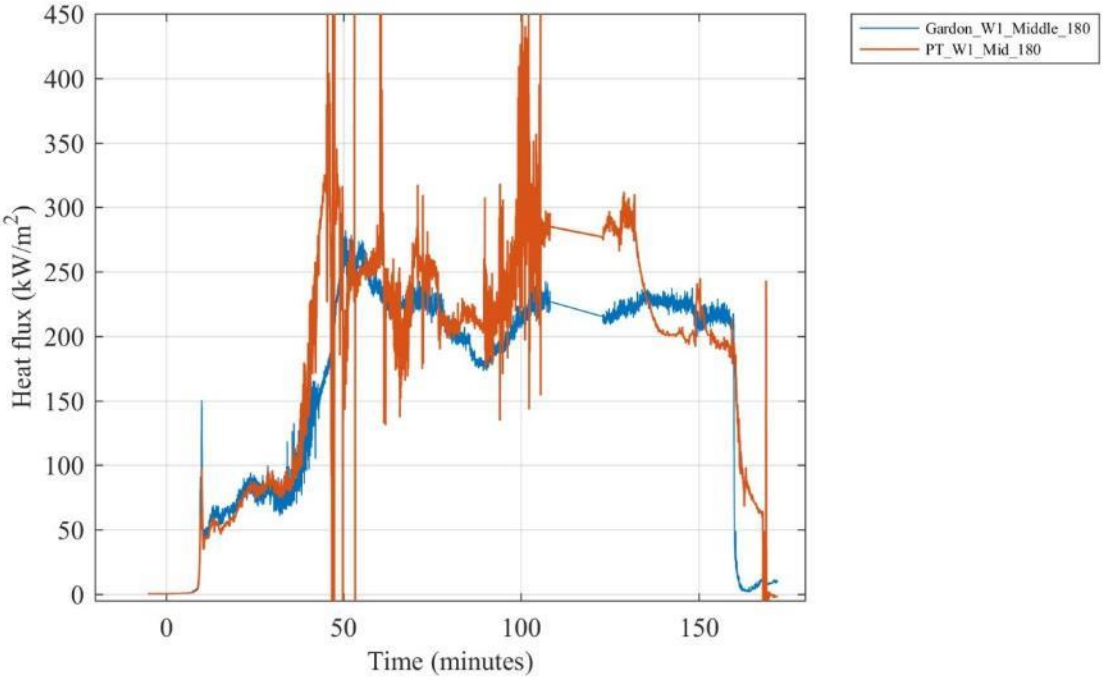

Figure J 20. Comparison of heat fluxes recorded by a collocated Gardon gauge, plate thermometer (PT) and differential flame thermometer (DFT) on Wall W1 at the middle of the compartment 1.8 m above the floor.

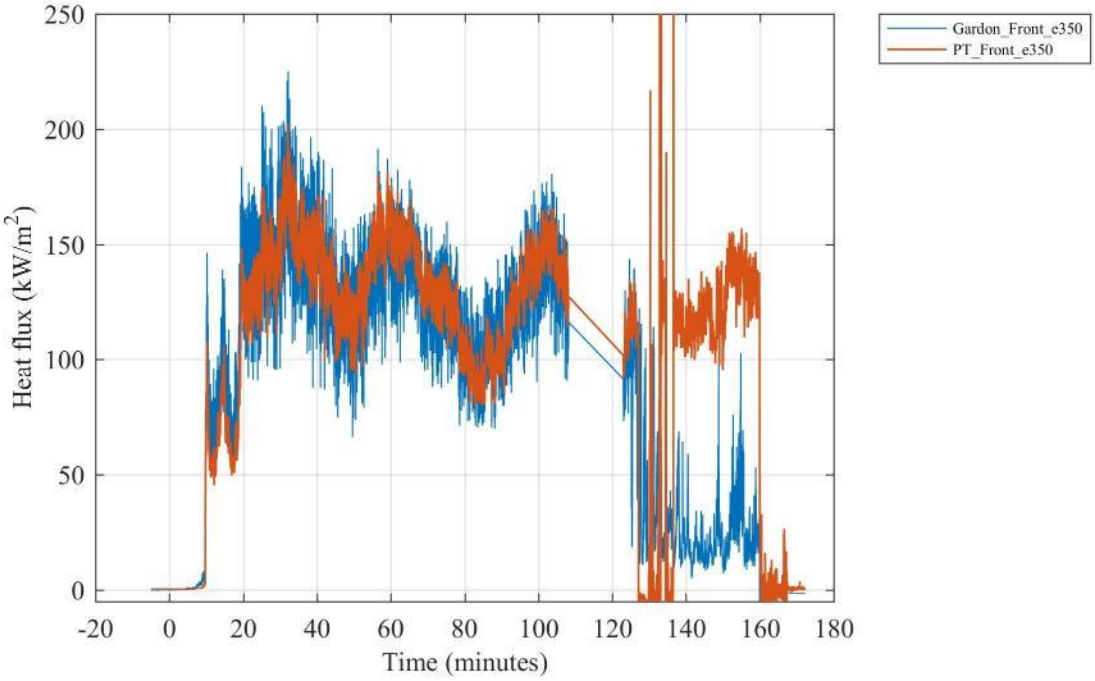

Figure J 21. Comparison of heat fluxes recorded by a collocated Gardon gauge and plate thermometer (PT) 350 cm above the floor above the doorway.

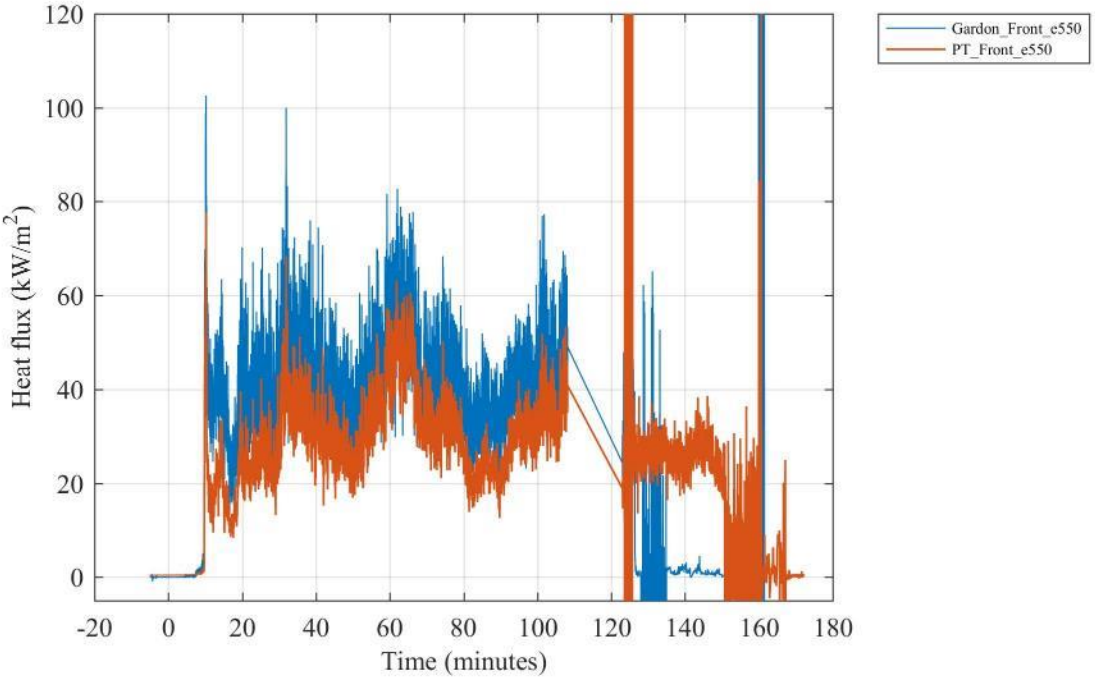

Figure J 22. Comparison of heat fluxes recorded by a collocated Gardon gauge and plate thermometer (PT) 550 cm above the floor above the doorway.

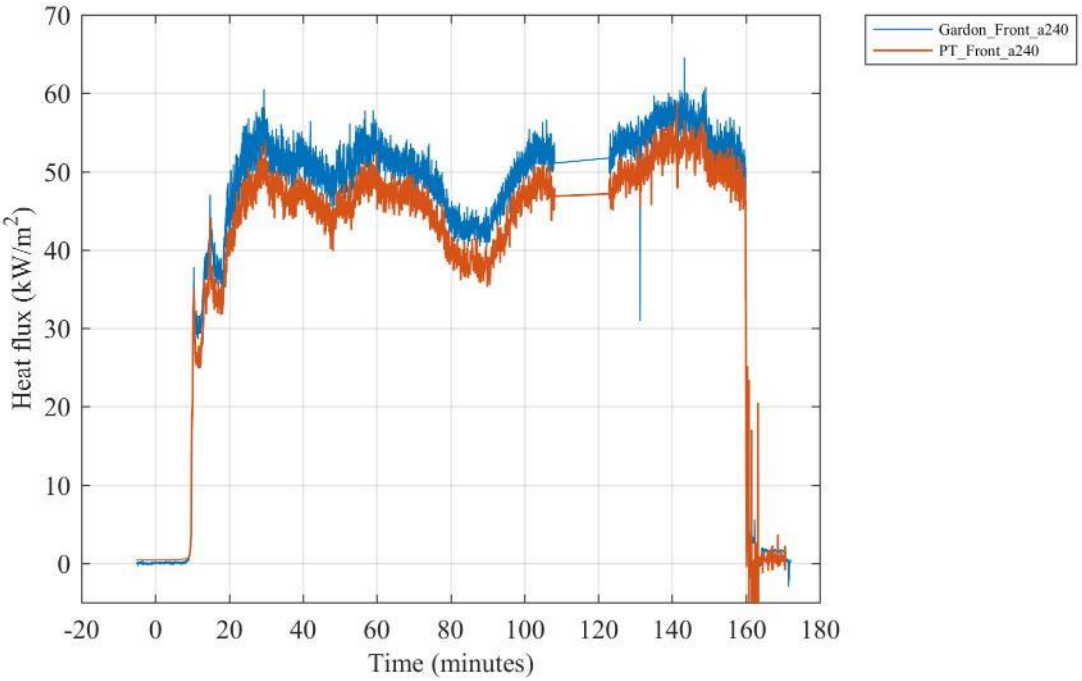

Figure J 23. Comparison of heat fluxes recorded by a collocated Gardon gauge and plate thermometer (PT) 240 cm from the doorway (facing doorway) and 150 cm above floor.

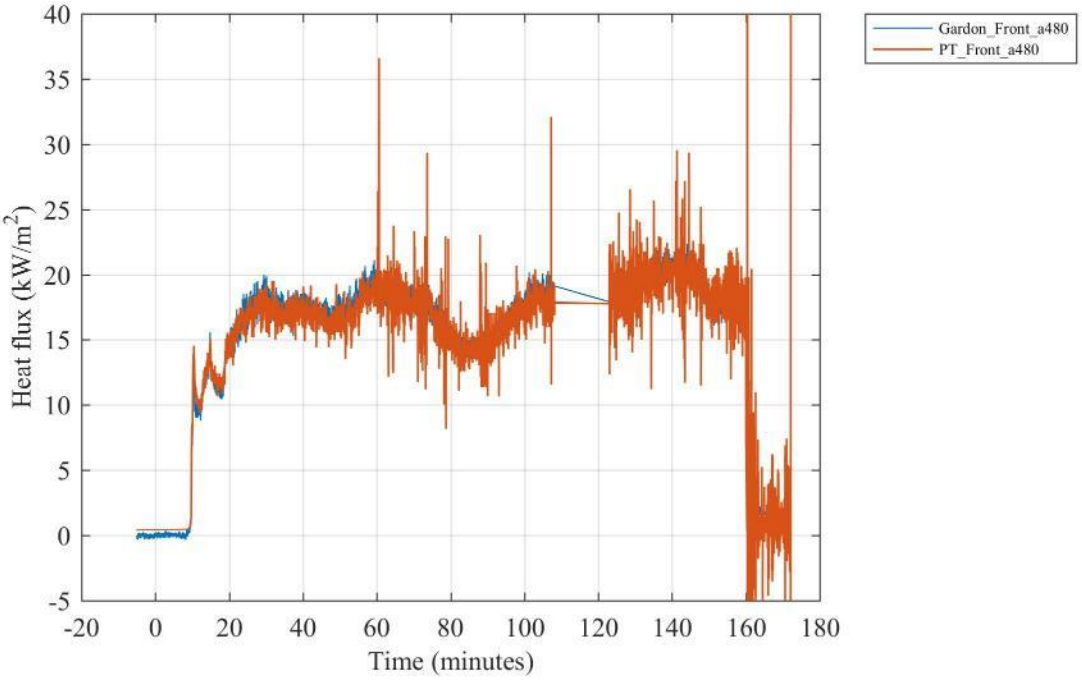

Figure J 24. Comparison of heat fluxes recorded by a collocated Gardon gauge and plate thermometer (PT) 480 cm from the doorway (facing doorway) and 150 cm above floor.

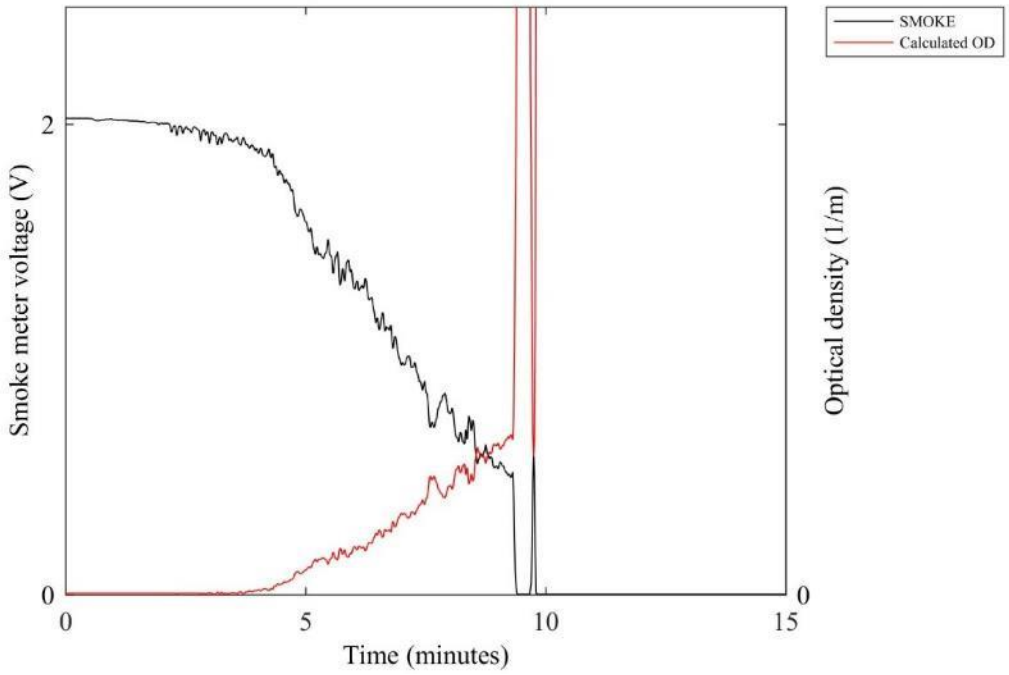

Figure J 25. Smoke meter voltage and calculated optical density (OD) from gas sampled at the center of the compartment 160 cm above the floor.

SENSOR DEFECTIVE

Figure J 26. Differential room pressure measured 210 cm above the floor at the center of the compartment.

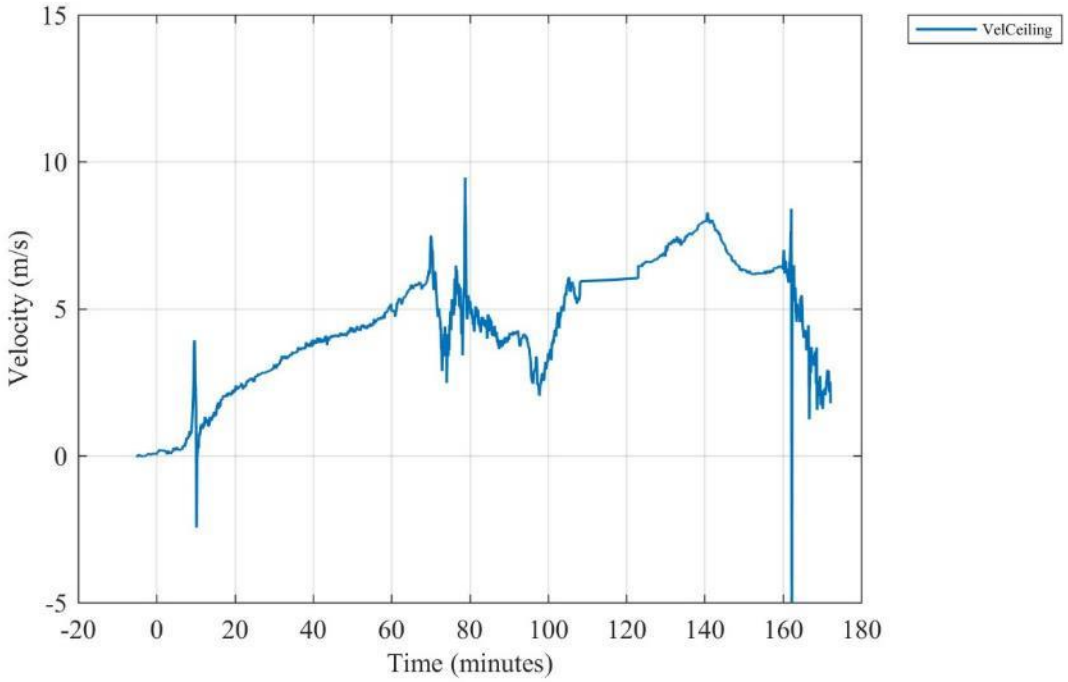

Figure J 27. Gas velocity measured 305 mm from the ceiling along the midline 227.5 cm from the back of the compartment (positive indicates flow out the door). [10 s moving average filter applied]

SENSORS DEFECTIVE

Figure J 28. Gas velocities measured in the doorway (positive indicates flow out the door). [10 s moving average filter applied]

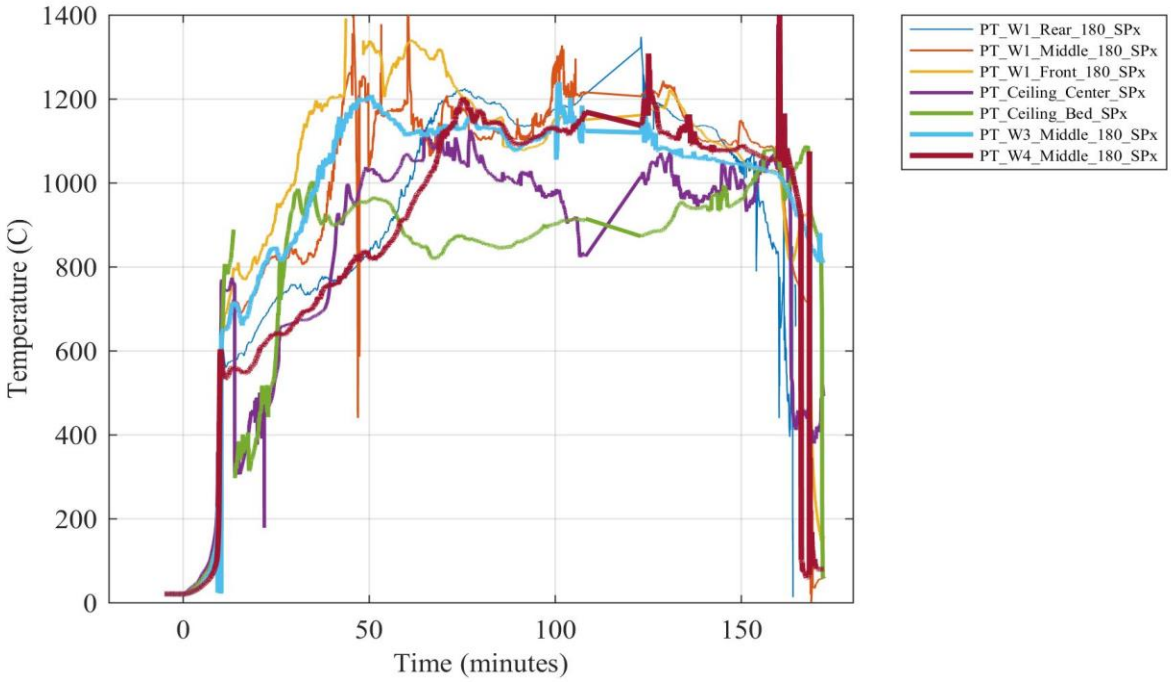

Figure J 29. Plate thermometer temperatures at various locations inside the compartment.

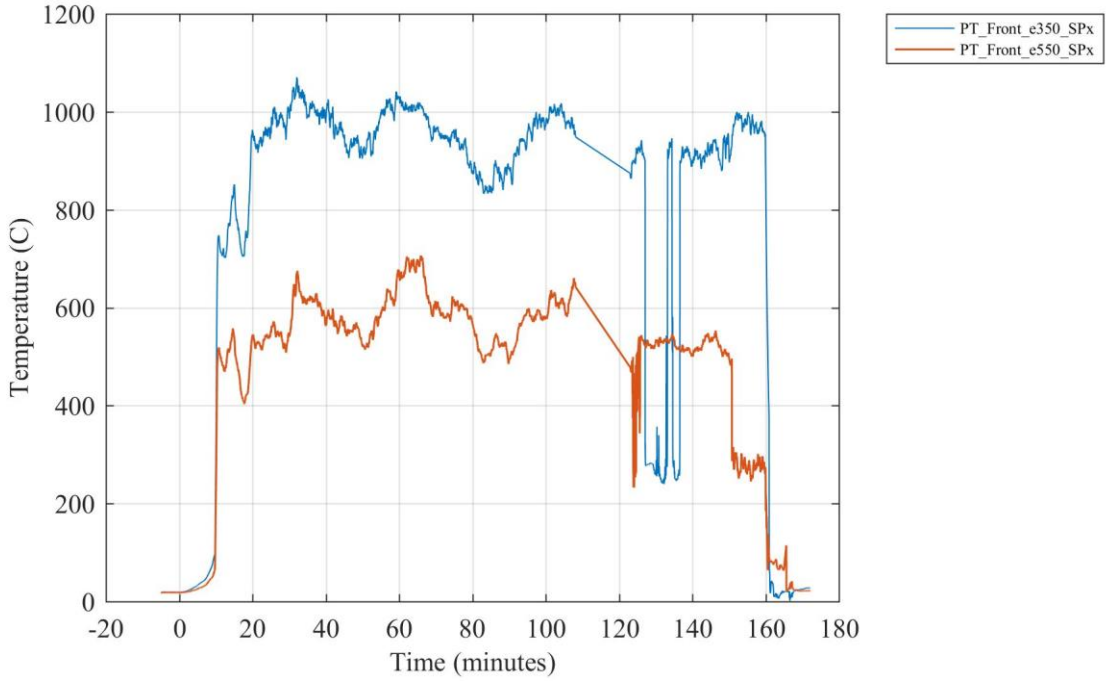

Figure J 30. Plate thermometer temperatures 350 cm and 550 cm above the floor above the doorway.

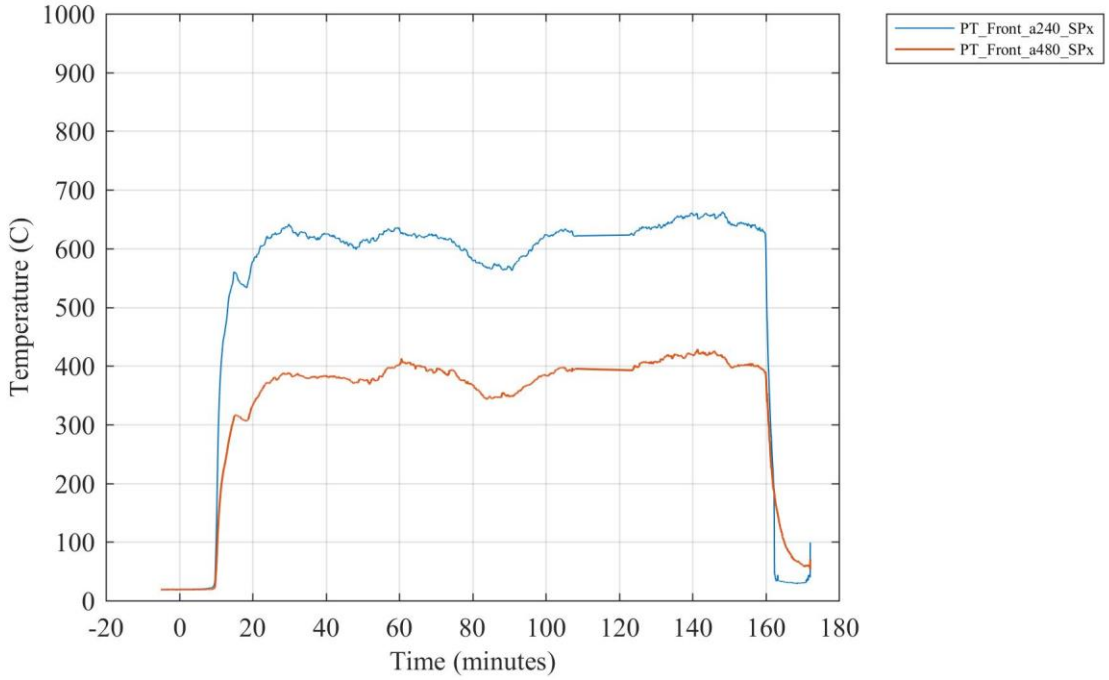

Figure J 31. Plate thermometer temperatures 240 cm and 480 cm from the doorway facing the opening.

Appendix K - Alarm activation times

Table K 1. Activation times of smoke alarms and heat alarms

Test ID	Activation time, s	
	Smoke alarm	Heat alarm
Test 1-1	126	210
Test 1-2	201	176
Test 1-3	327	173
Test 1-4	150	91
Test 1-5	109	149
Test 1-6	122	177
Mean	173	163
SD	82	40

Appendix L - Uncertainty of Measurements

The measurements presented in this report include length (structural element positions and dimensions, fuel positions and dimensions, charring depth, and instrument location), fuel mass, CLT moisture, calorimeter and burner heat release rates, gas species concentrations, differential pressure, optical density, temperatures, simulated thermal element (STE) response time, heat fluxes, gas flow velocities, and smoke and heat alarm response time. For each measurement, Type A and/or Type B uncertainties, combined standard uncertainties, and total expanded uncertainties were estimated. As defined in Taylor and Kuyatt (1994), Type A uncertainty was evaluated using statistical methods; Type B uncertainty was estimated by other means such as the information available in manufacturer's specifications, from past-experience, or engineering judgement. The combined standard uncertainty was estimated by combining the individual uncertainties using "root-sum-of-squares" (Taylor and Kuyatt, 1994). The expended uncertainty was then computed by multiplying the combined uncertainty by a coverage factor of 2 corresponding to an approximately 95 % confidence interval.

Table L-1 summarizes the components of the measurement uncertainty. All uncertainties are assumed to be symmetric (+/-) and to have a Gaussian distribution. The following definitions are used:

- *Precision*: The ability of the instrument to resolve information from the sensor.
- *Bias*: The uncertainty in the calibration of the sensor, the accuracy as published by the manufacturer, or other known sources of error.
- *Random*: Error due to random, unpredictable variations in the measurement process during a typical steady-state period.

For example, dimensional measurements were made using tape measures assumed to be readable with one's eye (*resolution*) to within 0.8 mm (1/32 in.) – half of the smallest marking – and to have a *bias* accuracy of 0.8 mm (1/32 in.), which is the manufacturer's published accuracy. The *random* error was based on repeat measurements.

Reference

Taylor, B. N., and Kuyatt, C. E. (1994). "Guidelines for Evaluating and Expressing the Uncertainty of NIST Measurement Results." NIST Technical Note TN-1297, Gaithersburg, MD.

Table L-1. Uncertainty in the experimental data.

Measurement / Component	Estimation Method	Component Standard Uncertainty	Combined Standard Uncertainty	Total Expanded Uncertainty
Structural element positions and dimensions, mm				
Precision	Type B	0.8		
Bias	Type B	0.8	2	5
Random (N=5)	Type A	2		
Fuel positions and dimensions, mm				
Precision	Type B	0.8		
Bias	Type B	0.8	13	25
Random (N=5)	Type A	13		
Charring depth, mm				
Precision	Type B	0.8		
Bias	Type B	0.8	2	3
Random (N=5)	Type A	1		
Instrument location, mm				
Precision	Type B	0.8		
Bias	Type B	0.8	5	10
Random (N=5)	Type A	5		
Fuel mass, kg				
Precision	Type B	0.001		
Bias	Type B	0.001	0.01	0.02
Random (N=5)	Type A	0.01		
CLT moisture, %				
Precision	Type B	0.1		
Bias	Type B	0.1	0.2	0.5
Random (N=5)	Type A	0.2		
Calorimeter heat release rate, % RD				
Precision	Type B	0.1		
Bias	Type B	4.5	7.4	14.8
Random (N=300)	Type A	5.9		
Burner heat release rate, % RD				
Precision	Type B	0.2		
Bias	Type B	0.6	0.8	1.6
Random (N=300)	Type A	0.5		
CO_2 gas species concentrations, % FS				
Precision	Type B	0.1		
Bias (Linearity)	Type B	1	2.8	5.6
Bias (Zero and span gas)	Type B	1		
Random (N=300)	Type A	2.4		
Differential pressure, Pa				
Precision	Type B	0.5		
Bias (Hysteresis and linearity)	Type B	0.6	1.1	2.3
Bias (Instrument temperature)	Type B	0.8		
Random, Pa (N=100)	Type A	0.13		
Optical density, % RD				
Precision	Type B	0.1		
Bias	Type B	10	10.2	20.5
Random (N=100)	Type A	2.2		

Measurement / Component	Estimation Method	Component Standard Uncertainty	Combined Standard Uncertainty	Total Expanded Uncertainty
Temperature (gas; bare bead thermocouple), % RD				
Precision	Type B	0.01		
Bias [a]	Type B	0.75	13.4	26.8
Random (N=300)	Type A	13.4		
Temperature (gas; sheathed thermocouple), % RD				
Precision	Type B	0.01		
Bias [a]	Type B	0.75	7.3	14.7
Random (N=300)	Type A	7.3		
Temperature (specimen; bare bead thermocouple), % RD				
Precision	Type B	0.01		
Bias [a]	Type B	0.75	3.1	6.2
Random (N=300)	Type A	3.0		
STE response time, s				
Precision	Type B	1		
Bias	Type B	0.1	1	2
Random	Type A	-		
Heat flux (Gardon), % RD				
Precision	Type B	0.01		
Bias	Type B	1.5		
Bias (Soot & dust)	Type B	10	11.2	22.5
Bias (Cooling water temperature)	Type B	0.5		
Random (N=300)	Type A	4.9		
Gas flow velocity, % RD				
Precision	Type B	0.01		
Bias (Probe constant)	Type B	5	7.6	15.2
Random (N=300)	Type A	5.7		
Smoke and heat alarm trigger timing, s				
Precision	Type B	1		
Bias	Type B	0.1	1	2
Random	Type A	-		

FS = full scale; RD = reading; N = number of samples

[a] The standard limit of error is the greater of +/- 0.75 % or 2.2 °C.